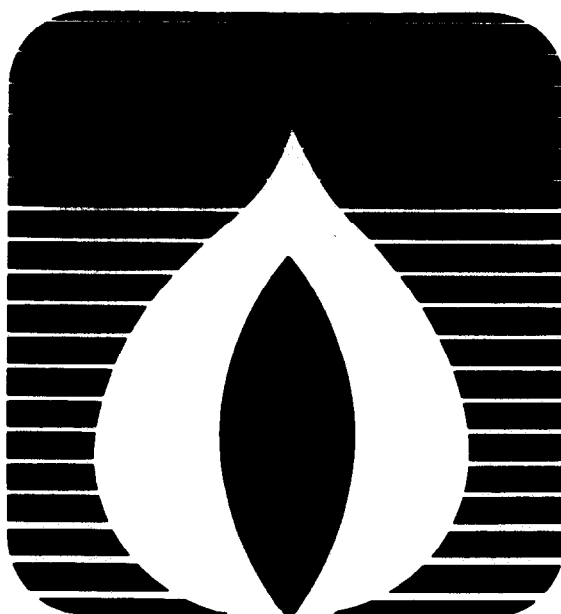


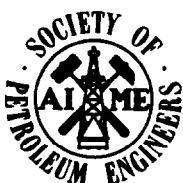
UNCONVENTIONAL GAS RECOVERY SYMPOSIUM

UGR FILE

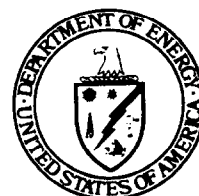
S357
*(S357)



May 18-20, 1980
Hilton-Gateway Center
Pittsburgh, Pennsylvania



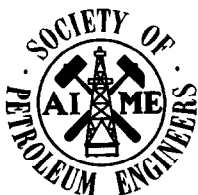
Sponsored Jointly
By The
Society of Petroleum Engineers of AIME
And The
U.S. Department of Energy



PROCEEDINGS
The First Annual Symposium on
UNCONVENTIONAL GAS RECOVERY

May 18 - 20, 1980
Hilton - Gateway Center,
Pittsburgh, Pennsylvania

Sponsored Jointly
by the
Society of Petroleum Engineers of AIME
and
U.S. Department of Energy



PUBLICATION RIGHTS RESERVED

All papers in this volume were prepared for the 1980 SPE/DOE SYMPOSIUM ON UNCONVENTIONAL GAS RECOVERY held in Pittsburgh, Pennsylvania, May 18-21, 1980. Permission to copy is restricted to an abstract of not more than 300 words. Illustrations may not be copied. The abstract should contain conspicuous acknowledgment of where and by whom the paper is presented. Publication elsewhere is usually granted upon request to the Executive Director, Society of Petroleum Engineers, 6200 N. Central Expwy., Dallas, Texas, U.S.A. Discussion of the paper is invited.

PREFACE

The objective of the SPE and DOE in organizing this symposium has been to bring together in a single annual meeting the best of the professional community engaged in unconventional gas recovery technology. The first venture will focus on discussions of the realities and potentials of unconventional gas sources and an exchange of technology developments.

Unconventional gas sources are expected to have an important impact on new gas supplies as technological developments rapidly emerge and become mature technologies in the recovery of natural gas from coal, tight formations, Devonian shale geopressured reservoirs and other alternative high-cost gas sources. It is hoped that this symposium will provide a state-of-art perspective on geology, exploration and production research, recovery technology and field test results.

The Keynote Session will examine the present status and projected future of unconventional gas production. The technical sessions have been arranged by the technology involved, rather than by gas sources, in order to have similar technologies presented in one session. The planning committee felt that this arrangement would be the most constructive method for presentation of the advances being made in technology. In recognition of the importance of how well new techniques work, one session is devoted to actual field results of various unconventional gas recovery projects.

Although much time and effort have been spent in organizing the program of this First Annual Symposium on Unconventional Gas Recovery, it has been a pleasure largely because of the excellent support offered by everyone involved. A very dedicated and hard working program committee contributed substantially to the quality of this symposium.

I would like to thank the Department of Energy, especially Hilma Barlow and Dee Dee Manilla who were so generous with their support, and many thanks to Janelle Stewart, Lisa Jolley, and Sabrina Rundle from SPE who have all been indispensable in helping to organize all aspects of this program. Finally, I thank every author whose work and ideas are presented in this symposium.

John L. Moore
Program Chairman

PROGRAM COMMITTEE

Lucio D'Andrea
U.S. Department of Energy

Robert W. Chase
Marietta College

Loyd E. Elkins
Petroleum Consultant

James H. Kennedy
INTERCOMP

Samuel L. Kimmel
Angerman Associates

John L. Moore, Chairman
Consolidated Natural Gas

Robert S. Ottinger
TRW, Inc.

T. Viswanathan
Gulf Research & Development

Robert L. Wise
U.S. Department of Energy

TABLE OF CONTENTS

SPE/8921 - <u>The Need and Urgency for Unconventional Gas</u> DOE <u>V.A. Kuuskraa, Lewin & Associates, Inc.</u>	9
SPE/8924 - <u>Natural Gas Potential of the New Albany Shale</u> DOE <u>Group (Devonian-Mississippian) in Southeastern Illinois</u> <u>R.M. Cluff and D.R. Dickerson, Illinois State Geological Survey</u>	21
SPE/8926 - <u>Preliminary Methane Resource Assessment of Coalbeds in</u> DOE <u>the Arkoma Basin</u> <u>H.H. Rieke III, TRW, Inc.</u>	29
SPE/8927 - <u>The Coal Bed Methane Potential of the Raton</u> DOE <u>Basin, Colorado</u> <u>C.M. Tremain, Colorado Geological Survey</u>	43
SPE/8928 - <u>The Coalbed Methane Resource of the Illinois Basin</u> DOE <u>P.L. Archer, TRW Energy Systems; D.D. Carr and D. Harper,</u> <u>Indiana Geological Survey</u>	51
SPE/8929 - <u>Geological Implications of Gas Production from</u> DOE <u>Insitu Gas Hydrates</u> <u>G.D. Holder, University of Pittsburgh; V.T. John and</u> <u>S.L. Yen, Columbia University</u>	59
SPE/8930 - <u>A Laboratory Investigation of Enhanced Recovery of Methane</u> DOE <u>From Coal by Carbon Dioxide Injection</u> <u>P.F. Fulton, C.A. Purente, B.A. Rogers, N. Shah, and</u> <u>A.A. Reznik, University of Pittsburgh</u>	65
SPE/8931 - <u>Effects of a No-Proppant Foam Stimulation Treatment on</u> DOE <u>a Coal Seam Degasification Borehole</u> <u>J.V. Mahoney, P.B. Stubbs, F.C. Schwerer III, and</u> <u>F.X. Dobscha, United States Steel Research</u>	73
SPE/8932 - <u>In Situ Stresses: The Predominant Influence on</u> DOE <u>Hydraulic Fracture Containment</u> <u>N.R. Warpinski, R.A. Schmidt, and D.A. Northrop,</u> <u>Sandia National Laboratories</u>	83
SPE/8933 - <u>The Mapping of Nitrogen Gas Induced Hydraulic Fracture</u> DOE <u>in Devonian Shale by Observation of the Associated</u> <u>Surface Deformation</u> <u>K.F. Evans, G.R. Holzhausen, and M.D. Wood, M.D. Wood, Inc.</u>	95
SPE/8934 - <u>In Situ Evaluation of Several Tailored-Pulse</u> DOE <u>Well-Shooting Concepts</u> <u>R.A. Schmidt, N.R. Warpinski, and P.W. Cooper,</u> <u>Sandia National Laboratories</u>	105
SPE/8936 - <u>Empirical Evaluation of Clinton Sand Well Performance</u> DOE <u>C.R. Skillern, TRW Energy Systems Group</u>	117
SPE/8937 - <u>A Wireline Hydraulic Fracturing Tool for the Determination</u> DOE <u>of In Situ Stress Contrasts</u> <u>M.D. Voegelé and A.H. Jones, Terra Tek, Inc.</u>	123
SPE/8938 - <u>Evaluation of Fractured Reservoir Rocks Using</u> DOE <u>Geophysical Well Logs</u> <u>W.H. Fertl, Dresser Atlas</u>	131
SPE/8940 - <u>Utilizing Well Interference Data in Unconventional Gas Reservoirs</u> DOE <u>W.K. Sawyer, West Virginia University; J. Alam and W.D. Rose*,</u> <u>Science Applications, Inc. (*presently with Institute of</u> <u>Gas Technology)</u>	137
SPE/8941 - <u>Finite Element Model Simulations Associated with</u> DOE <u>Hydraulic Fracturing</u> <u>S.H. Advani, The Ohio State University</u>	151

SPE/8942 -	<u>Effects of Various Parameters on Hydraulic Fracturing Geometry</u>	
DOE	M.E. Hanson, G.D. Anderson, and R.J. Shaffer, Lawrence Livermore National Laboratory	163
SPE/8943 -	<u>Elliptical Flow Equations for Vertically Fractured Gas Wells</u>	
DOE	B.W. Hale, Northwest Pipeline Corp.; and J. F. Evers, University of Wyoming	173
SPE/8944 -	<u>After the Technology, What Happens?</u>	
DOE	T.W. Merrill Jr., Industrial Energy Services Co.	181
SPE/8945 -	<u>Economics of Devonian Shale, Coal Seam and Similar Special Appalachian Gas Sources</u>	
DOE	R.M. Miller and N.E. Mutchler, Berger Associates	187
SPE/8946 -	<u>Utilization and Recovery Economics for Vertical Wells in Coalbed Methane</u>	
DOE	A. Gillies, A.J. Snygg, D. Dickehuth, and S.M. Howarth, TRW Energy Systems Group	199
SPE/8947 -	<u>Legal Aspects of Gas from Coalbeds</u>	
DOE	N.E. Mutchler, Berger Associates, Inc.; and H.R. Sachse, Sonosky, Chambers & Sachse	205
SPE/8948 -	<u>An Evaluation of the Geopressured Energy Resource of Louisiana and Texas</u>	
DOE	G. Samuels, Union Carbide Corp.	215
SPE/8949 -	<u>Second Generation Technology for the Production of Pipeline Quality Gas from Sanitary Landfills</u>	
DOE	F.C. Rice, Getty Synthetic Fuels, Inc.	225
SPE/8950 -	<u>An Economic Natural Gas Recovery Method for Wells With No Pipeline Connection</u>	
DOE	J.M. Burns, Texas Gas Transport Co. and Pressure Transport Inc.	229
SPE/8952 -	<u>Perspective on Devonian Shale Gas Exploration: U.S. DOE'S Eastern Tennessee Wildcat</u>	
DOE	C.S. Dean, U.S. DOE	237
SPE/8953 -	<u>Natural Gas From Tight Siltstones in the Catskill Clastic Wedge in West Virginia</u>	
DOE	J.F. Schwietering, West Virginia Geological and Economic Survey	245
SPE/8954 -	<u>Predicting the In-Situ Stress State for Deep Wells Using Differential Strain Curve Analysis</u>	
DOE	F.G. Strickland and N.K. Ren, Dowell Division of Dow Chemical	251
SPE/8955 -	<u>Earth Stress Relationships in the Appalachian Basin</u>	
DOE	S.F. McKetta, Columbia Gas System Service Corp.	259
SPE/8956 -	<u>Unconventional Exploration for Natural Fractures</u>	
DOE	W.M. Hennington, Mitchell Energy & Development Corp.	265
SPE/8957 -	<u>The Unique Methane Gas Deposit in Lake Kivu (Central Africa)--Stratification, Dynamics, Genesis and Development</u>	
DOE	K. Tietze, Federal Institute for Geosciences and Natural Resources	275
SPE/8958 -	<u>Preliminary Results of the Wells-of-Opportunity Geopressured-Geothermal Testing Program</u>	
DOE	R.L. McCoy, The Gruy Companies; J.H. Hartsock and R.J. Dobson, Gruy Federal, Inc.	189
SPE/8960 -	<u>Test Results of Stimulated Wells in Devonian Shales</u>	
DOE	R.M. Kumar and J.H. Hartsock, Gruy Federal, Inc.; K.H. Frohne, U.S. Dept. of Energy	297

SPE/8962 -	<u>Methane Recovery from Deep Unmineable Coal Seams</u>	
DOE	<u>L.D. Allred and R.L. Coates, Mountain Fuel Resources, Inc.</u>	307
SPE/8963 -	<u>Waynesburg College Multiple Coal Seam Methane</u>	
DOE	<u>Extraction Well</u>	
	<u>J.N. Kirr and G.E. Eddy, Waynesburg College; R. Rahsman,</u>	
	<u>Rahsman Geological Services; N.F. McGinnis, TRW, Inc.</u>	313
SPE/8964 -	<u>Influence of Coalbed Characteristics and Geology on</u>	
DOE	<u>Methane Drainage</u>	
	<u>G.L. Finfinger, L.J. Prosser Jr., and J. Cervik,</u>	
	<u>U.S. Bureau of Mines</u>	319
SPE/8965 -	<u>Completion Techniques and Production Data from Vertical</u>	
DOE	<u>Methane Drainage Boreholes, Jawbone Coalbed, Dickenson</u>	
	<u>County, Virginia</u>	
	<u>P.F. Steidl, M.A. Trevits, and W.P. Diamond, U.S. Bureau of Mines</u>	325
SPE/8966 -	<u>Determining the Feasibility of Using Vertical Boreholes to</u>	
DOE	<u>Drain Gas From the Pocahontas No. 3 Coalbed, Buchanan County, VA</u>	
	<u>M.A. Trevits, U.S. Bureau of Mines; W.L. Richards and H.A.G.</u>	
	<u>von Schonfeldt, Occidental Research Corp.</u>	329
SPE/8967 -	<u>Methane Drainage from the Mary Lee Coalbed, Alabama,</u>	
DOE	<u>Using Horizontal Drilling Techniques</u>	
	<u>J.H. Perry, L.J. Prosser Jr., and J. Cervik, U.S. Bureau of Mines</u>	335
SPE/8968 -	<u>Drilling Long Horizontal Coalbed Methane Drainage Holes</u>	
DOE	<u>from a Directional Surface Borehole</u>	
	<u>W.P. Diamond and D.C. Oyler, U.S. Bureau of Mines</u>	341
SPE/8969 -	<u>Advance Methane Control and Its Impact on Gas Emissions</u>	
DOE	<u>in the Pocahontas #3 Coal Seam</u>	
	<u>H.A. von Schonfeldt, B.R. Pothini, and G.N. Aul,</u>	
	<u>Occidental Research Corp.</u>	347
SPE/8971 -	<u>Analysis of the Coalbed Degasification Process At A Seventeen</u>	
DOE	<u>Well Pattern in the Warrior Basin of Alabama</u>	
	<u>K.L. Ancell, INTERCOMP; and S. Lambert, Dept. of Energy</u>	355
SPE/8972 -	<u>Seismic Velocity Analysis to Locate Shale Gas Wells</u>	
DOE	<u>J.St.A. Boyer III and N.A. Anstey, Donohue Anstey and Morrill</u>	371

THE NEED AND URGENCY FOR UNCONVENTIONAL GAS

by Vello A. Kuuskraa, Lewin & Assocs., Inc.

© Copyright 1980, Society of Petroleum Engineers

This paper was presented at the 1980 SPE/DOE Symposium on Unconventional Gas Recovery held in Pittsburgh, Pennsylvania, May 18-21, 1980. The material is subject to correction by the author. Permission to copy is restricted to an abstract of not more than 300 words. Write: 6200 N. Central Expwy., Dallas, Texas 75206

INTRODUCTION

Despite the nation's preoccupation with oil, the colorful, turbulent history of coal and the controversy surrounding nuclear energy, neither oil, coal or nuclear is now the dominant U.S. energy source--since the mid-1970's the largest domestic energy source has been natural gas.

In the past year, the nation consumed nearly 80 quads (quadrillion or 10^{15} BTUs) of energy with domestically produced natural gas providing approximately 19 quads (19 Tcf). In comparison, domestic oil production was 18 quads (3 billion barrels), coal production was 14 quads (600 million tons) and nuclear energy in the form of electricity was 3 quads (250 million kilowatt-hours).

Natural gas is an economically preferable substitute for oil and an environmentally more acceptable source than coal or nuclear for many uses, such as industrial heating. Further, increased domestic supplies of natural gas could reduce imports, lessen the U.S. dependence on foreign energy sources, and help the balance of payments.

The current constraint on natural gas usage is no longer stimulating demand but rather obtaining sufficient supply. Even though several early warnings were sounded in the 1960's and early 1970's, predicting curtailments of gas, these warnings were muted by econometric studies that forecast massive additions of natural gas if only prices were slightly increased.

Recent detailed geological studies, declining finding rates and the limited additions of new supplies in response to sharply higher prices corroborate the conclusion that the geological limits of the domestic conventional natural gas resource base are being reached and that future production from this source will decline.

The most promising hope for future additions to natural gas supplies is from the nontraditional sources such as frontier (offshore and arctic) areas, deep drilling, imports, and unconventional gas. This paper will discuss each of these future supply sources.

References and illustrations at end of paper.

THE DEMAND FOR ENERGY

Even with conservation and improved end-use efficiencies energy consumption is expected to increase from 78 quads in 1978 to about 100 quads by 1990. The changes in U.S. energy demand by sector, or market, are projected in Fig. 1.

The demand for natural gas is supply limited, with industrial firms deterred from its use by fear of curtailments and electrical utilities deterred by law. Assuming adequate supplies were available, the American Gas Association (AGA) and several demand models project an unconstrained gas demand of 25 to 30 quads (or Tcf). Thus, the critical issue for natural gas is supply and how it can be increased from domestic sources.

ESTIMATING FUTURE SUPPLIES OF NATURAL GAS

Three types of estimating techniques dominate any future projections of natural gas supplies--traditional, advocacy, and disaggregate analysis.

1. Traditional. The traditional approach to estimating energy supplies relies on econometric models, finding rates and an aggregate resource base, generally the latest official USGS study. The current validity of these techniques, however, is doubtful, given; (a) the fiasco resulting from the use of econometric models for the Project Independence Study in 1975;¹ (b) the dramatic recent changes that have taken place in the estimates of the lower-48 resource

¹Federal Energy Administration, Project Independence Report (Washington, D.C., November 1974). In their \$16.50 per barrel (1979\$) and accelerated development case, the Project Independence Study Group estimated domestic oil production would increase in 1985 to 18 million barrels per day and domestic natural gas production would be 24 Tcf per year and limited by demand.

base²; and, (c) the inability of "hindcasting" models to properly incorporate new geologic areas (e.g., offshore, deep gas) or unconventional resources.

The gas resource base used by traditionalists is (beyond the API proved reserves), the USGS 1976 estimate of 600 Tcf of inferred plus undiscovered recoverable reserves.³ The models in Fig. 2 project the future supplies and sources of gas.

2. Advocacy. A second set of projections are provided by advocacy groups such as industrial organizations and gas research institutes. While advocacy groups serve a valuable role and often provide information more timely than the traditionalists, the underlying assumptions in their forecasts must always be closely examined. Generally, the advocates use as their resource base the estimates of the Potential Gas Committee that over 1,000 Tcf of recoverable gas remains undiscovered, in addition to a proved and inferred reserves base of 400 Tcf.⁴ The problem with the advocacy group studies has been that few of the forecast increases in gas supplies have materialized despite five to ten fold real increases in gas prices.⁵

Two of the most thoughtful of the advocacy forecasts are those of AGA and the Gas Research Institute's "Gas Option." (See Fig. 3)

3. Disaggregate Analysis. While the two previous methods of forecasting seek to find statistical curves that describe production from an aggregate natural gas reserve base, a third set of forecasters reject the notion of a single, uniform resource base and question the value of trend line forecasts during major changes in prices, technology and the nature of the resource target. These forecasters rely heavily on detailed basin and reservoir data and geological assessments. They disaggregate the resource into the various gas sources and use engineering models to determine price and technology elasticities. Because of the massive data bases and the range of engineering and economic talent that must be assembled in making such forecasts, few such efforts have been attempted. The recent work by the National Petroleum Council on unconventional gas⁶ and the level of detail in Shell

²In 1976, the USGS issued its report, USGS Circular 725, that more than halved previous estimates of the domestic undiscovered natural gas resource base. Special U.S.G.S. studies of the offshore and selected onshore basins, conducted in 1978-79, further reduced the estimates of undiscovered natural gas.

³USGC Circular 725, op. cit.

⁴The Potential Gas Committee has repeatedly projected an undiscovered, recoverable natural gas reserve of 1,000 Tcf. However, the PGC has continually had to expand the geological base, by including deep waters and deeper horizons, to maintain its estimates. See Report of the Potential Gas Committee, 1979.

⁵New contract prices for intrastate and interstate natural gas in 1969 were \$0.20 and 0.26 per Mcf respectively. After adjusting for inflation, they would average about \$0.45 per Mcf (in 1979 dollars). Gas prices at the start of 1980 were between \$2.00 and \$4.00 per Mcf depending on applicable regulations.

Oil's recent supply forecasts are examples of disaggregated forecasts.⁷

A DISAGGREGATE FORECAST OF FUTURE NATURAL GAS SUPPLIES

The following forecast of natural gas supplies and the review of future unconventional gas sources is based largely on such a disaggregate geological and engineering approach.

1. Conventional Domestic Natural Gas Supplies

a. Lower 48

1) Existing Reserves. At the end of 1978, the lower 48 proved reserves were 174 Tcf and were being produced at a production to reserves (P/R) ratio of 1 to 10. With this proved reserves resource base and assuming a continuing 1 to 10 P/R ratio, it is relatively straightforward to project historic production from existing reserves to the year 2000. (See Fig. 4)

2) Inferred Reserves. The development of a natural gas field, by extension drilling and improvements in recovery efficiency, lead to adjustments in the size of the existing gas reserve. An examination and projection of this growth in gas reserves leads to the following estimates of gas production from inferred reserves. (See Fig. 5)

Ultimately 80 Tcf are anticipated to be added to lower 48 proved gas reserves by future development of already discovered fields.

3) New Discoveries. A major paradox exists in projecting new discoveries of natural gas. On one hand are the large undiscovered reserve estimates of the USGS and the Potential Gas Committee that project 400 to 1,000 Tcf of undiscovered recoverable natural gas. On the other hand, actual new discoveries during the past years have been low, despite four-fold increases in prices, as shown in Fig. 6.

The problem is not the amount of exploration drilling. The 1978 rate is four times that at the start of the decade, as shown on Figure I-1. The major problem is that the productivity of exploratory drilling has declined severely. New reserve additions per well have dropped from 4 Bcf per year in 1970 to 1 Bcf per well in 1978, as shown on Figure I-2.

Even after allowing for the growth of new discoveries through subsequent development drilling, only one half of the yearly production is being replaced.

⁶At the end of 1979, the National Petroleum Council was completing a detailed geological/engineering costing assessment of gas supplies from four unconventional sources -- tight gas, Devonian shales, methane from coal seams, and geopressed aquifers.

⁷One of the companies that has been in the forefront of detailed energy forecasts has been Shell Oil with its National Energy Outlook series. In 1978, they projected domestically produced gas supplies could decline to 15 Tcf per year by 1990, counter to much rosier forecasts provided by the bulk of the industry.

Given the recent reduced estimates of the conventional natural gas resource base, the limited gas recovery response to a tenfold price rise and a fourfold increase in drilling during the 1970's, and the continuing decline in exploratory drilling productivity, expectations of major gas supplies from new discoveries must be tempered. At best, the average yearly rate of new gas additions will stabilize at the 1978 levels. Less optimistically, new gas discoveries will follow the historically declining pattern. These two outcomes for new discoveries are shown on Figure I-3.

These new discoveries will grow by subsequent development drilling, similar to development growth of already discovered fields (through inferred reserves), as shown on Figure I-4. However, given that the new discoveries have been low, the base for subsequent development drilling is also limited. The estimates of future gas production from new discoveries is shown in Fig. 7.

b. Alaska. Currently, 26 Tcf of natural gas are in Prudhoe Bay and other smaller Alaskan reservoirs. Domestic use of this gas awaits the construction of a major, 4,000 mile pipeline. Assuming that the pipeline is built by 1990, at the currently planned 2.2 Bcf per day capacity, less than 1 Tcf per year would be available in the 1990-2000 period. However, the massive capital costs involved in the project, estimated at \$15 to \$20 billion dollars, dictate a high delivery cost, estimated at \$10.00 or more per Mcf.

This would make Alaska gas uneconomic unless rolled in with other lower priced gas and raises concerns as to who would bear the burdens of this higher cost gas. (A pipeline combining Alaskan gas with natural gas from the Canadian Mackenzie Delta/Beaufort Sea could lower these costs and expedite the availability of supplies from both sources). It is not likely that these concerns can be resolved in sufficient time to meet the current 1984 deadline. Assuming the U.S. is willing to subsidize this energy source, Alaskan gas could reach U.S. markets by 1990, as shown in Fig. 8.

c. Deep Gas. Considerable publicity has been given to the prospects of massive new gas supplies from formations below 15,000 feet. These estimates include 200 Tcf of recoverable reserves by the Potential Gas Committee; 80 Tcf in the Deep Andarko Basin (Oklahoma) alone. However, with 600 gas wells a year already being drilled to this depth, deep gas is essentially just a more challenging conventional target and has been included in the conventional gas reserves, estimated in Fig. 8.

The gas potential in horizons below 20,000 feet, labeled ultra and super deep, is still too speculative for inclusion in the projections.

2. Natural Gas Imports

Three sources of natural gas augment domestic supplies. These are: overland gas imports from Mexico and Canada and overseas gas imports of LNG.

a. Mexican Gas Imports. The U.S. euphoria over the increasingly large hydrocarbon reserves of Mexico, reported to be over 200 billion barrels of oil equivalent hydrocarbons, is not justified. Such large projections are not proven reserves. Rather, they should be classified as speculative anticipations and appear to be based on optimistic volumetric calcu-

lations.

Clearly, Mexico has a large amount of oil and gas. The estimates, in early 1979, placed the proved reserves at 34 billion barrels of oil and 35 Tcf of gas. However, it is not at all certain whether the U.S. will ever obtain access to more than a small fraction of the gas reserves. The Mexicans are converting their own industry to gas, the Mexican economy and population are growing, with a target economic growth rate of 7%, and, internal demand for gas is increasing rapidly. The newer prospects appear to be less gas prone (lower gas/oil ratios) and the current development schedule is straining internal capacity. Mexico has also stated that political and internal economic decisions rather than the size of the resource base will dominate decisions on exports. It may well be that the current 300 MMcf per day (0.1 Tcf per year) is the most the U.S. will be allowed to import from Mexico.

Projections for future natural gas imports from Mexico range from the current, essentially trivial levels, to a maximum based on Mexico's productive capacity and underlying reserves. However, even assuming highly successful exploration, less than 1 Tcf per year would be available in 1990 and internal demand would consume all available Mexican gas by the year 2000. (See Fig. 9)

b. Canadian Gas Imports. Canada currently exports about 1 Tcf annually to the U.S. and appears to have the capacity to remain the U.S.'s largest source for gas imports. With the additional exports authorized in late 1979 and early 1980, gas exports would rise slightly above this level through the mid-1980's. After that, unless new authorization is obtained and resources are committed, exports are scheduled to drop precipitously.

From a geological and resource perspective, Canada has the potential for becoming a major natural gas producer, primarily from its Frontier areas (Mackenzie Delta, Arctic Islands and East Coast Offshore) and from its unconventional gas (the tight gas sands of the Deep Basin). How much of this gas will be made available to the U.S. is uncertain and subject to numerous internal Canadian political decisions. The projections of gas imports from Canada would thus range from the currently authorized levels, as supplemented at the end of 1979, to the full technical potential, as shown in Fig. 10.

c. Liquefied Natural Gas (LNG). While the U.S. already has supply agreements that provide 0.4 Tcf per year of LNG imports, the capacity to substantially increase this amount is limited. The inaction by the U.S. government on LNG has led the bulk of the available gas reserves to be committed to European and Japanese markets. The remainder of the gas reserves are in highly uncertain areas for long term imports (Iran and the Soviet Union) or in geographically distant areas.

Using the recent LNG report by the Office of Technology Assessment as the primary source document, projections of U.S. LNG imports are shown in Fig. 11.

3. Summary of Conventional Gas Sources and Imports

The range of supply estimates for each conventional source of gas provides a useful boundary of antici-

pated outcomes, shown as the Low Case and High Case on Fig. 12. While prudent contingency planning for future energy supplies should heavily weight the projections of the Low Case, the likely outcome is somewhere between the Low and High Cases, labeled the Most Likely Case on Fig. 12.

Numerous assumptions and judgments, relevant to the natural gas situation in early 1980, are the basis for this Most Likely Case estimate. For example, the current U.S. policies give low priority to securing LNG imports while European and Japanese countries are aggressively signing long-term commitments. This dictates that, unless conditions change, future LNG imports will be closer to the Low rather than the High Case. A tabulation of the potential sources shows:

- o In 1990, domestic conventional gas production and imports would range from 12 to 17 Tcf with a Most Likely Case estimating 16 Tcf.
- o In 2000, these sources of natural gas have declined to a range of 9 to 15 Tcf, with a Most Likely Case estimate of 12 Tcf.

Even under the best conditions, conventional natural gas supplies will fall far short of potential gas demand. Filling as much of this gap as possible will depend on the promise and timeliness of the unconventional and synthetic sources of gas.

4. Synthetic/Unconventional Sources of Gas

Two sources of gas have the potential for appreciably closing the gap between demand and conventional supplies of natural gas; these are, synthetic gas from coal (or shale) and unconventional gas.

The technology for synthesizing gas exists, although it is unproven, limited and costly. The major technical challenge is to develop a pressurized, intrained-bed gasifier that can produce synthetic gas from the full range of U.S. coals. The major institutional challenge is to manage the massive scale introduction of medium (and possibly low) BTU gas as a substitute in the industrial sector for pipeline quality gas.

Unconventional gas is currently produced from the higher quality tight gas and Devonian shale deposits, providing about 0.9 Tcf per year. However, the gas recovery technology is inefficient and inadequate for unlocking the vast bulk of the more difficult, lower grade resource. The technical challenges vary by type of unconventional resource. However each type requires improvements in understanding the resource and its controlling characteristics and each type requires significant advances in well completion and stimulation technology.

To a major extent, the size of the gas potential from synthetic and unconventional sources is dependent on how rapidly the technologies develop. Given the imperfections in the R&D marketplaces and the limited capacity of the price mechanism to influence near-term private R&D investments in synthetic and unconventional gas technology, Federal incentives for R&D (like in Canada) or direct Federal investment in R&D will be required.

The Federal government has been reluctant to

establish incentives for technology or to make the necessary investment in R&D. For example, the unconventional gas program is only partly funded and the thrust of the proposed Energy Security Corporation is on building plants rather than on investing in future technology.

Because of this, major uncertainties and a wide range of outcomes characterize the potential of these supplementary gas sources.

a. Synthetic Gas

1) High BTU Gas from Coal

The pace at which synthetic gas enters the domestic market will depend greatly on the emergence and success of the Synthetic Fuels Corporation. Under a high track of world oil prices and assuming a market exists for high cost gas, total annual synthetic gas production from coal could be up to 0.5 Tcf by 1990 and range from 1 to 2 Tcf by the year 2000. (The production of SNG by reforming naphtha and LPG, is an energy inefficient conversion of an already valuable petroleum product and is not included in these estimates.) As a point of comparison, Shell and Exxon anticipate approximately 1 Tcf of synthetic gas by 1990.

2) Low and Medium BTU Gas from Coal

Low and medium BTU gas from coal will compete in a different energy market than pipeline quality gas and thus is not considered in these supply projections.

b. Unconventional Natural Gas Supplies

1) Size of the Resource

One of the largest potential additions to U.S. natural gas supplies could be from four unconventional natural gas sources--tight gas sands, Devonian shales, methane from coal seams, and dissolved methane in geopressured aquifers. The estimates of gas in-place for these four unconventional resources range widely, depending on what portions of the resource base are included, and are shown below:

- o Tight Gas Sands - 400-1,000 Tcf
- o Devonian Shales - 100-2,000 Tcf
- o Methane from Coal Seams - 200-700 Tcf
- o Geopressured Aquifers - 1,000-6,000 Tcf

While this gas is costly, the geologically better portions of the resource are already economic and projections of future prices appear adequate to render the resource economic. However, this resource is constrained much more by technology than by price and in general, after prices reach \$4.00 to \$5.00 per Mcf, the supply elasticities with current technology become very low. The major means for increasing supply and converting a modest gas source into a major resource is through the introduction of advanced gas recovery technology.

2) Potential Contribution

Estimates of the contribution of unconventional gas range widely and are highly dependent on assumptions about technology advances. The low side of the estimates assume a continuation of current capacity; the high side of the estimates assume accelera-

ted development and use of advanced technology, as shown in Fig. 13.

SUMMARY OF TOTAL GAS SOURCES

Considerable uncertainty exists in estimating energy supplies in the future. The three estimates of conventional gas supply, the Low, High and Most Likely Cases, are shown on Fig. I-5. Figure I-6 shows the

disaggregated sources that comprise the estimates in the Most Likely Case. Superimposed on the Most Likely Case, on Figure I-6, are the various estimates of gas supplies from unconventional and synthetic gas. Which of these futures will come about is dependent on how favorable the undrilled unconventional geology is and what choices we make in investing in the essential gas recovery and conversion technologies.

<u>Sector</u>	<u>Annual Consumption</u>	
	<u>(Quads or 10¹⁵ BTU)</u>	<u>1990</u>
Residential/Commercial	18	19
Industrial	22	33
Transportation	20	22
Conversion Losses/Adjustments	18	27
TOTAL Gross Energy Consumption	78	101

Source: Department of Energy EIA, Series C
1978 Annual Report to Congress

Fig. 1 - U.S. energy consumption.

	<u>EIA-78 Series C</u>		<u>Exxon - 1979</u>		
	<u>1985</u>	<u>1990</u>	<u>1985</u>	<u>1990</u>	<u>2000</u>
Domestic	18.4	17.9	15.7	15.1	11.3
Imported	1.9	2.0	2.0	2.6	2.8
Total	20.3	19.9	17.7	17.7	14.1

Source: Department of Energy, EIA, op. cit.,
Energy Outlook 1978-2000. Exxon Corporation, December, 1979.

Fig. 2 - Traditional forecasts of natural gas supplies (Tcf).

	AGA		GRI "Gas Options"	
	1985	2000	1985	2000
Domestic Lower 48	18.6	15.0	19.0	15.0
Alaska	0.8	3.6	0.9	1.5
Other (e.g., unconventional, synthetics, etc.)	1.4	8.8	1.6	12.5
Imports	<u>3.5</u>	<u>4.8</u>	<u>3.0</u>	<u>2.5</u>
TOTAL GAS SUPPLY	24.4	32.2	24.5	31.5

Source: Testimony by Dr. H. Linden before the Subcommittee on Energy and Power, U.S. House of Representatives, June 6, 1979.

Fig. 3 - Advocacy group estimates of natural gas supply (Tcf).

Year	Yearly Production (Tcf)		
	Onshore	Offshore	Total
1985	7.6	1.6	9.2
1990	4.3	0.9	5.2
2000	1.3	0.3	1.6

Fig. 4 - Estimates of production from existing reserves.

Year	Yearly Production (TCF)		
	Onshore	Offshore	Total
1985	2.2	0.5	2.3
1990	2.8	0.5	3.1
2000	2.3	0.4	2.7

Source: Enhanced Recovery of Unconventional Gas, Volume III, Lewin and Associates, Inc. 1978 (updated in 1980).

Fig. 5 - Estimates of production from inferred reserves.

Year	Gas Prices for New Contracts (\$/Mcf)		Lower 48 New Discoveries (Tcf)		
	Intrastate	Interstate	Onshore	Offshore	Total
1973	0.37	0.80			
1974	0.46	1.00	1.5	0.8	2.3
1975	0.57	1.40	1.5	1.1	2.6
1976	1.42	1.60	1.1	0.4	1.5
1977	1.42	1.90	1.2	1.0	2.2
1978	1.75	2.10	1.3	0.5	1.8

Source: Energy Future, op. cit.; API/AGA Blue Book, May, 1979.

Fig. 6 - Summary of natural gas prices and new discoveries for past six years.

<u>Year</u>	<u>Yearly Production (Tcf)</u>					
	<u>Onshore</u>		<u>Offshore</u>		<u>Total</u>	
	<u>Low</u>	<u>High</u>	<u>Low</u>	<u>High</u>	<u>Low</u>	<u>High</u>
1985	1.7	1.9	-	0.1	1.7	2.0
1990	2.3	2.8	0.2	0.6	2.5	3.4
2000	2.4	3.9	0.3	0.8	2.7	4.7

Source: Lewin and Associates, Inc.

Fig. 7 - Estimates of production from new discoveries.

<u>Year</u>	<u>Yearly Production (Tcf)</u>
1985	--
1990	0-0.8
2000	1.0

Fig. 8 - Estimates of production from Alaska.

<u>Year</u>	<u>Yearly Imports (Tcf)</u>
1985	0.1-0.5
1990	0.1-0.7
2000	0.1

Source: Future Mexican Oil and Gas Production. Lewin and Associates, Inc., 1979.

Fig. 9 - Estimates of natural gas imports from Mexico.

<u>Year</u>	<u>Yearly Imports (Tcf)</u>
1985	1.2-2.0
1990	0.3-2.5
2000	0-3.0

Source: Canadian Natural Gas: A North American Energy Source, Lewin and Associates, Inc., 1980.

Fig. 10 - Estimates of natural gas imports from Canada.

<u>Year</u>	<u>Tcf</u>
1985	0.4-0.8
1990	0.8-1.3
2000	0.8-1.8

Source: The Future of Liquified Natural Gas Imports (Draft), Office of Technology Assessment, U. S. Congress, 1979

Fig. 11 - Estimates of LNG imports.

	<u>Most Likely</u>	<u>Low</u>	<u>High</u>		<u>Most Likely</u>	<u>Low</u>	<u>High</u>
<u>1985</u>	<u>Case</u>	<u>Case</u>	<u>Case</u>	<u>1990 (continued)</u>	<u>Case</u>	<u>Case</u>	<u>Case</u>
o <u>Lower 48</u>				o Alaska	0.8	-	0.8
- Existing Reserves	9.2	9.2	9.2	o <u>Imports</u>			
- Inferred Reserves	2.7	2.7	2.7	- Mexico	0.5	0.1	0.7
- New Discoveries	<u>2.0</u>	<u>1.7</u>	<u>2.0</u>	- Canada	1.5	0.3	2.5
Sub-Total	13.9	13.6	13.9	- LNG	<u>1.3</u>	<u>0.8</u>	<u>1.3</u>
o Alaska	-	-	-	Sub-Total	3.3	1.2	4.5
o <u>Imports</u>				o Total Conventional Gas Supply*	<u>16</u>	<u>12</u>	<u>17</u>
- Mexico	0.3	0.1	0.5				
- Canada	1.5	1.2	2.0	<u>2000</u>			
- LNG	<u>0.5</u>	<u>0.4</u>	<u>0.8</u>	o <u>Lower 48</u>			
Sub-Total	2.3	1.7	3.3	- Existing Reserves	1.6	1.6	1.6
o Total Conventional Gas Supply*	<u>16</u>	<u>15</u>	<u>17</u>	- Inferred Reserves	2.7	2.7	2.7
				- New Discoveries	<u>4.0</u>	<u>2.7</u>	<u>4.7</u>
				Sub-Total	8.3	7.0	9.0
<u>1990</u>				o Alaska	1.0	1.0	1.0
o <u>Lower 48</u>				o <u>Imports</u>			
- Existing Reserves	5.2	5.2	5.2	- Mexico	-	0.1	0.1
- Inferred Reserves	3.3	3.3	3.3	- Canada	1.5	-	3.0
- New Discoveries	<u>3.0</u>	<u>2.5</u>	<u>3.4</u>	- LNG	<u>1.3</u>	<u>0.8</u>	<u>1.8</u>
Sub-Total	11.5	11.0	11.9	Sub-Total	2.8	0.9	4.9
				o Total Conventional Gas Supply*	<u>12</u>	<u>9</u>	<u>15</u>

* Total domestically produced gas supplies would be approximately 1 Tcf higher in 1985-1990 when unconventional gas sources are included.

Source: Lewin and Associates, Inc.

Fig. 12 - Estimates of U.S. gas supply from conventional sources - 1985-2000. (Tcf per year).

	<u>Current Technology</u>	<u>Advanced Technology</u>
1985	1	1-2
1990	1	2-4
2000	1	3-6

Fig. 13 - Estimates of production from unconventional gas in TCF.

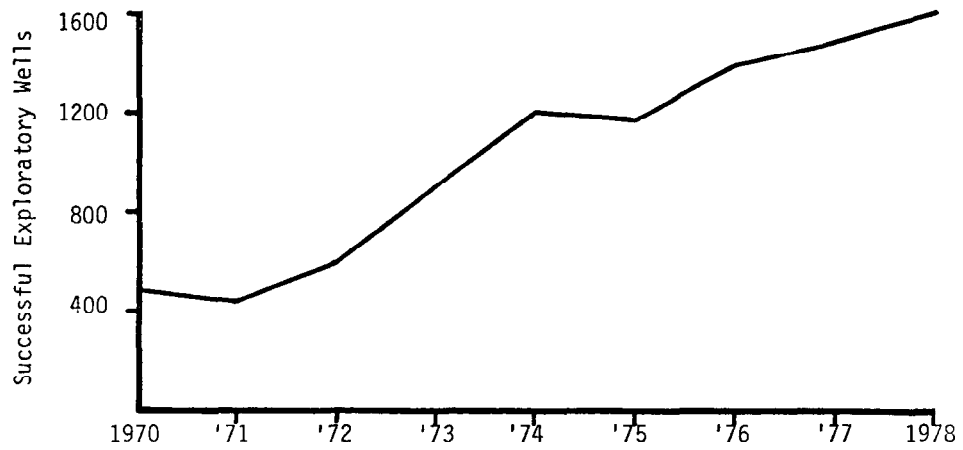


Fig. I-1 - Successful exploratory wells.

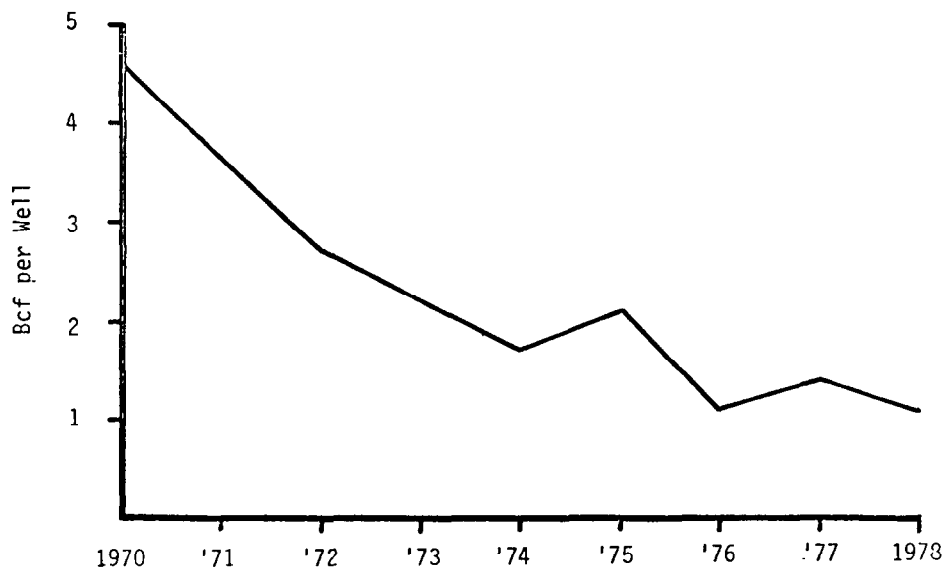


Fig. I-2 - Reserve additions per exploratory well.

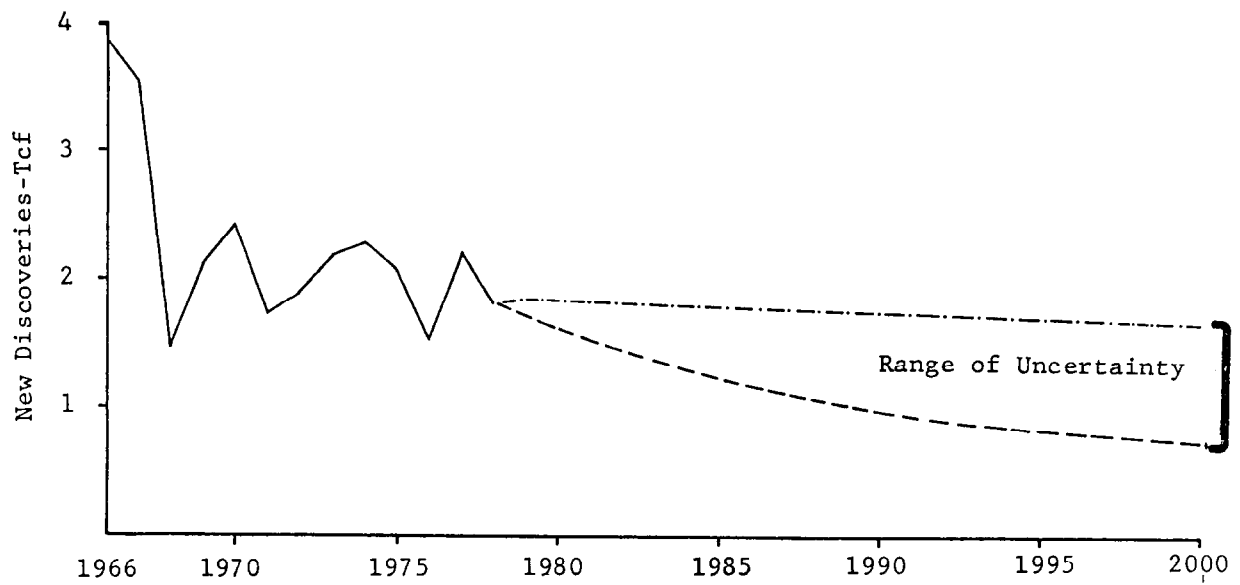


Fig. I-3 - Range of uncertainty in new discoveries. (First year new discoveries-lower 48.)

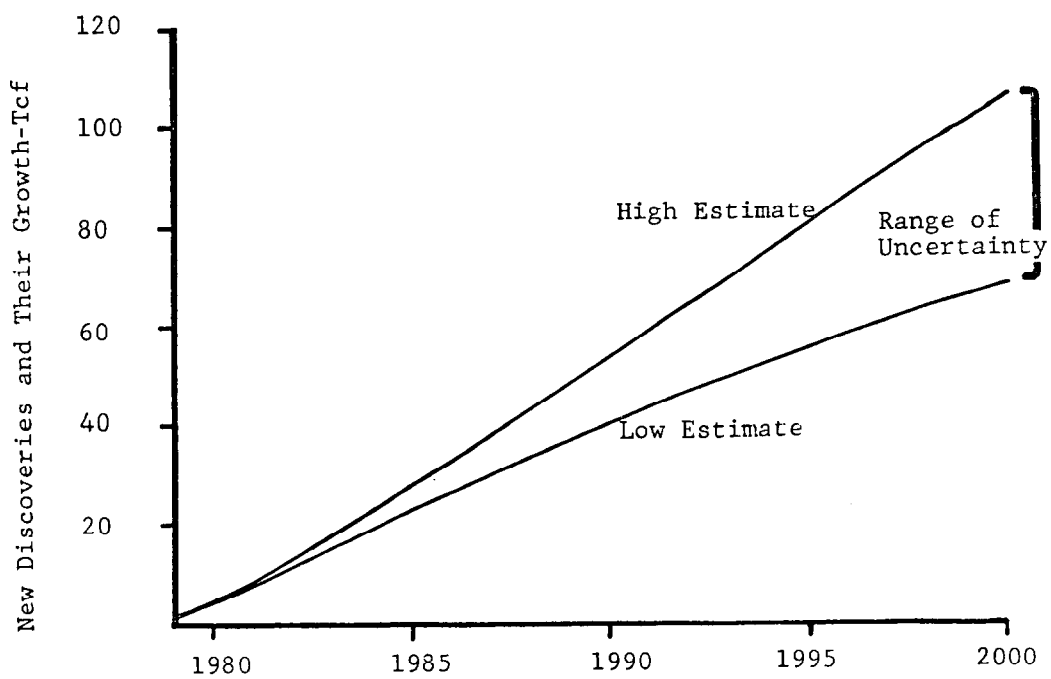


Fig. I-4 - Range of uncertainty in total new additions. (New discoveries and their growth-lower 48)

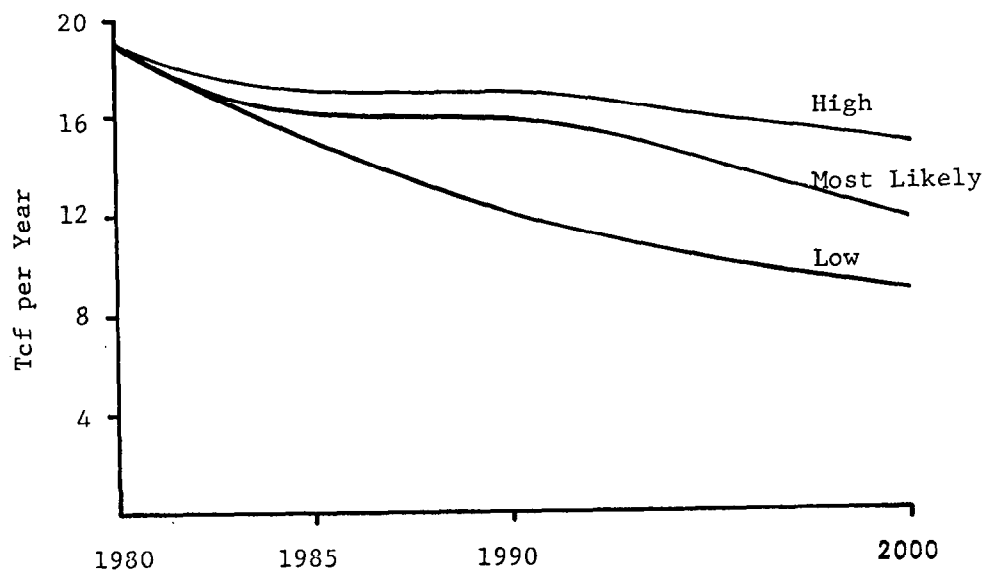


Fig. I-5 - Low, most likely and high case production from conventional gas.

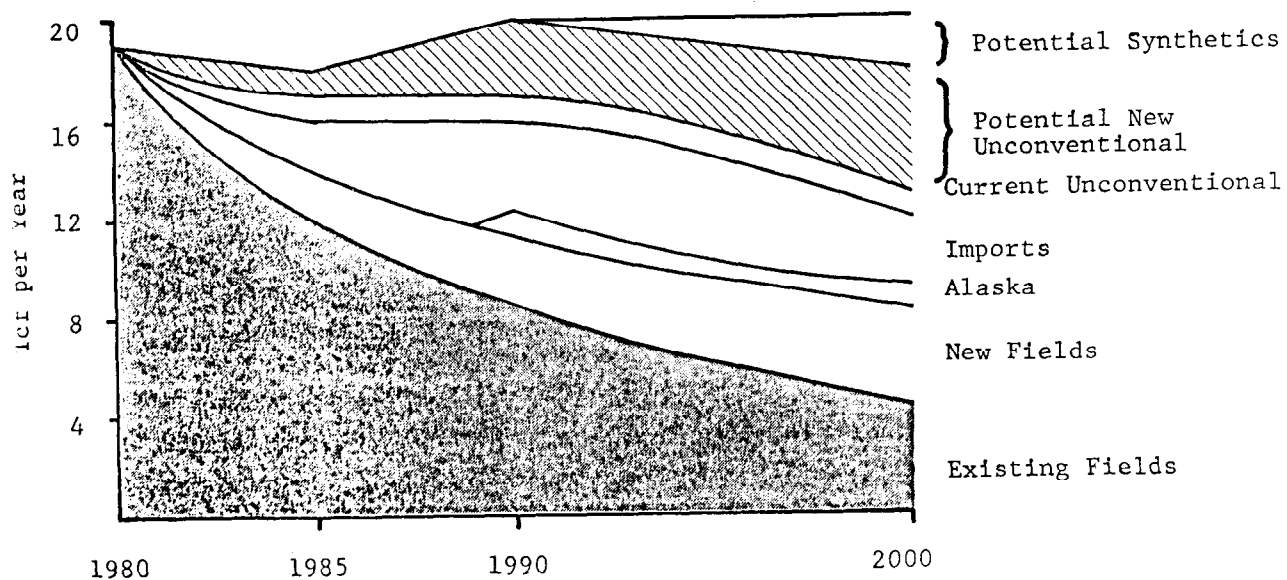


Fig. I-6 - Components of conventional gas production most likely case.

NATURAL GAS POTENTIAL OF THE NEW ALBANY SHALE GROUP (DEVONIAN- MISSISSIPPIAN) IN SOUTHEASTERN ILLINOIS.

by Robert M. Cluff and Donald R. Dickerson,
Illinois State Geological Survey.

This paper was presented at the 1980 SPE/DOE Symposium on Unconventional Gas Recovery held in Pittsburgh, Pennsylvania, May 18-21, 1980. The material is subject to correction by the author. Permission to copy is restricted to an abstract of not more than 300 words. Write: 6200 N. Central Expwy., Dallas, Texas 75206

ABSTRACT

Data from geologic and geochemical studies of the New Albany Shale Group indicate that a 19-county area of southeastern Illinois is a favorable area to explore for gas in Devonian shale. Devonian shale in this area is characterized by: 1) predominance of organic-rich, finely laminated black shale; 2) shale thickness of more than 45 meters; 3) sufficient thermal maturation of organic matter for oil and some gas generation, as indicated by vitrinite reflectances ≥ 0.5 percent; and 4) the presence of natural fracturing and faulting. Although gas shows have been encountered in several wells in this area that penetrate the Devonian shales, there has not been any commercial production of gas from shale in Illinois. Until 1979, no attempts had been made to complete or evaluate a shale gas well.

Core samples were taken in May 1979, from 5 meters of the upper part of the New Albany Shale in the Hobson Oil #2 Taylor well (Sec. 34, 1 S., 7 E., Wayne County) and in September through October 1979, from 72 meters of the upper part of the New Albany Shale (a complete section) in the G. T. Jenkins #1 Simpson well (Sec. 17, 3 S., 8 E., Wayne County). Seventy core samples were removed on-site at 1-meter intervals throughout both cores and were sealed in airtight metal canisters for off-gas analysis. The quantity of gas released after 34 days ranged from 0.16 to 2.40 m³ hydrocarbons/m³ of shale. These are minimal values and the actual in situ gas content of the shale may be two to four times greater. The highest gas contents were observed in the Grassy Creek Shale and in black shale intervals throughout the Selmer (Sweetland Creek) Shale. These gas-bearing intervals generally correspond with high radioactivity intervals on gamma-ray logs. Olive-gray and greenish-gray shales in the New Albany contained only moderate amounts of gas, as did the calcareous, laminated, black Blocher Shale at the base of the New Albany.

The average composition of the gaseous hydrocarbons was 70 percent methane, 19 percent ethane, 8 percent propane, 2 percent butane, and 1 percent heavier

hydrocarbons. This gas is richer in heavy hydrocarbons than is average "pipeline gas" and has a calculated average 46,200 kJ/m³ (1,240 BTU/ft³). The proportion of non-hydrocarbon gases is unknown and the calorific content of produced gas would necessarily be slightly lower.

The quantities of shale gas in core samples from southeastern Illinois are similar to those in core samples from gas-producing areas of Devonian shale in the Appalachian Basin; however, because the New Albany Shale is much thinner than its Appalachian Basin equivalents, the total gas resource is probably much smaller. Conventional rotary drilling with mud-based drilling fluids commonly causes extensive formation damage and accounts for the paucity of gas shows and completion attempts in the Devonian shales; therefore, commercial production of shale gas in Illinois will probably require novel drilling and completion techniques not commonly used by local operators.

INTRODUCTION

United States production of gas from Devonian black shales began in 1821 with the drilling of a well near Fredonia, New York. In the ensuing 159 years production from Devonian shales has extended into eastern Kentucky, southern and western West Virginia, and scattered areas of Pennsylvania, Ohio, New York, western Kentucky, and Indiana. Currently, about 9600 wells produce gas in the Appalachian Basin. One giant gas field, the Big Sandy Field in eastern Kentucky, has produced over 5.6×10^{10} m³ (2 tcf) of gas from Devonian shale.¹

The Devonian shales cover a broad area of the northeastern United States, extending westward into the Illinois Basin where they are called the New Albany Shale Group (Devonian-Mississippian). Although lithologically similar to the Devonian shales of the Appalachian Basin, the New Albany has produced gas in only a few small areas of Indiana and western Kentucky. No gas production is known from the New Albany in Illinois and few oil and gas operators in the Illinois Basin have considered the shales a commercial resource or a viable exploration target. Because of the great lateral extent and thickness of the shales,

References and illustrations at end of paper.

however, resource estimates of the total gas trapped within them are vast.

Producing gas from the shales has not been commercially attractive in the Illinois Basin because of technological constraints (the low production rates) and price regulations. If suitable technologies can be developed to recover the gas from these low permeability reservoirs and thereby increase the productive capacity of wells, then the Devonian shales might become an important source of natural gas in the near future.

In mid-1976, the Illinois State Geological Survey began a detailed study of the geology and geochemistry of the New Albany Shale in Illinois to evaluate its potential as a source of hydrocarbons, especially gas. This study, undertaken with partial support from the U.S. Department of Energy (DOE) Eastern Gas Shales Project, relied on studies of cores, drill cutting samples, and geophysical logs to evaluate the regional geology of the New Albany Shale and identify the broad areas where the potential for discovery of gas resources were best. In addition, DOE-funded drilling provided several cores of the New Albany Shale in Illinois and western Kentucky. Samples of these cores were collected at the coring site and quickly sealed in airtight canisters to determine the quantity of gas released from the shale and the composition of off-gases. These data allowed an evaluation of the magnitude of the gas resource and helped identify zones that are likely to be productive.

An economic evaluation of the potential of the New Albany Shale for commercial development is outside the scope of this report. Readers interested in such an evaluation should consult the recent report by the Devonian Shale Task Group of the National Petroleum Council for an in-depth economic analysis of shale gas production.²

GEOLOGIC EVALUATION

Previous studies of gas-bearing shales have shown that areas of gas production are related, at least partly, to four characteristics: regional facies patterns; areas of thick shale accumulation; the degree of thermal maturation of the organic matter in the shale; and the presence of extensive fracturing or faulting. Other factors may also be important, but they have not been well documented. One preliminary evaluation of the New Albany Shale in Illinois, using these four criteria, concluded that southeastern Illinois was the most favorable area for gas production.³

Depositional facies

Shale gas in the Appalachian Basin is usually obtained from black to brownish-black, laminated, organic-rich shales.¹ The gas in these shales originated from the thermal transformation (maturation) of the sedimentary organic matter dispersed throughout the shale matrix. Minor gas production from gray shales with low organic contents has been reported, but geologists generally believe that the gas originated in the black shales and migrated through natural fractures into the other zones. The dominant lithofacies of the New Albany Shale are similar in most respects to the Devonian shales of the Appalachian Basin.^{4,5,6}

The distribution of New Albany Shale facies forms a roughly concentric pattern around the depositional center of the basin. The cumulative thickness of organic-rich black shales, as interpreted from gamma ray logs,⁷ is greatest near the center of the ancestral Illinois Basin in southeastern Illinois and adjacent western Kentucky, and thins away from there in all directions (Fig. 1). Organic-poor, greenish-gray and olive-gray shales predominate in areas away from the basin center and are thickest in western and west-central Illinois. A broad transitional zone, where these two major facies belts interfinger and grade laterally into one another, trends northeast-southwest across central Illinois.

Shale thickness

Harris, de Witt, and Colton⁸ documented a close correlation between thickness of black shale accumulation and amount of gas production in the Appalachian Basin. They found that areas with the best production coincided with areas where the black, organic-rich shales exceeded 150 meters in thickness.

The entire New Albany Group attains a maximum thickness of approximately 143 meters (470 feet) in the Illinois Basin (Fig. 2). Clearly, if the shale must be thicker than this for commercial production of shale gas, then the entire Illinois Basin must be considered unfavorable. There are two broad regions where moderately thick shale was deposited in the Illinois Basin, however, and improved completion techniques might permit recovery of gas from such areas.

One of these depocenters, located in Iowa and extending into western Illinois, is not considered a likely area for gas accumulations because of the paucity of black shale (Fig. 1). The southern depocenter, located in southeastern Illinois and western Kentucky, is a more likely area because it coincides with the area of greatest black shale accumulation (Fig. 2).

The broad, thin area of New Albany sediments trending across central Illinois coincides with a transitional facies region having only marginal gas potential.

Thermal maturation

Numerous studies on the origin of petroleum and natural gas have established that the transformation of sedimentary organic matter to mobile hydrocarbons depends on burial time and temperature.⁹ The chemical and physical properties of the disseminated organic matter change in a progressive and systematic manner as hydrocarbons are generated; this process is termed "maturation." Several methods can measure the relative maturity of a potential hydrocarbon source rock; one of the best methods for organic-rich rocks is vitrinite reflectance.

Vitrinite, derived from the woody tissues of plants, frequently occurs as silt-sized detrital particles dispersed throughout the matrix of sedimentary rocks. The reflectance of light by vitrinite particles increases with increasing maturity and can be measured microscopically.¹⁰ Vitrinite reflectances are recorded as percentages of the

random reflectance of vitrinite under oil immersion, compared to glass standards of known reflectance. Usually, a vitrinite reflectance level of at least 0.5 percent is needed for a rock to attain the "mature stage" (mainly generation of oil with some co-generation of gas), and a level of at least 1.2 percent is needed to attain the "super mature stage" (mainly gas generation). Figure 3 is a map of iso-reflectance values in the New Albany Shale Group, based on samples from over 100 wells in Illinois.¹¹ Only the areas on this map with a reflectance greater than 0.5 percent are likely to have potential for gas production, and those areas with the highest reflectances are probably the most favorable. Note that the areas where reflectance exceeds 0.5 percent generally coincide with the areas of thickest New Albany sediments and the areas with greatest accumulation of black shale.

Faulting and fracturing

Natural fractures have been cited as a major pathway for gas migration and production in Appalachian gas fields.¹ Although their nature and importance are debatable, it is likely that extensive fracturing aids the flow of gas into a well and increases the volume of shale drained by any single well bore. Most of the major faulting in Illinois, including the Wabash Valley, Cottage Grove, and Rend Lake Fault Systems, and the Shawneetown Fault Zone, occur in southern and southeastern Illinois (Fig. 4). Extensive fracturing of rocks in these areas is known to exist, as evidenced by observations in coal mines and by the significant production of oil from fractured reservoirs in the New Harmony Field, White County. Mineralization along fracture systems is common in the Fluorspar District in extreme southeastern Illinois.

Area of greatest gas potential in Illinois

Our evaluation of these four major geologic criteria—depositional facies, shale thickness, thermal maturation, and known faulting and fracturing—indicates that a 19-county area of southeastern Illinois is geologically the most favorable area in Illinois for shale gas resources³ (Fig. 5). Although numerous oil and gas tests penetrate the Devonian shales in this region, especially in the northernmost counties, relatively few gas shows have been reported and there has never been any commercial production of gas from the shale. There are several possible reasons for the apparent lack of gas shows in Illinois:

1. Virtually all Devonian tests in southern Illinois are drilled with rotary tools. In Indiana and western Kentucky most reported gas shows have been from cable tool holes, wherein gas shows are more noticeable.
2. Mud logging units are not widely used in Illinois.
3. Operators in Illinois tend to exhibit little interest in Devonian shales; therefore, there are probably many gas shows that have not been reported. The marginal economics of shale gas production and the lack of production in Illinois may account for this lack of interest.
4. The Devonian shales beneath Illinois might not be gas bearing in many areas.

Except for a few inconclusive or negative drill stem tests of the Devonian shales in wells with gas shows, the producing potential of shale in southeastern Illinois was untested until recently. No data on gas release from shale cores were available that could be used to estimate the quantity of gas contained in the shale, or the most favorable stratigraphic zones for gas production. Without additional data on gas content or gas production, a geological evaluation must be limited to identifying broad areas that may hold gas; any quantitative analysis or commercial evaluation of the gas potential would be purely speculative.

ANALYSIS OF RELEASED GAS

In May 1979, Hobson Oil Company, an independent operator based in Flint, Michigan, cored 5 meters of the uppermost New Albany Shale in their #2 Taylor test (Sec. 34, T. 1 S., R. 7 E., Wayne County, Illinois). Four samples were removed on-site from this core for off-gas analysis. In September and October of 1979 the U.S. Department of Energy (through its subcontractor Gruy Federal, Inc.), funded coring of the entire New Albany Shale Group in the Gordon T. Jenkins #1 Simpson test (Sec. 17, T. 3 S., R. 8 E., Wayne County, Illinois). Sixty-six samples were removed for off-gas analysis from the 72 meters of Devonian shale recovered. These two cores provided the first data upon which a more conclusive assessment of the gas potential of the New Albany Shale in southeastern Illinois could be made.

Methods of gas analysis

Samples were collected at each coring site and sealed in airtight, reusable aluminum canisters for off-gas analysis. The time elapsed between coring the samples and sealing them in canisters varied from 4 to 6 hours, depending on the trip time out of the bore hole and the time required to break down the core barrel, remove the core, and make a brief lithologic description. The time of sealing, the air temperature, and the barometric pressure were recorded; then the sample canisters were transported to the laboratory to be stored at constant temperature (20°C).

The headspace pressure within each canister was monitored weekly until a relatively constant equilibrium pressure was attained. The quantity of gas released by each sample was calculated by Boyles Law using the final, stable headspace pressure. The volume of headspace was determined by weighing the volume of water displaced by the core sample and subtracting it from the known canister volume.

A significant portion of the gaseous hydrocarbons contained within the shale at its normal burial depth was probably lost prior to sealing the samples within their canisters, because of the sudden drop in confining pressure as the core is brought up to the surface, and the relatively long period between coring and sampling. The quantity of gas released from core samples should therefore be considered minimal values, and the actual in situ gas content is probably two to four times greater.

A small sample of gas was periodically removed by inserting a hypodermic needle through a rubber septum in each canister. Gas compositions for these samples were determined by gas chromatography using a dual phase column¹² for the separations (CTR

column, Alltech Associates, Inc.). A Perkin-Elmer Sigma 1 gas chromatograph system was used to analyze the headspace gas. A Perkin-Elmer Sigma 10 data processor was used to integrate peak areas and calculate both the total headspace gas and the hydrocarbon-only compositions from a single sample injection. A typical gas chromatogram for a New Albany Shale sample is shown in Figure 6.

Hobson Oil #2 Taylor core, Wayne County

This core provided the first positive evidence that the New Albany Shale contains significant quantities of gas in an area of Illinois. Hobson Oil notified the Illinois Geological Survey in May 1979 of their intent to cut a single 10-meter core through the New Albany Shale. The Survey agreed to describe, sample, and determine the gas content and composition for Hobson as part of our overall study of the shale. Five meters of core were recovered from the top of the New Albany Shale Group, all within a dominantly black shale formation known as the Grassy Creek Shale. Unfortunately, the entire length of the core was split by a single, near vertical fracture which resulted in severe jamming of the core barrel and prevented further coring. The gas released by four samples collected from this core ranged from 0.55 to 0.82 m³ hydrocarbon/m³ of shale. The gas was very wet, with over 25 percent ethane and heavier hydrocarbons (Table 1).

Hobson Oil hydraulically fractured the New Albany Shale and attempted to complete the #2 Taylor well as a gas producer; however, excessive water production, probably the result of a poor casing cement bond, resulted in abandonment of the fractured interval.

G. T. Jenkins #1 Simpson core, Wayne County

Because of the favorable indications of gas observed in the Hobson Oil well, the Illinois Survey urged DOE to give high priority to funding a complete New Albany core in Wayne County or some adjacent area of southeastern Illinois. Subsequently, Gordon T. Jenkins—a Fairfield, Illinois-based independent oil operator—agreed to core the entire New Albany Shale in his #1 Simpson test, just north of the town of Mill Shoals. A complete section of the New Albany, with several meters of overlying and underlying strata, was cored in this well during late September and early October 1979. Sixty-six samples taken at approximately 1-meter intervals were collected for off-gas analysis. The quantity of gas released after 34 days ranged from 0.16 to 2.40 m³ hydrocarbons/m³ of shale. The zones of shale with the highest gas content usually coincided with zones of high radioactive intervals (Fig. 7). Several sample canisters leaked for various reasons; therefore, the gas content of samples within the highest gamma-ray interval of the Grassy Creek Shale (near 5100 feet; Fig. 7) could not be accurately determined. Several black shale intervals of the Selmier Shale were relatively gas rich, while the Blocher Shale, a finely laminated, calcareous black shale at the base of the New Albany Group, contained little gas (Fig. 7). The low gas contents at the base of the New Albany Group suggest that the gas did not migrate into the shale from an underlying, undiscovered hydrocarbon reservoir.

The composition of the released hydrocarbons varied only slightly with stratigraphic position

within the shale (Fig. 7). On the average, the gas comprised 70 percent methane, 19 percent ethane, 8 percent propane, 2 percent butane, and 1 percent heavier hydrocarbons. Again, this gas is richer in heavy hydrocarbons than typical pipeline gas. The calculated calorific content of New Albany gas in Wayne County is 46,200 kJ/m³ (1240 BTU/ft³), which includes the four gas analyses from the Hobson Oil core. The actual calorific value of the produced gas would be slightly lower because an unknown percentage of carbon dioxide, nitrogen, and other non-hydrocarbon gases would probably be present. Jenkins did not attempt to complete this well as a gas producer and plugged back into a higher, oil saturated zone.

Other New Albany Shale cores in Illinois

Three cores of the New Albany Shale had been acquired previously in western and central Illinois as part of our research. For the most part, these cores identified broad areas where the New Albany has little or no potential for commercial production, rather than identifying areas where gas does occur. The two northernmost cores, located in Henderson and Tazewell Counties (Fig. 5), had no gas shows and released insignificant quantities of gas—less than 0.05 m³ hydrocarbon/m³ of shale. Although these quantities were very small, the amount of gas released correlated closely with the gamma-ray intensity (Figs. 8 and 9).

The third core was drilled at the northern edge of Loudon Oil Field in Effingham County, Illinois (Fig. 5). This core was located in an area where the New Albany is thin, and is just outside the 19-county area previously outlined as having favorable geologic characteristics for gas. Although moderate amounts of gas were released by the core samples (generally below 0.5 m³ gas/m³ of shale; Fig. 10), isotopic analyses suggest the gas is not indigenous to the shale but rather migrated upward from the underlying Devonian oil reservoir.¹³

CONCLUSIONS

The analysis of two cores from southeastern Illinois confirms our previous assessment of the gas potential of the New Albany Shale,³ which was based on stratigraphic and petrographic interpretations alone. These cores demonstrated that the New Albany contains gas in at least some areas of southeastern Illinois. The quantity of gas released compares favorably with gas-producing areas in the Appalachian Basin, where gas contents of 1.0 m³ hydrocarbon/m³ of shale are common. Broad areas of the Devonian shales in Illinois probably have little or no potential for commercial production of gas, based on both geologic data and off-gas analysis of three cores from these outlying areas. The total Devonian shale gas resource of any given area in Illinois is probably much less than that of a similar sized area in the Appalachian Basin because the New Albany is much thinner and the level of thermal maturation is generally lower. The total resource may still be appreciable; however, in our estimation a quantitative assessment of the resource is still premature because of limited data.

The widespread use of conventional rotary drilling with high density, mud-based drilling fluids in Illinois constitutes a major problem in evaluating the commercial potential for gas production from the New Albany Shale. Drilling muds cause

extensive formation damage to ultra-low permeability reservoir rocks such as shale, where even minor blockage of the few high permeability pathways available (including natural fractures) may be disastrous. The gas trapped within shales is released slowly, and at low pressures; thus the reservoir lacks the energy necessary to clean itself of drilling-induced damage. Unpublished studies in Kentucky and Indiana have shown that the proportion of natural gas shows in the Devonian shales is much higher in holes drilled with cable tools than in holes drilled with rotary tools. This suggests the possibility that drilling with cable tools and water, or, better yet, drilling with air may be the most satisfactory methods for drilling Devonian shale tests. Because of the numerous water saturated porous zones in the overlying Mississippian and Pennsylvanian, such techniques would probably require that a casing string be set prior to drilling into the New Albany Shale.

Furthermore, conventional drill stem testing of shales is probably of little value. Drill stem tests are of short duration and involve limited quantities of fluids; they are most satisfactory when evaluating rocks with high porosity and permeability. Production testing of Devonian shales should take several days or even weeks and will most likely require some type of stimulation technique such as massive hydraulic fracturing, to assess the commercial viability of an area. The expense and risk of setting casing and stimulating the shale to evaluate its potential for production will undoubtedly be major barriers to the development of this potential, but as yet untapped resource.

REFERENCES

- Hunter, Coleman D., and Young, David M.: "Relationship of Natural Gas Occurrence and Production in Eastern Kentucky (Big Sandy Gas Field) to Joints and Fractures in Devonian Bituminous Shale," Amer. Association of Petroleum Geologists Bull. (1953) v. 37, pp. 282-299.
- Devonian Shale Task Group of the National Petroleum Council Committee on Unconventional Gas Sources: Untitled draft of report on Devonian Shales (September, 1979; final report to be published spring, 1980) 102 p. plus appendices.
- Cluff, Robert M.: "A Preliminary Assessment of the Natural Gas Potential of the New Albany Shale Group in Illinois," Paper presented at 43rd Annual Meeting of the Kentucky Oil and Gas Association, Lexington, June 15, 1979. (Manuscript to be published in Technical Proceedings of the KOGA, by the Kentucky Geological Survey.)
- Harvey, R. D., White, W. A., Cluff, R. M., Frost, J. K., and DuMontelle, P. B.: "Petrology of the New Albany Shale Group (Upper Devonian and Kinderhookian) in the Illinois Basin: A Preliminary Report," Proceedings of the First Eastern Gas Shales Symposium, Morgantown, West Virginia, U.S. Dept. Energy MERC/SP-77/5 (October 17-19, 1977) pp. 239-265.
- Cluff, Robert M.: "Paleoenvironment of the New Albany Shale Group (Devonian-Mississippian) of Illinois," in press, J. Sedimentary Petrology.
- Nuhfer, Edward B., and Vinopal, Robert J.: "A Fabric-Element Based Classification for Low-Porosity-Shale Gas Reservoirs," Proceedings of the Third Eastern Gas Shales Symposium, Morgantown, West Virginia, U.S. Dept. Energy METC/SP-79/6 (October 1-3, 1979) pp. 485-498.
- Harper, John A., and Piotrowski, Robert G.: "Stratigraphy, Extent, Gas Production, and Future Gas Potential of the Devonian Organic-Rich Shales in Pennsylvania," Preprints for the Second Eastern Gas Shales Symposium, Morgantown, West Virginia, U.S. Dept. Energy METC/SP-78/6, v. 1 (October, 1978) pp. 310-329.
- Harris, Leonard D., DeWitt, Wallace, Jr., and Colton, G. W.: "What Are Possible Stratigraphic Controls for Gas Fields in Eastern Black Shale?" Oil and Gas J. (April 3, 1978) pp. 162-165.
- Tissot, Bernard P., and Welte, Dietrich H.: Petroleum Formation and Occurrence, A New Approach to Oil and Gas Exploration, Springer-Verlag, Berlin (1978) 538 p.
- Bostick, N. H.: "Microscopic Measurement of the Level of Catagenesis of Solid Organic Matter in Sedimentary Rocks to Aid Exploration for Petroleum and to Determine Former Burial Temperatures—A Review," Society of Economic Paleontologists and Mineralogists Special Publication 26 (1979) pp. 17-43.
- Barrows, Mary H., Cluff, Robert M., and Harvey, Richard D.: "Petrology and Maturation of Dispersed Organic Matter in the New Albany Shale Group of the Illinois Basin," Proceedings of the Third Eastern Gas Shales Symposium, Morgantown, West Virginia, U.S. Dept. Energy METC/SP-79/6 (October 1-3, 1979) pp. 85-114.
- Rendl, Thomas W., Anderson, James M., and Dolan, Richard A.: "A Dual-Phase GC Column," Amer. Lab. (January, 1980) pp. 60-68.
- Dickerson, D. R., and Coleman, D. D.: "Mode of Occurrence and Relative Distribution of Hydrocarbon Phases in Shale," in Geologic and Geochemical Studies of the New Albany Group (Devonian Black Shale) in Illinois, Illinois Geological Survey Annual Report to U.S. ERDA, Contract E-(40-1)-5203 (September 30, 1977) pp. 115-135.
- Cluff, R. M., Reinbold, M. L., and Lineback, J. A.: "The New Albany Shale Group of Illinois," Illinois State Geological Survey Circular, in review.
- Reinbold, M. L.: "Stratigraphic Relationships of the New Albany Shale Group (Devonian-Mississippian) in Illinois," Preprints for the Second Eastern Gas Shales Symposium, Morgantown, West Virginia, U.S. Dept. Energy METC/SP-78/6, v. 1 (October, 1978) pp. 443-454.
- Bassett, J. L., and Hasenmueller, N. R.: "The New Albany Shale and Correlative Strata in Indiana," Proceedings of First Eastern Gas Shales Symposium, Morgantown, West Virginia, U.S. Dept. Energy MERC/SP-77/5 (October 17-19, 1977) pp. 183-194.

NATURAL GAS POTENTIAL OF THE NEW ALBANY SHALE GROUP (DEVONIAN-MISSISSIPPIAN)

17. Schwalb, H. R., and Potter, P. E.: "Structure and Isopach Map of the New Albany-Chattanooga-Ohio Shale (Devonian and Mississippian) in

Kentucky: Western Sheet," Kentucky Geological Survey, Series X, 1:250,000 (1978).

TABLE 1
RELEASED GAS ANALYSIS AND HYDROCARBON COMPOSITION,
HOBSON OIL #2 TAYLOR CORE, WAYNE COUNTY, ILLINOIS

Depth to top of sample m (ft)	Off-gas, m ³ HC m ³ shale	C ₁ methane %	C ₂ ethane %	C ₃ propane %	C ₄ butane %	C ₅ pentane %
1474 (4834)	0.73	76.81	16.89	4.17	1.28	0.30
1476 (4838)	0.82	72.78	18.30	6.38	1.99	0.55
1477 (4843)	0.66	72.11	18.97	6.39	2.00	0.55
1478 (4846)	0.55	72.57	18.38	6.43	2.04	0.57
Averages	0.69	73.56	18.13	5.97	1.82	0.49

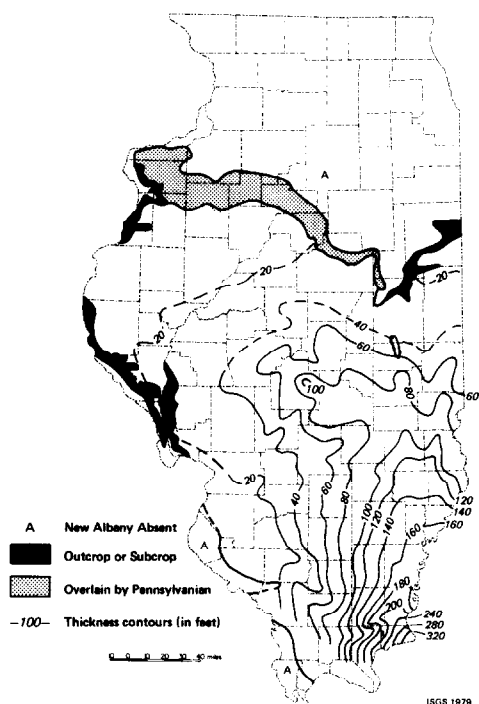


Fig. 1- Cumulative thickness of radioactive "black" shale within the New Albany Shale Group in Illinois. Radioactive shale has a log value >60 API units above a normal shale base line. From Cluff, Reinbold, and Lineback.¹⁴

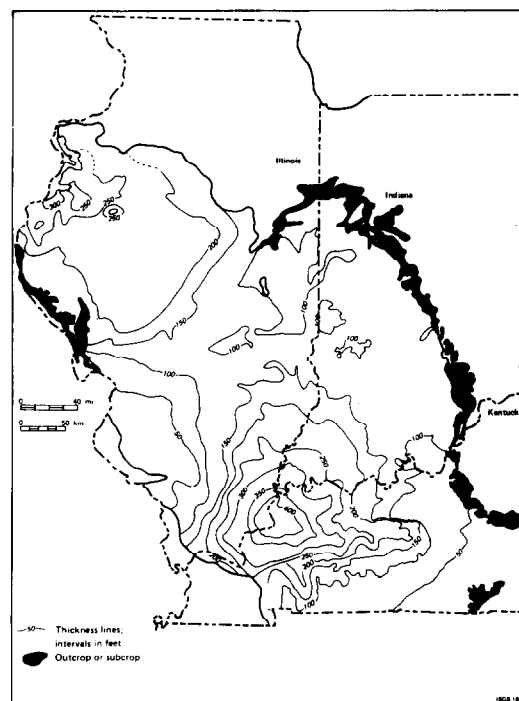


Fig. 2 - Thickness of the New Albany Shale group in the Illinois Basin; after Reinbold;¹⁵ Bassett and Hasenmueller;¹⁶ Schwalb and Potter.¹⁷

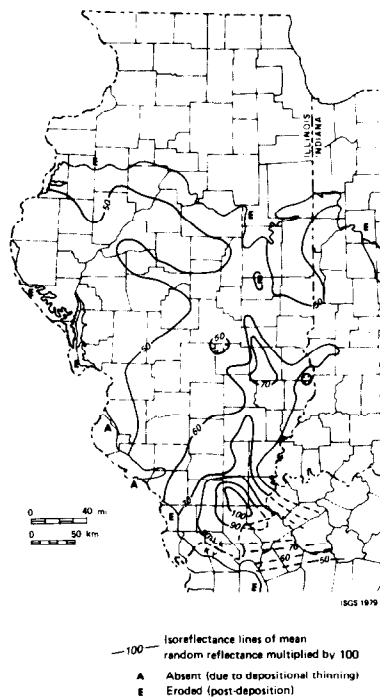


Fig. 3 - Mean random reflectance of vitrinite in the New Albany Shale Group (R_o percent $\times 100$). From Barrows, Cluff, and Harvey.¹⁰

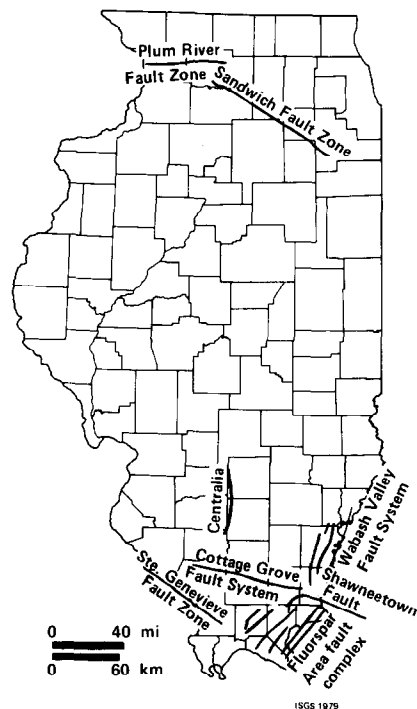


Fig. 4 - Major faults in Illinois.

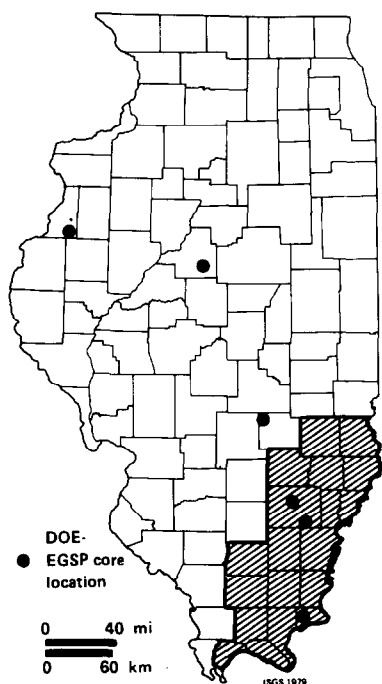


Fig. 5 - The 19-county area of most probable Devonian shale gas resources in Ill. Locations of cores sampled for off-gas analysis are shown.

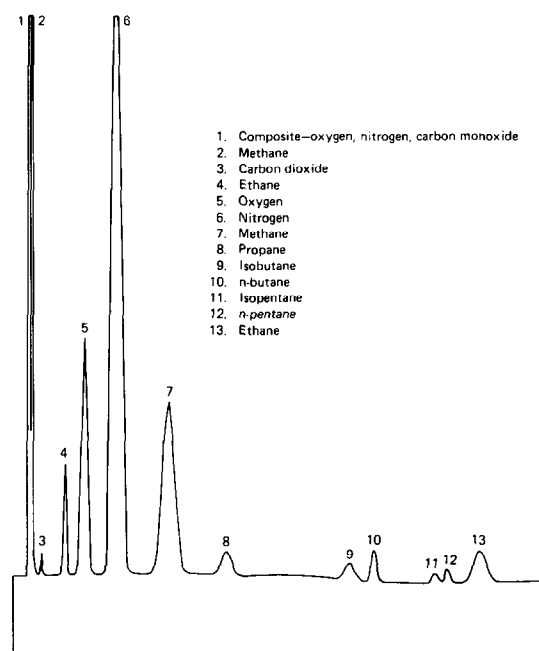


Fig. 6 - Typical GC chromatogram of a sample of gaseous hydrocarbons containing air. A CTR (Alltech Associates) column was used for separation. Analyzer conditions: inj. port --100°C; TCD--200°C; initial temp. --40°C (6 min. hold); temp. program 40°C to 140°C in 10 min. (3 min. hold); sample size: μ L.

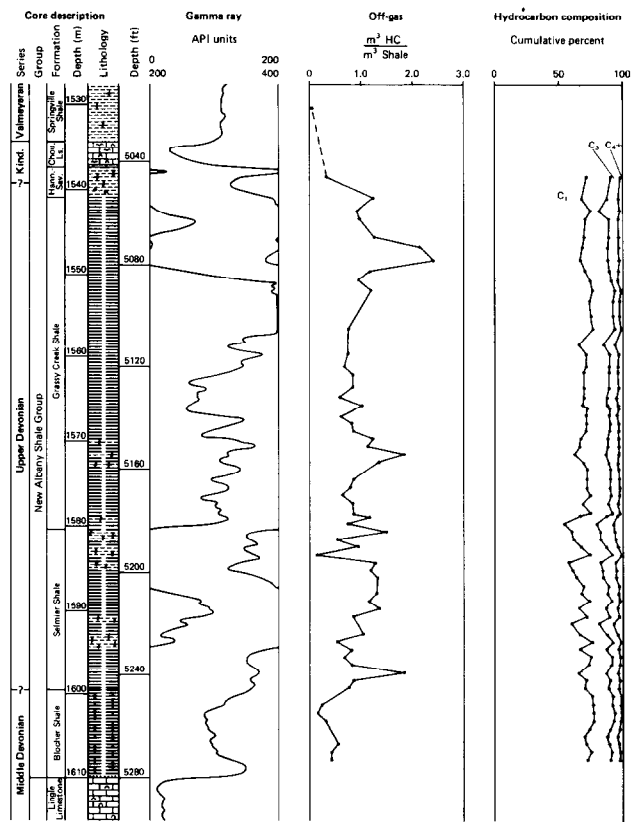


Fig. 7 - Released-gas analysis and core lithology, G.T. Jenkins #1 Simpson core, Wayne County, Illinois.

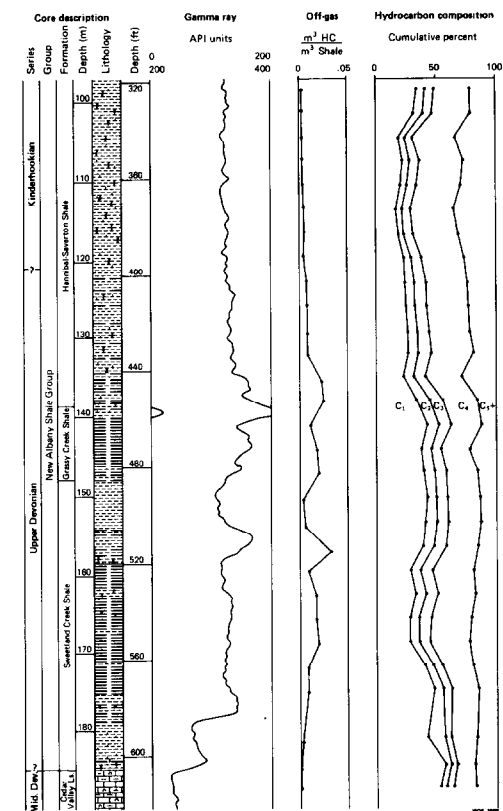


Fig. 8 - Released-gas analysis and core lithology, Northern Illinois Gas #1 RAR core, Henderson County, Illinois.

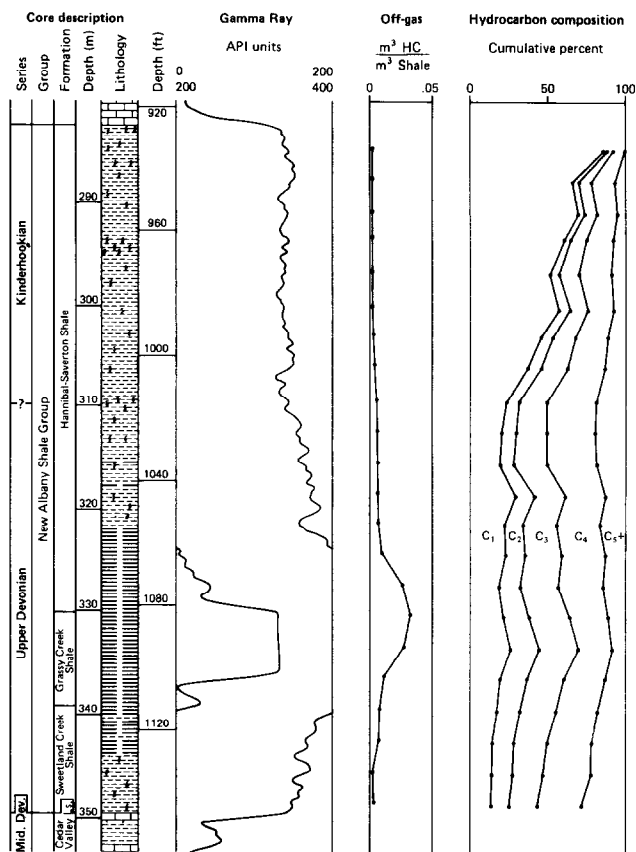


Fig. 9 - Released-gas analysis and core lithology, Northern Illinois Gas #1 MAK core, Tazewell County, Illinois.

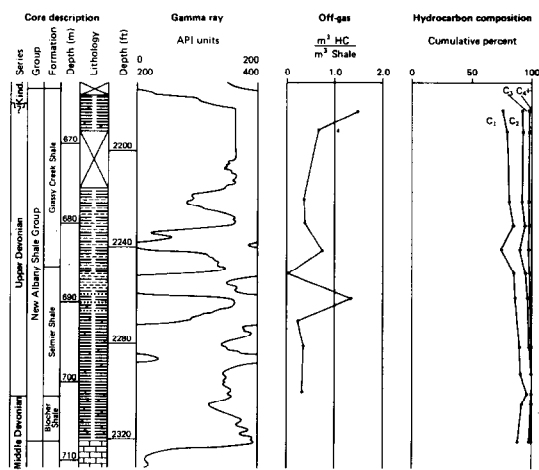


Fig. 10 - Released-gas analysis and core lithology, Tri-Star Production #1-D Lancaster core, Effingham County, Illinois.

PRELIMINARY METHANE RESOURCE ASSESSMENT OF COALBEDS IN THE ARKOMA BASIN

by Herman H. Rieke III, TRW, Inc.

© Copyright 1980, Society of Petroleum Engineers

This paper was presented at the 1980 SPE/DOE Symposium on Unconventional Gas Recovery held in Pittsburgh, Pennsylvania, May 18-21, 1980. The material is subject to correction by the author. Permission to copy is restricted to an abstract of not more than 300 words. Write: 6200 N. Central Expwy., Dallas, Texas 75206

ABSTRACT

Potentially recoverable quantities of methane from unconventional sources such as coalbeds have been largely excluded from potential gas supply surveys. This is attributable to the lack of data about the resource, technology and economics of its recovery. In order to provide answers, DOE initiated the Methane Recovery from Coalbeds Project (MRCP) to characterize the gas-in-place for various coalbeds and associated sediments. After the 1977 initiation of the MRCP, several other interested groups have supported various aspects of the project.

Results are presented from the first phase of a joint effort between DOE (METC), TRW, GRI, and Industry to investigate the coalbed methane resource in the Arkoma basin. This elongated narrow east-west sedimentary basin is located in east-central Oklahoma and in west-central Arkansas and contains extensive gaseous bituminous coal reserves of Pennsylvanian age. Preliminary gas-in-place resource estimates were made based on the volume of coal in-place and on direct methane desorption data. It has been conservatively estimated that the total coal resource of the basin is about 7.9 billion tons. Seven individual coal seams have been identified as being the most likely candidates to contain potential coalbed gas reservoirs. The majority of these coalbeds are continuous, but these beds do not maintain a constant thickness throughout the basin. Total gas contents, as determined by desorption tests on coal cores, range from 73 cubic feet per ton to 576 cubic feet per ton. The estimated unscaled in-place methane resource is 1.6 Tcf and is considered a low volumetric assessment for the basin. The estimated depth scaled in-place methane resource is 2.7 Tcf, 82 percent of which is contained in the Hartshorne coalbeds. Analyses of gas produced from the Hartshorne coals/Hartshorne Formation show a range of Btu values from 993 to 1118 in the western part of the basin.

A viable exploration rationale has been established for the Arkoma basin, based on various geological aspects, such as stratigraphy and structure, the depth of the coalbeds and the recent MRCP well tests. The described methodology of methane exploration is present along with the results. Redefined target-test areas in the basin have been delineated and are discussed.

INTRODUCTION

This study is a result of a cooperative effort between DOE (METC), TRW, GRI and the Natural Gas Industry to characterize and establish the methane resource associated with coalbeds in the Arkoma basin. These activities were initiated in 1979 as part of the Methane Recovery from Coalbeds Project (MRCP). Also, the USBM is doing a study in the Arkoma basin which will determine the effect of geology and occurrence of the emission of methane during mining operations (Iannacchione and Puglio, 1979).

The Arkoma basin encompasses an area of approximately 13,488 square miles in the south-central United States, approximately 41% of which is in the State of Oklahoma (Fig. 1). The basin is an east-west trending depression 250 miles long, 25 to 50 miles wide, and contains Pennsylvanian age and older sedimentary rocks. Except for large-scale faulting and folding in the trough portion of the basin, the shelf and sub-shelf are reasonably uncomplicated structurally. The shelf has been least disturbed by the Ouachita influence. Extensive Pennsylvanian age bituminous coal reserves and some semi-anthracite reserves are contained in the basin. Deepest coal bearing portions of the basin occur in a broad area centered around southern Pittsburg, central Latimer, southern Haskell, central Le Flore counties, Oklahoma and west-central Sebastian County, Arkansas. Because of the basin's central location and proximity to interstate pipelines, the Arkoma basin is an attractive potential gas resource area.

References and illustrations at end of paper.

A sedimentary basin approach is used as the basis for methane in coalbed estimates. This provides for a physical entity that can be characterized with a minimum amount of information early in the MRCP study. The regional geologic framework of the Arkoma basin described by Branan (1968) was utilized and modified as a first step to provide rational estimates of the in-place methane resource. Inasmuch as methane occurs in association with the coalbeds in the basin, the geological dimensions of the resource are defined by the extent of these coals. Hendricks et al. (1939) classical study on the coal geology of the basin helped establishing areal continuity of the coalbeds. The methane is held by adsorption within the coal and exists as free gas within the fractures (cleats) in the coalbed. Iannacchione and Puglio (1990) have shown that some of the coal-derived gas in the basin has migrated into associated sediments. The amount of gas in a coalbed is determined by the depth of burial, rank and the chemical nature of the coal. The largest volume of methane is associated with greater depths of burial and higher ranks of coal.

There is no ideal method for estimating the methane resource potential of a coal bearing basin. The coals in the Arkoma basin are considered to be moderate to highly gassy. The assessment method utilized in this study is compatible with the other basin evaluations in the project and with the technical resources and data base available. A range in methane contents was established and used in conjunction with the identified coal reserves to provide an estimate of the volume of methane in-place.

GEOLOGY

The basin contains upward to 30,000 ft (9,144 m) of sediments adjacent to the Ouachita system. Branan (1968) estimated that 40,000 cu mi (166,724 cu km) of sediments fill the basin. These sediments are predominantly of Pennsylvanian age and consist mostly of clastic marine/deltaic deposits with some cherty and marine limestones occurring in the Cambrian/Ordovician sequence.

Structural Framework

Rocks and coalbeds have been highly deformed by separate orogenic movements beginning during Atoka time (lower Pennsylvanian) and ending in the Permian. The Pre-Cambrian basement rocks have been depressed to depths greater than 25,000 feet in parts of the basin. Influence of the Ozark uplift and the Ouachita orogenic province has caused the Arkoma basin to possess many unique structural conditions. This has given rise to the reverse physiography in western Arkansas and eastern Oklahoma where the synclines form the mountains and the anticlines are expressed as valleys.

In order to explain the tectonics, Branan (1968) divided the Arkoma basin into three structural provinces, ranked in order of the influence of the Ouachita deformation (Fig. 1).

Zone 1 is at the forefront of the Ouachita Mountains in the trough area. Steep dips are common. The rocks are folded into a series of long, narrow anticlines, generally overthrust on the north. The Choctaw overthrust forms the southern boundary of the basin.

Zone 2 is an area of elongated and domal features, with little or no evidence of thrusting. This is known as the subshelf area.

Zone 3 is the basin shelf area where the Ouachita influence was slight, and only gentle folds characterize this portion of the basin. In Zone 3 in Oklahoma the outcropping beds are middle and upper Pennsylvanian. These rock units thicken southeastward; however, they have been elevated by the Ouachita disturbance and now dip northwestward.

There are two basic structural patterns affecting the target areas in the basin: (1) folding and northward overthrusting, and (2) block faulting. The stability of the Ozark Plateau on the north during basin subsidence caused tensional forces to develop which resulted in the evolution of major block faulting in the basin (Fig. 2). Disney (1960) reported that the anticlines occupy approximately 35 percent of the total basin area, whereas the synclines, being wider, account for approximately 65 percent of the area. These superficial folds diminish with depth and strike northeast to east. Structural expression below the Wapanucka Limestone (Morrowan, lower Pennsylvanian) is not related to the surface structure.

Directional permeability characteristics of coalbeds are generally dependent on the orientation of cleat fractures. Kissell (1972) demonstrated that a coalbed gives up gas at a higher rate from the face-cleat direction. Coal cleats do not always show the exact same orientation through a vertical sequence. That is to say the orientation of the butt and face cleats in the Secor coal could be different from those directions in the stratigraphically lower Hartshorne coalbed. These minor variations can be attributed to the competency and incompetency of the coalbed and the host rocks.

The structural character of the coals in the Arkoma basin, such as fracture or cleat (joint) density and orientation, have not been thoroughly investigated on a basin-wide scale. Iannacchione and Puglio (1979) reported on cleat directions that were measured at strip mines and surface exposures of coal in Le Flore County, Oklahoma. Cleat data were then analyzed by them using a method devised by Diamond et al. (1976). Results of these analyses show that the direction of the dominating face cleat varies from N 32°W to N 17°W, which is perpendicular to structural trends in that area of Le Flore County. Butt cleat directions vary from N 52°E to N 77°E and are generally parallel to structural trends in the area. The friability of the Hartshorne coalbed in eastern Oklahoma is due to close spacing of the cleat and the frequent occurrence of shear fractures with dips of 45° to 55° within the coalbed.

In summary the face cleats tend to be perpendicular to the axial trend of the Arkoma folds and probably formed as extension fractures. The butt cleats tend to be parallel to the axial trend and formed after compressive forces were released.

Stratigraphic Framework

Stratigraphic relationships are important in reconstructing the geological depositional environments of the coalbeds. Coalbeds are the most continuous lithotypes known and can be effectively used as key beds in lithostratigraphic correlation. Friedman (1978) developed a generalized geologic column showing coals and major key lithological beds in the Arkoma basin of Oklahoma (Fig. 3). This geologic column is preliminary and is changing as additional facts come to light from deep drilling and resource characterization studies of the coalbed methane resources which are in progress (Rieke, 1980).

The Desmoinesian age formations in the basin were deposited in a deltaic fashion. Apparently, the sediment sources were from eroding highlands to the northeast, north and northwest of the basin. Thin coalbeds appear in the central part of the basin in the upper Atokan section (Haley and Hendricks, 1972). These coalbeds become thicker and more widespread in the lower Desmoinesian section (Hartshorne and McAlester coals) providing the basin with a large coalbed resource.

Accurate coalbed correlation is an essential prerequisite to the determination of coal resources and reserves, especially those beds which are particularly gassy. Although some minor coals have been noted or described in the geologic literature of the Arkoma basin, they are not named and or shown in the geologic column (Fig. 3). These coals for the most part have been omitted from the present discussion because of insufficient basin-wide information and for resource calculations the coals are classified as "unnamed". It must be noted that these minor coals can be up to 3 feet thick in local areas (Rieke et al., 1980).

Strictly speaking the Hartshorne Sandstone forms the base of the commercial coal-bearing portion of the Pennsylvanian rock sequence in the coal basin. Friedman (1974) noted that there are certain stratigraphic sequences and correlation uncertainties in the McAlester-Hartshorne area of the Arkoma basin, such as the four coals present in the McAlester Formation above the Hartshorne coal and beneath the McAlester (Stigler) coal (Fig. 3). Rieke et al. (1980) has shown that these coals are associated with the Booch delta. At present the Booch coal resource is classified under "unnamed" beds. The McAlester coal appears to correlate with the Stigler coal and the upper McAlester coal appears to correlate with a "rider" coal above the Stigler. At least one additional coal is present above this rider coal in the McAlester Formation in Le Flore and Pittsburg counties, Oklahoma.

As many as four coals are present in the "Cavalal coal zone" in the lower part of the Savanna Formation in Le Flore County. A previously undetected coal occurs about midway between the Secor (Upper Witteville) coal and the Lower Witteville coal in Cavalal Mountain, Le Flore

County. This coal may be the one that is present 30-45 feet below the Secor in Pittsburg County in places where the Lower Witteville cannot be identified (Friedman, 1974).

An unnamed coal lies some 30 - 50 feet above the Secor Coal in Pittsburg County, and it may or may not be equivalent to the Mayberry Coal in Cavanal Mountain in Le Flore County. Another unnamed coal lies at least 100 feet stratigraphically above this "rider" of the Secor Coal.

Rieke et al. (1980) established 18 coal bearing zones in the MRCP Barringer No. 1-11 test well located in the Kiowa syncline, Pittsburg County, Oklahoma. Table 1 presents pertinent chemical and thickness data for these coals. Synthesis of offset well data indicates that there are lateral discontinuities in the coals within the Kiowa syncline. The characteristics and variability of the stratigraphy and depositional environments have been delineated for these coals in that area.

Depositional Framework

A delta is not deposited entirely at one time. It represents a history of progradation, maturation of older elements, and deposition throughout the delta. The control of these processes is dependent upon the geomorphic and tectonic framework, energy pattern, rates of sediment discharge and other physical conditions.

In the Arkoma basin the depositional pattern is one of major regressive progradations interrupting a continuous transgressive depositional period. This gave rise to the characteristic stratigraphic pattern in the basin.

Each sandstone has the general shape of a deltaic unit. Very few of these sandstones have been studied in detail in the basin's subsurface except those which show promise as oil or gas producing horizons in the Atokan series or in the Desmoinesian series on the shelf. The overall pattern and the basic depositional framework strongly suggest delta degradation as a result of excess sediment supply. This resulted in large deltaic complexes which have prograded out into the basin from various directions resulting in widespread coal deposition.

In the northwestern portion of the basin onlays are from south to north. The regularity of the transgression and the presence of excellent key beds provide the basis of a time-stratigraphic subdivision of the Atokan-Desmoinesian section of the Arkoma basin. Visser et al. (1971) stated that the unconformity separating Mississippian and Pennsylvanian strata disappears as one goes into the deeper part of the Arkoma basin, however, the unconformity is well developed on the shelf. No regional erosion surfaces have been recognized in the basin's trough. This suggests that warping and subsidence occurred in a progressive and regular manner, and it might not be necessary to involve tectonic events to explain the overall depositional pattern. The intermingling of the delta complexes gave rise to multiple coalbeds such as the lower, middle and upper Hartshorne coals.

It is not in the scope of this paper to reconstruct detailed depositional environmental patterns that spread over such a large area and represent the many different coal depositions; but a generalized pattern is presented in Table 2.

The distal portion of the delta is considered to be a neritic depositional environment, whereas, the term moderate denotes moderate water depths. Near signifies the delta slope and subaqueous delta top depositional environments and fluvial refers to the alluvial delta plain.

The relationship between coalbed continuity, thickness and depositional environment can be summarized; back barrier coals are thin and laterally discontinuous, lower delta plain coals are thin but continuous, upper delta plain coals are thick but laterally discontinuous and the transition zone between upper and lower delta plain provides a depositional environment for thick and wide spread coals. Further discussion about the individual deltas is contained in TRW's Arkoma Basin Report (Rieke, 1980).

COAL RESOURCE DATA BASE

In order to make reasonable estimates of the methane contained in the Arkoma coalbeds one has to establish the volume of coal present on a bed basis.

The volumetric assessment of the coalbed methane resource in the Arkoma basin is based on Friedman's 1974 study for the Ozarks Regional Commission which provides the data for the bituminous-coal resources and recoverable reserves of Oklahoma. The coal resource data for Arkansas is from Haley's 1977 study. The objectives of these coal-investigation studies were to obtain, evaluate, and provide basic information pertaining to the extent, thickness, depth of burial and quality of the coals. The coal resources for Oklahoma include those that are greater than 3,000 feet deep, and coalbeds greater than 12 inches thick, whereas the Arkansas data was not specified. Both data sets did not separate out the shallow (strippable) coals from the deep (non-strippable) coals. Only 9 percent of the remaining coal resources of Oklahoma are amendable to surface mining Friedman (1974). In addition shallow coals in the Arkoma basin can have very high methane contents (190 feet, 309 ft³/ton (9.6 cc/g), well DH-A17, Rock Island area of Le Flore County, Oklahoma.

Coal resources and reserves are classified according to standard procedure as measured, indicated, and inferred. These terms are categories of reliability based on geologic evidence and judgment. Friedman's data base consisted of 600 logs of boreholes drilled for coal since 1954, plus 10 boreholes drilled for the Ozarks Regional Commission Project, and earlier data published by the Oklahoma Geological Survey and the USGS. These coal datum points provide evidence of thickness, composition, continuity, depth, and altitude of coalbeds. The datum points may be at mine boundaries, in drill holes that penetrate coal, or at outcrops. In places where geologic evidence indicates impure or thin coalbeds or the absence of coal because of channel-sandstone erosional cutouts, post-Pennsylvanian erosion, or structural

faults coal resources are not computed in either measured, indicated, or inferred categories (Friedman, 1974).

Measured resources are those for which datum points are not more than 1/2 mile apart. An isolated datum point is considered to be the center of a circle whose radius is 1/4 mile, and this circle defines an area of measured resources.

Indicated resources are those for which datum points are not more than 1 1/2 miles apart. An isolated datum point is considered to be the center of a circle whose area of indicated resources is defined by a radius segment of 1/4 to 3/4 mile.

Inferred resources are those for which datum points are not more than 4 miles apart. An isolated datum point is considered to be the center of a circle whose area of inferred resources is defined by a radius segment of 3/4 to 2 miles.

For Oklahoma, Friedman plotted coal datum points on base maps compiled from 7.5-minute topographic-quadrangle maps at a scale of 1:24,000, on county road maps and geologic maps at a scale of 1:63,360, and on published geologic maps at a scale of 1:31,680. These datum points are located by 1/4 1/4 section, township, and range, within a geographic accuracy of about 50-100 feet. The datum points were obtained by Friedman from previous work published in the geologic literature, coal-mine maps surveyed by engineers, recent coal-test boreholes, coal faces exposed in active mines, and coal outcrops, but these points were not determined from geophysical well log records. Mine slopes, drifts, shafts, and mine boundaries also were taken as datum points. Arcs or circles were drawn around all datum points, delineating the measured, indicated, and inferred, resources and reserves. Although coal deposits were judged by Friedman to exist in geologic continuity with adjacent resources, these deposits have not been included in the tonnage figures of resources if they were more than 2 miles from a datum point. This has been done to adhere as closely as possible to the criteria established by the U.S. Geological Survey, which have been used conservatively by Trumbull (1957) in maintaining the standard method of determining coal resources and reserves (Friedman, 1974).

A coal resource base of about 7.9 billion tons of bituminous coal remains in the Arkoma basin. This estimate is conservative due to the lack of information about deep buried coalbeds and minor (unnamed) laterally discontinuous coals.

MRCP WELL TESTS

To date there have been four MRCP type I test wells in the Arkoma basin. These tests were performed during the past 1 1/2 years in the initial target areas. The four tests are:

- Brown Estate #1-2, Pittsburg Co., OK - Subshelf - Lilypad Creek Anticline
- Barringer #1-11, Pittsburg Co., OK - Trough - Kiowa Syncline

- Day #1-14, Haskell Co., Ok - Trough - Sanbois Syncline
- USBLM/USBR DH-A17, Le Flore Co., Ok - Trough - Greenwood Syncline

MRCP data on the methane gas content of the Arkoma basin coals is presently limited to coring and well testing in Pittsburg, Haskell and Le Flore counties, Oklahoma. In Pittsburg County, the upper Hartshorne, lower Hartshorne, the Booch and the McAlester coals were conventionally and side-walled cored in two wells between the depths of 1905 and 4630 feet. The coal core samples were desorbed for approximately five months using the USBM's direct method. Total gas contents for the upper Hartshorne coal and Booch coals were 73 and 211 ft³/ton (2.3 cc/g and 6.6 cc/g), respectively. In Le Flore County, Oklahoma, the upper Hartshorne coal was sampled at a depth of 192 feet and found to contain 309 ft³/ton (9.6 cc/g). Variability in gas content cannot always be directly related to coalbed depth, inasmuch as some of the gassier coals were from shallower horizons. Gas contents are thought to be related to various geologic controls, such as the chemical character, thickness, permeability of the coals and structural history of the specific area.

GAS RESOURCE ASSESSMENT

The results of the direct core desorption tests were used to provide a rough preliminary estimate of the methane resource. MRCP test results have shown that the measured gas content of the coals range from a low value of 73 ft³/ton to a high value of 309 ft³/ton (2.3 cc/g to 9.6 cc/g). The Hartshorne coals in Oklahoma are the most frequently sampled coalbeds. The USBM have measured total gas contents in the Hartshorne coals that range from 350 ft³/ton (10.9 cc/g) to 570 ft³/ton (17.8 cc/g). MRCP measured values are 211 ft³/ton (6.6 cc/g) to 232 ft³/ton (7.3 cc/g) for Booch coals and 131 ft³/ton (4.1 cc/g) for the McAlester coal. The lower values are from the coals located in the western part of the basin on the subshelf where the coalbeds are thinner and not as well developed.

USBM Studies

Iannacchione and Puglio (1979) calculated the total volume of methane contained within the upper and lower Hartshorne coals for Haskell and Le Flore counties, Oklahoma. Their study used the results of the USBM desorption tests Hartshorne coals. Estimation of the Hartshorne gas content was based on a total gas versus depth relationship (Fig. 4). This relationship is used in conjunction with overburden and coal isopach maps to scale the resource. The methane content of the Hartshorne coals within these two counties was calculated to be between 1.1 and 1.5 trillion cubic feet of gas. This estimate was based on a reserve of 2,330 to 3,120 million short tons of coal in place (Iannacchione and Puglio, 1979).

MRCP Results

The total methane content of any coalbed area can be calculated by multiplying the total tonnage estimated for that area by the methane content per

unit weight determined by the direct gas desorption method (McCulloch et al., 1975). Based on the data in Table 3 it is possible to present reasonable ranges for the minimum and maximum expected in-place gas resource of the coals in the Arkoma basin. Gas in-place estimates were calculated on a county basis and on a bed basis for the Arkoma basin. Table 4 presents the minimum in-place gas resource of 1.58 Tcf based on a minimum average methane content of 200 ft³/ton (6.2 cc/g). Two hundred cubic feet per ton is considered to be the average natural gas content of coal. The following coalbeds were included:

- Lower Hartshorne
- Upper Hartshorne
- Hartshorne Undivided
- McAlester (Stigler)
- McAlester (Stigler) Rider
- Charleston - Arkansas
- Cavanal
- Paris - Arkansas
- Lower Witteville
- Secor
- Unnamed

It is reasonable to assume that the methane resource contained in these coalbeds should be much higher, inasmuch as no depth scaling for the gas content was made such as was done by Iannacchione and Puglio (1979) in this initial approximation. An average gas content of 450 ft³/ton (14.1 cc/g) would give an unscaled upper limit for the methane gas resource of about 3.55 Tcf. This value is an average derived from data shown in Fig. 5. Recent MRCP drilling activities in the Arkoma basin have also delineated areas which contain more coal than previously thought, such as encountered in the Barringer and the Day wells, Pittsburg and Haskell counties, Oklahoma. The extent of these new coal reserves have not been determined and therefore are not included in the present assessment.

Depth scaling of the Hartshorne coal resource was made using Fig. 4 for Haskell, Latimer and Le Flore counties, Oklahoma and for Sebastian County, Arkansas and the coal resource data from Friedman (1974). The scaled gas-in-place resource was calculated to be 2.73 Tcf for the basin. Table 5 compares the depth scaled resource values with the unscaled values. Results from this table show a strong shift in the preponderance of the Hartshorne gas resource from 69% (unscaled) to 82% (scaled). Uncertainties still exist in the variation of the gas content values with respect to:

- area
- depth

Future testing activities will hopefully establish the variation in the coalbed gas content with depth for the western, central and eastern parts of the Arkoma basin.

Gas Composition

The gas from the Arkoma coalbeds and associated sediments is not pure methane. Table 6 provides some selected typical gas compositions of samples taken from producing wells in the Hartshorne Formation. The gas bearing zones in the Hartshorne wells are closely associated with the Hartshorne coals by either being right above the coalbeds, between or directly below them.

Thermal quality of the gas being produced from the Hartshorne Sandstone/Hartshorne coals in the S. McAlester Gas Field, Kiowa syncline, Pittsburg County, Oklahoma ranges from 1097 to 1119 Btu's. Pure methane has a heat content of 1012 Btu's per cubic foot at 60°F and atmospheric pressure. The range in the thermal values of 993 to 1118 Btu's would give a thermal energy resource somewhere between 1.57×10^{15} to 1.76×10^{15} Btu's for the basin using the assumed minimum resource value. By using the scaled resource value of 2.73 Tcf the range is from 2.71×10^{15} to 3.05×10^{15} Btu's.

Carbon Isotope Values

The USBM collected and analyzed samples of the desorbing gas from the upper Booch (Barringer No. 1-11 well) and the upper Hartshorne (DH-A17 well) coals cores. The δC^{13} values are similar to those values from gas in medium-volatile bituminous Hartshorne coals as analyzed by Iannacchione and Puglio (1980).

TARGET AREA SELECTION

An initial target area of approximately 5300 square miles of the Arkoma basin was selected for early testing in the MRCP. This area was thought to contain ample opportunities for testing those coals having the greatest potential for commercialization of the coalbed methane resource.

A detailed investigation completed this year surveyed the available resource data and the results of MRCP testing. As a result of this study, the initially defined target area has been redefined to concentrate further on the gas-in-place in deep lying Hartshorne and McAlester coalbeds. Further resource characterization detailing the variability of the coals' total gas contents is needed in order to properly evaluate their contribution to the total coalbed methane resource of the basin. The following criteria were developed and used in redefining areas with the greatest potential methane resource.

- Thick coalbeds have higher methane contents.
- Higher the coal's rank, greater the amount of thermally generated methane present in the coalbed.
- Lower the fixed carbon values for bituminous coal, the higher the remaining methane content in the Arkoma basin coalbeds.

- Fixed carbon values in the Arkoma basin coals are related to structural deformation.
- Coals in anticlines have a higher percentage of fixed carbon than the coals in adjacent synclines.
- Anticlines in the basin are narrower than the synclines indicating more deformation.
- More deformation - more fractures - more gas loss to surrounding sediments.
- Anticlines occupy approximately 35 percent of the total basin area.
- Synclines occupy 65 percent of the total basin area.
- Methane content in the Hartshorne coalbeds increases with depth of burial.
- Thick Hartshorne sand development thin lower Hartshorne coalbed.
- Optimum conditions for gas in coalbeds - Look for:
 - Broad synclines
 - Thick coalbeds
 - Deeply buried coalbeds
- Optimum conditions for gas in coal associated sediments - Look for:
 - Narrow anticlines
 - Thick coalbeds
 - Fractured rocks

Recommendations for completing the delineation of the Arkoma coalbed methane resource base area are:

- Type I tests (conventional gas or oil wells being drilled to potential reservoirs below the coal):
 - Cavanal syncline (Le Flore County, Oklahoma)
 - Cavanal syncline (Sebastian County, Arkansas)
 - Lehigh syncline (Coal County, Oklahoma)
- Type III tests (well drilled expressly for completion as a production well from coalbeds):
 - Kiowa syncline (Pittsburg County, Oklahoma; Barringer No. 1-11 well)
 - Sanbois syncline (Haskell County, Oklahoma; Day No. 1-14 well)
 - Cavanal or Lehigh syncline as needed.

It is recommended that a minimum of three type I test wells be planned in these chosen target areas (Fig. 5). In addition at least one type III well test should be conducted in the Kiowa syncline, Pittsburg County, Oklahoma to test the deep McAlester and Hartshorne coals. Once these target areas have been adequately tested an evaluation of the resource data should be made to determine the requirements for, or value of, additional type I testing in the Arkoma basin. Type III testing, if sufficient gas is found, should be planned for the purpose of gathering specific reservoir and production data from these coalbeds.

CONCLUSIONS

Although the presented methane data are derived from a relatively small data base, it appears that the measured methane content of the coalbeds in the Arkoma basin is low to moderate (73 to 211 ft³/ton; 2.3 to 6.6 cc/g) in the northwest subshelf area, moderate to high (200 - 570 ft³/ton; 6.2 to 17.8 cc/g) in the central trough, and unknown in Arkansas. There appears to be a general increase in the gas content within the trough portion of the basin towards the east.

On the basis of information gathered in this report, a rational was developed that redefined those areas in the Arkoma basin which hold a higher probability for early commercial coalbed methane gas production. One of the key considerations in this response to this requirement is understanding the relationships between geologic structure, coal rank and variation of total gas content with respect to depth and location.

In summary:

1. The in-placed methane resource
 - Unscaled
 - Minimum 1.6 Tcf
 - Maximum 3.6 Tcf
 - Scaled
 - Most likely 2.7 Tcf
2. Measured desorbed gas content of Arkoma coals range from 73 ft³/ton (2.3 cc/g) to 570 ft³/ton (17.8 cc/g).
3. The amount of gas which is producible is undetermined.
4. Total coal resource base (measured, indicated and inferred) is 7.9 billion tons.
5. Measured and inferred coal resource values are low for the basin and need to be updated owing to the recent MRCP well tests.
6. Majority of the gas in-place is contained in two distinct coal measures
 - Hartshorne coals 69% to 82%
 - McAlester coals 21% to 12%

7. Thermal values (dry) of gas produced from associate sediments range from 993 to 1118 Btu's.

UNIT CONVERSION

To obtain the corresponding SI units:

Multiply Btu by 1.055 to obtain kJ

Multiply ft by 0.3048 to obtain m

Multiply ft³ by 0.0283 to obtain m³

Multiply ft³/ton by 0.0312 to obtain cc/g

Multiply ton by 0.9071 to obtain Mg

REFERENCES

- Branan, C. B., Jr., 1968, Natural gas in Arkoma basin of Oklahoma and Arkansas: Am. Assoc. Petrol. Geol., Memoir No. 9, pp. 1616-1635.
- Diamond, W. P., C. M. McCulloch, and B. M. Bench, 1976, Use of Surface Joint and Photolinear Data for Predicting Subsurface Coal Cleat Orientation. USBM RI 8120, 13 pp.
- Disney, R. W., 1960, Subsurface Geology of the McAlester Basin, Oklahoma: Univ. Okl., Ph.D. Diss., 116 pp.
- Friedman, S. A., 1974, Investigation of the Coal Reserves in the Ozarks Section of Oklahoma and their Potential Uses. Oklahoma Geol. Surv., Norman, OK, 117 pp.
- Friedman, S. A., 1978, Des Moinesian Coal Deposits in part of the Arkoma Basin, Eastern Oklahoma. Amer. Assoc. Petrol. Geol. Field Guidebook, Oklahoma City Geol. Soc., Oklahoma City, OK, 62 pp.
- Haley, B. R. and Hendricks, T. A., 1972, Geology of the VanBuren and Lavaca Quadrangles Arkansas-Oklahoma. U. S. Geol. Surv., Prof. Paper 657-A, 41 pp.
- Hendricks, T. A., Knechtel, M. M., Dane, C. H., Rothrock, H. E. and Williams, J. S., 1939, Geology and Fuel Resources of the Oklahoma Coal Field. U. S. Geol. Surv., Bull. 874, 300 pp.
- Iannacchione, A. T. and Puglio, D. G., 1979, Methane content and geology of the Hartshorne coalbed in Haskell and LeFlore counties, Oklahoma. USBM RI 8407, 14 pp.
- Iannacchione, A. T. and Puglio, D. G., 1980, Geological association of coalbed gas and natural gas from the Hartshorne Formation in Haskell and LeFlore counties, Oklahoma. Comp. Renda, IX Intern. Congr. of Carb. Strat. and Geol., Urbana, Ill. In press.
- Kissell, F. N., 1972, The Methane migration and storage characteristics of the Pittsburg, Pocahontas No. 3, and Oklahoma Hartshorne Coalbeds. USBM RI 7667, 22 pp.

PRELIMINARY METHANE RESOURCE ASSESSMENT OF COALBEDS IN THE ARKOMA BASIN

McCulloch, C. M., J. R. Levine, F. N. Kissell, and M. Deul, 1975, Measuring the Methane Content of Bituminous Coalbeds. USBM RI 8043, 22 pp.	Desmoinesian coals in the Kiowa syncline, Pittsburg County, Oklahoma, Geol. Soc. Amer. Abstr., Vol. 16, No. 1, 16 pp.
Moore, B. J., 1976, Analyses of natural gases. USBM IC 8749, 94 pp.	Trumbull, J. V. A., 1957, Coal resources of Oklahoma: U.S. Geol. Surv. Bull. 1042-J, pp. 307-382.
Rieke, H. H., III, 1980, Arkoma Basin Report (Draft). TRW Energy Systems Group, Morgantown, WV, prepared under Contract DE-AC21-78MC08089.	Visher, G. S., Sandro, S. B. and Phares, R. S., 1971, Pennsylvanian Delta Patterns and Petroleum Occurrences in Eastern Oklahoma. Am. Assoc. Petrol. Geol., V. 55, No. 8, pp. 1206-1230.
Rieke, H. H., III, Galliers, F. G., and Friedman, S. A., 1980. Stratigraphic relationship of	

Table 1

Summary of coalbed data derived from geophysical well logs for the Barringer No. 1-11 well, Pittsburg County, Oklahoma.

NAME	DEPTH INTERVALS	CARBON WT PCT	ASH WT PCT	MOISTURE WT PCT	COAL SEAM THICKNESS FT.	CUMULATIVE THICKNESS FT.
■ UNNAMED BOGGY COAL	446.375 - 447.500	62.50	37.50	0.00	1.13	1.13
UNNAMED BOGGY COAL	465.250 - 467.125	64.06	31.56	4.37	1.88	3.01
■ SECOR RIDER	940.375 - 941.125	62.14	32.86	5.00	0.75	3.76
SECOR	994.125 - 998.000	37.70	41.41	20.62	3.87	7.67
UNNAMED BOGGY COAL	1050.000 - 1053.250	41.11	35.74	23.15	3.25	10.88
L. WITTEVILLE	1180.375 - 1181.125	47.14	37.86	15.00	0.75	11.63
■ UNNAMED SAVANNA COAL	1904.750 - 1905.625	67.50	32.50	0.00	0.88	12.51
U. CAVANAL	2128.125 - 2128.750	69.17	22.50	8.33	0.63	13.14
L. CAVANAL	2131.125 - 2132.250	81.00	19.00	0.00	1.13	14.27
UNNAMED SAVANNA COAL	2173.500 - 2174.000	45.00	45.00	10.00	0.50	14.77
■ UNNAMED MCALESTER COAL	2768.125 - 2769.500	49.58	39.58	10.83	1.37	16.14
UNNAMED MCALESTER COAL	2856.500 - 2857.750	34.55	54.09	11.36	1.25	17.39
UNNAMED MCALESTER COAL	3108.500 - 3109.500	52.78	38.33	8.89	1.00	18.39
MCALESTER RIDER	3168.875 - 3170.000	59.00	35.00	6.00	1.13	19.52
MCALESTER	3213.375 - 3217.000	57.00	21.83	21.17	3.63	23.14
U. BOOCH*	3651.000 - 3652.500	45.39	35.00	19.62	1.50	24.64
■ M. BOOCH*	3880.250 - 3883.625	27.14	41.07	31.79	3.37	28.01
LOWER HARTSHORNE	4629.625 - 4632.750	50.58	30.58	18.85	3.13	31.14

*UNOFFICIAL NAME

■ SHALY-COAL OR CARBONACEOUS SHALE

Table 2

Generalized depositional environments in the Arkoma basin. Western section includes Atoka, Coal and Pittsburg counties, Oklahoma; Central section includes Haskell, Latimer, Le Flore counties, Oklahoma and Sebastian and Scott counties, Arkansas; Eastern section includes Crawford, Franklin, Johnson and Logan counties, Arkansas.

MODEL	WESTERN	CENTRAL	EASTERN
Boggy	Near to fluvial	Fluvial	Missing
Savanna	Near to fluvial	Near to fluvial	Fluvial
McAlester	Moderate to near to fluvial	Near to fluvial	Fluvial
Hartshorne	Near to fluvial	Near to fluvial	Near to fluvial
Atoka	Distal	Moderate to near	Near to fluvial

Table 3

Methane data from coals sampled in the Brown Estate No. 1-2 and Barringer No. 1-11 wells Pittsburg County, Oklahoma and the DH-A17 well, Le Flore County, Oklahoma.

Coalbed	Depth Ft.	Lost Gas cc/g	Desorbed Gas cc/g	Residual Gas cc/g	Total Gas Content (cc/g)	(ft ³ /ton)
McAlester	1905	1.407	2.683	0	4.09	131
Booch	2130	3.514	3.087	0	6.60	211
Upper Hartshorne	2733	0.630	1.639	0	2.27	73
Booch		0.76	5.59	0.9	7.25	232
Upper Hartshorne	196	0.08	8.37	1.2	9.65	309

Table 4

Total Remaining Bituminous Coal and Coalbed Methane on a County Basis, Arkoma Basin, in Arkansas and Oklahoma.

County	State	Remaining Coal 1,000 Short Tons	Average Gas Content BCF	
			200 cf/ton (6.25 cc/g)	450 cf/ton (14 cc/g)
Atoka	Oklahoma ¹	29,619	5.92	13.33
Coal		292,875	58.58	131.79
Haskell		1,513,681	302.74	681.16
Hughes		Not Known	—	—
Latimer		841,968	168.39	378.89
LeFlore		1,973,362	394.67	888.01
Muskogee		61,199	12.24	27.53
Pittsburg		1,383,832	276.77	622.72
Sequoyah		27,146	5.43	12.22
Subtotal	Oklahoma	6,123,682	1,224.74	2,755.65
Crawford	Arkansas ²	289,900	57.98	130.46
Franklin		212,400	42.48	95.58
Johnson		59,400	11.88	26.73
Logan		41,400	8.28	18.63
Scott		104,200	20.84	46.89
Sebastian		1,063,000	212.60	478.35
Subtotal	Arkansas	1,770,300	354.06	796.29
Total	Arkoma Basin	7,893,982	1,578.80	3,552.29

¹As of January 1, 1974.

²As of January 1, 1977.

Table 5
Percentage distribution of the methane
resource in the Arkoma coalbeds

	Unscaled	Scaled
Hartshorne Coals	68.9%	82.3%
McAlester Coals	20.9	12.4
Charleston Coal	0.8	0.3
Cavanal Coal	2.0	1.1
Paris Coal	0.5	0.3
Lower Witteville Coal	0.8	0.4
Secor Coal	5.2	2.9
Unnamed Coals	0.9	0.3
	100.0%	100.0%

Table 6
Gas sample analysis from the Hartshorne Formation in Oklahoma

	Smalley No. 1-12	German No. 1	Stipe No. 1-4	Roberts No. 1
County	Coal	Pittsburg	Pittsburg	Pittsburg
Field	Ashland S	McAlester S	McAlester S	Featerston NW
Location	Sec. 12, T.3N., R.11E.	Sec. 33, T.5N., R.15E.	Sec. 4, T.4N., R.15E.	Sec.3, T.7N., R.17E.
Owner	Continental Oil Co.	Mustang Prod. Co.,	Mustang Prod. Co.	Potts Stephenson Expl.Co.
Completed	Not Given	Not Given	3/74	05/26/76
Sampled	09/30/76	10/73	9/75	10/12/76
Formation	Penn-Hartshorne	Penn-Hartshorne	Penn-Hartshorne	Penn-Hartshorne
Depth, Feet	3320	3290	3838	2502
Wellhead Pressure, PSIG	500	823	124	585
Open Flow, MCFD	5300	Not Given	Not Given	3900
Component, Mole PCT				
Methane	85.40	90.88	88.66	94.60
Ethane	3.10	6.17	6.97	3.80
Propane	1.50	2.18	2.53	0.70
N-Butane	0.40	0.38	0.41	0.10
Isobutane	0.20	0.26	0.30	Trace
N-Pentane	0.10	0.06	0.09	0
Isopentane	0.10	0.10	0.09	0.10
Hexanes Plus	0.10	0.04	0.10	Trace
Nitrogen	8.30	0.39	0.36	0.60
Oxygen	0.30	0	0	Trace
Argon	0.10	ND	ND	Trace
Carbon Dioxide	0.30	0.14	0.43	Trace
Helium	0.12	0.06	0.05	0.04
Heating Value (Dry)	993	1102	1118	1052
Reference	Moore, 1977	NA	NA	Moore, 1977

ND Not Determined NA Not Applicable


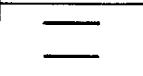




SYSTEM	SERIES	GROUP	FORMATION (THICKNESS IN FEET)	SKELETAL COLUMN	COAL OR OTHER KEY BEDS
P E N N S Y L V A N I A N	D E S M O I N E S I A N	C A B A N I S S	SENORA Psn 150-900		CROWEBURG MORRIS ERAM
			0-375 STUART SH. THURMAN SS. 0-250		
		K R E B S	BOGGY Pbg 125-2140		Secor Rider SECOR
			SAVANNA Psv 180-2500		Bluejacket Sandstone LOWER WITTEVILLE (ROWE) UPPER CAVANAL Sam Creek Limestone CAVANAL
			McALESTER Pma 140-2830		Spaniard Limestone Tamaha Sandstone UPPER McALESTER (Stigler Rider) McALESTER (STIGLER) Cameron Sandstone Warner Sandstone
			HARTSHORNE Phs 3-360		HARTSHORNE { UPPER LOWER

Fig. 3 - Generalized geologic columns.

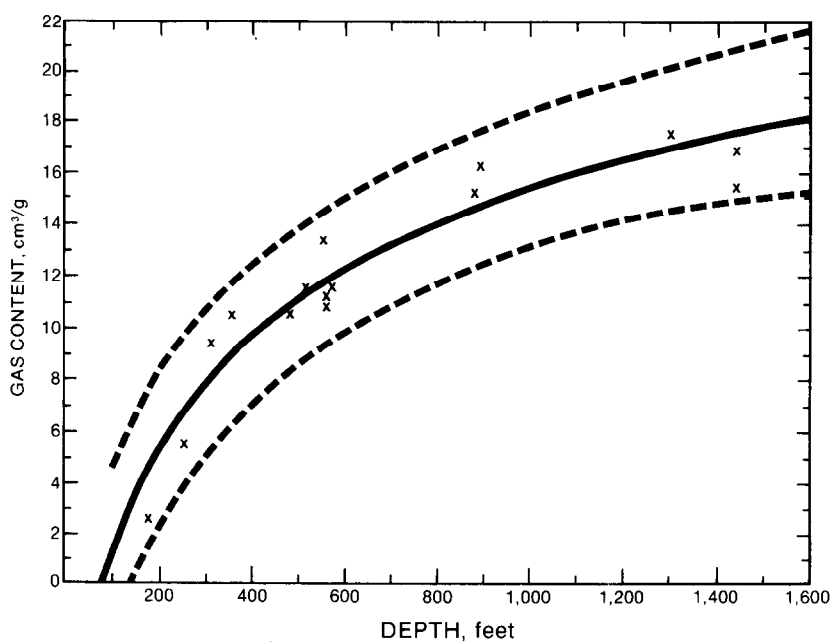


Fig. 4 - Changes in total gas content of the Hartshorne coalbed with dep #1.

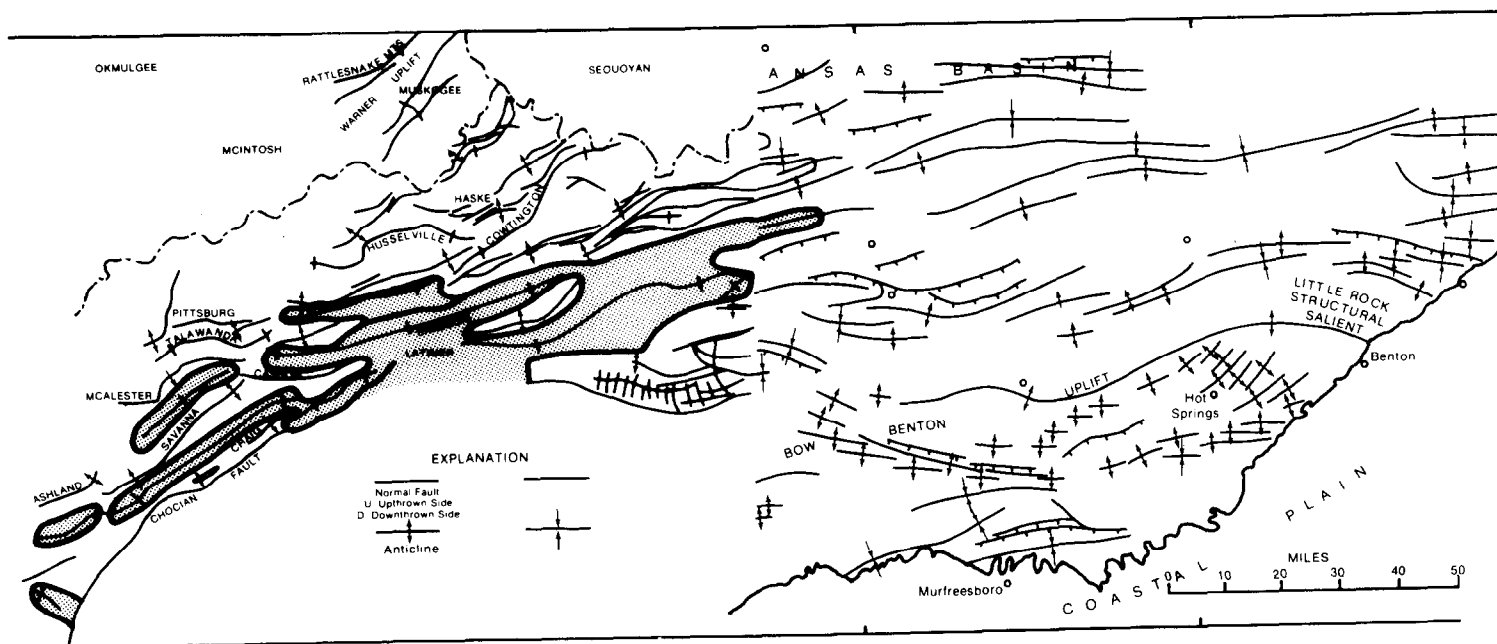


Fig. 5 - Redefined target areas in the Arkoma Basin.

THE COAL BED METHANE POTENTIAL OF THE RATON BASIN, COLORADO

by Carol M. Tremain, Colorado Geological Survey

This paper was presented at the 1980 SPE/DOE Symposium on Unconventional Gas Recovery held in Pittsburgh, Pennsylvania, May 18-21, 1980. The material is subject to correction by the author. Permission to copy is restricted to an abstract of not more than 300 words. Write: 6200 N. Central Expwy., Dallas, Texas 75206

ABSTRACT

In order to determine the coal bed methane potential of the Raton basin, Colorado Geological Survey personnel studied the geography, the geology, the history of oil and gas exploration, and the coal resources and past production in the Raton coal region. Data gathered during study of the above disciplines, along with direct measurements of the coals' gas content, can be used to estimate the methane potential of the Raton basin.

INTRODUCTION

Coal has been mined commercially in the Colorado portion of the Raton basin since 1870¹; reports of methane gas occurrences in the coal mines date back to the same period. Oil and gas exploration in the region began late in the last century. Explorationists encountered methane gas as they drilled through coal zones; they even tested some coal beds. Today coal mines, coal core holes, and oil and gas tests are still encountering large amounts of coal-derived methane. If the amount and source of this gas could be better defined, possible coal mining hazards could be predicted and an untapped gas source utilized.

In 1975, the U.S. Bureau of Mines provided the Colorado Geological Survey with a grant to gather data on the methane potential of the coal beds of Colorado. During this grant, Survey geologists located 32 historically gassy mines and recorded methane emission rates from operating mines. In addition, Survey geologists began using the U.S. Bureau of Mines "direct method" of desorbing (or measuring the gas emitted by) fresh coal core samples to determine the total gas content of a coal.

Today, this research continues under two grants - a U.S. Department of Energy Grant entitled "Evaluation of the Methane Potential of Unmined/Unminable Coalbeds in Colorado" and a Colorado Oil and Gas Conservation Commission grant entitled "Conservation of Methane from Mined/Minable Gaseous Coal Beds". Forty one coal core samples from the Raton coal region alone, have or are being desorbed. In addition, the geography, geology,

oil and gas resources, and coal resources of the region are being studied to provide a framework for the methane data.

GEOGRAPHY

The Raton basin is a 241 x 193 km (150 x 120 mi.) north-south trending structural basin in southeastern Colorado and northeastern New Mexico (Fig. 1). The area of the Colorado portion of the basin is approximately 12,950 km² (5000 mi.²). The basin is bounded by the Sangre de Cristo Mountains to the west, the Wet Mountains and the Apishapa uplift to the north and northeast, and the Sierra Grande-Las Animas arch to the east and southeast.

The coal bearing region in Colorado is a 2850 km² (1100 mi.²) area in Las Animas and Huerfano Counties. The region is a plateau within the basin edged by the cliff-forming outcrop of the Trinidad sandstone. The elevation of the coal region ranges from 2130 m (7000 ft) in the east to 2740 m (9000 ft) in the west; the highest point is West Spanish Peak at 4152.29 m (13,623 ft). The plateau is dissected by the Purgatoire, Huerfano, Cuchara, and Apishapa Rivers (all eastward draining tributaries of the Arkansas River) (Fig. 1).

The largest towns of the region occur where these rivers flow onto the plains: Trinidad (population 9901) on the Purgatoire, Walsenburg (population 4329) on the Cuchara, and Aquilar (population 699) on the Apishapa.² Important land uses include grazing cattle and sheep, dry farming (at intermediate elevations), irrigation farming (along larger streams), lumbering (in the mountains), and coal mining.

The climate of the coal region is dependent on the elevation and ranges from semiarid in the plains to subhumid in the mountains. Most precipitation occurs as thundershowers from April through September; there is a dry spell in June.

Vegetation is also elevation dependent. Eighty percent of the area is in the foothills vegetation zone of open coniferous forests and grasslands. Eighteen % is in the mountain zone of coniferous forests

References and illustrations at end of paper.

and aspen groves. Less than two % is in the subalpine zone of dense coniferous forests and less than one % is in the alpine zone of sparse vegetation above timberline.¹

Access to the coal region is by railway and highways as shown in Figure 1. The two gas pipelines in the region are also shown in this figure.

STRATIGRAPHY

The formations present in the Raton Mesa coal region range from Precambrian to Recent in age and are listed in the stratigraphic chart (Fig. 2). The total sediment thickness is 4570-7620 m (15,000-25,000 ft) on the west side of the region and 3048 m (10,000 ft) on the east. Late Paleozoic and early Mesozoic strata form an eastward thinning wedge 3660-6100 m (12,000-20,000 ft) thick in the west to 2130 m (7000 ft) thick in the east. Overlying late Cretaceous strata are approximately 914 m (3000 ft) thick.³

During much of Cretaceous time, the coal region was under a vast Cretaceous sea extending from the Gulf of Mexico to Canada. The uppermost Cretaceous strata and Tertiary strata record the northeastward regression of the Cretaceous sea and rise of the Rocky Mountains during the Laramide revolution. The late Cretaceous to Tertiary strata which bear upon the coal bed methane potential of the region are described below.

Pierre Shale

The Pierre shale is a Cretaceous marine shale widespread throughout the Great Plains and 490-700 m (1600-2300 ft) thick in the study area. The easily weathered shale forms valleys and lowlands around the coal region.

The main body of the shale is a dark gray to black, non calcareous, bentonitic, fissile shale 400-700 m (1300-2300 ft) thick. It contains a few thin limestone lenses and septarian concretions. This part of the formation was deposited in a neritic environment and represents the maximum transgression of the Cretaceous sea.

The upper 60-90 m (200-300 ft) of the Pierre is buff to gray, fine to medium grained shaly sandstones interbedded with gray to black, silty and sandy shales. It is highly burrowed and was deposited in a prodelta environment forming a gradual transition with the overlying and intertonguing Trinidad sandstone.

Trinidad Sandstone

The Trinidad sandstone is a 0-90 m (0-300 ft) thick ledge-forming sandstone roughly correlatable with the Pictured Cliffs sandstone in the San Juan basin of southwestern Colorado and the Fox Hills sandstone of the Denver basin to the north. Recent workers, Billingsley⁴ and Manziolillo⁵, divide the sandstone into an upper fluvial zone and a lower delta front sandstone. Earlier workers considered the Trinidad a beach sand formed along the western margin of the northeasterly retreating Cretaceous sea.

According to Billingsley and Manziolillo, the lower Trinidad is a buff to light gray, coarsening upward, very fine to fine grained quartz sandstone. It usually exhibits tabular bedding, ball and pillow structure, and littoral to shallow neritic fossils

such as Halymenites and Ophimorpha.

The upper Trinidad is a fining upward, medium to fine grained sandstone. It is more porous and permeable than the lower; Matuszczak⁶ reported a maximum porosity of 21% and permeability of more than 200 md in this zone. Billingsley and Manziolillo interpret it as a salt marsh estuarine or distributary channel facies due to: 1) its lack of burrowing, 2) scour contact and high angle cross stratification, 3) fine to medium grain size, 4) subaqueous shrinkage cracks, 5) lag deposits, 6) indistinct bedding, and 7) upward decrease in grain size. It intertongues with the overlying Vermejo formation. Figure 3 is a structure map on the top of the Trinidad sandstone.

Vermejo Formation

The Vermejo formation is a 0-17 m (0-550 ft) thick fresh water delta plain formation of Late Cretaceous age. It forms gentle slopes and subsequent stream valleys between the sandstones of the underlying Trinidad and overlying Raton formation.

According to Harbour and Dixon⁷, the Vermejo formation is composed of 60% shale, 30% sandstone, and 10% coal. The shales are gray to black, carbonaceous and silty. The sandstones are buff, gray and gray green in color; they are composed of fine grains of quartz (with some weathered feldspar, mica, and ferromagnesium minerals) cemented by clay and calcium carbonate. The coals are high volatile A to low volatile in rank and are composed of vitrain with lesser durain and fusain; they have cubic or prismatic cleat and are bright and friable. Both sandstone and coals are often discontinuous and lenticular.

Raton Formation

The Raton formation is a 0-520 m (0-1700 ft) thick continental formation of Late Cretaceous and Paleocene age. It overlies and intertongues with the Vermejo formation.

This formation is composed of sandstones, silty shales, carbonaceous shales, coals, and conglomerates deposited in a flood plain environment. The sandstones are light gray to buff in color and thin to massive bedded; they are composed of very fine to medium, subangular to subrounded, grains of quartz (with some feldspar, ferromagnesium minerals and rock fragments) that are cemented by calcium carbonate and clay. The gray to black shales grade from pure claystone into siltstone and from carbonaceous shales into coal. A well cemented 0-76 m (0-250 ft) conglomerate composed of chert, quartzite, granite, gneiss, and quartz pebbles forms the base of the Raton formation. The friable coals are high-volatile C to low-volatile in rank and are mostly vitrain with some durain and fusain; they have cubic or prismatic cleat and a dull to bright luster. The sandstones and the conglomerate form benches in outcrop while the thicker shales form lowlands.

Poison Canyon Formation

The Poison Canyon formation is a 0-760 m (0-2500 ft) thick Paleocene age formation. It unconformably overlaps the Raton, Vermejo, Trinidad and Pierre formations in the north and intertongues with the Raton formation in the south.

It is formed of arkosic sandstones, conglomerates,

thick shales, and minor coals deposited in a piedmont environment. It differs from the Raton formation in that: 1) the sandstones are coarser grained and contain unweathered pink feldspar, 2) the shales are yellow and not carbonaceous, and 3) the coals are thin, rare, and lignitic.

IGNEOUS ROCKS

Igneous rocks cut all the formations described above. Stocks, laccoliths, sole injections, flows, plugs, dikes and sills emplaced during Tertiary and Quaternary time, occur throughout the coal region. The composition of the rocks varies from basic to silicic.

Prominent stocks include: 1) the granodiorite and syenodiorite porphyritic Spanish Peaks at townships 30 and 31 south, ranges 67 and 68 west (Tps. 30 and 31 S., Rs. 67 and 68 W.), 2) the syenodiorite porphyritic Dike Mountain at T. 28 S., R. 69 W., and 3) the granite porphyritic White Peaks at T. 31 S., R. 69 W. Laccoliths include the syenodiorite porphyritic Black Hills at T. 27 S., R. 68 W., and the granitic cored Morley dome⁸ at the intersection of Tps. 33 and 34 S., Rs. 63 and 64 W. Plugs include the latitic Goemmer Butte T. 30 S., R. 68 W.

Basic to silicic dikes .6-18 m (2-60 ft) thick and up to 30 m (100 ft) high radiate from the Spanish Peaks and Dike Mountain and fill east-west joints throughout the coal region. Dike fed sills, centimeters to 90 m (inches -300 ft) thick, occur throughout the region, often replacing coals. Basaltic flows, most extensive south of Trinidad, form the Raton Mesas.

STRUCTURE

The Raton basin is a north-south trending, structural and sedimentary basin. The western limb dips steeply at 20-90°, the eastern limb dips gently at 2-10°, and the interior is almost horizontal. The main syncline is split in the Colorado portion by the Greenhorn anticline (a south plunging nose extending off the Wet Mountains) into the La Veta Syncline on the west and the Delcarbon syncline on the east. The basin formed in Pennsylvanian time during the orogeny that created the Ancestral Rocky Mountains and was rejuvenated during the Late Cretaceous-Early Tertiary Laramide orogeny.

Anticlines bound the basin. The Sange de Cristo Mountains to the west and the Wet Mountains to the north are both Late Cretaceous asymmetric anticlines with exposed Precambrian crystalline cores; they are bounded by faults on the side facing the basin. The Apishapa uplift on the northeast and the Las Animas-Sierra Grande uplifts to the east and southeast are broader anticlinal uplifts.

The coal region lies in the interior of the basin. It contains several minor anticlinal features all having eroded crests of Pierre shale. These features include: 1) the Tercio anticline at Tps. 34 and 35 S., R. 68 W., 2) the Ojo anticline at T. 29 S., R. 69 W., and 3) the Alamo dome at section 34, T. 27 S., R. 68 W.

Both normal and reverse faults occur in the coal region. Normal faults are not widespread, but occur in "isolated groups of small displacements"¹—usually less than 15 m (50 ft). Long thrust faults lie mainly to the east of the coal region and "involve the coal bearing and younger formations only locally"¹.

OIL AND GAS PRODUCTION

There are four fields capable of production in the Raton basin. Model dome (Tps. 20 and 30 S., R. 60 W.) produced helium from the Permian Lyons formation (refer Fig. 2). Sheep Mountain (Tps. 27 and 28 S., Rs. 69 and 70 W.) contains several shut in wells capable of producing carbon dioxide gas from the Dakota formation. Gardner, a one well oil field at T. 26 S., R. 79 W., has produced 373 m³ (2348 barrels) of oil, and 64,713 m³ (2250 MCF) in five years of production from the Codell sandstone. Garcia, a gas field at Tps. 33 and 34 S., R. 62 W., produced 44,064 x 10⁴ m³ (15,561 MMCF) of gas from fractured Pierre shales before it was abandoned; it is currently the target of renewed exploration.

None of the above fields are within the coal region of the Raton basin. Structures tested within the coal region itself include the Alamo dome, the Ojo anticline, the Morley dome, and the Tercio anticline. Wells in each have exhibited shows (Fig. 4) but not commercial production rates.

However, the drilling density in the coal region is low with only one well per 130 km² (50 sq. mi.)⁹ Possible traps that may exist include: 1) coals and methane charged channel sands in the Vermejo and Raton formations, 2) stratigraphic traps in the more porous and permeable zones of the Trinidad sandstone and hydrodynamic entrapment of gas in the Trinidad sandstone at basin center, 3) entrapment of gas in the Vermejo, Trinidad and Raton formations where they are truncated by the unconformity on the northwestern side of the basin (Fig. 3), 4) fracture traps in the Pierre and Niobrara shales, and 5) traps formed by the eastward facies changes and pinching out of the Trinidad sandstone, Dakota sandstone, and Pennsylvanian strata.

Problems that have hindered exploration and production in the basin to date include: 1) low formation permeabilities, 2) subnormal formation pressures, 3) formation damage in reservoirs containing swelling clays, 4) the lack, until recently, of logging programs capable of detecting porosity and hydrocarbon saturation in clay filled reservoirs.

COAL RESOURCES AND PRODUCTION

The commercial coal of the coal region is contained in the Raton and Vermejo formations in coal beds up to 4.3 m (14 ft) thick. However, the beds are discontinuous and can seldom be traced more than a few miles. Therefore, coal "zones" are used for correlation purposes rather than coal beds.¹⁰

Two coal fields exist in the coal region - the Trinidad field and the Walsenburg field. Trinidad field coals are generally of coking quality; Walsenburg field coals are generally steam coals. The Huerfano-Las Animas County line is usually taken as the boundary between these fields although coal quality actually increases gradually from north to south (Fig. 5).

Cumulative production from the region as of 1/1/79 was 228,117,523 Mg (251,522,676 short tons).¹⁰ Production during 1978 was 603,500 Mg (665,245 short tons).¹⁰ Remaining reserves as of 1/1/77 were 609.15 x 10⁶ Mg (671.47 million short tons).¹⁰ Three hundred twenty seven mines are on record as having operated in the region¹⁰; 9 mines are currently operating 2 in the Walsenburg field and 7 in the Trinidad field.

METHANE IN COAL

Specific instances of methane occurrence in Raton region coals include the following examples:

- 1) Hollis Fender¹¹ recorded 32 coal mines with reported occurrences of gas. These mines are shown in Figure 6.
- 2) The Allen Coal Mine emitted an average of 11,610 m³/d (410 MCFD) of methane during the period 1974-1976.
- 3) The Energetics Healy No. 13-8 in Sec. 8, T. 31 S., R. 65 W., reported background gas of 100% methane throughout the coal interval.
- 4) Filon Exploration Corporations No. 1 Zeles Hope, at Sec. 31, T. 31 S., R. 65 W., recovered some burnable gas after fracturing a 1.52 m (5 ft) Raton formation coal.
- 5) Thirty five completed "direct method" tests on coal core samples indicate methane in the coal of up to 15.37 cm³/g (492 ft³/ton). (See Table 1.)

"DIRECT METHOD" TEST

In the Bureau of Mines direct desorption method, a sample of coal approximately 1,000 g in weight is obtained from a conventional core and is sealed in a desorption cannister (usually made of plastic or aluminum) immediately after the core has been removed from the core barrel. The gas emitted by the coal is measured daily (by water displacement in an inverted graduated cylinder [Fig. 7]) until emission (desorption) ceases. The gas lost from the coal between the time it was first penetrated by the core bit and the time it was encapsulated in the cannister is estimated using a "back calculation" method. After desorption, the residual gas in the coal is measured (by the same water displacement method) after the coal is crushed in a sealed ball mill at the U.S. Bureau of Mines' Pittsburgh (Bruceton) facility. The estimated lost gas, plus the measured desorbed and residual gas, are added to give the total in-place gas content (in cm³/g or ft³/ton) of the coal bed. (Refer to McCulloch and others, ref. 12 for a more complete description of this method.)

After completion of the residual gas measurements, the samples are sent to the Department of Energy's Pittsburgh laboratory for proximate, ultimate, and related analyses and to the U.S. Geological Survey in Denver for geochemical (including trace-element) analyses. In addition, if the samples emit sufficient gas during the initial days of desorption, a gas sample is drawn from the inverted graduated cylinder into an evacuated gas bomb for hydro-carbon analysis.

"DIRECT METHOD" RESULTS

As mentioned above, the Colorado Geological Survey has completed 35 "direct method" tests on coal samples from the Raton coal region. Total gas contents of the 27 Trinidad field samples range from 0.07 cm³/g (2 ft³/ton) to 15.37 cm³/g (492 ft³/ton). Total gas contents from the 8 Walsenburg field samples range from 0.14 cm³/g (5 ft³/ton) to be 2.05 cm³/g (66 ft³/ton).

The gassiest samples in the region (nos. 4, 5, 6, and 10, Table 1) are of medium-volatile rank and were taken from a depth of 305 m (1000 ft) or greater. Methane contents of the 8 gas samples analyzed ranged from 46.14% to 98.98%; heating values ranged from 4139-8873 kcal/m³ (465-997 Btu/ft³).

Exploration for Coal Bed Methane

As can be seen from the above data, the direct desorption method can locate coals with high methane contents if a coal core is available. In addition, a gas detector can detect gassy coal beds as they are being drilled as shown in Danilchik et al.¹³

However, conventional formation evaluation logs will not detect a gassy coal zone since coal beds are highly resistive and since coals produce very high porosity readings on neutron, sonic, and density logs regardless of the coals' gas content. In addition, drill stem tests in coals are often unsuccessful because of the low pressures of the coal beds. (See Tremain¹⁴ for some examples).

Certain maps can help delineate areas of high coal bed methane potential. A map of "direct method" gas contents and gas detector shows combined with a coal isopach map, such as Figure 8, will indicate high potential areas. In an area without desorption measurements, a coal rank map, such as Figure 5, will indicate the higher rank and thus more likely gassy coals. In the Raton coal region where the coal bearing formations are close to the surface, an overburden map (such as Danilchik's¹³) is needed; such a map permits omission of the coals with less than 305 m (1000 ft) of overburden (from which the methane has escaped) from resource calculations.

RESOURCE ESTIMATIONS

Estimates of the methane resources of the entire Raton Mesa coal region await completion of overburden maps. The overburden maps will then be combined with coal isopach maps, coal rank maps, and "direct method" gas contents to estimate methane resources. (Remaining coal reserves mentioned earlier cannot be used for methane resource calculations since these reserves only include coal with less than 305 m (1000 ft) of overburden. Desorption data (see Table 1) indicate such coals have lost much of the gas which they generated during the coalification processes.)

However, the methane resources of a promising 3 m (10 ft) coal have been estimated at 8.8×10^9 m³ (311 BCF) in a 140 km² (54 mi²) area. A coal sample from this bed has a "direct method" gas content of over 15.6 cm³/g (500 ft³/ton) and the gas emitted by a nearby sample was 99% methane.

CONCLUSIONS

The methane potential of a coal region and commercial application of the gas can be revealed by a detailed basin study. Such a study can illuminate the following considerations:

Geography

- 1) the climate, highways, and terrain that could affect a drilling program
- 2) the location of gas lines and population centers that would affect gas markets

Stratigraphy

- 1) the location, extent, trend, and continuity of coal and other reservoirs
- 2) the recognition of geologic section during drilling

Structure

- 1) the determination of overburden on the coals

Oil and Gas Production

- 1) the location of any coal gas shows
- 2) the problems that could be encountered during drilling
- 3) the existence of oil and gas traps in non coals

Coal Resources and Production

- 1) the location of gassy mines
- 2) the location of high ranking (and likely gassy) coals

Direct Method Tests

- 1) in-place gas contents
- 2) gas quality

REFERENCES

1. Johnson, Ross B.: "Coal Resources of the Trinidad Coal Field in Huerfano and Las Animas Counties, Colorado," U.S. Geological Survey Bull. 1112-E (1961) p. 129-180.
2. Colorful Colorado - State Highway Map, Colorado Dept. of Highways.
3. Wood, G.H., Jr., Johnson, R.B., and Dixon, G.H.: "Geology and Coal Resources of the Starkville - Weston Area, Las Animas County, Colorado," U.S. Geological Survey Bull. 1051 (1957) 68 p.
4. Billingsley, Lee T.: "Stratigraphy and Clay Mineralogy of the Trinidad Sandstone and Associated Formations (Upper Cretaceous), Walsenburg Area, Colorado," M.S. thesis, Colorado School of Mines (1977) 105 p.
5. Manziolillo, Claudio D.: "Stratigraphy and Depositional Environments of the Upper Cretaceous Trinidad Sandstone, Trinidad Aguilar Area, Las Animas County, Colorado," M.S. thesis, Colorado School of Mines (1976) 147 p.
6. Matuszczak, R.A.: "Trinidad Sandstone Interpreted, Evaluated, in Raton Basin, Colorado-New Mexico." The Mountain Geologist, vol. 6, no. 3 (1969) p. 119-124.
7. Harbour, R.L., and Dixon, D.H.: "Coal Resources of Trinidad-Aguilar Area, Las Animas and Huerfano Counties, Colorado," U.S. Geological Survey Bull. 1072-G (1959) p. 445-489.
8. Bench, Bernard M.: "Drilling for Methane Gas in the Fishers Peak Area, Las Animas County, Colorado," U.S. Bureau of Mines Information Circular (1979) 26 p. (unpublished).
9. Dolly, E.D., and Meissner, F.F.: "Geology and Gas Exploration Potential, Upper Cretaceous and Lower Tertiary Strata, Northern Raton Basin, Colorado," in Exploration Frontiers of the Central and Southern Rockies, Rocky Mountain Association of Geologists (1977) p. 247-270.
10. Boreck, D.L., and Murray, D.K.: "Colorado Coal Reserves Depletion Data and Coal Mine Summaries," Colorado Geological Survey Open-File Report 79-1 (1979) p. 47-50.
11. Fender, Hollis B., and Murray, D. Keith: "Data Accumulation on the Methane Potential of the Coal Beds of Colorado," Colorado Geological Survey Open-File Report 78-2 (1978) 25 p.
12. McCulloch, C.M., Levine, J.R., Kissell, F.M., and Deul, Maurice: "Measuring the Methane Content of Bituminous Coal Beds," U.S. Bureau of Mines Report of Investigations 8043 (1975) 22 p.
13. Danilchik, Walter, Schultz, Janet E., and Tremain, Carol M.: "Content of Methane in Coal from Four Core Holes in the Raton and Vermejo Formations, Las Animas County, Colorado," U.S. Geological Survey Open-File Report 79-762 and Colorado Geological Survey Open-File Report 79-3 (1979) 19 p.
14. Tremain, Carol M.: "The Coal Bed Methane Potential of the Raton Basin, Colorado," Colorado Geological Survey Open-File Report 80-4 (1980) (in preparation).
15. Goolsby, S.M., and Reade, N.S.: "Evaluation of Coking Coals in Colorado," Colorado Geological Survey Resource Series 7 (1979) 72 p.

TABLE 1
DESORPTION RESULTS, RATON MESA COAL REGION
COLORADO

FIELD	TEST NO.	FORMATION	DEPTH (m)	TO BED (ft)	SAMPLE WEIGHT (g)	DESORBED GAS (cm ³)	LOST GAS (cm ³)	RESIDUAL GAS (cm ³ /h)	TOTAL GAS (cm ³ /g)	(ft ³ /ton)	APPARENT RANK OF COAL	% METHANE IN GAS (AIR FREE)	HEATING VALUE OF GAS (kcal/m ³)	(Btu/ft ³)
T R I N I D A D W A L S E N B U R G	1	Raton	246.89	810.0	2319	3086	370	0.10	1.59	51	an ¹	66.78	6282	698
	2	Raton	252.37	828.0	1098	755	130	0.0	0.81	26	hvcB ²	--	--	--
	3	Raton	321.11	1053.5	2308	4731	480	0.0	2.26	72	hvb ³	91.75	8233	925
	4	Raton	324.03	1063.1	1710	9441	850	0.01	6.03	193	mvb ⁴	83.34	7485	841
	5	Vermejo	515.48	1691.2	1600	14255	3400	0.04	11.07	354	mvb	46.14	4139	465
	6	Vermejo	546.20	1792.0	1724	18098	8300	0.06	15.37	492	mvb	97.16	8722	980
	7	Raton	94.24	309.2	1461	3390	170	0.16	2.60	83	lvb ⁵	--	--	--
	8	Raton	146.97	482.2	1057	2031	890	0.0	2.76	88.4	mvb	--	--	--
	9	Raton	152.31	499.7	767	2719	1110	0.0	4.99	160	mvb	--	--	--
	10	Vermejo	222.32	729.4	1768	10176	3300	0.33	7.95	254	mvb	98.98	8873	997
	11	Vermejo	30.63	100.5	808	158	170	0.30	0.71	23	mvb	--	--	--
	12	Vermejo	51.18	167.9	553	1057	800	0.20	3.56	114	mvb	--	--	--
	13	Vermejo	218.11	715.6	876	88	--	1.35	1.45	46	hvaB ⁶	--	--	--
	14	Vermejo	246.89	810.0	1051	74	115	0.0	0.18	6	hvaB	--	--	--
	15	Vermejo	247.65	812.5	1657	56	65	0.0	0.07	2	hvaB	--	--	--
	16	Vermejo	261.37	857.5	1107	4409	280	0.60	4.84	155	hvaB	81.62	7316	822
	17	Vermejo	265.02	869.5	1661	6589	360	0.40	4.58	147	hvaB	81.49	7307	821
	18	Vermejo	266.70	875.0	1223	3183	100	0.50	3.20	102	hvaB	--	--	--
	19	Vermejo	264.57	868.0	1035	505	70	0.60	1.16	37	hvaB	--	--	--
	20	Vermejo	265.94	872.5	1122	220	10	0.14	0.40	13	hvaB	--	--	--
	21	Vermejo	293.13	961.7	753	260	130	0.61	1.13	36	hvaB	--	--	--
	22	Vermejo	293.80	963.9	1014	270	70	0.69	1.03	33	hvaB	--	--	--
	23	Vermejo	306.48	1005.5	1152	745	130	0.44	1.20	38	hvaB	--	--	--
	24	Vermejo	308.70	1012.8	796	445	170	1.90	2.70	86	hvaB	--	--	--
	25	Vermejo	313.67	1029.1	809	320	90	1.20	1.71	55	hvaB	--	--	--
	26	Vermejo	313.94	1030.0	938	335	160	1.11	1.64	52	hvaB	--	--	--
	27	Vermejo	313.94	1030.0	478	847	200	0.65	2.84	91	hvaB	--	--	--
	28	Vermejo	33.83	111.0	1049	51	75	0.36	0.93	30	hvcB	--	--	--
	29	Vermejo	47.24	155.0	1211	82	241	0.41	1.08	35	hvcB	--	--	--
	30	Raton	205.65	674.7	315	185	300	0.10	1.60	53	hvaB	--	--	--
	31	Raton	273.10	896.0	352	157	370	0.0	1.50	48	hvaB	--	--	--
	32	Vermejo	346.47	1136.7	549	134	550	0.80	2.05	66	hvaB	--	--	--
	33	Vermejo	306.81	1006.6	369	32	300	0.0	0.90	29	hvaB	--	--	--
	34	Vermejo	308.64	1012.6	584	54	30	0.0	0.14	5	hvaB	--	--	--
	35	Vermejo	327.20	1073.5	257	48	90	0.0	0.54	17	hvaB	--	--	--

1 anthracite
2 high-volatile C bituminous coal
3 high-volatile B bituminous coal

4 medium-volatile bituminous coal
5 low-volatile bituminous coal
6 high-volatile A bituminous coal

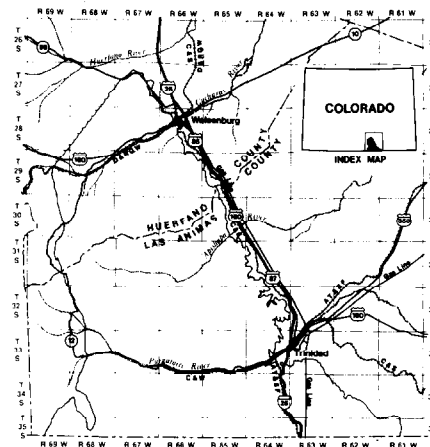


Fig. 1 - Index map of Raton Mesa coal region, Colorado.

GEOLOGIC AGE		FORMATION	THICKNESS (feet)	LITHOLOGY	OIL AND GAS SHOWS	
QUATERNARY		Recent	0 -30	Alluvium; basalt flows		
TERTIARY	MIOCENE	Devils Hole	25 -1300	Water - laid tuff volcanic conglomerate		
	Oligocene	Farisita	0 -1200	Arkosic conglomerate		
	EOCENE	Huerfano	0 -2000	Variegated shale, conglomeratic sandstone		
		Cuchara	0 -5000	Massive red conglomeratic sandstone with thin variegated shale		
	PALEOCENE	Poison Canyon	0 -2500	Coarse arkosic sandstone and conglomerates with thin shales	*	
MESOZOIC	LATE CRETACEOUS	Raton	0 -1700	Thin coalbeds, sandstone, basal conglomerate, shale	● *	
		Vermejo	0 -550	Sandstone, Shale, coal	*	
		Trinidad sandstone	0 -300	Fine-grained beach sand	● *	
		Pierre shale	1600 -2300	Grey marine shale, sandy shale, sandstone	● *	
	EARLY CRETACEOUS	Niobrara	560 -630	Marine shale, limestone	● *	
		Carlile shale	165 -235	Dark grey marine shale	*	
		Greenhorn limestone	38 -80	Thin bedded limestone		
		Graneros shale	185 -385	Dark grey marine shale	● *	
		Dakota sandstone	100 -150	Grey massive sandstone	● *	
		Purgatoire	100 -150	Continental shale, sandstone	● *	
		JURASSIC	Morrison		Continental sandstone, shale	●
			Ralston, Todilto	100 -600	Marine sediments, gypsum	
	Entrada		Beach sandstone		●	
	TRIASSIC	Johnson Gap	10 -700	Limestone conglomerates		
		Dockum group of formations	0 -1200	Red sandstone, calcareous shales, thin limestones		
PALEOZOIC	PERMIAN	Bernal	<150	Continental sediments		
		Glorieta	0 -200	Marine sandstones		
		Yeso	0 -250	Red silt, shale, sandstone		
	PENNSYLVANIAN	Sangre de Cristo	250 -5400	Variegated shales, arkose, conglomerates, thin marine limestones	●	
	PRECAMBRIAN	Precambrian	Basement rocks	Crystalline, igneous, and metamorphic		

Fig. 2 - Stratigraphic chart of Raton Mesa coal region, Colorado.

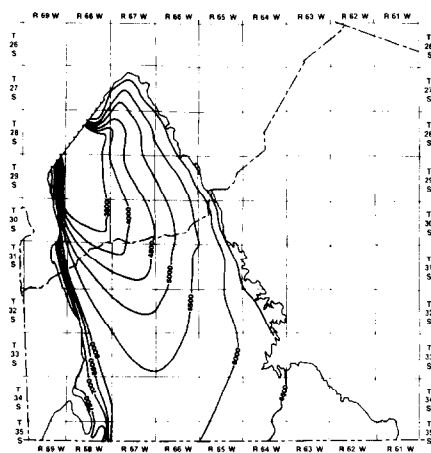


Fig. 3 - Structure map of Trinidad sandstone, contoured in feet above sea level.

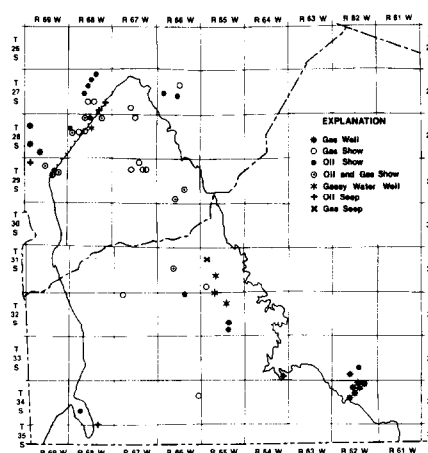


Fig. 4 - Oil and gas shows.

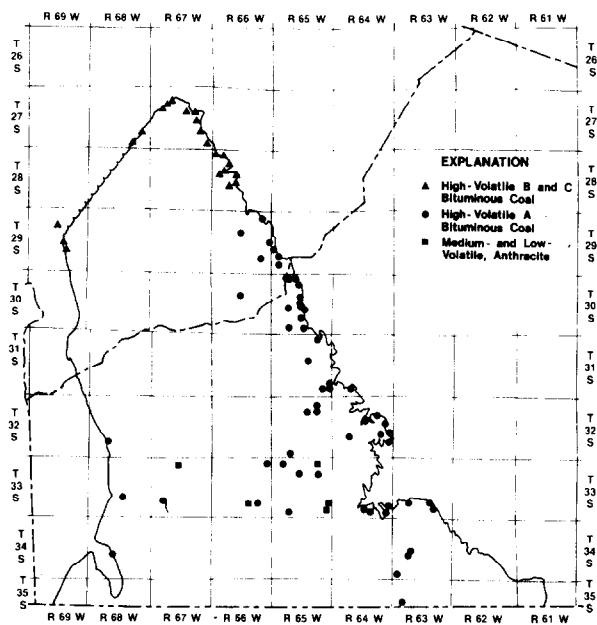


Fig. 5 - Coal rank map, after Goolsby and Reade¹⁵.

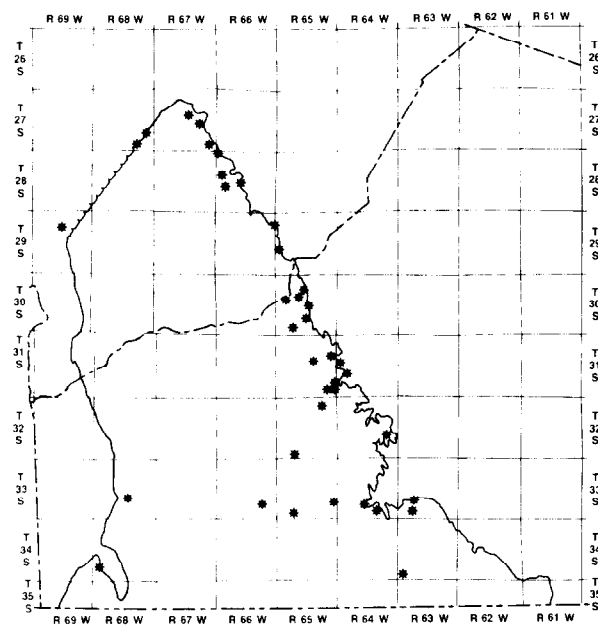


Fig. 6 - Gassy mines, after Fender and Murray¹¹.

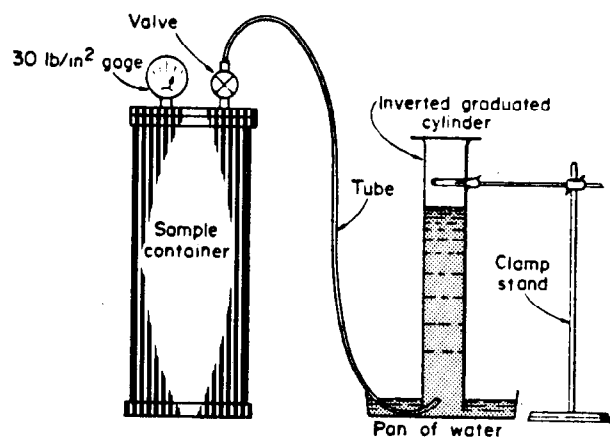


Fig. 7 - Desorption equipment after McCulloch et al¹².

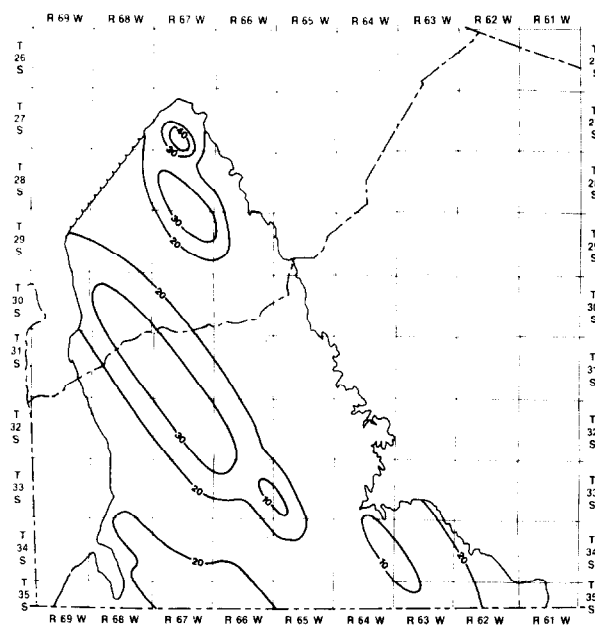


Fig. 8 - Total coal isopach map of Vermejo Formation, contoured in ft.

THE COALBED METHANE RESOURCE OF THE ILLINOIS BASIN

by Paul L. Archer, TRW Energy Systems; Donald D. Carr and Denver Harper, Indiana Geological Survey,

This paper was presented at the 1980 SPE/DOE Symposium on Unconventional Gas Recovery held in Pittsburgh, Pennsylvania, May 18-21, 1980. The material is subject to correction by the author. Permission to copy is restricted to an abstract of not more than 300 words. Write: 6200 N. Central Expwy., Dallas, Texas 75206

ABSTRACT

A program was initiated to determine the extent of the coalbed methane resource and the location of the most favorable resource areas within the Illinois basin, and to obtain a better understanding of the relationships between selected variables and the gas content of coals. Preliminary gas in-place resource estimates are made based on coal desorption data and the most favorable resource areas are outlined. Limited and/or poor data precluded establishing relationships between various geological-chemical/physical parameters and coal gas content. Further investigations are required to determine such relationships and to define what percentage of this resource is producible.

INTRODUCTION

Coalbed gas has been of concern to the coal industry as a safety hazard since the early days of underground mining in the 19th century. Only recently, however, has methane, the major component of this gas, been considered a potential source of energy. In late 1977, the United States Department of Energy (DOE) initiated the Methane Recovery from Coalbeds Project (MRCP), to characterize and to investigate and develop means to extract the coalbed methane resources of this country. This paper discusses work performed in conjunction with the MRCP and research efforts conducted by the Indiana Geological Survey within the Illinois basin, or Eastern Interior Coal Region.

Adequate evaluation of the methane resource in coal of the Illinois basin involves answering two questions. First, what regions of the basin hold the greatest potential for commercialization of this resource? This question was initially addressed by an intensive literature search, communication with state geological surveys and the U.S. Bureau of Mines (USBM), and by using proposed geologic criteria. These efforts resulted in identification of potential "gassy" target areas. Recent and current activities include coring and

testing in these target areas with the hope of identifying smaller regions containing the best potential for commercialization.

The second question is: What set of geologic/chemical/physical conditions exist which cause coal seams in certain areas to be "gassy" while in other areas they are not? The approach taken to answer this question has been strictly empirical; a computer program designed to perform multiple variable statistical analyses of the data is being used at the Indiana Geological Survey. Early efforts have been inconclusive, but it is hoped that as more information is generated and added to the data base significant relationships between gas content and various parameters can be determined.

REGIONAL COAL DISTRIBUTION

The Illinois basin contains extensive bituminous coal reserves in Pennsylvanian age rocks. The U.S. Geological Survey has estimated that the total coal resource of the Illinois basin might be 3.3×10^5 kg (365 billion short tons). More than 75 individual coal seams have been identified in this area, 20 of which are mined. A general stratigraphic correlation of major coal seams in the basin is provided in Figure 1. The majority of the coals are not continuous and do not maintain constant thicknesses. Individual seams range from 5 cm to 4.6 m (a few inches to 15 ft) in thickness. The coals outcrop at the basin periphery and dip gently towards the deeper portions in southeastern Illinois and western Kentucky. Lower and upper Pennsylvanian coals are thin and discontinuous making them a relatively unattractive gas reservoir while the middle Pennsylvanian coals are thick, generally continuous, and provide the major reserves of the basin. The greatest cumulative thickness of coal seams presumably occurs in the southeastern portion of the basin (near the tri-state Illinois, Kentucky, Indiana boundary) where the thickest Pennsylvanian section occurs. All Illinois basin coal seams are covered by less than 914 m (3,000 ft) of overburden, and the major coals are within 457 m (1,500 ft) of the surface.

References and illustrations at end of paper.

The Springfield-Harrisburg (No. 5) coal in Illinois and its correlatives, Springfield V in Indiana and No. 9 coals in Kentucky are the most extensive and uniformly thick coals in the Illinois basin; estimated coal reserves are over 6×10^4 kg (67 billion short tons). The Herrin (No. 6) coal is also thick and extensive in Illinois and contains estimated coal reserves of over 7×10^4 kg (77 billion short tons). Some deeper coals contain combined reserves estimated at over 3.5×10^4 kg (39 billion short tons). These include the Colchester (No. 2), which is uniformly present over the entire basin, and the Davis (No. 6) and Mannington (No. 4) which occur primarily in Kentucky.

ACQUISITION OF RESOURCE DATA

Generally all coal contains methane either as free gas in fissures (cleats) or as adsorbed gas on coal surfaces or in pore spaces. This gas is trapped in the coal either during breakdown of organic matter during coalification¹, or during vertical migration of gases from deeper source rocks. The amount of methane gas in coal has usually been considered a function of the rank and depth of burial of the coal; the greater the rank or depth of burial the higher the gas content of the coal.

Coals of the Illinois basin region are not "gassy" relative to many coals in Appalachian coal fields. Because of this, few tests of the gas content of coals in this region have been made (the coal resource, however, is quite well defined based on rather extensive coal exploration and production and oil and gas drilling records). A gross indication of "gassy" areas comes from mine ventilation records compiled by the USBM² (Table 1). Figure 2 illustrates the location of mines and the associated ventilation of gas relative to tons of coal produced. Similar indications of potential "gassy" areas are determined by reviewing records of mine explosions or by talking with "old-time" miners.

The best data concerning the specific methane content of coals, however, comes from desorption of coal samples collected during coring operations. The procedure for this testing was developed by the USBM and is referred to as the "direct method" of coalbed gas determination³; this procedure is currently being used by the Bureau and others with only slight modification. Basically, as soon as the core retrieval equipment arrives at the surface the coal sample is sealed in an air tight can. An estimate is made of the "lost" gas during coring operations and gas emitted from the coal, primarily because of the change in pressure conditions, is measured on a regular basis until the emission or desorption rate is very low. At that point the coal is crushed, causing any remaining (or trapped) gas to be released. The "lost" gas the desorbed gas and remaining gas volumes are totaled to provide an estimate of the specific gas content of the coal sample. It should be noted that although these data may give reasonable estimates of the in-place gas content of coals, no relationship between this information and the productive capabilities of a coal zone(s) in a well has been established. Actual field production tests need to be performed and correlated with laboratory desorption data in order to generate a reasonable estimate of the recoverable resource.

Data providing estimates of the gas contents of Illinois basin coals have come primarily from studies of the USBM, Indiana and Illinois geological surveys, and from recent MRCP coring operations conducted by TRW. Limited data has also been provided by coal operators - generally this information is difficult to obtain. The available data is summarized in Table 2. Distribution of the data throughout the basin is illustrated in Figure 3. In the Illinois basin area, total gas emitted during mine operations is typically on the order of 4 to 7 times the gas indicated to be present in the coal from USBM "direct method" determinations.

Since 1975, the Indiana Geological Survey has conducted a program of measuring the methane content of coals in Indiana. The Indiana Survey owns and operates its own drilling rig; their use of a wire-line coring system allows rapid withdrawal of freshly cored coal from the hole. To date thirty-two samples have been recovered from 7 holes in Indiana (Figure 4).

TRW, integrating contractor for the DOE/MRCP, contracted and conducted 5 coal coring operations in the Illinois basin over the past eighteen months (Figure 5). Three of these operations were conducted in a "piggyback" mode where the principle operator was drilling to a deeper conventional target. During these operations, TRW personnel planned and supervised all coring and testing operations deemed necessary to evaluate the coal and methane resource. TRW paid all costs associated with those operations not previously planned by the principle operator, and indemnified the operator for any potential losses he might have incurred as a result of this testing. Experience has shown that once a person becomes familiar with and known to the oil and gas operators in a certain region these modes of testing and types of agreements can be readily consummated.

Additional information concerning the potential methane resource of coals comes from predrainage or degasification tests prior to coal mining operations. Again, the relative low gas content of Illinois basin coals has precluded the requirement for these operations in this region. However, as mining activity moves towards deeper virgin coal areas, methane is becoming more of a problem and predrainage a more viable option. The only predrainage or degasification test to date in the Illinois basin was performed by the USBM in Jefferson Co., Illinois. Five vertical boreholes were drilled and stimulated at an average depth of 223 m (733 ft) in the Herrin (No. 6) coalbed. Although a drop in methane concentration was observed when the borehole was passed during mining, the holes produced an insignificant amount of gas. According to the USBM⁴, who give a complete discussion of the predrainage test, the gas flow increased from an initial 3 to 1311 m³ (10 to 4,300 cu ft) per day.

IDENTIFICATION OF TARGET AREAS

An initial target area of approximately 2.4×10^4 (9,100) of a possible 9.6×10^4 m² (37,000 mi²) containing coal bearing rocks in the Illinois basin was selected for early testing in the MRCP (Figure 6). This area was thought to contain those coals having the greatest potential for

early commercialization of the coalbed methane resource. The following criteria were used to select the initial target area:

- Physical and chemical characteristics of coal (i.e., fixed carbon percent volatiles, percent sulfur, etc.)--Higher rank coals generally contain more methane.
- Seam depth (> 122 m or 400 ft)--Deeper coals are more likely to have retained the methane.
- Total effective coal thickness (~ 4.5 m or 15 ft)--Higher total production per well possible on basis of multiseam completion.
- Individual seam thickness (minimum of 1.5 m or 5 ft for shallow beds)--To minimize need for multiple fracturing.
- Extent (contiguous basin)--Allow extrapolation of results to a wider area.

A detailed investigation completed this past year incorporated additional resource data and the results of recent coring operations and desorption tests⁵. As a result of this study, the initial MRCP target area was redefined (Figure 7). Selection of the redefined areas, believed to better represent the most attractive resource areas within the Illinois basin, was based on criteria similar to that given above but also included gas content and structural setting considerations. The criteria used were:

- Areas reporting exceptionally gassy coals
- Areas having the thickest cumulative section of coal
- Areas having the highest coal rank
- Areas whose major coal units are at the greatest depths
- Areas where some structural deformation has potentially enhanced coal porosity and permeability.

Target Area A, located in western Kentucky, contains a thick section of deep coals in a highly disturbed structural belt. Target Area B, in southeastern Illinois and southwestern Indiana contains previously reported gassy coals, and thick coal sections at considerable depths. The boundaries outlining these areas are somewhat arbitrary, but generally reflect the extent to which the best combination of the criteria exists.

Field tests were performed this past fall and winter in both target areas. These tests are currently being evaluated to determine if the rationale used to select the target areas is valid. The target areas defined by the MRCP will be continually revised to reflect increased knowledge and understanding of where the best coalbed gas resource might exist. It is hoped that ultimately prime target areas can be much more narrowly defined and that possibly different regions of the basin can be ranked relative to their potential for producing methane gas from coal.

RESOURCE ESTIMATES

The potential in-place methane resource from selected coalbeds in the Illinois basin can be estimated from desorption data generated by the USBM, the Illinois and Indiana State Surveys, and field tests performed under the MRCP (see Table 2). The Herrin (No. 6) and the Springfield-Harrisburg (No. 5) coals and their correlatives in Indiana have been sampled most often. The estimated gas content of the Herrin (No. 6) ranges from 1 to 3.9 cc/gm (32 to 125 ft³/ton) of coal. A similar range of values, 1 to 4.6 cc/gm (32 to 147 ft³/ton), has been calculated for the Springfield-Harrisburg (No. 5) coals. The variability in gas content data for a particular seam is both real, due to variable geologic/chemical/physical conditions, and artificial, due to incorrect or non-uniform treatment of the samples and data. Although recent efforts have been performed under generally uniform conditions, a major problem exists in trying to recognize analytically bad data points and eliminating them so that evaluation and estimates of gas contents are not biased. Because of this problem, and the fact that the data base is relatively limited, it is difficult to make accurate resource estimates of methane in coal in the Illinois basin. A detailed resource estimate requires much better knowledge of the physical and chemical character (including rank, thickness of coal, porosity, etc.) of each coal throughout the basin, the geologic history of specific regions, and how each of these parameters affect the methane content of the coal.

Nevertheless, for the purposes of an initial rough estimate of the in-place gas resource the values in Table 2 are used. Minimum and maximum expected in-place gas resources for the Danville, Herrin, Springfield-Harrisburg, and their equivalent coals (Figure 1) were calculated on a simple volumetric basis for the whole basin (Table 3). The minimum in-place gas resource for these 3 seams is greater than 142 MMm³ (5 Tcf). It is reasonable to assume that the methane contained in major deeper coals (Colchester, Davis, etc.) may add significantly to this figure. Estimates of gas resources in the redefined target areas were made using a modest 2.2 cc/gm (70 ft³/ton) as the specific gas content of the coals. On this basis target area A is estimated to contain 31 MMm³ (1.1 Tcf) of gas and target area B is estimated to contain 37 MMm³ (1.3 Tcf). Assuming the typical cumulative thickness of coals is 4.6 m (15 ft) in area A and 3 m (10 ft) in area B, the gas resource estimate is on the order of 110 Mcf/acre-ft and 64 Mcf/acre-ft respectively for these areas. It should be emphasized here that these numbers only reflect the coalbed gas resource in-place. The volume of gas that could actually be produced from coal is unknown at this time. Productivity will, of course, be affected by the degree to which the necessary (favorable) reservoir and economic conditions exist.

DISCUSSION

The desorption data indicate that the gas content of particular coalbeds can be highly variable. Unfortunately there is no ready explanation for this variability. The often accepted rule that deeper and higher rank coals have the greater gas content has only been true in some instances. In many cases it is obvious that other parameters

THE COALBED METHANE RESOURCE OF THE ILLINOIS BASIN

affect the amount of gas present in a coalbed. Detailed resource estimates and an understanding of coalbed gas accumulation can only be obtained if relationships between gas content and the chemical and physical properties and geologic setting (history) of the coal are established. Once empirical or theoretical relationships are outlined for a given coal region it becomes possible to predict, without costly and time consuming core analysis, those areas which are likely to have the best coalbed gas resource. Previously suggested controls on gas content which need to be investigated are coal rank, depth, permeability and porosity of the coal, degree of fracturing, distance to outcrop, permeability of adjacent strata, and the adsorptive capacity of the coal⁶. The depth of burial basically controls the temperature and pressure conditions of the coal which in turn affects its capacity to adsorb gas. The adsorptive capacity of coal is also a function of fixed carbon, volatile matter, moisture, and mineral matter percentages. The type and permeability of adjacent strata may play a significant role in determining the gas content of the coal. Permeable surrounding rocks may allow coalbed gas to escape, or permit the migration and accumulation of natural gas from other sources^{7,8}. In the latter case, the coalbed is simply acting as a host or "conventional" reservoir rock.

The Indiana Geological Survey recently began to investigate the relationship between some of these parameters and the gas content of coals in the Illinois basin. A multi-variable statistical analysis approach is being used in this study. The parameters, seam thickness, depth, ash, moisture, sulfur, volatile, fixed carbon contents, and heating value (Btu) are independently tested against the observed desorbed gas value. Computer generated x-y scatter diagrams are analyzed statistically to determine the extent of linear relationships. Any correlation between parameters that might exist has not been seen. Possibly, establishment of relationships may be precluded at this time because of the limited availability of and the poor quality of some data. It is hoped that broad relationships will become apparent as additional data and variables are added to the system.

CONCLUSIONS

This evaluation of the coalbed methane resource of the Illinois basin has produced the following conclusions:

1. Gas content of coal is generally low (< 100 cc/gm).
2. The deepest parts of the basin in southeastern Illinois, southwestern Indiana, and western Kentucky probably have the greatest potential for commercialization of this resource.
3. The in-place coalbed methane resource for the entire basin exceeds 5 and may be as high as 20 Tcf; the resource in the MRCP target areas exceeds 2.4 Tcf.
4. The amount of gas which is producible is undetermined.
5. Gas content can vary tremendously; further investigation of the chemical/physical/geologic controls over gas generation, migration, and accumulation are required before relationships between these parameters and gas content can be established and used for predictive purposes.

REFERENCES

1. Kim, Ann G.: "Estimating Methane Content of Bituminous Coalbeds from Adsorption Data," U.S. Bureau of Mines, RI 8245 (1977).
2. Irani, M. C., Jansky, J. H., Jeran, P. W., Hassett, G. L.: "Methane Emission from U.S. Coal Mines in 1975, A Survey," U.S. Bureau of Mines, IC 8733 (1977).
3. McCulloch, C. M., Levine, J. R., Kissell, F. N., Deul, M.: "Measuring the Methane Content of Bituminous Coalbeds," U.S. Bureau of Mines, RI 8043 (1975).
4. Elder, C. H., Deul, M.: "Hydraulic Stimulation Increases Desgasification Rate of Coalbeds," U.S. Bureau of Mines, RI 8047 (1975).
5. TRW: "Illinois Basin Report," Draft to DOE-METC under contract (DE-AC21-78MC08089), (1979).
6. Kim, Ann G.: "Experimental Studies on the Origin and Accumulation of Coalbed Gas," U.S. Bureau of Mines, RI 8317 (1978).
7. Iannacchione, Anthony T., Puglio, Donald G.: "Geological Association of Coalbed Gas and Natural Gas from the Hartshorne Formation in Haskell and Leflore Counties, Oklahoma," U.S. Bureau of Mines, in preparation.
8. Popp, John T.: personal communication (1979).

TABLE 1
Gas Emission Data from Coal Mines in the Illinois Basin

NAME OF MINE	COUNTY	COALBED	AVERAGE DEPTH OF SHAFT OR SLOPE (FT.)	AGE OF WIRE (YR.)	COAL PRODUCTION (TONS/DAY)	CUBIC FT. OF GAS TON OF COAL MINED (CF/TON)	YEAR DATA COLLECTED
Orient #3	Jefferson, IL.	Herrin (No. 6)	800	27	9,670	186	1973
Orient #6	do	do	530	4	8,950	113	1971
Inland	do	do	735	10	9,500	125	1975
Old Ben #21	Franklin, IL.	do	666	16	6,200	258	1975
Old Ben #24	do	do	660	11	8,000	237	1975
Old Ben #26	do	do	658	8	8,600	208	1975
Peabody #10	Saline, IL.	do	325	24	15,800	89	1975
Crown	Montgomery, IL	do	600	25	8,400	124	1971
Fies	Hopkins, KY	No. 11	200	24	4,200	296	1973
Wabash	Wabash, IL	Harrisburg (No. 5)	768	3	6,800	206	1975

(From Irani, et al. 1977)

TABLE 2
Methane Desorption Data from the Illinois Basin

COALBED	STATE	COUNTY	DEPTH (FT)	DESORBED GAS ¹ (cc/gm)	REMAINING GAS [*] (cc/gm)	TOTAL GAS CONTENT (cc/gm)	(FT ³ /TON)
Shelbyville (7)	Illinois	Coles	504	0.1	0.1 (BM)	0.2	8
Danville (No. 7)	do	Clay	984	0.9	0.4 (BM)	1.3a	40**
do	do	Coles	983	2.0	0.7 (BM)	2.7	87
do	do	Marion	864	0.7	0.1 (BM)	0.8	26**
Herrin (No. 6)	do	Clay	1035	0.6	0.4 (BM)	1.0a	32**
do	do	Coles	1067	1.0	0.5 (BM)	1.5	48
do	do	Franklin	~650	1.7	—	—	53
do	do	do	~650	2.3	—	—	72
do	do	do	~650	2.2	—	—	69
do	do	Jefferson	733	1.8	0.1 (CB)	1.9	61
do	do	Marion	698	0.9	0.2 (BM)	1.1	35**
do	do	Wayne	900	1.2	0.7 (G)	1.9	61
do	do	do	969	1.6	1.8 (G)	3.4	109
do	do	White	781	3.5	0.4 (BM)	3.9	125
Brier Hill (No. 5A)	do	Clay	1075	0.5	0.5 (BM)	1.0	32**
do	do	Marion	727	0.4	0.3 (BM)	0.7	22**
Harrisburg (No. 5)	do	Clay	1090	0.9	0.3 (BM)	1.2	38**
do	do	Coles	1092	0.8	1.0 (BM)	1.8a	58
do	do	Franklin	~700	1.2	—	—	38
do	do	do	~700	2.2	—	—	70
do	do	do	~700	1.9	—	—	62
do	do	Jefferson	793	0.8	0.2 (CB)	1.0	32
do	do	Marion	732	0.8	0.1 (BM)	0.9a	26**
do	do	Wayne	1010	2.4	1.3 (G)	3.7	118
do	do	do	1066	1.4	1.3 (G)	2.7	86
do	do	White	908	2.4	0.5 (BM)	2.9	93
Colchester (No. 2)	do	Peoria	133	0.6	0.5 (G)	1.1	35
Seelyville	do	Clay	1352	1.1	0.4 (BM)	1.5	48**
do	do	Wayne	1287	1.3	0.7 (G)	2.0	64
do	do	do	1290	1.5	1.6 (G)	3.1	99
Danville (VII)	Indiana	Knox	339	3.0	1.5 (G)	4.5	144
do	do	do	413	2.2	1.4 (G)	3.6	116
do	do	Posey	467	Desorption in progress			
do	do	do	506				
do	do	Sullivan	145	0.7	0.2 (BM)	0.9	29
Herrin	do	Gibson	580	1.8	1.1 (G)	2.9	93
do	do	Posey	518	Canister leaked			
do	do	do	582	Desorption in progress			
Hymers (VI)	do	Knox	361	0.9	0.8 (G)	1.7	55
do	do	do	422	2.2	1.4 (G)	3.6	116
do	do	Sullivan	178	1.1	0.2 (BM)	1.3	42
Coal Va	do	do	238	1.8	0.3 (BM)	2.1	67
Coal Vb	do	Knox	522	1.9	1.2 (G)	3.1	100
Springfield (V)	do	Gibson	665	2.7	1.8 (G)	4.5	144
do	do	Knox	420	2.7	1.9 (G)	4.6	147
do	do	do	536	2.5	1.7 (G)	4.2	134
do	do	Posey	616	0.4	0.4 (BM)	0.8	26
do	do	do	665	Desorption in progress			
do	do	Sullivan	261	2.1	0.3 (BM)	2.4	77
Houchin Creek (IVa)	do	Posey	728	1.4			
do	do	do	772	Desorption in progress			
Survant (IV)	do	Knox	695	2.8	1.9 (G)	4.7	149
do	do	Posey	787	1.5			
do	do	do	827	Desorption in progress			
Colchester (IIIa)	do	do					
Seelyville (III)	do	Gibson	994	1.3	0.9 (G)	2.2	70
do	do	Posey	892	Desorption in progress			
do	do	do					
do	do	Sullivan	?	2.2	0.3 (BM)	2.5	80
Coal #13	Kentucky	Webster	1200	Desorption in progress			
Coal #9	do	do	1305				

^a Data is average of two or more samples

^{*} Method of determination is indicated

(BM) — Gas released by crushing sample in ball mill

(G) — Graphical method as in USBM RI 8043.

(CB) — Gas released in crushing box

^{**} MRCP data

¹ Desorbed gas includes estimated "lost" gas

TABLE 3

Estimated In-Place Coalbed Gas Resource
(1 March 1980)

COAL SEAM	GAS CONTENT CUBIC FT./TON	GAS RESOURCE CUBIC FT.	
		MINIMUM	MAXIMUM
Danville (and equivalents)	40 — 116	5.83×10^{11}	1.69×10^{12}
Herrin (and equivalents)	32 — 125	2.47×10^{12}	9.64×10^{12}
Springfield-Harrisburg (and equivalents)	32 — 147	2.16×10^{12}	9.91×10^{12}

Illinois		Indiana		W. Kentucky	
Modest Fm		Shelburn Fm		Lisman Fm	
Carbondale Fm	Danville (No. 7)* Jamestown* Herrin (No. 6)*	Dugger Fm	Danville (VII) Hymera (VI) Herrin		No. 14 No. 13 No. 12
	Briar Hill (No. 5A)* Springfield-Harrisburg (No. 5)*	Petersburg Fm	Springfield (V)		No. 11 No. 10 No. 9
	Summum (No. 4)* Shawneetown Coal*	Linton Fm	Houchin Creek (IVa) Survant (IV)		Upper Well (No. 8b) No. 8
	Colchester (No. 2)*		Colchester (IIIa)		Schultztown
Spoon Fm	Seelyville* DeKoven* Davis* Murphysboro New Burnside Bidwell Rock Island (No. 1)*	Staunton Fm	Seelyville (III) Buffaloville		DeKoven Davis (No. 6)
Abbott Fm	Willis	Brazil Fm	Minshall Upper Block Lower Block	Tradewater Fm	Mining City (No. 4) Mannington
	Reynoldsburg				
Caseyville Fm.	Gentry	Mansfield Fm	Mariah Hill Blue Creek St. Meinrad Pinnick French Lick		Bell
				Caseyville Fm.	Main Nolin

* Modified from Kosanke et al., 1960.

Figure 1 Stratigraphic correlation of principal coal seams in the Illinois Basin (after table 3, Illinois Geol. Survey Min. Note 67)

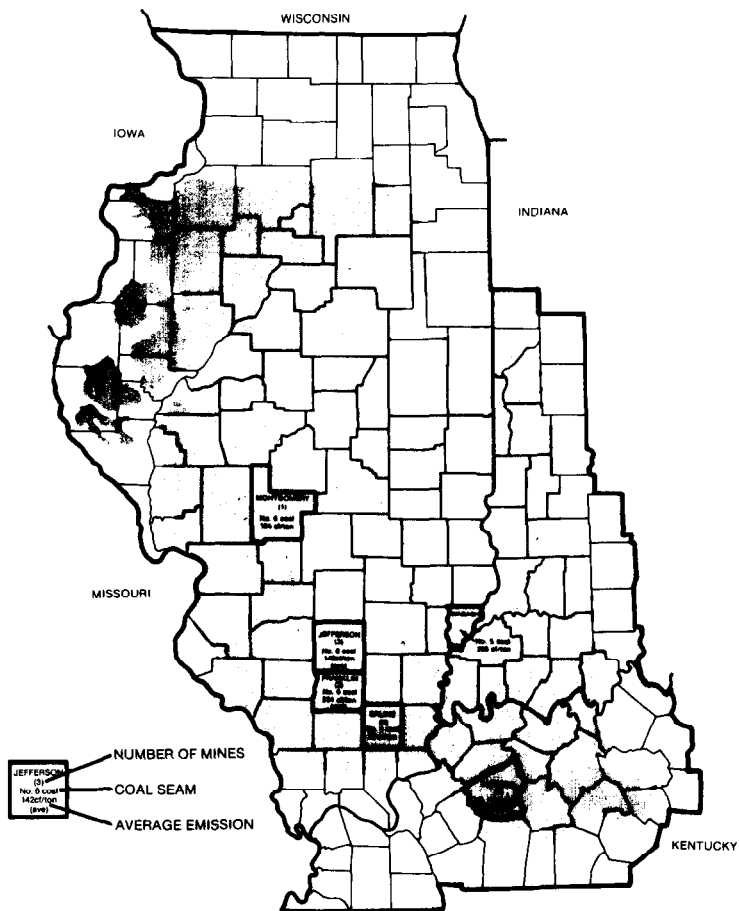


Figure 2 Illinois basin map locating coal mines, by county, and the amount of gas emitted per ton of coal mined

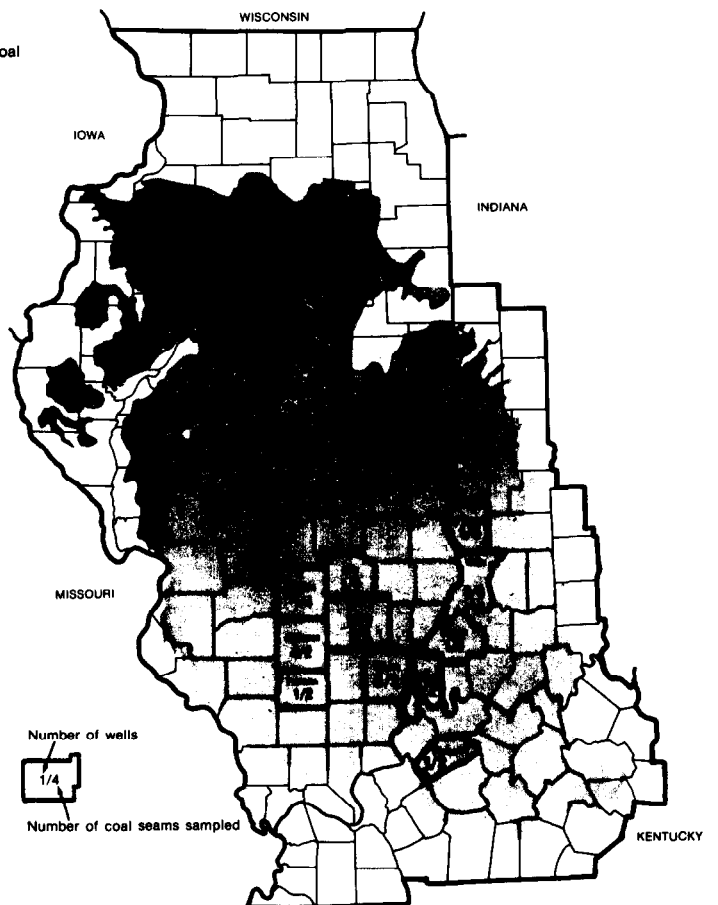


Figure 3 Illinois basin map locating counties in which methane desorption data are available

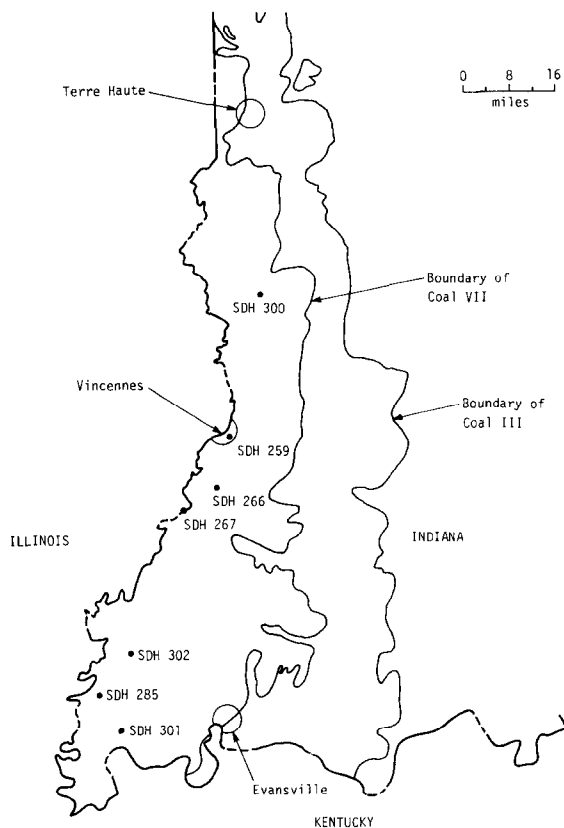


Figure 4 Location of drill holes in Indiana from which samples of coal have been obtained for determination of methane content

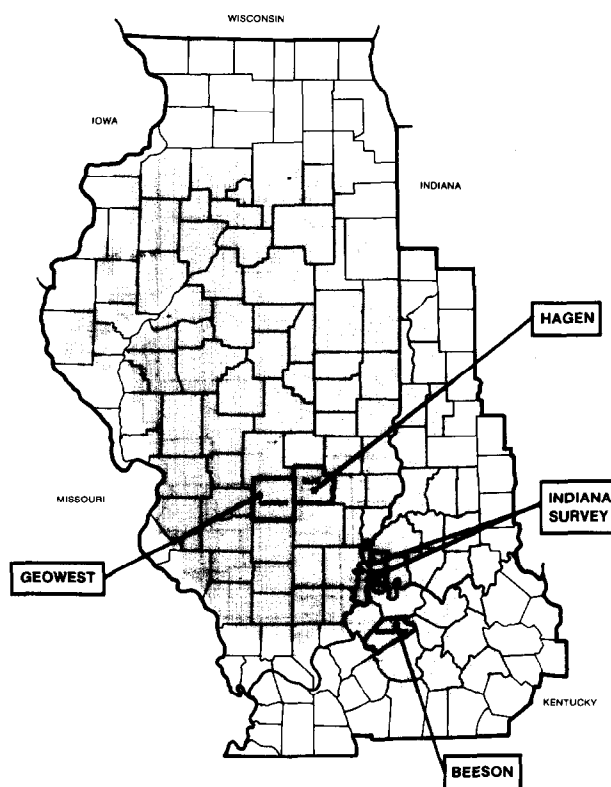


Figure 5 Location of MRCP wells

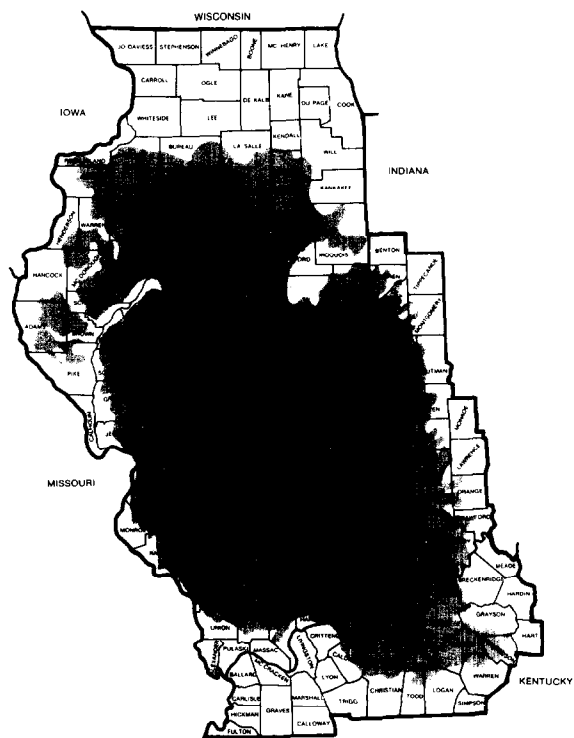


Figure 6 Initial Illinois Basin coalbed methane target area

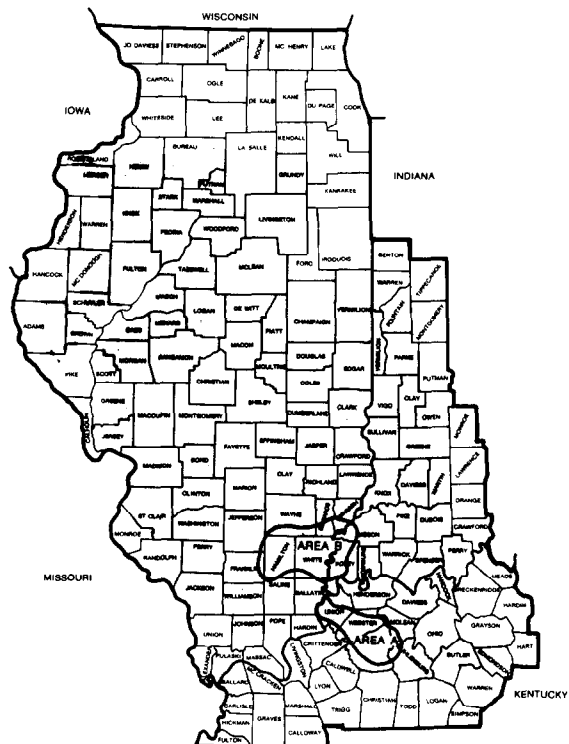


Figure 7 Redefined Illinois Basin coalbed methane target areas

GEOLOGICAL IMPLICATIONS OF GAS PRODUCTION FROM IN-SITU GAS HYDRATES

by G.D. Holder, U. of Pittsburgh; V.T. John and S. Yen, Columbia U.

© Copyright 1980, Society of Petroleum Engineers

This paper was presented at the 1980 SPE/DOE Symposium on Unconventional Gas Recovery held in Pittsburgh, Pennsylvania, May 18-21, 1980. The material is subject to correction by the author. Permission to copy is restricted to an abstract of not more than 300 words. Write: 6200 N. Central Expwy., Dallas, Texas 75206

ABSTRACT

Natural gas hydrates are believed to exist in large quantities in arctic regions and beneath the earth's oceans. Efficient thermal recovery of gas through hydrate dissociation is dependant on the geological and thermal conditions of the hydrate reservoir. Calculations for a steam injection recovery technique indicate the process is energy efficient and that a strong potential exists for gas production from hydrates.

INTRODUCTION

Gas hydrates are crystalline ice-like compounds composed of water and natural gas. Until recently, studies on hydrates were directed towards preventing their formation in natural gas pipelines¹. The apparent discovery of natural gas hydrates in arctic regions², and under the sea floor³, has brought about interest in their study as a potential source of clean energy. Hydrates have also been shown to exist in oil bearing reservoirs.⁴ In such reservoirs, the presence of hydrates is important not only as a potential source of free gas, but also in the way they affect oil production. Hydrates will block reservoir pores and will selectively remove high vapor pressure components such as methane, thus increasing oil viscosity and reducing the driving force for oil production.⁵

The existence of hydrates in the earth therefore, has diverse implications. Recent estimates indicate that as much as 10^{18} m³ of natural gas may exist as in-situ hydrates⁶. While there is no certainty that hydrated gas can be produced economically, the potential of this resource clearly demands evaluation.

This paper examines the potential for recovering gas from naturally occurring hydrates. Factors to be considered in such a study are a) the location of the hydrate fields, b) the purity of hydrates in the reservoir, c) the type of media in which hydrates form, d) thermodynamic conditions of temperature, pressure and composition, e) thermal properties of the reservoir.

References and illustrations at end of paper.

Based on these considerations, calculations were made to determine the energy needed to dissociate hydrates and the amount of gas recovered per kmole of hydrate dissociated.

NATURE OF GAS HYDRATES

Two structures of gas hydrates called structure I and structure II are known to form from mixtures of water and light gases. Each of these structures has two approximately spherical cavities of different diameter as shown in Table 1. Not all the cavities need be occupied by gas molecules to produce a stable hydrate, but a completely unoccupied lattice phase is metastable and does not exist.

The thermodynamic behavior of gas hydrates is illustrated by the phase diagram for methane-ethane-water hydrate forming mixtures (Figure 1). A gas of any indicated composition will form hydrates at pressure-temperature points above the corresponding curve. Below the curve, hydrates will decompose; high pressures and low temperatures favor hydrate formation.

The enthalpy of formation of gas hydrates, from water and free gas can be approximated by a modification of the Clapeyron equation.

$$\Delta H_{Diss} = z RT^2 \frac{d \ln P}{dT} \dots \dots (1)$$

The derivative $d \ln P/dT$ is the slope of the semi-logarithmic P-T graph shown in Figure 1. Calculation of the enthalpy of formation is important because it gives the energy required to dissociate the hydrates.

The hydrates which form in the earth are likely to be structure I hydrates only when pure methane is present. Structure II hydrates will generally form in the presence of even small quantities of heavier gas constituents such as propane. The amount of gas in the hydrate does not generally depend on the structure; structure I has one cavity for every 5-3/4 water molecules and structure II has a cavity for every 5-2/3 water molecules. Occupation of all the cavities of either structure results in a maximum gas concentration, 15 percent, in the hydrate phase. Table 2 shows the composition of the hydrate that would be in

equilibrium with a natural gas containing 97% methane, 2% ethane and 1% propane.⁷ As this table indicates, the hydrate phase gas composition depends upon the formation temperature. The presence of propane causes structure II to form and greatly enhances the stability of the hydrate by lowering the dissociation pressures; hence structure II hydrate can exist under a considerably wider range of geological P-T conditions than can structure I.

A basic model to predict hydrate equilibria was first developed by van der Waals⁸. The model with some modifications⁷, serves as the basis for hydrate equilibrium calculations to determine the conditions at which hydrates may form within the earth.

HYDRATES IN SUB-SURFACE ENVIRONMENTS

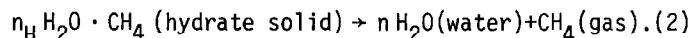
Occurrences of continental hydrates are found primarily in regions of thick permafrost, where the temperature at any given depth within the earth is relatively low. Katz⁹ reported that Alaskan reserves of hydrates exist at depths of 200 to 1300 m. The estimates are based upon actual temperature profiles and an assumed hydrostatic head. If an overburden pressure provides a greater pressure at every depth, the probable range of hydrate existence would increase. Temperature profiles indicate hydrate existence, due to the dissimilar thermal properties of hydrates, water, and ice. Hydrates have a lower thermal conductivity than water or ice and hence effect a characteristic temperature gradient.

The possible existence of gas hydrates in marine sediments was suggested by Stoll¹⁰ to explain unusually high seismic velocities and anomalous reflectors in gas-rich sediments on the Blake-Bahama outer ridge, off the coast of Florida. The average acoustic wave velocity in the sediment based on the most obvious correlation between seismic reflections and lithologic changes was found to be over 2 km/sec, which is high when compared to velocities in sediments with similar porosity and grain size that contain no gas. Milton⁶ has suggested that the anomalous reflectors are due to the presence of an isothermal surface which itself is indicative of a phase transition that would exist for hydrate-gas-water equilibrium. At present, it is felt that the anomalous reflectors that have been observed are located at depths where the temperature-pressure conditions correspond to a gas-water-hydrate equilibrium curve such as shown in Figure 1.

Experimental studies by Makogon¹¹ to simulate hydrate formation in porous rock found that factors influencing hydrate formation are a) the degree of moisture saturation of the rock, b) the gas-water contact area and c) the capillary radii of the pores. In particular, the capillary effect of the porous rock causes the vapor pressure of the water to decrease and consequently causes the hydrate forming pressure to increase.

HYDRATE DISSOCIATION

The dissociation of hydrates to gas and water can be represented by



where n_H has a value approaching 6 for hydrates of natural gas. The enthalpy change associated with the

transition is about 63 kJ per mole of methane dissociated.

As has been predicted by Katz⁹ and verified in drilling operations, rapid dissociation of hydrates cannot be effected, simply by relieving the pressure in a hydrate reservoir. The energy for hydrate dissociation has to be supplied by an internal source. The energy required to produce one cubic meter of gas from hydrates represents about seven or eight percent of the heating value of the gas produced. The exact ratio of the energy recovered to the energy input will depend on the composition of the gas recovered and on the heat losses incurred in transferring the dissociation energy to the hydrate phase.

The energy efficiency of hydrate production can be estimated by making an energy balance over the reservoir volume in which the hydrates are dissociated¹². In this model, it is assumed that steam is injected into the hydrate containing reservoir, causing the hydrates to dissociate in the vicinity of the injection string bottom. A further assumption is that the region of dissociation is continuous, and has a spatially uniform temperature T_R , which will be higher than the surrounding temperature. Figure 2 is a schematic of steam injection in a hydrate reservoir, showing the interface between the gas-water region and the hydrate region. An energy balance over the control volume considered, gives

$$\Delta H_S \dot{M}_S = \Delta H^* \dot{M}_G + \frac{d}{dt} \dot{M}_R H_R \quad \dots \quad (3)$$

The term on the left represents the enthalpy change of the steam from the time it enters the reservoir to the time it leaves as water. The first term on the right represents the enthalpy change of the water and gas in the hydrate phase as it dissociates from hydrates at temperature T_H , forming gas and water at the reservoir temperature T_R . If \dot{M}_G is the flow rate of recovered gas, and α , the fraction of dissociated gas left unrecovered, then $\dot{M}_G/(1-\alpha)$ is the total rate of dissociation. The enthalpy change associated with this transition is $[\Delta H_{Diss} + (C_{pg} + n_H C_{pw})\Delta T] \dot{M}_G/(1-\alpha)$ and a comparison with the second term in equation 2 indicates that ΔH^* can be expressed as

$$\Delta H^* = [\Delta H_{Diss} + (C_{pg} + n_H C_{pw})\Delta T] / (1-\alpha). \quad \dots \quad (4)$$

In the above analysis, \dot{M}_S and \dot{M}_G are assumed to be constant steam injection and gas production rates. For the actual case, the quantities could be considered to be averaged over the duration of steam injection and hydrate dissociation.

The last term in equation 3 represents the change in sensible heat of the reservoir media, for total dissociation of the hydrates within the control volume. This sensible heat change is given by

$$\frac{d}{dt} \dot{M}_R H_R = \left[\frac{1-\phi}{\phi} \right] \frac{n_H}{(1-\alpha)} \frac{\rho_R}{\rho_{H_2O,H}} C_{pR} \Delta T \dot{M}_G \quad \dots \quad (5)$$

where $(1-\phi)$ is the 'effective' porosity of the reservoir. The total heat balance can now be written as

$$\Delta H_S \dot{M}_S = (\Delta H^* + C_p^* \Delta T) \dot{M}_G \quad \dots \quad (6)$$

where

$$C_p^* = \left[\frac{1-\phi}{\phi} \right] \frac{n_H}{(1-\alpha)} \frac{\rho_R}{\rho_{H_2O,H}} C_{pR} \dots \dots \dots (7)$$

Equation 7 indicates that C_p^* , the effective reservoir heat capacity, depends on α , the fraction of dissociated gas that is not recovered. While a certain amount of gas will remain trapped in the porous medium, an efficient steamflood would displace most of the dissociated gas. A lower limit on the quantity of gas recovered can be calculated by assuming gas recovery at a pressure equal to the equilibrium pressure at the corresponding depth, and complete displacement of residual water from the control volume. A sample calculation was done (Appendix) assuming a basis of 100 cubic meters of reservoir volume initially occupied by hydrates at equilibrium conditions of 6900 kPa and 283 K. The final conditions correspond to the 100 cubic meters of reservoir volume occupied by gas at the same pressure and temperature. The upper limit on α in this case is 0.46. In actuality, the final pressures attained are much less than equilibrium pressures. The presence of residual water also decreases the reservoir volume available to the gas. These two factors lead to increased gas recoveries and much lower values of α .

Typical properties of hydrates and hydrate reservoirs are given in Table 3. Using these properties, a comparison of the sensible heat terms shows that

$$C_{pg} \approx 0.1(n_H C_{pw})$$

$$(n_H C_{pw}) \approx 0.1 \left[\frac{1-\phi}{\phi} \right] \frac{n_H}{(1-\alpha)} \frac{\rho_R}{\rho_{H_2O,H}} C_{pR} \dots \dots \dots (8)$$

That is, the heat gained by the reservoir media is much greater than the sensible heat gained by the water or gas. C_p^* , the effective heat capacity of the reservoir media is hence more important than the heat capacity of the dissociated hydrates. From the data of Table 3, C_p^* is calculated to have a value between 25 and 6700 kJ/K for every kmole of gas produced. For numerical purposes, C_p^* is assigned a value of 1250 kJ/kmol·K

Figures 3 through 5 show how the steam requirement per kmole of gas produced varies with latent heat and the reservoir temperature increase. Figure 3 shows the energy input to output ratio, expressed here in kg of steam/100 m³ of gas, as a function of the combined latent and sensible heats of hydrate dissociation. In this figure the average reservoir temperature increase is assumed to be 30 °K. The value of ΔH_S is the amount of latent heat of the steam given up to the reservoir. If ΔH_S is 2330 kJ/kg, then all of the latent heat is transferred to the reservoir. If ΔH_S is 1860 kJ/kg, then 80 percent of the heat is transferred to the reservoir. If ΔH_S is 1400 kJ/kg, 60 percent is transferred. The remaining 20 percent, or 40 percent are considered to be heat losses.

Figures 4 and 5 show similar curves for average reservoir temperature increases of 50°K and 70°K respectively. It is unlikely that temperature increases as large as 70°K would be required since hydrates will generally dissociate at temperatures less than 298°K. A 70°K increase would imply a normal reservoir temperature of 228°K which is highly unlikely in any region. However, in order to effect a rapid rate of gas production, some increase above the hydrate equilibrium dissociation temperature will be required.

Figure 6 shows how the input to output energy ratio depends upon the modified reservoir heat capacity, C_p^* . As Equation 7 shows, this term incorporates ϕ , the fraction of the reservoir containing hydrates, and α , the fraction of the dissociated gas that is recovered. The upper line in Figure 6 represents a case where forty percent of the steam energy is lost, with the reservoir temperature raised 70°K. Above a limiting value of C_p^* (≈ 4200 kJ/kmol K), the energy produced is less than the energy input. The lower line represents a case wherein heat losses are negligible. For such cases, it is likely that a net energy production will be obtained for values of C_p^* as high as 8000 kJ/kmol·K.

CONCLUSIONS

The thermodynamic evaluation presented, indicates that hydrates, if they exist in a pure enough state, have good potential for producing gas with a greater energy content than is needed to break down the hydrates. The produceability of a reservoir depends on the geological factors that determine the amount of hydrates formed. Reservoir porosity influences both heat requirements and recovery flow rates of dissociated gas. Other important factors are the thermal properties of the reservoir which determine the efficiency of thermal injection, and thermal properties of hydrates. At this point, only estimates can be made of the heat quantities involved. It is clear however that if future research finds that reservoir conditions are favorable, then the production of gas from hydrate fields is certainly viable from a thermodynamic viewpoint.

NOMENCLATURE

C_{pg}	= gas heat capacity - kJ/kmol·K
C_{pR}	= reservoir media heat capacity - kJ/kg·K
C_{pw}	= water heat capacity - kJ/kmol·K
C_p^*	= reservoir effective heat capacity - kJ/kmol K
ΔH_{Diss}	= enthalpy of dissociation - kJ/kmol CH ₄
ΔH_R	= reservoir media enthalpy - kJ/kg
ΔH_S	= steam enthalpy change - kJ/kg
ΔH^*	= effective gas-water enthalpy change - kJ/kmol CH ₄
\dot{M}_G	= recovery rate of gas - kmol/s
\dot{M}_R	= reservoir mass
\dot{M}_S	= mass flow rate of steam - kg/s
n_H	= number of water molecules/gas molecule in the hydrate phase
p	= pressure - kPa
t	= time - s
T	= temperature - K
T_H	= hydrate dissociation temperature - K
T_R	= reservoir temperature within the control volume - K
z	= gas compressibility factor
ΔT	= $T_R - T_H$ = reservoir temperature increase
α	= fraction of dissociated gas that is not recovered
ρ_R	= reservoir media density - kg/m ³
$\rho_{H_2O,H}$	= density of water in the hydrate phase - kmol/m ³
ϕ	= fraction of reservoir containing hydrates - m ³ hydrate/m ³ reservoir

GEOLOGICAL IMPLICATIONS OF GAS PRODUCTION FROM INSITU GAS HYDRATES

ACKNOWLEDGEMENT

Acknowledgement is made to the Donors of the Petroleum Research Fund, administered by the American Chemical Society, for partial support of this research. Partial support was also provided by the United States Department of Energy.

REFERENCES

1. Hammerschmidt, E. G.: "Formation of Gas Hydrates in Natural Gas Transmission Lines", Ind. & Eng. Chem. (August, 1934), v. 26, pp. 851-855.
2. Bily, C., and Dick, J. W. L.: "Naturally Occurring Gas Hydrates in the McKenzie Delta, N. W. T.", Bull. Can. Pet. Geo. (September, 1974), v. 22, pp. 340-352.
3. Bryan, G. M.: "Insitu Indications of Gas Hydrates", in 'Natural Gases in Marine Sediments', Kaplan, I. R., ed., Plenum Press, New York (1974), pp. 195-225.
4. Holder, G. D., Katz, D. L., and Hand, J. H.: "Hydrate Formation in Subsurface Environments", Am. Assoc. of Pet. Geo. Bull. (June, 1976), v. 60, n. 6, pp. 981-994.
5. Verma, V. K., Katz, D. L., Hand, J. H., Holder, G. D.: "Denuding Hydrocarbon Liquids of Natural Gas Constituents by Hydrate Formation", J. Pet. Tech. (February, 1975), v. 27, pp. 223-226.
6. Milton, D. J.: "Methane Hydrate in the Sea Floor - A Significant Resource", paper presented at the Future Supply of Nature-made Petroleum and Gas Conference, Luxemburg, Austria, 1976.
7. Holder, G. D.: "Multi-Phase Equilibria in Methane-Ethane-Propane-Water Hydrate Forming Systems", Ph.D. Dissertation (1976), Univ. Mich., Ann Arbor.
8. Van der Waals, J. H., and Platteeuw, J. C.:

"Clathrate Solutions", Adv. Chem. Phys. (1959), v. 2, pp. 1-57.

9. Katz, D. L.: "Depths to which Frozen Gas Fields may be Expected", J. Pet. Tech. (April, 1971), v. 24, pp. 557-558.
10. Stoll, R. D., Ewing, J., and Bryan, G. M.: "Anomalous Wave Velocities in Sediments Containing Gas Hydrates", J. Geophys. Res. (March, 1971), V. 76, n. 8, pp. 2090-2094.
11. Makogon, Yu. F.: "Hydrates of Natural Gas", 1974; Translated by Cieslewicz, W. J., 1977.
12. Yen, S. L.: "Thermal Recovery of Natural Gas from Gas Hydrates", M.S. Thesis (1979), Columbia University, New York.

APPENDIX 1

Example calculation of the upper limit for α , the fraction of dissociated gas that is not recovered:

Basis: 100 m³ of hydrate at equilibrium conditions of 6900 kPa (about 750 m depth) and 283 K.

The density of water in the hydrate phase, assuming structure II formation is 44 kmol/m³.

The density of gas in the hydrate, assuming 94 percent occupation of the cavities (hydrate number of 6) is 44/6 or 7.3 kmol/m³.

The amount of gas within the reference volume (100 m³) at hydrate condition is 730 kmol. At the end of the dissociation and recovery process, the reference volume is assumed to be occupied by gas at 6900 kPa and 283 K. These are taken as 'worst case' conditions.

The amount of gas within the reference volume is 337 kmol, assuming a gas compressibility factor of 0.87 (from compressibility charts for methane gas). Hence α maximum is 337/730 or 0.46. This factor would decrease in a nearly linear fashion with pressure.

Table 1

Lattice Properties of Structure I and
Structure II Hydrates

	Structure I	Structure II
Number of Large Cavities/Unit Cell	6	16
Number of Small Cavities/Unit Cell	2	8
Number of Water Molecules/Unit Cell	46	136
Large Cavity Diameter, m	8.60 E-10	9.46 E-10
Small Cavity Diameter, m	7.88 E-10	7.82 E-10

Table 2

Calculated Composition of Structure II Hydrate in Equilibrium with
a Natural Gas Containing 97% CH₄, 2% C₂H₆, and 1 % C₃H₈
Formation Pressures are also given

Temperature (K)	Pressure (k Pa)	Composition in Hydrate			
		CH ₄	C ₂ H ₆	C ₃ H ₈	H ₂ O
277.8	2234	8.2	0.2	4.1	87.5
283.3	4447	9.9	0.2	3.5	86.4
288.9	9770	11.0	0.2	2.9	85.9
294.4	26958	12.3	0.2	2.0	85.5
300.0	54434	12.7	0.2	1.8	85.3

Table 3

Typical Properties of Hydrates and Hydrate Reservoirs

Parameter	Range	Typical	Units
ϕ	0.1 - 0.8	0.2	m ³ hydrate/m ³ reservoir
α	0 - 0.2	0.1	fraction of dissociated gas not recovered
n_H	5 - 7	6	kmol water/kmol hydrate gas
$\rho_R C_{pR}$	800 - 3800	1200	kJ/m ³ media K
$\rho_{H_2O,H}$	44 - 45	45	kmol/m ³

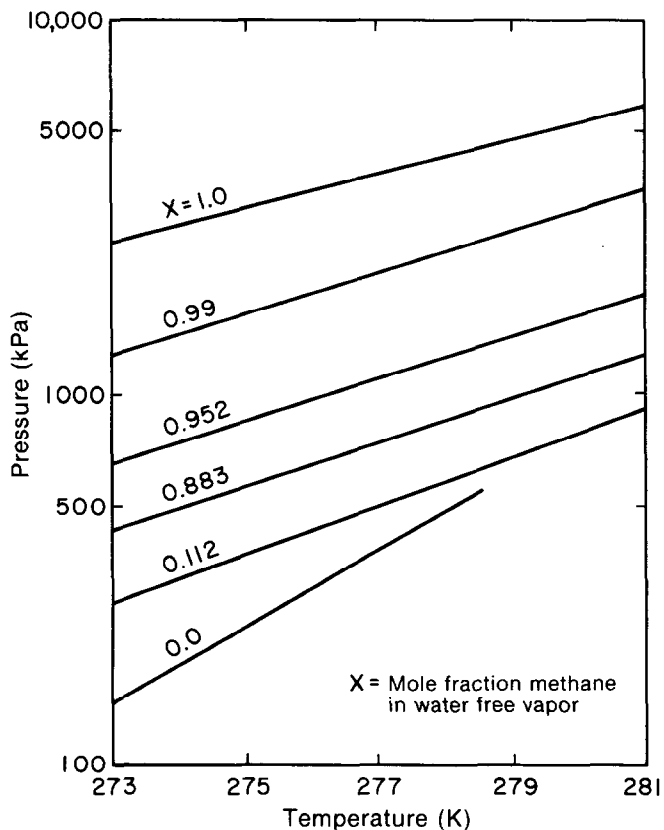
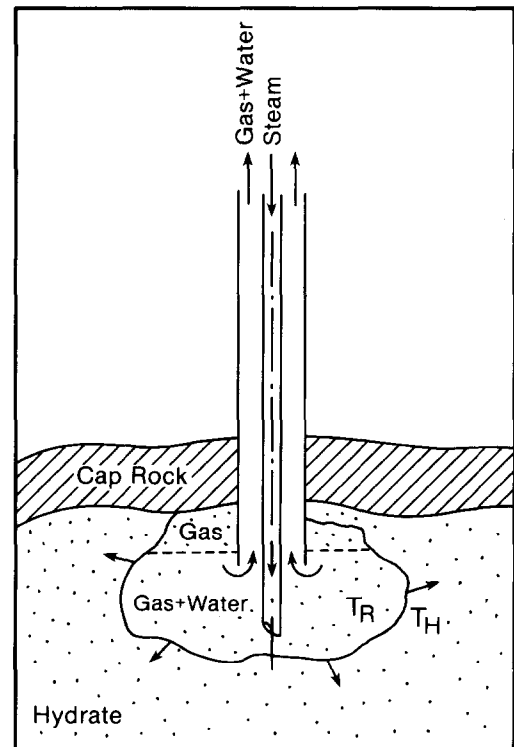
Fig. 1 - Dissociation pressures of Methane-Ethane Hydrates⁷.

Fig. 2 - Schematic of steam injection into a hydrate reservoir.

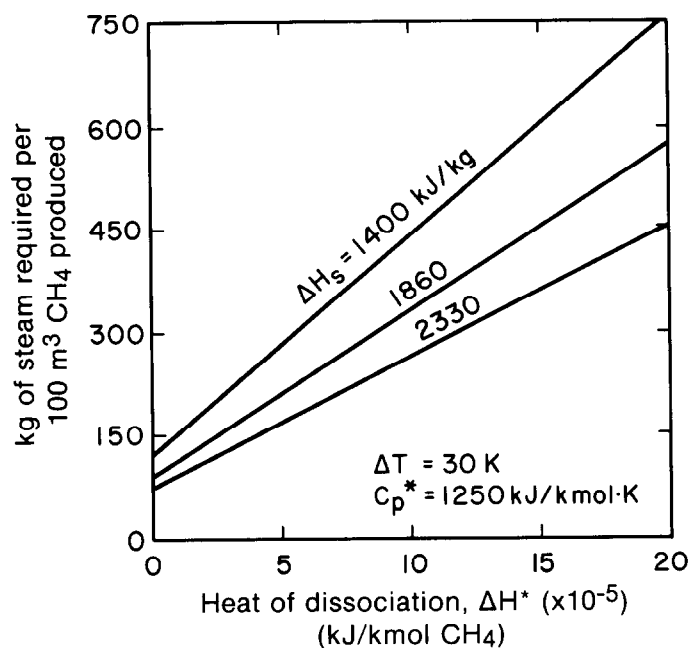


Fig. 3 - The effect of the latent heat of hydrate dissociation on the amount of steam required per kmole of gas produced. Case I.

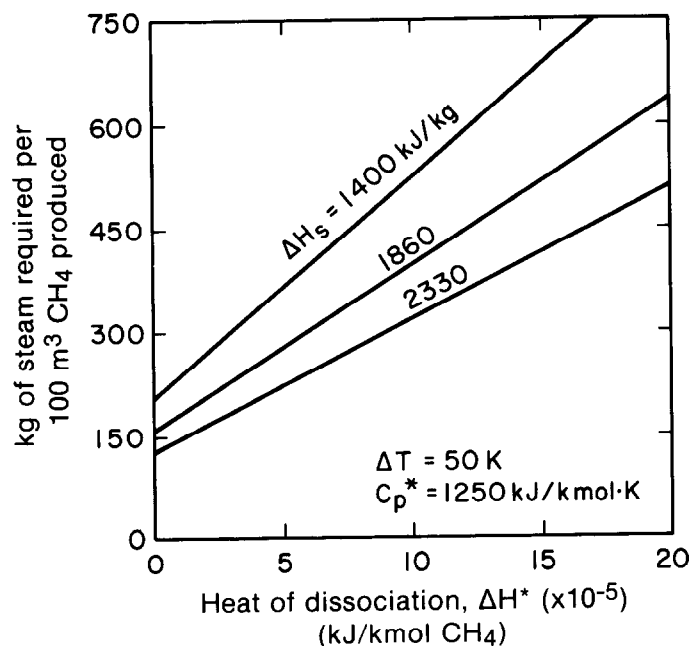


Fig. 4 - The effect of the latent heat of hydrate dissociation on the amount of steam required per kmole of gas produced. Case II.

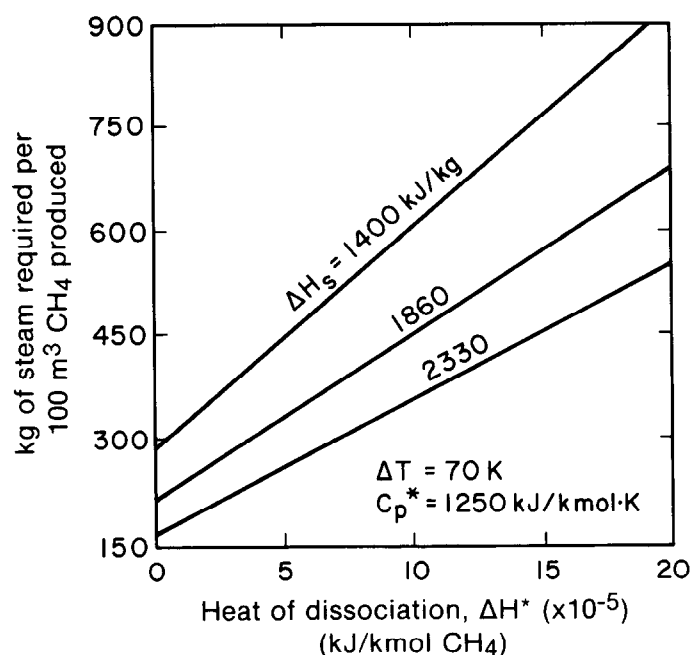


Fig. 5 - The effect of the latent heat of hydrate dissociation on the amount of steam required per kmole of gas produced. Case III.

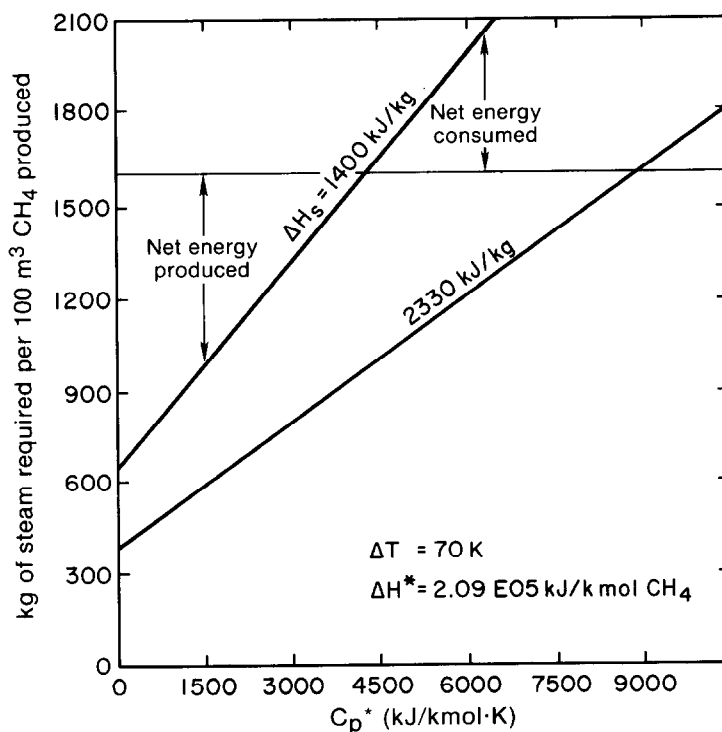


Fig. 6 - The effect of the modified reservoir heat capacity on the amount of steam required for hydrate dissociation.

A LABORATORY INVESTIGATION OF ENHANCED RECOVERY OF METHANE FROM COAL BY CARBON DIOXIDE INJECTION

by Paul F. Fulton, Carol A. Parente, Bruce A. Rogers, Nitin Shah, and A.A. Reznik, Univ. of Pittsburgh

© Copyright 1980, Society of Petroleum Engineers

This paper was presented at the 1980 SPE/DOE Symposium on Unconventional Gas Recovery held in Pittsburgh, Pennsylvania, May 18-21, 1980. The material is subject to correction by the author. Permission to copy is restricted to an abstract of not more than 300 words. Write: 6200 N. Central Expwy., Dallas, Texas 75206

ABSTRACT

An experimental procedure for determining the effectiveness of CO₂ injection into methane-containing coal samples for the purpose of enhancing methane production is described. Experimental results on both dry and water saturated samples reveal that CO₂ injection greatly enhances both production rate and recovery efficiency. Most effective is a cyclic CO₂ injection-gas production technique which recovered essentially all of the adsorbed methane in the 3½" core samples used in the experiments.

INTRODUCTION

The coal which lies buried beneath the United States at depths of less than 3000 feet is thought to contain nearly 300 trillion standard cubic feet of pipeline quality gas.¹⁻⁵ This exceeds the current proved gas reserves in the U.S. and represents a significant possible supplement to dwindling supplies. The natural gas found in virgin coal beds is predominantly methane,⁶ usually exceeding 80%. Very small percentages of ethane, propane, butane and pentane have been detected. Carbon dioxide and nitrogen may be as high as 15% in gas from virgin coal. Most of the gas present in coal beds is adsorbed on the coal surfaces and desorption is normally a very slow process.

In addition to the desirability of producing this gas as an energy source there is the added important advantage from a safety standpoint of demethanating a coal bed prior to mining. Attempts to produce the gas in coal through vertical well bores by pressure draw-down have generally not been commercially successful because of low production rates.^{7-13,22} Differing theories on the transport of gases through coal have been proposed by Cervik¹⁴, Kissel^{15,16,17}, Skidmore and Chase¹⁸ and Kuuskraa, et. al²¹ to explain these low production rates. None of these has concluded that desorption rate is the mechanism which controls production rates from wells drilled into coal beds.

References and illustrations at end of paper.

A key publication by Every and Delosso in 1972¹⁹ showed that carbon dioxide proved to be very effective in displacing methane from crushed coal under laboratory imposed flow conditions at ambient temperature. This led to the proposal that competitive adsorption-desorption of methane by carbon dioxide might provide an efficient means for rapid degassification of coal beds and thereby increased recovery rates of methane from vertical well bores. This paper describes a laboratory procedure for measuring the effectiveness of carbon dioxide in replacing methane from 3½" diameter samples of Pittsburgh coal and also presents the experimental results.

EXPERIMENTAL PROCEDURE

The coal from the Pricetown mine in West Virginia was delivered in large lumps which were then stored under water until cored for use in the experiments.

The experimental apparatus is represented schematically in Figure 1 and pictorially in Figure 2. The pressure vessels used were 4 inch (10.16 cm) I.D. and 12 inches (30.48 cm) long. The vessels were designed for operating pressures of 100 psi (4.78 Pa) and 200 psi (9.56 Pa). The coal samples were cut to diameters of 3½ or 3 ¾ inches (8.89 or 9.555 cm) and varying lengths between 2 to 4 inches (5.08 to 10.16 cm) and stacked in the vessels to a total height of approximately 11½ inches (29.21 cm). The system was evacuated for several hours. Methane was expanded from a constant volume pressure cylinder into the vessel containing the coal resulting in methane adsorption on the coal surfaces. As methane was being adsorbed, the pressure in the system declined and the amount of methane adsorbed was determined by material balance. At some arbitrarily selected time, usually six to eight days, the pressure in the system was noted, and the amount of adsorbed methane calculated. In some cases, in order to get a greater quantity of methane adsorbed, the pressure was increased and the process repeated several times. When the desired amount of methane had been adsorbed the excess gas in the vessel was vented to atmospheric pressure. At this point the natural desorption production cycle was begun and continued until no more gas was being produced, or was stopped after some arbitrarily chosen time interval.

The produced gas was collected and measured in inverted water-filled graduated cylinders.

At this point the experimental procedure varied. On some of the dry samples additional methane was added or in others the CO₂ was injected without the additional methane. The carbon dioxide was added in the same manner as was the methane but was adsorbed much faster. Again, material balance made possible a calculation of the amount of CO₂ adsorbed on the coal. Either when the pressure in the system had stabilized or at any arbitrarily selected time, the gases in the cylinder were vented and collected for volumetric determination and the composition determined by gas chromatography. Gases desorbed from the coal at atmospheric pressure over a period of time were collected as before and the composition of the produced gases determined. The data collected to this point made possible a comparison of methane production by natural desorption with that by CO₂ enhancement.

On some of the samples the CO₂ was injected in a cyclic manner with each CO₂ injection followed by a short period of CO₂ adsorption and then methane production. As many as six such cycles were used in order to get maximum methane recovery. The experiments were stopped when the produced CO₂/methane ratio became excessive.

The procedure was modified somewhat for experiments on samples containing water. Following the period of methane adsorption, the coal was surrounded by water and the pressure increased by applying methane pressure for several days. It was reasoned that the combination of pressure and imbibition would result in a significant water saturation in the coal. The excess water was then removed from the vessels and the same production-CO₂ injection-production cycle as with dry coal samples was followed.

DATA AND RESULTS

The results will be presented and discussed separately for dry coal samples and those containing water.

DRY SAMPLES

The results of the first experimental testing by the authors of the effectiveness of CO₂ injection in enhancing methane recovery are discussed in detail by Parente.²⁰ Typical of the many results from these first experiments using dry coal samples is that shown in Figure 3: Note that measurable natural desorption had ceased after five days. Because the CO₂ adsorption time was five days and because the data indicate that methane was being desorbed during this period, the enhanced production curve was started with day five. The tremendous increase in produced methane by CO₂ enhancement was very encouraging.

At this point the equipment was modified and the experimental procedure adjusted somewhat to make possible a quantitative determination of the gases adsorbed on the coal samples at various times in the experimental process. It is this equipment and procedure that is detailed in the section EXPERIMENTAL PROCEDURE.

With this modified equipment, four separate pressure vessels were filled with coal cores and a different quantity of methane adsorbed on each sample, depending on the initial pressure in the vessels.

Results of production by natural desorption are shown in Figures 4 and 5 for Samples 1 and 4 with injection pressures of 45 and 195 psia respectively. Results from those experiments with injection pressures of 88 and 142 psia followed a similar pattern. The experiments were arbitrarily stopped at the end of 8 days in the interests of time, even though in the case of Sample 4, it was still producing. A summary of the results of this portion of the experiments are shown in Table 1.

There followed a second six day methane adsorption cycle to replace that which was produced. This resulted in somewhat more adsorbed methane in each sample than at the beginning of the natural desorption cycle. Carbon dioxide was injected into each vessel at the same pressure used for methane and again allowed to adsorb for six days. A comparison of the pressure history during the first methane adsorption and CO₂ adsorption periods is shown in Figure 6. Note the much more rapid adsorption rate for the CO₂ as indicated by the rapid decline in pressure. After about thirty six hours the pressure had stabilized, indicating either that all of the CO₂ that could be adsorbed at that pressure had been adsorbed, or that CO₂ was being adsorbed at approximately the same rate as methane was being desorbed, or a combination of the two. Subsequent work will include analysis of the gas composition during this period.

Production history for the CO₂ enhancement cycle for two of the samples is also shown in Figures 4 and 5. Results from all four samples are tabulated in Table 2. Note that Sample 4 produced considerably more methane than had been adsorbed at the beginning of the CO₂ injection. Again the additional methane production is considerable while the amount of CO₂ produced during the period is much less than the methane. It is significant to note that the greatest portion of the methane production occurs during the release of pressure following the CO₂ adsorption.

Finally, some of the samples were subjected to a cyclic operation where each of several injection cycles was followed by a production cycle. Results of one such experiment are shown in Figure 7 and a summary of the data for two such experiments are shown in Table 3.

At the end of six injection-production cycles the amount of methane recovered from Sample 1 was almost 7 times that produced by natural desorption. At the end of four cycles before the produced CO₂/methane became excessive almost six times as much methane had been produced than by natural desorption.

Significantly, as shown in Table 3, both samples produced considerably more methane than had been calculated to be adsorbed at the beginning of the experiment. This, plus the earlier similar example (Sample 4), led to the obvious conclusion that significant amounts of the original in-situ methane remained adsorbed on the coal six months or so after it was mined. Except for the one or two days that may have elapsed between mining the coal and delivery to our laboratory and the elapsed time of the experiments the coal was immersed in water. Table 3 shows significant quantities of CO₂ remained adsorbed on the coal at the termination of the experiment. This could be significant in coal mining.

WATER SATURATED SAMPLES

Obviously since all coal beds are water-saturated it is essential to evaluate the effectiveness of this recovery technique on samples containing water.

The initial experiments with water-saturated samples were performed on previously dried samples that were evacuated and saturated with water and then subject to methane pressure to allow methane adsorption. Because of the water present, significantly less methane was adsorbed than in the dry samples. Nevertheless, the results as typified by Figure 8 were just as encouraging as with the dry samples.

The amount of methane adsorbed on the samples typified by Figure 8 is considerably less than one would expect to find in-situ in most Pittsburgh seam coals. In order to get more methane adsorbed, the procedure described in the final paragraph of EXPERIMENTAL PROCEDURES was used. Repetitive methane adsorption cycles on Sample 6 were used to obtain a methane content of 11813 cc, equivalent to 167 SCF/Ton of coal. This represents more gas than had been adsorbed at the start of any other of the tests. Production by natural desorption was continued for 38 days by which time 56% of originally adsorbed gas had been produced. (See Figure 9.) This was followed by the usual CO₂ injection and a production cycle totalling 18 days during which an additional 10% of the methane was produced, resulting in a total recovery of 67%. This is a much lower recovery percentage after 56 days than attained from dry coal samples after only a 12 total day CO₂ injection-production cycle. It is quite probable that this experiment could have been considerably speeded up by earlier injection of the CO₂ and that additional methane would have been produced from additional CO₂ injection cycles. This experiment was useful in establishing experimental technique and at the same time providing additional evidence that the method will produce additional methane in water-saturated cores.

As a final experiment, a core was cut from a lump of coal that had been immersed in water for over six months since it was delivered from the mine. The core was cut with water as the circulating fluid (and therefore remained water saturated) and immediately placed in a pressure vessel with no methane being added. The objective was to determine how much of the original in-situ methane had remained in the coal. Of course, no methane was produced by natural desorption so a cyclic CO₂ injection program was followed with the results shown in Figure 10. A total of almost 2800 cc (40 SCF/Ton) on methane was produced after three cycles covering a period of 95 days. In retrospect the CO₂ injection time could have been considerably shortened, as could the production cycle since most of the production takes place in the first few days of each cycle. The same recovery probably could have been attained in 20-30 days.

Considerably greater quantities of CO₂ than methane were produced. At least a part of this may be due to the deliberately excessively large quantities of CO₂ adsorbed. Also significant amounts of nitrogen were produced. This latter probably resulted from exposure of the coal to air during the time between mining and submersion in water in the laboratory.

Considerable importance can be attached to the results of this experiment. They show that the very tightly adsorbed "hard-to-recover" methane in a water saturated coal can be recovered by the CO₂ enhancement process.

CONCLUSIONS

1. The data suggest that desorption rate plays a significant role in the rate of production of methane from coal samples of the size used in these experiments.

2. On dry coal samples a single CO₂ injection is a very effective mechanism for enhancing the recovery of adsorbed methane from coal. It not only increases the recovery efficiency but equally important, it increases the rate of recovery. Recovery efficiency appears to increase with CO₂ injection pressure within the limits of these experiments (45-200 psia).

3. A cyclic CO₂ injection-gas production system is capable of completely stripping the coal of its adsorbed methane.

4. Significant quantities of CO₂ remain adsorbed on the coal after cyclic injection (see Table 3).

5. An experimental procedure for determining the effectiveness of CO₂ enhancement of methane production from water saturated coal samples has been demonstrated.

6. Experiments completed to date give positive indication that the method will lead to increased methane recovery rates and recovery efficiency in water saturated samples.

7. Even the very strongly adsorbed "hard-to-recover" residual methane is desorbed as a result of CO₂ injection.

8. Considerable additional experimental work needs to be done before conclusions can be drawn concerning the applicability of the technique to the enhanced recovery of methane from coal beds.

ACKNOWLEDGEMENTS

Much of this work was funded by the Morgantown Energy Technology Center of the United States Department of Energy. We also acknowledge support from the Exxon Educational Foundation for partial funding of the contribution of Bruce Rogers to this effort.

REFERENCES

1. Irani, M. C., Jeran, P. W., and Deul, M., "Methane Emission from U.S. Coal Mines in 1973, A Survey," USBM IC 8659, 1974.
2. Deul, M., and Kim, A. G., "Coal Beds: Source of Natural Gas," Oil and Gas Journal, June 16, 1975.
3. Tilton, J. G., "Gases from Coal Deposits," Natural Gas from Unconventional Geologic Sources, National Academy of Sciences Contract E(49-18)-2271, 1976.
4. Little, A. D., "Economic Feasibility of Recovering and Utilizing Methane Emitted from Coal," USBM PB-24-728, 1975.
5. TRW Energy Systems Group, "Systems Studies of Energy Conservation: Methane Produced from Coal Beds," ERDA Contract E(46-1)-8042, January 1977.
6. Kim, A. G., "The Composition of Coal Bed Gas," USBM R17762, 1973.
7. Elder, C. H. and Deul, M., "Hydraulic Stimulation Increased Degasification Rate of Coal Beds," First National Coal Association Underground Mining Symposium, Louisville, KY, 1975.

A LABORATORY INVESTIGATION OF ENHANCED RECOVERY OF METHANE FROM COAL BEDS BY CO₂ INJECTION

<p>8. Chase, R. W., "Degasification of Coal Seams Via Vertical Boreholes: A Field and Computer Simulation Study," Ph.D. Thesis, The Pennsylvania State University, 1979.</p> <p>9. Diamond, W. P., Oyler, D. C., and Fields, H. H., "Directionally Controlled Drilling to Horizontally Intercept Selected Strata, Upper Freeport Coal Bed, Greene County, PA," USBM R18231, 1977.</p> <p>10. Fields, H. H., Krickonic, S., Sainato, A., and Zabetakis, M. G., "Degasification of Virgin Pittsburgh Coal Bed Through Large Borehole," USBM R17800, 1973.</p> <p>11. Fields, H. H., Perry, J. H., and Deul, M., "Commercial Quality Gas from a Multipurpose Borehole," USBM R1 8025, 1975.</p> <p>12. Chase, R. W., "Natural Gas Production From Coal Seams," SPE Paper No. 6629 presented at Society of Petroleum Engineers Regional Meeting, Pittsburgh, PA, October 1977.</p> <p>13. Deul, M., and Elder, C. H., "Degasification Through Vertical Boreholes in Methane Control in Eastern U.S. Coal Mines," USBM IC 8621, 1973.</p> <p>14. Cervik, J., "Behavior of Coal-Gas Reservoirs," SPE Paper No. 1973 presented at Eastern Regional Meeting of Society of Petroleum Engineers, November 1967.</p> <p>15. Kissell, F. N., "The Methane Migration and Storage Characteristics of the Pittsburgh,</p>	<p>Pocahontas No. 3, and Oklahoma Harshorne Coal Beds," R1 7667, 1972.</p> <p>16. Kissell, F. N. and Edwards, J. C., "Two Phase Flow in Coal Beds," USBM R1 8066, 1978.</p> <p>17. Thimons, C. D., and Kissell, F. N., "Diffusion of Methane Through Coal," Fuel, Vol. 52, October 1973.</p> <p>18. Skidmore, D. R. and Chase, R. W., Joint Communication, West Virginia University, 1977.</p> <p>19. Every, R. L., and Dell'osso, Jr., L., "A New Technique for the Removal of Methane From Coal," Canadian Mining and Metallurgy Bulletin, March 1972.</p> <p>20. Parente, C. A., "Methane Production from Coal by Carbon Dioxide Adsorption," M.S. Thesis, Chemical and Petroleum Engineering Department, University of Pittsburgh, 1978.</p> <p>21. Kuuskraa, V. A., Hammershaimb, E., and Doscher, T. M., "The Controlling Mechanism of Methane Gas From Coal Beds", Proceedings of the Second Annual Methane Recovery from Coal Beds Symposium, April 1979, Morgantown Energy Technology Center, U.S. Department of Energy, NTIS-METC/SP-79/9.</p> <p>22. Shoemaker, H. B., Rennick, G. E., Wise, R. L. and Gilmore, D. W., "Methane Production from Snodgrass No. 2, Pricetown, W. Va.," Proceedings of the Second Annual Methane Recovery from Coal Beds Symposium, April 1979, Morgantown Energy Technology Center, U.S. Department of Energy, NTIS-METC/SP-79/9.</p>
--	--

TABLE 1

METHANE PRODUCTION BY NATURAL DESORPTION

Sample No.	1	2	3	4	5
Initial CH ₄ Pressure, psia	44.45	88.20	141.70	194.50	45.30
CH ₄ Adsorbed, cc (SCF/TON)	1302 (18.88)	2762 (39.28)	4056 (58.28)	4873 (69.05)	1368 (18.94)
CH ₄ Natural Production, cc (SCF/TON)	346 (5.02)	1128 (16.04)	2240 (32.19)	3647 (51.68)	253 (3.50)
Recovery Efficiency % Adsorbed CH ₄	27	41	55	75	18

TABLE 2

ENHANCED METHANE PRODUCTION DATA
(SINGLE STATE CO₂ INJECTION)

Sample No.	1	2	3	4	5
Total CH ₄ Adsorbed Prior to CO ₂ Injection, cc (SCF/TON)	1536 (22.27)	3070 (43.65)	4527 (65.05)	4976 (70.50)	1115 (15.44)
Initial CO ₂ Pressure, psia	49.20	90.45	145.70	204.70	103.70
Total CO ₂ Adsorbed, cc (SCF/TON)	1980 (28.71)	4117 (58.55)	6434 (92.45)	8199 (116.19)	4487 (62.10)
Enhanced CH ₄ Production, cc (SCF/TON)	547 (7.93)	2178 (30.98)	4203 (60.40)	6571 (93.11)	724 (10.02)
Recovery Efficiency %	36	71	93	132	65
CH ₄ Remaining in Coal, cc (SCF/TON)	989 (14.34)	892 (12.68)	324 (4.66)	-1595 (-22.61)	391 (5.42)
CO ₂ Production, cc (SCF/TON)	36.3 (0.53)	306 (4.35)	1255 (18.04)	3222 (45.65)	229 (3.16)
CO ₂ Remaining in Coal, cc (SCF/TON)	1944 (28.19)	3811 (54.20)	5179 (74.41)	4977 (70.53)	4258 (58.94)

TABLE 3

MULTI-CYCLE CARBON DIOXIDE ENHANCED PRODUCTION DATA

	Cycle #2		Cycle #3		Cycle #4		Cycle #5	Cycle #6
	Sample #1	Sample #5	Sample #1	Sample #5	Sample #1	Sample #5	Sample #1	Sample #1
CO ₂ Pressure psia	49.40	101.70	49.20	102.70	100.30	102.10	100.10	99.70
Total CO ₂ Adsorbed, cc (SCF/TON)	3889 (56.39)	8558 (118.45)	5775 (83.74)	11468 (158.72)	10082 (146.18)	12847 (177.80)	13164 (190.88)	14829 (215.03)
CH ₄ Enhanced Production, cc (SCF/TON)	415 (6.02)	411 (5.69)	485 (7.03)	207 (2.87)	481 (6.97)	134 (1.86)	267 (3.87)	169 (2.45)
Cumulative CH ₄ Production, cc (SCF/TON)	962 (13.95)	1388 (19.21)	1447 (20.98)	1595 (22.08)	1928 (27.95)	1729 (23.94)	2195 (31.82)	2364 (34.27)
CH ₄ Remaining in Coal, cc (SCF/TON)	575 (8.32)	-20 (-0.27)	89 (1.29)	-227 (-3.15)	-392 (-5.68)	-361 (5.00)	-659 (-9.55)	-828 (-12.00)
CO ₂ Production cc (SCF/TON)	70.8 (1.03)	777 (10.75)	148 (2.15)	2190 (30.31)	842 (12.21)	2360 (32.67)	2282 (33.08)	2476 (35.90)
Cumulative CO ₂ Production, cc (SCF/TON)	107 (1.56)	1005 (13.91)	255 (3.71)	3195 (44.22)	1097 (15.92)	5555 (76.89)	3379 (49.00)	5855 (84.90)
CO ₂ Remaining in Coal, cc (SCF/TON)	3818 (55.31)	7782 (107.70)	5627 (81.59)	9278 (128.42)	9240 (133.97)	10487 (145.14)	10882 (157.14)	12353 (179.12)

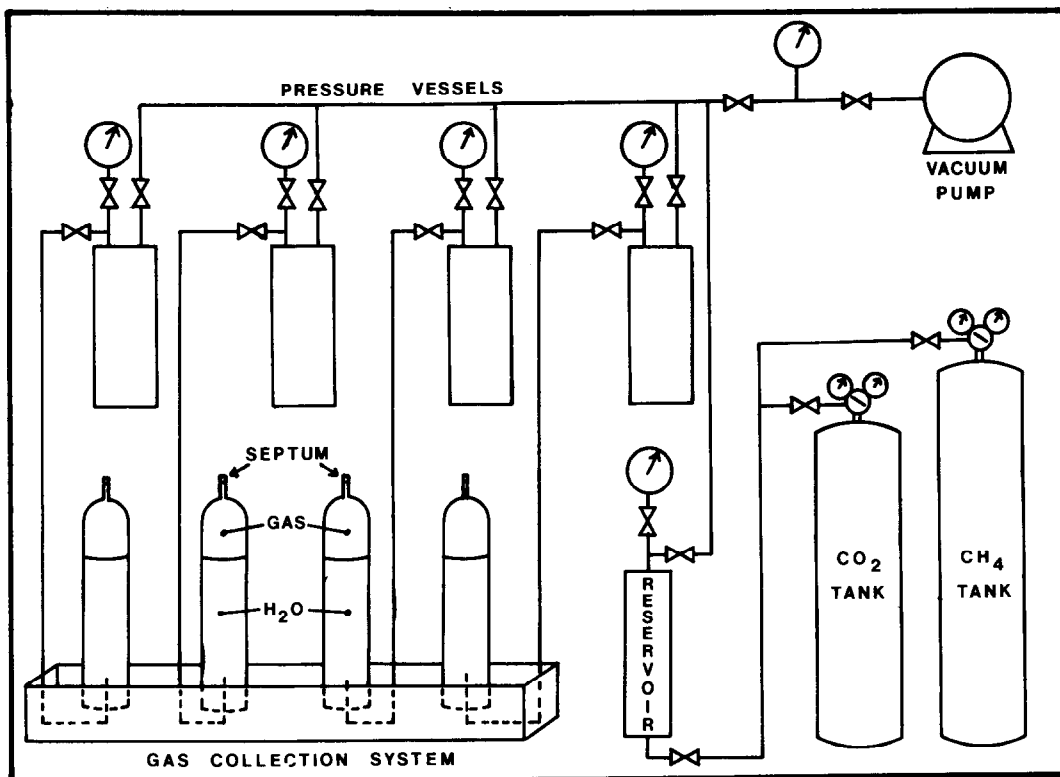


Fig. 1 - Sketch of experimental layout.



Fig. 2 - Photo of experimental equipment.

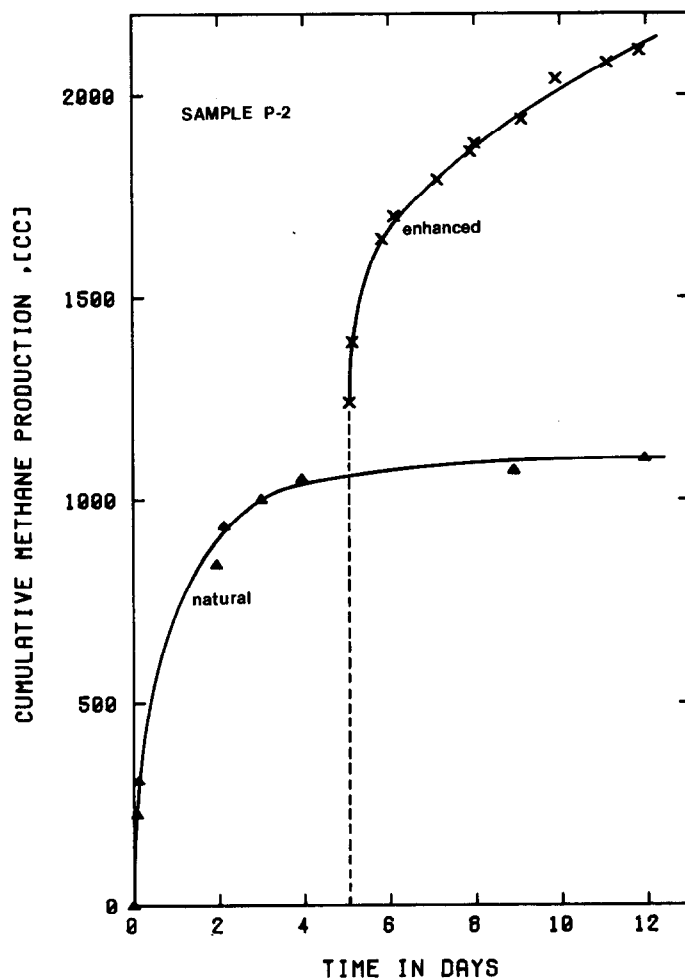


Fig. 3 - Typical results of preliminary experiments - dry core.

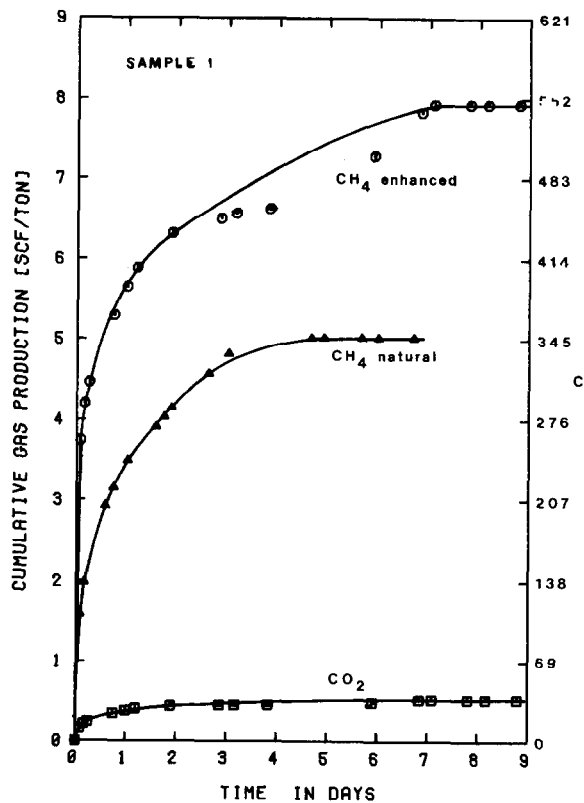


Fig. 4 - Comparison of CH₄ production by natural desorption and CO₂ enhancement, dry core - inj. press. = 45 psia.

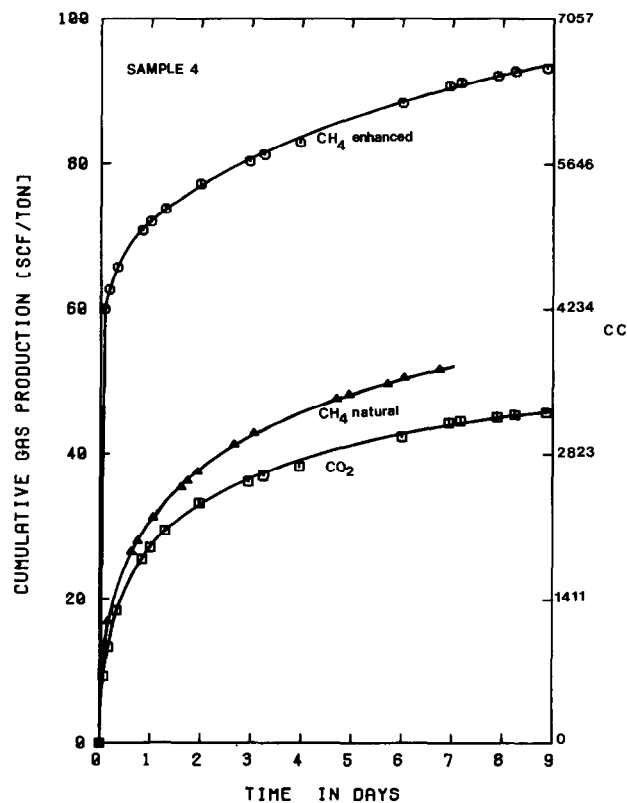


Fig. 5 - Comparison of CH₄ production by natural desorption and CO₂ enhancement, dry core - inj. press. = 195 psia.

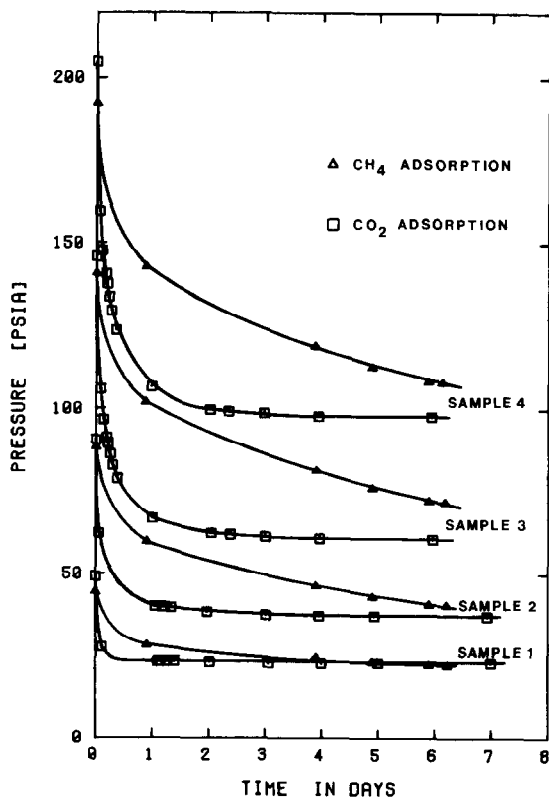


Fig. 6 - Adsorption pressure history - methane and CO₂ cycles.

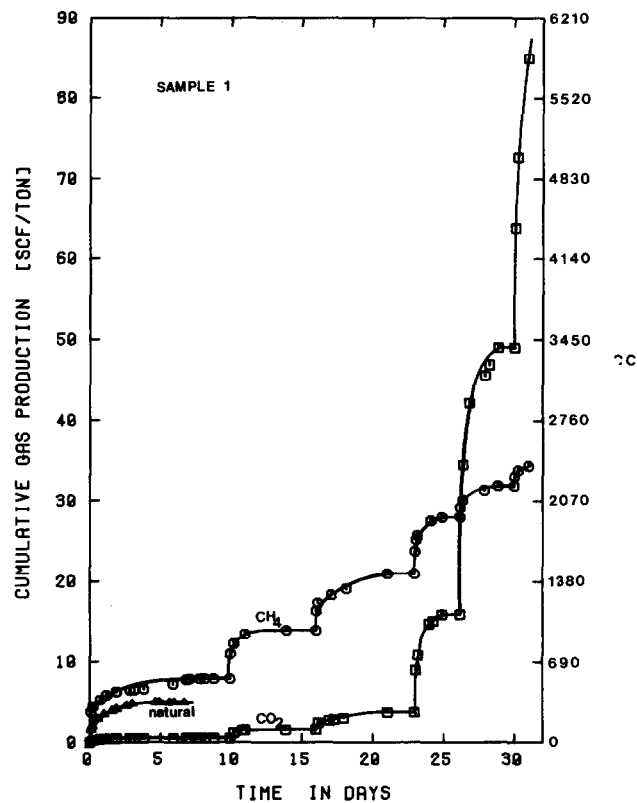


Fig. 7 - Production history - cycle CO₂ injection on dry coal sample.

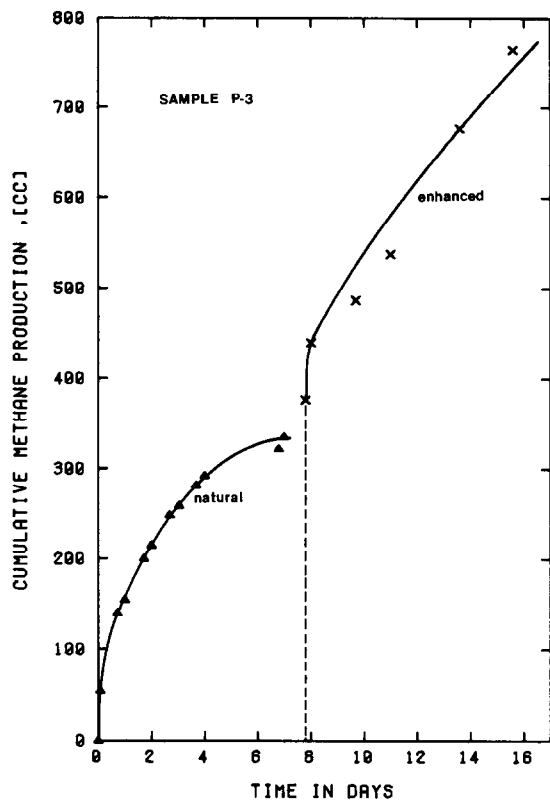


Fig. 8 - Preliminary results - water saturated sample No. P-3.

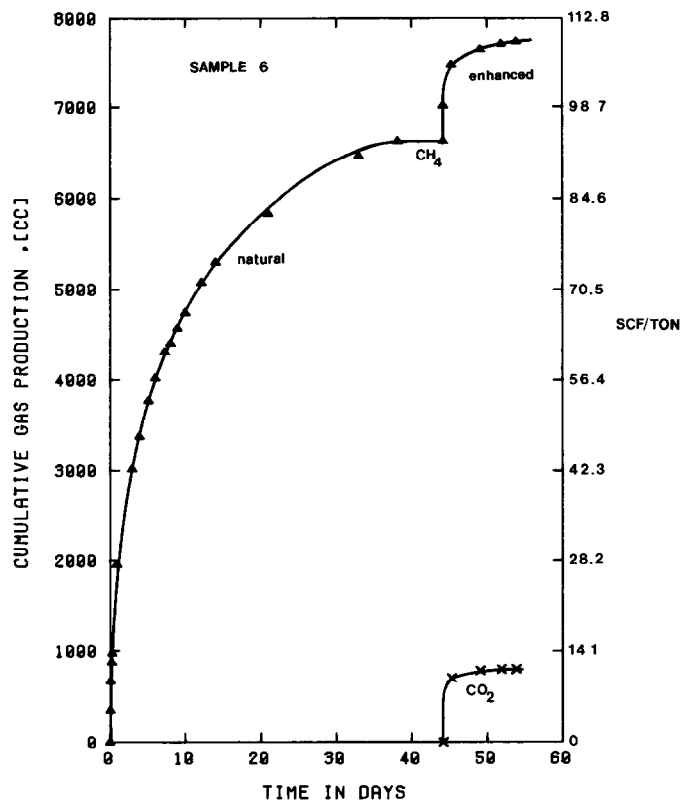


Fig. 9 - Production history - water saturated sample No. 6.

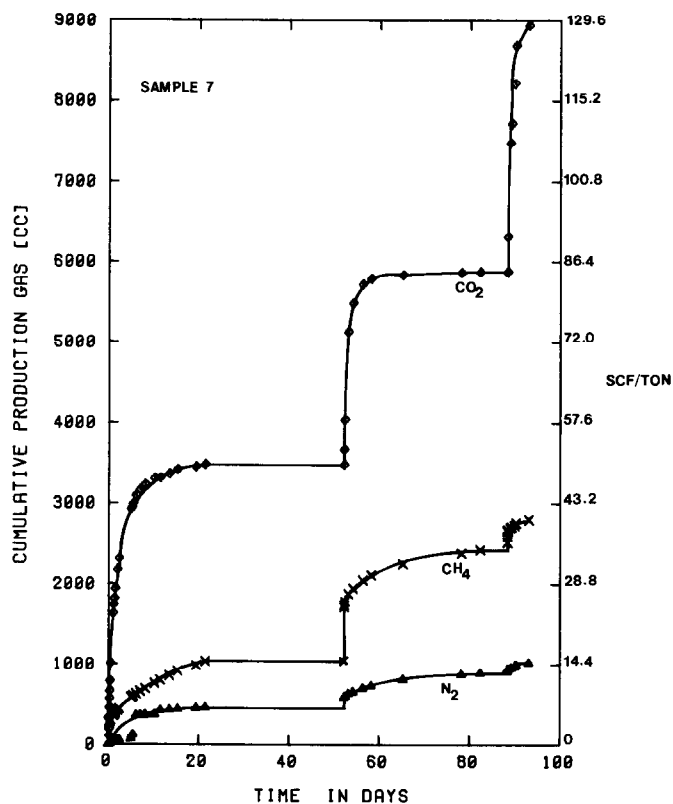


Fig. 10 - Production history - water saturated sample containing only residual in-situ methane.

EFFECTS OF A NO-PROPPANT FOAM STIMULATION TREATMENT ON A COAL SEAM DEGASIFICATION BOREHOLE

by James V. Mahoney, P.B. Stubbs, F.C. Schwerer III
and F.X. Dobscha, U.S. Steel Research

This paper was presented at the 1980 SPE/DOE Symposium on Unconventional Gas Recovery held in Pittsburgh, Pennsylvania, May 18-21, 1980. The material is subject to correction by the author. Permission to copy is restricted to an abstract of not more than 300 words. Write: 6200 N. Central Expwy., Dallas, Texas 75206

ABSTRACT

A vertical borehole drilled into a friable coal seam was stimulated by using 53,000 gallons (200.6 m³) of foam. Proppant materials were omitted from the treatment fluids and colored, fluorescent pigments were included. The borehole produced 6.6 MMcf (187,000 m³) of methane at an average rate of 49 Mcfd (1390 m³/d) during its 4-½ month lifetime. After the wellbore was mined through, both vertical and horizontal fracture surfaces were found to be decorated with fluorescent material. No significant penetration of the fluid into the overlying strata was found.

INTRODUCTION

Foam hydraulic stimulation treatments have been used to increase methane production from vertical degasification boreholes at U.S. Steel's Oak Grove Mine, near Birmingham, Alabama. Fifteen boreholes, in an area approximately two miles northeast of the active workings, have each been stimulated by using approximately 50,000 gallons (190 m³) of sand-laden foam fluid. Despite very low daily gas output from two of these holes, the average production for the 15 has been in excess of 70 Mcfd (2000 m³/d) for the past 11 months.¹⁾ Cumulatively, more than 450 MMcf (1.07 x 10⁶ m³) of methane has been removed by these degasification holes.

Before foam-stimulated degasification holes can be accepted as part of the standard sequence for development of gassy mines, two major problems must be solved. The most important of these is the potential detrimental influence of the stimulation treatment on the integrity of the strata overlying the coal. In this regard, previous experiences at Oak Grove have not been encouraging. Around two boreholes which had been stimulated with small treatments (~20,000 gallons) [76 m³], cracks were observed in the mine roof immediately above the coal-seam portions of the fracture.²⁾ Although no serious problems have been encountered to date, mine personnel are concerned that these cracks may present difficulties during pillar extraction. The second problem is the excessive operating expenses experienced for the boreholes stimulated with sand-

laden foam treatments. Sand flow-back into the wellbore has resulted in premature degradation of the dewatering equipment, abundant downtime, and the need for repetitive clean-out procedures. Each of these occurrences could seriously jeopardize the cost effectiveness of this treatment design.

Proppant and Injection Rate Criteria

Sand, or an alternative proppant, has traditionally been blended into the stimulation fluid to prevent the ground stresses of the formation from "closing" the induced fracture after the fluid pressure has been released.³⁾ Production characteristics of the boreholes at Oak Grove, however, suggest that the closure stresses in the Blue Creek coal seam are significantly less than those encountered in the strata for which stimulation treatments have traditionally been designed. It is, therefore, conceptually possible that a treatment conducted without proppant might provide gas productions comparable to those recorded on the existing sand-propped boreholes. Obviously, such a treatment would eliminate the sand-related operating problems that have been encountered.

More importantly, sandless fluid treatments provide an opportunity to fracture at lower injection rates and thereby test the theoretically developed prediction that lower fluid injection rates are more likely to confine the induced fracture within the coal zone. Very generally, fractures will extend when the frac fluid pressure exceeds the sum of the tensile strength of the solid matrix and the total opposing earth stress. If, as suspected, the tensile strength of the naturally cleated coal matrix is significantly less than that of the boundary material, or if horizontal earth stresses are significantly lower in the bounding strata than in the coal seam, then fractures would propagate more easily in the coal seam and containment of the fracture could be achieved by regulating the treatment pressure. Unfortunately, during the injection process the bottom hole pressure is likely to be significantly greater than the extension pressure at the crack tip. A pressure difference of this nature can result from frictional stresses associated with fluid flow in the fracture. For large pressure drops, the propagation pressure of the

References and illustrations at end of paper.

boundary material may be exceeded at the wellbore and the fracture may propagate out of zone. This source of pressure drop has been recognized for a long time in the oil-country hydrofracture literature; however, it assumes increased importance in hydrofracture of relatively shallow coal seams with correspondingly lower earth stresses and fracture propagation pressures.

In a design model currently being developed,* this "viscous pressure loss" responds to the fluid injection rate according to a power relationship that is determined by the nature of the fluid flow, laminar or turbulent. In either case, the pressure loss can best be kept to a minimum by injecting the stimulation fluids at very low rates. Treatments containing high-density solids, such as sand, require injection rates sufficiently high to suspend and transport the proppant material. The foam treatments conducted by U.S. Steel at the Oak Grove site ensured solids suspension by employing an injection rate of approximately 10 barrels per minute ($0.03 \text{ m}^3/\text{s}$). As previously mentioned, the areas around two such holes have been mined through and, in each case, fractures were observed in the roof rock. A treatment conducted without any proppant, on the other hand, could employ injection rates as low as 2 barrels per minute ($0.005 \text{ m}^3/\text{s}$) with standard commercial equipment.

Site Selection, Borehole Installation, and Stimulation Treatment

Our desire to test both the gas-production and fracture containment properties of a no-proppant foam-stimulation treatment required that the hole be placed sufficiently close to active mining to allow near-term mine-through. The hole, on the other hand, would have to be remote enough to provide near virgin reservoir conditions and at least six months of production before intercepted by mining. To satisfy these requirements, the borehole was sited above a six-entry section approximately 1500 feet (460 m) in advance of active mining, Figure 1. Eventual inspection of the wellbore and the area affected by the treatment was facilitated by targeting the borehole to penetrate the Blue Creek coal seam in an entry immediately adjacent to the planned left return air course. The borehole was identified as No. 1-West.

Site preparation began on November 1, 1978, and by November 28, No. 1-West was ready for testing and stimulation. The borehole consisted of approximately 40 feet (12 m) of grouted 8-5/8-inch (219 mm) casing to protect ground water, 1102 feet (336 m) of grouted 6-5/8-inch (168 mm) casing to isolate overlying formations, and a 5-7/8-inch (149 mm) diameter open-hole segment approximately 56 feet (17 m) in length.

A suite of geophysical logs (caliper, gamma ray, and bulk density) was used to assess the borehole conditions and stratigraphy of the open hole segment. Descending from the bottom of the casing (Figure 2), No. 1-West comprised 34 feet (10 m) of shale overburden, 2.5 feet (0.8 m) of Mary Lee coal seam, 6 feet (1.8 m) of shale parting, 5.5 feet (1.7 m) of Blue Creek Seam, and 8 feet (2.4 m) of fireclay material underlying a thin shale parting used as the mine floor. An additional assessment of the total borehole length was made by using a submersible television camera that had an integral light source and could be lowered from the surface. Besides the immediate monitor output, this system provided a video recording that allowed comparisons to be made with similar recordings obtained

at later dates. The initial video inspection indicated that the entire open-hole segment was concentric, all the noncarbonaceous strata were tight and unjointed (within the 1/32-inch (0.07 mm) camera resolution), and the two coal seams were somewhat porous and cleated although very little spalling had occurred during drilling.

Before No. 1-West was stimulated, a horizontal notch was eroded at approximately the midpoint of the producing formation, the Blue Creek coal seam. The notching procedure consisted of pumping a slurry containing 2 pounds (0.9 kg) of 20- by 40-mesh (0.84 mm by 0.42 mm) sand per gallon ($3.8 \times 10^{-3} \text{ m}^3$) of water through two 3/16-inch-diameter (4.8 mm) nozzles located at the target depth. Slurry injection began at 2 bbl/min ($19 \text{ m}^3/\text{h}$) and was eventually increased to 2.75 bbl/min ($26.3 \text{ m}^3/\text{h}$). An average wellhead pressure of 1800 psi (12.4 MPa) was recorded during slurry pumping. Throughout the injection period the slurry tubing was rotated at approximately 4 rpm. Within 11 minutes of initial injection, coal particles were observed in the effluent emitted from the annular space between the borehole casing and the slurry tubing. Cumulatively, the notching process consumed 2268 gallons (8.58 m^3) of water and 5500 pounds (2495 kg) of sand over a 27-minute period. The effect of the procedure was assessed by a second television survey. Beginning at the midpoint of the coal seam and extending to the interface with the bottom material, a large cavity had been eroded through a full 360-degree arc. The maximum radius of the cavity was greater than the 15-inch (38.1 cm) radius-of-view of the camera.

In preparation for the treatment, a 10-foot-long (3 m) inflatable packer was attached to the frac tubing and positioned in the hole such that all strata above the Blue Creek Seam would be isolated from the hydraulic stimulation pressure. The sealing element of the packer extended from 1/2 foot (0.15 m) into the top of the Blue Creek Seam to 1/2 foot above the Mary Lee Seam. As on previous boreholes, formation breakdown was initiated with clear water. Injection began at 1/4 bbl/min ($2.38 \text{ m}^3/\text{h}$) and was increased by 1/4 bbl/min ($2.38 \text{ m}^3/\text{h}$) increments until fracture initiation was achieved at a pumping rate of 1-1/4 bbl/min ($11.9 \text{ m}^3/\text{h}$). A breakdown pressure of 1000 psig (6.9 MPa) was measured at the wellhead.

While preparations were being made to resume the treatment with foam, water was observed flowing out of the wellhead from the annular space between the borehole casing and the frac tubing. Because the treatment thus far had represented the least disruption of the formation that was physically possible, it was decided to delay the foam treatment long enough to determine whether a fracture had already been created upward, beyond the extent of the packer element. Before the packer was removed, however, 10 barrels (1.6 m^3) of fresh water containing 3 gallons (0.01 m^3) of red fluorescent paint and 1 pound (0.45 kg) of fluorescein dye were injected into the hole. Another 10 barrels (1.6 m^3) of water were injected to flush the tubing and to push the paint into the formation. In total, only 2200 gallons (8.33 m^3) of water were injected during this aborted treatment.

The use of fluorescent paint as a tracer material had been an integral part of the planned treatment. The siting of No. 1-West would eventually allow extensive inspection of a large area around the borehole and, therefore, the fluorescent paint would act as an easily detectable means to identify the path of the

*U.S. Steel Research project

frac fluids. Along these lines, the red fluorescent paint used toward the end of the water-injection phase would help to resolve the effect of this small treatment.

When the packer was removed, two 180-degree opposed, longitudinal impressions were observed along a 6-foot (1.8 m) length of the rubber sealing element. The impressions, which were approximately 1/16 inch (1.6 mm) in width (see Figure 3), appeared to be artifacts of cracks in the wellbore. This possibility was confirmed by a third television survey that revealed two score marks in the wellbore extending in a vertical direction from the top of the Blue Creek Seam through the "middleman" to the base of the Mary Lee Seam. It was impossible from the video survey to ascribe any parting width to these cracks. Possibly, the pressure used to inflate the packer element was sufficient to cause separation and may have actually created the cracks sometime prior to fluid injection.

After the packer was replaced at its previous location, the formation was stimulated with 53,000 gallons (200 m³) of 75 percent quality foam containing blue fluorescent paint and fluorescein dye.* Blue fluorescent paint was included to distinguish the penetration of the foam treatment from that of the earlier water treatment. Foam injection began at 2 bbl/min (19 m³/h) and was increased every half hour in 1 bbl/min (9.5 m³/h) increments until 5 bbl/min (47.8 m³/h) was reached. At this point the injection rate was maintained constant for 1-½ hours. The injection sequence was completed at 6 bbl/min (57 m³/h) for a similar 1-½ hour period. During the treatment, the maximum wellhead pressure of 2000 psig (13.8 MPa) was recorded at this latter rate.

Two hours after completion of the treatment, the wellhead valve was opened to allow the stimulation fluids to flow back through a 32/64-inch (13 mm) choke. The effluent was a water/foam mixture that was emitted in a 40-foot (12 m) arc. After 12 hours the initial pressure of 750 psig (5.2 MPa) behind the choke had decreased to approximately 300 psig (2.1 MPa). Within 1-½ days the effluent changed from the water/foam mixture to mainly gas, with occasional minor unloadings of water. The hole was allowed to produce gas for nine more days before it was intentionally flooded so that the packer could be removed and the dewatering equipment installed.

Production History

Immediately prior to activation of the dewatering equipment on February 13, 1979, all surface valves in the gas-production line were closed to prevent gas flow beyond the wellhead. Experience at Oak Grove has indicated that a shut-in wellhead is very effective in controlling the severity of the unloading episodes that are likely to occur during the initial production period. (The term unloading refers to those instances when water from the wellbore and the immediate reservoir area is rapidly carried to the surface by large volumes of expanding coalbed gas.¹⁾) Gas and water velocities are sufficiently high during unloading to transport solid debris from the bottom of the borehole to the surface. The moving solids invariably cause mechanical breakdown of the dewatering equipment.

*The paint concentration was maintained at 1 gallon/80 barrels of foam and fluorescein was added at a concentration of 1 pound/80 barrels of foam.

With a shut-in wellhead, the gas that is produced as the water column in the wellbore is lowered causes a pressure buildup near the surface. This increasing wellhead pressure partially compensates for the decreasing hydrostatic pressure and effectively reduces the vertical gas velocity in the wellbore.

Sixteen hours after the dewatering pump on No. 1-West was started, enough gas had been produced to create a wellhead pressure in excess of 125 psig (0.86 MPa). To prevent subsequent unloading, the surface valves were slowly opened over a period of 4 days, and by February 22 the hole was producing 81 Mcfd (2300 m³/d) against a back pressure of 66 psig (0.05 MPa) (see Figure 4). For the first 76 days of operation, No. 1-West was produced against an average wellhead pressure of 28 psig (0.19 MPa). During this same period the recorded gas flows decreased nearly linearly to a value of 21 Mcfd (595 m³/d). As is evident in Figure 4, significant deviations from a monotonic decline were observed on March 9 and between April 10 and May 1. The later calendar period coincides with our efforts to rapidly reduce the back pressure from approximately 20 psig (0.14 MPa) to zero. The possibility exists that the gas production was reflecting abrupt changes in the reservoir conductions brought about by alterations of the wellhead pressure. Unfortunately, no cause is evident for the deviation on March 9, but this event appears suspiciously similar to the production curves observed at other boreholes during minor unloading episodes.

Except for a brief initial period, water production for the first three months remained relatively constant at 300 gal/day (1.14 m³/d) with the pump located approximately 22 feet (6.7 m) above the producing formation. On May 8 the pump was lowered 25 feet (6.7 m) so that the inlet was located at the midpoint of the Blue Creek coal seam. Water production immediately increased to 1058 gal/day (4 m³/d), but declined over a 12-day period to nearly its previous value. Within three days of lowering the pump, gas production increased from 26 Mcfd (736 m³/d) to more than 70 Mcfd (1980 m³/d) and was no longer characterized by a monotonic decline curve. Although the gas flows again began to decline after a brief stabilization period, the magnitude of the daily production remained more than four times that extrapolated from the previous decline curve.

Between May 13 and 15, the dewatering pump was inoperative and, consequently, the gas production was observed to decrease. One week later the gas production again demonstrated a precipitous decline. At the same time, the wellhead pressure gauge began to register a value of 1 psig (6.9 kPa). The pressure gauge used on this hole, however, was inappropriate for accurate measurement at low values and it is entirely possible that as much as 5 psig (35 kPa) back pressure was imposed on the hole until June 27. On this date the pump was removed from the hole in preparation for mine-through. No. 1-West was still producing 35 Mcfd (990 m³/d) even though mining operations were within 95 feet (29 m). Gas production continued without dewatering equipment until July 3 when the active face intercepted the borehole. During its 4-½ month production lifetime, No. 1-West removed a total of 6.6 MMcf (187,000 m³) of methane at an average rate of 49 Mcfd (1390 m³/d).

Production Events Associated with Mine Development

While No. 1-West was being installed, the coal seam segment of the borehole was approximately 1500 feet (457 m) in advance of active mining. Soon after the dewatering equipment had been activated, the development section was within 1250 feet (381 m) of the hole and was advancing at an average rate of 65 feet (20 m) per week. This moving boundary had associated with it a drainage distance or effective reservoir area. The gas contained within this area was transported to the mined regions of the section. Earlier measurements at another location indicated that the effective drainage distance extended much more than 500 feet (152 m) into the undeveloped coal. Large drainage distances can be partially justified by the high pressure gradients thought to exist at Oak Grove and the potential existence of a very permeable crushed zone that could surround areas of active mining.⁴⁾ Contributing to the pressure gradients are the below-atmospheric pressures created at the mine perimeter by the "exhausting" ventilation system of the mine, and the measured virgin seam gas pressure in excess of 400 psi (2.8 MPa).⁵⁾

It could be expected, then, that at some time the effective reservoir area of the advancing section would overlap that of No. 1-West and the two drainage points would compete for the stored methane. As the moving boundary approached the hole, the increasing level of competition might cause a production decline curve similar to that observed. Furthermore, once interference of the two reservoir areas occurred, any changes in the rate of face advance might be reflected in the slope of the gas decline curve.

Figure 5 compares the gas production with the changing distance between the borehole and the working area. The mine advance curve (dotted line) during the time corresponding to the first 76 days of gas production has been segmented into three periods. Each period represents a time during which the mine advance was relatively constant on a weekly basis.

For the four-week period between February 19 and March 18, period A, mining operations moved toward the borehole at an average rate of 75 feet (23 m) per week. During this same time, the gas production declined from the maximum rate of 81 Mcfd (2300 m³/d) to approximately 52 Mcfd (1500 m³/d), a decrease of nearly 1040 cf (29.5 m³) for each day of the period. The following four weeks (B), the mine advanced at an average rate of 50 feet (15 m) per week with a corresponding production decline of only 482 cf (13.7 m³) for each day of the period. A high rate of advance was again established by the mine for the next two weeks (C). Unfortunately, this period coincides with the previously discussed erratic gas production. Nonetheless, a general correlation is still evident between the rate of advance and the declining gas production.

Although the above causal description provides a tidy explanation for the observed production decline, caution should be exercised when attaching emphasis to it. As has been indicated, No. 1-West was influenced by a wide variety of parameters that significantly altered the gas production. The suggested effect of mine advance was less pronounced and, therefore, more speculative than the other influencing parameters. Some additional data exist, however, that support the concept of interfering reservoir areas. After the hole was stimulated and prior to installation of the dewatering equipment, the hole produced gas at high rates for nine days before being intentionally "killed" by

flooding the wellbore with water. Considering relative-permeability concepts and the behavior of other degas holes at Oak Grove, it is likely that the water content of the coal seam had already been appreciably reduced in the vicinity of the wellbore. The most probably drainage point in this region would have been the mine section approximately 1400 feet (427 m) away.

In-Mine Analysis of the Fracture Pattern

Mining operations intercepted No. 1-West on July 12, 1979, and continued a westerly development of the section for another 450 feet (137 m). A slight deviation of the mining plan was required to reveal the borehole which, after coal extraction, was located very close to the southeast corner of a support pillar. Figure 6 is a representation of this area immediately after mine-through. Near the borehole a large cavity had been effectively eroded by the abrasi-jetting procedure. The cavity's lower extremity, which was located 12 inches (30.5 mm) above the floor material, was nearly horizontal and was covered with 2 inches (51 mm) of sand. Although only one third of the original cavity remained, it appeared to have been symmetrically conical with a base radius of 36 inches (914 mm) and a height of nearly 23 inches (584 mm).

The effect of the stimulation treatment on the mined interval and the immediate overburden was analyzed by making repeated inspections of all the exposed areas within the section. A long-wavelength, ultra-violet light rated permissible for coal-mine service was used to reveal the fluorescent material that had been included as part of the treatment design. Around the vicinity of the borehole, two features became instantly evident; both vertically and horizontally oriented surfaces were decorated with red and blue fluorescent paint. A few feet to the northeast of the borehole, vertical fractures were observed to be propagated through the upper half of the coal seam. The fractured zone was approximately 3 feet (0.91 m) wide at this point and contained numerous parallel surfaces - one of which is depicted in Figure 6. Most decorated planes within this zone had an azimuthal strike that nearly coincided with the predominant face-cleat direction, N61°E.

Except for the inner perimeter of the wellbore and one very tight roof joint within 8 feet (2.4 m) of the hole, no evidence could be found of possible fracture penetration into the upper roof rock. The two 180-degree opposed cracks observed within the wellbore extended from the top of the Blue Creek Seam through the rock parting to the bottom of the Mary Lee coal seam (refer to Figure 2) and probably were responsible for the impressions that had been observed on the rubber packer element.

The observed horizontal decoration was confined to the slickensided surfaces of two coal stringers found at the top of the mined interval. As shown in Figure 7, the mined interval generally included the 5.5 feet (1.7 m) of Blue Creek coal and two 4- or 5-inch-thick (102 or 127 mm) carbonaceous shale layers separated by the coal stringers. These slickensided coal surfaces demonstrated very little adhesion to the surrounding strata and appeared to have prevented upward growth of the induced fractures. It was not uncommon to observe an abrupt termination of the vertically decorated planes wherever they abutted one or the other coal stringer.

Inspection of these slickensided surfaces around

the perimeter of each support pillar in the section indicated that the region affected by horizontal penetration of the fracture fluids described an elliptical area, as shown in Figure 8. The curves that best surround the decorated regions are composed of two separate elliptical lobes. The lobe with northeast axis of symmetry has semiaxes of 230 (70.1 m) and 88 feet (26.8 m) while the semiaxes of the southwest lobe are 240 (73.2 m) and 105 feet (32.0 m). Both axes of symmetry trace a strike of N63°E, which nearly corresponds to the strike of the observed vertical fracture planes. The total area circumscribed by both ellipses amounts to approximately 71,000 square feet (6600 m²).

A similar detailed analysis of the vertical surfaces decorated with fluorescent paint provided both an estimate of the total "fracture length"* and a possible explanation for the displacement of the larger elliptical lobe away from the wellbore. Figure 9 depicts with arrowheads each location in the developed section where fluorescent paint was observed along vertical surfaces. Except for the solid arrowheads, the strike of these planes closely approximated the most predominant face-cleat direction at Oak Grove. As indicated earlier, the vertically decorated surfaces were often found to occur as numerous parallel planes in a zone spanning a few feet. This observation was particularly true within the areas circumscribed by the ellipses. Outside the elliptical areas, on the other hand, the vertically decorated fracture wings were generally confined to a single plane. The height of these planes decreased as the distance from the wellbore increased. This shrinkage generally occurred from the bottom of the fracture so that, at their extremities, the decorated surfaces had a total height of only a few inches and were completely confined to the upper portion of the mined interval.

Fracture-height differences were also observed between the two wings. The fracture comprising the northeast trending wing were mainly confined to the upper 3 feet (0.91 m) of the mined interval. Those comprising the southwest wing, however, had propagated for most of their total length with a floor-to-roof extent. The maximum observed lengths of the two wings were 315 (11.0 m) and 370 feet (12.9 m), respectively. It is interesting to note in Figure 9 how these extreme points are located almost exactly along the projected symmetry axes of the ellipses.

The observations made at the locations indicated by the solid arrowheads provided a possible explanation for the fracture displacement away from the wellbore in the southwest. These three points represent the only areas in the entire section where evidence was found that fracture fluids had penetrated along the butt-cleat direction, that is, approximately normal to the direction of the face cleats. It is theorized that as the fractures proceeded out from the wellbore in the favored direction, they intercepted this region of preexisting butt fractures and some treatment fluid was directed normal to the previous fracture growth. The fluid directed along butt fractures would probably intersect numerous face cleats and growth could be reinitiated along the favored direction.

*For our study, caution should be exercised when relating all the vertically decorated planes to the "fracture length". Because coal contains natural fractures (cleats), the potential existed for the fluorescent treatment fluids to penetrate the formation without creating new matrix separation. Wherever this might have occurred, the decorated surfaces should not be considered part of the fracture length.

This scenario not only helps to explain the displacement of the symmetry axis but also rationalizes why more vertical fractures over a larger area were observed toward the southwest. In the main, the decorated surfaces northeast of the borehole were found very close to the projection of the symmetry axis. Toward the southwest, however, vertically decorated surfaces were found throughout the inscribed area of the ellipse. This region was apparently influenced by the butt fractures. Outside this region, the fractures were considerably more confined to the vicinity of the symmetry axis.

In total, the patterns outlined by the horizontally and vertically decorated surfaces, as shown in Figures 8 and 9, respectively, provided the most comprehensive analysis obtained to date of coal-seam penetration by treatment fluids. The fluorescent tracer technique was found to be so sensitive, in fact, that some question exists as to whether or not all the decorated surfaces were truly part of the fracture length. Fluid leak-off has always been a primary concern when designing stimulation treatments for coal seams and might have been responsible for decorating a significant portion of the surfaces observed in our study.

Conclusions

Because of some combination of (1) local geologic conditions, (2) effective horizontal abrasi-jetting, and (3) a low-rate foam treatment without proppant, this specific hydrofracture design yielded a degasification borehole with a gas production schedule acceptable for coal seam degasification. Additionally, this single treatment did not propagate the induced fractures into the overlying strata and may offer technology which will allow production of gas without dangerous damage to the strata above and below the seam. The inclusion of fluorescent pigment into the stimulation design was an effective method of tracing the penetration of the treatment fluids.

Near-mine boreholes are influenced by a set of reservoir conditions that are distinct from those influencing more remote boreholes. The dehydration of the coal seam by the ventilation air and the negative relative pressure within the mine rapidly reduce the water saturation in the reservoir area and initiate early gas production. These effects make it imperative to operate the borehole with a minimum of back pressure. Similarly, the dewatering pump should be placed at or below the producing formation to reduce this component of the bottom hole pressure and to increase the relative permeability of the coal seam.

ACKNOWLEDGEMENTS

The authors express sincere appreciation to S.W. Lambert, Technical Project Officer, of the Department of Energy and to M. A. Trevits of the Bureau of Mines for their valuable technical assistance. Also, we wish to recognize the U.S. Department of Energy for cooperation and support through the cost-sharing Contract No. ET-75-C-01-9027.

EFFECTS OF A NO-PROPPANT, FOAM STIMULATION TREATMENT
ON A COAL SEAM DEGASIFICATION BOREHOLE

REFERENCES

- | | |
|---|---|
| <p>1) P. B. Stubbs, F.X. Dobscha, and J.V. Mahoney, "Degasification of the Blue Creek Coal Seam at Oak Grove Mine", Proc. of the Second Annual Methane Recovery for Coalbeds Symposium (April 1979), METC/SP-79/9, 96-113.</p> <p>2) S.W. Lambert and M.A. Trevits, "Methane Drainage Ahead of Mining Using Foam Stimulation - Mary Lee Coalbed, Alabama", U.S. Department of Energy Report of Investigation PMTC-3(79), January 1979, 1-22.</p> <p>3) S.W. Lambert, M.A. Trevits, and P.F. Stiedl, "Vertical Borehole Design and Completion Practices Used</p> | <p>to Remove Methane Gas from Mineable Coalbeds", U.S. Department of Energy Report of Investigation - To be released.</p> <p>4) F.N. Kissel, "The Methane Migration and Storage Characteristics of the Pittsburgh, Pocahontas No. 3, and Oklahoma Hartshorne Coalbeds", U.S. Bureau of Mines Report of Investigations 7667, 1972.</p> <p>5) C.H. Elder, and M. Deul, "Degasification of the Mary Lee Coalbed Near Oak Grove, Jefferson County, Alabama, by Vertical Borehole in Advance of Mining", U.S. Bureau of Mines Report of Investigations 7968, 1974, 1-21.</p> |
|---|---|

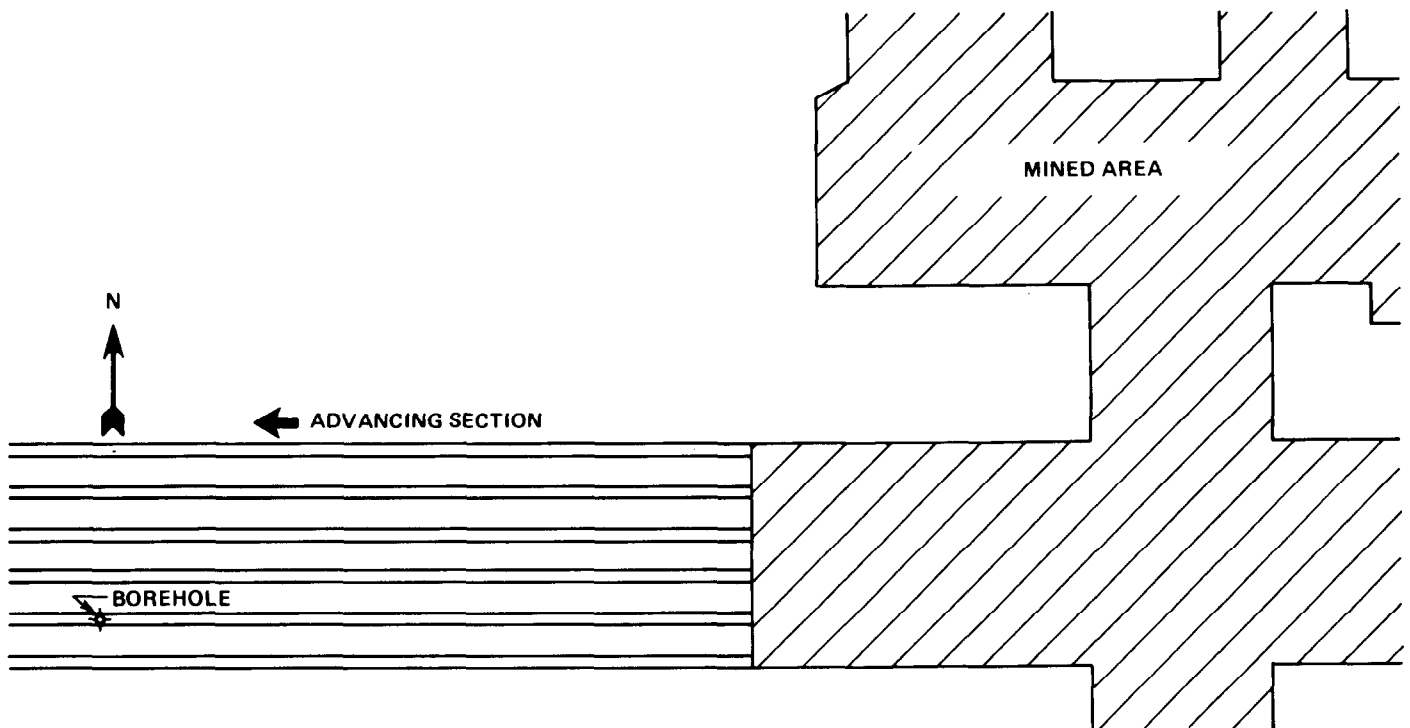


Fig. 1 - The region of Oak Grove Mine around the Degas Borehole No. 1-West.

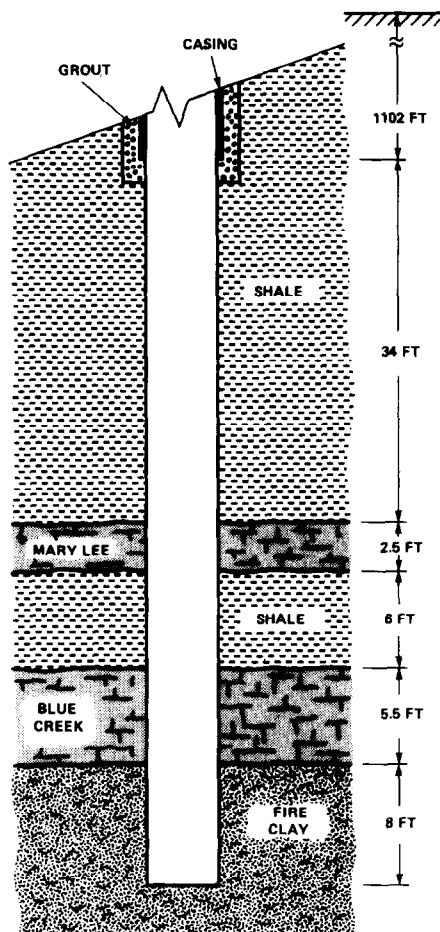


Fig. 2 - Stratigraphy of the open-hole segment.

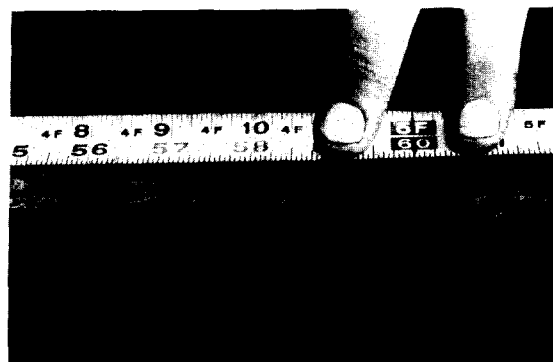


Fig. 3 - The crack impression remaining on the rubber packer element.

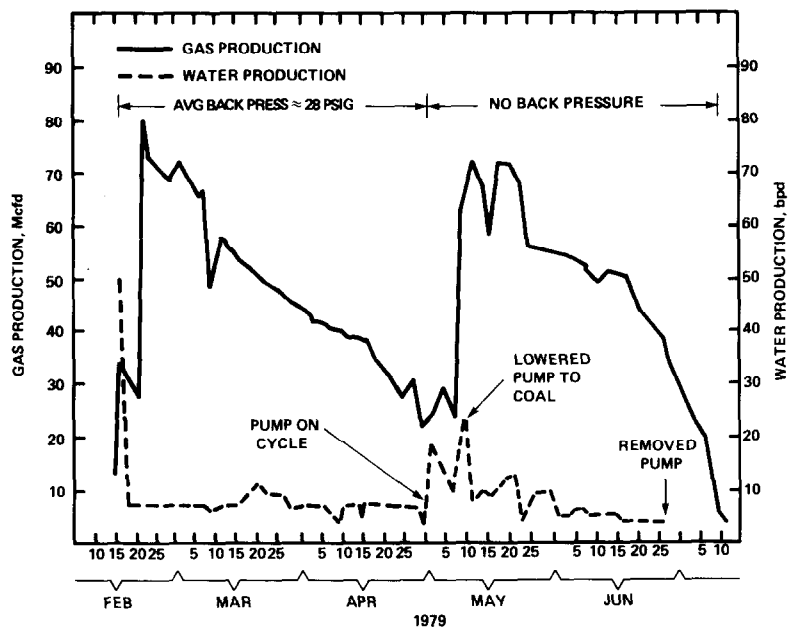


Fig. 4 - Gas and water production curve.

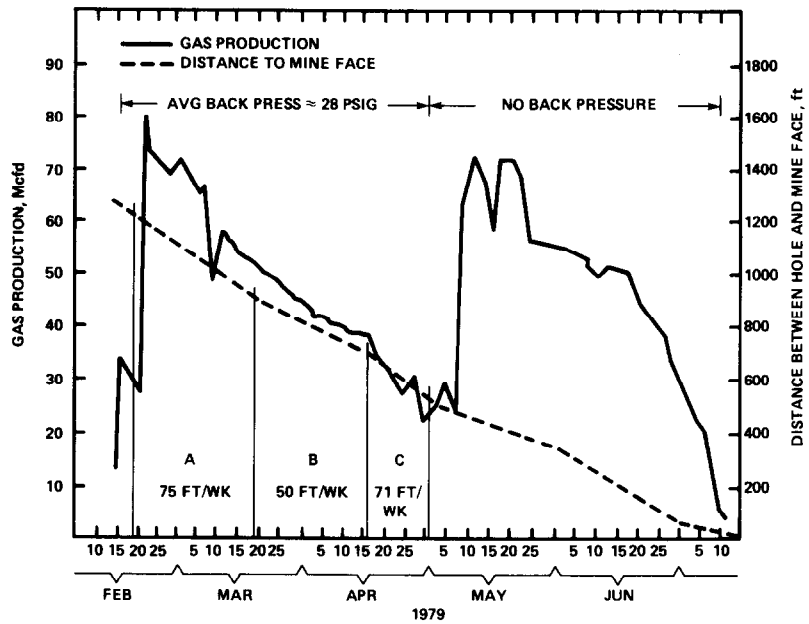


Fig. 5 - Gas production related to the advancing section boundary.

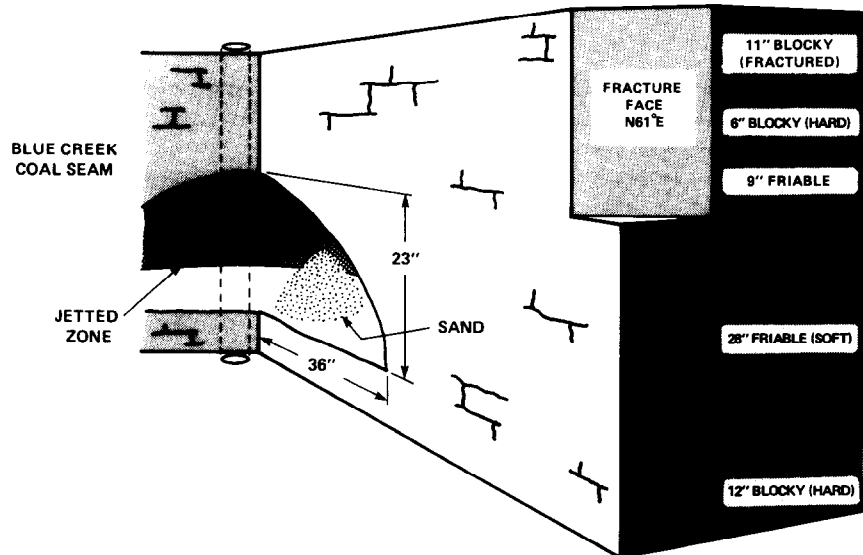


Fig. 6 - Coal seam segment of the borehole immediately after mine-through.

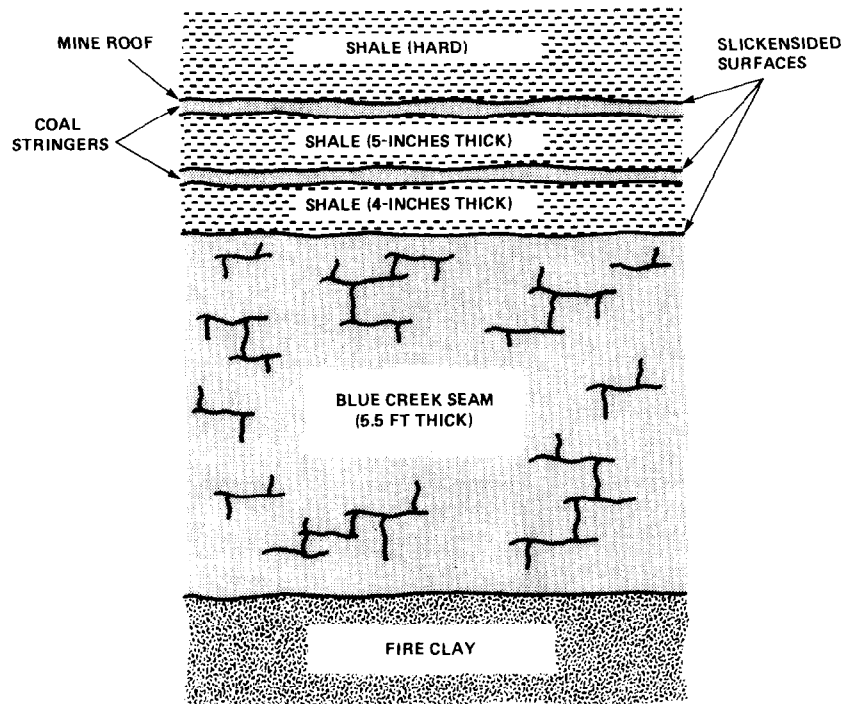


Fig. 7 - Stratigraphy of the mined interval and the immediate boundary layers.

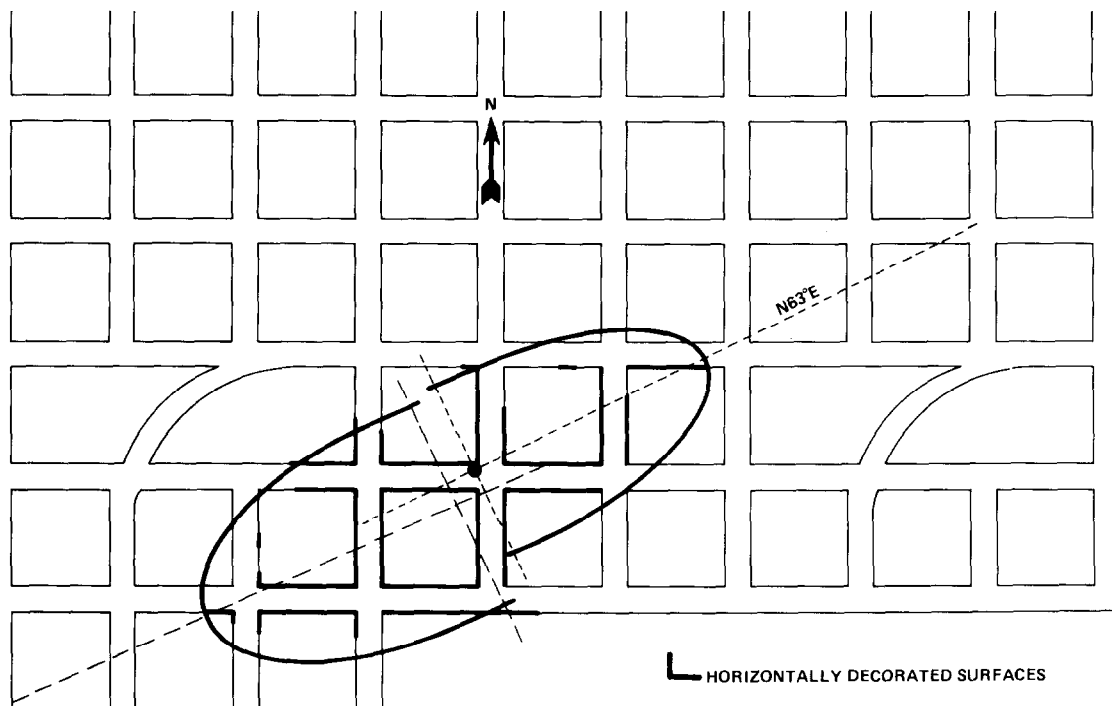


Fig. 8 - Areas where horizontal surfaces were observed to be decorated with fluorescent paint.

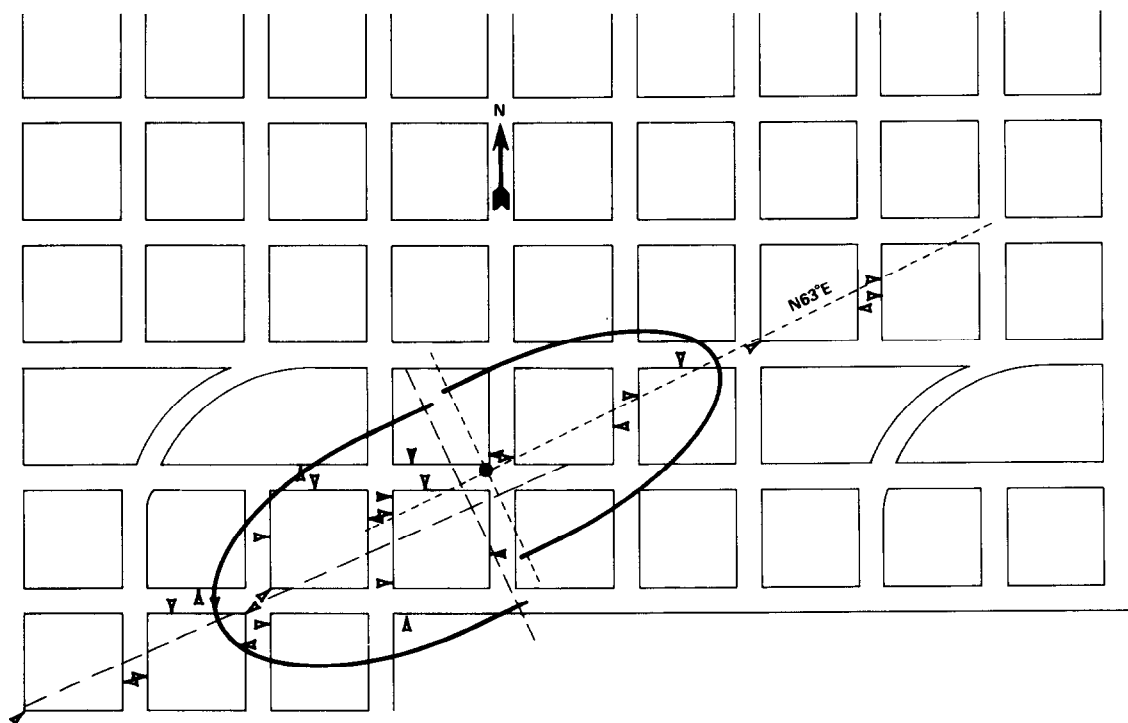


Fig. 9 - Locations where vertical surfaces were observed to be decorated with fluorescent paint.

IN SITU STRESSES: THE PREDOMINANT INFLUENCE ON HYDRAULIC FRACTURE CONTAINMENT

by Norman R. Warpinski, Richard A. Schmidt and
David A. Northrop, Sandia National Laboratories.

6

This paper was presented at the 1980 SPE/DOE Symposium on Unconventional Gas Recovery held in Pittsburgh, Pennsylvania, May 18-21, 1980. The material is subject to correction by the author. Permission to copy is restricted to an abstract of not more than 300 words. Write: 6200 N. Central Expwy., Dallas, Texas 75206

ABSTRACT

In situ experiments, which are accessible by mineback, have been conducted to examine the parameters that control hydraulic fracture containment. These experiments show conclusively that material property differences at an interface are insufficient to arrest crack growth. Present models that predict the fracture should be contained at the interface because the stress intensity factor at the fracture tip goes to zero as the interface is approached are inadequate, and an improvement is suggested.

However, sharp increases in the minimum principal in situ stress (as may occur at faults) and steep gradients in that stress have been shown to be effective barriers to crack propagation. Examples of fractures terminating at faults and parting planes illustrate how discontinuities in the in situ stress can arrest fracture growth. Furthermore, experiments were conducted in a formation which contained a steep gradient in the minimum principal in situ stress and which was overlain by a formation with a factor of five greater modulus. In each case, fractures were observed to terminate at regions of high minimum principal stress but to propagate readily into the higher modulus formation.

INTRODUCTION

Hydraulic fracturing has been used extensively for more than thirty years to stimulate the production of natural gas from many different reservoir rocks. Most of these treatments were small since their primary purpose was to link the wellbore to the undamaged reservoir rock, a distance ranging from a few meters to a few tens of meters depending on the conditions. With the increasing depletion of the conventional natural gas reserves, attention has been focused on producing gas from unconventional

gas resources such as tight gas sands and Devonian shales.

At the present time, stimulation of these formations is being attempted by massive hydraulic fracturing, at least an order of magnitude scaleup of conventional fracturing treatments. Here it is proposed that fractures of over 1000 m length be propagated in the low-permeability, gas-bearing formations to provide a high conductivity path for the gas to reach the wellbore. Unlike small conventional treatments in which the fractures are only propagated a short distance, it is imperative that the large and massive hydraulic fractures be contained largely to the pay zone. Obviously, if only a small portion of the fracture surface is in contact with the reservoir rock, the result may well be an uneconomic well in a reservoir that, in fact, has sufficient resources if stimulated correctly. Detrimental results will occur should the fracture break into a water-bearing zone.

When referring to massive hydraulic fracturing in the tight gas sands, containment may refer to confinement of the fracture to specified intervals comprised of both gas-bearing, sandstones lenses and surrounding shale zones or to the usual concept of confinement within a single reservoir zone. In either case, the study of the containment of hydraulic fractures is directed toward determining the parameters and the conditions which will limit the height of a fracture and control its direction of propagation so that the necessary fracture lengths will be obtained. Implicit in these studies is the presumption that sufficient understanding of these conditions will allow operators to alter treatment parameters to help control containment, at least in those formations where there is already some propensity for containing the fractures. If this is not possible, then, it still may be possible to define, a priori, those zones that will most likely provide economic production due to

References and illustrations at end of paper.

favorable fracture growth (or containment) conditions.

BACKGROUND

The parameters that are considered to have some effect on the containment of hydraulic fractures have been detailed previously in the literature. A difference in elastic modulus between the reservoir rock and the barrier rock is usually singled out as the primary mechanism controlling containment. In their work on composite materials, Cook and Erdogan¹ calculated the stress intensity factor for a two-dimensional crack approaching an interface between two materials with different elastic moduli. Simonson et al.² and Rogers et al.³ applied these results to hydraulic fracturing and observed that since the stress intensity factor, K , at the tip approaches zero as a fracture in a lower modulus material propagates toward a higher modulus material, the fracture will tend to be arrested. Conversely, for a fracture propagating in a higher modulus material toward a lower modulus material, they observed that K becomes large as the interface is approached, and the fracture should "snap" through the interface.

Erdogan and Biricikoglu⁴ also determined stress intensity factors for a crack that has penetrated the interface, although their analysis was not strictly applicable since it requires a different internal pressure on either side of the interface in proportion to the modulus difference. Hanson et al.^{5,6} performed a similar analysis and found that K at the tip of a crack that has just penetrated an interface shows the reverse of that described previously. That is, the stress intensity factor jumps to zero just as a low modulus material is penetrated from a high modulus material. This then would indicate that containment would be expected in either situation. If taken in the strictest sense, these calculations would predict fracture arrest at all material interfaces and yet cracks are known to be capable of propagating through composite materials.

One principal difficulty with these analyses is that the fracture criterion relies solely on the value of the stress intensity factor. K is defined as the strength of the square-root singularity in stress at the crack tip, but the nature of this singularity changes as an interface is approached. When the crack reaches the interface, the singularity is no longer square-root and K goes to zero; but the stresses remain singular (infinite). Other singularities now dominate the fracture growth.

In addition, the existing analyses do not include a model for the crack tip process zone. A model that describes the microcrack zone at a crack tip is available⁷ and could be used along with the stress analysis and a realistic fracture criterion. This might provide a more realistic assessment of the actual effect that material interfaces have on fracture growth.

Daneshy⁸ conducted laboratory experiments and found that differences in rock properties were insufficient to stop fracture growth at an interface. He suggested that barriers may need to be defined as formations that reduce vertical fracture growth rather than prevent it altogether.

Daneshy⁸ further suggested that fracture containment may be more a result of the nature of the interface itself rather than any difference in material properties, but he thought that this would be most often the case at shallow depths where the bonding is likely to be weaker. Teufel⁹ and Hanson et al.^{5,10} performed laboratory experiments to study crack growth near both bonded and unbonded interfaces. They showed that, for unbonded interfaces, the stress normal to the interface (thus the friction along the interface and the ability to transmit shear) was the determining parameter for crack arrest or continued propagation. In experiments with bonded interfaces, Hanson et al.^{5,10} determined that the strength of the two materials relative to the strength of the interface is important for crack propagation.

Simonson et al.² studied the effect that in situ stress variations have on fracture propagation. They showed that a layer of greater in situ stress would provide an effective barrier because of the increase in the fracturing pressure necessary to continue propagating a fracture in this layer. The effectiveness of the barrier would, of course, depend on the difference in stress in the two regions. They also showed that the upward or downward migration of the fractures can be influenced by the hydrostatic gradient of the frac fluid relative to the vertical gradient of the minimum horizontal in situ stress. Cleary¹¹ suggested that an effective stress differential between the porous reservoir rock and the impermeable barrier can be obtained by drawing down the reservoir. This results in a reduced pore pressure and a reduced lateral confining stress so that the fracture would preferentially propagate in the lower stress reservoir rock.

Brechtel et al.¹² found significant differences in in situ stress between the Benson sandstone and adjacent shale layers, and they suggested treatment parameters to utilize this difference to control fracture height. Jones et al.¹³ found considerable stress differences between various Devonian shale layers which might act as significant barriers. Hanson et al.⁶ calculated an idealized stress field around lenses of different material properties from the surrounding formation and found that sizeable differences in in situ stresses should be expected under these conditions.

While all of these theoretical studies and laboratory experiments offer insight to the problem of containment, it is clear that such idealized results are not easily applied directly. This paper presents the results of realistic in situ experiments which have been conducted in an existing tunnel complex at the U. S. Department of

Energy's Nevada Test Site to examine hydraulic fracture behavior under many different conditions.¹⁴⁻¹⁶ These facilities are ideal for hydraulic fracturing experiments because they provide a realistic in situ medium with the appropriate boundary conditions (in situ stresses, no free surfaces) yet still allow for detailed examination of the created fractures and geological features through mineback. A detailed physical description can be obtained through photography and mapping, and this can be correlated with measured geologic properties, in situ stress distributions, fluid behavior and the operational parameters of the test. Although the various volcanic tuffs in which these fractures are propagated are not the sandstones and shales usually encountered in gas reservoirs, proper application of rock mechanics principles allows the extrapolation of these results to gas well conditions.

In this paper, the results of many hydraulic fracturing experiments are correlated to assemble a clearer picture of the factors which influence containment. These results clearly show that a material property difference between the reservoir rock and the bounding formation is not sufficient to contain the fracture. It will be shown, however, that the minimum in situ stress offers the predominant influence on the propagation of hydraulic fractures. Not only does the orientation of the minimum in situ stress dictate the orientation of the fracture, but steep gradients and discontinuities in the magnitude of this stress can act as barriers to fracture propagation.

EXPERIMENTS, RESULTS AND DISCUSSION

Five large-scale hydraulic fracture experiments ($>2 \text{ m}^3$ of fluid) and nearly 200 small-scale experiments^{14,15,16} ($<0.6 \text{ m}^3$ of fluid) have been performed in the past five years to study important fracture phenomena. Many of these tests were conducted in regions having uniform physical properties, small variations in in situ stress and few natural fractures or faults. The results from these tests were excellent and clearly reflected the homogeneity of the medium. The fractures propagated perpendicular to the minimum principal in situ stress, the created fracture area usually was found to be approximately the design value, and there was little anomalous fracture behavior. These results are probably typical of the situation frequently encountered in small conventional treatments in blanket sands and are indicative of the reasons for the good success that has often been obtained from such treatments.

Recent efforts, however, have been concentrated on determining the effects of layered formations on hydraulic fracture behavior, particularly those conditions which limit vertical fracture growth, or contain, the fracture. The results of several experiments are discussed in light of either material property-interface effects or minimum in situ stress effects in the following two sections.

A. MATERIAL PROPERTY DIFFERENCES ARE INCAPABLE OF CONTAINING HYDRAULIC FRACTURES

A significant part of the experimental research has centered on fracture behavior near interfaces to determine if material property differences between adjacent layers can act as a barrier to fracture propagation. If, as the models suggest, the stress intensity factor at the tip does tend to zero as the higher modulus material is approached, then, regardless of in situ stress variations, the fracture should be arrested before it penetrates the higher modulus material. In a formation interface fracture experiment¹⁴ designed to test this concept, a grout-filled fracture (35 m^3 at $0.0159 \text{ m}^3/\text{sec}$ in a 2 m open hole zone of a vertical hole) was initiated below an ash-fall tuff/welded tuff interface with significant differences in material properties as shown in Figure 1. Although the interface is not discrete (3 m transition zone), at the immediate contact between the ash-fall tuff and the transition zone there is a factor of five difference in elastic modulus and a factor of fifteen difference over a few meters. All interfaces between the ash-fall tuff and welded tuff are well bonded.

During mineback, it was found that the fracture which was initiated in the ash-fall tuff zone propagated through the interface into the higher modulus material everywhere that it contacted the interface. The fracture did not change orientation as it propagated across the interface. There were, however, significant width changes in regions of differing modulus with the larger width found in low modulus regions. Figure 2 shows this fracture propagating through the interface at a location near the tip of one wing of the fracture. The lower rock unit is the ash-fall tuff and above it is the basal ash flow unit (see Figure 1). As can be seen, the interface apparently had little effect on fracture propagation except where local irregularities, such as the hard lithic shown in Figure 2, obstructed crack propagation. Figure 3 shows this fracture in the opposite wing from Figure 2. Here, the entire transition region is shown, from the ash-fall tuff at the bottom to the densely-welded tuff at the top. Neither the interfaces nor the transition zone offered any resistance to propagation of the fracture into the high modulus region.

Figure 4, which shows the results of an exploratory coring program to determine the overall geometry of the fracture, illustrates the minimal influence of the interface and the high modulus layer on vertical propagation. The fracture is generally penny-shaped with a greater tendency for downward growth rather than horizontal extension. The propagation of the fracture into the high modulus layer clearly demonstrates that a material property interface will not arrest the vertical growth of a hydraulic fracture.

To further examine this problem, a series of small scale experiments were designed to confirm these results under more controlled conditions. These tests used small volumes ($0.2\text{--}0.6\text{ m}^3$) of dyed water at low flow rates ($0.1\text{--}0.5\text{ dm}^3$ per sec for a 1.5 m fracture interval) and fractures were initiated from nearby horizontal boreholes drilled below the same interface. In one borehole, six different zones were fractured at 0.5 dm^3 per sec with 0.6 m^3 of dyed water and then mined back to observe fracture behavior, particularly at the interface. As shown in Figure 5, each zone was at a different distance below the interface in the ash-fall tuff, varying from 0.15 to 1.0 m below.

In all six zones, the fracture propagated upwards through the interface rather than in the ash-fall tuff. Figure 6 shows one zone where the fracture propagated upwards through the basal ash-flow unit (factor of five greater modulus) and into the vitric unit where it intersected some natural fractures and filled some of them. (There are several strands of the fracture near the borehole, but this appears to be a common occurrence and is often observed during mineback.) Figure 7 shows a different zone where the fracture is nearly parallel to the mineback face. Only a small part of the fracture is exposed in this photo, but it clearly breaks through the interface. These experiments were conducted at very low flow rates and indicate that rate effects are probably not important for containment.

The results of these mineback experiments consistently show that the predictions of the idealized two dimensional analyses presented in the background section (e.g., Simonson et al.² and Rogers et al.³) are incompatible with the real physical mechanisms governing fracture behavior at a material property interface. Material property interfaces do not provide an effective mechanism for fracture containment.

Although fractures may not be contained at a material property interface as Daneshy⁸ suggests, high modulus layers may still provide containment in a sense by restricting fracture growth in that layer. Since the fracturing pressure above the minimum in situ stress level should be proportional to the elastic modulus, it will require, under similar conditions, considerably more pressure to fracture in a higher modulus material than in a lower modulus reservoir rock. One would expect that although the fracture may break through the interface, it may not propagate a great distance due to increasing viscous losses. The fracture should prefer to propagate in the direction of least resistance, such as in the lower modulus material, unless in situ stresses or other parameters dictate otherwise. In the large-scale formation interface fracture experiment, however, even this type of restricted growth was not evident.

B. VARIATION OF THE MINIMUM IN SITU STRESS IS THE PREDOMINANT FACTOR CONTROLLING FRACTURE GROWTH

In addition to the previously mentioned six small scale fractures which were conducted near the interface, 29 other small scale fractures were conducted in this same vicinity to delineate the vertical and horizontal distribution of the in situ stress and to determine its effect on fracture growth and geometry. In these experiments, hydraulic fractures were typically initiated with a small breakdown pump ($15\text{--}40\text{ dm}^3$) to determine the minimum principal in situ stress in a localized region near the borehole: The minimum principal in situ stress is equal to the instantaneous shut-in pressure after fracturing.¹⁷ (For brevity in the following discussion, in situ stress will refer to the minimum principal in situ stress.) Thus, in regions of interest (i.e., near an interface), many small volume fractures can be conducted to provide a detailed in situ stress distribution.

The distribution of the in situ stress near, and particularly below, the interface is shown in Figure 8. It can be seen that there are very large variations in the in situ stress distribution over distances of a meter. The data labeled CFE-1 were obtained from the previously discussed six small-scale fracture experiments. CFE-2 was a similar set of fractures conducted approximately 12 m from CFE-1, and the CFE-3 and CFE-4 data are from a location approximately 12 m on the opposite side of CFE-1. It can be seen that two significant in situ stress irregularities exist below the interface, and in both cases the in situ stresses increase by a factor of two to three.

The effects of these in situ stress anomalies can be clearly seen in the fractures shown in Figures 6 and 7. The volume of dyed water which was injected into each fracture was sufficient to create penny-shaped fractures of 6-10 m radius; however, the fractures propagated downward only to a position about 1.0 m below the interface. They preferentially propagated horizontally outwards and upwards into a material of much higher modulus. The location of fracture termination at a point 1.0 m below the interfaces correlates well with the location of the upper in situ stress "peak" seen in Figure 8. It is clear that the region of greater in situ stress terminated fracture growth and provided the observed containment feature. This same behavior was observed in all six fractures of CFE-1. As can be seen in Figure 6, near the location of fracture termination, the cracks are generally impregnated with more dye than any other location. This indicates that the fractures probably propagated to this point at an early time and remained inflated during pumping even though crack propagation had terminated in that direction. Fluid continued to leak off resulting in a heavy dye residue along the fracture surface.

The ability of the in situ stresses to restrict fracture growth was particularly evident in several fractures initiated between the stress peaks. Figure 9 shows a vertical fracture which was propagated with 0.2 m^3 of fluid at 0.125 dm^3 per sec and should have resulted in a fracture of about 5 m radius. However, the fracture, which can be seen on the right side of the photo, was restricted to a 1 m interval between points corresponding to the upper CFE-3, 4 and the CFE-2 stress peaks shown in Figure 8. The hole in the lower center is where the fracture was initiated. (The fracture is vertical but appears otherwise because of the curved mineback surface.)

The stress peaks appear to shift vertical position somewhat with horizontal location. However, they are an ever present feature in this region.

The largest value of the minimum stress recorded was 8 MPa in CFE-2 compared to a background level of about 3 MPa. Although the maximum recorded stress in CFE-3 and CFE-4 is only about 5 MPa, the maximum value of stress at the peaks may have been missed due to the paucity of data points. In fact, the very high pressures recorded during fracturing near both of these peaks indicate that the highest value of the minimum stress is probably 6-8 MPa in both areas. It should also be noted that this discrepancy may be due to errors arising from the finite size of the initial breakdown pump fracture. This results in an instantaneous shut-in pressure which may be the lowest minimum in situ stress in contact with the fracture surface or some average of the stress distribution. This is a problem only in areas with widely varying stress magnitudes.

The results from all the tests are similar to Figures 6, 7, and 9, and they are shown schematically in Figure 10. Generally, the fractures which were initiated above or below the in situ stress peaks propagated away from the high in situ stress regions as in Figures 6 and 7. The only exceptions to this were those fractures which were initiated very close to the in situ stress peaks. These often propagated through the high in situ stress region, but this may be due to borehole effects. A number of fractures which were initiated between the in situ stress peaks were totally confined to that area as in Figure 9. These tests resulted in rectangular fractures which were only about 1 m in height since they were confined by the regions of greater in situ stress. However, several fractures which were initiated between the in situ stress peaks eventually broke out of that region. Apparently they were so restricted that the fracturing pressure became sufficiently elevated to allow the fractures to break through one of the in situ stress peaks. In general, the results of these experiments demonstrate the overwhelming importance of in situ stresses in controlling fracture height.

Other experiments have also demonstrated the predominant influence of in situ stresses in limiting fracture growth. A sand-propped fracture¹⁶ was conducted in a region which was found to have a large number of faults, fractures, and significant variations in in situ stresses (both orientation and magnitude). Approximately 6 m^3 of a polymer water gel with 20-40 mesh sand in three stages (each stage had a different color and concentration of sand) were pumped into a 1.2 m open-hole zone at 0.01 m^3 per sec. As shown in Figure 11, the experiment was designed with sufficient volume to create fractures 15 m high by 100 m total length. Although one obviously does not expect the fracture to be of rectangular shape, this provides a useful reference for analyzing fracture growth patterns. The fracture was then mined back at the elevation of the fracture interval, and these results were correlated with geologic features which affected fracture behavior. The cross hatching outlines the boundary of the mineback, and the shaded area indicates where the fracture was observed. Clearly, the majority of the fluid and sand was forced downward.

On the left side, from 1-2 m from the borehole, the fracture terminated at a fault. In a few locations the fracture did break through the fault, but propagated less than 1 m past, as seen in Figure 12. There was no sand found in the fault, but small amounts of the fluid gel were found. Since the fracture did break through the fault in some locations, it was not the character of the fault interface itself that arrested fracture growth; only a significant increase in in situ stresses across the fault could have terminated the fracture. On the other side of this borehole, the fracture intersected another fault, but upon crossing this fault, the fracture changed direction by $\sim 45^\circ$. Here, the magnitude of the minimum in situ stress was probably the same or less, but the orientation of these stresses deviated by $\sim 45^\circ$ across the fault.

The behavior of the fracture at the top boundary is also interesting. Near the top of the zone where the fracture was initiated, a parting plane (unbonded, bedding-plane interface between two similar materials) terminated the upward propagation of the fracture, as shown in Figure 13. There are two possible reasons for this. First, a fracture can be terminated by an unbonded interface, as shown by Daneshy.⁷ However, in this case there is nearly 430 m of overburden which should give a sufficient normal force for friction to provide a mechanism for transmitting shear. Furthermore, in many locations the fracture did break through the interface, but in these cases it only propagated a few cm across. This indicates that the friction is indeed sufficient to allow the fracture to propagate across, but that something else is restricting growth. It appears that the unbonded interface at this location reflects a discontinuity in the in situ stress, such as would be found at a fault. In this situation the termina-

tion of the fracture can be attributed to a stress discontinuity across the parting plane, with a greater stress in the upper layer.

The stresses in this region were investigated using small volume hydraulic fractures (minifrac) to determine the magnitude of the minimum principal in situ stresses and mineback to provide the stress orientations. It was found that the magnitudes of the stresses differ considerably across faults (up to 2 MPa) and mineback also showed significant changes in orientation as the minifrac crossed faults. Although the exact values of the stress changes across these faults could not be determined (the mineback perturbs the stresses in the nearby region so stress measurements after the fact must be made at least 10 m away), the results showed that the type of stress irregularities needed to produce a fracture with the observed characteristics did indeed exist.

The preponderance of evidence from the mineback of hydraulic fractures points to in situ stress gradients as being the only mechanism that is capable of containing hydraulic fractures. Mineback results as well as laboratory experiments⁸ have shown that a material property interface is insufficient to arrest fracture growth. Although it has been demonstrated that an unbonded interface will arrest a fracture,⁸ other experiments^{5,9} have shown that a sufficiently large normal force across the interface will presumably provide enough frictional force to allow the fracture to propagate through. Only at very shallow depths would the overburden stress be too small to allow this to occur.

Mineback experiments have shown that discontinuities in the minimum principal in situ stress (e.g., faults) and steep gradients in this stress can arrest fracture growth. Field experiments,^{11,12,18} calculations⁶ and mineback experiments have shown that significant differences in the minimum in situ stress can exist in both the same formation and in different strata. In many cases these differences may be exploited to control the height of a hydraulic fracture. However, this would require determination of the stress distribution through techniques such as minifrac.

Although it may be possible to preferentially propagate the fracture upwards or downwards by varying the density of the fluid,² in practice this may be only occasionally successful because of the slight variation in stress due to the gradient of hydrostatic pressure relative to the gravitational gradient of the minimum principal in situ stress. When compared to the magnitude of in situ stress variations that can occur due to tectonics or lenticular inclusions, the effect of the density gradient is very small.

CONCLUSIONS

Mineback experiments have provided insight into the mechanisms that are responsible

for controlling hydraulic fracture growth. It has been demonstrated that material property differences are insufficient to arrest a fracture at an interface. The present two-dimensional analyses of crack behavior at an interface which predict containment are inadequate. It will be necessary to link a realistic failure criterion with the stress analysis to properly model the mechanisms operating in this problem.

However, these experiments have shown that the minimum in situ stress is the predominant influence on hydraulic fracture containment. Fractures are arrested wherever there is a sufficiently large discontinuity (e.g., fault) or gradient in this stress. Determination of the minimum in situ stress variations is imperative in a region where containment is desired. Thus, development of improved in situ stress measuring tools or techniques for use in oil or gas wells should be a high priority for future research.

ACKNOWLEDGEMENTS

The authors extend their thanks to William Vollendorf, Sharon Finley, many other Sandia personnel and the skilled mining crew who conducted these tests, evaluations and mining operations in G tunnel. This project is supported by the Office of Oil and Gas, United States Department of Energy.

REFERENCES

1. Cook, T. S. and Erdogan, F. "Stresses in Bonded Materials with a Crack Perpendicular to the Interface," International Journal of Engineering Sciences, Vol 10, 1972, p 677-697.
2. Simonson, E. R., Abou-Sayed, A. S. and Clifton, R. J., "Containment of Massive Hydraulic Fractures," Society of Petroleum Engineers Journal, February, 1978, p 27-32.
3. Rogers, L. A., Simonson, E. R., Abou-Sayed, A. S., and Jones, A. H., "Massive Hydraulic Fracture Containment Analysis Utilizing Rock Mechanics Considerations," Proceedings of the Massive Hydraulic Fracturing Symposium, Feb 28 - March 1, 1977, University of Oklahoma, Norman, OK.
4. Erdogan, F. and Biricikoglu, V., "Two Bonded Half Planes with a Crack Going Through the Interface," International Journal of Engineering Sciences, Vol. 11, 1973, p 745-766.
5. Hanson, M. E., Anderson, G. D., Schaffer, R. J., Hearst, J. R., Haimson, B. and Cleary, M. P. "LLL Gas Stimulation Program, Quarterly Progress Report, April through June 1978," Lawrence Livermore Laboratory Report UCRL - 50036-78-2, July 26, 1978.

6. Hanson, M. E., Anderson, G. D., Shaffer, R. J., Emerson, D. O., Swift, R. P., O'Banion, K., Cleary, M. P., Haimson, B., Knutson, C. F., and Broadman, C. R., "LLL Gas Stimulation Program, Quarterly Progress Report, July through September, 1978," Lawrence Livermore Laboratory Report WCRL-50026-78-3, November 6, 1978.
7. Schmidt, R. A., "A Microcrack Model and Its Significance to Hydraulic Fracturing and Fracture Toughness Testing," 21st U. S. Symposium on Rock Mechanics, Rolla, Missouri, 1980.
8. Daneshy, A. A., "Hydraulic Fracture Propagation in Layered Formations," Society of Petroleum Engineers Journal, February, 1978, p 33-41.
9. Teufel, L. W., "An Experimental Study of Hydraulic Fracture Propagation in Layered Rock," PhD dissertation, Texas A&M University, August, 1979.
10. Hanson, M. E., Anderson, G. D., Shaffer, R. J., Emerson, D. O., Heard, H. C., and Haimson, B. C., "Theoretical and Experimental Research on Hydraulic Fracturing," Proceedings, Fourth Annual DOE Symposium on Enhanced Oil and Gas Recovery & Improved Drilling Methods, August 29-31, 1978, Tulsa, OK.
11. Cleary, M. P., "Rate and Structure Sensitivity in Hydraulic Fracturing of Fluid-Saturated Porous Formations," Proceedings, 20th U. S. Symposium on Rock Mechanics, June 4-6, 1978, Austin, TX, p 127-142.
12. Brechtel, C. E., Abou-Sayed, D. S., and Jones, A. H., "Fracture Containment Analysis Conducted on the Benson Pay Zone in Columbia Well 20538-T," Proceedings, Second Eastern Gas Shales Symposium, October 1978, Morgantown, West Virginia.
13. Jones, A. H., Abou-Sayed, A. S., and Rogers, L. A., "Rock Mechanics Aspects of MHF Design in Eastern Devonian Shale Gas Reservoirs," Proceedings, Third ERDA Symposium on Enhanced Oil, Gas Recovery & Improved Drilling Methods, August 30-31, Sept. 1, 1977, Tulsa, OK.
14. Tyler, L. D. and Vollendorf, W. C., "Physical Observations and Mapping of Cracks Resulting from Hydraulic Fracturing In Situ Stress Measurements," SPE 5542, Dallas, TX, Sept. 28 - Oct. 1, 1975.
15. Warpinski, N. R., Northrop, D. A., and Schmidt, R. A., "Direct Observation of Hydraulic Fractures: Behavior at a Formation Interface," Sandia Laboratories Report, SAND78-1935, October, 1978.
16. Tyler, L. D., Vollendorf, W. C., and Northrop, D. A., "In Situ Examination of Hydraulic Fractures," presented at Third ERDA Symposium for Enhanced Oil and Gas Recovery and Improved Drilling Methods, Tulsa, OK, Aug. 30 - Sept. 1, 1977.
17. Kehle, R. O., "The Determination of Tectonic Stresses through Analysis of Hydraulic Well Fracturing," Journal of Geophysical Research, Vol. 69, No. 2 Jan, 1964, p 259-273.
18. Wyman, R. E., Holditch, S. A., and Randolph, P. L., "Analyses of an Elsworth Hydraulic Fracture-Alberta, Canada," SPE 7935, 1979 SPE Symposium on Low-Permeability Gas Reservoirs, May 20-22, 1979, Denver, Colorado.

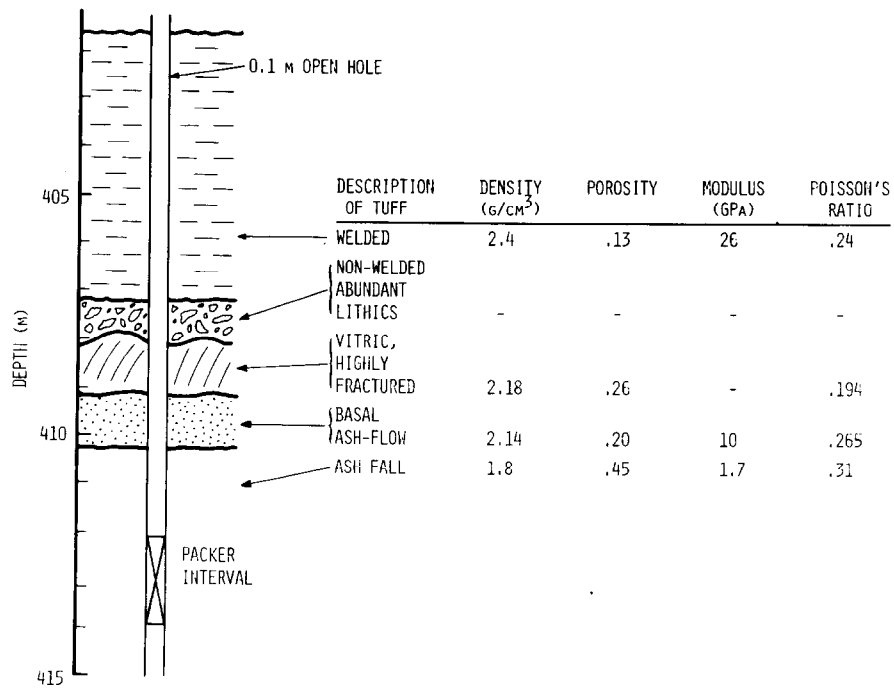


Fig. 1 - Formation interface fracture experiment.

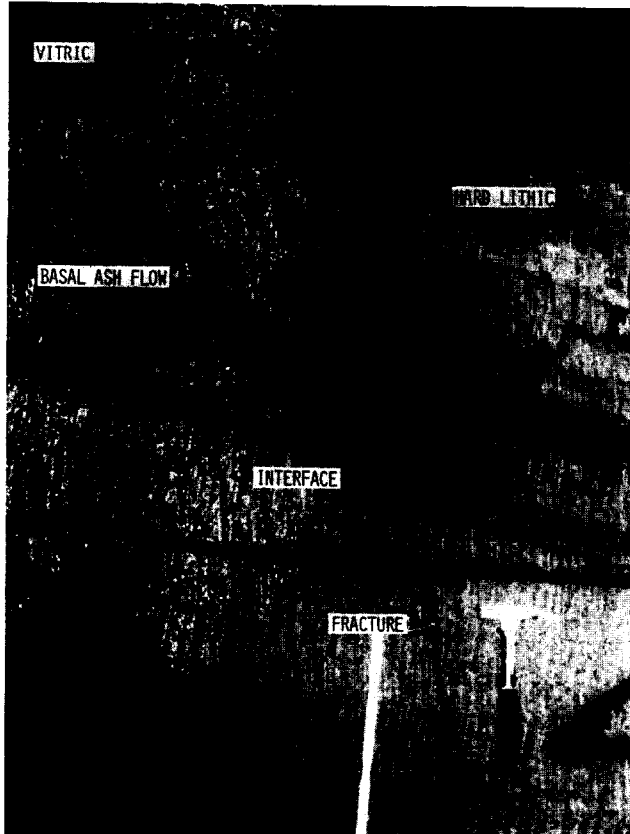


Fig. 2 - Grout fracture at the interface.

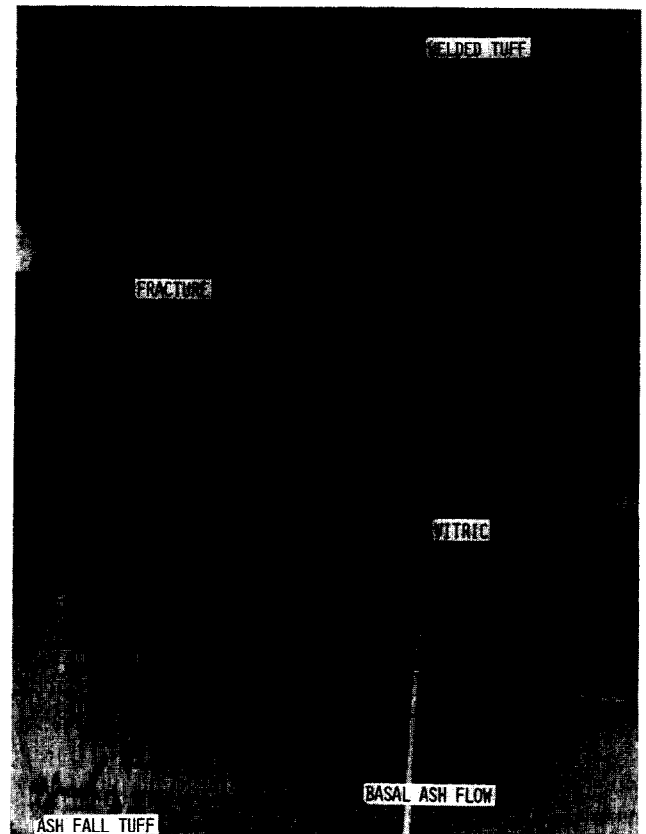


Fig. 3 - Grout fracture propagating entire transition zone.

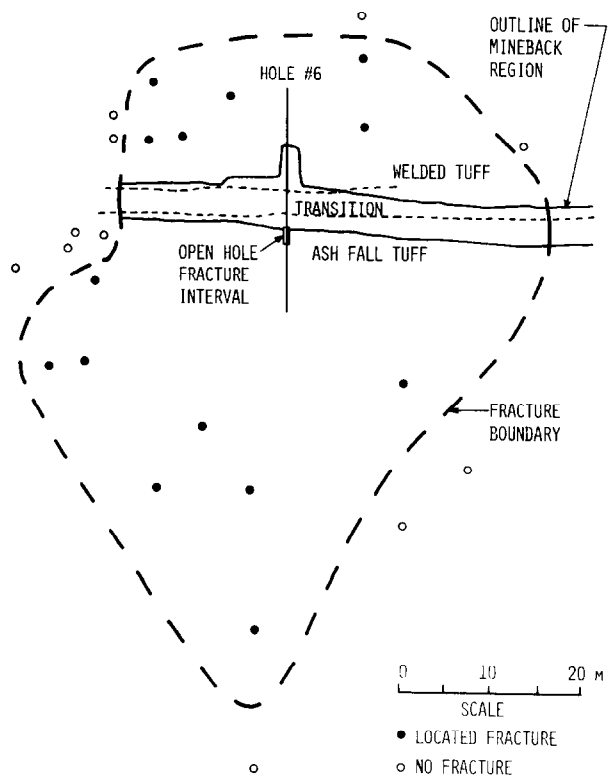
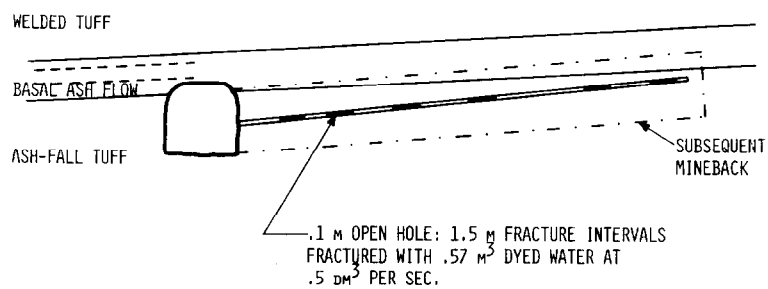


Fig. 4 - Formation interface fracture experiment coring results.



PROPERTIES	DENSITY (G/CM ³)	POROSITY	MODULUS (GPA)	PERMEABILITY (μM ²)
BASAL ASH-FLOW	2.1	.22	8.6	4.9 X 10 ⁻⁶
ASH-FALL	1.7	.45	1.7	1.4 X 10 ⁻⁴

Fig. 5 - Interface test series.

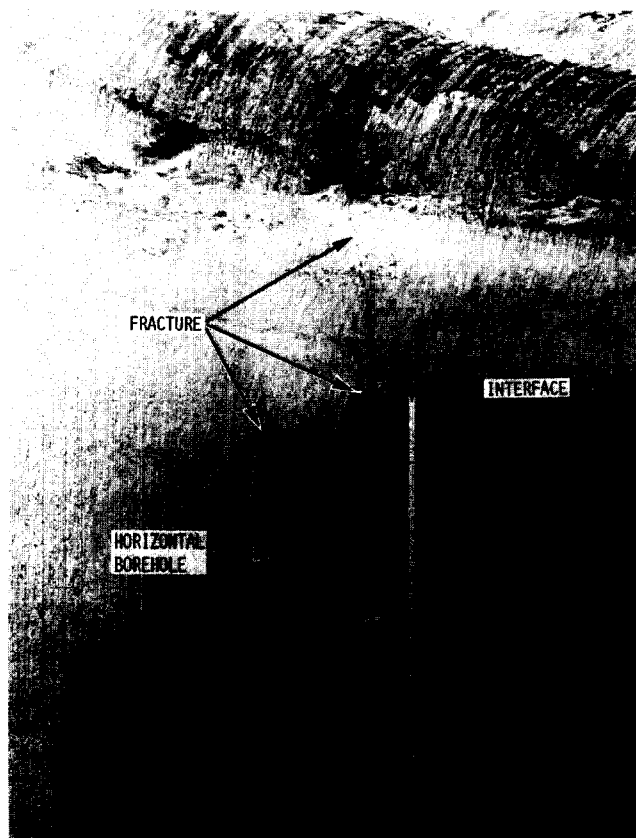


Fig. 6 - Dyed-water fracture at the interface.

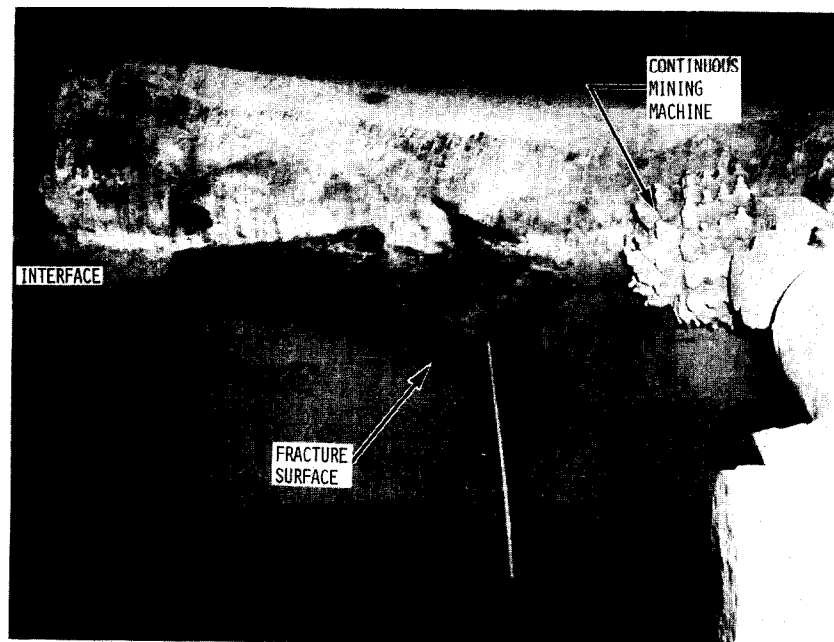


Fig. 7 - Dyed-water fracture at the interface.

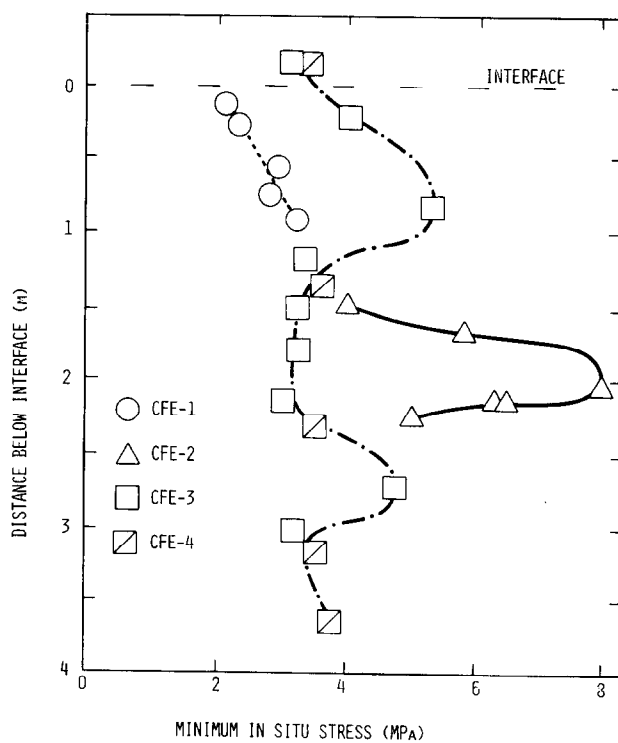


Fig. 8 - Vertical variations in the minimum principal in situ stress.

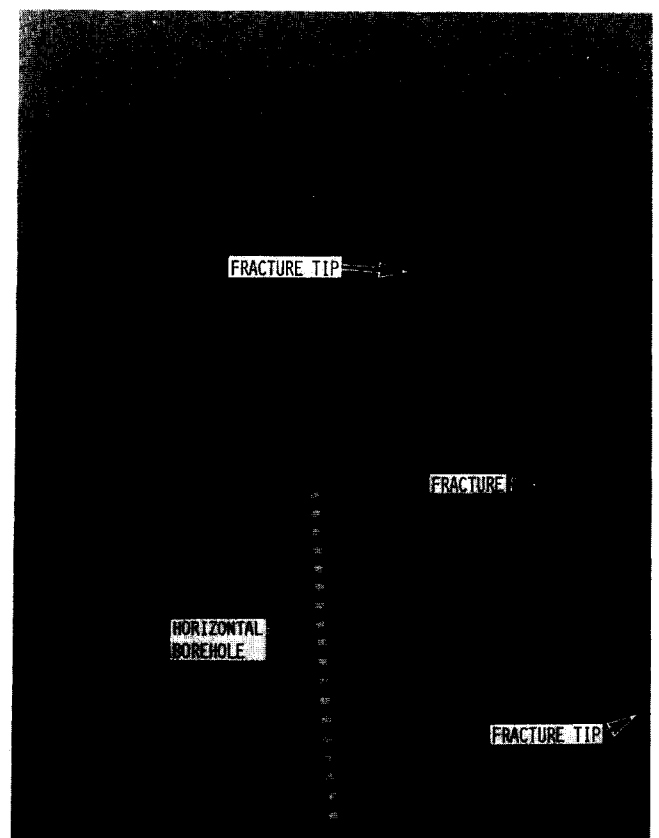


Fig. 9 - Dyed-water fracture confined by in situ stresses.

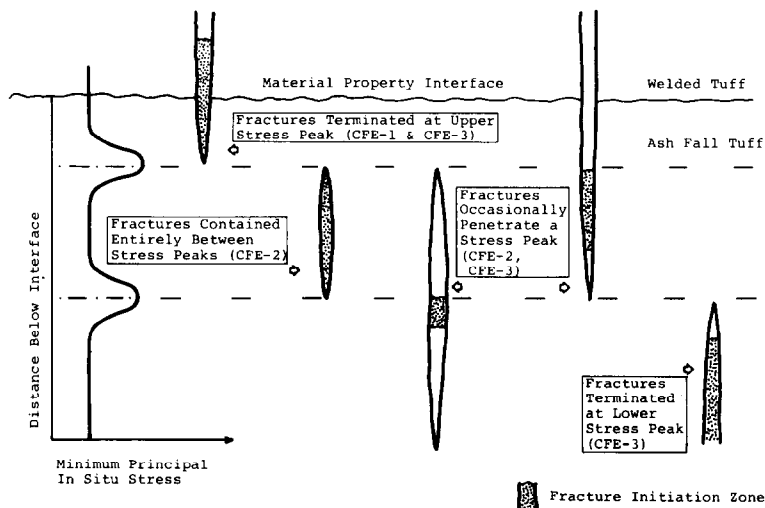


Fig. 10 - Schematic of the effect of in situ stresses on hydraulic fractures.

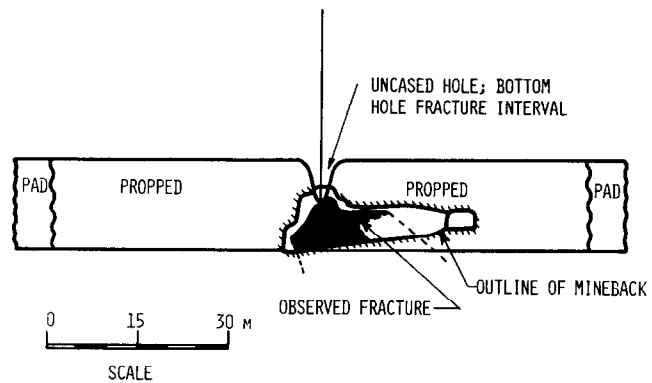


Fig. 11 - Mineback of sand-propped fracture.

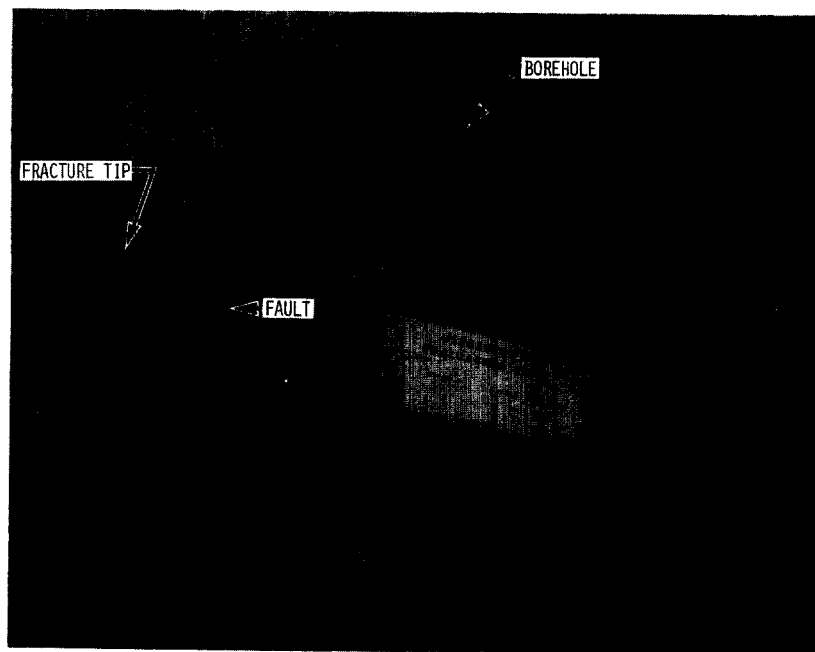


Fig. 12 - Sand-propped fracture terminating near a fault.

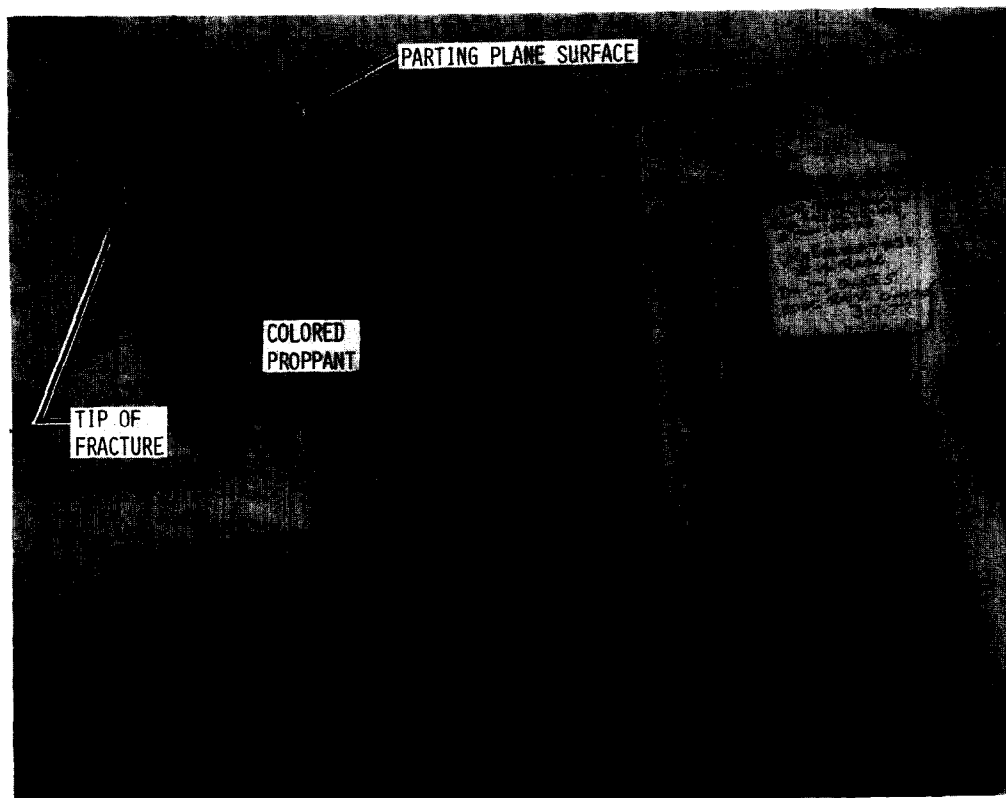


Fig. 13 - Sand-propped fracture terminating at a parting plane.

THE MAPPING OF NITROGEN GAS INDUCED HYDRAULIC FRACTURES IN DEVONIAN SHALE BY OBSERVATION OF THE ASSOCIATED SURFACE DEFORMATION

by Keith F. Evans, Gary R. Holzhausen, and
Milton D. Wood, M.D. Wood, Inc.

This paper was presented at the 1980 SPE/DOE Symposium on Unconventional Gas Recovery held in Pittsburgh, Pennsylvania, May 18-21, 1980. The material is subject to correction by the author. Permission to copy is restricted to an abstract of not more than 300 words. Write: 6200 N. Central Expwy., Dallas, Texas 75206

ABSTRACT

The growth of a hydraulic fracture was monitored by observation of the ensuing deformation of the Earth's surface. It is shown that breakout from the initial sub-vertical fracture plane of orientation N62°E occurred during the treatment. The data is consistent with the physically plausible interpretation that the breakout occurred into the horizontal plane after a fracture height of 600 ft [183 m] above the 1100 ft [336 m] deep injection point had been attained. Independent evidence supports this result.

INTRODUCTION

Production enhancement of gas from wells draining low permeability formations such as the Devonian shale sequence is commonly attempted using the technique of hydraulic fracturing. The problem of designing such fractures to optimize the resulting yield has underlined the need for a more thorough understanding of the fracturing process itself. To this end, several wells penetrating the Devonian shale have been selected for intensive study during fracturing treatments. The studies, which are largely being coordinated by Sandia National Laboratories (SNL), involve the application of a wide variety of diagnostic technologies capable of supplying information pertinent to identifying the behavior of the fracture during treatment and the principal factors which influence this behavior.

This paper presents the results of applying one such technology, the fracture mapping technique (FRAC-MAP) of M. D. Wood, Inc. (MDWI), to determine the geometrical characteristics of the fracture resulting from nitrogen gas injection into the 1100 ft [335 m] deep Black #1 Well, which penetrates the Devonian shale in Know County, Ohio. During the treatment, which lasted from 16:47 to 17:15 hours (Standard Central Time) on October 22, 1979, the well received 9.68×10^5 std ft³ [(2.59×10^4 std m³) (0°C, 1 atm)] of nitrogen at a temperature of 114°F [45.7°C] and

pressure of 1300 psi [8962 kPa]. No proppant was used. The well was offered to the research program by its owners, Thurlow Weed & Associates, after its production had slowly declined from an initial 3.2×10^4 std ft³/D [8.6×10^4 std m³/D] after drilling in 1975, to zero by the end of 1977. During this period of production, the well was open hole for the entire Devonian shale section (Figure 1), and had suffered neither explosive nor hydraulic stimulation treatments. It is not known whether the bulk of production came from the shale matrix or from sets of high-angle natural fractures which have been identified as intersecting the well (Bob Trump, personal communication). The well was recased prior to the experiment, as shown in Figure 1.

Other diagnostic technologies included, in the Black #1 Well experiment included a logging and coring program², lineament analysis³, seisviewer⁶ imagery⁷, borehole television⁸, nitrogen analysis⁶, and finally, a prototype downhole seismic recording system developed by SNL¹ which, like the MDWI FRAC-MAP technique, attempted to monitor continuously the growth of the fracture during treatment. The results of these analyses, copies of which can be obtained from either SNL or Morgantown Energy Technology Center, Morgantown, W. Virginia, will be drawn upon for interpretive support of the MDWI analysis here presented.

THEORY

The underlying principle of the FRAC-MAP technique is to determine the deformation field at the Earth's surface that ensues from the growth of a hydraulic fracture or other dislocation source at depth. This time-evolving deformation field can then be used in conjunction with models derived from elastic continuum theory to resolve geometric features of the fracture; the so-called "inverse" problem. The extent to which fracture geometry can be recovered from the data depends principally upon the completeness of the data in describing the actual sur-

References and illustrations at the end of paper.

face deformation field, and the degree to which the well environs conform to an homogeneous elastic half-space of known properties. A well chosen array of eight or so deformation field sample points is usually adequate to resolve the broad-scale features of fracture, such as height, length, orientation, and depth.

The deformation field is sampled with an array of shallow borehole tiltmeters. It is found that measurement of the spatial gradients of the displacements themselves, are the most practical method of accurately sampling the deformation field. Hence, borehole tiltmeters, which are both rapid to install and produce good quality data within a week of installation, are employed. The noise level of the instruments is determined principally by their immediate environment, which gives rise to thermo-elastic and other ground noise of local origin. Nonetheless, a well installed instrument is capable of resolving the principal solid earth tides (3×10^{-8} radian) although the presence of such may not be immediately obvious from simple inspection of the data.

SITE GEOLOGY AND ROCK ELASTIC PARAMETERS

The shallow lithology about the well region is shown in Figure 1. Bedding of all formations is approximately horizontal. The surface layer of about 200 ft [61 m] thickness consists of a dark sandy loam, and is underlain by glacial sands and gravels down to a depth of about 550 ft [168 m]. Beneath this lies the Devonian shale, which has alternating layers of hard black shale and slightly softer gray shale of varying thicknesses. There is clear evidence that the shale contains high-angle faults of approximate orientation N70°E (core analysis and seismviewer imagery results).

The permeability of the shale is generally low and does not facilitate rapid diffusion of fluids through pore space. The density of the shale, as measured by a Birdwell borehole compensated log, is rather consistent at 165 lb/ft³ [2.65×10^3 kg/m³]. The elastic parameters of Devonian shales, taken from other locations but of identical density, have been measured using dynamic techniques on cores taken from 1,000 ft [305 m] depths (Hugh Hert personal communication). They are found to be:

$$\begin{aligned} \text{Poisson's Ratio } \nu &= 0.25 - 0.30 \\ \text{Shear Modulus } \mu &= 1.5 \times 10^6 \text{ psi } [1.0 \times 10^7 \text{ kPa}] \\ &\quad (\text{measured } \perp \text{ to bedding}). \\ \mu &= 3.0 \times 10^6 \text{ psi } [2.0 \times 10^7 \text{ kPa}] \\ &\quad (\text{measured } // \text{ to bedding}). \end{aligned}$$

The shale is clearly anisotropic and appears more resistant to fractures opening vertically than those opening horizontally. The correct value of shear modulus applicable to the bulk behavior of the formation (rather than a core sample) is difficult to determine. The core-determined value is invariably an overestimate which is attributed to a class of cracks and imperfections that are present in the bulk rock but not in the core sample. The values of shear modulus for cores of the shale taken from 300 feet and 1,000 feet depths did not change appreciably (Hugh Hert personal communication). With these points in mind, the following values of shear modulus will be adopted in the following analysis:

$$\begin{aligned} \text{Vertical cracks: } 2.5 \times 10^6 > \mu > 1.5 \times 10^6 \text{ psi} \\ &\quad [1.7 \times 10^7 > \mu > 1.0 \times 10^7 \text{ kPa}] \\ \text{Horizontal cracks: } 1 \times 10^6 > \mu > 5 \times 10^5 \text{ psi} \\ &\quad [0.6 \times 10^7 > \mu > 0.3 \times 10^7 \text{ kPa}] \end{aligned}$$

INJECTION WELL CHARACTERISTICS AND SURFACE TILTMETER ARRAY CONFIGURATION

The injection well was 7 inches [17.8 cm] in diameter, and extended to a depth of 1,120 ft [341 m] the upper 1,055 ft [322 m] of which was cased. Additionally, the casing was perforated between 1,000 and 1,030 ft [305-314 m]. Only layers of black shale were exposed in the uncased sections of the wellbore (Figure 1).

Eight tiltmeters circumscribed the wellbore, each at a radial distance of approximately 390 ft [119 m]. A plan view of the site, including tiltmeter locations, is shown in Figure 2. The tiltmeter locations were chosen to optimize the signal expected from a fracture centered at a depth of 1100 ft [335 m].

A shallow water table contributed significantly to the background noise level monitored by some of the instruments. The noise level on instruments #6, #7, and #8 was sufficiently high to effectively disable them; consequently they are not used in the analysis. The noise level on the other five instruments, however, proved to be acceptable at the periods of interest, and numerous conclusions could be drawn from the data collected from these instruments.

TILOMETER DATA

The data used in the analysis are presented in Figure 3. Specifically, Figures 3a-3e represent the surface tilts recorded at instrument sites #1 to #5, respectively (Figure 2) during a 2.5-hour time window containing the injection operation. The two dashed vertical lines mark the time of formation breakdown and shut-in. Each instrument has two channels representing tilt in a direction toward or away from the wellbore (radial axis), and tilt perpendicular to this direction (tangential axis). Figure 3f shows the wellhead gas pressure, and Figure 3g the volume flow rate of the gas at 114°F [45.7°C] into the wellbore. Both the records were obtained from devices located at the wellhead.

For purposes of calculating the effective fracture-forming gas volume injected, the wellhead flow data must be corrected for the difference between wellbore and "in-fracture" temperatures and pressures. It is likely that at some feet away from the injection point the gas has cooled to the formation temperature of about 50°F [10.2°C]. The in-fracture pressures are more difficult to estimate, due to possible dynamic pressure gradients within the fracture system; however, it is known that breakdown occurred at 900 psi [6205 kPa] and that the wellhead gas pressure of 1300 psi [8962 kPa] was unlikely to be maintained at any appreciable distance from the injection point. Thus, an in-fracture gas pressure of 900 psi [6205 kPa] is adopted. The resulting fracture forming gas volume corrected for temperature and pressure is 15,500 ft³ [440 m³].

ANALYSIS: Structure

Inspection of the suite of tilt waveforms shown in Figure 3 suggests that the tilt event associated with the injection operation consists of three phases. Within each phase the evolution of the tilts is gradual and consistent, but between phases the evolution of the tilt field is radically different. This behavior suggests that the nature of growth of the hydraulically induced fracture differs markedly between phases, but remains essentially constant during a specific phase. The phases are marked in Figure 3 by the vertical solid lines. Phase I begins at breakdown (16:49), and is succeeded by Phase II at 17:07. Phase 2 terminates at shut-in, and the post-shut-in response is termed Phase 3 for consistency. During Phase I, which is the longest, six-tenths of the total gas volume were injected. In the analysis, each of the three phases is examined separately.

ANALYSIS: Phase 1: 16:51 - 17:07

During this phase, a fracture-forming gas volume, (at 900 psi [6205 kPa] and 50°F [10.2°C]) of 9.184 ft³ [263 m³] was injected into the formation. For the purpose of calculating the injection rate at the bottom of the wellbore, a pressure of 1,300 psi [8,962 kPa] and a temperature of 90°F [32°C], as indicated by a downhole thermistor operated by SNL, are used. The initial injection rate of 48 ft³/min [22.6 dm/s] was maintained until formation breakdown, after which the rate was stepped to 360 ft³/min [170 dm/s] and then 528 ft³/min [249 dm/s] (Figure 3g). The wellbore pressure rose in proportion to the step increments and maintained a constant level until shut-in at 17:15. Examination of the tilt records (Figure 3) shows the tilt amplitudes recorded by all instruments (with the exception of #5) to be rather uniformly increasing throughout the phase, following which there is a pronounced change in the sense of tilt. The transition from Phase 1 to Phase 2 is most evident at the northeastern instruments #1, #2, and #3. The residual (accumulated) tilt vector at each site at the end of Phase 1 is shown in Figure 4.

Minimum Dimensions of Fracture

A minimum bound on the lateral dimensions of the fracture can be deduced by assuming the fracture to have propagated radially from the injection point throughout Phase 1. The only assumption made which may possibly lead to an overestimate of fracture dimensions is that of negligible leakoff. However, the constantly high injection pressure, together with the low permeability of the formation, suggest that leakoff into fissures, joints, and formation was not dramatic.

For given fracture volume, V , and internal pressure, p , the radius, a , of the corresponding penny-shaped fracture in an infinite isotropic and homogeneous, linear elastic medium is found to be (Perkins and Kern, 1960):

$$a = \left\{ \frac{3\mu V}{8p(1-\nu)} \right\}^{1/3} \quad \dots (1)$$

where μ is shear modulus and ν Poisson's ratio. The maximum width, w , of the fracture is (Perkins and Kern, 1961):

$$w = \frac{4p(1-\nu)a}{\pi \mu} \quad \dots (2)$$

$$\begin{aligned} \text{and using the values } \mu &= 9 \times 10^5 \text{ psi } [6.2 \times 10^6 \text{ kPa}], \\ &= 0.25, \\ V &= 9.3 \times 10^3 \text{ ft}^3 [263 \text{ m}^3] \end{aligned}$$

$$\begin{aligned} \text{we have } a &= 1.9 \times 10^4 p^{1/3} \text{ inches } [9.18 \times 10^4 p^{-1/3} \text{ cm}] \\ w &= 0.02 p^{2/3} \text{ inches } [0.014 p^{2/3} \text{ cm}] \end{aligned}$$

The appropriate pressure here is the difference between the fracture fluid pressure and the in-situ stress acting perpendicular to the fracture plane, which acts to close the fracture. Initial formation breakdown occurred under modest pumping rates at a downhole pressure of 900 psi [6204 kPa], which thereafter increased to 1,300 psi [8962 kPa] as a result of the order of magnitude increase of injection rate (Figure 3f,g). Assuming breakdown pressure was approximately equal to the in-situ stress normal to the fracture plane, a driving pressure of 400 psi [2757 kPa] acted in the immediate vicinity of the injection point during most of the treatment period. Such a high pressure need not necessarily have extended appreciable distances from the wellbore; indeed, consideration of the fracture toughness of rocks makes it extremely unlikely that the driving pressures operating near remote fracture edges would exceed tens of psi. Bounds on fracture toughness that embrace most common geologic materials are presented in Figure 5, and show that near edge driving pressures of between 5 and 12 psi [35-83 kPa] might be expected to exist once the fracture has become large.

Using uniform pressures of 400 and 5 psi [1757 and 35 kPa] as upper and lower bounds on driving pressure, equations 1) and 2) yield a minimum fracture radius of 214 ft [66 m] with a fracture width of 1.09 inches [2.77 cm] at the wellbore, and a maximum (wet) fracture radius of 926 ft [282 m] having a fracture width of 0.06 inches [0.15 cm] at the wellbore. Any driving pressure gradient that resulted in a fall from 400 psi [2757 kPa] at the wellbore to 5 psi [35 kPa] at the fracture edges would produce a fracture of radius and width intermediate between those above. Analysis of the surface tilt field in the following sections places an upper bound on the average driving pressure of 38.5 psi [265 kPa]. Consideration of the probable containment of vertical fracture growth can only strengthen the conclusion that the fracture propagated laterally some considerable distance beyond the limits of the array.

Strike of Fracture

From Figure 4 it is evident that the direction of tilting on the instruments in the eastern part of the array during Phase 2 was perpendicular to a direction of N62°E. The sense of these tilts corresponds to those anticipated to result from a long, high-angle fracture of strike N62°E and dipping to the NW. The precise angle of dip can be found by considering the relative amplitudes of the tilts, and is discussed in the following section. The observed tilt vectors on instruments in the southwest quadrant are generally consistent with this orientation. The direction of tilt at site #5 is not well defined, but the small tilt amplitude at this site is consistent with a fracture strike of roughly ENE-WSW. The direction of tilt at site #4 suggests a fracture strike of N59°E to the south-

west of the wellbore.

Height and Dip of Fracture

It is unlikely that a sizeable hydraulic fracture will grow as an expanding penny-shaped rupture. The effects of faulting, bedding, interfaces, the in-situ stress gradients and pore pressure drawdown are known to influence hydraulic fracture growth. The fracture of interest here, a fracture in a horizontally bedded medium, might be expected to have its vertical progress checked, or at least retarded, by the effects of bedding interfaces and overburden pressure gradients. Clearly, restriction of fracture height would lead to even greater lateral propagation, and the surface tilts occurring a mere 400 ft [122 m] from the wellhead would ostensibly be the same as those generated by an infinitely long fracture. The surface tilts at this radius would then be dependent only upon the vertical geometry of the fracture and could be used to estimate the latter, providing the elastic properties of the medium are known.

Pollard and Holzhausen (1979)¹⁰ have derived a model to calculate the free-surface displacements and tilts due to a buried infinitely long fracture of arbitrary dip, α ; height (along fracture), $2a$; and depth to center, d ; subject to an increase in uniform internal fluid pressure, p . The predicted amplitudes of the surface tilts are found to be directly proportional to p and inversely proportional to the shear modulus, μ , of the medium.

Unfortunately, the uncertainty in the value of both of these parameters is too great to constrain fracture height appreciably from the absolute values of tilt. However, the form of the tilt field is dependent only upon relative fracture geometry and hence, assuming the depth of injection remains at the center of the fracture during growth, the height and orientation of fracture may be inferred from the relative amplitudes of the surface tilts.

The ratio of tilt observed to tilt predicted for a range of fracture heights is shown in Figure 6. The ratios are normalized such that instrument #2 always has the value of unity. The dips of the various fractures plotted are all 87° . Changing the dip by 1° either side of 87° produced unreasonable discrepancies between the tilt ratios for instruments #1, #2, and #3. The graph indicates that the observed tilt residuals on instruments #1, #2, and #3 can be reproduced almost exactly by a suitably pressurized fracture of half-height 600 ft [183 m] having a dip to the northwest of 87° . Insufficient data points are available in the southwest quadrant to tightly constrain the height and orientation of the southwest fracture lobe by this technique. It is of note that a fracture height of 600 ft [183 m] would place the top of the fracture near the top of the shale sequence (Figure 1). This unconformity may act to prevent further vertical growth.

Driving Pressure

Having used the form of the surface tilt field to constrain the fracture height, the predicted absolute amplitude for a 600 ft [183 m] high fracture may be compared with the observed to determine the quotient p/μ . Figure 7 shows a plot of quotient

value versus fracture height for instrument #1. Instruments #1, #2, and #3 will, of course have the same quotient value only when the fracture height is 600 ft [183 m]. The value of the quotient for this fracture height is $p/\mu = 0.65 \times 10^{-5}$.

Now, for a vertical fracture in the horizontally bedded shale sequence, the appropriate bounds on the shear modulus are: $10 \times 10^{-5} < \mu < 25 \times 10^{-5}$ psi [$6.9 \times 10^{-4} < \mu < 17.0 \times 10^{-4}$ kPa].

Hence, for a quotient value of 0.65×10^{-5} , the resulting bounds on driving pressure are:

$$6.5 < p < 38.5 \text{ psi } [45 < p < 265 \text{ kPa}].$$

It should be emphasized that the above values represent the possible range of uniform pressures operating in the fracture, and as such must be understood to be averages taken over any gradients in gas pressure. That appreciable gradients exist is certainly true, for, as has already been noted, the fracture edge driving pressure is limited by the fracture toughness, K_{IC} , of the rock to be less than 12 psi [84 kPa] (Figure 5). The maximum value of mean driving pressure of 38.5 psi [265 kPa] was deduced from the surface tilts at a distance of 350 ft [107 m] from the wellbore. Consequently they must be taken as suggesting that the 400 psi [2753 kPa] driving pressure at the injection point did not extend appreciably from the wellbore; or that, if it did, it was localized within a narrow band of low impedance flow. Two mechanisms which could give rise to pressure gradients might be of importance here, namely viscous forces within the nitrogen, and fluid leakoff into open joints, fissures, and pore space.

ANALYSIS: Phase 2; 17:07 - 17:15

The total volume of fracture forming gas injected during this phase amounted to 6215 ft³ [176.3 m³]. The transition from Phase 1 is identified by a sudden change in the previously consistent tilt rates and directions recorded by all instruments (Figure 3). The change is especially rapid on instruments #1, #2, and #3, and presumably indicates those instruments to be closer to the source. The onset of Phase 2 undoubtedly marks a change in the evolution of the fracture growth. Wellbore pressure and flow rate remained undisturbed both during and following the transition, presumably due to a high pressure gradient about the injection point effectively decoupling the wellbore pressure from that within much of the fracture volume. Thus, any sudden depressurization of the fracture due to intersection with an open fissure or joint would not necessarily produce a change in pressure at the wellbore.

The fracture event during Phase 2 is complex in nature and does not admit to simple deduction from the measured tilt field. The problem, which is of a general nature for multiple event fractures, is that no single point through which fracture is known to pass (e.g. injection point) can be identified. The data does not lend itself to quantitative analysis, and hence only brief speculative arguments which are qualitatively consistent with the observed tilts are presented here.

The residual tilt vectors accumulated during Phase 2 are shown in Figure 7. Comparison with those resulting from Phase 1 reveals an approximate reversal in trend on instruments located in the northeast quadrant, and might be interpreted as resulting from partial collapse of the fracture opened during the initial phase. This behavior would be anticipated were the fracture to have intersected a high-permeability natural fracture system at the end of Phase 1, and the sharpness of the reversals on instruments #1, #2, and #3 suggests that this intersection would have occurred to the northeast of the wellbore. The deviation of the tilt directions from that of an exact reversal of the trend of Phase 1 could then be explained by the widening of a high-angle (steeply dipping) fracture system to the northeast of the instruments by gas pressure. The fracture system would be required to strike in a broadly southerly direction. The tilt vectors from instruments #4 and #5 do not conform particularly well to this scheme. It should be emphasized that the above interpretation is only qualitatively consistent with the data and is not well constrained. Tilt vectors from sites located further to the northeast would be required to test the hypothesis.

An alternative interpretation to the above is that the fracture ceased to grow vertically at the end of Phase 1 and instead, flipped over into the horizontal plane. Physically this could occur as soon as the fracture edge propagated vertically to a depth where the minimal principal stress direction changed from horizontal to vertical. The depth may be easily evaluated, assuming the breakdown pressure is marginally greater than the minimum principal in-situ stress, which is then approximately horizontal and less than or equal to about 900 psi [6205 kPa] at the depth of injection. Let us define the following:

- $P_H(z)$ = minimum horizontal principal stress at depth z
- $P_H(0)$ = minimum horizontal stress at the earth's surface
- $P_V(z)$ = vertical (overburden) principal stress at depth z
- ν = Poisson's ratio
- ΔP_V = overburden pressure gradient.

Assuming that lateral confinement prevents horizontal strain at depth, we find from Hooke's Law that

$$P_H(z) = P_H(0) + \frac{\nu(z)\Delta P_V}{(1-\nu)} \quad \dots (4)$$

Using values $z = 1100$ ft [335 m], $\nu = 0.25$, $P_V = 1.15$ psi/ft [26 kPa/m], $P_H[1100 \text{ ft}] = 850$ psi [$P_h(335 \text{ m}) = 5860$ kPa], we get

$$P_H(0) = 428 \text{ psi [2950 kPa]}.$$

Thus, the depth at which the minimum principal stress changes from horizontal to vertical is given by:

$$P_V = P_H, \text{ which, upon substitution, becomes}$$

$$z\Delta P_V = 428 \text{ psi} + \frac{\nu\Delta P_V}{(1-\nu)} \quad [2950 \text{ kPa} + \frac{\nu\Delta P_V}{(1-\nu)}]$$

and the depth is

$$z = 558 \text{ ft [170 m]}.$$

The overburden pressure at this depth is 642 psi [4426 kPa]. The fracture may have thus propagated slowly vertically until its upper edge was about 558 ft [170 m] below the ground surface, at which time it began to propagate horizontally. This interpretation fits well with the analysis of Phase 1. The tilt residuals on all instruments in Figure 8 (not just #1, #2, and #3, as in the first interpretation) have the form suggestive of a horizontal fracture propagating perpendicularly from an initial subvertical fracture that strikes approximately ENE-WSW.

ANALYSIS: Phase 3; 17:15 (Shut-in)

At the time of shut-in, 9.68×10^5 std ft³ [2.59×10^4 std m³ (0°C, 1 atm)] of gas had been injected downhole, and the pressure in the wellbore was 1300 psi [8962 kPa]. As this pressure considerably exceeds in-situ compression perpendicular to the planes of the fractures that had been formed, continued fracture advance might be anticipated until the system reached equilibrium conditions under uniform pressure. That this occurred is evident from the tiltmeter data.

The wellhead pressure record shows an initially constant decay over a period of three minutes, from 1300 psi [8962 kPa] down to 1000 psi [6550 kPa] over the next 33 minutes. A short, eight-minute blowback at the wellhead reduced the pressure to 900 psi [6205 kPa], where it remained for 12 hours. It is likely that the initial rapid decline was associated with continuing fracture advance.

The tilt records are not entirely consistent with the pressure behavior. Tilting continued on all instruments for three minutes after shut-in, in roughly the same sense as before shut-in. However, instruments #1, #2, #3, and #4 continued to register changing tilts for up to seven minutes following shut-in. The timing of the records shown in Figure 3 is good to within 30 seconds, so the effect is real.

The residual tilt vectors accumulated during the ten minutes following shut-in are shown in Figure 9.

DISCUSSION AND CONCLUSIONS

Analysis of the surface tiltmeter array data indicates the fracture resulting from the injection of 15,500 ft³ [440 m³] of fracture forming nitrogen gas at a depth of 1100 ft. [335 m] to be a complex structure. During the first 16 minutes of injection, the fracture propagated from the wellbore as a bi-lobed near-vertical feature of dipping 87° to the northwest. The strike of the northeastern lobe was approximately N62°E. That of the southwestern lobe was approximately S59°W. The strike of the northeastern lobe is accurate to ±1°, that of the southwestern lobe is less precise due to low instrument density. The derived azimuth is in excellent agreement with the orientation of maximum post-frac microseismic activity, as monitored by the downhole seismic sensor package of SNL. Inter-

estingly, this direction corresponded to the likely azimuth of the natural fracture systems that intersected the well as suggested by seisviewer imagery, the downhole seismic sensor package and core analysis. The implication would seem to be that the induced fracture may well have exploited pre-existing fracture systems, at least near the wellbore.

Fracture height in the vicinity of the northeastern instruments, as deduced from the pattern of surface tilting, is placed at 600 ft [183 m] above the injection point. The depth of extent is placed similarly at 600 ft [183 m] but is much less certain owing to the decreased sensitivity of the instruments to fracture deeper than the point of injection. Fracture height to the southwest of the wellbore is probably slightly less than 600 ft [183 m]. Lateral extent of fracture cannot be determined, other than to place it greater than about 800 ft [244 m] from the wellbore in the northeastern direction at least. It is likely that the 1300 psi [8962 kPa] pressure in the wellbore during injection did not extend appreciably from the injection point.

A significant change in fracture growth occurred 16 minutes after injection commenced and persisted until shut-in, eight minutes later. The nature of the change has not been uniquely identified, although it is certain that a change in the plane of fracture advance occurred. Gas entry into a pre-existing fracture system oblique to the plane of the existing fracture and lying to the northeast of the instrument array presents one possibility. However, this would require the fracture system to be similarly oblique to the plane of the natural fracture systems observed in the wellbore. A physically more attractive, albeit provocative, interpretation of the tilt field is that it results from a breakout of the fracture into the horizontal plane at a depth of roughly 500 ft [153 m] near the wellbore. Analysis of the in-situ overburden stress gradient shows this behavior to be possible once the fracture has attained a height of approximately 600 ft [183 m]. Considerable support for the interpretation is provided by the observation that the Wade 2 well, lying 1500 ft [4572 m] from the well in a direction S61E (Figure 2), suffered contact with the nitrogen gas during some stage of the treatment (Tad Weed, personal communication). Clearly, the original subvertical fracture plane cannot have direct contact with the Wade #2 well.

NOMENCLATURE

- a = half height of fracture (or radius of circular fracture)
- α = dip of fracture
- d = depth to center of fracture
- K_{IC} = fracture toughness of shale
- L = distance measured along flow line
- μ = shear modulus of shale
- ν = Poisson's ratio
- p = driving pressure of fracture fluid
- $P_h(z)$ = minimum horizontal stress at depth z
- $P_v(z)$ = vertical (overburden) principal stress at a depth z.
- ΔP_v = overburden pressure gradient
- Q = flow rate of fluid from wellbore
- r = distance of an in-fracture "field" point from the wellbore

- V = volume of fracture
- w = maximum width of fracture

ACKNOWLEDGEMENTS

The Black #1 Well Project was jointly funded by DOE/Morgantown Energy Technology Center (METC) and the Gas Research Institute (GRI). The well was made available by Thurlow Weed and Associates and the work performed by MDWI was funded by Sandia National Laboratories (SNL). The authors would particularly like to thank Tad Weed, Phil Henry and Bob Dewey of Thurlow Weed or Associates, Mike Wilson of Halliburton Services, Bob Trump of Gulf Research and Development, Carl Schuster and crew from SNL, Al Youst of METC and John Sharer of GRI for providing enthusiastic co-operation and discussion. Credit is also due to the field crew and staff of M. D. Wood, Inc. for their most essential contribution to this project.

REFERENCES

- 1) Birdwell Division of Seismograph Services Corporation. Suite of logs performed on Black #1 Well, Knox County, Ohio. DOE:METC Unconventional Gas Recovery Program, Open-file Report, 1979.
- 2) Unknown. Analysis of cores taken from Beckholt #1 Well, Knox County, Ohio. DOE:METC Unconventional Gas Recovery Program, Open-file Report, 1979.
- 3) Schafer Exploration Company. Lineament analysis for the region in the vicinity of Black #1 Well, Knox County, Ohio. DOE:METC Unconventional Gas Recovery Program, Final Report, December 15th, 1979.
- 4) Schafer Exploration Company. Analysis of borehole seisviewer data taken from Black #1 Well, Knox County, Ohio. DOE:METC Unconventional Gas Recovery Program, Final Report, January 19th 1979.
- 5) Records in the possession of: Alan Joust, Morgantown Energy Technology Center, Morgantown, W. Virginia, 1980.
- 6) Analytical Research Associates Incorporated. Nitrogen analysis of samples taken from wells in the vicinity of Black #1 Well, Knox County, Ohio, DOE:METC Unconventional Gas Recovery Program, Open-file Report, 1979.
- 7) Sandia National Laboratories. Gas Research Institute: Improved Fracturing. Quarterly Report. Sandia No. SAND-80-0591, February 1980
- 8) H. Hert, Lawrence Livermore Laboratories, Livermore, California.
- 9) Perkins, T. K. and Kern, L. R. "Widths of hydraulic fractures", J. Pet. Tech. (Sept, 1961) 937-949.
- 10) Pollard, David D. and Holzhausen, Gary R.. "On the mechanical interaction between a fluid-filled fracture and the Earth's surface," Tectonophysics, (1979), 53, 27-57.

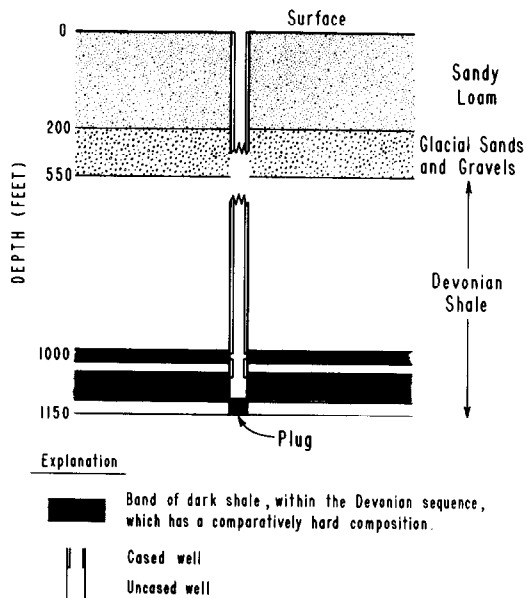


Fig. 1 - Cross-section through Black #1 well showing strata through which the wellbore passes.

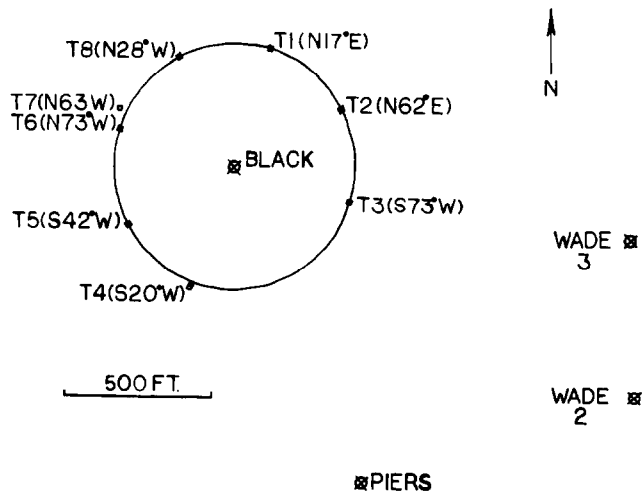


Fig. 2 - Plan view of site showing neighboring wells (T1-T8) and the location of the tillimeters.

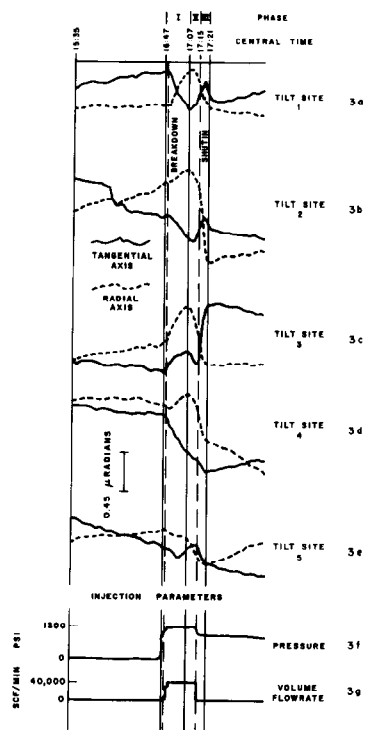


Fig. 3 - Till waveforms observed during injection. Solid vertical lines delineates phase of fracture growth.

07-DEC-79 AOA NITROGEN FRAC: PHASE 1 H.O. MOOD, INC.

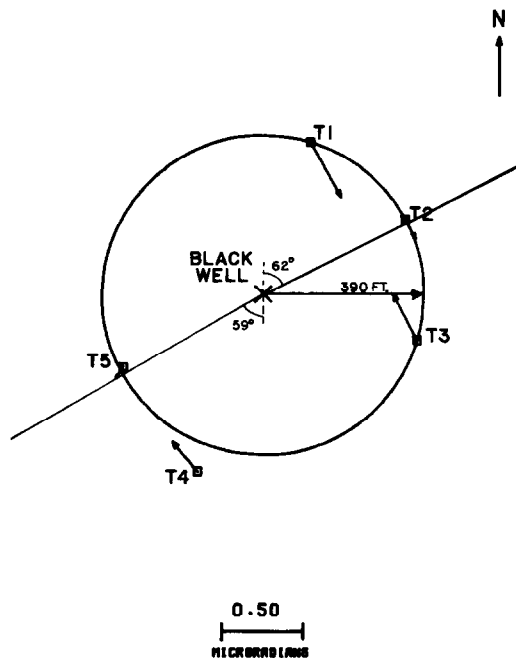


Fig. 4 - Till vector residuals at the end of phase 1.

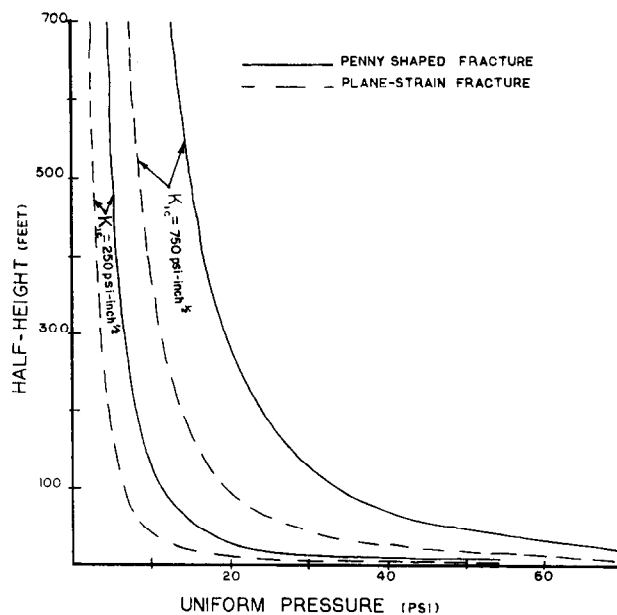


Fig. 5 - Bounds on driving pressure and fracture height placed by the possible range of fracture toughness of the rock.

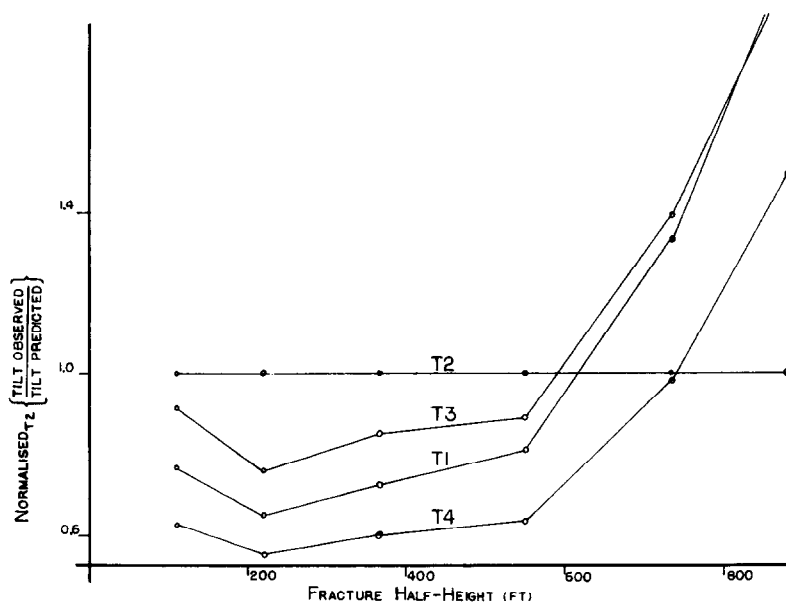


Fig. 6 - Plot of the ratio of tilt observed to that predicted for each instrument from a buried fracture of dip 87° and strike $N 62^\circ E$ for a variety of fracture heights. For a given height, the ratios for all instruments have been normalised so as to make the ratio for #2 equal to unity. The ratios shown are thus independent of driving pressure and shear modulus.

30-OCT-79

AOA FRAC PHASE 2

M.D. WOOD, INC.

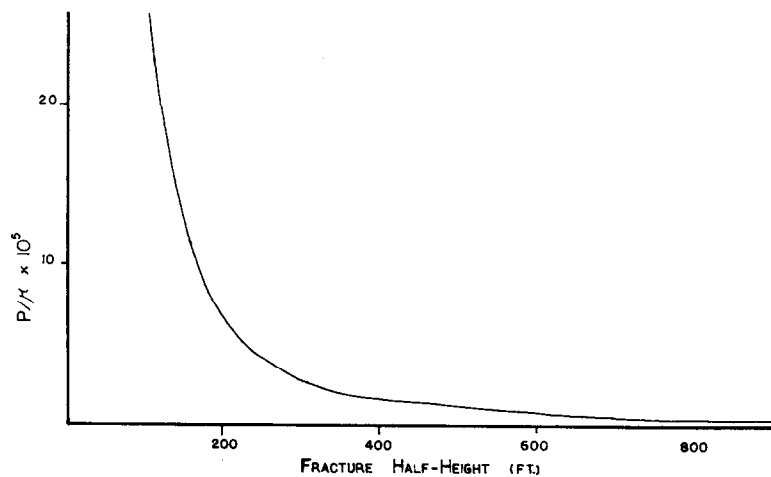


Fig. 7 - Plot of P/K values required to satisfy observed tilts for a fracture of variable height and appropriate dip, strike, etc.

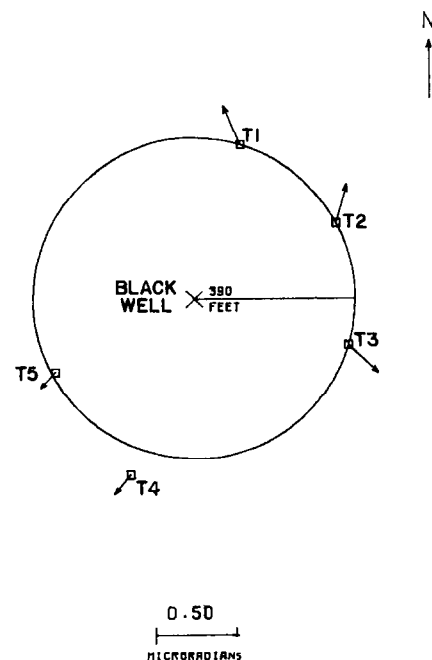


Fig. 8 - Residual tilt vectors accumulated during phase 2.

30-OCT-79

AOA FRAC PHASE 3
H.O. HOOD, INC.

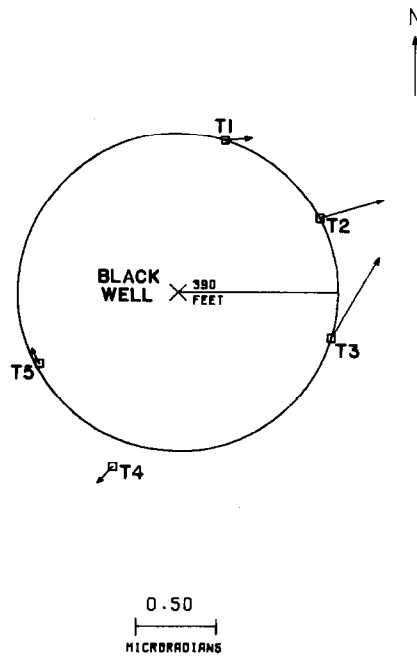


Fig. 9 - Residual tilt vectors accumulated during phase 3.

IN SITU EVALUATION OF SEVERAL TAILORED-PULSE WELL-SHOOTING CONCEPTS

by Richard A. Schmidt, Norman R. Warpinski and
Paul W. Cooper, Sandia National Laboratories

This paper was presented at the 1980 SPE/DOE Symposium on Unconventional Gas Recovery held in Pittsburgh, Pennsylvania, May 18-21, 1980. The material is subject to correction by the author. Permission to copy is restricted to an abstract of not more than 300 words. Write: 6200 N. Central Expwy., Dallas, Texas 75206

ABSTRACT

Dynamic stimulation techniques that produce multiple fracturing in a wellbore are being investigated for enhanced gas recovery. Multiple fracturing appears to be especially promising for stimulating naturally-fractured reservoirs, such as the Devonian shales, since this may be the most effective technique for connecting a wellbore to a pre-existing fracture network. Previous studies have demonstrated that detrimental effects can occur with high-strength explosive techniques and that these effects can be avoided through the use of propellants.^{1,2} The use of propellants and other so-called tailored-pulse techniques depend on a controlled pressure-time behavior to minimize wellbore damage and maximize fracture growth by gas penetration.

This paper describes a series of five full-scale tests performed to evaluate various multi-frac concepts. The tests were conducted at the Nevada Test Site in cased, horizontal boreholes drilled in ash-fall tuff from a tunnel under 430 m of overburden. This site provides both realistic in situ conditions for the tests and access to the stimulated regions by mineback which permits direct observation of results. The five tailored-pulse concepts tested involve:

- Case A - a decoupled explosive,³
- Case B - a decoupled explosive with propellant booster,³
- Case C - a small-diameter propellant charge with pressurized water pad,⁴
- Case D - three successive shots of Case C, and
- Case E - a full-diameter charge of a progressively-burning propellant.²

While direct observation by mineback is highly beneficial, evaluation and analysis

References and illustrations at end of paper.

of these test results also depended heavily on other diagnostics. Thirty-six stressmeters and accelerometers were fielded in the surrounding rock to record the dynamic disturbances, and each borehole contained transducers to measure the actual cavity pressures. Pre-test and post-test evaluations include TV log, caliper log, and permeability measurements. Permeability, which evaluates the effectiveness of the created fracture network to transmit fluids, was determined by analysis of constant-pressure, water-injection tests and the subsequent pressure decline after shut-in.

Results show a large increase in formation permeability for Case E, modest increases for Cases B, C, and D and a decrease for Case A that appears due to the formation of a stress cage. A comparison of Case E results with previous tests suggests a multiple fracture criterion based on pressure rate with little effect of peak pressures.

INTRODUCTION

Oil and gas wells have been stimulated with high-energy explosives since the late 1800's. It appears, however, that the term "well shooting" originated many years before this in days when a water well was sometimes rejuvenated by shooting a rifle down the well. Well shooting as discussed herein refers to any rapid release of energy from a chemical reaction in a wellbore for the purpose of stimulating production, presumably by fracturing the reservoir rock. This includes explosives (solid, liquid, and gas) and propellants that deflagrate rather than explode. In a broad sense, well shooting has been applied in several geotechnical fields; e.g., preparation of oil shale beds for true in situ processing, preparation of underground mineral deposits for solution mining, etc.

Problems of wellbore damage, safety hazards, and unpredictable results have

reduced the relative number of wells stimulated by high-strength explosives. In recent years hydraulic fracturing has been favored, and sophisticated techniques, equipment, fracturing fluids, and proppant have been developed to optimize the hydraulic fracturing process.

Unfortunately, similar efforts toward general understanding and process optimization have been lacking for well shooting. However, recent findings (summarized in Ref. 1) have shed new light on the process of dynamic wellbore fracturing. These findings indicate that vast improvements may be possible using "tailored-pulse" loading techniques.

Tailored-pulse loading involves using propellants, decoupled explosives, or explosive gases to produce a controlled, but rapid, release of energy. This concept is more fully described in a later section, but first the general behavior and limitations of conventional well shooting with high-strength explosives need to be described to understand better the benefits derived from tailored-pulse loading.

GENERAL BEHAVIOR OF A DEEPLY-BURIED CHARGE

One important aspect common to most well shooting configurations is the fact that there is no free surface near enough to the charge to affect the behavior. The phenomena associated with deeply-buried charges, as they are called, differ significantly from those of blasts that occur near a free surface as in excavations, quarries, and road cuts.

Briefly, the high pressures of a detonation in a wellbore are known to be sufficient to cause the nearby rock to yield and compact (plastic flow). When the stress wave passes, the rock unloads elastically leaving an increased borehole diameter and a residual stress field which is compressive near the wellbore. Figure 1 depicts these general steps that take place during such an event.

The creation of this residual stress field is closely analogous to the process of autofrettage or the "gun barrel problem" in which pressure vessels are often over-pressurized sufficiently to yield the inside wall and develop residual compressive stresses that help prevent crack growth during service. The zone of highly compacted rock with its associated residual compressive stresses is sometimes referred to as a stress cage, and the phenomena is sometimes called the bladder effect. Fracturing caused by high pressure gas may also be inhibited in this situation since fines are created during the compaction process that can plug newly formed cracks and prevent gas penetration. Some or all of these effects may actually cause decreased permeability near the wellbore and are probably responsible for many well-shooting failures.

The existence of residual stress regions around boreholes that have been subjected to

explosive detonations is a well documented phenomenon. Most of these observations have been made with regard to field experiments at the Nevada Test Site^{1,5} as well as laboratory experiments⁶ and computer code calculations^{1,5,7} for the purpose of understanding containment of underground nuclear blasts. This general behavior of a deeply-buried charge, however, is rather universal since it has been demonstrated to occur for detonations ranging from a one pound charge of TNT to a nuclear detonation of several kilotons. Further description of these general phenomena and details of the supporting evidence can be found in Ref. 1.

TAILORED-PULSE LOADING

ADVANTAGES

With the basic knowledge that the bladder effect impedes fracture growth near an explosively loaded cavity, one might wonder how conventional well shooting would ever enhance production. Experience has shown, however, that improved production is sometimes realized. There are several reasons for such results, including the possibility that explosive stimulation may at times be capable of removing skin damage, and that leakage paths may be formed that connect the cavity to the region outside the stress cage. Situations can also occur in which the stress cage will break up and slough into the wellbore. These possibilities are not necessarily predictable or applicable in all formations. It would, of course, be desirable if reliable procedures could be developed to replace conventional well shooting.

Several viable alternatives to explosive well shooting have been considered and tested in recent years that show promise of substantial improvement.²⁻⁴ An approach that has received considerable attention is to tailor the pressure-time behavior of the explosive or a suitable propellant so as to keep the maximum pressure and the loading rate below a level that would cause the rock to crush and undergo plastic flow. The intent here is to avoid entirely the formation of a stress cage while still loading at a sufficiently high rate to produce multiple fractures from the wellbore. Unfortunately, the proper combination of loading parameters that will produce optimal multiple fracturing and avoid the formation of a stress cage are not, as yet, well known.

Tailored-pulse loading of a wellbore has several advantages over hydraulic fracturing that make this technique attractive in certain situations. For example, hydraulic fractures, which are propagated at pressures that are slightly higher than the minimum in situ stress and pumping times that are on the order of hundreds of seconds, typically produce only a single fracture whose orientation is perpendicular to the minimum principal stress.^{8,9} Higher wellbore pressures, such as are achieved in tailored-pulse loading, are needed to drive cracks in less favorable directions with respect to the in

situ stresses in order to produce multiple fractures.

Multiple fractures may be highly desirable in naturally fractured reservoirs such as Devonian shale for reasons depicted in Figure 2. The production from an unstimulated well, Figure 2a, depends strongly on the number of fractures intersected. Hydraulic fracturing typically produces a single fracture that is likely to run parallel to most of the existing fractures, Figure 2b, since its orientation is governed by in situ stresses that probably also govern the pattern of the natural fractures. Multiple fractures may not extend as far as a hydraulic fracture but may link the well to more, natural fractures, Figure 2c.

In addition, tailored-pulse loading with propellants are likely to produce little formation damage due to the interaction of fluids with the rock. Very little water is produced by these materials, and the products have very little time to react with the rock. Some hydraulic fracturing fluids, on the other hand, are known to cause swelling in shale and other deleterious effects.

Cost is also a factor that may make tailored-pulse techniques very attractive, particularly in marginal wells that probably are not promising enough for expensive hydraulic fracturing treatments. Igniting an explosive or a propellant charge in a well requires very little equipment or time when compared to even a small hydraulic fracture job.

CONCEPTS

Several tailored-pulse concepts rely on the use of propellants which deflagrate rather than detonate. Unlike explosives, the burn front in these materials travels slower than the sound speed, and the burning rate can be varied over a wide range. Pressure-time behavior of propellants differ from explosives in that peak pressures are lower, and burn times are longer. Total energy available, however, is similar in both materials (typically 4kJ/g).

One of the first tailored-pulse concepts investigated was a decoupled explosive such as that used for Case A.³ A conventional explosive is used, but the charge diameter is some eight times less than the wellbore diameter. The charge is surrounded by water, and the peak pressure reaching the rock after detonation is thus mitigated, presumably to a value below the yield stress. The total explosive energy, however, is limited by the small diameter of the charge.

The concept employed in Case B uses the same decoupled explosive in conjunction with a small propellant charge.³ The decoupled explosive is designed to initiate multiple cracks and the propellant is then burned to drive water into these cracks to extend them. The propellant is essentially a rocket motor that burns for several seconds. Some

field testing has been performed using this device but results are inconclusive.

Case C is a small diameter (4cm) pressure-insensitive propellant charge that is designed both to initiate and propagate multiple cracks.⁴ A typical rise time is 3 ms with a burn time of 0.5 s. This device is also designed to push water into the cracks ahead of the gas generated by the propellant reaction products. It has been used in the field as a cleaning tool and as a fracture initiating device to reduce the breakdown pressure for hydraulic fracturing. The number and size of the fractures created by this tool are largely unknown. Case D was three successive shots using the same configuration as Case C.

Case E consists of a gas-producing, progressively-burning propellant with a suitable rise time to initiate and propagate multiple fractures while avoiding the damage of a stress cage.^{2,10} This concept differs from the others in three main areas: 1) A full-diameter charge is used that fills the wellbore to maximize the energy released. 2) Lightweight gas products from the propellant itself, rather than water, are pushed into the created fractures. This maximizes the speed in which fractures are penetrated and pressure loaded. 3) The propellant is of the progressively-burning type in that the burning rate increases as material is consumed. This allows energy to be saved and not released until it is most needed, later in time, when fractures are long and system volume is large.

MULTI-FRAC TEST SERIES

FEASIBILITY STUDY

Experiments to investigate tailored-pulse concepts have been conducted in a tunnel complex at the Nevada Test Site. The tunnel facility provides a means of performing realistic tests of deeply-buried charges in rock formations at depth and yet allows for direct observation of resulting fracture behavior by mining back to uncover the test bed itself. The purpose of this test series is two-fold: (1) evaluate and compare several tailored-pulse concepts in a controlled test bed to determine the ability of each to produce multiple fractures and to enhance formation permeability and (2) provide data for testing and verification of various modeling schemes presently being used to describe the complex behavior of tailored-pulse loading.

The feasibility of performing such experiments was demonstrated previously in a test series conducted on Gas Frac.² Three canisters, each containing propellant with markedly different burning rates, were ignited in grouted horizontal holes drilled in a water-saturated ash-fall tuff formation. The results of the three tests showed phenomenologically different behavior as depicted in Figure 3. The slowest-burning propellant created a single fracture similar to a hydraulic fracture, the intermediate-rate

propellant produced extensive multiple fractures, and the fast-burning propellant produced explosive-type behavior as evidenced by an enlarged borehole and minimal fracturing.

TEST SETUP

The previous Gas Frac tests were not instrumented except for a pressure transducer to measure dynamic cavity pressures. The five tests described below make up the so-called Multi-Frac Test Series and involved thirty-six stressmeters and accelerometers to measure rock formation response as well as pressure transducers to record dynamic cavity pressures. Along with direct observation by mineback, post-test evaluation included a reentry into each test zone for borehole television log, caliper log, and permeability measurements. The caliper log is intended to detect the degree of borehole enlargement (indicating plastic flow) and the permeability test is designed to measure the effectiveness of each test to increase the formation's ability to transmit fluids (i.e., conductivity of fracture network). The rock formation is a water-saturated ash-fall tuff having material properties as listed in Table 1.

The experiments were all conducted in 15 cm diameter, nearly horizontal holes drilled 12.2 m deep from a tunnel drift as depicted in Figure 4. The holes were spaced 6.1 m apart. Experiments A and B were conducted with 3.05 m of open hole and 9.15 m of casing while Experiments C, D, and E had 6.1 m of open hole and 6.1 m of casing. The mineback (not completed as of this writing) is planned so that half of each test zone will be mined out and examined thoroughly, leaving any fracture patterns occurring at the midpoint displayed on the right rib of the tunnel (Figure 4). All test setups were similar and a cross-section of the Case B configuration is seen in Figure 5.

Rock mass instrumentation consisted of an array of stressmeters and accelerometers as depicted in Figure 6. This array of gages was fielded only for Experiments B, D, and E. The stressmeters were special, strain-gaged, borehole-inclusion stressmeters.¹¹ Two of these transducers were set and preloaded in each instrumentation hole to measure diametral deformations in the radial and transverse directions. Calibration of these gages was accomplished by static loading of a block of ash-fall tuff that contained a gage mounted in a hole drilled in the sample. Commercially available accelerometers were also set and preloaded in a similar fashion to measure radial and transverse accelerations. (Note that transverse accelerations would not be expected in a symmetric displacement field but could result from motions due to the dynamic propagation of a nearby crack.)

SPECIFIC TEST CONFIGURATIONS

The device fielded in Experiment A was simply a 2 cm diameter by 3 m long PVC tube filled with 2.3 kg of Comp C4 explosive. This was centralized in the hole and the

cavity filled with water under atmospheric pressure. The water contained a blue dye to stain the created fractures and to ease identification and mapping during mineback. Dynamic cavity pressure was measured in this experiment using both Kulite* sensors and specially designed ytterbium paddle gages¹² located near the end of the casing section (Figure 5). The Kulite gage model HKM-375, is a piezoresistive integrated sensor. This gage has a 200 MPa pressure range and consists of a miniature silicon member on which a temperature compensated wheatstone bridge is atomically bonded. The miniaturization results in a natural frequency of 400 kHz.

Experiment B involved the same Comp C4 explosive setup but also contained a 2.7 kg charge of propellant. This relatively slow-burning propellant charge consisted of a single, internal-star rocket grain ignited with a black-powder-filled spit tube and housed in a sealed aluminum canister. The canister was located in the casing section against the bulkhead and was designed to act as a dynamic plunger to push the dyed water down the casing and into fractures initiated by the explosive charge. The fire set was designed to ignite the propellant charge first and then to detonate the explosive 70 msec later by which time the propellant would have reached sufficient pressure. Transducers fielded in this experiment to measure the dynamic cavity pressure event included Kulite and ytterbium gages at the end of the casing section and a fluid-coupled-plate gage¹³ located at the bulkhead near the propellant canister. The sensing element used in the fluid-coupled-plate transducer is the same Kulite gage mentioned previously.

The device used for Experiments C and D consisted of a 2 cm diameter by 6.1 m long soft aluminum tube filled with 2.3 kg of propellant which was ignited at one end. The device was centralized in the test hole and the cavity filled with dyed water. The water was pressurized statically to 3.4 MPa using a hydraulic pump just prior to these shots in order to simulate the containment from a 300 m column of water. Dynamic cavity pressure was measured in each of these shots by means of Kulite gages located near the end of the casing section.

The device fielded in Experiment E included a number of design improvements over the previous configuration.² The device (Figure 7) consisted of six canisters, each 12.7 cm diameter by 1 m long that screwed together. The canisters were made of perforated plastic tubes with a heat-shrinkable vinyl covering to make the unit watertight. Each canister contained 9.1 kg of M5 multi-perf propellant grains with a 1 mm web thickness. This propellant was ignited by means of a 3.2 cm diameter perforated-steel primer tube that runs through the center of each canister and becomes a continuous igniter when the units are screwed together. The

*Kulite Semiconductor Products, Inc., Ridgefield, NJ.

primer tube contained an explosive and igniter which provided ignition along the entire 6 meter length in less than 1 msec. The primer tube itself was initiated with an exploding bridge wire device as were all other experiments.

Since the propellant burns cleanly, several bags containing carbon black were taped to the outside of the canisters (Figure 7) to act as crack markers so that the created fractures would be more visible during mineback. Also, a number of 1.3 cm diameter ceramic spheres and 0.6 cm diameter cylinders were taped to this device in hopes that they would be propelled into the fractures and thereby act as dynamic crack width indicators when located during mineback. (These spheres and cylinders were used in the other experiments as well.) The assembly was placed in the dry 6.1 meter test section and sealed with a grout plug. The opposite end of the test zone contained a fluid-coupled plate transducer to measure dynamic cavity pressure.

Estimates of the grout-to-casing and grout-to-rock shear strength indicated that sufficient load-carrying capacity was available to contain these shots (refer to Figure 5). However, a strong-back brace was added as a backup measure (Figure 8). The brace was designed to transmit the load from the casing and bulkhead to the opposite tunnel rib if complete containment was not achieved. All shots were fired remotely and were monitored by close-circuit television.

All shots were fired using a capacitive discharge unit which dumps to an exploding bridge wire. Data was recorded in a separate instrumentation trailer using a 50 kHz analog system with voltage-controlled-oscillator and multiplexer. The analog data was recorded on magnetic tape and later digitized, reduced, and plotted.

RESULTS AND DISCUSSION

Note: Reduction and analysis of the test data and mineback evaluation were not complete at the deadline of this paper. Thus, the results and conclusions presented here are preliminary.

All shots were fired successfully except Experiment B. On that test, the propellant charge was ignited as planned. After a 70 msec delay, a signal was sent to the explosive charge, but detonation did not occur. Post-shot evaluation disclosed that the exploding bridge wire was intact, but that the detonation cables had been severed in two places by the propellant charge, preventing the bridge from receiving the impulse required.

Pressure-time and stress-time records from Experiment D are displayed in Figure 9. The stress-time behavior is for radial and transverse stress at a location 1 m from the test section. Note that the pressure-time record shows a second pressure peak that occurs 9 msec after the first. This corres-

ponds to the transit time of the stress pulse propagating from the gage to the steel bulkhead and back. This second pulse is also observed in the stress records.

Peak borehole pressure is seen to be 46 MPa. If this pressure were assumed constant and confined to the borehole, a 0.32 MPa stress would be expected at the 1 m stressmeters (with radial stress being compressive and tangential being tension). Peak stresses, however, were much higher: 1.06 MPa tangential tension and 2.16 MPa radial compression. Wave-code analysis indicates that little dynamic effect is present in this rate regime. Note that the tangential and radial stress become nearly equal in magnitude at late times as expected from quasi-static analysis. The discrepancy is likely due, instead, to pressure escaping from the borehole and loading the created fractures, thereby strongly affecting the loading configuration.

Preliminary results of stressmeter data from Experiment E indicate that stresses were more than 10 times larger than calculated from assumptions of a static borehole pressure. This discrepancy must be a result of substantial gas penetration into fractures and is consistent with observations of extensive fracturing detected in this experiment as discussed later.

A pre-test and post-test evaluation of in situ permeability was made for each test to indicate the capability of each device to increase the formation's ability to transmit fluids. Since this water-saturated ash-fall tuff formation has no "reservoir" pressure, per se, measurements were made by pressurizing each zone with water at a constant pressure of 2.8 MPa and recording the decay of flow with time. The flow rate data could then be fit to give the appropriate parameters which characterize the porous media and boundary conditions. However, since flowing time was always greater than a few minutes, the analysis was greatly simplified by an approximate logarithmic equation. The inverse of the flow rate ($1/q$) is plotted against the logarithm of time, and the permeability is determined from the slope of this line by

$$K = \frac{(185.7)\mu}{H(P_0 - P_\infty)m}$$

where

K is permeability in md
 μ is viscosity in kPa·s
 H is zone length in m,
 $P_0 - P_\infty$ is injection over-pressure in kPa, and
 m is slope in $(\text{cm}^3/\text{sec})^{-1}/\text{cycle}$

An example of this measurement scheme is displayed in Figure 10. The pressure decay after shut-in was also analyzed in a manner similar to that for a standard pressure buildup record in a gas well.

Results of the pre-test and post-test permeability measurements are presented in Table 2. Each value of permeability is the average of the flow test and the shut-in. A large permeability enhancement is seen for Experiment E which is a clear indication of extensive fracturing. Experiments B, C, and D display a moderate increase in permeability. Experiment A, however, produced a decrease in formation permeability. This is apparently due to the creation of a stress cage (the bladder effect) even though the explosive was "decoupled" from the formation by an 8 to 1 ratio of hole diameter to charge diameter.

These observations are consistent with post-test TV logs. Several, wide radial fractures were seen in the log of Experiment E, and a few narrow fractures were seen in C and D. While no fractures were seen in the log of Experiment B, a single hydraulic-type fracture is expected here due to the very low pressure-loading rate of the propellant used. The presumption of a stress cage in Experiment A was confirmed in the TV log by the observation of an enlarged, distorted borehole with no apparent fractures.

Closed circuit television of Experiment E also showed indications of extensive fracturing. Shortly after ignition, a gas-driven fracture apparently reached an instrumentation hole located 2 m from the test section, which then pressurized the hole and propelled a 3 m long grout plug across the tunnel. Shortly after this another fracture apparently reached the test section of Experiment C (see Figure 4) 6.1 m away and propelled water and debris out of that hole. These observations were confirmed upon reentry in the tunnel when significant levels of combustion gas (carbon monoxide) were monitored coming out of these holes.

An enlightening comparison can also be made among the three previous Gas Frac shots² and Experiment E. Pressure-time characteristics and observed fracture behavior are compared in Table 3. Note that a good correlation between pressure rate and resulting behavior exists while no such correlation occurs with peak pressure. This indicates that pressure rate may be the governing parameter in determining whether resulting behavior is hydraulic fracturing, multiple fracturing, or explosive compaction. A preliminary closed-form analysis was performed that indicates the pressure rates in GF2 and Experiment E were low enough such that tangential stress at the borehole wall begins and remains tensile. On the other hand, the pressure rate of GF3 was sufficiently high to cause tangential compression initially. These initial compressions probably delay the tensile failure until after the compaction process has begun causing the bladder effect. This suggests a multiple fracture criterion that is based on a pressure rate being less than a value that would produce tangential compressive stress at the borehole wall. This criterion was previously suggested by Bligh as a means to avoid explosive compaction.¹⁴

CONCLUSIONS

These experiments have shown that multiple fractures can be created from a borehole while avoiding the formation of a stress cage by using an appropriately designed tailored-pulse technique. In particular, results of TV logs, permeability tests and other indirect data showed that the Case E technique produced a highly stimulated zone around the wellbore; Case B, C, and D resulted in a modest stimulation; and Case A, which apparently induced a stress cage to be formed in this rock even though it was a decoupled charge, actually decreased the formation permeability.

The results of these tests and previous experiments suggest that a multiple fracture criterion be based on borehole pressure-loading rate. Peak pressure conditions may not be important if loading-rate requirements are adequate.

Finally, these tests show the value of carefully designed in situ experiments for evaluating stimulation techniques. Instrumentation such as stressmeters, accelerometers, and pressure transducers can be fielded in critical locations, evaluation techniques such as TV and caliper logs and permeability tests can be conveniently employed, and ultimately, mineback can provide a complete diagnosis of the resultant fracture patterns.

ACKNOWLEDGEMENTS

Appreciation is extended to all who worked on the Multi-Frac Test Series with special thanks to Tom Laws for field engineering, Jack Schwarz for mechanical design, Rod Shear, Mike Burke, and Gary Miller for instrumentation and data acquisition, Lew McEwen and Fred Shoemaker for arming and firing, Bob Beyatte for data reduction, Sharon Finley for mineback evaluation and Clarence Huddle for material property measurements. The excellent work of the skilled mining crew at the Nevada Test Site is also acknowledged. The authors would also like to thank Stuart McHugh of SRI International for initial wave code calculations that helped determine gage settings. This investigation was sponsored under the Eastern Gas Shales Project which is managed by R. L. Wise and C. A. Komar, Morgantown Energy Technology Center. This work was supported by the United States Department of Energy (DOE) under contract number DE-AC04-76000789.

REFERENCES

- Schmidt, R. A., Boade, R. R., and Bass, R. C., "A New Perspective on Well Shooting - The Behavior of Contained Explosions and Deflagrations," Proceedings of 1979 Society of Petroleum Engineers Annual Technical Conference and Exhibition, SPE 8346 (1979).

2. Warpinski, N. R., Schmidt, R. A., Cooper, P. W., Walling, H. C., and Northrop, D. A., "High-Energy Gas Frac: Multiple Fracturing in a Well-bore," Proceedings of 20th U. S. Symposium on Rock Mechanics, Austin, TX, (1979).
3. Moore, E. T., Mumma, D. M., and Seifert, K. D., "Dynafrac - Application of a Novel Rock Fracturing Method to Oil and Gas Recovery," Physics International Final Report 827, April 1977.
4. Fitzgerald, R. and Anderson, R., "Kine-Frac: A New Approach to Well Stimulation," ASME Paper 78-PET-25, ASME Energy Technology Conference and Exhibition, Houston, TX, November 5-19, 1978.
5. Smith, C. W., Bass, R. C., and Tyler, L. D., "Puff 'n Tuff, A Residual Stress - Gas Fracturing Experiment," Proceedings of 19th U. S. Symposium on Rock Mechanics, Stateline, Nevada (1978).
6. Florence, A. L., and Gates, R. W., "Explosive Cavity Residual Stress Experiment," 76-3702-2, Stanford Research Institute, Menlo Park, CA (1976).
7. Boade, R. R., Stevens, A. L., Harak, A. E., and Long, A., "Bed Preparation Concepts for True In Situ Oil Shale Processing: An Evaluation of Current Technology," Proceedings of the 1979 Society of Petroleum Engineers Annual Technical Conference and Exhibition, SPE 8447 (1979).
8. Howard, G. C., and Fast, C. R., Hydraulic Fracturing, Society of Petroleum Engineers of AIME Monograph Series, Dallas, TX, (1970).
9. Northrop, D. A., Warpinski, N. R., Schmidt, R. A., Smith, C. W., "Stimulation and Mineback Experiment Project - The Direct Observation of Hydraulic and Explosive Fracturing Tests," Proceedings of the Fourth Annual DOE Symposium on Enhanced Oil and Gas Recovery, Tulsa, OK, August 1978, p. E-4.
10. Schmidt, R. A., Warpinski, N. R., and Northrop, D. A., "In Situ Testing of Well-Shooting Concepts," Proceedings of Third Eastern Gas Shales Symposium, Morgantown, WV (1979).
11. Cook, C. W. and Ames, E. S., "Bore-hole-Inclusion Stressmeter Measurements in Bedded Salt," Proceedings of 20th U. S. Symposium on Rock Mechanics, Austin, TX, (1979).
12. Ginsberg, M. J., Grady, D. E., Decarli, P. S., and Rosenberg, J. T., "Effects of Stress on the Electrical Resistance of Ytterbium and Calibration of Ytterbium Stress Transducers," Stanford Research Institute, DNA 3577F, Menlo Park, CA (1973).
13. Cook, C. W. and Ames E. S., "Pressure Measurements in Harsh Environments," Proceedings of the 25th International Symposium of Instrument Society of America, May 7-10, 1979, Anaheim, CA.
14. Bligh, T. P., "Principles of Breaking Rock Using High Pressure Gases," Advances in Rock Mechanics, Proceedings of the Third Congress of the International Society for Rock Mechanics, Denver, CO, 1974, Vol. II, Part B, p. 1421.

TABLE 1
ASH-FALL TUFF MATERIAL PROPERTIES

DENSITY	1.8 gm/cm ³
POROSITY (WATER FILLED)	40%
PERMEABILITY	SEE TABLE 2
ELASTIC MODULUS	5 GPa
COMPRESSIONAL WAVE VELOCITY	2.1 mm/ μ s
SHEAR WAVE VELOCITY	1.2 mm/ μ s
TENSILE STRENGTH	700 kPa
COMPRESSIVE STRENGTH (UNCONFINED)	30 MPa
FRACTURE TOUGHNESS	400 kPa \sqrt{m}

TABLE 2
PERMEABILITY ENHANCEMENT

CASE	TAILORED-PULSE CONCEPT	PRE-TEST PERMEABILITY (md)	POST-TEST PERMEABILITY (md)	FACTOR OF INCREASE	OBSERVATIONS FROM TV LOG
A	DECOUPLED EXPLOSIVE WITH WATER PAD	0.20	0.05	0.25	ENLARGED, DIS- TORTED BOREHOLE
B	DECOUPLED EXPLOSIVE* WITH PROPELLANT PUSHER (WATER PAD)	0.83	5.6	7	NO FRACTURES APPARENT
C	SMALL DIAMETER PROPELLANT WITH PRESSURIZED WATER PAD	0.0015	0.008**	5**	MULTIPLE FRACTURES (VERY NARROW)
D	THREE SHOTS OF CASE C WITH PRESSURIZED WATER PAD	0.007	0.034	5	MULTIPLE FRACTURES (NARROW)
E	FULL BORE, PROGRESSIVELY- BURNING PROPELLANT WITH AIR PAD	0.014	25.0	1800	MULTIPLE FRACTURES (WIDE)

*EXPLOSIVE DID NOT DETONATE

**SOME PERMEABILITY INCREASE MAY BE DUE TO FRACTURE CAUSED BY EXPERIMENT E

TABLE 3
PRESSURE LOADING CHARACTERISTICS VS. OBSERVED BEHAVIOR

	EXPERIMENT	PEAK PRESSURE (MPa)	PRESSURE RATE (kPa/ μ s)	RESULTING BEHAVIOR
PREVIOUS GAS FRAC TEST SERIES ²	GF1	43	0.6	HYDRAULIC FRACTURE
	GF2	95	140	MULTIPLE FRACTURES
	GF3	~200	>10,000	EXPLOSIVE STRESS CAGE
	EXPERIMENT E	250	430	MULTIPLE FRACTURES

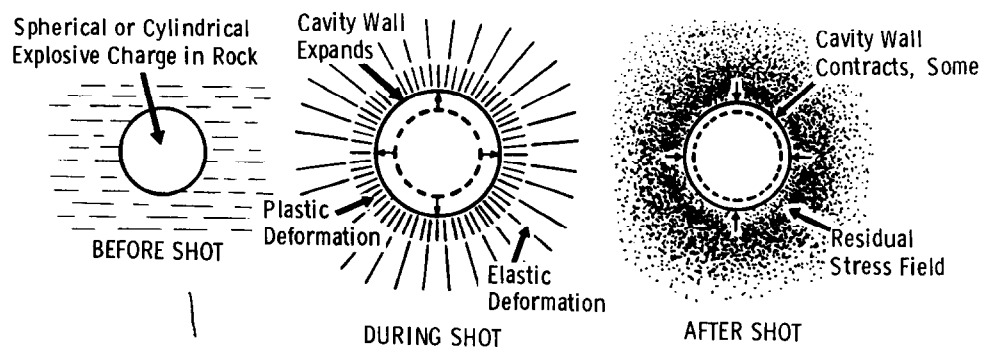


Fig. 1 - General behavior of deeply-buried charge.

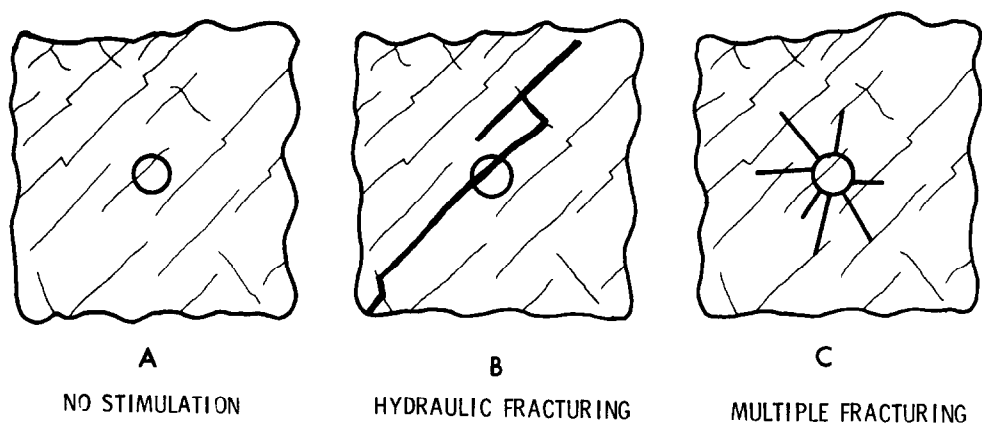


Fig. 2 - Stimulation of naturally fractured reservoir.

	GF1 "SLOW"	GF2 "INTERMEDIATE"	GF3 "FAST"
LOADING RATE (kPa/ μ s)	0.6	140	>10,000
PEAK PRESSURE (MPa)	43	95	>~200
PULSE DURATION (msec)	900	9	~1

MINEBACK
OBSERVATION
(SCHEMATIC)

1
METER

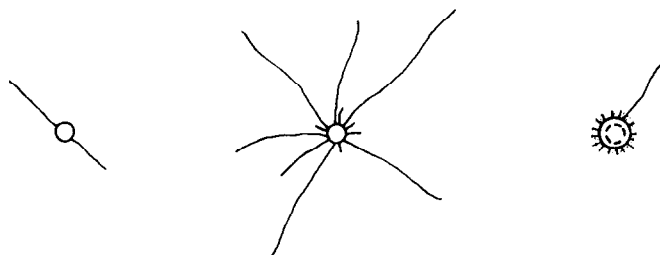


Fig. 3 - Results of gas frac experiments².

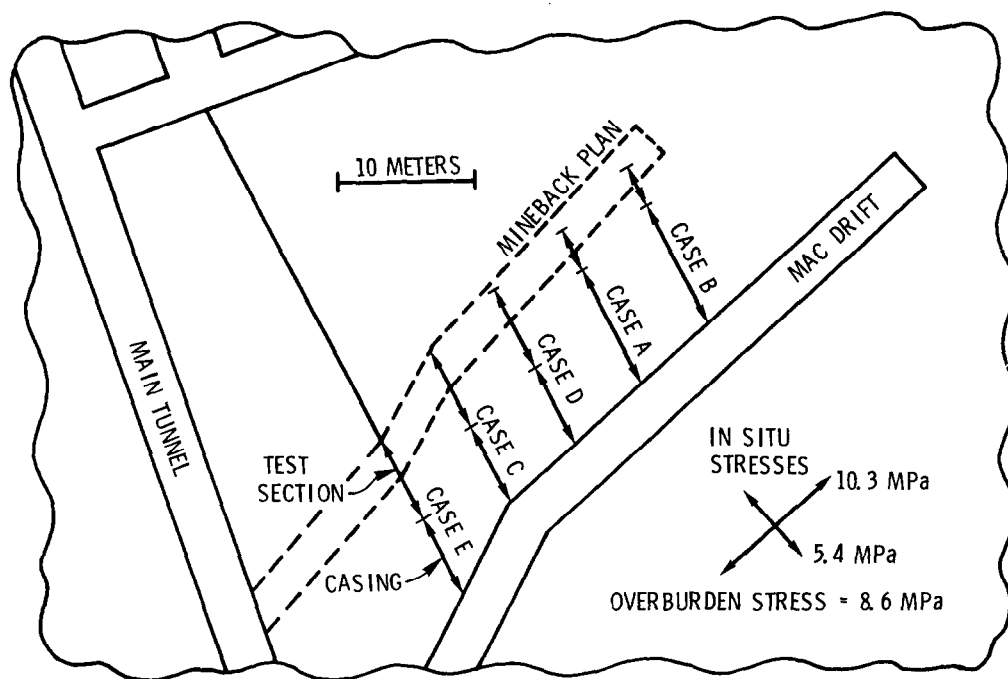


Fig. 4 - Tunnel plan for multi-frac test series.

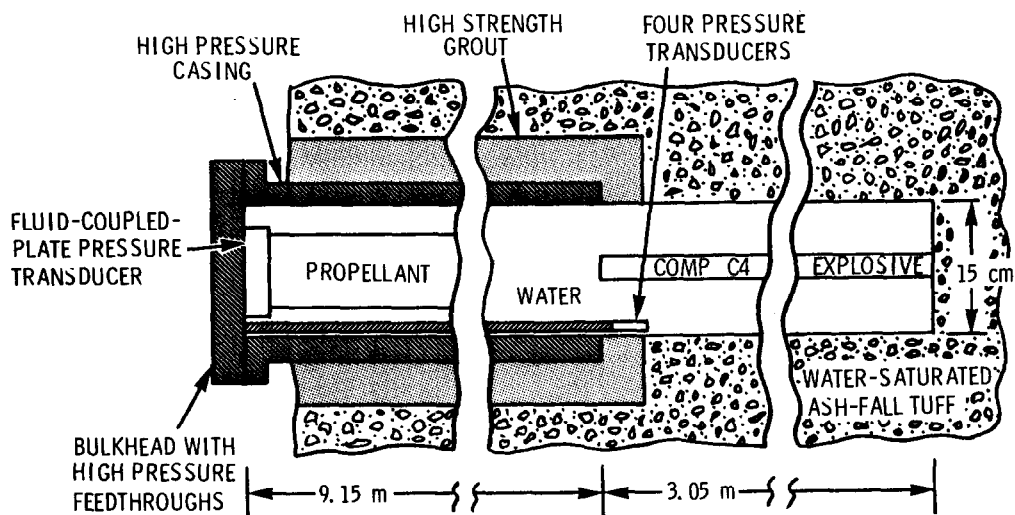


Fig. 5 - Cross section of test setup for experiment B.

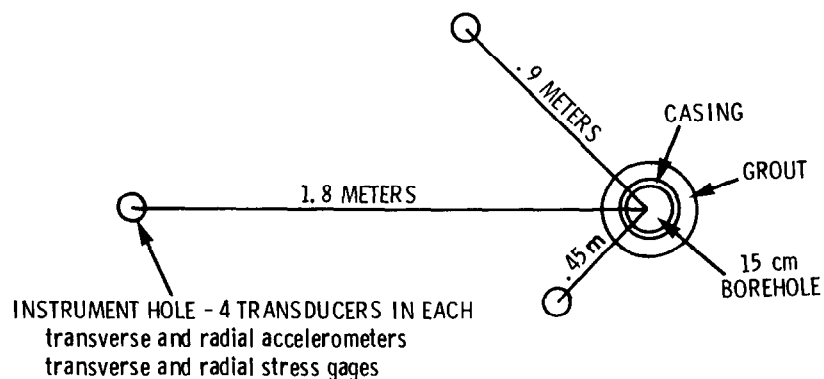


Fig. 6 - Layout of instrumentation holes.

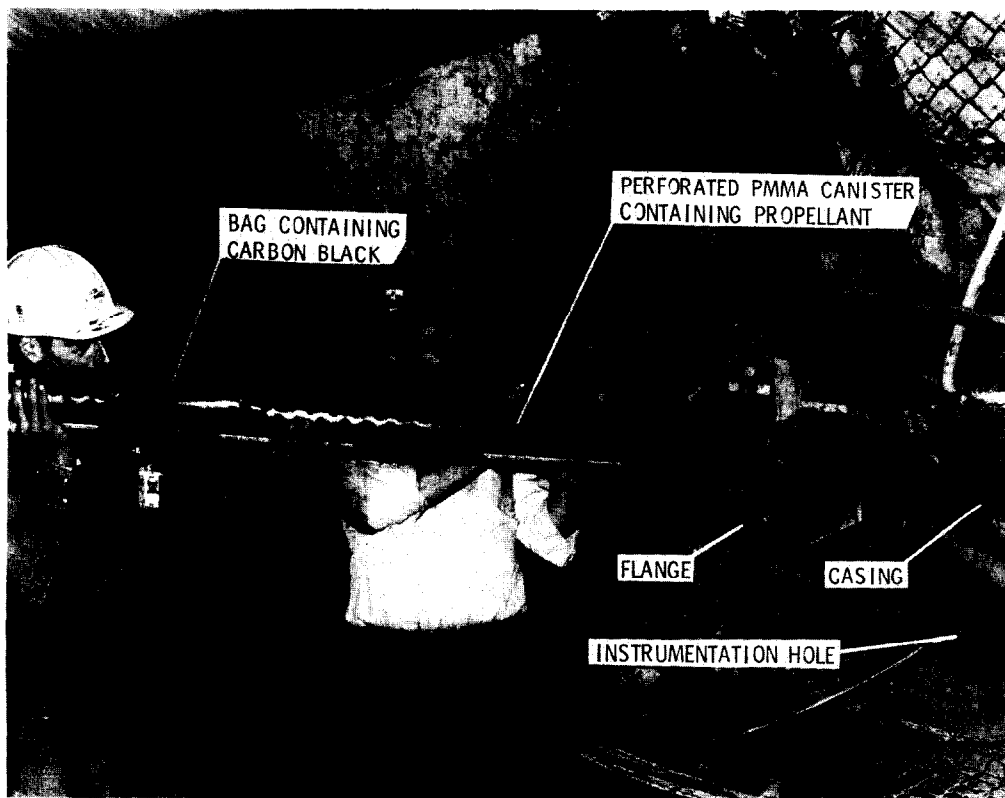


Fig. 7 - Loading of propellant device for experiment E.

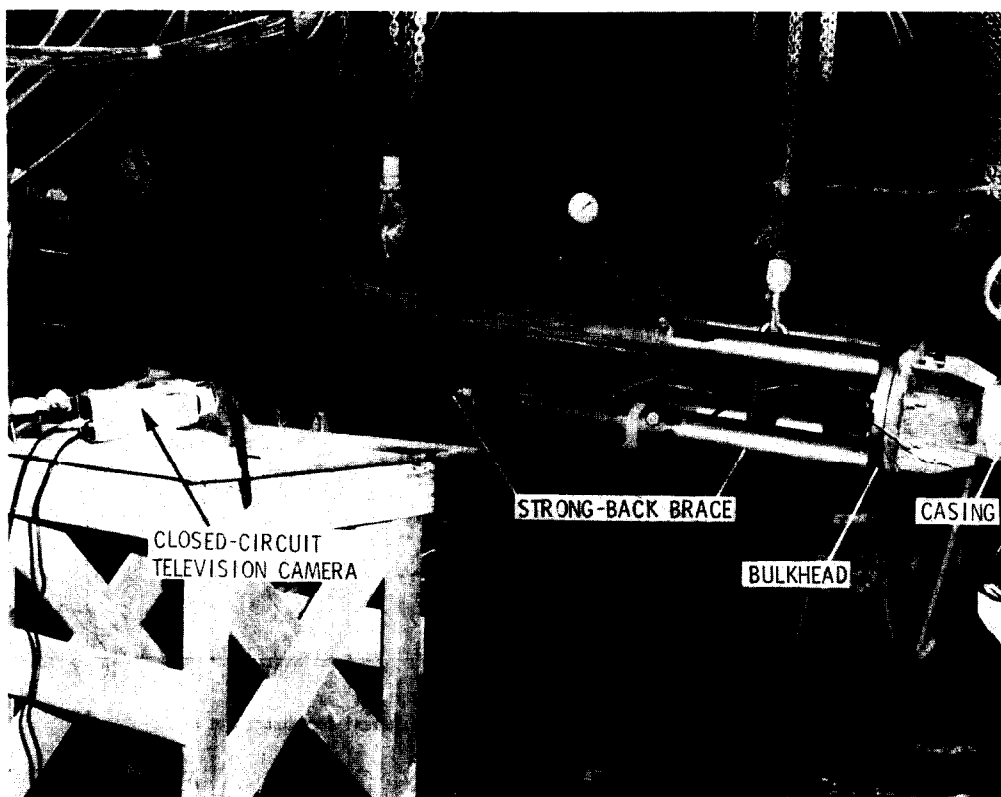


Fig. 8 - Typical view of experiment ready for arming and firing.

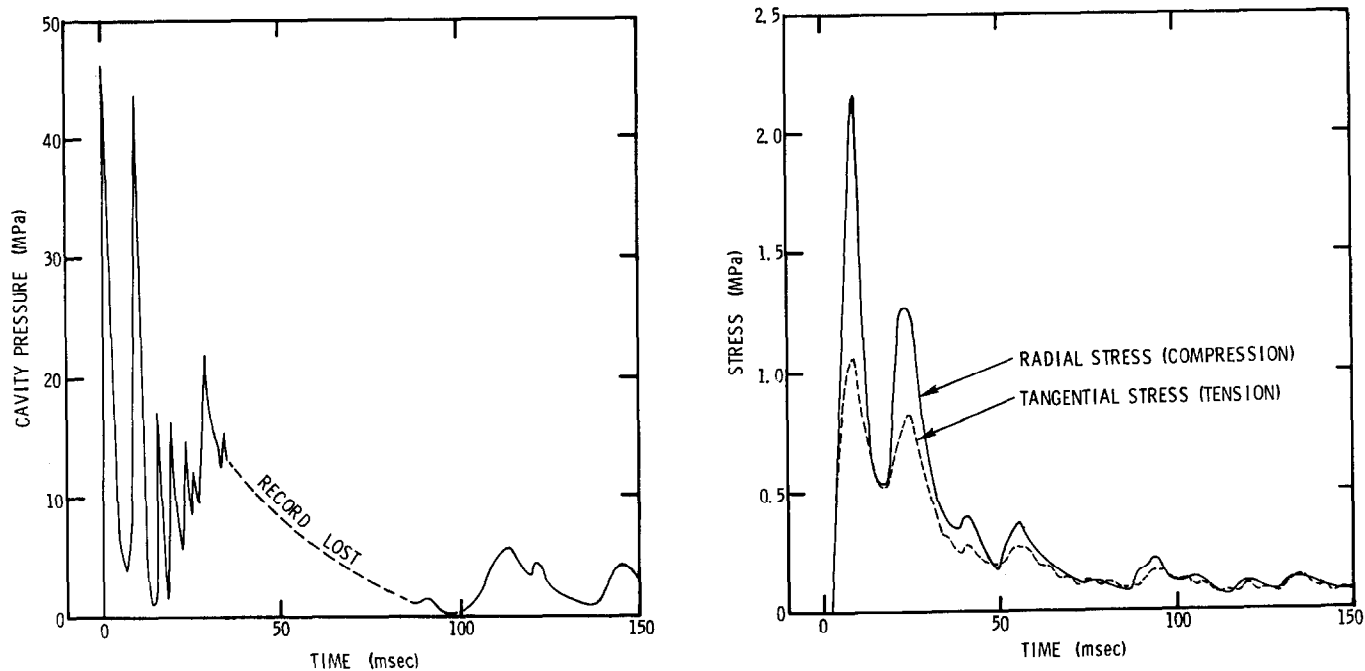


Fig. 9 - Record of cavity pressure and stress at 1 m for experiment D.

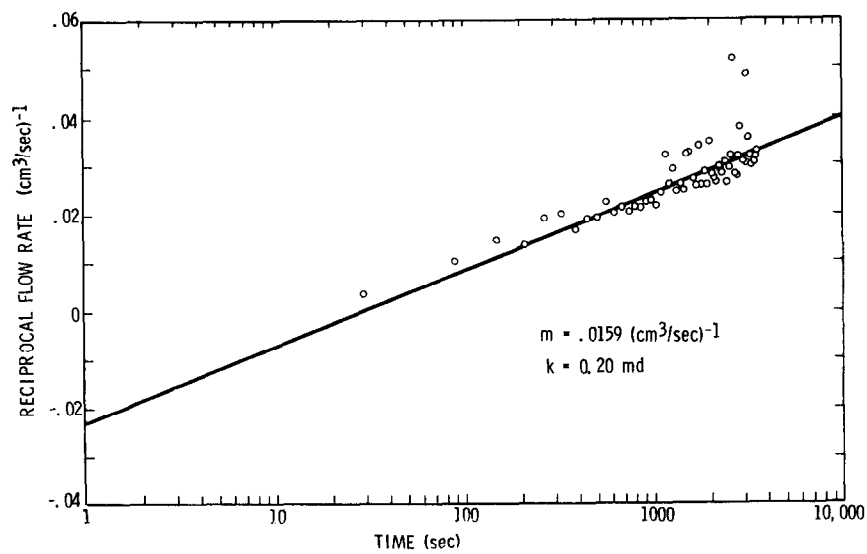


Fig. 10 - Pre-shot permeability measurement for experiment A.

EMPIRICAL EVALUATION OF CLINTON SAND WELL PERFORMANCE

by Charles R. Skillern, TRW Energy Systems Group

© Copyright 1980, Society of Petroleum Engineers

This paper was presented at the 1980 SPE/DOE Symposium on Unconventional Gas Recovery held in Pittsburgh, Pennsylvania, May 18-21, 1980. The material is subject to correction by the author. Permission to copy is restricted to an abstract of not more than 300 words. Write: 6200 N. Central Expwy., Dallas, Texas 75206

ABSTRACT

The production economics of tight to near-tight formations such as the Clinton sands of Ohio have become increasingly marginal due to rapidly increasing well costs and geologically less favorable areas to drill. To evaluate the potential for improved well performance, the Gas Research Institute (GRI) sponsored the empirical investigation of historical Clinton sand well performance presented herein.

The study is based on well data from 303 wells in northeastern Ohio which were drilled between 1963 and 1974. All the wells were single-completions stimulated by hydraulic fracturing for which at least five years of uninterrupted production data are available. The data are believed to be representative of Clinton wells in the 1963 to 1974 time frame and were selected only on account of availability. Statistical regression methods were used to determine well parameters which impact individual well performance. The five-year cumulative production (first five years) for each of the 303 wells was used as the dependent variable in a multivariable linear regression equation, with the statistically significant well parameters as independent variables.

The empirical regression equation was used to estimate average well performance (five-year cumulative production) for geographically oriented subsets of the 303-well data base with varied levels of stimulation treatment volume. Significant variations in well performance are demonstrated as a function of apparent geologic variations and variations in stimulation treatment volume. Historical production (303 wells) could have been increased by 15 percent through use of near-optimum stimulation treatment volumes. A method is proposed which utilizes the statistical regression methods of the study, in conjunction with exploratory drilling in areas which are geologically similar to those represented by the data base, to assist in optimizing future Clinton sand production.

References and illustrations at end of paper.

INTRODUCTION

The Silurian-age Clinton sands represent the primary gas and oil producing formation in Ohio. The formation consists primarily of quartz, with feldspar, calcite and clays appearing as secondary minerals, and are interfingered with the red Queenston shale. The producing areas are generally tight to near tight with an average effective permeability of $1 \times 10^{-5} \mu\text{m}^2$ (0.1 md)¹ and widely varying porosity. For the data set of this study, porosity ranged between 5 and 13 percent. Gross sand thickness may locally exceed 37 m (120 ft), but the net pay thickness values in the data set ranges between 2 m and 18 m (7 ft and 60 ft).

Clinton sand gas production is generally from stratigraphic traps where porosity and permeability are sufficiently developed. Since about 1960 conventional hydraulic fracturing has become the accepted stimulation method for achieving reliable production results. Stimulation treatment volumes for the data set of this study ranged between 80 m³ and 640 m³ (500 bbl and 4,000 bbl) with up to 34,000 kg (75,000 lb) of sand proppant. Most Clinton wells are fractured with a low viscosity (less than 20 Pa·s) fluid containing as much sand as can be transported by the fluid.

Gas production from the Clinton sands typically involves initial production levels of $1.4 \times 10^5 \text{ m}^3/\text{a}$ to $1.4 \times 10^7 \text{ m}^3/\text{a}$ ($5 \times 10^3 \text{ Mcf/yr}$ to $5 \times 10^5 \text{ Mcf/yr}$) with uninterrupted production intervals ranging from 15 to 25 years. The historical dry hole factor is about 9 to 10 percent following stimulation, an important economic consideration. According to a recent industry estimate of producible resource remaining, only about 20 percent of the resource has been produced to date.² However, the future economic viability may be less attractive than in the past in view of gas prices not keeping pace with the inevitably higher extraction costs.

This investigation utilizes a comprehensive set of historical well data to provide an assessment of the impacts of measured well parameters on well performance. The empirical evaluation results form the

basis for estimating stimulation treatment volumes which maximize production in new areas geologically similar to those represented within the data base.

METHODOLOGY

The variations in performance (well productivity) among wells in the same field of a tight formation such as the Clinton sands are due to:

- Geological variations within the field
- Limitations of available stimulation techniques employed
- Well drilling, stimulation and completion operational factors

The geological variations of course are not controllable; however, some degree of control is available to operators regarding choice of an appropriate stimulation method and the proper execution of overall well operations. The purpose of this study is to identify pertinent effects of measured well parameters on well performance using measured well parameters of 303 wells drilled between 1962 and 1974 in north-eastern Ohio (Figure 1). The original data set contained well data on 328 wells of which one well was not placed on line and sufficient well data were not available for another 24 wells; the remaining wells thus comprise the data base. The specific well data available for each well are listed in Table 1.

As indicated in Table 1, monthly well production for at least five years are available for each of the 303 wells in the data set. Consequently, the five-year cumulative production (Q) for each well was arbitrarily selected as the measure of individual well performance for the study. To assess the effects of measured and observed well parameters on Q, standard statistical regression methods were employed. These consisted of an exploratory evaluation whereby subsets of selected variables were plotted versus Q to provide an initial understanding of key variables, followed by a formal multivariable linear regression analysis. The regression analysis utilized various combinations and functional forms of selected well parameters as independent variables with the well performance parameter Q as the dependent variable.

Initially in the exploratory phase, the 303 wells were grouped over ranges of pertinent variables such as rock pressure, net pay thickness and stimulation treatment volume to identify well subsets for narrow bands within each variable range. Plots were made of the average values of subsets of 25 wells or more for particular variables versus the corresponding averaged values of five-year cumulative production Q. Although most of these resulted in essentially random distributions, a few showed useful relationships. The most important of these is the total stimulation treatment volume (sand laden fluid plus pad and displacement water) versus Q shown in Figure 2. The humped shape of those plots provided the first clue as to the importance of stimulation treatment volume regarding well performance. The next step was to utilize the results of the trend plots in the statistical regression phase.

The regression analysis utilized an empirical production function of the form:

$$Q = f(x, y, z) \quad (1)$$

where

x is a vector of geologic variables such as net pay thickness, rock pressure, depth and porosity

y is a vector of stimulation variables such as treatment volume, sand quantity, and hydraulic horsepower

z is a vector of operational variables such as well performance variations with time and learning curve effects

Q is the five-year cumulative production.

The regression analysis was performed in a stepwise fashion, using increasingly more significant sets of variables and functional forms as independent variable terms in the regression equation. As new independent variable terms were found to be improvements over previous terms, the least significant terms were replaced with the new terms. Student t values for the hypothesized independent variable terms were used to estimate the statistical significance, i.e., terms with lowest t values were replaced by new terms which demonstrated higher t values. Improvements in the overall statistics of the successive regression equations were determined from increases in the correlation-coefficient squared (r^2) and F-test for the ratio of variances for observed and estimated values of Q. Increased values of these indicate statistically stronger combinations of independent variables.

ANALYSIS RESULTS

Through the above process, the following equation emerged as the best overall representative of the empirical data base:

$$\begin{aligned} [\ln Q]^{-1} = & C_0 + C_1 X_1^2 + C_2 X_2^{0.7} + C_3 X_3^2 + C_4 X_2 \ln X_4 \\ & + C_5 X_6 / X_1^2 + C_6 Y_1^2 + C_7 Y_1 X_2 + C_8 Y_1^2 X_2 \\ & + C_9 Y_1 X_3 + C_{10} Y_1^2 X_3 + C_{11} (Y_1 / X_6)^2 \\ & + C_{12} \text{IND} Y_1^2 + C_{13} Z_2 + C_{14} \ln Z_3 \end{aligned} \quad (2)$$

A summary of the statistics for Equation 2 is presented in Table 2.

Some of the derived terms in Equation 2 require further clarification. The locational variables X_2 and X_3 , were oriented to the geometry of the well field (Figure 1) by regression of the latitude versus longitude for wells within the field. Those variables, defined by a simple latitude-longitude coordinate rotation, represent the effects of unmeasured factors such as permeability and fracture intensity that vary systematically over the field. The post-1967 learning curve index, IND, is a bilevel constant set to zero for years prior to 1967 and set to one for years after 1967. The product of IND and Y_1^2 is a measure of increasingly effective stimulation practice (per specified treatment volume) after 1967. The seasonal index, Z_2 , is also a bilevel constant set to one for wells brought on line during winter months (January to April) and set to zero otherwise; that index accounts for wells being initially produced at capacity during winter months and not otherwise. The time index, Z_3 , is the difference

between the year a well is placed on line and the empirical reference, 1961.5. The negative effect of the natural log of that variable accounts for decreased production in later years due to drilling more favorable areas in early years.

A comparison of the well parameters used in Equation 2 with the total set of well parameters in Table 1 shows that many parameters in Table 1 do not appear in the equation. The excluded parameters either showed little or no correlation with well performance or simply demonstrated less significance than those excluded. An implicit guideline for the acceptance of any hypothesized independent variable term in the development of Equation 2 is that it exhibited a student t value corresponding to a confidence level of at least 90 percent (i.e., a 90 percent probability of being a non-random effect). Further details regarding Equation 2 and its derivation may be obtained from Reference 3.

The usefulness of Equation 2 lies in its well performance estimation capability. To assess that feature, the overall Clinton well set was arbitrarily divided into groupings of wells by county with which to make average well performance estimates (Table 3). As indicated in Table 3, the number of wells per county ranged from two wells to 146 wells and for well subsets greater than about 10, the estimation error is less than 10 percent.

A further use of Equation 2 is to anticipate performance variations due to changes in geology (i.e., as a function of geographical location) over the well field and variations in well performance for different stimulation volumes as reflected in Figure 2. That was accomplished for each of three counties (Tuscarawas, Portage, and Guernsey) in the following manner. Equation 2 was first calibrated with the observed average well performance in Table 3 using a bias term which eliminated the estimation error. The equation was then used to estimate the average well performance, Q , using specified values for the total treatment volume over the range of historical values (Figure 3). As seen in Figure 3, optimum well performance for each of the counties is obtained at values of stimulation treatment ranging between 120 m^3 and 240 m^3 (750 bbl and 1,500 bbl).

An overall evaluation of the 303-well data set showed that near-optimal stimulation treatment volumes were utilized for about half the wells. In most instances the non-optimum performance resulted from "over kill" stimulation volumes. The overall effect is that about 15 percent greater average well productivity would have been possible through use of near-optimum treatment volumes for all the wells.³

The demonstrated estimation results presented in Table 3 and Figure 3 offer a potentially useful tool for the evaluation of new producing areas and optimization of production potential of favorable areas, provided the new areas exhibit similar geologic characteristics as those represented within the empirical data base.

PROPOSED APPLICATION

An important finding of this study is that "more is not necessarily better" relative to hydraulic fracturing treatment volumes in the Clinton sands. As indicated, a 15-percent greater five-year cumula-

tive production from the 303 wells of the data base would have been possible through use of near-optimum levels of total stimulation treatment volume. The proposed application which follows makes use of the empirical results to promote optimal production from future Clinton sand gas wells using the proven hydraulic fracturing technique of the data base.

Equation 2 does not lend itself to extrapolations beyond the empirical data from which it was derived for the following reasons:

- The data base spans a wide range of geological conditions which tends to lower the r^2 value and potential usefulness in a restricted geologic setting.
- Many terms in the equation such as the locational variables and associated terms apply only to the geographic region of the data base.

The first limitation can be overcome by partitioning the data base in well subsets which represent specific geologic conditions identified within the overall field, and deriving separate regression equations such as Equation 2 for each well subset. Reliable statistical and corresponding extrapolative qualities can be maintained with as few as 25 to 30 wells.⁴ The second limitation may be partially or totally overcome by the partitioning, provided the geologic characteristics for a specified well set are relatively consistent, thus eliminating the need for locational variables. If that is not possible, averaged values of appropriate locational parameters can be used to represent areas expected to have similar geologic features.

Using the above guidelines, sets of regression equations can be developed for geologic areas represented by the empirical data base and possible extensions thereof. In a new area, measured well parameters from exploratory or nearby productive wells and available geologic correlation data such as developed by Pepper, de Witt, Jr., and Everhart⁵ could be compared with similar data for the historical data base to determine the specific historical area which matches the new one. The corresponding regression equation for an acceptable match would then be available as an evaluation tool for the new area.

SUMMARY

The results of this study demonstrate the usefulness of statistical regression techniques for relating measured well parameters to well performance when sufficient well data are available. The Clinton sand data show wide variations in average well performance as a function of geologic variations and variations in stimulation treatment volume. The proposed method for extending the results to new producing areas provides an evaluation tool whereby improved production from future Clinton wells may be possible.

ACKNOWLEDGEMENTS

The work described was sponsored by the Gas Research Institute (GRI) under Contract 5011-310-0107. The support of Consolidated Natural Gas Company in Pittsburgh in making available the necessary well records and that of Mr. C. A. Komar

of the Department of Energy, Morgantown Energy Technology Center, in assimilating the detailed well data are gratefully acknowledged.

NOMENCLATURE

C_i	= Regression equation coefficients ($i = 0, 14$)
Q	= Five-year cumulative production
X_1	= Rock pressure after fracture
X_2	= Location along main field axis
X_3	= Location away from main field axis
X_4	= Porosity
X_6	= Net Pay Thickness
Y_1	= Total sand-laden treatment volume
IND	= Post-1967 learning curve index
Z_2	= Seasonal index
Z_3	= Time Index (year - 61.5)

REFERENCES

1. Jennings, Jr., A. R., Darden, W. G., "Gas Well Stimulation in the Eastern United States" SPE 7914 presented at the 1979 SPE Symposium on Low-Permeability Gas Reservoirs, May 20 - 22, 1979.
2. Private Industry Communication, 1979.
3. "Clinton Sands Analysis," Analysis of Tight Formations, GRI-79/0021, Volume II, March, 1980.
4. "Devonian Shale Analysis," Analysis of Tight Formations, GRI-79/0021, Volume III, March, 1980.
5. Pepper, James F., de Witt, Jr., Wallace, and Everhart, Gail M., "The 'Clinton' Sands in Canton, Dover, Massillon, and Navarre Quadrangles, Ohio," United States Geological Survey Bulletin 1003, 1953.

TABLE 1
CLINTON SAND WELL PARAMETERS

- | | |
|--|---|
| <ul style="list-style-type: none"> • Latitude and Longitude • Date on Line • Monthly Gas Production (5 Years) • Producing Zone • Net Pay Thickness • Depth to Top of Pay Zone • Porosity • Instantaneous Shut in Pressure • Open Flow After Fracture • Rock Pressure After Fracture (Surface Shut-In Pressure) | <ul style="list-style-type: none"> • Treatment Volume • Total Water Volume (Sand Laden Treatment Volume Plus Pad and Displacement Water) • Sand Quantity • Hydraulic Horsepower • Injection Rate • Breakdown Pressure • Average Treatment Pressure |
|--|---|

TABLE 2
LINEAR REGRESSION FUNCTION* FOR CLINTON SAND DATA SET

Variable	Symbol	Functional Form	Regression Coefficient	Confidence Level**
Dependent				
Five-Year Cumulative Production	Q	$[1nQ]^{-1}$		
Constant Term	—	—	$C_0 = 0.811 \times 10^{-1}$	
Independent				
Geological				
Rock Pressure (RPSI)	X_1	X_1^2	$C_1 = -0.829 \times 10^{-8}$	> 0.9995
Projection Along Main Axis (PROJ)	X_2	$X_2^{0.7}$	$C_2 = 0.126 \times 10^{-2}$	> 0.9995
Projection Away From Main Axis (PROJ2)	X_3	X_3^2	$C_3 = 0.396 \times 10^{-5}$	0.983
Porosity (PORP)	X_4	—	—	
PROJ, Porosity (PORP)	X_5	$X_5 \ln X_5$	$C_4 = -0.508 \times 10^{-4}$	0.995
Net Pay Thickness (NEPAY)	X_6	—	—	
NEPAY, RPSI	X_7	X_6/X_1^2	$C_5 = -0.239 \times 10^3$	0.999
Stimulation				
Total Water Volume (SLF)	Y_1	Y_1^2	$C_6 = 0.719 \times 10^{-8}$	0.981
SLF, PROJ	Y_2	$Y_1 X_2$	$C_7 = -0.188 \times 10^{-6}$	> 0.9995
SLF, PROJ	Y_3	$Y_1^2 X_2$	$C_8 = 0.872 \times 10^{-10}$	> 0.9995
SLF, PROJ2	Y_4	$Y_1 X_3$	$C_9 = 0.226 \times 10^{-6}$	0.976
SLF, PROJ2	Y_5	$Y_1^2 X_3$	$C_{10} = -0.183 \times 10^{-3}$	0.998
SLF, NEPAY	Y_6	$(Y_1/X_6)^2$	$C_{11} = -0.153 \times 10^{-6}$	0.927
Operational				
Learning Curve, POST-67	Z_1	$INDY_1^2$	$C_{12} = -0.845 \times 10^{-8}$	0.992
Seasonal Index (WIN)	Z_2	Z_2	$C_{13} = -0.194 \times 10^{-2}$	0.992
Time Index (Year - 61.5)	Z_3	$\ln Z_3$	$C_{14} = 0.729 \times 10^{-2}$	> 0.9995

* Regression Statistics: F-Test for Ratio of Measured and Estimated Q Variances = 10.4; Correlation Coefficient (γ) Squared = 0.337

** Student t Test of Hypothesized Regression Term

TABLE 3
ESTIMATED FIVE-YEAR CUMULATIVE PRODUCTION OF CLINTON SAND WELL SUBSETS

Aggregate Well Set	Number Wells	Estimated Average 5-Year Cumulative Production Q_E , Mcf	Measured Average 5-Year Cumulative Production Q_M , Mcf	Percent Error $\frac{Q_E - Q_M}{Q_M} \times 100$
Overall	303	120.176	120.154	0.0183*
Tuscarawas	146	104.383	101.082	3.2
Portage	80	129.090	131.494	-1.8
Guernsey	27	159.986	168.564	-5.1
Muskingum	15	161.619	154.039	4.9
Noble	12	144.885	132.043	9.7
Stark	10	93.072	137.904	-32.5
Morgan	6	334.392	157.478	112.3
Columbia	3	145.631	51.179	184.6
Ashtabula	2	20.087	17.430	15.2
Geauga	2	105.646	83.756	26.1
Mahoning	2	147.076	110.808	32.7

* Residual Regression Error



Fig. 1 - Map of Ohio with outline of 328 well gas field.

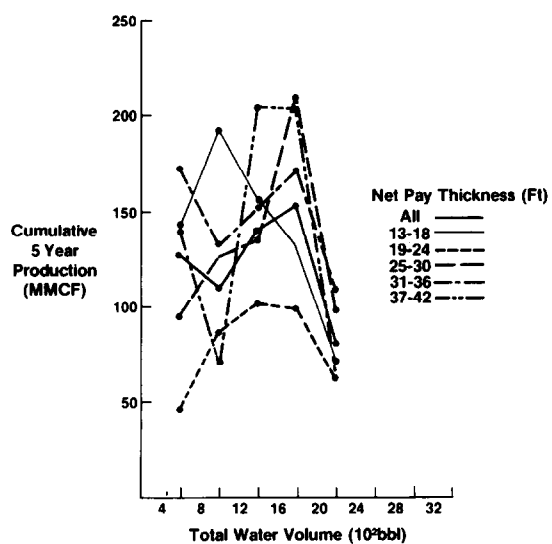


Fig. 2 - Data trend plot: production versus total water volume.

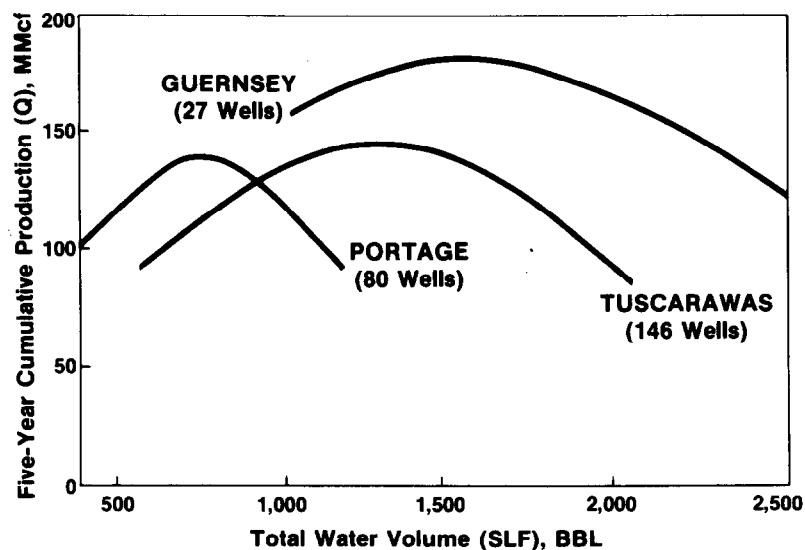


Fig. 3 - Interaction between stimulation and well location.

A WIRELINE HYDRAULIC FRACTURING TOOL FOR THE DETERMINATION OF IN SITU STRESS CONTRASTS

by Michael D. Voegelé and Arfon H. Jones,
Terra Tek, Inc.

This paper was presented at the 1980 SPE/DOE Symposium on Unconventional Gas Recovery held in Pittsburgh, Pennsylvania, May 18-21, 1980. The material is subject to correction by the author. Permission to copy is restricted to an abstract of not more than 300 words. Write: 6200 N. Central Expwy., Dallas, Texas 75206

ABSTRACT

A significant amount of research has been devoted in the past few years to the study of fracture containment in stimulation of low permeability gas reservoirs. One finding of this research is that vertical fracture growth is controlled by contrasts in the *in situ* stress state. A knowledge of the variation of horizontal stress with depth would aid in the design of well stimulation.

The only method available today for determining *in situ* stress at depths greater than about 200 meters is a small scale hydraulic fracturing technique; stress calculations are based upon several relatively simple measurements; however, at present the economics of sending the tool downhole on a tubing string are unfavorable. To overcome this problem the design of a self contained tool which operates on a standard seven conductor wireline cable has been undertaken by Terra Tek, Inc.; funding is being provided by the U. S. Department of Energy, Morgantown Energy Technology Center. A major goal of the design effort is to build the tool primarily with commercially available components. The basic tool consists of a downhole hydraulic power supply control unit, straddle packers and pressure transducer; it has been designed to function in cased or open holes. Additionally, the tool design incorporates a fracture detection device so that orientation can be determined.

In conjunction with the tool design a laboratory investigation utilizing 1 meter cubic samples is being pursued to study the mechanics of stress determination in cased boreholes. Since there is very little published literature on the determination of *in situ* stresses through perforated casing, it is hoped that the laboratory investigations will allow stress determinations in cased wells with the same degree of reliability that now exists for stress determinations in open holes.

INTRODUCTION

As a method of utilizing our nation's energy resources, attention has been focused, in recent years, on the huge gas reserves that exist in massive, low permeability reservoirs. The technique that has been utilized to stimulate these relatively thin, low permeability intervals is a large volume hydraulic fracturing treatment with an effective treatment radius approaching 100 percent of the drainage radius. The stimulation of a reservoir with the intent to obtain a large treatment radius is known as a Massive Hydraulic Fracture (MHF) treatment. Hydraulic fracturing treatments are common in production well stimulation, but typically do not achieve the extensive treatment radius; these do not qualify as MHF treatments. In order to achieve a large radial distance of propped fracture, vertical fracture growth must be inhibited by some means. Many of the reservoirs for which MHF treatments are contemplated possess strong natural boundaries but in other instances some method of controlling the vertical fracture growth must be implemented.

The application of fundamental fracture mechanics principles to the analysis of fracture propagation in MHF treatments is leading to the rapid development of both qualitative and quantitative predictions of hydraulic fracture growth. Significant input parameters in these analyses are found to be the *in situ* material properties and the *in situ* stress state.

Simplified two dimensional analyses of the problem indicate that as a fracture growing in the pay zone approaches the interface between the pay zone and the adjacent layer its growth in the vertical direction will be impeded if: (1) the shear modulus of the adjacent layer is greater than that of the pay zone; or (2) the minimum *in situ* stress of the adjacent layer is greater than the minimum *in situ* stress in the pay zone (Simonson, *et al.*, 1976). Analysis of data from numerous MHF projects indicates that favorable moduli contrasts are the exception rather than the rule. Knowledge of *in situ* stress fields offers the key to better design of fracture treatments and control of fracture growth. Techniques for measurement of *in situ* stress variation within a gas reservoir must be developed into a routine test that is both economic and acceptable to well operators before significant advances in fracturing treatment design technology can be made.

References and illustrations at end of paper.

Pertinent *in situ* material properties normally can be obtained with some degree of precision through the use of geophysical logs supplemented by a lab testing program. *In situ* stress measurements on the other hand are difficult to obtain and presently only one technique, hydraulic fracturing, can be used to obtain this data at depths greater than about 200 meters. At the present time, *in situ* stress measurements are too expensive and time consuming to perform on a regular basis. Additionally, operators are often reluctant to trip tools into wells and perform operations that could conceivably result in the loss of the well.

This paper describes a research program that is in the initial stages of designing and evaluating the use of wireline tools for measuring *in situ* stress by hydraulic fracturing. The use of wireline tools could significantly reduce the cost of these stress measurements by drastically reducing the test preparation time required to set high pressure tubing to the required depth. Additionally, the research program is evaluating the possibility of measuring *in situ* stresses through perforated casing thus reducing the chances of losing a well. A laboratory program of simulated *in situ* stresses, casing and cementing will attempt to demonstrate the feasibility of such measurements.

The combination of reduced test time through the use of wireline tools and minimal well damage by fracturing through perforated casing should allow hydraulic fracturing measurements to be made on a routine basis in almost all exploratory wells.

The design of any downhole tool is a complex process. The tool must be able to perform its function under a variety of harsh downhole conditions, thousands of feet deep inside a very expensive hole in the ground. If it is to be useful and therefore used regularly, it must be economically feasible to build, relatively quick and easy to use, and most importantly, it must be reliable in that it can be removed from the borehole without damaging the well.

A list of expected design requirements for this particular tool reveals some of the problems to be solved:

1. Hole depths from near surface to 10,000 feet (3000 m) deep.
2. Boreholes that are dry or filled with water, drilling mud, or other liquids.
3. Corresponding variable working pressures from atmospheric to several hundred atmospheres.
4. Boreholes that are smooth, deteriorated, washed out, straight, crooked, cased or uncased through a wide variety of rock.
5. Downhole operating temperatures from surface conditions to geothermal (100°C).
6. If possible, the tool should be able to function on a standard cable currently used for other purposes.

WIRELINE TOOL DESIGN

The wireline hydraulic fracturing tool concept will be considered as a combination of four subsystems listed below:

1. Packers to isolate test section. Lynes inflatable packers were considered for each

design as shown in Figures 1 thru 4.

2. Pumping and wireline system (the wireline selected will be based on final selection of the mode of pressurization).
3. Fracture detection system for both cased and open hole.
4. Telemetry and control system.

Isolation Packers

After considering the various design problems and possible solutions for the proposed tool, it becomes clear that the major obstacle that must be solved is the design of the high pressure liquid supply system. The pressure system should be capable of supplying sufficient flow at the required pressure to satisfy the requirements of the test to be performed. The flow rate must be large enough so that pressure builds up rapidly before the fracture occurs. Too low of flow rate will allow the fluid to simply migrate into the rock through existing pores. Clearly, the larger the test section for a given rock, the higher the flow rate required for fracturing. Hence, the smallest allowable test section should be used, consistent with practical and theoretical considerations. A practical limit for the maximum pump pressure to be used downhole may well be around 5500 psi. This is also the maximum differential pressure at which available packer systems can operate in an open borehole. Somewhat higher pressures may be allowable in cased boreholes, due to better sealing conditions for the packers. If we assume the pressure system will supply liquid at a pressure increase of 5500 psi, the energy required (neglecting inefficiencies) is about 3.2 horsepower for each gallon per minute of flow rate required. If the overall efficiency is 70 percent and 2 GPM are required, the energy to be supplied is over 9 horsepower or about 6800 watts of electricity.

Pumping System

The simplest solution in terms of the pumping requirements would be to generate the fluid power at the ground surface and conduct it downhole through a high pressure conduit that is an integral part of the wireline. This method would allow use of many different types of pumps since space is not limited. Although this simplifies the downhole portion of the tool, it complicates the wireline cable. The requirement of 10,000 feet of continuous high pressure tubing can be met with present day technology, but additional equipment is needed to handle it (i.e., straighten it as it is placed into the well). Other problems are covered later in the discussion. High pressure thermoplastic conduit is presently available and seems to be a better possibility. Another option would be to use small diameter metal, rubber, or plastic tubing built into the wireline to recharge a pressure storage tank downhole. A small tube could not provide the necessary flow rates for fracturing directly without downhole storage.

The alternative to a surface pump is to create or have stored downhole the pressure needed for the experiment. The most obvious method is to generate the needed fluid power downhole by means of an electric pump or a pump-intensifier. This method requires a more complex control system but has the advantage of a simplified wireline cable design. Another possibility is a tool carrying its own energy source.

Another significant problem to be considered in the design of any pressurization system for this tool is the fluid supply method. If the tool is used in a dry hole, no liquid is available to be pumped. In holes filled with drilling mud, brine or other corrosive or abrasive liquid, it may well be desirable to use liquids (or possibly gases) other than those in the borehole. In some cases, to avoid possible damage to the formation, it may be necessary to provide the desired fluid for the fracture.

If the needed fluid cannot be taken from the borehole, it must be supplied to the tool either from a downhole reservoir or from a fluid tube in the wireline. The only other alternative is to filter or treat the borehole fluid in some way to make it suitable or use it as is and suffer the increased maintenance problems. The following discussion is intended to point out the considerations involved for each choice.

Clearly, for most tool options, the simplest method of test fluid supply would be to use liquid from the borehole. Although this choice does not apply directly to dry boreholes, liquid would be "dumped" down the borehole after the packers are set. However, since many boreholes are dry because they cannot tolerate liquid, it would probably not be acceptable to put unconstrained liquid in most dry boreholes.

For wet holes, there are a variety of liquids that might be found in the borehole. For drilling mud, the options are very limited. The mud will contain cuttings that would be difficult to filter since most drilling muds would plug any filtering system that could remove the abrasives. Many muds are so viscous that they could be pumped only by positive displacement pumps to avoid cavitation. With all things considered, a system that could pump drilling mud successfully would be so specialized that it would probably require considerable alteration to be used with any other liquid.

The various components discussed to this point do not readily lend themselves to a simple categorization scheme whereby the "ideal" component can be selected. Accordingly, the general tone of this portion of the paper has been to accept the fact that each pressurization component has desirable characteristics with respect to the task at hand and attempt to document these significant operating characteristics in light of operation in wet or dry holes as well as surface or downhole operation.

It is possible to select, from the components presented, four basic pressurization systems for consideration. The following is an enumeration of these systems.

1. A submergible pump based pressurization system similar to standard oil field production equipment. This pressurization system has the advantage of the ability to generate high flow rates and pressures downhole but suffers from the requirement of a special cable, special handling equipment and high wattage requirements, as well as the need for a fluid filled borehole.
2. A surface pressurization system incorporating standard triplex or air-powered pumps. This type of pressurization system can literally be used in any borehole and has a much simplified downhole control system.

The major disadvantage of this system is the requirement of a custom wireline cable incorporating a fluid conductor.

3. A small downhole gear type pump such as those used to pump hydraulic fluid. This type of system could probably not use most borehole fluids and thus would require a reservoir. The reservoir would also allow it to be used in a dry hole. The pump should be functional on a standard wireline but the limited reservoir capacity would probably make any tool based on this system a "one shot" tool. However, if the borehole is fluid filled and the borehole fluid is relatively debris free, the system can possibly use the borehole fluid directly and the reservoir can be eliminated.
4. A gas reservoir operated system supplying the fluid power. This pressurization system could also be incorporated on a tool built on a standard wireline cable. It must be used with a reservoir and thus would probably be configured as a "one shot" tool.

Surface controlled inflation packers are available which can be used in a 6.25 inch (16 cm) diameter borehole. These packers can be inflated with either gas or liquid. The potential problems with inflating this type of packer from the surface are that it would require a conduit in the wireline cable to inflate them and if liquid is used to set them the hydrostatic head from the fluid in conduit would almost ensure that the packers would not deflate. If a gas was used to inflate them this would not be a problem. The availability of fluid pressure generated downhole would alleviate the need for a separate inflation line coming in from the surface. This type of packer would also simplify the design of the wireline tool since it would not be necessary to move the inner mandril.

Telemetry System

There are many variables that must be taken into account before a telemetry system is finally chosen and implemented. FM/FM telemetry is a frequency-sharing scheme whereby all transducer or signal-conditioner outputs are monitored continuously and transmitted simultaneously on a common r-f carrier, but at different subcarrier frequencies. On the other hand, pulse amplitude modulation, pulse duration modulation, and pulse code modulation are time-multiplex or time-division schemes. That is, the signal conditioner outputs are monitored or sampled at routine intervals by a commutator. These samples are then transmitted on a common r-f carrier at a common subcarrier frequency. It appears that FM/FM telemetry for the tool and task at hand is best suited because of this continuous monitoring. Thus, if failures occur a record has a better chance of indicating problem areas. (The above comment has to be tempered somewhat for pulse code modulation since this technique has some distinct advantages as will be discussed). FM/FM telemetry has some other unique advantages over the other schemes such as noise rejection. In a noisy environment where pumps, motors, etc., are active, an FM/FM system will succeed where others will fail.

As the number of signal channels increase (greater than about eight or ten) the pulse code modulation (PCM) technique becomes more attractive than FM/FM. In these cases, sampling rates can be held high with essentially no loss in data. However, PCM typically requires a digital computer for use as a recording device to be highly efficient. A digital word can be sampled and acquired by the digital computer for subsequent processing and storage.

It appears that the choice of a telemetry system for the wireline hydraulic fracturing tool is basically a function of the number of signal channels. The FM/FM system is probably slightly less expensive and the component parts more readily available but is probably a better choice only for a small number of signal channels. If the chosen tool design incorporates more than about 10 signal channels PCM becomes the more attractive option. The final telemetry system choice will depend upon the other tool components and can be made as the tool design progresses.

Fracture Detection Equipment

There are three basic approaches to the problem of selection of a fracture detection device for incorporation in the wireline hydraulic fracturing device, namely: (1) select a tool capable of detecting fractures in both open and cased holes and incorporate it as part of the tool package; (2) select two basic tools, one of which is capable of detecting fractures in open holes and one of which is capable of detecting fractures in cased holes, and design the total tool package such that these two components can be easily interchanged; and, (3) design the fracture detection device to be run in on a separate wireline before and after the hydraulic fracturing experiment.

Option one is clearly the desired goal of the project while option two probably involves extremely difficult logistics and the development of complicated control systems. Option three must, however, be considered as a viable alternative in the tool design, particularly in light of the findings of this study.

The fracture detection devices investigated in this study are summarized in Table I; operating restrictions and pertinent comments are also summarized. The evaluation matrix used to assess probable tool performance and adherence to design goals is presented in Table II. The matrix addresses nine parameters for each of the logging tools which cover the spectrum from hole type and tool availability through several functional characteristics pertinent to the project goals. An examination of the Tables and in particular the notes accompanying Table II will aid in following the subsequent discussion.

To strictly meet the project requirements the tool in question must have an "X" in each of columns one through six; however, if the lack of an "X" in column five or six can be remedied by a relatively simple tool modification or special operating technique, this is so indicated by an "X" in column seven. Table II thus indicates that only three tools, the Sandia Passive Seismic tool, the radioactive tracer tool, and the Radial Differential Temperature tool meet all of the requirements of the project. All three tools will probably function in both open or cased holes, are commercially available and possess sufficient horizontal resolution to define fracture orientation. Two of the tools, the Radial Differential

Temperature tool and the tracer tool, however, have, in light of available information, never been used to determine fracture location and orientation; their primary function has been to locate producing zones or orient perforating guns. The Sandia Passive Seismic tool, on the other hand, was specifically designed to detect fractures created by hydraulic fracturing and is also the only device that detects fractures away from the borehole. It appears to be a logical tool choice for incorporation in the wireline tool but it must be remembered that there has been little field testing.

The choice for a fracture detection device for the wireline tool is thus a difficult one. When considering that it probably is not possible to build a single tool for use in all possible circumstances, it becomes evident that the final tool design chosen for consideration may well be configured for specific applications.

PROPOSED TOOL DESIGNS

Careful consideration of the requirements and possibilities for a wireline fracturing tool has consistently suggested that no single tool is the best solution to all possible downhole conditions. Indeed, the tool design should be selected based on the actual conditions for which it will be used most of the time. The major hole conditions that must be considered in selecting the tool are whether or not the hole is cased which can affect the fracture detection device; whether or not the borehole is fluid filled which dictates the need for a reservoir; and the most serious, the type of borehole fluid. That is not to say that a given tool cannot be designed to allow for simple modifications on site. These changes make possible a tool that could be used effectively in a wide variety of conditions.

Theoretical considerations and practical limits are also a major factor in shaping the final design. As mentioned several times, the size of the test section between the packers will have a great effect and will weigh heavily in the final design.

The following tools are suggested as good combinations of available components. The final selection should be based on a careful consideration of the intended use, the boreholes available for testing and their character (casing, fluid conditions, etc.) and the overall economics, including available equipment such as pumps, motors and wireline cable. The tools are presented randomly - each has advantages depending on the conditions of use. Each tool design is described and a diagram of the tool is included. The control system for each tool is also presented.

1. A modified version of a standard oil field submersible pump, Figure 1. The tool is large [3000 lbs (13.3 kn); 70 feet (21 m) long] and has as its major disadvantages its cost and the requirement of a special wireline cable and power supplies. The tool will only work in fluid filled boreholes but has the advantage of the ability to perform numerous tests before being brought to the surface.
2. A tool with a surface fluid power supply, Figure 2. This tool is compact [1000 lbs. (4.5 kn); 15 feet (4.5 m) long]

but it also requires a special wireline cable to transmit fluid downhole. This tool will work in dry boreholes and has much simplified control circuitry.

3. A tool with a self-contained fluid reservoir utilizing a hydraulic gear pump, Figure 3. This tool could use borehole fluid but filtration requirements are excessive for other than clean water. The tool is designed to run from a standard wireline but the reservoir capacity limits downhole testing time. The size of the tool is about 500 lbs. (2.2 kn), and 24 feet (7.5 m) long.
4. A tool with a self-contained reservoir utilizing a high pressure gas reservoir regulated for output pressure, Figure 4. This tool also will run from a standard wireline cable but cannot use reservoir fluid without a complicated recharging system. Additionally, the high pressure reservoir must be brought to the surface frequently for recharging. The size of the tool is about 600 lbs. (2.7 kn), and 30 feet (9 m) long.

These four tool designs incorporate the primary options available for use in a wireline hydraulic fracturing tool. As noted, each has desirable characteristics and the final selection of any of these tools can only be made on the basis of most frequently encountered borehole conditions. Accordingly, these designs are presently under review by a panel of consultants; the final design selected for development will incorporate their suggestions.

ACKNOWLEDGEMENT

The research described in this paper was funded by the U. S. Department of Energy, Morgantown Energy Technology Center; the contract administrator was Mr. C. A. Komar. Their support is gratefully acknowledged.

REFERENCE

Simonson, E. R., Abou-Sayed, A. S. and Clifton, R. J.: "Containment of Massive Hydraulic Fractures," paper number SPE 6089 presented at the 51st Annual Fall Technical Conference and Exhibition, Society of Petroleum Engineers of AIME, New Orleans, Oct. 3-6, 1976.

TABLE 1
SUMMARY OF FRACTURE DETECTION TOOLS

Logging Tool	Status	Open Hole	Cased Hole	Restrictions	Comments
Borehole Televiwer	used commercially	yes	no	fluid filled borehole only	some interpretation problems
Dipmeter	used commercially	yes	no	conductive mud required	highly unreliable in locating vertical fractures
Sandia Passive Seismic	used by Sandia	yes	yes		has potential for incorporation of simple orientation determination method
Circumferential Acoustic Log	built, but not in use	yes	?	fluid filled borehole only	has potential for use in cased hole but needs development work
Acoustic Pulse-Echo	used commercially	yes	no		will not detect fracture passing through borehole
Horizontal Spinner	used commercially	yes	yes	tool in packed off region	modification needed to enable fracture detection and orientation
Magnetic Induction	Concept only	yes	no		preliminary design complete but development discontinued
Circumferential Resistivity	developed but not available	yes	no	conductive mud	results of research projects have not been released
Borehole Television	used commercially	yes	no	clear fluids required	units small enough to scan 6" borehole lack pressure hardening
Radio-active Tracers	used commercially	yes	yes	radioactive material handling	very complex hole cleaning required to eliminate background noise.
Impression Packer	used commercially	yes	no		a wireline version must be developed to be feasible.
Ultrasonic Spectroscopy	laboratory only	yes	no	need material properties	has potential for determining stress state as well as orientation
Borehole Wall Displacements	commercially used	yes	no		caliper systems do not possess adequate sensitivity
Gamma Ray	commercially used	no	yes	radioactive material handling	laboratory and field work required to prove method
Cement Bond	commercially used	no	yes	fluid filled hole	laboratory and field work required to prove method
Radial Differential Temperature	commercially used	yes	yes	single Licensee using tool	temperature anomaly created by fluid cooling pump motor
Noise Log	commercially used	yes	yes		directional capabilities are not developed but refer to Sandia Passive Seismic.

TABLE 2

EVALUATION MATRIX FOR FRACTURE DETECTION DEVICES

	1	2	3	4	5	6	7	8	9
	Cased	Open	Commercial	Std.App.	Directional	Function	Modify	Resolution	Straddle
Televiewer		X	X	X	X	X			
Dipmeter		X	X	X		X			
Pass Seismic	X	X	0	X	X	X			
CAD		X	0	X		X	X	X	
Pulse-Echo		X	X	X	X				
Spinner	X	X		X	X		X		X
Mag. Ind.		X		X	X	X			
Circ. Res.		X		X	X	X			
Television		X	X	X	X				
Tracer	X	X	X	X	X	X			
Impression		X	X	X	X		X		
Spectroscopy		X		X	X	X			X
Gamma	X		X	X		X	X		
Bond	X		X	X					
RDT	X	X	X	X	X	X			
Noise	X	X	X	X					X

NOTES

- i) An "X" in a column indicates that the tool meets the corresponding specification below.

Column

1. Tool detects fractures in a cased borehole.
2. Tool detects fractures in an open borehole.
3. Tool is commercially marketed by service companies.
4. Application of logging device is standard.
5. Tool has sensitivity in horizontal plane.
6. Tool meets specified operating requirements and at the present level of assessment will enable the detection of fractures and will indicate orientation.
7. Tool can be modified to meet requirements of 4, 5, 6 and 8.
8. Resolution of tool is poor, typically $\pm 45^\circ$.
9. To function properly tool must be configured within the packed off region of test.

- ii) An "0" in Column 3 indicates that although a tool is not in commercial use per se, it is developed, has been used in the field and is available.

- iii) Details upon which judgment used in assessing the tools was made can be found in the complete tool descriptions preceding this summary.

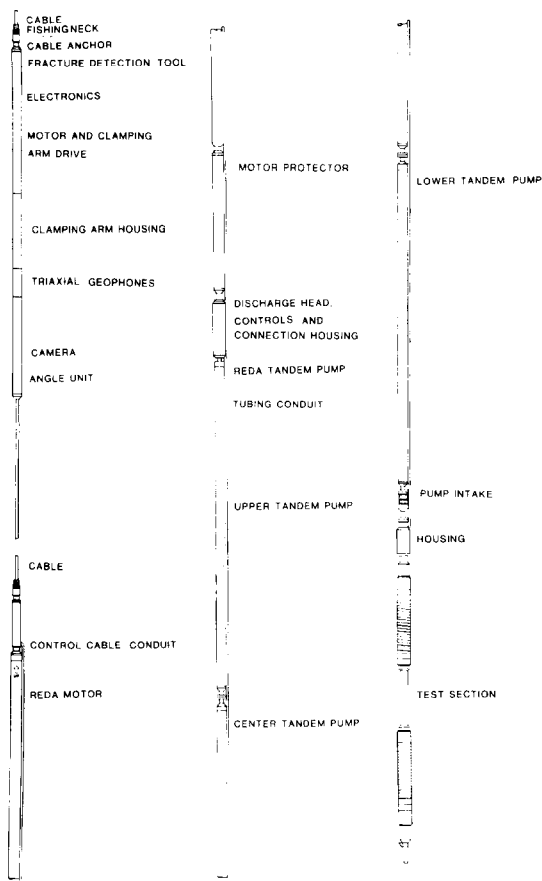


Fig. 1 - Tool No. 1 - Modified oil field submersible pump.

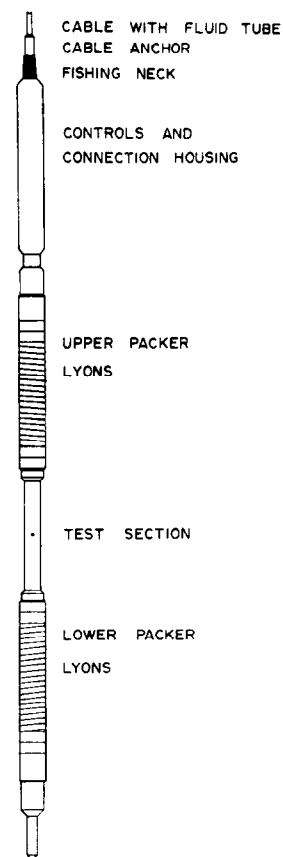


Fig. 2 - Tool No. 2 - surface generated fluid pressure.

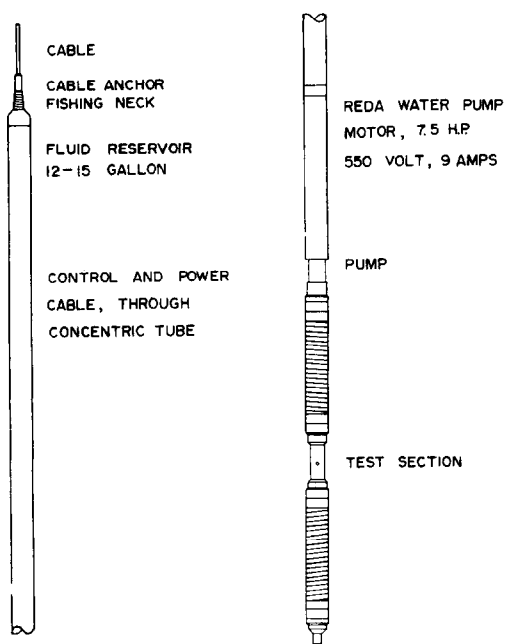


Fig. 3 - Tool No. 3 - Hydraulic gear pump and reservoir.

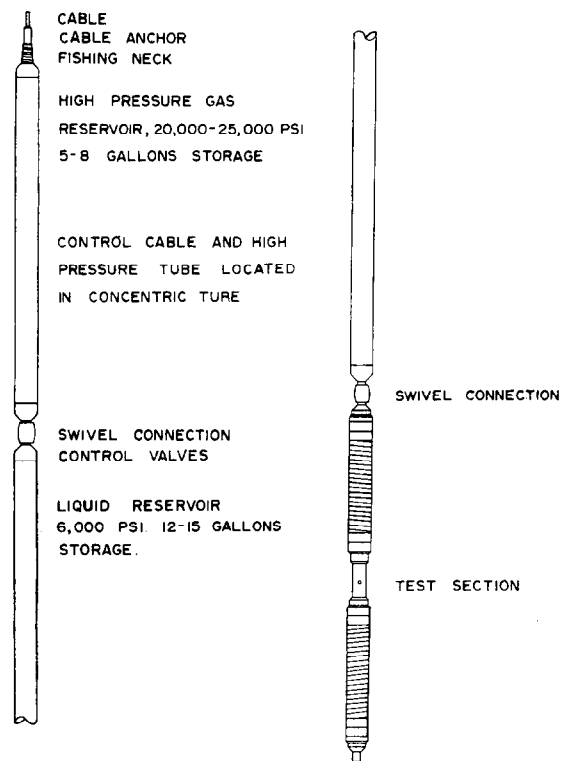


Fig. 4 - Tool No. 4 - High pressure gas reservoir.

EVALUATION OF FRACTURED RESERVOIR ROCKS USING GEOPHYSICAL WELL LOGS

by Walter H. Fertl, Dresser Atlas

© Copyright 1980, Society of Petroleum Engineers

This paper was presented at the 1980 SPE/DOE Symposium on Unconventional Gas Recovery held in Pittsburgh, Pennsylvania, May 18-21, 1980. The material is subject to correction by the author. Permission to copy is restricted to an abstract of not more than 300 words. Write: 6200 N. Central Expwy., Dallas, Texas 75206

ABSTRACT

Recent economic forecasts place recoverable crude oil reserves from fractured reservoir rocks in excess of 40 billion stock tank barrels. Hence, over the past few years the petroleum industry has exhibited an ever increasing interest in fractured reservoirs.

The present discussion summarizes wireline logging techniques applicable in the detection of fractured reservoir rocks and reviews their advantages and possible limitations.

INTRODUCTION

Natural fracture systems may be encountered in various lithologies, including sandstones, shales, carbonates, igneous and metamorphic reservoir rocks. Natural fracture systems not only control performance and state of depletion in reservoirs under primary, secondary, or tertiary recovery schemes; greatly control wellbore pattern of production and injection wells; affect exploration concepts, drilling operations, casing seat selection, cementing and completion techniques, etc.

Natural fracture systems can be identified, studied, and evaluated by proper selection and combination of several techniques. These include surveys from space, areal reconnaissance, surface geology, seismic information, core analysis, down-hole cameras, inflatable packers, geophysical well analyses, well testing, and production behavior.

The present discussion focuses on the use of well logs to identify the presence, determine extent, and/or evaluate the porosity of open, natural fracture systems and, hence, highly permeable zones.

References at end of paper

Basically, fracture porosity--which frequently ranges from less than 0.05% up to 5.5% -- is primarily controlled by the width, length, area, spacing, and surface roughness of the fracture. Natural fracture systems, their porosity, orientation, morphology, spacing, and continuity are much dependent on the mode of origin.

Fracture systems fall into two main categories, artificial (i.e. induced, shear, extension, tensile) fractures and natural ones. Recently, natural fracture systems (1) have been classified as tectonic features, which are structure related, (2) regional fractures, (3) contractional fractures, which are not restricted to geologic structures, result from desiccation, syneresis (tension, extension, "chicken-wire" fractures), thermal gradients (columnar jointing in igneous rocks), mineral phase changes (calcite to dolomite), and (4) surface-related fractures, which may result from unloading, release of stored stress and strain, unsupported boundaries, and weathering effects.

Furthermore, natural fractures may be open or healed. Healed or sealed fractures are filled with minerals (such as calcite) precipitated over geologic time from circulating subsurface waters. Nevertheless, sealed fracture systems are frequently weakness places favorable to hydraulic well stimulation. Concentrating a properly engineered well stimulation effort at a closed natural fracture system present at and within vicinity of the wellbore often establishes communication with an open fracture system at some distance from the wellbore.⁽²⁾

RESPONSE OF WELL LOGS IN FRACTURED FORMATIONS

Presence of a single natural fracture or a massive fracture system can cause minor to significant departures^(3,4,5,6) from the "normal" well log response. Such anomalies may be recorded by mechanical, electrical, acoustic, nuclear, radioactive, and temperature logging devices as a function of borehole conditions, drilling mud characteristics and fracture-related reservoir properties.

Downhole Cameras

Several attempts have been reported ^(7,8) to use downhole cameras in gathering direct information as to fractures, hole size and shape, bed boundaries, etc. Application of cameras appears to be limited to empty, gas-filled wellbores and downhole temperatures less than 200°F.

Temperature Log

In case the "cooler" mud invades the "hotter" formation, a cooling effect will indicate fractured intervals. The resulting log response is similar to temperature profiles observed in injection wells.

Basically, a fracture-related temperature anomaly will depend on the temperature differential between drilling mud and formation and the thermal conductivities of both media. Numerous temperature logging devices are available to the petroleum industry, including a radial differential temperature log.⁽⁹⁾

Caliper

Fractured formations may exhibit one of two basic patterns on any caliper log, (a) an indication of thick mud cake build-up, particularly when using circulation loss material or heavily weighted mud, and (b) borehole elongation observed preferentially in the main direction of fracture orientation over fractured zones (but not over entire length of very long hole-sections). Fracture-related "washout" indication may result from "chipping" while drilling these fractured intervals.

In case of the dual caliper on high-resolution diplogs one can also monitor the rotation of the logging tool. In vertically fractured zones, tool rotation may essentially stop or, depending on the fracture system, tool rotation will at least slow down.

However, in using caliper logs as possible fracture indicators one has to be fully aware of inherent design criteria, such as number, type, length, and configuration of pads and springs, prior to making sweeping interpretive conclusions.⁽¹⁰⁾

Spontaneous Potential (SP) Curve

Frequently the SP-curve appears to be affected by fracturing. Erratic negative SP-deflections are caused by delectokinetic (streaming) potential effects. Such observations have not only been made in exploring for oil and gas, but also in the evaluation of metamorphic and igneous rocks in geothermal resource assessments.⁽¹¹⁾

Natural Radioactivity

Gamma ray log. Frequently observed gamma ray increases, without concurrently higher formation salinity, has been explained by deposition of uranium salts along fracture surfaces.⁽²⁾

Gamma ray spectral data, as recorded by the

Spectralog, for in addition to the total gamma ray counts, provides information as to the individual gamma rays emitted by potassium-40 (K^{40}), the uranium series nuclide bismuth-214 (Bi^{214}) and the thorium series nuclide thallium-208 (Tl^{208}).

In presence of organic matter, hydrogen sulfide, sulfur dioxide, and the available uranium ions transported by migrating formation waters will precipitate as UO_2 , with tuffaceous, arkosic, and granitic rocks being among the probable sources of uranium. Precipitated uranium may concentrate along fault planes, fracture and fissure systems of some lateral extent.

Collaborating field experiences ^(2,6,12,13) have been reported for the Austin Chalk, Eagle Ford Shale, and Buda Lime in the Cretaceous Carbonate Trend of Texas, carbonates of West Texas, fractured reservoirs in the Niobrara, Mancos, and Pierre formations of Cretaceous age in Colorado and New Mexico, the localized highly productive Woodford Shale in Oklahoma, Devonian Shales in the Appalachian Basin, the productive Monterrey Shales of Miocene age in California, etc.

One has, however, to keep in mind that gamma ray spectral data does not differentiate between open and closed fractures.

Density Log

Since density logs measure total reservoir porosity in carbonates, fractures will decrease the recorded bulk density. Particularly affected is the count rate at the short detector and, hence, the correction $\Delta\rho$ -curve.

However, such anomalies assume the tool's pad to be in contact with the fracture, no major tool rotation occurs (otherwise "fractures come and go" on multiple repeat runs), and the unfavorably low count rate and, therefore, poor repeatability in low porosity formations is recognized.

In other words, such probable fracture identification needs to be confirmed by other techniques.

Furthermore, presence of large fractures filled with baryte containing heavy mud can be observed due to the drastic increase in the photoelectric cross-sectional number.⁽⁵⁾

Neutron Logs

Similar to a density log, any neutron-type log also measures total reservoir porosity in carbonate rocks. While the repeatability of these tools is good in low-porosity formations, a neutron log by itself is not a reliable fracture indicator.

Acoustic Logging

Several acoustic logging concepts are available which lend themselves to fracture identification.

In dual-receiver and BHC acoustic logging systems, "cycle skipping" may occur at any receiver. This causes the measured travel time to be either too long, too short, or correct. Such "cycle-skipping" may occur when the attenuation

in a formation is abnormally high (due to under-compaction, light hydrocarbons, or fractures) or when the mud is gas-cut. In hard rock (i.e. fast formations) cycle skipping is a good fracture indicator.

Fractures are known to significantly reduce the amplitude of the formation signal, with the amplitude loss being a function of dip angle of fracture, number of fractures intersected by well-bore, shape of fracture faces, extent and nature of material in fracture, etc. Basically, the compressional amplitude is little affected by fractures having dip angles less than 20° or more than 85°, whereas the shear amplitude is largely decreased by horizontal or near-horizontal fractures. Acoustic wave train recordings, such as Signature logs, and Variable Density, etc., can be used in fracture evaluations.

The compressional acoustic measurement is essentially unaffected by subvertical fractures, whereas shear velocity and amplitudes are significantly affected.

Interpretation, however, is not always straight-forward since many formation-and bore-hole-related parameters, and particularly tool excentering, may greatly affect the tool response.

Sidewall Acoustic Log. The acoustic section, of this tool consists of a transmitting transducer and two receiving transducers and is contained in a pad approximately two feet in length, with a receiver spacing of 6 inches.⁽¹⁴⁾ The sidewall acoustic tool has successfully recorded continuous logs of both shear and compressional wave transit time. Application to fracture identification is apparent and has been successfully field tested in Texas, California, Canada, and elsewhere.

Long-Spaced Acoustic. Long spacing tools assist in separation of various wave types. For example, formation compressional and shear interval transit time logging based on wide-band transducers and a long spacing between transmitter and an array of four receivers plus signal processing can be performed automatically in a minicomputer.⁽¹⁵⁾

Borehole Televiewer. This acoustic logging tool provides a continuous, 360° scanning of the amplitude of the reflected signal in fluid-filled wellbores as affected by the nature and geometry of the borehole wall. Fractured intervals are characterized by amplitude reduction of the reflected signal.

Length and direction of fracture systems intersecting the wellbore can be determined. Field experience with this acoustic-type system, which is available on limited basis only, has been reported for both petroleum and geothermal reservoir evaluation.^(16,17)

Circumferential Acoustic Logging. By utilizing a number of radial transmitters and receivers in a horizontal plane the acoustic transmission properties along the borehole wall can be measured. Attenuation effects of fractures on this transmission are then measured. Such circumferen-

tial acoustic concepts specifically apply to detection and evaluation of vertical fractures.^(18, 19) Prototypes are currently in the field test stage.

Noise Logs. This logging device basically consists of a microphone which transmits the recorded sound to the surface panel, where the acoustic spectrum is decomposed into several frequencies. These noise levels assist in estimates of the axial flow rate past the logging tool for single-phase flow, flow rate from perforations for single-phase or gas/liquid flow, pressure drop across a plugged perforation, and sand production rate from perforations.^(20,21)

We have also successfully used noise logs, such as the Sonar Log, as fracture indicator in tight gasbearing formations in the Sonora area, Texas, and elsewhere.

Resistivity logs

Whereas induction-type logs will be little affected (with the exception perhaps of a major horizontal fracture containing saturated salt water), invaded fractures offer a preferential current path for normal electrode and focused resistivity logs.

Therefore, in fresh muds the Dual Induction-Focused log will qualitatively indicate fractures, with the shallow curve reading resistivity values less than those of the deep or medium induction curve.

In the case of subvertical, unidirectional fracture systems a deep laterolog should read significantly higher than the shallow curve. However, this observation is not exclusive to fractured zones.

R_{xo} -log responses, such as marked conductivity anomalies, may be indicative of fractures. However, loss of pad contact with the borehole wall in rugose or highly deviated wells may result in similar response. Furthermore, the R_{xo} -pad has to face the fracture to "see" it, and fractures may "come and go" on multiple repeat runs due to tool rotation.

Diplog (Dipmeter)

In resistive formations the diplog will show significant anomalies toward low resistivities in the presence of fractures. Due to tool rotation, some of these anomalies may not again show up on repeat runs. Furthermore, severe boreholes rugosity and resulting loss of pad contact, shale breaks, etc., may show diplog response similar to that in the presence of fractures. Whereas vertical fracture may appear as long anomalies on one or two electrode curves. Horizontal fractures, appear as short anomalies on all four curves.

In a recent dipmeter log study of 23 wells in Alberta, Canada,⁽²²⁾ the presence of steeply dipping fractures has been defined and the vertical length and azimuth of fractured zones intersected by the boreholes has been investigated based on the measurement of the azimuth of hole cross-section elongation of zones overbreak where the drill bit encountered a fracture. Of a total of 246 caved zones in 23 wells, located throughout Alberta, over 90% showed a preferential breakout parallel with one of the

principal joint sets observed at outcrops.

Fracture Identification Log

Fracture recognition using dipmeter data is improved by a special presentation format of the recorded data, such as the Fracture Identification Log (FIL)(23). This, for example, may include the four original dipmeter curves, and displays of two (1&2, 3&4) or four (1&2, 3&4, 2&3, 4&1) curve displays.

Initially applied in the fractured Cretaceous Carbonates, Texas, the FIL is now used in many areas.

Crossplots

Crossplotting of porosity logging data has been utilized since the early 1960's. Whereas computer processing allows quick and easy data handling, hand plotting still provides an effective check for the experienced log analyst.

Binary (Two-Mineral) Porosity Model

Complex Reservoir Rocks. Two basic mineral constituents are present. The mathematical solution requires, in addition to the unity equation, only two of the three basic porosity response functions listed below. Ambiguity exists in certain crossplots due to non-linear dolomite response of neutron-type logs.

$\rho_b, \phi_N = f$ (type and bulk volume percentage of rock matrix components, porosity, fluid in pore space, shale)

$\Delta t = f$ (type and bulk volume percentage of rock matrix components, porosity, fluid in pore space, shale, secondary porosity)

$1.0 = \text{Porosity} + E$ (bulk volume matrix components) = Unity Equation

A brief review of the three possible porosity log crossplot combinations leads to the following conclusions:

DEN(Y) vs. AC(X), ρ_b vs. Δt

Such crossplots provide: shaliness definition; evaporite determination (anhydrite, halite, polyhalite; gypsum in clean, non-gasbearing zones); poor porosity resolution; definition of ρ_{sh} , Δt_{sh} , (M_{sh})_{cal}; light hydrocarbon, gas gypsum shift the points towards NW; shales and compaction effects shift points towards E; secondary porosity shifts trend towards W; borehole rugosity, washouts shift trend towards N.

NEU(Y) vs. AC(X), ϕ_N vs. Δt

This crossplot exhibits good porosity and lithology (quartz, calcite, dolomite) resolution in clean, waterbearing intervals; resolution of gypsum in clean, non-gasbearing zones; shales trend towards NE (easily seen on z-plots); definition of Δt_{sh} , ϕ_{Nsh} ; compaction shifts towards E; light hydrocarbons and gas shift towards S; gypsum, hole rugosity, washouts (use

caliper z-plot) shift towards N; secondary porosity shifts toward W.

DEN(Y) vs. NEU(X), ρ_b vs. ϕ_N

This important and quite frequently used crossplot provides: satisfactory resolution of porosity; basic insensitivity to lithology (simple approximation $\phi = 0.5 (\phi_{DEN} + \phi_{NEU})$, both in limestone units); good lithology resolution for quartz, calcite, and dolomite; no secondary porosity effect since both logs measure total porosity; shales, gypsum trend towards E, NE; definition of ρ_{sh} , ϕ_{Nsh} , (N_{sh})_{cal}; light hydrocarbon and gas trend towards NW; gypsum determination in clean (or shale-corrected) reservoirs void of gas; non-linear dolomite response of Neutron Log.

Ternary (3-Mineral) Porosity Model

M(Y) vs. N(X) or Litho-Porosity Crossplot

This crossplot is a two-dimensional display of all three porosity log responses in complex reservoir rocks. M and N are lithology-dependent parameters, but essentially independent of primary porosity. Non-linearity of neutron response in low-porosity dolomite requires three pseudo-matrix points for dolomite. All matrix point locations also vary with the type of neutron logs and fluid in the borehole. However, the scaling of constituents in ternary mineral models is more complex than for binary mineral combinations, since M and N values are defined by the tangents of the matrix-to-fluid-point lines.

Basically however:

$M = f(\Delta t_f, \Delta t, \rho_b, \rho_f) \cdot 0.01$ = slope in AC vs. DEN crossplot

$N = f(\phi_{Nf}, \phi_N, \rho_b, \rho_f)$ = slope in NEU vs. DEN crossplot

M vs N crossplot (24) can be used for lithology determination, lithology trends, gas detection, clay mineral classification, etc. Each mineral has a unique set of (M,N) values and the concept is applicable to ternary and binary mineral models. Additional superimposed effects include; gas trend shifts to NE, secondary porosity shifts to N, gypsum shifts to NNW, shales shift to S, SW, etc.

Formation Factor (F) versus Porosity (ϕ)

For some time it has been recognized that extremely low values for the cementation exponent, m, may characterize fractured intervals.(25)

Along this line a statistical approach (26) has been proposed recently for detecting natural fracture systems in complex reservoir rocks of very low matrix porosity. The minimum logging suite required in using this technique consists of resistivity and either a density or neutron log.

The method has been already successfully field tested in the fractured Cretaceous carbonate rocks of Southeast Mexico and Venezuela.

A similar concept has been applied in the evaluation of low-porosity carbonates at Malossa, Italy.(27) Crossplots of the apparent formation

factor (F) from deep-resistivity logs (when $S_w = 1.0$) or microresistivity logs ($S_w \leq 1.0$) versus reservoir porosity (ϕ), both on logarithmic scales will define the cementation exponent, m , as the slope of a straight water line with its origin at $\phi=F-1.0$. In the Malossa field study the fractured intervals exhibit m -values of 1.4 and lower.

Statistical Approach

A statistical method initially proposed for determination of water saturation in intergranular rocks has also proved useful in fractured reservoir rocks.^(25,28)

The technique is based on the parameter P , a function of resistivity and porosity response, which has been found empirically to exhibit a square-root-normal distribution for zones 100-percent saturated with water, whereas hydrocarbon zones deviate from this distribution.

Secondary Porosity Index

Acoustic wave propagation by-passes sub-vertical fractures (if present) and essentially responds to primary porosity (ϕ_{AC}), whereas density (ϕ_D) and neutron logs (ϕ_N) measure total porosity. Hence, comparison of total and primary porosity does provide an estimate of secondary porosity index (SPI), such as $SPI = \phi_{ND} - \phi_{AC}$.

The SPI-Index defines fracture plus vugular porosity. Fracture-related secondary porosity indication, with only a minor fracture system present, may become rather unreliable.

Flowmeter (Spinner) Surveys

Continuous flowmeter surveys can be used for metering fluid flow rates within open or cased wellbores. Significant production volume changes in fractured versus otherwise tight formations can be located.

Miscellaneous Concepts

Drillstem tests, radioactive tracers, log-inject-log methods, impression packers, ultrasonic spectroscopy,⁽²⁹⁾ magnetic induction,⁽³⁰⁾ acoustic pulse-echo logging,⁽³¹⁾ borehole passive seismic system,⁽³²⁾ are additional concepts in actual field use, prototype testings, or in the conceptual stage.

CONCLUSIONS

1. Several log-derived fracture indicators are available to the industry.
2. These fracture indicators are based on variations and contrast in electrical, acoustic, nuclear and radioactive formation properties, temperature, hole size, etc.
3. No unique, universally reliable log-derived fracture evaluation technique exists.
4. Reliable fracture evaluation requires a sufficient number of properly selected well logs.

REFERENCES

1. Nelson, R.A., 1979, Natural Fracture Systems: Description and Classification, Am. Assoc. Petro. Geol., 63(12): 2214-2232.
2. Fertl, W.H., Stapp, W.L., Vaello, D.B., Vercellino, W.C., 1978, Spectral Gamma Ray Logging in the Texas Austin Chalk Trend, SPE-7431, 53rd Ann. Fall Meeting, Houston, Texas, Oct. 1-3; also Journal Petr. Tech., 1980, 32 (3): 481-489.
3. Shanks, R.T., Kwon, B.S., DeVries, M.R., Wichmann, P.A., 1976, A Review of Fracture Detection With Well Logs, SPE 6159, 51st Ann. Fall Meeting, New Orleans, La., Oct 3-6.
4. Aquilera, R., Van Poolen, H.K., 1979, Naturally Fractured Reservoirs, 13 installments, Oil & Gas Journal, December 18, 1978 to June 4, 1979.
5. Suau, J., Gartner, J., 1979, Fracture Detection From the Logs, 6th SPWLA European Formation Evaluation Symposium, London, U.K., March.
6. Heflin, J.D., 1979, Fracture Detection in West Coast Reservoirs Using Well Logs, SPE 7976, California Regional Meeting, Ventura, California, April 18-20.
7. Fons, L.C., 1960, Downhole Camera Helps Solve Production Problems, World Oil, 151; 150-152.
8. Dempsey, J.C., Hickey, J.R., 1958, Use of Downhole Camera for Visual Inspection of Hydraulically Induced Fractures, Procedures Monthly, April 18-21.
9. Cooke, C., 1978, Radial Differential Temperature Logging - A New Tool for Detecting and Treating Flow Behind Casing, SPE 7558, 53rd Annual Fall Meeting, Houston, Texas, October 1-3.
10. Kading, H.W., 1977, Computer Caliper, Finger Prints of the Hole, from Austin Chalk to Ellenburger, Paper P, Transactions SPWLA, p.12.
11. Sethi, D., Fertl, W.H., 1979, Geophysical Well Logging Operations and Log Analysis in Geothermal Well Desert Peak No. B-23-1, DOE-LASL Report, p.69.
12. Fertl, W.H., 1979, Gamma Ray Spectral Data Assists in Complex Formation Evaluation, Transactions SPWLA, 6th European Formation Evaluation Symposium, London, March 1979; also Dresser Atlas Publication #3335, February 1979.
13. Fertl, W.H., Rieke, H.H., 1979, Gamma Ray Spectral Evaluation Techniques Identify Shale Reservoirs and Source Rock Characteristics, SPE 8454, 54th Annual Fall Meeting, Las Vegas, Nevada, September 23-26.
14. Guy, J.O., Smith W.D.M., Youmans, A., 1971, The Sidewall Acoustic Neutron Log, Paper X, Transactions SPWLA.
15. Aron, J., Murray, J., Seeman, B., 1978, Formation Compressional and Shear Interval Transit

- | | |
|---|--|
| <p>Time Logging by Means of Long Spacings and Digital Techniques, SPE 7446, 53rd Annual Fall Meeting, Houston, Texas, October 1-3.</p> <ol style="list-style-type: none"> 16. Zemanek, J., Caldwell, E.E., Glenn, E.E., Holcomb, S.V., Norton, L.J., Strauss, A.J.D., 1969, The Borehole Televiewer - A New Logging Concept for Fracture Location and Other Types of Borehole Inspection, Journal of Petroleum Technology, 21(6): 762-774. 17. Keys, W.S., 1979, Borehole Geophysics in Igneous and Metamorphic Rocks, Paper O, Transactions SPWLA. 18. Koerperick, E.A., 1975, Evaluation of the Circumferential Microsonic Log - A Fracture Detection Device, Transactions SPWLA. 19. Vogel, C.B., Herholz, R.A., 1977, The CAD, A Circumferential Acoustic Device for Well Logging, SPE 6819, 52nd Annual Fall Meeting. 20. McKinley, R.M., Bower, F.M., Rumble, R.C., 1973, The Structure and Interpretation of Noise from Flow Behind Cemented Casings, Journal of Petroleum Technology, 16(3): 329-338. 21. McKinley, R.M., Bower, F.M., 1979, Specialized Applications of Noise Logging, Journal of Petroleum Technology, 31(11): 1387-1395. 22. Babcock, E.A., 1978, Measurement of Sub-surface Fractures from Dipmeter Logs, American Association of Petroleum Geology, 62(7): 1111-1126. 23. Beck, J., Schultz, A., Fitzgerald, D., 1977, Reservoir Evaluation of Fractured Cretaceous Carbonates in South Texas, Paper M, Transactions SPWLA. 24. Burke, J., Campbell, R., Schmidt, A., 1969, | <p>The Litho-porosity Crossplot, The Log Analyst, 25-43, November-December.</p> <ol style="list-style-type: none"> 25. Aguilera, R., 1974, Analysis of Naturally Fractured Reservoirs from Sonic and Acoustic Logs, Journal of Petroleum Technology, 26(11): 1233-1238. 26. Gomez - Rivero, O., 1978, The F-ϕ-m Cross Plot - A New Approach for Detecting Natural Fracture in Complex Reservoir Rocks by Well Log Analysis, Paper D, Transactions SPWLA, p.18. 27. Suau, J., Roccabianca, R., Cipni, M., Boyeldieu, C., Spila, M., 1978, Evaluation of Very Low Porosity Carbonates, Malossa, Italy, Transactions SPWLA. 28. Porter, C.R., Pickett, G.R., Whitman, W.W., 1969, A Statistical Method for Determination of Water Saturation From Logs, Transactions SPWLA. 29. Agpson, J.R., 1978, The Potential Application of Ultrasonic Spectroscopy to Underground Site Characteristics, Paper E-25, 48th Annual International Meeting, Society of Exploration Geophysicists, San Francisco. 30. Landt, J.A., 1978, A Magnetic Induction Technique for Mapping Vertical Conductive Fractures: Theory of Operations, LASL Report UC-66 b, July. 31. Edwards, R.C., Mitchell, T.H., 1978, Field Research Experiment for New Site Exploration Techniques Acoustic Pulse-echo and Through-transmission Surveys, USDOT Contract, DOT-FH-11-9268. 32. Schuster, C., 1978, Detection Within the Seismic Signals Created by Hydraulic Fracturing, SPE 7448, 53rd Annual Fall Meeting, Houston, Texas, October 1-3. |
|---|--|

UTILIZING WELL INTERFERENCE DATA IN UNCONVENTIONAL GAS RESERVOIRS

by W.K. Sawyer, West Virginia Univ.; J. Alam,
Science Applications, Inc.; and W.D. Rose,
Institute of Gas Technology

© Copyright 1980, Society of Petroleum Engineers

This paper was presented at the 1980 SPE/DOE Symposium on Unconventional Gas Recovery held in Pittsburgh, Pennsylvania, May 18-21, 1980. The material is subject to correction by the author. Permission to copy is restricted to an abstract of not more than 300 words. Write: 6200 N. Central Expwy., Dallas, Texas 75206

ABSTRACT

This paper describes the use of a dual porosity radial gas flow simulator for estimating values for the key parameters controlling gas production from the Devonian shale or similar unconventional resource. Using best estimates from the literature on shale fracture and matrix properties as a starting point, the model is used to history match production decline and cumulative production data from a Devonian shale well in Meigs County, Ohio. Three sets of parameters were obtained which gave good agreement with the production data. Utilizing simulated pressures at a distance of 96 feet (29.3 m) as a third matching parameter, it was possible to distinguish between the three cases and thus obtain a "more unique" match.

From the results obtained it is concluded that interference data can provide additional information needed for determining the key parameters that control shale well deliverability.

INTRODUCTION

Devonian shale wells have produced in the Appalachian Basin for 50 to 100 years with very low but sustained productivity. In recent years there has been a large effort by government and private industry to develop and implement improved techniques for recovering a greater percentage of gas from this important resource. A part of this effort involves the development of mathematical models with predictive capability so that various alternative production schemes can be investigated and accurate forecasts of additional recovery can be made.

Most Devonian shale reservoirs are believed to consist of a very tight, low porosity shale matrix with high storage capacity and low flow capacity coupled with a relatively high flow capacity natural fracture system of very low storage capacity. As pointed out by Smith et al¹ the weight of all available evidence favors the position that the shale matrix provides the major contribution of the recoverable gas.

The Kucuk-Sawyer model² was used in this study in an effort to approximate the key parameters controlling gas production from a particular shale well in Meigs County, Ohio. The model was used in the history mode so that observed and simulated data were plotted for immediate comparison. Parameters were adjusted manually until good agreement between observed and simulated production decline and cumulative production curves was obtained.

Good matches were obtained for three sets of the following parameters: (1) fracture porosity, (2) fracture permeability, (3) fracture spacing, (4) matrix porosity, and (5) matrix permeability. In an attempt to obtain "more uniqueness" the simulated pressures at a distance of 96 feet (29.3 m) were compared for three "matches". It was found that, for each of the three sets, pressures were significantly different. Thus the possibility of utilizing interference data from offset wells to delineate storage and flow properties of the Devonian shale is inferred. Details of the matching procedure and the sensitivity to the various parameters are presented.

BACKGROUND

Warren and Root³ and Kazemi⁴ have presented models and techniques for analysis of naturally fractured reservoirs for the flow of compressible liquids. Kazemi et al⁵ also studied the pressure behavior of an observation well in a naturally fractured reservoir with an adjacent well produced at a constant rate. It was found that the early time response was substantially different from that of an equivalent homogeneous reservoir. Crawford et al⁶ analyzed more than twenty field-measured pressure buildup curves in a reservoir known to be naturally fractured and concluded that the Warren and Root model³ adequately described the buildup response and is therefore useful in determining effective (fracture system) permeability.

In 1976 DeSwaan⁷ presented an analytical model for a naturally fractured reservoir which does not involve the Warren and Root parameters. In discussing various methods of analysis of well test data from

References and illustrations at end of paper.

fractured reservoirs, Aquilera and van Poolen⁸ suggests that DeSwaan's method may be a more practical engineering tool.

Later Najurieta⁹ presented an approximate solution for the model proposed by DeSwaan and showed that the behavior of a uniformly fractured reservoir can be fully described by four parameters, each of which is a function of two or more of the five basic reservoir parameters (fracture and matrix permeability, fracture and matrix porosity, and fracture spacing or matrix element size). More recently, the method has been extended by Najurieta¹⁰ to interference testing in naturally fractured reservoirs when boundary effects are present.

In general, all these techniques can be applied to the evaluation of naturally fractured gas wells. For example, at pressures less than 2000 psi (13,790 kPa) the product p_z usually is essentially constant and methods developed for compressible liquids can readily be used for gas by using pressure squared¹¹ and converting flow rates to gas units.

Adams et al¹² presented a complete evaluation of gas well test data from a fractured carbonate reservoir. However, the observed pressure buildup behavior was not in accordance with the earlier models of Warren and Root³ and Kazemi^{4,5}. Adams et al¹² theorized that the observed behavior was possibly due to the well being in communication with the fracture system only through the relatively tight matrix.

Under the assumption that gas recovery from the Devonian shale depends on transport of gas from within the shale matrix to a natural fracture system and subsequently through the fracture system to a producing well, the above studies provide a basis for studying pressure and production behavior in Devonian shale wells. However, shale matrix permeability is so low that the phenomenon of gas slippage^{13,14} or "Klinkenberg effect" must be considered. Also it has been shown that, for crushed samples, the surfaces of the powdered shale can contain large amounts of adsorbed gas which is released simply by pressure reduction¹⁵.

To rigorously account for dual porosity effects and the nonlinearities introduced by gas slippage and adsorption/desorption, to provide the capability of studying the effects of variable wellbore conditions, and to be able to simulate interference data, a numerical model has recently been developed² for predicting performance in Devonian shale or other unconventional gas reservoirs.

INITIAL PARAMETERS ESTIMATION

Fracture System

Muskat¹⁶ first presented the equation which relates fracture width, spacing and permeability for parallel fissures

$$k_f = 8.33 \times 10^9 \frac{w_f^3}{S} \quad (1)$$

The fracture permeability calculated from Eq. 1 will yield high values if fissures are partially filled with carbonate, pyritic or other material.

Fracture porosity can be estimated using the differential change in volume of a square block of shale matrix as illustrated in Figure 1. Using two sides of each block to avoid duplication it is seen that

$$\phi_f = \frac{2w_f}{S} \quad (2)$$

Smith¹ has reported fracture spacings of at least 10 feet (3.05 m) based on core analysis and observations of over 2500 feet (762.0 m) of Devonian shale from Lincoln County, West Virginia and Martin County, Kentucky. Table 1 gives fracture porosity and permeability values according to Eqs. 1 and 2 for reasonable values of effective fissure width. The extremely low values of porosity indicate how small the fracture storage capacity may be in comparison with that of the shale matrix. Even if the fissures are much wider but partially filled, small porosities would still result. For example, fissures 300 cm apart and 0.1 cm wide with a "fissure porosity" of 25% would still only give a bulk fracture porosity of 0.00016.

Shale Matrix

Shale matrix porosities near the area of the well used in this study have been reported in the range of 0.5 to 8 percent¹⁷. Since matrix porosity primarily determines "recoverable" gas content which can be estimated independently from outgassing experiments, this parameter normally should only be varied over a narrow range.

The reader may take exception to the claim that gas content is determined simply by matrix porosity instead of adsorbed gas. However, it is the authors collective opinion based on available evidence to date that sorption isotherms measured on crushed samples give unrealistically high gas contents so far as recoverable gas is concerned. For example, examination of the data of Thomas and Frost¹⁸ indicates an adsorbed gas content of about 6 (Scf/cu. ft.) at 675 psi (4654 kPa). However, a low matrix porosity for a core sample of 0.5 percent will give a gas content of about 0.2 at this pressure which is often used as an average value for the entire Appalachian Basin. If we add an adsorbed gas content of 6 we get an unreasonably high value compared to outgassing experiments reported¹⁸. Apparently, the sorption isotherms involve "low mobility" gas which possibly could only be produced by heating to a high temperature to break down the kerogen. Experiments are planned on both whole core and crushed samples to clarify if and how this low mobility gas can be produced.

Shale matrix permeabilities near the area of the study well have been reported¹⁹ from 10^{-3} to 10^{-9} the millidarcies (10^{-6} to 10^{-12} μm^2). Flow through the shale matrix is often considered to be Fickian diffusion. The relationship between the diffusion constant and darcy permeability is given below and derived in the appendix.

$$k = \frac{14,700 D \phi \mu}{P} \quad (3)$$

Since most diffusion experiments are conducted at low pressure and the product ϕu is on the order of 10^{-4} we see that the permeability in millidarcies is about 0.1D. Smith²⁰ has reported an average diffusion coefficient of $6.8 \times 10^{-8} \text{ cm}^2/\text{sec}$ for Devonian shale samples from Ohio and West Virginia. The highest value measured was $4.7 \times 10^{-7} \text{ cm}^2/\text{sec}$ and the lowest (measurable) value was $9.1 \times 10^{-10} \text{ cm}^2/\text{sec}$. Using Eq. 3 at one atmosphere with ϕu equal to 10^{-4} gives matrix permeability in the range 9.1×10^{-11} to $4.7 \times 10^{-8} \text{ md}$ (9.0×10^{-14} to $4.6 \times 10^{-11} \mu\text{m}^2$).

Jones et al.¹⁴ has presented experimental data on Klinkenberg parameters for low permeability gas sands. He found that, for true permeabilities in the range 10^{-1} to 10^{-5} md (10^{-4} to $10^{-8} \mu\text{m}^2$) the Klinkenberg number in psi is given by

$$b = 12.64 k_L^{-.33} \quad (4)$$

In the absence of specific data on b values for the Devonian shales, Eq. 4 was used in this study for both fracture and shale matrix permeabilities.

In summary, the initial parameters used in this study, based on the above considerations, are given in Table 2.

FIELD DATA

The well selected for this study is located in Chester Township, Meigs County, Ohio and will be referred to as Well A. The well was drilled to a total depth of 3273 feet (997.6 m) and completed in July, 1956 with $3\frac{1}{2}$ inch (.0088 m) tubing set at 2774 feet (845.5 m). The producing formation is the brown shale with a gross thickness of 410 feet (125 m). The entire interval was shot with 4050 pounds (1837 kg) of borehole explosives. Initial wellhead pressure was 638 psi (4399 kPa) with an Initial Open Flow of 54 MCFD ($1529 \text{ m}^3/\text{day}$).

Using a gas gravity of 0.60 and a reservoir temperature of 100°F (37.8°C) the gas property data given in Table 3 was obtained using standard correlations in the literature. The initial formation pressure was estimated to be 684 psi (4716 kPa) by using the initial wellhead pressure and a gas gradient of 0.014 psi/ft. (.317 kPa/m) to get the midpoint reservoir pressure.

Average production rates and cumulative production data were available from 1956 to 1972. Table 4 gives the 17 year production history of the well. During this time the well was flowed against a line pressure which varied from 207 to 263 psi (1427 to 1813 kPa).

SIMULATION STUDY

Using the numerical model² and gas property and reservoir data from the previous section, a simulation study was initiated in an effort to determine what combinations of parameters would result in a history match of the 17 year production history. Initial parameter estimates are given in Table 2 and have been previously discussed.

A well spacing of 40 acres ($1.62 \text{ E} + .05 \text{ m}^2$) was used in this study. Although no regular spacing exists in the area studied, it was observed that

Well A and an adjacent well at a distance less than 2000 feet (609.6 m) have distinct pressure histories, possibly indicating production from different reservoirs. With a 40 acre ($1.62 \text{ E} + .05 \text{ m}^2$) area, 410 feet (125 m) thick and a matrix porosity of 0.5 percent the initial gas in place is 173 MMSCF ($4.90 \times 10^5 \text{ m}^3$) at 684 psi (4716 kPa) which is nearly three times the well's productivity in 17 years.

It was anticipated at the beginning of the study that several combinations of parameters would give a reasonable match of the well's production history. Moreover, it was expected that, due to the different fracture-matrix interactions with different parameter combinations, observed pressures a short distance away would be distinct, at least for some of the sets of matching parameters. In this manner, it was hoped that a more unique set of parameters could be found.

Three good matches were obtained using three different sets of parameters. As expected, each of the matches yielded distinctly different pressures at an offset distance of 96 feet (29.3 m). Table 5 gives the matching parameters and the simulated offset pressures after 14 years of production.

Figures 2 through 7 show the good agreement between the simulated and actual production decline and cumulative production curves for the three matches. For purposes of plotting, the production rate data in Table 4 was adjusted back in time to the mid-year point, except for the first year in which the well was only on line 115 days. This was assumed to be the last 115 days of the year and the production rate was adjusted back 57.5 days. Cumulative production data was given at the end of each year so no adjustment was required.

Figure 8 shows the pressure versus time history at a distance of 96 feet (29.3 m) for each of the three matches (based on performance of the flowing well). The model performance indicates significantly different pressures over the entire producing life of the active well. This strongly suggests the need and importance of an offset well program as an adjunct to single well testing in the Devonian shale.

Figures 9 through 14 show the sensitivity of Match No. 2 to fracture and matrix permeability and fracture spacing. Curves for both rate and cumulative production are shown for each case. In Figure 9 we see that, with all other parameters constant, fracture permeability controls the production performance for the first few years but has little effect after about 10 years. This indicates that at late times fracture spacing and matrix permeability controls well productivity.

Figures 11 and 13 indicate that production rate is very sensitive to both fracture spacing and matrix permeability. Moreover, the effect of a two-fold change in matrix permeability has nearly the same effect as a change of 200 cm in fracture spacing. This is not surprising since the permeability-radius product appears in radial differential form of Darcy's law. Of course a change in either permeability or radius will cause an adjustment in pressure gradient at the fracture-matrix interface and hence one would not expect to obtain identical performance by maintaining the product constant.

Figures 10, 12, and 14 show the integrated or cumulative effect of changes in k_f , S , and k_m . In all cases the change in cumulative production with time is approaching a constant value since the production rates become nearly constant after about 12 years. Of more importance is the greater sensitivity to matrix permeability and fracture spacing as compared to fracture permeability.

Figure 15 shows the rate sensitivity of Match No. 3 to the Klinkenberg factor. The effect is dramatic but not surprising when one considers that gas slippage is likely to be very significant in porous media with permeabilities as low as those used in this study.

Figure 16 shows the rate sensitivity of Match No. 3 to skin factor. All matches were conducted with a constant skin factor of 4.0 to account for possible damage due to water invasion and/or a "stress cage" as a result of the borehole stimulation. As can be seen, skin damage has a dramatic effect during the first two or three years but little effect thereafter. With a constant wellbore pressure, the pressure drop across the damaged zone must decrease as the rate decreases and hence will eventually become very small for low rates, as is the case here.

DISCUSSION

It has been shown that the Kucuk-Sawyer model² will simulate actual Devonian Shale well production performance data for reasonable values of the five basic reservoir parameters:

- Fracture porosity
- Fracture permeability
- Fracture spacing
- Matrix porosity
- Matrix permeability

That the values are indeed reasonable can be seen by comparing the matching parameters (Table 5) with values obtained from Eqs. 1 to 3 which are presented in Table 2. Note, in particular, that the parameters from Match No. 2 agree well with values of fracture porosity and permeability and fracture spacing from Eqs. 1 and 2.

The values of matrix permeability in Table 5 also agree very well with values predicted by Eq. 3 using measured diffusion constants on the Devonian shale. In addition, matrix porosity values used to match production performance are consistent with laboratory values measured on shale samples from an area nearby at about the same depth as Well A.

It should be mentioned that desorption of gas was not used in this study. To obtain a match with a sorption isotherm like or similar to the data presented by Thomas and Frost¹⁵, either fracture spacing would have to be unrealistically large (greater than 2000 cm) and/or matrix permeability would have to be unrealistically low (less than 10^{-10} md or 10^{-13} μm^2). Under these conditions, the adsorbed gas is "locked up" in the matrix and cannot flow into the fracture system enough to make a significant contribution to well productivity. However, in other more thermally mature organic rich areas desorption may play a significant role.

To test the possibility of a single porosity system it was attempted to match the production data from the subject well by running the model in the single porosity mode. A fair match was obtained using an area of 160 acres ($6.47 \times 10^5 \text{ m}^2$) with a porosity and permeability of .00085 and .015 md ($1.5 \times 10^{-5} \mu\text{m}^2$), respectively. However, the match was not as good as any of the dual porosity matches presented and, based on field pressure measurements (no communication with well less than 2000 feet (609.6 m) away), an area of 160 acres ($6.48 \times 10^5 \text{ m}^2$) is too high for Well A.

The major significance of this study is the finding that pressure data at a nearby observation well helps to "zero in" on a set of unique parameters which match actual performance at an active or reference well. However, one qualification needs to be made here. In a previous sensitivity analysis with the active well flowing at a constant rate in an infinite acting reservoir, no additional information could be obtained by using simulated pressures at any distance from the flowing well. Although no field data was used in this previous study, the authors' experience to date would indicate that it may be necessary for the active well to be finite-acting in order for unique pressure behavior to occur at an observation well. However, this is of little concern at this point since many Devonian wells apparently produce from a fairly small drainage area and/or low volume fracture system and hence must necessarily be finite-acting after a short production period. Thus history matching both production and well test data to delineate relationships between the five basic reservoir parameters seems to be a viable tool for many Devonian shale reservoirs.

As an example of how this work could be extended, suppose fissure width could be assumed constant over a particular area. Equation 1 indicates that the same performance should be obtained so long as the product $k_f S$ is constant. In this case, one parameter has been eliminated and the task of matching performance has been simplified. If average fracture spacing can be determined from observations of core material, both k_f and S become known and two parameters have been eliminated.

Najurieta⁹ indicates that reservoir performance is determined by four parameters, each of which is a function of two or more of the five basic reservoir parameters. The relationships given by Najurieta as well as Eqs. 1 to 3 are planned to be studied and used in the numerical model to analyze well test data from additional shale wells. Both interference data as well as data at the active well will be analyzed in an effort to determine relationships between the basic reservoir parameters. The work presented in this report provided the necessary first step in utilizing interference data in that it showed the existence of unique pressures at observation wells for sets of parameters which give essentially the same behavior at the active or reference well.

CONCLUSIONS

The work presented has accomplished several things. First, to some extent it has validated the Kucuk-Sawyer model² in that the model has been shown to accurately simulate the production performance of a Devonian shale well using realistic parameters

based on laboratory data and observations.

Second, the potential has been demonstrated for using interference data in conjunction with data at an active or reference well in order to delineate a "more unique" set of basic reservoir parameters which control gas recovery and productivity from the Devonian shale.

Third, it was found that gas slippage can have a significant effect on gas production from the Devonian shale. Additional laboratory work is needed in order to quantify the magnitude of the Klinkenberg factor for Devonian shales.

Finally, this study has shown evidence that Devonian shale production may occur from relatively small finite-acting reservoirs and that more likely these shales have a dual porosity system. This is based on the fact that a good single porosity match could not be obtained and that a dual porosity match could only be obtained in an area sufficiently small to be finite-acting.

NOMENCLATURE

- A = Area, ft.² (m²)
 b = Klinkenberg factor, psi (kPa)
 C = Concentration, gm/cm³ (kg.m⁻³)
 D = Diffusion constant, cm².sec⁻¹ (m².sec⁻¹)
 k = Permeability, md (μm²)
 p = Pressure, psi (kPa)
 q = Volume flow rate, cm³.sec⁻¹
 Q = Mass flow rate, gm.sec⁻¹
 S = Fracture spacing, cm (m)
 w = Fracture width, cm (m)
 z = Gas deviation factor, dimensionless
 μ = Viscosity, cp (Pa.s)
 ρ = Density, gm/cm³ (kg.cm⁻³)
 φ = Porosity, fraction

(SPE preferred SI units in parenthesis)

Subscripts

- f = Fracture
 m = Matrix

ACKNOWLEDGEMENTS

This work was done in part under contract number: DE-AT21-78MC08216 to DOE/METC.

The authors gratefully acknowledge the aid and encouragement given by Mr. Charles A. Komar, Project Manager of the Eastern Gas Shales Project and Mr. K-H. Frohne, section leader, production technology at the DOE Morgantown Energy Technology Center (METC).

The authors thank the management of Science Applications, Inc., Morgantown for permission to present this paper.

REFERENCES

1. Smith, E. C., Cremean, S. P., and Kozair, G.: "Gas Occurrence in the Devonian Shale", paper SPE 7921 presented at the 1979 SPE Symposium on Low Permeability Gas Reservoirs, Denver, Colorado, May 20-22, 1979.
2. Kucuk, F., and Sawyer, W.: "Modeling of Devonian Shale Gas Reservoir Performance", Proceedings of Third Eastern Gas Shales Symposium, U.S. Department of Energy, Morgantown, West Virginia, October 1-3, 1979.
3. Warren, J. E., and Root, P. J.: "The Behavior of Naturally Fractured Reservoirs", Soc. of Pet. Eng. J. (September, 1963) 245-255; AIME, 228.
4. Kazemi, H.: "Pressure Transient Analysis of Naturally Fractured Reservoirs with Uniform Fracture Distribution", Soc. of Pet. Eng. J. (December, 1969) 451-462; Trans., AIME, 246.
5. Kazemi, H., Seth, M. S., and Thomas, G. W.: "The Interpretation of Interference Tests in Naturally Fractured Reservoirs with Uniform Fracture Distribution", Soc. of Pet. Eng. J. (December, 1969) 463-472; Trans., AIME, 246.
6. Crawford, G. E., Hagedorn, A. R., and Pierce, A. E.: "Analysis of Pressure Buildup Tests in a Naturally Fractured Reservoir", Paper SPE 4558 presented at the 48th Annual Fall Meeting of the Society of Petroleum Engineers of AIME, Las Vegas, Nevada, September 30 - October 3, 1973.
7. DeSwaan, A. O.: "Analytic Solutions for Determining Naturally Fractured Reservoir Properties by Well Testing", Soc. of Pet. Eng. J. (June, 1976) 117-222.
8. Aguilera, R. and vanPoolen, H. K.: "Several Techniques Evaluate Well Test Data", The Oil and Gas Journal (January 22, 1979) 68-73.
9. Najurieta, H. L.: "A Theory for the Pressure Transient Analysis in Naturally Fractured Reservoirs", Paper SPE 6017 presented at the 51st Annual Fall Meeting of the Society of Petroleum Engineers of AIME, New Orleans, Louisiana, October 3-6, 1976.
10. Najurieta, H. L.: "Interference and Pulse Testing in Uniformly Fractured Reservoirs", Paper SPE 8283 presented at the 54th Annual Fall Meeting of the Society of Petroleum Engineers of AIME, Las Vegas, Nevada, September 23-26, 1979.
11. Aziz, K., Mattar, L., Ko, S., and Brar, G. S.: "Use of Pressure, Pressure-Squared or Pseudo-Pressure in the Analysis of Transient Pressure Drawdown Data from Gas Wells", Journal of Canadian Petroleum Technology (April-June, 1976) 58-65.

12. Adams, A. R., Ramey, H. J., and Burgess, R. J.: "Gas Well Testing in Fractured Carbonate Reservoir", J. of Pet. Tech. (October, 1968) 1187-1194.
13. Rose, W. D.: "Permeability and Gas-Slippage Phenomena", Trans., AIME (1948) V. 28, 127-135.
14. Jones, F. O., and Owens, W. W.: "A Laboratory Study of Low Permeability Gas Sands", Paper SPE 7551, presented at SPE Symposium on Low Permeability Gas Reservoirs, Denver, Colorado, May 20-22, 1979.
15. Thomas, J., Jr., and Frost, R. R.: "Internal Surface Area and Porosity in Eastern Gas Shales from the Sorption of Nitrogen, Carbon Dioxide, and Methane", in proceedings of First Eastern Gas Shales Symposium, Morgantown, West Virginia, October 17-19, 1977, (U.S. DOE, MERC/SP-77/5).
16. Muskat, M.: The Flow of Homogeneous Fluids Through Porous Media, McGraw-Hill Book Company, Inc., New York (1937).
17. Kalyoncu, R. S., and Snyder, M. J.: "Characterization and Analysis of Devonian Shales as Related to Release of Gaseous Hydrocarbons". Battelle Laboratory Quarterly report to DOE/METC, (April 19, 1978).
18. Smith, E. C.: "A Practical Approach to Evaluating Shale Hydrocarbon Potential", Preprints for Second Annual Eastern Gas Shales Symposium, U.S. Department of Energy, Morgantown, West Virginia, METC/SP-78/6, Volume II.
19. Zielinski, R. E., and Nance, S. W.: "Physical and Chemical Characterization of Devonian Gas Shale", Mound Facility Quarterly Status Report to DOE/METC, December 31, 1979.
20. Smith, R. O.: "Diffusion Experiments on Cored

Samples of Devonian Shale", Preprints for the Second Eastern Gas Shales Symposium, U.S. Department of Energy, METC/SP-78/6, Volume 1.

APPENDIX

Using the ideal gas law, Equation 3 may be derived from Darcy's Law for fluid flow and Fick's Law of diffusion as shown below. First, we express Darcy's Law in terms of mass flow using fluid density

$$\rho q = - \frac{kA}{\mu} \rho \frac{dp}{dx} \quad (A-1)$$

Then we use the concentration-density relationship

$$C = \phi \rho \quad (A-2)$$

and the ideal gas law

$$\rho = \frac{pM}{RT} \quad (A-3)$$

in Fick's Law

$$Q = - DA \frac{dC}{dx} \quad (A-4)$$

$$\text{to get } Q = - DA \frac{\phi M}{RT} \frac{dp}{dx} \quad (A-5)$$

Combining Equations A-1 and A-5 and using A-3 gives

$$\frac{k}{\mu} = \frac{D\phi}{p} \quad (A-6)$$

which is equivalent to Equation 3 in the text. It should be noted that units are consistent with Equations A-2 in Darcy units, Equation A-3 in cgs units, T in degrees Kelvin and R=82.05 ml-atm/deg-mole. Thus, in Equation A-6 D is in cm²/sec, p is in atmospheres, μ is in cp, and k is in darcys.

Unfortunately, Smith's²⁰ relationship between Darcy permeability and diffusion is erroneous. It appears that Smith²⁰ did not convert the Darcy flow rate to mass flow before comparing with the diffusion equation.

TABLE 1
FRACTURE POROSITY AND PERMEABILITY VALUES
FROM EQUATIONS 1 AND 2

<u>w_f = .001 cm</u>		
<u>S, cm</u>	<u>φ_f</u>	<u>k_f, md (μm²)</u>
30	.000667	.278 (2.74E-04)
100	.000020	.083 (8.19E-05)
300	.000007	.028 (2.76E-05)
1000	.000002	.008 (7.90E-06)
<u>w_f = .002 cm</u>		
30	.000133	2.22 (2.19E-03)
100	.000040	.667 (6.57E-04)
300	.000013	.222 (2.19E-04)
1000	.000004	.067 (6.51E-05)

TABLE 3
GAS PROPERTY DATA

TABLE 2 INITIAL PARAMETER ESTIMATES BASED ON LABORATORY DATA		Pressure, psi (kPa)	z-Factor	Viscosity, cp (Pa.s)
		15 (103)	.998	.0126 (1.26E-05)
Fracture Porosity	.000007	100 (689)	.988	.0127 (1.27E-05)
Fracture Permeability, md (μm ²)	.025 (.025E-03)	200 (1379)	.977	.0127 (1.27E-05)
Fracture Spacing, cm	300 cm	300 (2068)	.960	.0128 (1.28E-05)
Matrix Porosity	.025	400 (2758)	.948	.0129 (1.29E-05)
Matrix Permeability; md (μm ²)	10 ⁻⁸ (10 ⁻¹¹)	500 (3447)	.937	.0129 (1.29E-05)
Klinkenberg Parameter, psi (kPa)	12.64 k ^{-.33} (87.10 k ^{-.33})	600 (4137)	.925	.0130 (1.30E-05)
		700 (4826)	.915	.0131 (1.31E-05)
		800 (5516)	.900	.0131 (1.31E-05)
		900 (6205)	.890	.0132 (1.32E-05)
		1000 (6895)	.880	.0133 (1.33E-05)

TABLE 4
PRODUCTION DATA -- WELL A

<u>Year</u>	<u>Production Rate, MCFD ($M^3 \cdot day^{-1}$)</u>	<u>Cumulative Production, MCF (M^3)</u>
1956	25.9 (7.33E-01)	2,983 (8.447E+01)
1957	22.6 (6.40E-01)	10,633 (3.0109E+02)
1958	18.3 (5.18E-01)	17,254 (4.8858E+02)
1959	15.0 (4.25E-01)	22,396 (6.3418E+02)
1960	12.1 (3.43E-01)	26,425 (7.4827E+02)
1961	10.7 (3.03E-01)	30,264 (8.5698E+02)
1962	10.4 (2.94E-01)	33,662 (9.5320E+02)
1963	9.2 (2.6E-01)	36,895 (1.0448E+03)
1964	9.7 (2.7E-01)	40,301 (1.1412E+03)
1965	8.6 (2.4E-01)	43,409 (1.12292E+03)
1966	8.6 (2.4E-01)	46,450 (1.3153E+03)
1967	7.8 (2.2E-01)	49,256 (1.3948E+03)
1968	8.5 (2.4E-01)	52,321 (1.4816E+03)
1969	8.9 (2.5E-01)	55,515 (1.5720E+03)
1970	6.4 (1.8E-01)	57,828 (1.6375E+03)
1971	4.2 (1.2E-01)	59,329 (1.6800E+03)
1972	4.5 (1.3E-01)	60,938 (1.7256E+03)

TABLE 5
MATCHING PARAMETERS AND OFFSET PRESSURES (96 ft. or 29.3 m)
AT 5060 DAYS

<u>No.</u>	<u>ϕ_f</u>	<u>$k_{f, md} (\mu m^2)$</u>	<u>S, cm</u>	<u>ϕ_m</u>	<u>$k_{m, md} (\mu m^2)$</u>	<u>$P, psi (kPa)$</u>
1	.20E-03	.025 (2.47E-05)	1000	.005	.20E-07 (1.97E-11)	332 (2289)
2	.20E-05	.050 (4.93E-05)	450	.005	.10E-07 (9.9E-12)	293 (2020)
3	.15E-02	.020 (1.97E-05)	500	.015	.25E-08 (2.5E-12)	362 (2496)

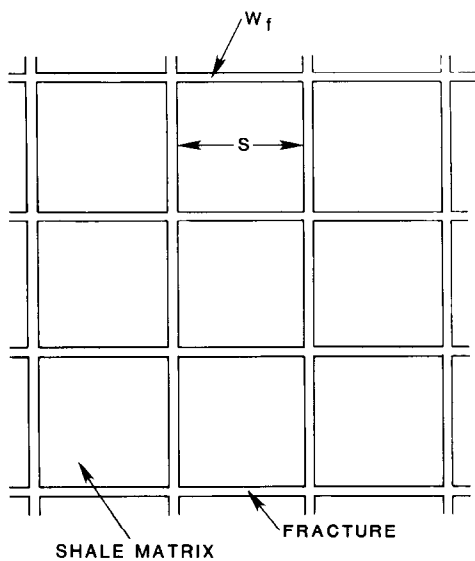


Fig. 1 - Relating fracture width and spacing to bulk fracture porosity.

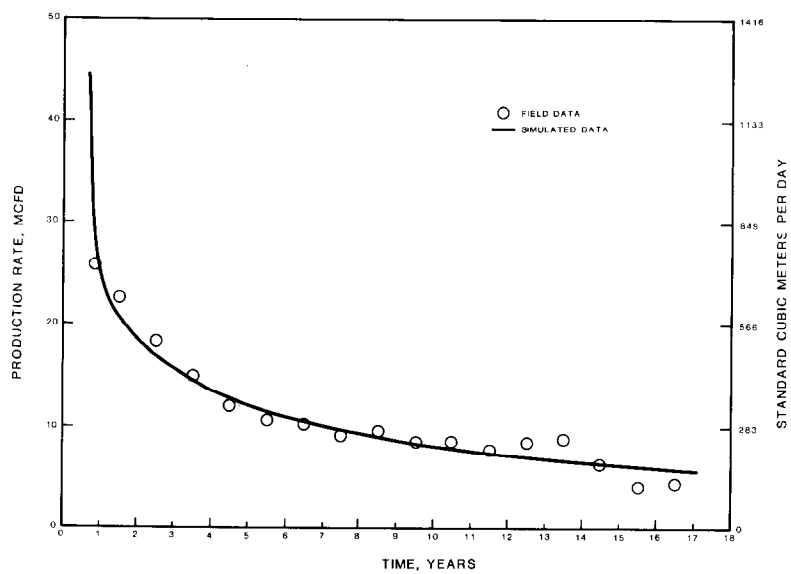


Fig. 2 - Simulated and actual production decline - Match No. 1.

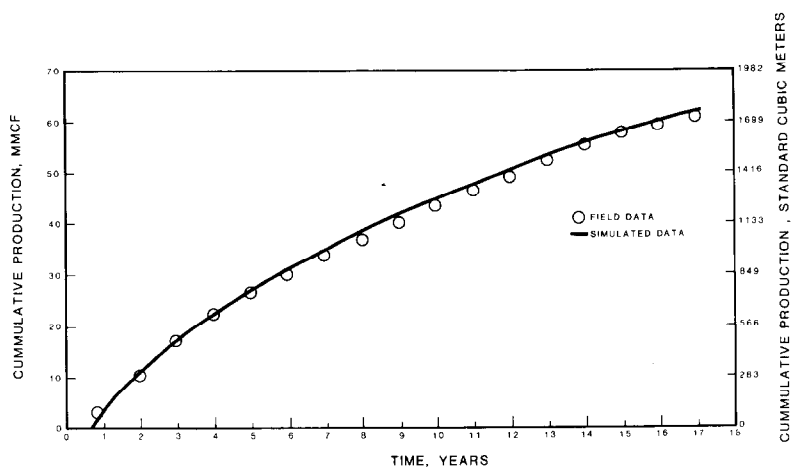


Fig. 3 - Simulated and actual cumulative production - Match No. 1.

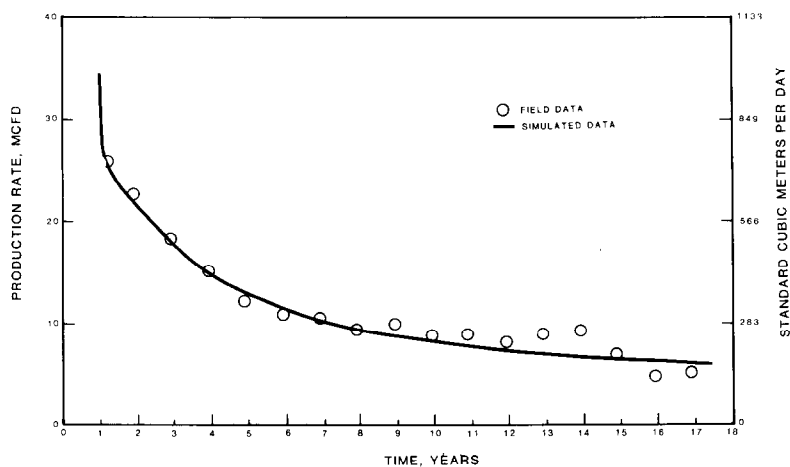


Fig. 4 - Simulated and actual production decline - Match No. 2.

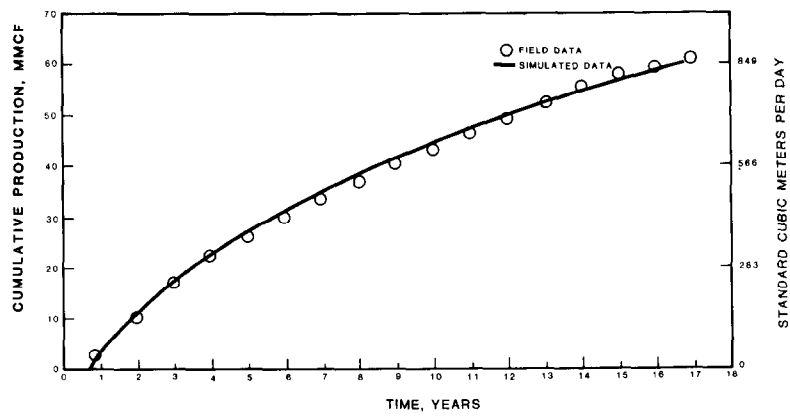


Fig. 5 - Simulated and actual cumulative production - Match No. 2.

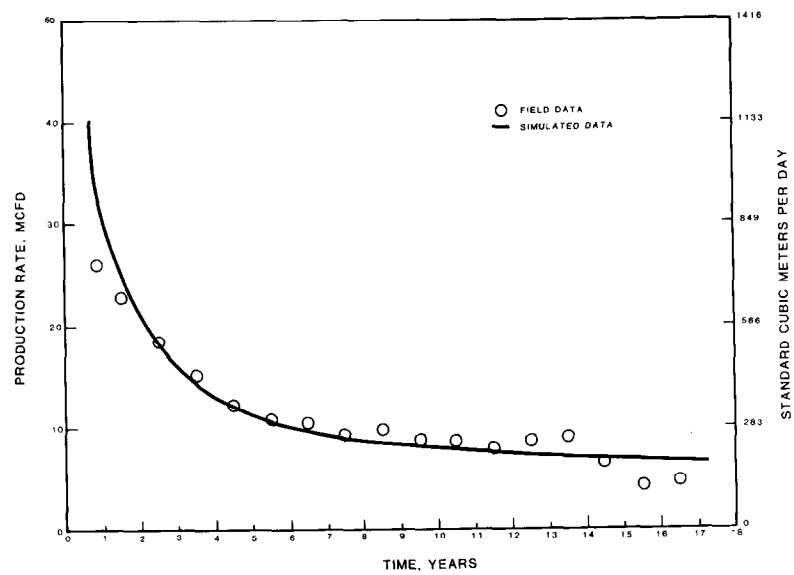


Fig. 6 - Simulated and actual production decline - Match No. 3.

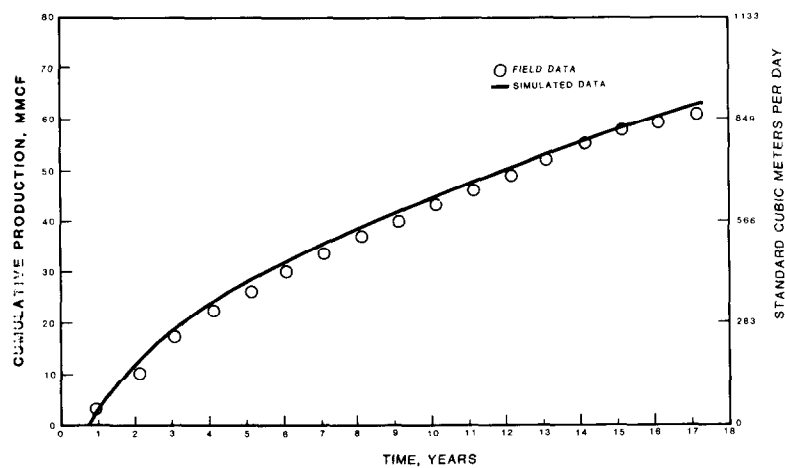


Fig. 7 - Simulated and actual cumulative production - Match No.3.

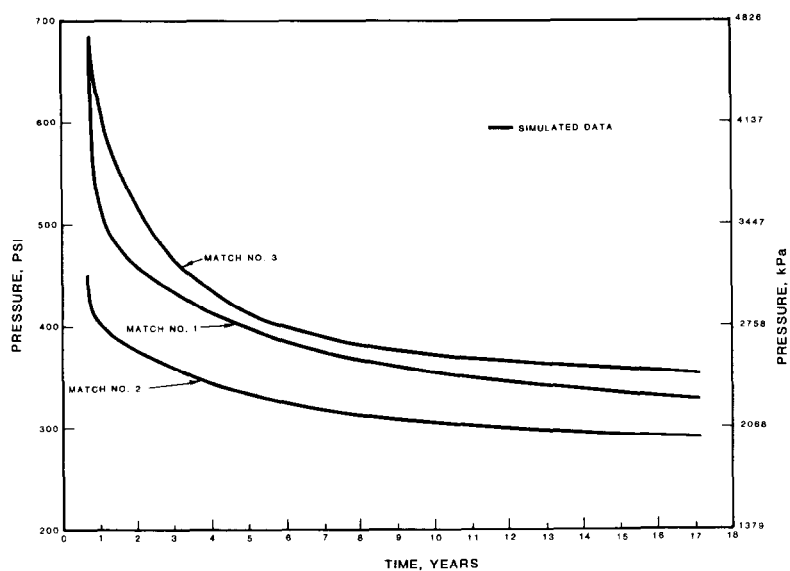


Fig. 8 - Simulated pressure history at offset distance of 96 ft.(29.3m).

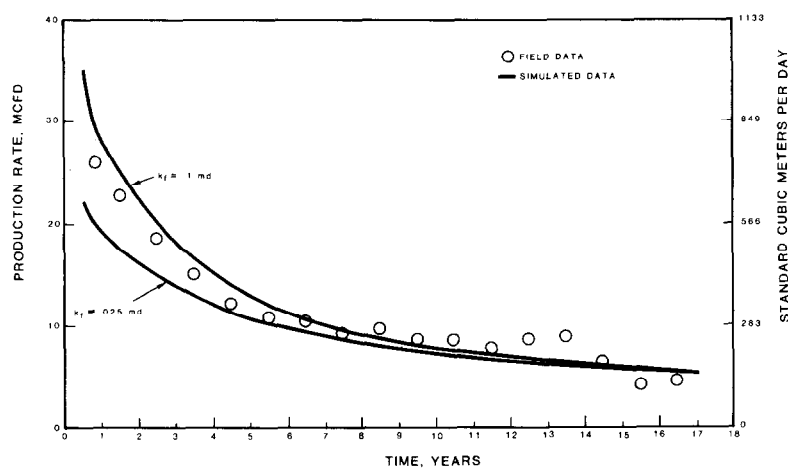


Fig. 9 - Production rate sensitivity to fracture permeability - Match No. 2.

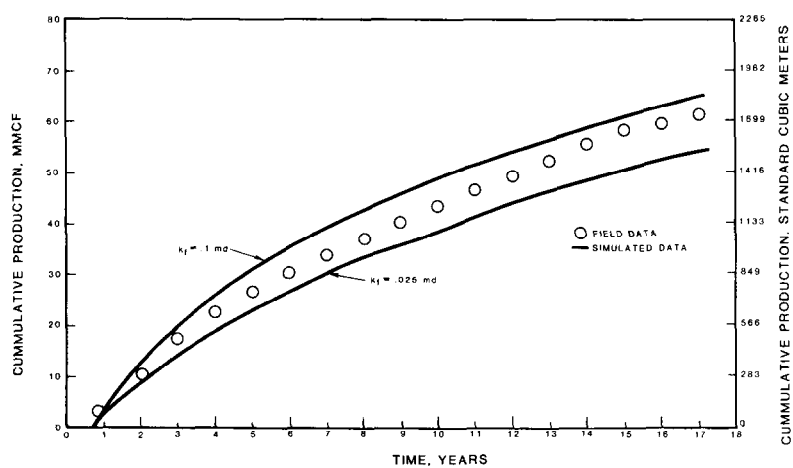


Fig. 10 - Cumulative production sensitivity to fracture permeability - Match No.2.

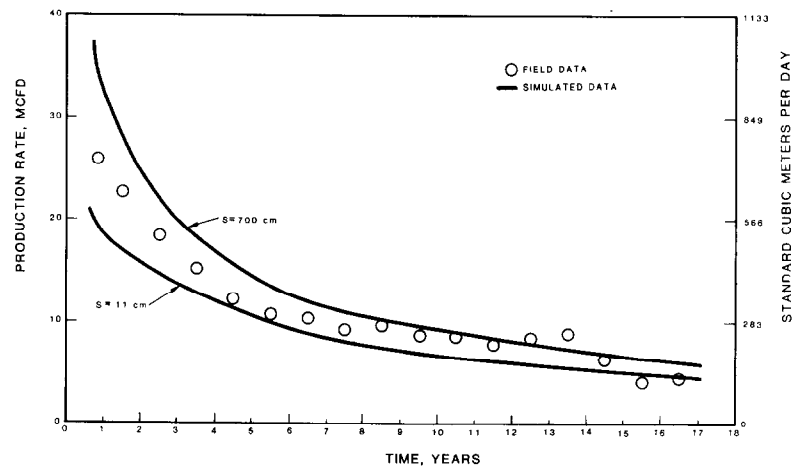


Fig. 11 - Production rate sensitivity to fracture spacing - Match No. 2.

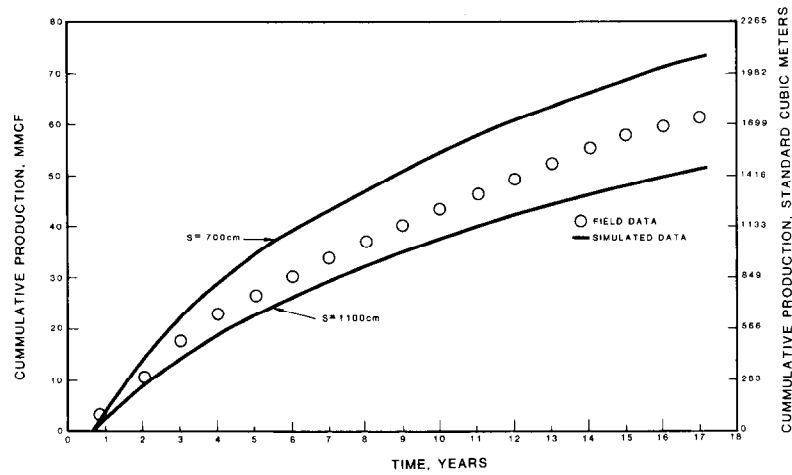


Fig. 12 - Cumulative production sensitivity to fracture spacing - Match No. 2.

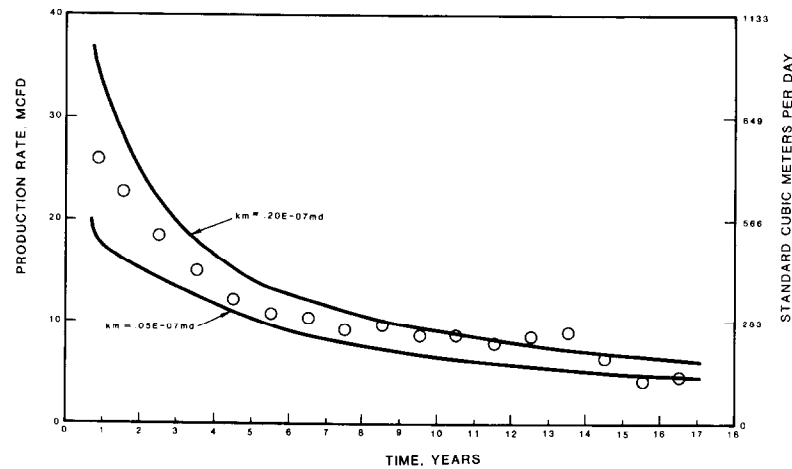


Fig. 13 - Production rate sensitivity to matrix permeability - Match No. 2.

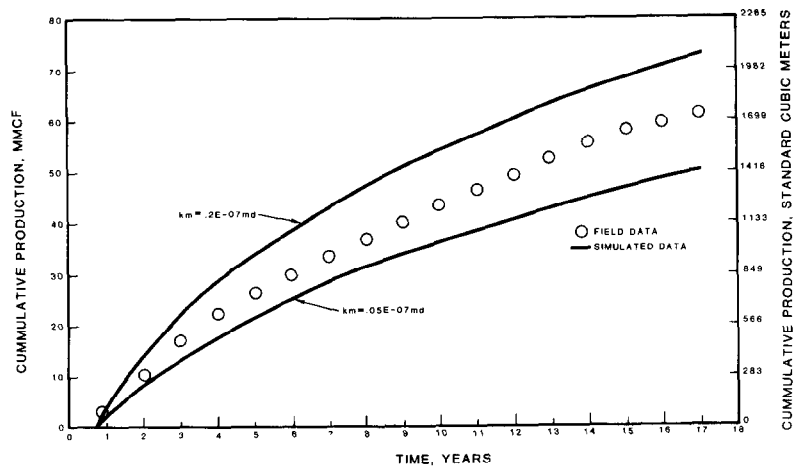


Fig. 14 - Cumulative production sensitivity to matrix permeability - Match No. 2.

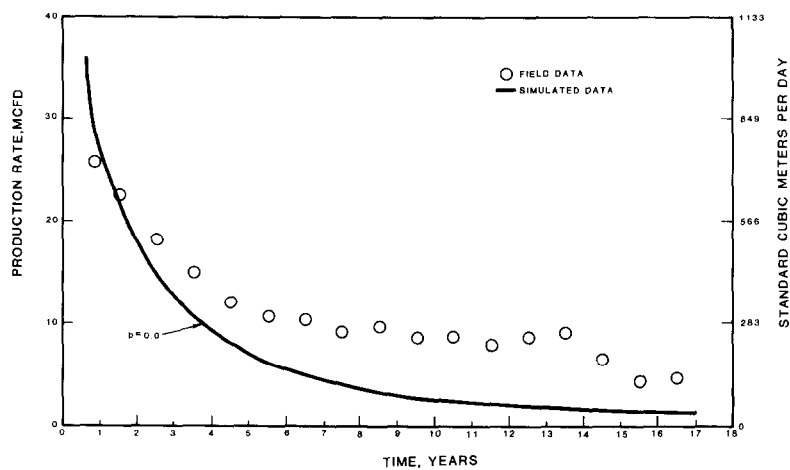


Fig. 15 - Production rate sensitivity to Klinkenberg factor - Match No. 3.

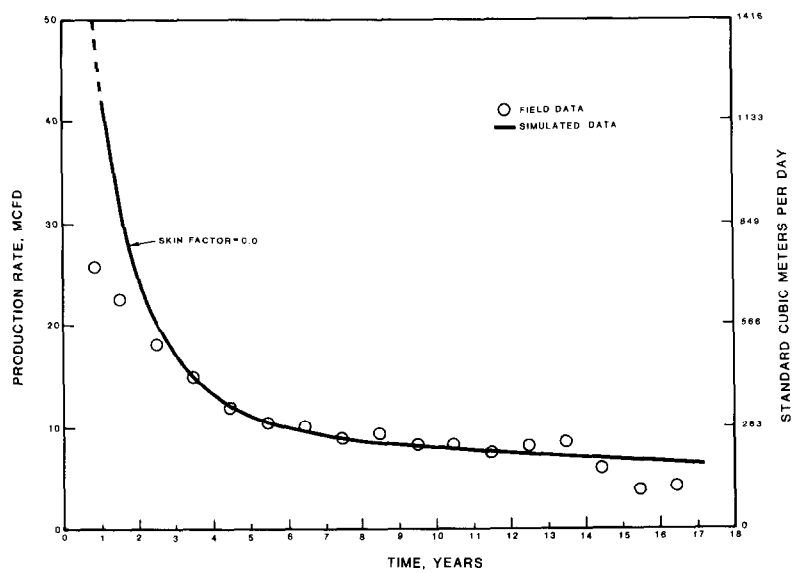


Fig. 16 - Production rate sensitivity to skin factor - Match No. 3.

FINITE ELEMENT MODEL SIMULATIONS ASSOCIATED WITH HYDRAULIC FRACTURING

by Sunder H. Advani, Ohio State University

This paper was presented at the 1980 SPE/DOE Symposium on Unconventional Gas Recovery held in Pittsburgh, Pennsylvania, May 18-21, 1980. The material is subject to correction by the author. Permission to copy is restricted to an abstract of not more than 300 words. Write: 6200 N. Central Expwy., Dallas, Texas 75206

ABSTRACT

Recent emphasis on the recovery of unconventional gas resources has focussed efforts on the development and testing of innovative well stimulation techniques. The design of optimum hydraulic fracturing treatments, for specified reservoir conditions, requires sophisticated models for predicting the induced fracture geometry and interpreting governing mechanisms.

This paper presents methodology and results pertinent to hydraulic fracture modeling for the Eastern Gas Shales Program (EGSP). The presented finite element model simulations extend available modeling efforts and provide a unified framework for evaluation of fracture dimensions and associated responses. Examples illustrating the role of multi-layering, in situ stress, joint interaction, and branched cracks are given. Selected comparisons and applications are also discussed.

INTRODUCTION

The selection and design of stimulation treatments for Devonian shale wells has received considerable attention in recent years^{1,2,3}. The production of natural gas from such tight Eastern petroliferous basins is dependent on the vertical thickness of the organically rich shale matrix, its inherent fracture system density, anisotropy, and extent, and the communication link characteristics of the induced fracture system(s). The investigation of stimulation techniques based on resource characterization, reservoir property evaluation, theoretical and laboratory model simulations, and field testing is a logical step toward the development of commercial technology for optimizing gas production and related costs.

This paper reports the formulations, methodology, and results associated with analytical simulations of hydraulic fracturing for the Eastern Gas Shales Project (EGSP). The presented model extends

work reported by Perkins and Kern⁴, Nordgren⁵, Geertsma and DeKlerk⁶, and Geertsma and Haafkens⁷. The simulations provide a finite element model framework for studying vertical induced fracture responses with the effects of multi-layering and in situ stress considered. In this context, recent studies addressing specific aspects of this problem are due to Brechtel et al⁸, Daneshy⁹, Cleary¹⁰, and Andersen et al¹¹. The use of finite element model techniques for studying mixed-mode fracture problems encountered in dendritic fracturing and vertical fracture-joint interaction is also illustrated here along with the application of suitable failure criteria.

VERTICAL HYDRAULIC FRACTURE MODEL FORMULATIONS

Coupled structural, fracture mechanics, and frac fluid response models for predicting hydraulically induced fracture responses have been previously reported^{12, 13}. These simulations incorporate specified reservoir properties, in situ stress conditions, and stimulation treatment parameters. A shortcoming of this modeling effort is that finite element techniques are utilized for the structural and stress intensity simulations while a finite difference approach is employed for evaluating the leak-off and frac fluid response in the vertical crack. A consistent framework for conducting all simulations using finite element modeling is formulated here.

The steady state and transient fracture width response, governed by the frac fluid variables, multilayering, and minimum effective horizontal in situ stress, is initially determined by combining the formulations and solutions presented by Geertsma and Haafkens⁷ and Advani et al¹². The plane strain vertical crack model is illustrated in Figure 1 with fluid coupling provided by the crack interface pressure. The one dimensional fluid flow conservation of mass equation, as applied by Nordgren⁵ on the basis of the Perkins and Kern model⁴, for an isotropic porous-permeable elastic medium is

$$\frac{E}{128(1-\nu^2)} \frac{\partial^2 w^4}{\partial x^2} - \frac{\partial w}{\partial t} = \frac{8C}{\pi \sqrt{t-\tau}(x)} \quad (1)$$

References and illustrations at end of paper.

along with the initial condition $W(x,0) = 0$ and the boundary conditions

$$W(x,t) = 0 \text{ for } x > L(t)$$

and

$$-\left(\frac{\partial W^4}{\partial x}\right)_{x=0} = \frac{256\mu(1-\nu^2)Q}{\pi E}$$

for a two sided fracture.

The steady state solution and finite difference results for the transient problem in Equation (1) have been presented by Nordgren⁵ and Geertsma and Haafkens⁷. The discretized finite element weak form of the extended version of the width equation (1), obtained by using the Galerkin procedure, is

$$K_{ij}(a) \dot{a}^j(t) + C_{ij} \dot{a}^j(t) + F_i(t) = 0 \quad (2)$$

where

$$K_{ij}(a) = \frac{E}{32(1-\nu^2)(2H)\mu} \int N_{i,x}^T (N_k a^k)^3 N_{j,x} dx$$

$$C_{ij} = \int N_i^T N_j dx$$

$$F_i(t) = \frac{8C}{\pi} \int \frac{N_i}{\sqrt{t-\tau(x)}} dx$$

where N_i is the selected interpolation function associated with the i -th node defined by

$$W(x,t) \approx N_i(x) a^i(t)$$

and commas designate differentiation.

For the steady state problem, the appropriate equation is

$$K_{ij}(a) a^j + F_i(t) = 0 \quad (3)$$

with

$$K_{ij} = \frac{E}{128(1-\nu^2)(2H)\mu} \int N_{i,x}^T N_{j,x} dx$$

$$F_i = \frac{8C}{\pi} \int \frac{N_i}{\sqrt{t-\tau(x)}} dx$$

where N_i is defined by

$$W^4(x,t) \approx N_i(x) a^i(t)$$

Equation (3) is the familiar linear stiffness-force matrix formulation. On the other hand, the non-linearity inherent in the stiffness matrix for Equation (2) requires the solution of a non-linear set of algebraic equations. The isotropic medium steady state and transient width profiles are modified for the multi-layered geometry by introducing the width scaling coefficient¹³. Subsequent cumulative leak-off computations are based on the width response. The fracture height and length evaluations require determination of the vertical crack stress intensity factor and application of the percentage leak-off volume¹².

VERTICAL HYDRAULIC FRACTURE MODEL SIMULATIONS

The steady state and transient width profile evaluations with the shape functions defined by

$$N_1(x) = (1-x)/2, \quad N_2(x) = (1+x)/2$$

require computations entailing the discretized matrix form of Equations (3) and (2) respectively.

For the steady state case, the width profile is obtained without difficulty for specified parameters. Figures 2a and 2b compared the steady state finite element width and pressure profiles with the "exact" Perkins and Kern⁴ solution outlined by Geerstma and Haafkens⁷. The selected parameters are:

Pump rate $Q = 10$ bbl/min ($1.6\text{m}^3/\text{min}$),
Total Injected Volume $V = 2000$ bbl (318m^3),
Fracture Height $2H = 100$ ft (30.48m),
Fluid Loss Coefficient $C = 0.0015$ ft/min^{1/2},
($0.00046\text{m}/\text{min}^{1/2}$), Ratio $\nu = 0.20$, Shear
Modulus $G = E/2(1+\nu) = 2.6 \times 10^6$ psi (17.94 GPa).

Discrete algorithms are developed for the transient case with the non-linear system of Equations (3) considered at time intervals (t_n, t_{n+1}). The resulting non-linear algebraic equations are solved by the Newton-Raphson method. For each time interval, the time rate of change of the width vector is approximated by

$$\dot{a}^* = (a_{n+1} - a_n)/\Delta t \quad (4)$$

at a specified time t^* defined by

$$t^* = (1-\xi)t_n + \xi t_{n+1}, \quad \xi \in [0,1]$$

Also, a corresponding linearized form of the width vector is assumed, namely

$$\tilde{a}^* = (1-\xi)a_n + \xi a_{n+1} \quad (5)$$

Substitution of Equations (4) and (5) into (3) yields

$$[K(\tilde{a}^*) + \frac{1}{\xi \Delta t} C] \tilde{a}^* + [F - \frac{1}{\xi \Delta t} (Ca_n)] = 0 \quad (6)$$

The suitable application of the Newton-Raphson solution technique, following a curtailed Taylor series expansion, does not require iterations within a time step since all the quantities are evaluated only at the onset of the time step. These ongoing computations indicate that the transient width and percentage leak-off response approach the steady state case.

The extension of the preceding simulations of the width profile to the case of a multi-layered formation with different in situ stresses on the layers necessitates development of scaling curves. These curves incorporate the layer elastic moduli ratio, vertical fracture penetration, and in situ stress differential across the layers. Figures 3a and 3b reveal the developed fracture width scaling curves obtained from finite element simulations of the plane strain model (Figure 1). The determined isotropic width magnitudes can be converted to the layered case by multiplication with the appropriate scale factor. The corresponding fracture height is obtained by computing the stress intensity factors associated with the frac fluid pressure and tectonic

loading (Figures 4a and 4b)¹². Figure 5 illustrates typical effective pressure versus fracture height penetration curve deduced from Figures 4a, 4b for a specified ratio of E_2/E_1 . With the fracture width, height, and percentage leak-off determined, the time dependent fracture length can be computed using an iterative volume balance for the frac fluid. The evaluated fracture width and length, employing the finite difference frac fluid simulations and finite element structural modeling¹³, compare favorably with the results obtained by Geertsma and DeKlerk⁶, Perkins and Kern⁴, and Nordgren⁵. Good agreement between the frac fluid response using the previously developed finite difference and presented finite element simulations is similarly obtained.

MIXED MODE HYDRAULIC FRACTURE MODEL SIMULATIONS

Relatively few investigations have been conducted on mixed mode fracture propagation in hydraulic fracture applications since a single vertical fracture is generally considered in the analysis. However, simulations associated with dendritic fracturing or vertical crack-interface joint interaction entail mixed mode conditions.

The principal novelty in dendritic fracturing is the procedure of stopping the injection of frac fluid and subsequently relieving the fluid pressure by allowing the fluid to flow back¹⁴. It is rationalized that more fractures are created, that there is a tendency for branching fracture, and that spalling of the formation is induced. Predictive calculations for spalling depths for specified minimum horizontal stress, tensile strength, pore pressure, and injection pressure have been reported¹³. Figure 6 illustrates the selected dendritic fracture model with a primary fracture and secondary crack subjected to in situ and pressure loading. Stress intensities and stress contours, using the finite element method, are obtained for this model under frac fluid pressure, minimum horizontal stress, and maximum horizontal stress loadings. Table I illustrates the computed stress intensity factors for these loadings with $c/b = 0, 0.25, 0.50, 0.75$ and 1.00 . The magnitude of the normalized mode II stress intensity factor contributes significantly to the secondary crack propagation. For example, it can be demonstrated that the quantity $K_{eff} = [(K_I^b)^2 + (K_{II}^b)^2]^{1/2}$ exceeds K_{IC} for $0 \leq c/b \leq 0.075$ with $S_y/P = 2$, and $S_x/P = 1$. Various mixed mode fracture propagation criteria are discussed in the subsequent text. Stress contours, resulting from frac fluid pressure loading, are typically illustrated in Figures 7a and 7b.

Another example of mixed mode conditions results from the interaction of the induced vertical fracture with a joint. Figure 8 illustrates a vertical crack intersecting with a horizontal joint at the bi-material interface. The shear tractions at the joint interface coupled with the interaction of frac fluid pressure and tectonic stress can produce conditions favorable to crack propagation at the joint tip. For the case of the joint subjected solely to a uniform shear stress τ , the computed values of $K_I/\tau\sqrt{a}$ and $K_{II}/\tau\sqrt{a}$ at the joint tip are -0.198 and 0.593 . These values when superposed with the in situ and frac fluid pressure stress intensity response can induce joint tip fracture propagation under mixed mode conditions.

Several mixed mode fracture initiation criteria

are available in the literature. Ingraffea¹⁵ has presented a comparison of the maximum hoop tensile stress¹⁶, minimum strain energy density¹⁷, and the maximum energy release rate theories¹⁸. In addition, a fracture criterion for rock media with the effects of crack closure and frictional effects has been recently developed by Advani and Lee¹⁹. These criteria are reviewed below

(i) Maximum Tensile Hoop Stress Theory

In this theory fracture envelope is governed by

$$\cos \frac{\theta}{2} \left[\frac{K_I}{K_{IC}} \cos^2 \theta - \frac{3}{2} \frac{K_{II}}{K_{IC}} \sin \theta \right] = 1 \quad (7a)$$

where the fracture angle θ is governed by

$$K_I \sin \theta + K_{II} (3 \cos \theta - 1) = 0 \quad (7b)$$

(ii) Minimum Strain Energy Density Theory

Fracture initiation for this theory with $\nu = 0.2$ is governed by

$$\begin{aligned} & K_I (2.2 - \cos \theta) (1 + \cos \theta) \\ & + 4 K_I K_{II} \sin \theta (\cos \theta - 0.6) \\ & + K_I^2 [3.2 (1 - \cos \theta) \\ & + (1 + \cos \theta) (3 \cos \theta - 1)] = 2.4 K_{IC}^2 \end{aligned} \quad (8a)$$

with

$$\begin{aligned} & K_I^2 \sin \theta (2 \cos \theta - 1.2) + 4 K_I K_{II} (\cos 2\theta - 0.6 \cos \theta) \\ & + K_{II}^2 (1.2 - 6 \cos \theta) \sin \theta = 0 \end{aligned} \quad (8b)$$

(iii) Maximum Strain Energy Release Rate

The fracture locus for this theory is defined by

$$\left(\frac{K_I}{K_{IC}} \right)^4 + 6 \left(\frac{K_I}{K_{IC}} \right)^2 \left(\frac{K_{II}}{K_{IC}} \right)^2 + \left(\frac{K_{II}}{K_{IC}} \right)^4 = 1 \quad (9)$$

(iv) Crack Closure and Frictional Effects Theory

This theory, based on the maximum circumferential stress, includes the effects of crack closure and frictional effects. The failure threshold is defined by

$$\left(\frac{K_{II}}{2K_{IC}} \right)^2 + \left(\frac{K_I}{K_{IC}} \right) = 1 \quad (10)$$

Reasonable correlation of this theory with available experimental data for rock media has been obtained.

Figure 9 reveals the variation between the theories defined by Equations 7, 8, 9 and 10. The selection of a specific theory, say for Devonian shale or Pittsburgh coal, requires controlled mixed mode experiments. Its subsequent application to dendritic fracturing or joint interaction provides rationale and guidelines for field experiments.

MODEL APPLICATIONS AND DISCUSSION

Fracture geometry predictions for several hydraulic fracture experiments are being conducted using the presented vertical fracture finite element model simulations. Computations on selected Columbia Gas Co. experiments²⁰ in Lincoln County, West Virginia have been performed for the stimulated zones associated with Well #20401, 20402, 20403. In addition, criteria for vertical containment of the fracture in the desired pay zone have been developed in terms of the local effective bottom hole treatment pressure.

We consider here the example of foam fracturing of Well #20403 in the interval 3851 to 4031 ft (1174 to 1229 m). The computed in situ stress are $\sigma_{OVBD} = 3590$ psi (24.77 MPa), $\sigma_{HMIN} = 1589$ psi (10.96 MPa), and $\sigma_{HMAX} = 2528$ psi (17.44 MPa). The following data is assumed:

Foam quality 0.80, adjusted flow rate of 38 BPM (6.08 m³/min), treatment time of 150 min, effective pressure of 341 psi (2.35 MPa), shear modulus $G = 2.0 \times 10^{10}$ psi (13.8 GPa), Poisson's ratio $\nu = 0.2$, and a fluid loss coefficient of 0.0001 ft/ $\sqrt{\text{sec}}$ (0.0003 m/ $\sqrt{\text{sec}}$ on the basis of reservoir permeability, foam compressibility, and viscosity).

Available data on the differential in situ stress across the formation layers²⁰ yields a fracture height of 320 ft (55.72 m). The computed fracture width and resulting fracture length for this massive hydraulic fracture treatment are 0.28 in (0.007 m) and 2025 ft (617.4 m).

The mixed mode fracture simulations suggest the effectiveness of dendritic fracturing for reservoirs with a large number of secondary fracture, joint systems, and/or relatively isotropic horizontal stress fields for enhancing secondary crack/joint propagation. In this context, the potential of dendritic fracturing for methane recovery from bituminous coal beds appears attractive in view of orthogonal butt cleat-face cleat - bedding plane fracture systems. Spalling of the fractured coal for enhancement of proppant characteristics does not appear to be a significant factor. Vertical migration of the fracture in the overburden can be possibly minimized by discrete control of the treatment pressure and/or alteration of the local effective minimum horizontal stress by means of successive pressure draw downs followed by fracture propagation in stages.

CONCLUSIONS

The theoretical simulations of the induced crack opening mode and mixed mode fracture propagation responses provide interpretive and quantitative information on the governing hydraulic fracture mechanisms and geometry. Several characteristics for the assignment of conventional, foam, or dendritic fracture treatments for specific reservoir properties have recently emerged^{13,20,21}. These factors include the consideration of fracture density and extent, shale thickness, in situ stress gradient, energy assist mechanisms, well clean-up, shale-frac fluid interaction, proppant selection, and fracture height control. Preliminary results indicate that correlations with the prevailing in situ stress index are promising diagnostic indicators for fracture treatment selection and design. The comprehensive develop-

ment of an economical strategy, however, requires extensive and controlled field testing with supporting comparative and predictive analyses on reservoirs exhibiting extreme ranges of the significant variables.

NOMENCLATURE

a^i	Width vector component
C	Fluid loss coefficient
C_{ij}	Transient width coefficient
E	Elastic modulus
$F_i(t)$	Leak-off forcing function
G	Shear modulus
h	Half pay zone height
H	Half fracture height
K_I, K_{II}	Mode I and II stress intensity factors respectively
K_{IC}	Critical Mode I stress intensity factor
K_{ij}	Stiffness matrix
L	Fracture length
N_i	Interpolation function
Δp	Effective pressure
S_x, S_y	Horizontal in situ stresses
Q	Injection rate
W	Fracture width
t	Time
x	Co-ordinate in direction of fracture propagation
$\Delta\sigma$	Horizontal in situ stress differential
ν	Poisson's ratio
μ	Fluid viscosity
$\tau(x)$	Fluid loss delay time
τ	Joint shear stress

ACKNOWLEDGEMENT

The support of the U.S. Department of Energy under Contract No. DE-AC 21-79 MC10514 is gratefully acknowledged.

REFERENCES

1. Komar, C.A.: "Development of a Rationale for Stimulation Design in the Devonian Shale", SPE Paper No. 7166, 1978.
2. Cremean, S.P.: "Novel Fracturing Treatments in the Devonian Shale", MERC/SP-77/5, pp. 288-308.
3. McKetta, S.F.: "Investigation of Hydraulic Fracturing Technology in the Devonian Shale", MERC/SP - 78/6, Vol I, pp. 25-34.
4. Perkins, T.K. and Kern, L.R.: "Widths of Hydraulic Fractures", Journal of Petroleum Technology, 1961, pp. 937-949.
5. Nordgren, R.P.: "Propagation of a Vertical Hydraulic Fracture", Society of Petroleum Engineers Journal, V. 253, 1972, pp. 306-314.
6. Geertsma, J., and DeKlerk, F.: "A Rapid Method of Predicting Width and Extent of Hydraulic Induced Fractures", Journal of Petroleum Technology, 1969, pp. 1571-1581.
7. Geertsma, J., and Haafkens, R.: "A Comparison of the Theories for Predicting Width and Extent of Vertical Hydraulically Induced Fractures", Journal of Energy Resources Technology, V. 101, 1979, pp. 8-19.

- | | |
|--|---|
| <p>8. Brechtel, C., Abou-Sayed, A., and Clifton, R.J.: "In Situ Stress Determination in the Devonian Shales (IRA McCOY 20402) within the Rome Basin", Terra Tek Report TR 76-36, July 1976.</p> <p>9. Daneshy, A.A.: "Hydraulic Fracture Propagation in Layered Formations", SPE Paper No. 6088, 1976.</p> <p>10. Cleary, M.P.: "Primary Fractures Governing Hydraulic Fractures in Heterogeneous Stratified Porous Formations", ASME Paper No 78-PET-47, 1978.</p> <p>11. Andersen, G.D., Hanson, M.E., Shaffer, R.J.: "Theoretical and Experimental Analyses of Hydraulic Fracturing", METC/SP-79/6, pp. 225-246.</p> <p>12. Advani, S.H. et al: "Hydraulic Fracture Modeling for the Eastern Gas Shale Project", METC/SP-78/6, pp. 84-98.</p> <p>13. Advani, S.H. et al: "Rock Mechanics Aspects of Hydraulic Fracturing in the Devonian Shale", In Press, Proceedings 21st U.S. National Symposium on Rock Mechanics, 1980.</p> <p>14. Kiel, O.M.: "Hydraulic Fracturing Process Using Reverse Flow", U.S. Patent #3,933,205, 1976.</p> <p>15. Ingraffea, A.R.: "On Discrete Fracture Propagation in Rock Loaded in Compression", Proceedings First Internal Conference on Numerical Methods</p> | <p>in Fracture Mechanics, Editors Luxmoore, A.R. and Owen, D.R.J., pp. 235-248, 1978.</p> <p>16. Erdogan, F., and Sih, G.C.: "On the Crack Extension in Plates Under in Plane Loading and Transverse Shear", Journal of Basic Engineering, V 85, 1963, pp. 519-527.</p> <p>17. Sih, G.C.: "Strain-Energy-Density Factor Applied to Mixed Mode Crack Problems", International Journal of Fracture Mechanics, V 10, 1974, pp. 305-321.</p> <p>18. Hellen, T.K., and Blackburn, W.S.: "The Calculation of Stress Intensity Factors for Combined Tensile and Shear Loading", International Journal of Fracture Mechanics, VII, 1975, pp. 605-617.</p> <p>19. Advani, S.H., and Lee, K.Y.: "Thermo-Mechanical Failure Criteria for Rock Media", Proceedings 20th U.S. Symposium on Rock Mechanics, 1979, pp. 19-25.</p> <p>20. Cremean, S. et al: "Massive Hydraulic Fracturing Experiments of the Devonian Shale in Lincoln County, West Virginia", Final Report Columbia/DOE Contract E (46-1) - 8014, January 1979.</p> <p>21. Komar, C.A., Yost, A.B., and Sinclair, A.R.: "Practical Aspects of Foam Fracturing in the Devonian Shale", SPE Paper No. 8345, 1979.</p> |
|--|---|

TABLE 1

Estimates Stress Intensity Factors for Dendritic Fracture Model

c/b	0.00			0.25			0.50			0.75			1.00		
Loading	P	S_x	S_y	P	S_x	S_y	P	S_x	S_y	P	S_x	S_y	P	S_x	S_y
$K_I^b/[P, S_x, S_y]\sqrt{a}$	0.762	-0.460	-0.320	0.730	-0.465	-0.280	0.672	-0.473	-0.217	0.590	-0.483	-0.120	0.489	-0.488	-0.021
$K_{II}^b/[P, S_x, S_y]\sqrt{a}$	-0.510	-0.030	0.547	-0.592	-0.040	0.630	-0.472	-0.026	0.500	-0.300	-0.0130	0.360	-0.248	-0.025	0.257
$K_I^e/[P, S_x, S_y]\sqrt{a}$	-	-	-	1.025	0.210	-1.310	1.471	0.193	-1.681	1.710	0.150	-1.874	1.839	0.107	-1.966

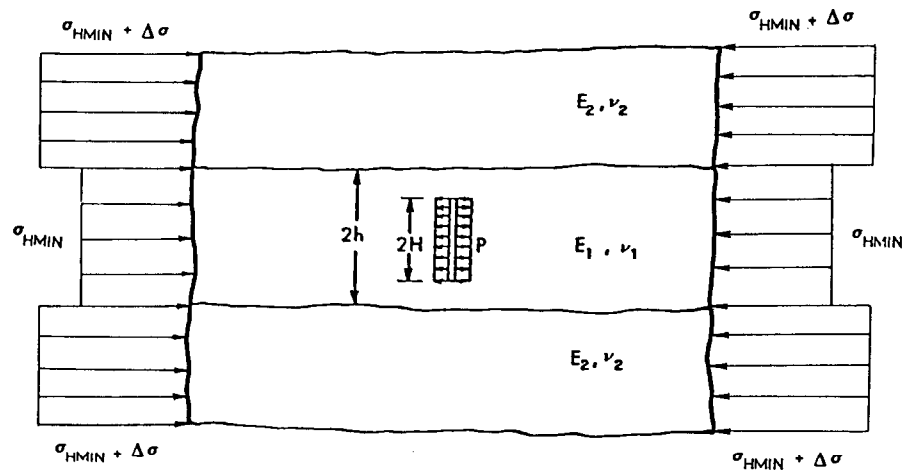


Fig. 1 - Plane strain model idealization of vertical crack model.

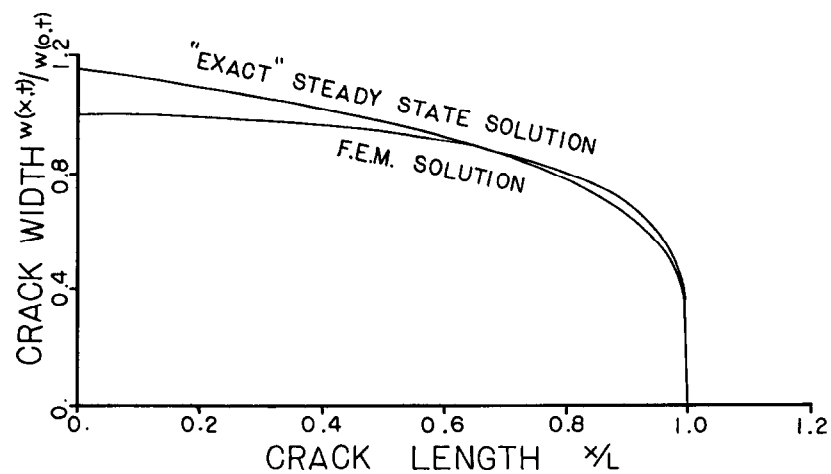


Fig. 2a - Comparison of steady state width profiles.

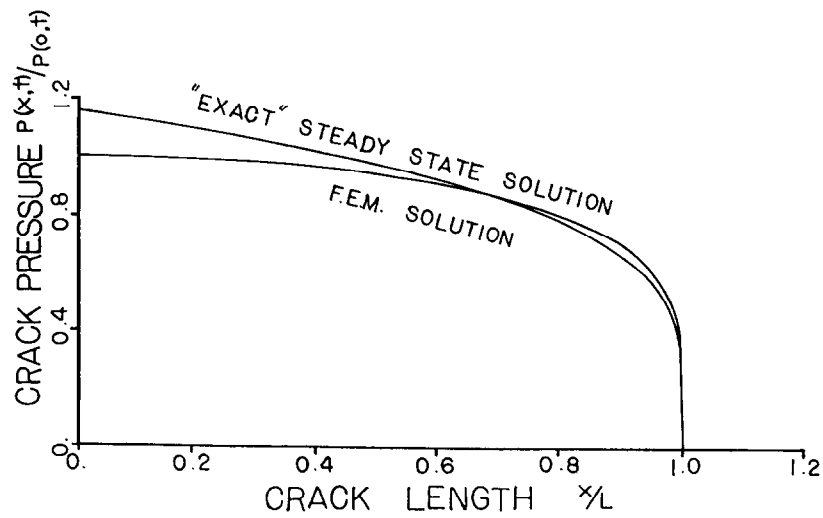


Fig. 2b - Comparison of steady state pressure profiles.

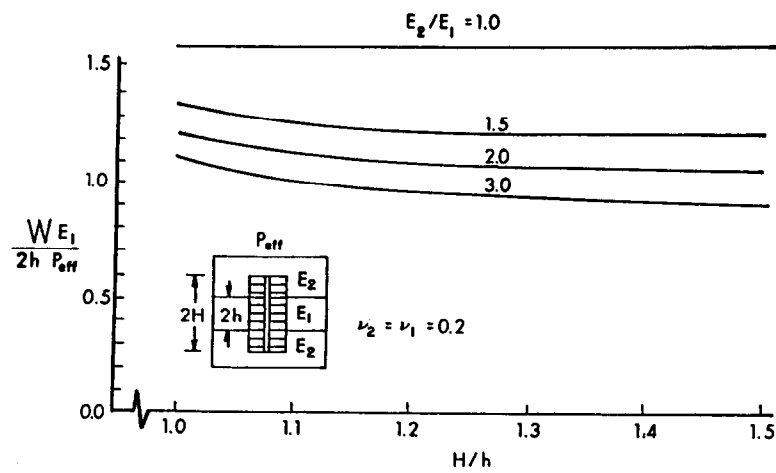


Fig. 3a - Fracture width plots for induced pressures.

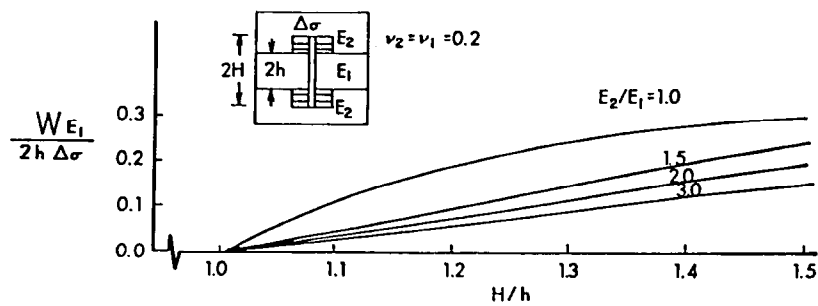


Fig. 3b - Fracture width plots for in situ stress differentials.

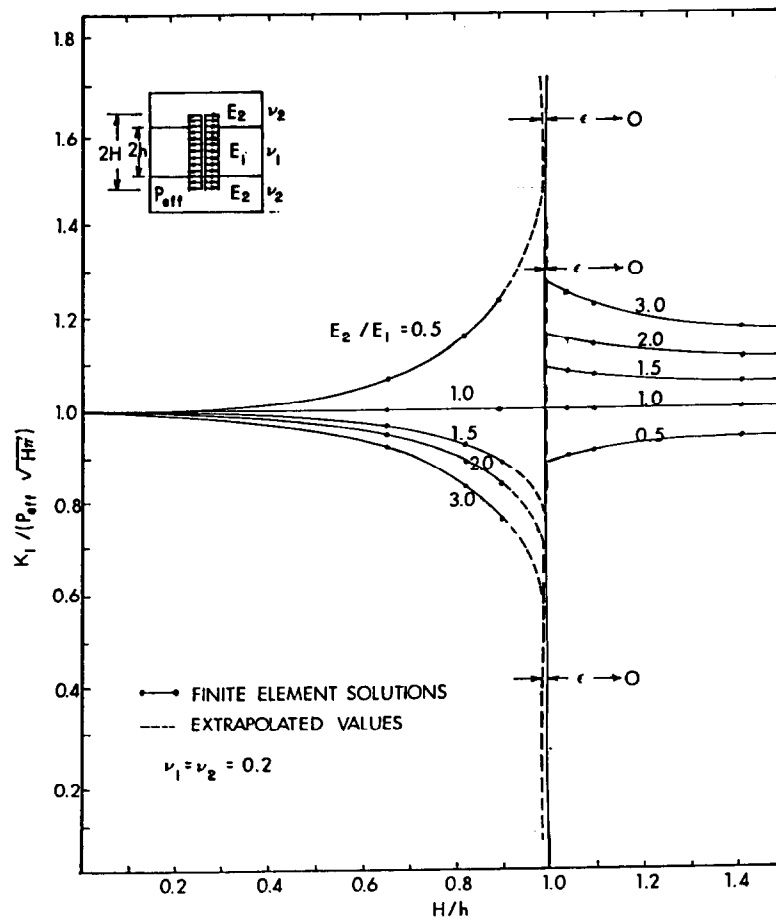


Fig. 4a - Stress intensity factor plots for induced pressures.

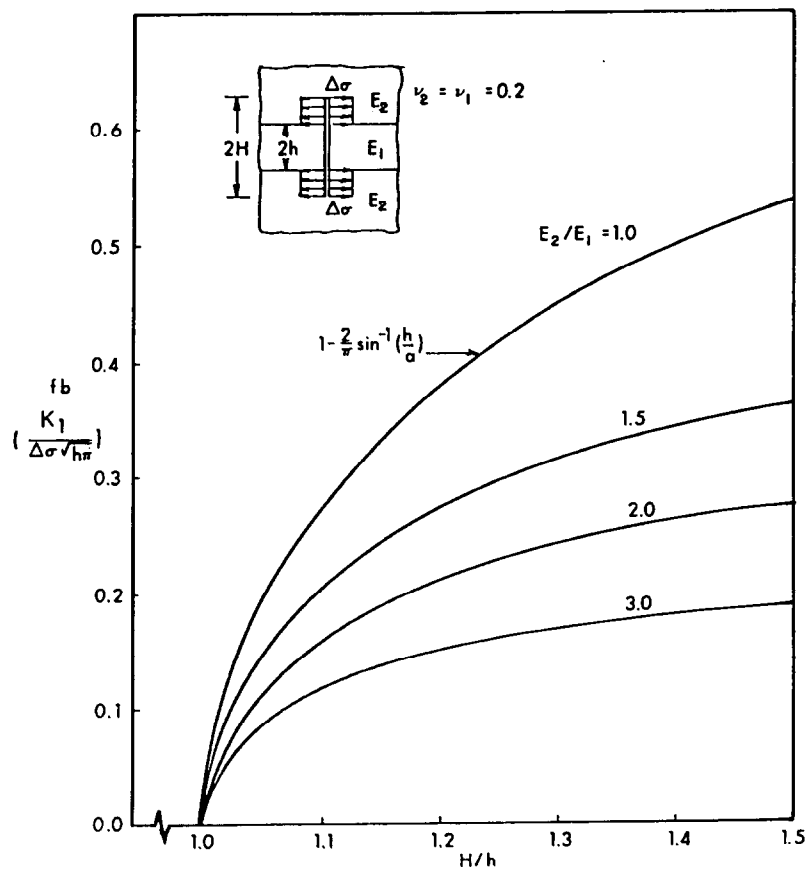


Fig. 4b - Stress intensity plots for in situ stress differentials.

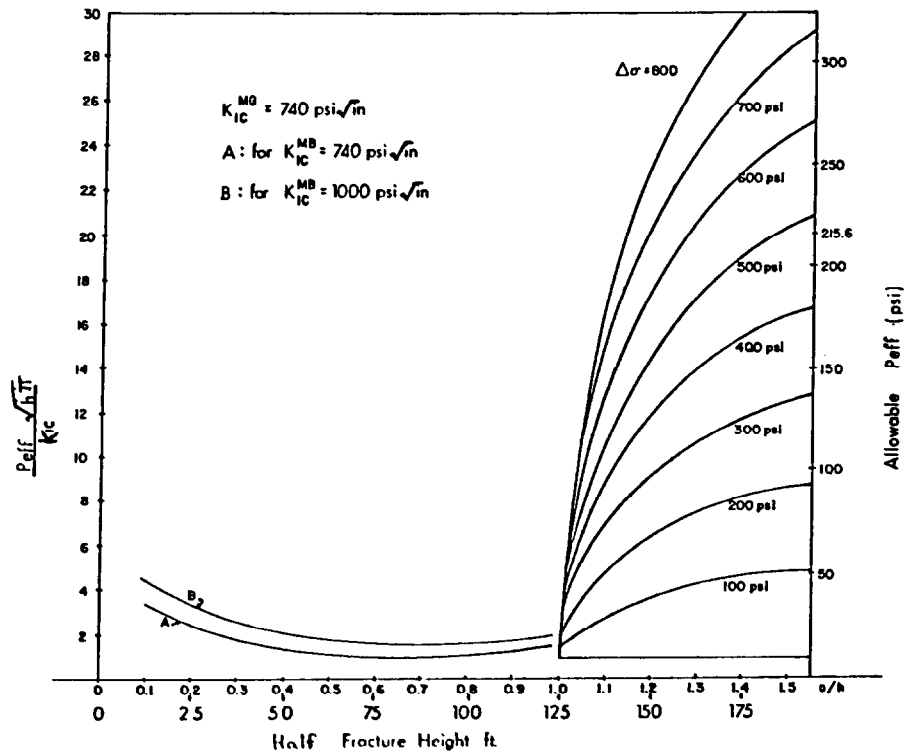


Fig. 5 - Effective pressure versus fracture height for $E_2/E_1 = 1.25$.

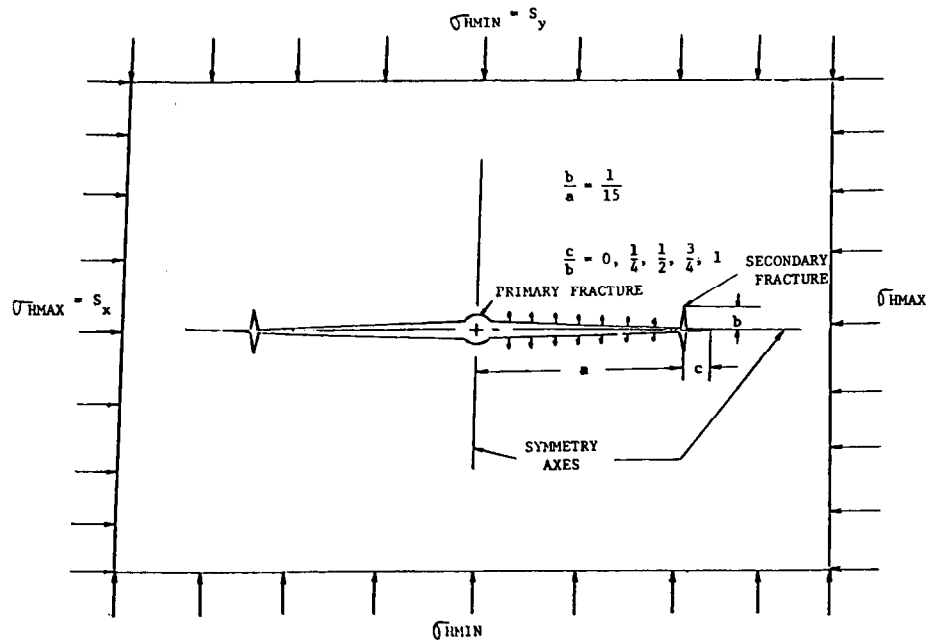


Fig. 6 - Two dimensional dendritic fracture model.

BRNCH CRCK

SIGMA σ_{xx}

□	-2500.00
○	-2000.00
△	-1500.00
+	-1000.00
×	-500.00
◇	0.00
⊕	500.00
⊗	1000.00
Υ	1500.00
⋈	2000.00
✱	2500.00

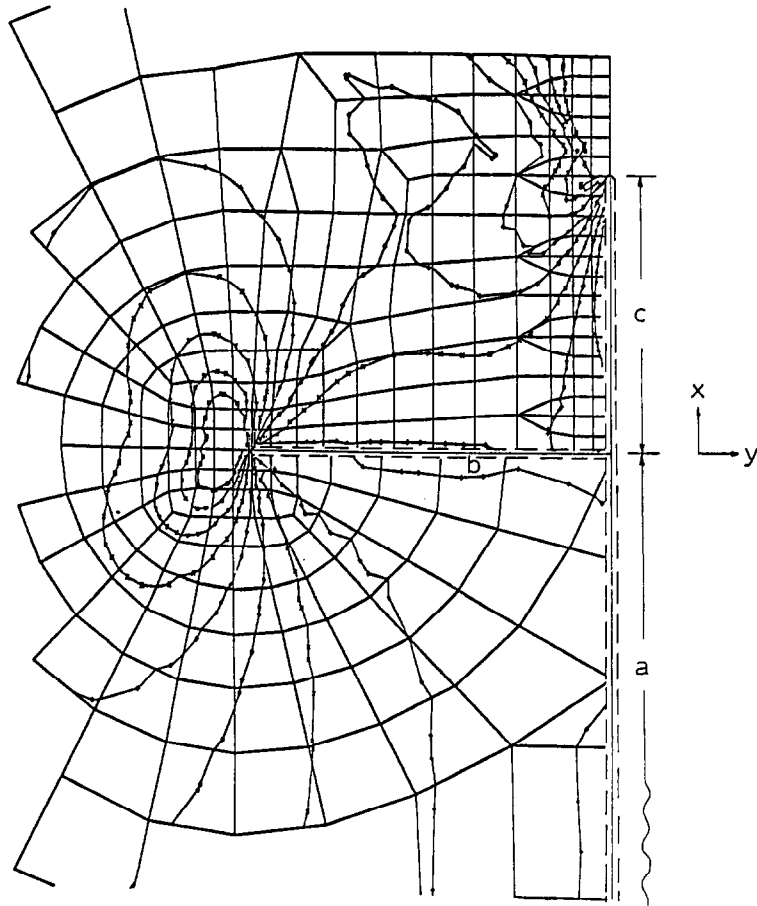


Fig. 7a - Stress contours σ_{xx} induced by frac fluid pressure loading $p = 1000$ psi (6.9 MPa).

BRNCH CRCK

SIGMA σ_{yy}

□	-2000.00
○	-1000.00
△	0.00
+	1000.00
×	2000.00
◇	3000.00
⊕	4000.00
⊗	5000.00
Υ	6000.00
⋈	7000.00
✱	8000.00

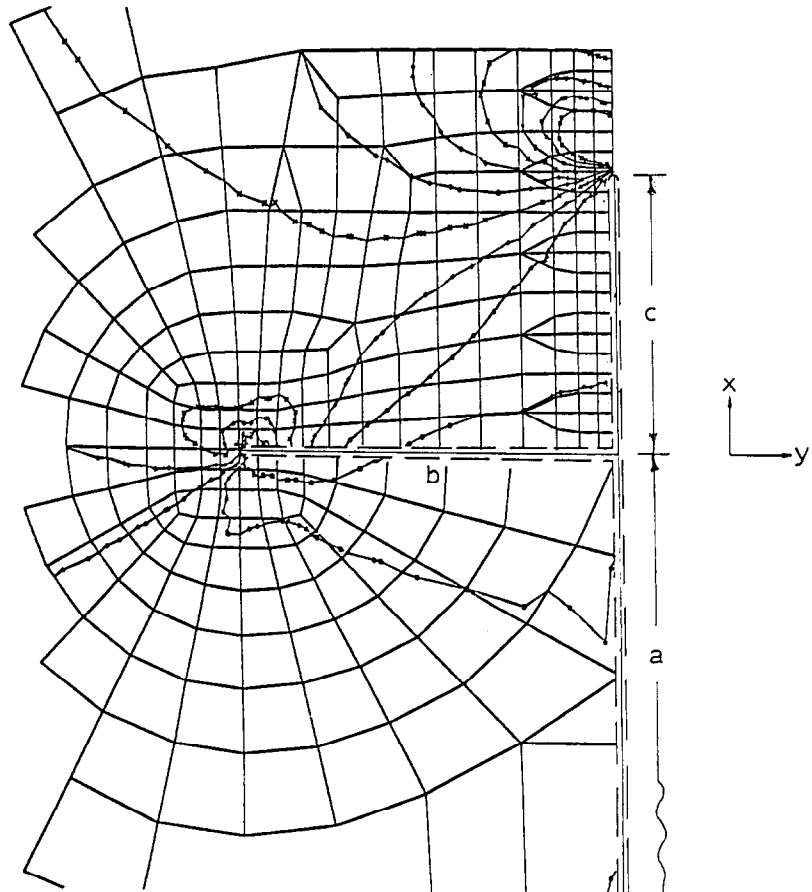


Fig. 7b - Stress contours σ_{yy} induced by frac fluid pressure loading $p = 1000$ psi (6.9 MPa).

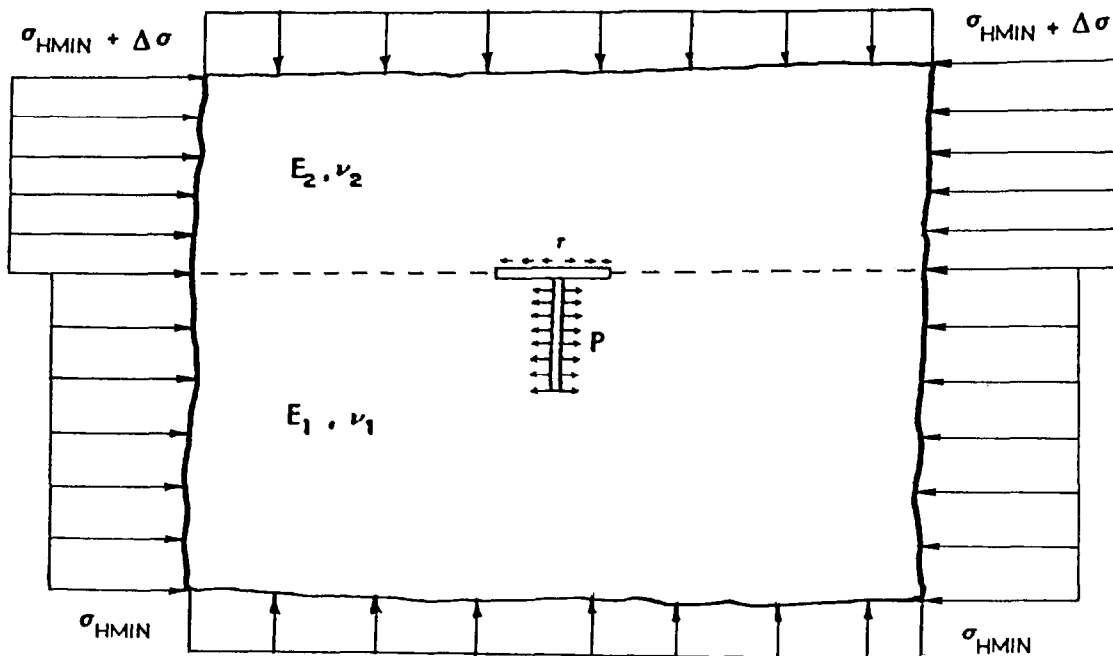


Fig. 8 - Joint interaction at Bi-material interface ($E_2/E_1=1.25$) and vertical crack model.

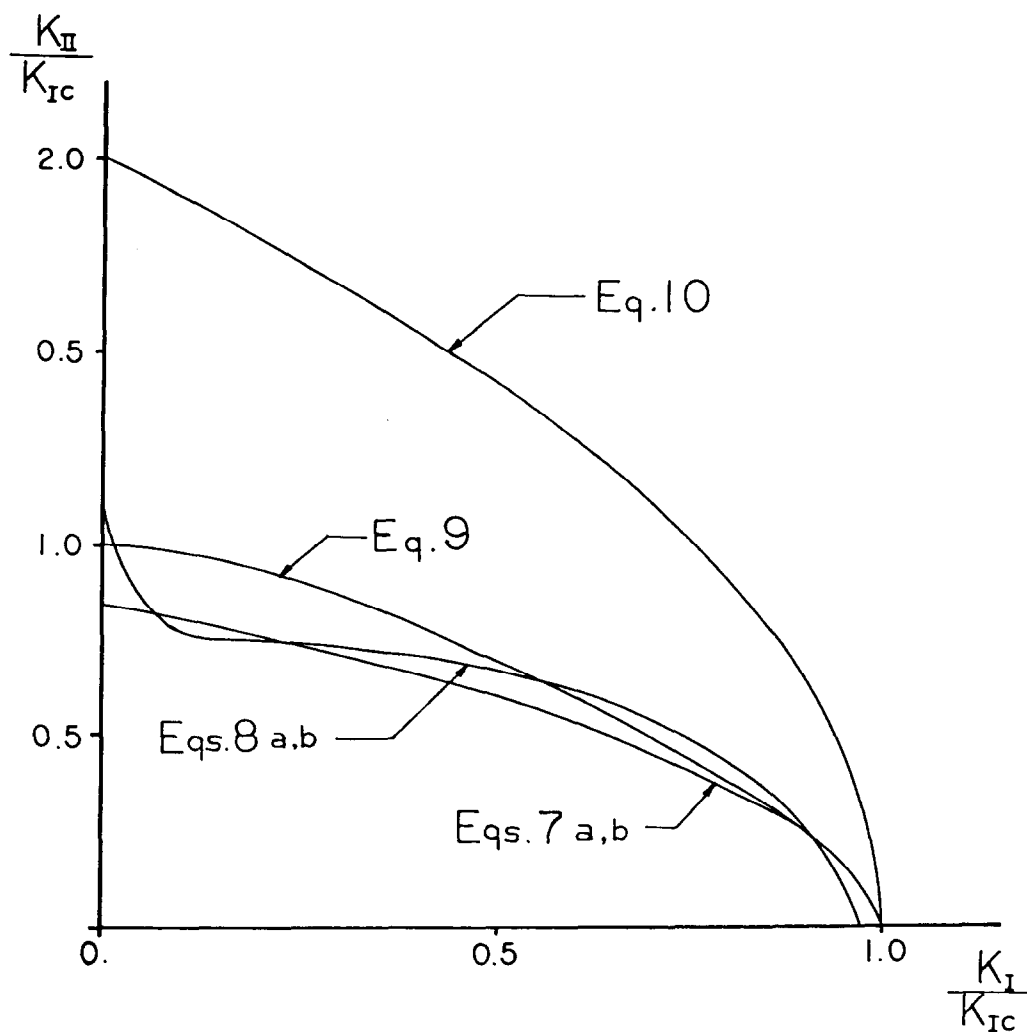


Fig. 9 - Comparison of mixed mode fracture theories.

EFFECTS OF VARIOUS PARAMETERS ON HYDRAULIC FRACTURING GEOMETRY

by Merle E. Hanson, Gordon D. Anderson, and Ronald J. Shaffer, Lawrence Livermore National Laboratory

This paper was presented at the 1980 SPE/DOE Symposium on Unconventional Gas Recovery held in Pittsburgh, Pennsylvania, May 18-21, 1980. The material is subject to correction by the author. Permission to copy is restricted to an abstract of not more than 300 words. Write: 6200 N. Central Expwy., Dallas, Texas 75206

ABSTRACT

We are conducting a theoretical-experimental program on the hydraulic fracturing process. A primary objective of the program is to determine those reservoir properties or characteristics which can control the created fracture geometry. Theoretical models have been applied to analyze some aspects of the dynamics of fracturing near material interfaces. The results of these calculations indicate that variation of material properties across a well bonded interface can cause dynamic material response resulting from the fracturing which could enhance propagation across the interface. Effects of friction have also been analyzed theoretically; however, in the frictional calculations the wave mechanics have been ignored. These calculations have shown that frictional slip along the interface tends to draw a pressurized fracture toward the interface; this motion tends to reduce the chances of penetrating the material across the frictional interface.

Small scale laboratory experiments are performed to study the effects of frictional characteristics on hydraulic fracture growth across unbonded interfaces in rocks. Various lubricants and mechanical preparation of the interface surfaces are used to vary the coefficients of friction on the interface surfaces. It is found that the frictional shear stress that the interface surface can support determines whether a hydraulically driven crack will cross the interface. Experiments are also being performed to study the effects of pre-existing cracks, which perpendicularly intersect the unbonded interface, on hydraulic crack growth across the interface. It is also found that the presence of these pre-existing cracks impedes the propagation of the hydraulic fracture across the interface. These experimental results on the effects of friction on the interface and the effects of pre-existing cracks on hydraulic fracture penetration of interfaces are consistent with the predictions of the numerical model calculations.

INTRODUCTION

Massive hydraulic fracturing (MHF) is a primary candidate for stimulating production from the tight gas reservoirs in the United States. Hydraulic fracturing has been widely used as a well completion technique for about 30 years. MHF is a more recent application that differs from hydraulic fracturing in that more fluid and proppant are pumped to create more extensive fractures in the reservoir. Application of MHF to increase production from the tight reservoirs has provided mixed and, in many cases, disappointing results, especially in lenticular reservoirs. For MHF to be successful in enhancing the production of gas from tight reservoirs, it is important that the fractures be emplaced in productive reservoir rock providing large drainage surfaces in the low permeability material and conductive channels back to the wellbore. We are then faced with the problem of containing fractures in a given formation.

Under the Department of Energy's Unconventional Gas Recovery program Lawrence Livermore Laboratory is conducting a research program to study the hydraulic fracture process. The general goal of this research is to determine if and to what extent the reservoir parameters control the geometry of the created fractures. From theories implied¹ and demonstrated²⁻⁴ hydraulic fractures propagate perpendicular to the least principal stress. Hence, except for very shallow applications, the fractures will be primarily vertical with the azimuthal orientation controlled by the in-situ stress. The vertical gradient in the horizontal stresses could also be a factor in the control of the shape or vertical extent of fractures. There have also been speculations that the stratigraphy, especially where the elastic material properties vary from layer to layer, could be effective in containing the vertical extent of fractures. Additionally, interfacial properties such as extent of loading, normal load, and friction will also play an important role in

inhibiting or enhancing the growth of the created fractures across the interfaces. Existing fractures and faults can also be important to the growth and final geometry of the propped fracture. To determine if and to what extent these effects are operative in controlling the geometry of the created fractures requires both theoretical and experimental analyses.

The study of interface fracturing characteristics is important for other hydrofracturing applications as well. Penetration of an interface can be required to open up a large pay zone, especially in lenticular reservoirs. Penetration is undesirable when an aquifer must remain isolated.

In our research program two-dimensional numerical models have been constructed to analyze fracturing in an elastic, layered, jointed continuum. Pore-pressure effects and changes in pore pressure resulting from porous flow have been coupled to the elastic calculations⁵ using the descriptions due to Terzaghi.⁶ Porous flow effects in pressurized fractures are reported in Hanson et al.⁷ The elastic part of the model was formulated using bilinear forms⁸ with the fractures simulated in the elements using techniques similar to that of Hanson and Sanford,⁹ Hanson,¹⁰ Shaffer et al.,¹¹ and Shaffer.¹² The model can accommodate more than one elastic material so that the effects of layering, and changes in elastic properties from layer to layer can be studied. Stresses resulting from the inclusion of layers and lenses have been studied for some simple geometries.⁷

In some cases, wave propagation effects are ignored to speed up the calculations. Fracture propagation in these cases is then analyzed as a succession of equilibrium states. We assume that this approximation is valid in the continuum sense because the body wave speeds are much larger than the macroscopic propagation velocity of a hydraulically driven fracture. For example, a fracture is driven on the order of 2000 ft (610 m) in 5 to 8 h, while an elastic wave traverses this distance in 200 ms. Therefore, we assume that at a given time the elastic continuum is in a quasi-equilibrium state with the fracture.

In addition, we have conducted experiments¹³ in which hydraulically driven cracks are initiated in limestone and sandstone. We are studying the conditions that cause or prevent a crack from crossing an interface between these materials. It has been shown^{7,14,15} that the mechanical properties of the two adjacent materials and the shear strength of the interface influence whether a crack will cross an interface. Currently we are conducting experiments on unbonded interfaces to determine threshold normal stresses required for fracture penetration and to determine the coefficient of friction for various surface characteristics and water content.

THEORETICAL MODELS

The equations of motion for an elastic continuum can be written as

$$\text{and} \quad \begin{aligned} \frac{\partial \sigma_x}{\partial x} + \frac{\partial \tau_{xy}}{\partial y} &= \rho \frac{\partial^2 u}{\partial t^2} \\ \frac{\partial \sigma_y}{\partial y} + \frac{\partial \tau_{xy}}{\partial x} &= \rho \frac{\partial^2 v}{\partial t^2} \end{aligned} \quad (1)$$

where t is time, ρ is density, τ_{xy} is the shear stress, and σ_x and σ_y are normal stresses and u and v are displacements in the x and y directions, respectively. The stresses are related to the strains with the constitutive relations:

$$\begin{pmatrix} \sigma_x \\ \sigma_y \\ \tau_{xy} \end{pmatrix} = \begin{bmatrix} 2\mu + \lambda & \lambda & 0 \\ \lambda & 2\mu + \lambda & 0 \\ 0 & 0 & \mu \end{bmatrix} \begin{pmatrix} \frac{\partial u}{\partial x} \\ \frac{\partial v}{\partial y} \\ \frac{\partial u}{\partial y} + \frac{\partial v}{\partial x} \end{pmatrix} \quad (2)$$

where μ and λ are the Lamé constants. Then a unique problem is specified by supplying the proper initial and boundary conditions.

We discretized Equations (1) in space with bilinear forms.⁸ When the displacements are time independent, this discretization leads to a stiffness matrix that relates point forces to point displacements. We relax this matrix with an iteration scheme that is a variation of the incomplete Cholesky-conjugate gradient method by Kershaw.¹⁶ We also use this iteration scheme to solve the mass matrix that arises in time dependent problems.

Equilibrium Crack Growth Near a Frictional Interface. Some reservoir characteristics which can exert control on fracture geometry include changes in material properties across a material interface and frictional slip along existing fractures and poorly bonded bedding planes. We have previously reported results of analyses on some of the effects on fracturing near material interfaces.^{7,17} In shallow reservoirs, frictional slip along an existing fracture or along poorly bonded bedding planes can effectively arrest propagation. Variations in the frictional coefficient can modify the path of the fracture. For example, the fracture geometry may display a sharp step due to frictional variation along a discontinuity.

We have been applying two-dimensional equilibrium models to study some aspects of fracture propagation as a fracture approaches a frictional discontinuity at right angles to the axis (direction of propagation) of the fracture. The equilibrium equations used to describe the elastic continuum are:

$$\text{and} \quad \begin{aligned} \frac{\partial \sigma_x}{\partial x} + \frac{\partial \tau_{xy}}{\partial y} &= 0 \\ \frac{\partial \sigma_y}{\partial y} + \frac{\partial \tau_{xy}}{\partial x} &= 0 \end{aligned} \quad (3)$$

with the constitutive relations shown in Eq. (2) above.

The frictional stress which the interface can support is defined by

$$\tau_f = \beta \sigma_n \quad (4)$$

where σ_n is the normal stress across the interface, and β is the coefficient of friction. The shear stress is calculated in the interface coordinate system and compared to τ_f . If the shear stress is greater than the frictional stress, slippage is allowed to occur through an iteration process until the shear stress and the frictional stress are balanced.

The effect of a frictional interface on a pressurized fracture as the crack propagates toward the interface has been analyzed. Analysis of the penetration of the interface will be the subject of future work. The geometry of the fracture and the interface used in the calculations is shown on Figure 1. The pressure in the crack was constant and the material on both sides of the interface was identical. Poisson's ratio was equal to 0.25. The ratio of the effective pressure in the crack to Young's modulus for the material (P_c/E) was 1.5×10^{-3} . Changes in pore pressure due to leakage of fluid from the crack into the surrounding material was ignored. The fracture tip distance from the interface, δ , has been normalized with respect to the fracture length. We have completed calculations for five ratios of $\tau_f/P_c = \gamma$.

Figure 2 shows the normalized Mode I stress intensity factor as a function of δ for the values of $\gamma = 0.033, 0.067, 0.1, 0.133$ and 0.167 . As expected, when the scaled distance from the crack tip to the interface is greater than 1, the effects of the frictional interface on the pressurized crack are small. The stress intensity factor is seen to increase both as the pressurized fracture approaches the interface and as the frictional coefficient becomes smaller. This is because relative motion along the interface increases in the same manner. Frictional stress along the interface changes as the fracture nears the interface. This happens when the normal stress across the interface is reduced because the material ahead of the fracture is driven toward the tip and hence the normal stress across the interface is reduced. The largest change in the frictional stress occurs ahead of the tip where it decreases to very small values when the scaled distance is less than 0.2. Increasing the initial frictional stress along the interface delays slip until the fracture is closer to the interface; however, the stress intensity factor increases at a higher rate once slip occurs.

Dynamic Crack Growth Near a Bonded Interface.

Several calculations were made with our time-dependent finite-element model in order to quantify the changes in material response due to variations in densities and elastic moduli across an interface. In the problem geometry of Fig. 3, a

crack initiates at $x = 0, y = 0$, propagates bilaterally at half the dilatational wave speed along $y = 0$ for a distance "c" and stops. The densities and elastic moduli are subscripted to differentiate between their values on either side of the interface. The elapsed time from crack initiation to stopping is defined as t_b , and the strain in the z direction is set to zero. The result, shown in Figures 4 to 6, is the time history of the vertical displacement (v) of a point just behind the final position of the right crack tip.

For all calculations the Lamé constants of material 1 were set to 0.3 Mbar (30 GPa) and the density of material 1 was 2.7 gm/cm^3 . In the first set of calculations, all the Lamé constants were set equal. Three calculations were made, corresponding to three values of the density of material 2: $\rho_2 = \rho_1/9, \rho_1$, and $9\rho_1$. Hence, for the second calculation, the medium is homogeneous and the interface does not exist. The results of these three calculations are shown in Fig. 4. The displacement in the y direction has been nondimensionalized with the final half crack length and the problem time t is nondimensionalized with the time required to break so that $t/t_b = 1$ is the time the crack stops. For this set of calculations the crack stopped at $c/L = 0.6$, so that Fig. 3 is drawn to scale. As seen in Fig. 4, the variation in material response is small even for a large variation in density.

In Fig. 5, the same density variation was used, but the crack propagated up to the interface ($c/L = 1.0$). Here the variation in material response is larger than in the previous case, but is still small when compared to the maximum displacement. There is also a difference seen in the character of the curve for the smallest value of ρ_2 when Fig. 5 is compared to Fig. 3. This crossing over of the curves occurs long after the crack stops.

In the next set of calculations, the density was uniform ($\rho_2 = \rho_1$), and the Lamé constants for the second material were assigned the values 10 GPa, 30 GPa, and 90 GPa. The results from these three calculations are shown in Fig. 6. As in the previous case, the crack propagated to the interface ($c/L = 1.0$). Changing the elastic constants by a factor of three causes large changes in the material response.

We conclude that, even though wave reflection and transmission at an interface are controlled by density and elastic moduli changes across that interface, a change in elastic moduli causes a much larger variation in material response than a change in density does. It should be noted that, in Figs. 4 and 5, all the curves converge as the time becomes large; i.e., density variation is strictly a dynamic effect. This is not true of the variation in elastic constants; i.e., all the curves in Fig. 4 will approach different values as t becomes large.

LABORATORY EXPERIMENTS

Small scale laboratory experiments are being performed to guide and corroborate the theoretical models. These experiments are not intended to simulate in-situ hydraulic fracture stimulation of a reservoir. They are highly idealized experiments in which specific parameters are controlled for comparison with the prediction of the theoretical models. At the present time the results are more qualitative than quantitative with regard to the modeling.

The rocks used in the experiments are Indiana limestone and Nugget sandstone from Utah. These two materials were chosen because they represent two different rock types. The limestone is a porous rock (~15%) relatively weak in compression and the sandstone is a stronger less porous (~3%) rock. Some mechanical properties are summarized in Table 1.

Two types of experiments are performed. One of the experiments treats the conditions of load under which a hydraulic fracture will cross an unbonded interface and the other measures the friction between the interface surfaces. These techniques have been described previously¹³ but a brief description will be repeated here. The hydraulic fracture experiment is shown in Fig. 7. Here prismatic blocks of the rock to be studied are stacked between the platens of a press. As can be seen in Fig. 7, the sides of the blocks are unconfined so that the load acts only across the interfaces between the blocks. Generally the stack consists of three blocks with the fracturing fluid injected into the center block. The prismatic blocks which are nominally 2"x4"x4" are machined flat with opposite faces parallel to insure uniform distribution of the applied load. The fluid is pressurized through an injection tube which is cemented by epoxy in an injection hole drilled into the center of the block. The experiment then consists of pressurizing the fluid until breakdown occurs and observing under which conditions of applied load and interface condition the hydraulic fracture, which is initiated in the block with the injection tube, will cross the interface and enter the adjacent block.

The frictional experiment is shown in Fig. 8. This apparatus consists of a hydraulic vise which squeezes together a sandwich of three blocks. The magnitude of the applied load is measured by a pressure transducer. A vertical ram applies a force to the center block which eventually causes it to slide between the two outer blocks. This load is measured by a load cell. The frictional properties of the interface are then given by the vertical load necessary to initiate motion under a given horizontal load. This frictional property depends upon the preparation of the sliding interface.

Static-friction measurements. Static frictional curves in which applied frictional stress to initiate slip is plotted against normal stress for several surface finishes on Indiana limestone and Nugget sandstone have been previously presented.¹³ It was found there that the presence of water decreased friction in the sandstone and increased friction in the limestone. More recently we have employed lubricants to further reduce the

friction effects. Two lubricants found to be quite effective are HI-TEMP C-100, Anti-Ball Lubricant* and 630-AA Lubriplate.**† A friction plot for Indiana limestone is presented in Fig. 9. It is seen that these lubricants significantly reduce the frictional load necessary to initiate slip below that for wet and dry surfaces. Similar reductions were found on Nugget sandstone surfaces. These data and extrapolations thereof are used to estimate the shear frictional stress that an interface can support when it is under a load in one of the hydraulic fracture experiments.

Hydraulic fracture-interface experiments. The purpose of the hydraulic fracture-interface experiments is to gain an understanding of the parameters that determine whether or not a fluid driven crack will cross an interface and penetrate the adjacent rock structure. This knowledge has application in the placement of hydraulic fractures for optimum reservoir stimulation. Among these parameters are the frictional properties of the interface and the presence of existing fractures near the interface. Some results from these interface experiments have been reported.¹³ It was found that for the Indiana limestone and the Nugget sandstone there exists a critical threshold normal stress across the interface below which the crack will not penetrate the interface into the adjacent rock. These normal stress thresholds (normally 4.5 MPa and 5.5 MPa for the limestone and sandstone respectively) were converted to threshold shear stresses from the friction curves such as in Fig. 9. More recent hydraulic fracture-interface experiments in which the lubricants were applied to the interface have been performed. As one would expect, the effect of the lubricant was to increase the threshold normal stress. The results from these experiments are summarized in Table 2. As can be seen from the table, the threshold frictional shear stress decreases with increasing threshold normal stress as the interface frictional coefficient decreases due to lubrication. This decrease in the threshold shear stress that the interface must support could be due to the fact that a greater difference in principal stresses exists because of the increased applied normal load.

*Manufactured by FEL-PRO, INC., Skokie, IL.

**Manufactured by Fiske Bros. Refining Co., Neward, NJ, and Toledo, OH.

†Reference to a Company or product name does not imply approval or recommendation of the product by the University of California or the U.S. Department of Energy to the exclusion of others that may be suitable.

A change in the frictional properties of an interface such as one region having a lower coefficient of friction than an adjacent region can also influence crack propagation across the interface. Fig. 10 shows the result of an experiment in which a 3/4-inch strip of the C-100 lubricant was coated on an otherwise smooth, dry limestone interface parallel to the fluid injection tube. The opposite interface contained no lubricant whatever. The three block stack was placed in a press and a load in excess of the threshold for cracks to cross the interface was applied. As can be seen in the figure, at the interface with the lubricated strip the crack reached the interface within the strip and then continued into the adjacent block laterally displaced to the edge of the lubricated zone. At the interface containing no lubricant the crack continued directly across the interface. Analysis indicates that if a crack tip is approaching the neighborhood on an interface where the coefficient of friction suddenly increases, a concentration of shear stress will occur at the discontinuity. This shear stress concentration makes crack initiation across the interface more likely at the discontinuity than directly across the interface and this is what is qualitatively shown in Figure 10. This experiment again demonstrates that frictional characteristics at the interface affect the geometry of fracture growth.

Calculations have been performed to assess the effects of existing cracks near an interface on the growth of a fluid driven crack across that interface.⁷ Using the Mode I stress intensity factor as a criterion for crack growth, the results showed that the presence of cracks on the opposite side of the interface from the approaching fluid driven crack had the same effect as lowering the elastic modulus across the interface. Having the elastic modulus suddenly drop across the interface was shown to have the effect of drawing the fluid driven crack to the interface but inhibiting the growth on the opposite side of the interface into the adjacent material. Experiments have been performed to simulate the geometry of these calculations. The standard three prismatic limestone block setup with two interfaces, one on each side of the injection tube, was used as shown in Fig. 11. However, one of the outer blocks was actually three smaller blocks sitting parallel to give the effect of two perpendicular cracks intersecting the interface as shown in Fig. 11a. The block assembly was then placed in a press and a load greater than the threshold load for crack penetration was applied. As seen in Fig. 11b, the crack crossed the lower interface into the solid block but terminated at the interface which was intersected by the existing cracks. Again this experiment qualitatively agrees with the prediction of the theoretical model.

CONCLUSIONS

The equilibrium model when applied to an unbonded interface which can support friction shows that as the friction decreases the pressurized crack has a greater tendency to grow toward the interface. The effect of lowering the coefficient of friction at the interface has a similar effect on crack growth as lowering the elastic modulus of the material on the opposite side of the interface. The

small scale experiments are consistent with this result and also indicate that decreasing friction reduces the tendency for the crack to cross the interface.

Dynamic calculations of the material displacement as a propagating crack approaches and stops at or near an interface show that the effect of a change of elastic modulus across the interface is much greater than the effect of a density change. Results of this type of study have potential application in determining the rate of fracture growth for optimum reservoir stimulation.

The small scale laboratory experiments are designed to check for consistency with the predictions of the theoretical model and to point out phenomena which must be included in the models. These experiments have shown that the frictional characteristics of interfaces are important in crack growth across interfaces. These frictional effects could be important in stimulation of shallow reservoirs. An abrupt change in the frictional characteristics of an interface can produce an abrupt change in the growth path of a pressure driven crack. Finally, both the analysis and the small scale laboratory experiments indicate that the presence of existing cracks in the vicinity of an interface influence crack growth. The existing cracks appear to effectively lower the elastic modulus of the material in which they are contained.

REFERENCES

1. Hubert, M. King, Structural Geology (Hafner Publishing Company, New York, 1972).
2. Haimson, B., Hydraulic Fracturing in Porous and Nonporous Rocks and Its Potential for Determining In-Situ Stresses, PhD Thesis, University of Minnesota (1968).
3. Daneshy, A. A., "True and Apparent Direction of Hydraulic Fractures," SPE Paper 3225, Society of Petroleum Engineers (Dallas 1971).
4. Hanson, M. E., et al., "LLL Gas Stimulation Program Quarterly Progress Report, October 1977-December 1977," Lawrence Livermore Laboratory Rept. UCRL-50036-77-4 (1978).
5. Hanson, M. E., and Shaffer, R. J., "Some Continuum Considerations of the Hydraulic Fracturing Process," Lawrence Livermore Laboratory Rept. UCRL-80360 (1978). Paper presented at 19th U.S. Symposium on Rock Mechanics, May 1978, Lake Tahoe, NV.
6. Jaeger, J. C., and Cook, N. G. W., Fundamentals of Rock Mechanics, (Chapman and Hall, London 1969).
7. Hanson, M. E., and Shaffer, R. J., "Some Results from Continuum Mechanics Analysis of the Hydraulic Fracture Process," SPE 7942, AIME 1979.
8. Petschek, A. G., and Hanson, M. E., "Difference Equations for Two-Dimensional Elastic Flow," J. Comp. Phys. 3, 307 (1968).

EFFECTS OF VARIOUS PARAMETERS ON HYDRAULIC FRACTURE GEOMETRY

- | | |
|---|--|
| <p>9. Hanson, M. E., and Sanford, A. E., "Some Characteristics of a Propagating Brittle Tensile Crack," Geophys. J. R. Astr. Soc. 24, 231 (1971).</p> <p>10. Hanson, M. E., "Some Effects of Macroscopic Flaws on Dynamic Fracture Patterns Near a Pressurized Driven Fracture," Int. J. Rock Mech. Min. Sci. and Geomech. Abstr. 12, 311 (1975).</p> <p>11. Shaffer, R. J., et al., "Laser-Induced Fractures in Silicon, Flaw Interaction Studies and Fracture in Granular Materials," Air Force Weapons Laboratory, Kirtland Air Force Base Rept. AFWL-TR-74-267 (1976).</p> <p>12. Shaffer, R. J., <u>Source Functions for Frictional Transient Shear Slip</u>, PhD Thesis, New Mexico Institute of Mining and Technology, Socorro, NM (1978).</p> <p>13. Anderson, G. D., "The Effects of Mechanical and Frictional Rock Properties on Hydraulic Fracture Growth Near Unbonded Interfaces," SPE</p> | <p>Paper 8347, AIME, 1979.</p> <p>14. Jones, A. J., Abou-Sayed, A. S., and Rogers, L. A., "Rock Mechanics Aspects of the MHF Design in Eastern Devonian Shale Gas Reservoirs," Enhanced Oil, Gas Recovery and Improved Drilling Methods Conference, Tulsa, OK, Aug.-Sept. 1977.</p> <p>15. Daneshy, A. A., "Hydraulic Fracture Propagation in Layered Formations," SPE Paper 6088, AIME, 1976.</p> <p>16. Kershaw, D. S., "The Incomplete Cholesky-Conjugate Gradient Method for the Iterative Solution of Systems of Linear Equations," Lawrence Livermore Laboratory Rept. UCRL-78333, Rev. 1 (1977).</p> <p>17. Shaffer, R. J., M. E. Hanson, and G. D. Anderson, "Hydraulic Fracturing Near Interfaces," Lawrence Livermore Laboratory Rept. UCRL-83419. Presented at ASME Energy & Technology Conf., New Orleans, Feb. 3, 1980.</p> |
|---|--|

TABLE 1
MECHANICAL PROPERTIES OF ROCKS⁽¹³⁾

Material	Strength (MPa)	Compressive Strength (MPa)	Bulk Modulus (GPa)	Poisson Ratio	Initial Density (Mg/m ³)
Nugget sandstone	3.7-7.5* 6.3-8.6**	230.0	11.7	.07	2.55
Indiana limestone (dry)	4.7-5.9	62.0	11.3	.115	2.28
Indiana limestone (saturated)	1.9				2.45

* Perpendicular to bedding.

** Parallel to bedding.

TABLE 2

THRESHOLD STRESSES FOR CRACK GROWTH ACROSS
UNBONDED INTERFACES (MPa)

ROCK	LUBRICANT			
	DRY	WATER	630-AA	C-100
Indiana limestone	4.5	3.4	9.7	15.2
	(2.4)	(2.4)	(2.3)	(2.0)
Nugget sandstone	5.5	6.5	---	11.7
	(2.8)	(2.6)	---	(2.0)

Upper entry is normal stress

Lower entry in parenthesis is shear stress from friction plots.

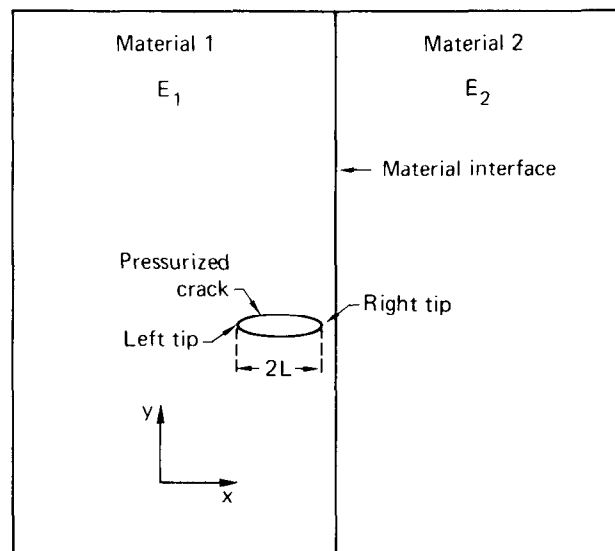


Fig. 1 - Geometry of a fracture near an interface for equilibrium studies.

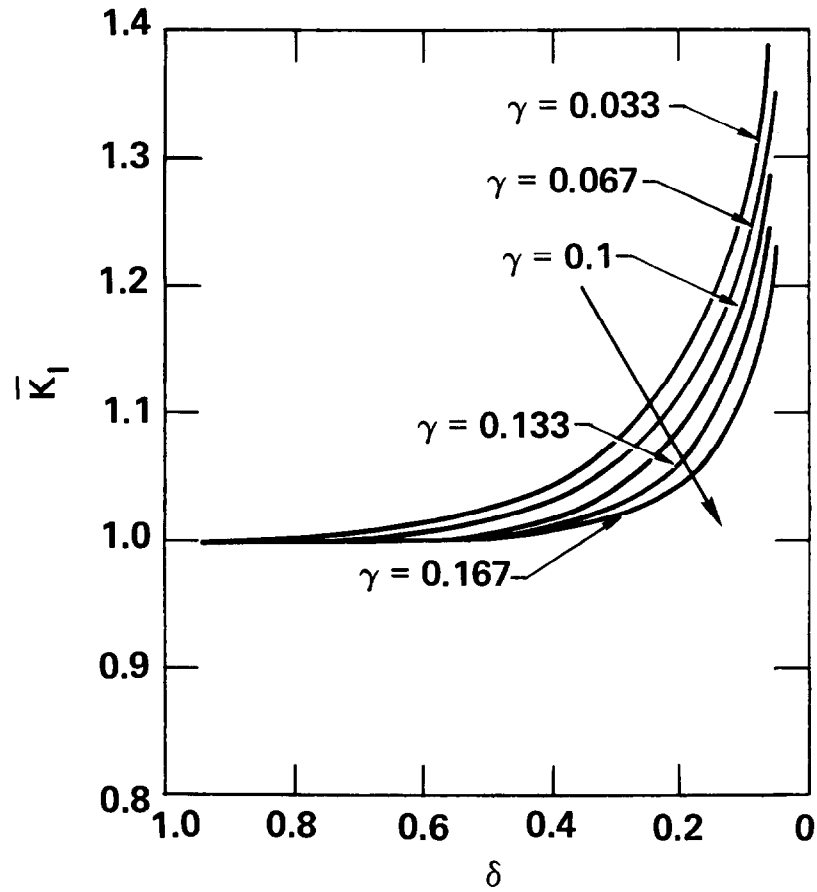


Fig. 2 - Variation in Mode I stress-intensity factor as crack approaches a frictional interface for variations in frictional stress along interface.

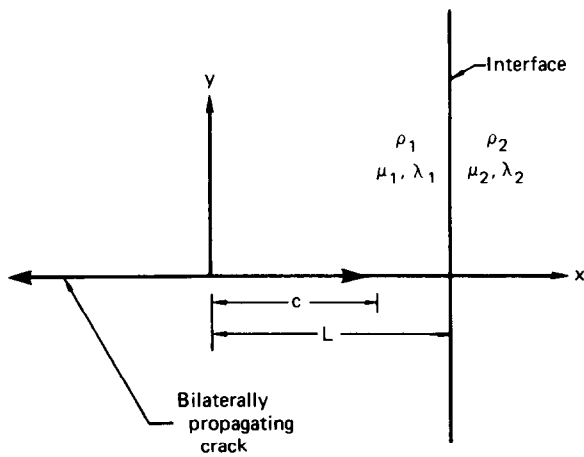


Fig. 3 - Problem geometry for time dependent crack propagation near an interface.

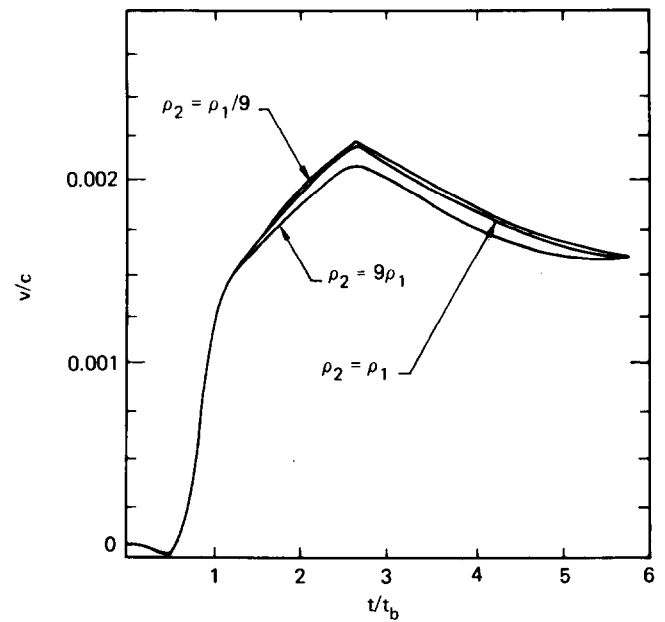


Fig. 4 - Displacement perpendicular to the crack when $c/L = 0.6$ (the crack does not reach the interface).

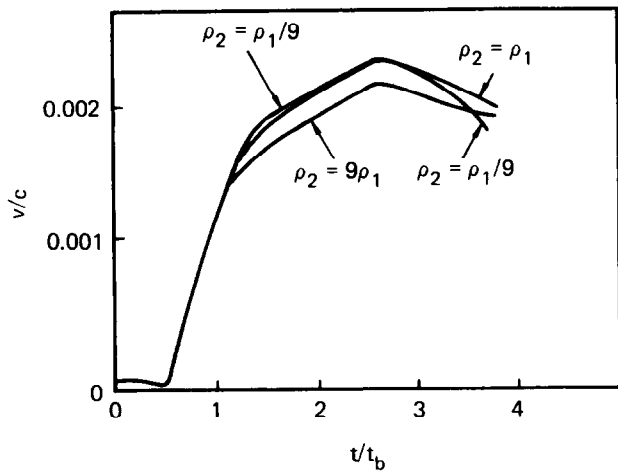


Fig. 5 - Displacement perpendicular to the crack when $c/L = 1.0$ (the crack reaches the interface).

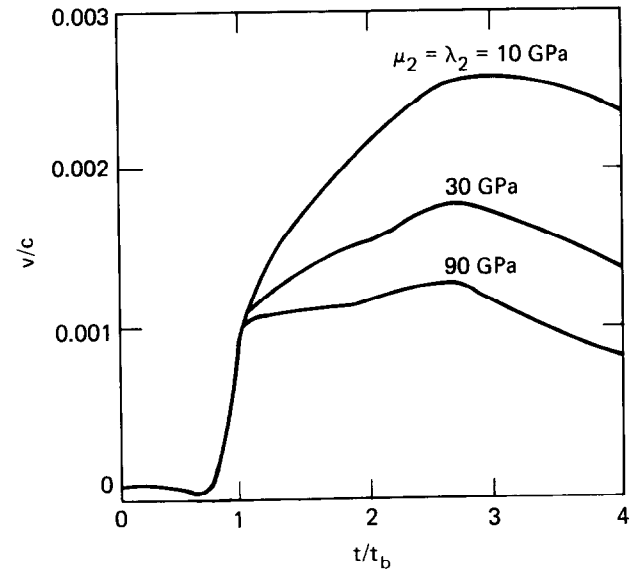


Fig. 6 - Displacement perpendicular to the crack when the density is constant across the interface and $c/L = 1.0$.



Fig. 7 - Hydraulic fracture - interface experimental setup.



Fig. 8 - Friction experiment setup.

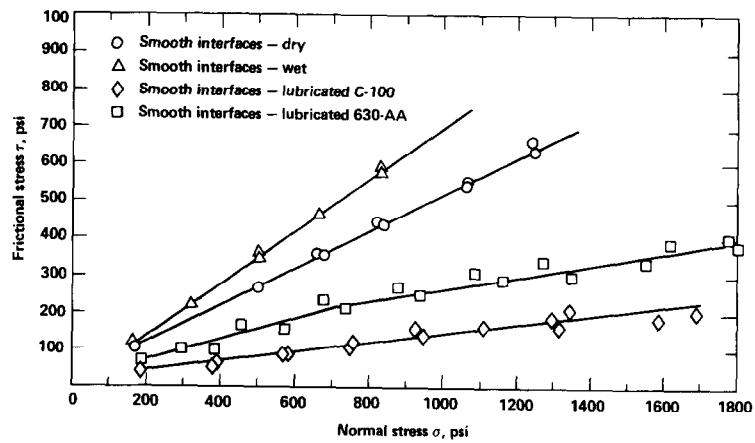


Fig. 9 - Static friction plot for different surface conditions of Indiana limestone.

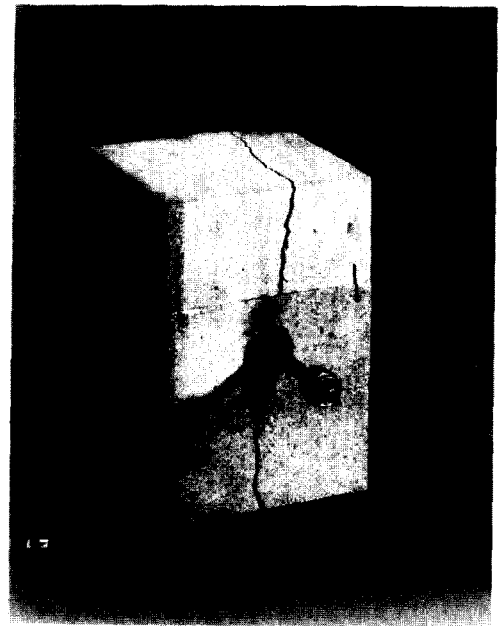


Fig. 10 - Effect of low friction region on growth across an unbounded, loaded interface.

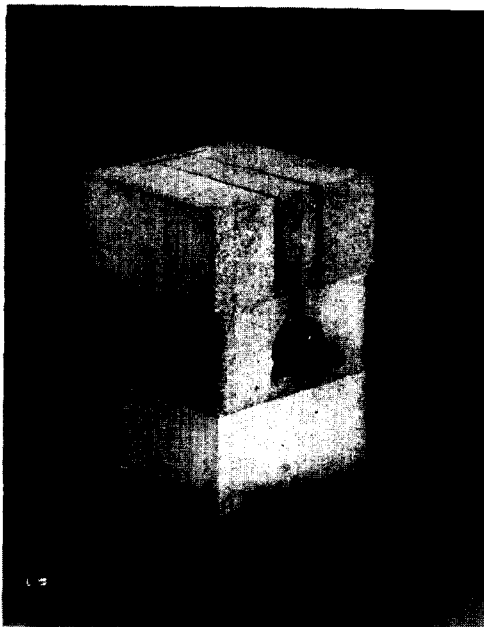
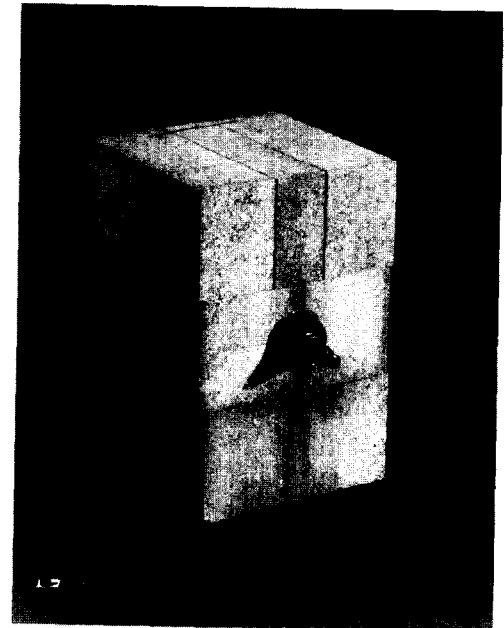


Fig. 11 - Effect of perpendicular cracks intersecting an interface on crack growth across the interface.



ELLIPTICAL FLOW EQUATIONS FOR VERTICALLY FRACTURED GAS WELLS

by Brent W. Hale, Northwest Pipeline Corp.;
and J.F. Evers, University of Wyoming

© Copyright 1980, Society of Petroleum Engineers

This paper was presented at the 1980 SPE/DOE Symposium on Unconventional Gas Recovery held in Pittsburgh, Pennsylvania, May 18-21, 1980. The material is subject to correction by the author. Permission to copy is restricted to an abstract of not more than 300 words. Write: 6200 N. Central Expwy., Dallas, Texas 75206

ABSTRACT

A set of elliptical equations is developed for use in understanding and evaluating vertically fractured gas wells in low permeability gas sands. The equations are designed for use with short term flow tests at either constant rate or constant pressure test conditions.

The relationship of elliptical equations to radial equations is discussed. Elliptical equations are found to be an improvement over radial equations because they effectively account for both early time linear flow and late time radial flow. A method for determining true permeability where radial flow cannot be established is presented. Test conditions allowing calculation of fracture damage, fracture length and permeability from a single test are presented. Test conditions preventing permeability determination are discussed.

Transient well test analysis methods suited for field evaluation of tight gas wells are presented with examples. Equations designed for use with hand-held calculators allow on-site well evaluations without computers. Estimates of production rates, stabilization time, drainage area and drainage volume may also be made.

INTRODUCTION

Much new Rocky Mountain Area gas is being produced from tight gas sands. These wells often prove to be uneconomical unless they are hydraulically fractured. After fracturing the wells, testing is generally required to insure that sustained production will justify the cost of a pipeline connection. Current practice generally involves a flow test ranging from several hours to several days. A corresponding pressure build-up often ranges from a day to a week or more. Using a well test involving hours to forecast many years performance can be very misleading if not done with care.

A basic understanding of elliptical equations can yield a great deal of useful information from short flow and buildup tests. It also helps set limits on what information can be expected from a test and what cannot be expected.

References and illustrations at end of paper.

THE ELLIPTICAL EQUATION

The generalized elliptical flow equation¹ combines linear properties of early time behavior with the radial properties of late time flow in a single equation. Written using the real gas pseudo-pressure², $m = 2 * \int (p * dp / (u(p) * z(p)))$, it is

$$Q_{sc} = \frac{\pi T_s KH (M_i - M_{xf})}{P_s T \{ S_{xf} + \ln(\sqrt{\pi t_{Dxf}} + \sqrt{1 + \pi t_{Dxf}}) \}} \quad \dots (1)$$

Elliptical dimensionless pressure for a constant rate drawdown is:

$$P_D = \ln(\sqrt{\pi t_{Dxf}} + \sqrt{1 + \pi t_{Dxf}}) \quad \dots (2a)$$

Elliptical dimensionless pressure for a constant pressure drawdown is:

$$R_{QD} = E \ln(\sqrt{\pi t_{Dxf}} + \sqrt{1 + \pi t_{Dxf}}) \quad \dots (2b)$$

Dimensionless time is:

$$t_{Dxf} = Kt / \phi \mu c_x f^2 \quad \dots (3)$$

Fracture damage is:

$$S_{xf} = \pi T_s KH \Delta M_s / P_s T Q_{sc} \quad \dots (4)$$

Equation 1 can be rewritten using dimensionless pressure as:

$$Q_{sc} = \frac{\pi T_s KH (M_i - M_{xf})}{P_s T (S_{xf} + P_D)} \quad \dots (5)$$

For early time in a vertically fractured well, T_{Dxf} is small. P_D is approximated by $(3.14 * T_{Dxf})^{.5}$. This is the linear P_D function and represents linear flow. As t_{Dxf} becomes large, P_D can be approximated by $.5 * \ln(3.14 * 4 * t_{Dxf})$. This is a radial P_D function.

The elliptical dimensionless pressure function is derived by considering the properties of vertical fractures and fluid flow through a porous media. Use of the coordinate transformation $w = \arcsin(z)$ and conformal mapping results in steady state isobars which are ellipses. Figure 1 shows isobars mapped in the X-Y plane as ellipses.^{3,4,5} The same isobars are mapped in the U-V plane as rectangles. In the U-V plane, all flow is linear. A fracture extends from $-X_f$ to $+X_f$ with the wellbore at the center. 'A' is a major semiaxis. 'B' is a minor semiaxis. X_f , A and B are related by:

$$X^2 = A^2 - B^2 \quad \dots (6)$$

The steady state fluid flow equation is:

$$\frac{\delta^2 M}{\delta X^2} + \frac{\delta^2 M}{\delta Y^2} = 0 \quad \dots (7)$$

The steady state solution, giving the total pressure drop from the external ellipse to the fracture is:

$$Q_{sc} = \frac{T_s KH (M_i - M_{xf})}{P_s T \ln \left\{ \frac{A_e + B_e}{A_{xf} + B_{xf}} \right\}} \quad \dots (8)$$

The steady state dimensionless pressure function is:

$$P_D = \ln \left\{ \frac{A_e + B_e}{A_{xf} + B_{xf}} \right\} \quad \dots (9)$$

As X_f becomes smaller, A becomes equal to B and Equation 9 reduces to $\ln(A_e/B_e)$, which is the dimensionless pressure term for radial flow. As X_f becomes larger, B approaches zero. Equation 9 becomes B_e/X_f , which is the dimensionless pressure term for linear flow. The steady state elliptical dimensionless pressure function has both linear and radial properties based on fracture length.

The unsteady state Equation 2a is derived from Equation 9 by letting a moving steady state boundary represent the unsteady state effects. Dimensionless time at this moving boundary is defined as:

$$t_{De} = Kt/\phi \mu c B^2 \quad \dots (10)$$

At a dimensionless time of $1/\pi$, flow is steady state and t_{Dxf} is related to B and X_f by:

$$B^2/X_f^2 = \pi t_{Dxf} \quad \dots (11)$$

Equation 2a results from combining Equations 11 and 9. Equation 2b is Equation 2a times E, the elliptical integral of the second kind.⁶ This additional pressure drop is associated with constant pressure tests. This elliptical integral varies in value from 1.0 when radial effects dominate to $\pi/2$ when linear effects dominate. Since constant pressure production is most common for tight gas wells, it should be used.

Fracture damage, Equation 4, is a zone of reduced permeability around the fracture. Dimensionless pressure drop across this zone is constant. Real pressure drop is proportional to the flow rate. Fracturing and permeability alteration are not combined into a single

term, as is done with radial equations.⁷ The two effects can be better understood if identified separately. Many tight gas sands are extremely sensitive to fracture fluids. Accurately measuring this sensitivity should help in selecting the best available treatment procedures.

GAS WELL TESTING

For a comprehensive well test, both linear and radial flow properties must be measured. The radial flow as observed on a Horner pressure buildup plot of $m(p)$ versus $\log \{(T+dT)/dT\}$ gives permeability. A radial slope, M_r , can only be measured if radial flow is observed. The equation is:

$$KH = \frac{Q_{sc} P_s \ln \sqrt{t_0}}{\pi T_s M_r} \quad \dots (12)$$

Linear flow effects are used to measure fracture length. A linear slope, M_l , is measured from a plot of $m(p)$ versus $(T+dT)^{0.5} - dT^{0.5}$. For a constant pressure drawdown, the equation is:

$$X_f = \frac{P_s T Q_{sc}}{2 T_s M_r H} \sqrt{\pi/\phi K \mu c} \quad \dots (13a)$$

For a constant rate drawdown, the equation is:

$$X_f = \frac{P_s T Q_{sc}}{T_s M_r H} \sqrt{1/\phi K \mu c \pi} \quad \dots (13b)$$

In tight gas wells, radial flow is often absent or not well established. This causes a continuously increasing Horner slope. In the absence of a correct Horner straight line, the maximum slope should be measured at the end of the pressure buildup. An apparent permeability is determined from this slope which is an upper limit to permeability.

For partially established radial flow, permeability correction charts, Figures 2 and 3, have been found useful. The correction, which is similar to the Russell and Truitt correction⁸, is a function of dimensionless flow time, t_{Df} , and of the steady state radius of investigation, $\ln\{(A+B)/X_f\}$. The permeability correction has no upper limit. Use of the charts is iterative because both true permeability and fracture length are unknown. A value of t_{Df} is estimated based on the apparent Horner permeability. $\ln\{(A+B)/X_f\}$ is calculated using Equation 2a or 2b. t_{Dxf} is dimensionless shut-in time based on the estimated value of t_{Df} . After a correction factor is obtained, a corrected KH will yield a corrected t_{Df} . The two values for t_{Df} will not converge if flow is completely linear. This is normally true for correction factors of more than 3.0.

For completely linear flow, Equation 12 sets an upper limit on KH. Equation 13a or 13b sets a lower limit on X_f . All late time points will lie on a straight line of a plot of $m(p)$ versus $(T+dT)^{0.5} - dT^{0.5}$. When late time points fall below the straight line, flow is being influenced by radial effects. If no straight line is observed, linear flow either does not exist or is masked by wellbore storage and fracture damage.

Fracture damage, S_{fx} , is measured on the plot of

$m(p)$ versus $(T+dt)^{0.5} - dt^{0.5}$. At $dt = 0$, fracture damage is the difference of the extrapolated line and the final flowing pressure. Negative fracture damage or permeability increase has not been observed by the authors.

Reservoir boundaries are not likely to influence short term flow tests of tight gas wells. The radius of investigation generally extends no more than 30 meters from the fracture. When a boundary is reached, years are likely to have passed with flow rates being so low that the boundary will have only a minor effect on recoverable reserves.

Total gas in place for a tight gas well depends on boundary distances. Economic recovery is dependent on fracture length and permeability. A well may easily reach uneconomic rates before reaching a physical boundary. In this case, the pressure coning around the fracture is the total reserve of the well. There is no depletion at a physical boundary. All production comes from the zone of reduced pressure near the fracture. Using Equation 9, this pressure coning can be calculated. For large fractures, coning depletion can approach 40% of the original gas in place. When this happens, economic gas in place is determined by permeability and by hydraulic fracturing.

If the distance to a boundary can be predicted, boundary effects on a deliverability projection can be calculated. Deliverability after boundaries are encountered is best estimated using type curves or computer models. Type curves based on elliptical geometry are shown in Figures 4 and 5. Type curves using different boundary conditions have been published.^{9,10} Equations 14 and 15 relate fracture length and exterior elliptical geometry to drainage area. The area of a drained ellipse is given by:

$$\text{Area} = \pi AB = \frac{\pi X_f^2}{4} \left(\left\{ \frac{A+B}{X_f} \right\}^2 - \left\{ \frac{X_f}{A+B} \right\}^2 \right) \quad \dots (14)$$

If the area is known, $(A+B)/X_f$ is given by:

$$\frac{A+B}{X_f} = \left(\frac{2AB}{X_f^2} + \left\{ \left(\frac{2AB}{X_f^2} \right)^2 + 1 \right\}^{1/2} \right)^{1/2} \quad \dots (15)$$

TEST DATA INTERPRETATION

Test data for a San Juan Basin Mesaverde well is given in Table 1. Figure 6 is a Horner plot of the pressure buildup. The Horner slope is increasing. No radial flow is expected. Figure 7 is a linear square root plot of the same data. The late time points lie on the straight line confirming the absence of radial flow. Early time points show some fracture damage which is not serious. Table 2 presents evaluation results. The apparent permeability is at least twenty times the true permeability. Figure 8 shows a production and test history. The forecast based on the test is about 20% low. The total rate change from testing to production is about thirty-fold.

Figure 9 shows a Wyoming gas well with 44,000 hours of production. There is no sign of radial flow and no boundary effects. The slope of $\frac{1}{2}$ on this log-log plot is characteristic of linear flow. If boundaries are not encountered, the reserve will be less than 40% of the original gas in place. Infill drilling may well be justified in this area. Many wells

behave like this Wyoming well. It is this type of behavior which lead the authors to search for equations which more reliably predict tight gas well behavior than do radial equations.

CONCLUSIONS

As tighter gas sands are developed in the future, elliptical flow equations will become more important. As gas becomes more valuable and development more costly, they will serve as a useful diagnostic tool to improve the industry's performance. Conclusions reached by the authors are:

1. Elliptical equations adequately model tight gas wells.
2. Horner pressure buildup analysis yields correct permeability only if flow is radial.
3. Fully developed radial flow may never occur in tight gas wells.
4. Horner permeability can be corrected to true permeability only if flow is influenced by radial effects.
5. Completely linear flow allows an upper bound to be set on permeability and a lower bound to be set on fracture length.
6. Coning depletion may be up to 40% of OGIP prior to onset of boundary effects.

NOMENCLATURE

A	= exterior elliptical major semi-axis
A_{xf}	= fracture face elliptical major semi-axis
B	= exterior elliptical minor semi-axis
B_{xf}	= fracture face elliptical minor semi-axis
C	= gas compressibility
E	= elliptical integral of the second kind
H	= net pay
K	= permeability
K_a/K	= ratio of apparent permeability to true permeability
$m, m(p)$	= real gas pseudo pressure
m_i	= initial real gas pseudo-pressure
m_e	= real gas pseudo-pressure at the external boundary
m_{xf}	= real gas pseudo-pressure at the fracture face
M_l	= slope of linear square root plot
M_r	= slope of Horner plot
P_s	= pressure - standard
P_D	= pressure - dimensionless
Q_{sc}	= standard flow rate
R_{QD}	= reciprocal dimensionless rate
R_{QDt}	= total reciprocal dimensionless rate
S_{fx}	= fracture face damage
t	= time
t_{Dxf}	= dimensionless time for a vertically fractured well
t_{De}	= dimensionless time at steady state boundary

T = formation temperature
 T_s = standard temperature
 X_f = fracture half length
 ϕ = Porosity - gas filled
 μ = viscosity
 ΔM_s = pseudo-pressure drop in the damaged zone

ACKNOWLEDGEMENTS

Parts of this paper were completed as fulfillment of a Masters Degree requirement at the University of Wyoming. The authors also acknowledge the assistance of Northwest Pipeline Corporation in providing well test data used in the paper.

REFERENCES

1. Hale, Brent W.: "Elliptical Flow Systems in Vertically Fractured Gas Wells", Masters Thesis, University of Wyoming, Dept. of Petroleum Eng., 1979.
2. Al-Hussainy, R. and Ramey, H.J., Jr.: "The Flow of Real Gases Through Porous Media", JPT, May, 1966.
3. Chen, Shing-ming: "A Numerical Model For Gas Flow in Vertically Fractured Reservoirs with Stress-Sensitive Fractures", Masters Thesis, University of Wyoming, Dept. of Petroleum Eng., 1976.
4. Kucuk, F., and Brigham, W.E.: "Transient Flow in Elliptical Systems", SPE Paper 7488.
5. Prats, M.; Hazebrock, P. and Strickler, W.R.: "Effect of Vertical Fractures on Reservoir Behavior - Compressible Fluid Case", SPEJ, June, 1962.
6. Abramowitz, M. and Stegun, I.A.: "Handbook of Mathematical Functions", Dover Publications, Inc., New York, Ninth Printing.
7. Mathews, C.S. and Russell, D.G.: "Pressure Build-up and Flow Tests in Wells", Monograph Series, Society of Petroleum Engineers of AIME, Vol. 1, Dallas.
8. Russell, D.G. and Truitt, N.E.: "Transient Pressure Behavior in Vertically Fractured Reservoirs", JPT, October, 1964.
9. Earlougher, R.C.: "Advances in Well Test Analysis", AIME Monograph, Vol. 5.
10. Cinco, H. and Samaniego, F.: "Effect of Wellbore Storage and Damage on the Transient Pressure Behavior of Vertically Fractured Wells", SPE Paper 6752.

T A B L E 1

Well Name	San Juan Basin Mesaverde
Perfed Interval	1618 m to 1639 m
Fracture Treatment	1.89 m ³ 15% HCl
Fracture Treatment	31750 kg 20-40 sand
Fracture Treatment	303 m ³ water
Depth of Interest	1628 m
Air Pressure	83 K Pa
Gas Gravity	0.5910 (Air = 1.000)
Mol Fraction CO ₂	0.023
Mol Fraction N ₂	0.001
Mol Fraction H ₂ S	0.0
Flow Hours	20.0
Wellhead Temperature	16°C
Reservoir Temperature	60°C
Critical Pressure	4695 K Pa
Critical Temperature	195 K

WELLHEAD PRESSURE K Pa	PSEUDO PRESSURE K Pa/s * E-15	ELAPSED TIME - HOURS - Δt
8060	5.37	Initial Pressure
7867	5.13	2 hrs. @ 29411 m ³ /D
7957	5.28	" " " 0 m ³ /D
7605	4.85	" " " 43976 m ³ /D
7846	5.13	" " " 0 m ³ /D
7322	4.55	" " " 58927 m ³ /D
7695	4.94	" " " 0 m ³ /D
7026	4.23	" " " 73341 m ³ /D
6274	3.46	12 " " 65865 m ³ /D
6481	3.67	.083
6557	3.74	.167
6612	3.80	.250
6647	3.83	.333
6681	3.86	.417
6715	3.90	.500
6750	3.94	.583
6764	3.96	.750
6805	4.00	1.000
6846	4.04	1.250
6881	4.08	1.500
6909	4.11	1.750
6950	4.15	2.000
6964	4.16	2.250
6984	4.18	2.500
7012	4.14	2.750
7033	4.24	3.000
7060	4.26	3.500
7080	4.29	3.750
7108	4.32	4.000
7136	4.34	4.500
7184	4.40	5.000
7536	4.80	6.000
7681	4.94	25.000
7763	5.04	49.000
8060	5.37	74.000

T A B L E 2

WELL EVALUATION RESULTS FOR A WYOMING WELL

TS = 16°C PS = 101.5 K Pa

Final M ³ /D	67196
Temp - °K	333
Net Pay - meters	8.8
Pore - meters	.664
Viscosity - Pa/s	.000014
Comp - V/V/K Pa	.000116
Square Root Slope	409E12
Horner Slope	2120E12
Shut-In Hours	59
Damage - K Pa/s	209E12
Dimensionless Damage	0.012
(KH) _a - μm ² /m	.01574
(KH) _a /KH	23.2+
KH - μm ² /m	.00068
K - μm ²	.000077
XF - meters	436+
(A+B) / XF	2.25+
M ² Drained	890308+
OGIP - M ³	53.0E6
Produced - M ³	8.2E6

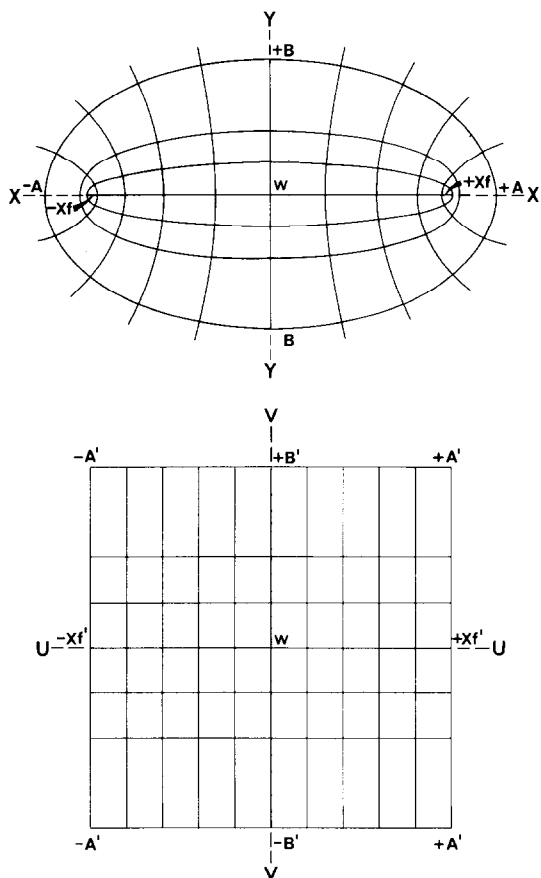


Fig. 1- Conformal transform of an Elliptical system.

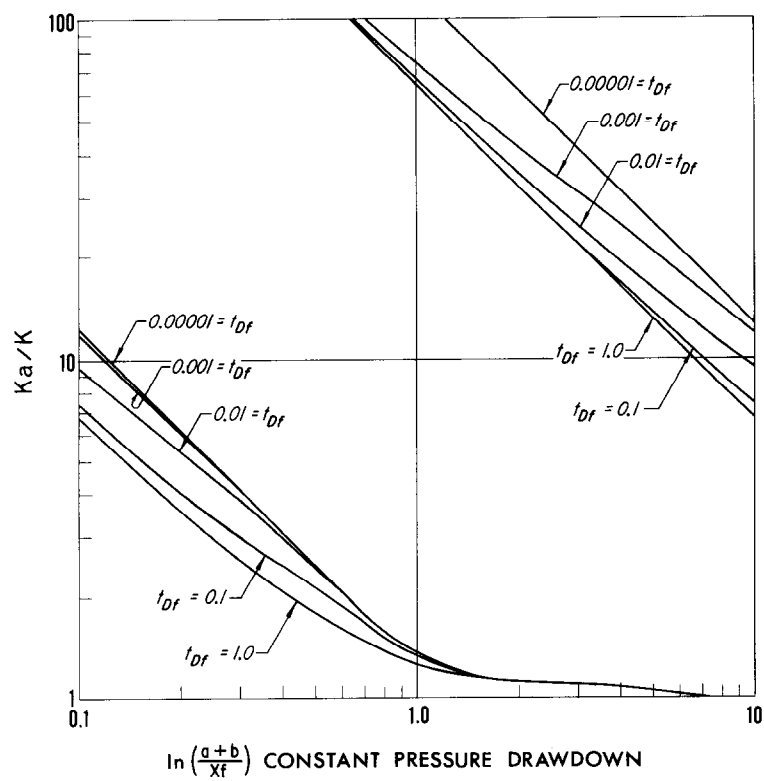


Fig. 2 - Horner permeability correction for Elliptical flow.

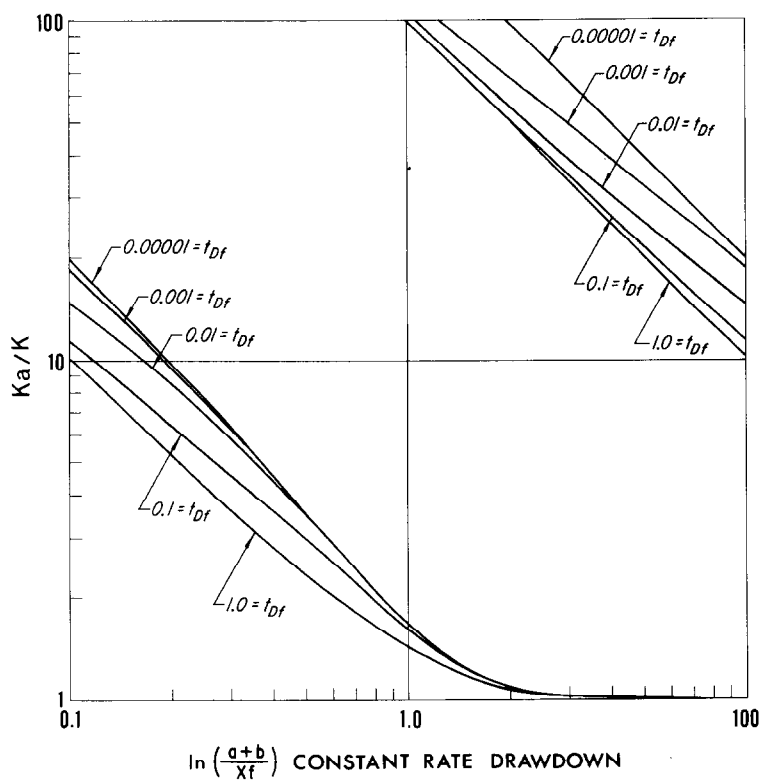


Fig. 3 - Horner permeability correction for Elliptical flow.

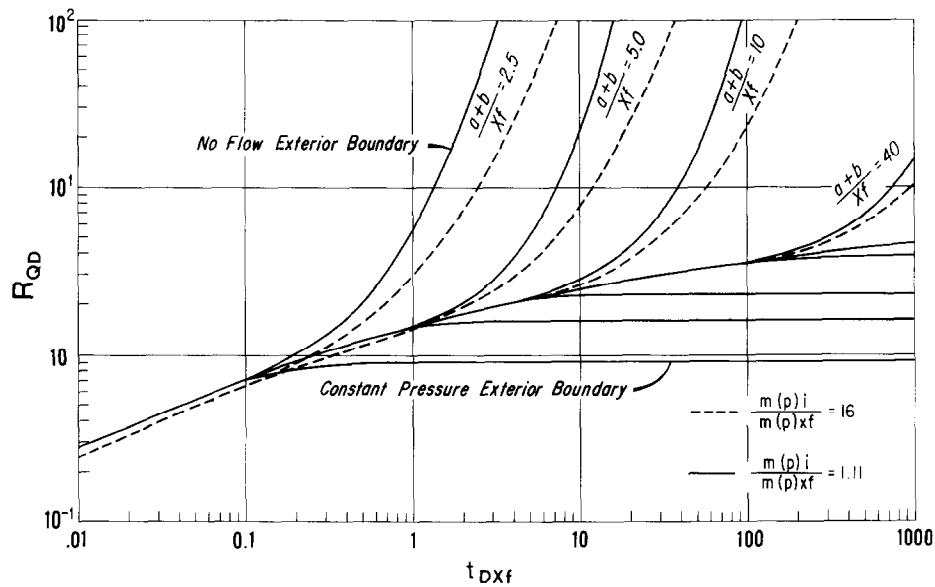


Fig. 4 - Reciprocal dimensionless rate for Elliptical flow.

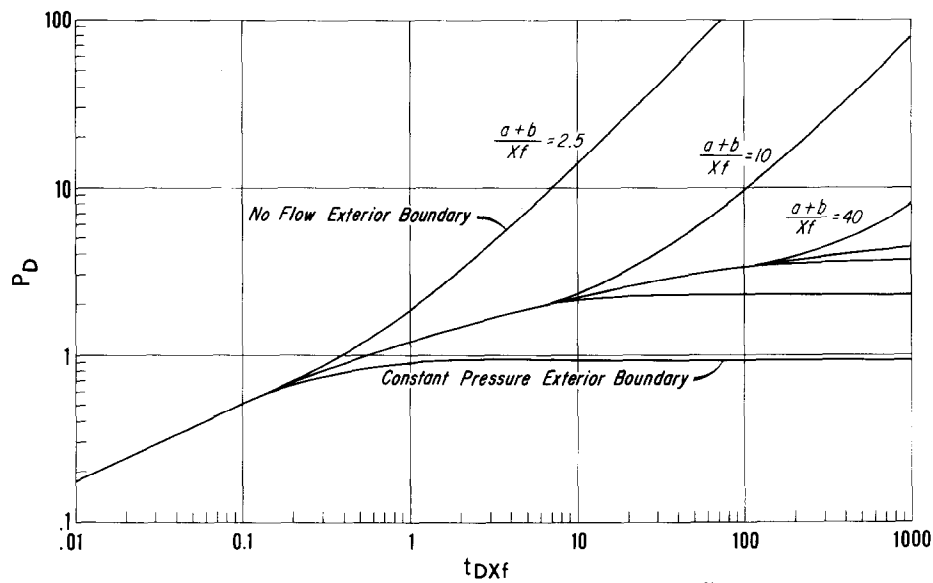


Fig. 5 - Dimensionless pressure for Elliptical flow.

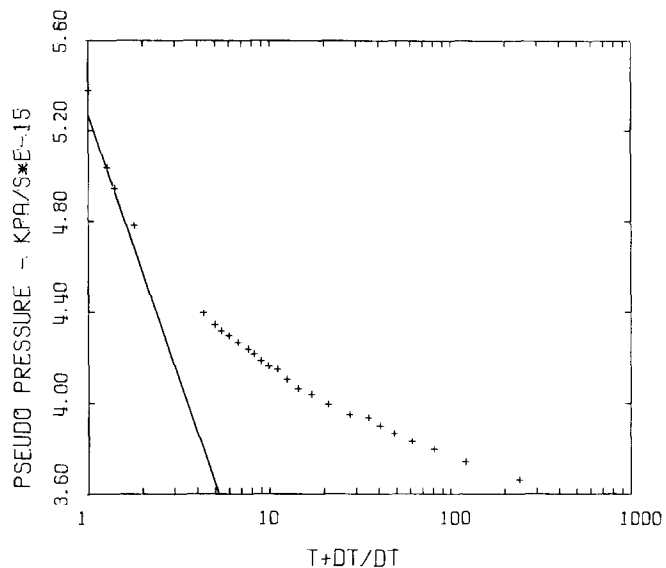


Fig. 6 - Horner plot for a San Juan Basin Mesaverde well.

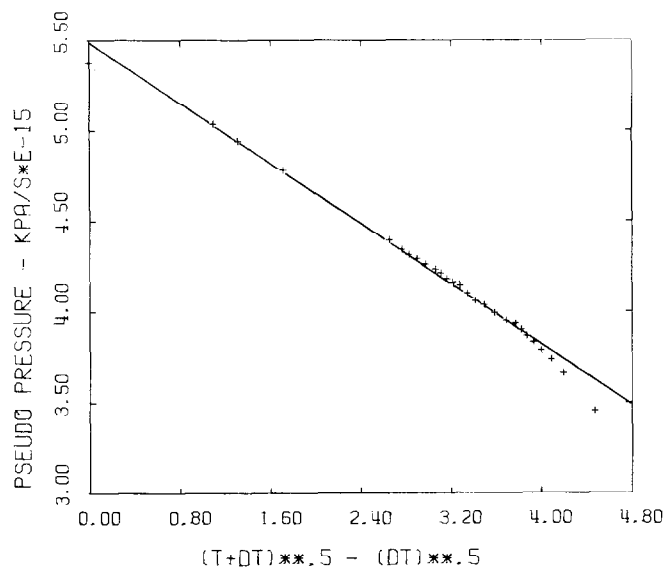


Fig. 7 - Linear plot for a San Juan Basin Mesaverde well.

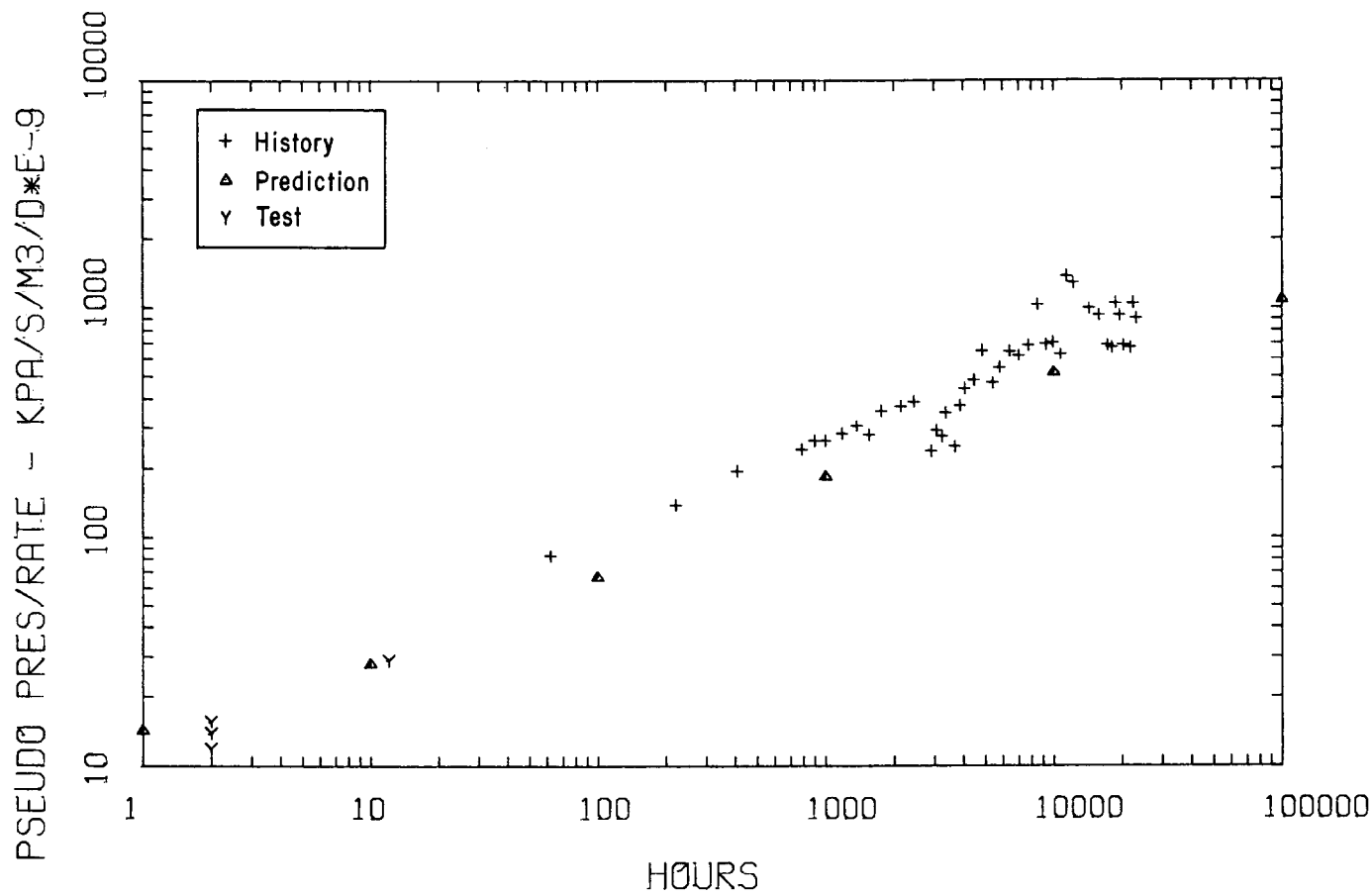


Fig. 8 - Production history for a San Jaun Vasin Mesaverde well.

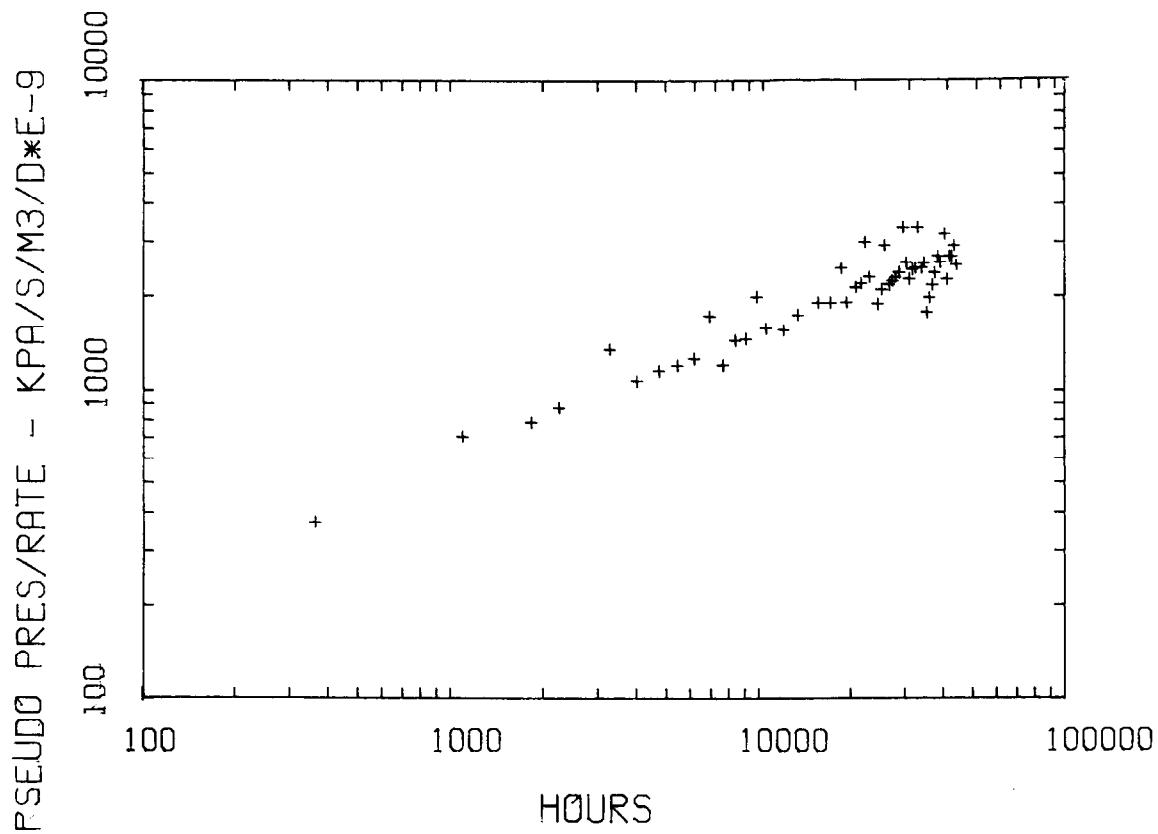


Fig. 9 - Production history for a Wyoming well.

AFTER THE TECHNOLOGY, WHAT HAPPENS?

by Timothy W. Merrill, Jr., Industrial Energy Services Co.

© Copyright 1980, Society of Petroleum Engineers

This paper was presented at the 1980 SPE/DOE Symposium on Unconventional Gas Recovery held in Pittsburgh, Pennsylvania, May 18-21, 1980. The material is subject to correction by the author. Permission to copy is restricted to an abstract of not more than 300 words. Write: 6200 N. Central Expwy., Dallas, Texas 75206

INTRODUCTION

An underlying premise to the Unconventional Gas Recovery (UGR) Program seems to be: given adequate technological solutions and proper economic incentive, the marketplace can accommodate any and all volumes of produced gas. My paper explores this hypothesis by examining the gas industry infrastructure as it exists today in the Appalachian Basin.

The UGR Program as structured by the Department of Energy (DOE) identifies four unconventional gas sources: methane recovery from coal beds, eastern gas shales, western gas sands, and geopressurized aquifers. The third category - western gas sands - may have evolved from a category which had been called "tight gas basins" in a report written by Lewin and Associates, Inc. (published in summary form in *The Oil and Gas Journal*, June 12, 1978, under the title "Vast Potential Held by Four 'Unconventional' Gas Sources.") On August 29, 1979 (Docket No. RM79-76) the Federal Energy Regulatory Commission (FERC) issued its Notice of Proposed Rulemaking in which it proposed to implement Section 107(b) and (c)(5) of the Natural Gas Policy Act (NGPA). Those sections of the NGPA charged FERC with setting incentive prices for gas produced under such conditions which present extraordinary risks or costs. The FERC has identified that gas produced from tight formations may indeed present such extraordinary risks and costs. Although the initial proposed rulemaking identified only western sand formations as qualifying for a tight sands definition, the tight sand definition guidelines would encompass - in some peoples' minds - certain Appalachian sands.

Thus, it might be argued that three of the UGR programs (methane recovery from coal beds, eastern gas shales, and "tight sand formations") have particular relevance for the Appalachian gas producing, transmission, distribution, and gas usage industries. To proceed with the technology of UGR without a thorough knowledge of these industries may constitute a major oversight. Why invent a perfect mousetrap if no one wants it? It is conceivable that the technology to produce Devonian shales will be established someday and the price "right," but the gas not be produced for lack of a market. If such a conclusion seems incredible, I

suggest that such a condition exists today. Conventional gas drilling programs in the Appalachian Basin are currently being either stabilized or reduced. Gas purchasers are not paying NGPA ceiling prices though we are all well aware that better than ceiling prices are being paid for other "commercial" sources of gas (Canadian, Mexican, LNG). The reason for such an apparent inconsistency lies not in any conspiracy theory or monopolistic domination, but in the history of Appalachian gas production and in its current industry infrastructure.

HISTORY

Few at this symposium need to be reminded that the gas and oil industry began here in the Appalachian Basin. However, unless one is currently participating in the Appalachian play, he probably is unaware - or is disparaging of - the extent of oil and gas activity in the Basin.

Soon after the turn of the century - or more specifically, Spindletop - the Appalachian oil and gas industry was consigned to the minor leagues. Hydrocarbon finds never or rarely equalled in volume the giants of the southwest. Pittsburghers, by providing the financial support for Spindletop, were in a way responsible for the inevitable march to the Southwest. The Gulf Building at the corner of Grant and Seventh stands as a significant symbol of the onetime national oil and gas industry dominance provided by Appalachians.

Those who remained continued to drill and produce oil and gas. Over the past 120 years, approximately 40 Tcf of gas and 3.1 billion barrels of oil have been produced from the Appalachian Basin. Relative to current national annual oil and gas consumption levels (20 Tcf and 6.5 billion bbls.) it is easy to see why the Appalachian Basin is not synonymous today with the oil and gas industry.

Yet such statistics hide two important facts: the Appalachian Basin's relatively high share of the total number of producing oil and gas wells, and the relatively small percentage of the Basin's potential which

References and illustrations at end of paper.

has been developed to date. About 42 percent of the country's producing gas wells and 17 percent of the producing oil wells are located in the Appalachian Basin. In 1978, 31 percent of all the gas wells drilled in the country were drilled in the Basin; and yet, historic and current production is only from 10 to 12 percent of the Basin's total volume of sediments according to one source.

Most "conventional" gas drilling in the Basin occurs in the shallow sands down to depths of three and four thousand feet in New York, Pennsylvania and West Virginia and to 6,500 feet in Ohio. These sands have long been considered marginal in that production is rarely greater than 200 Mcf per day in the first year of production and the decline curve is fairly steep during the first few years of production. "Conventional" drilling has gone to 'deeper' targets such as the Oriskany and Rose Run, and given the potential for higher prices, these targets are experiencing a renewed interest (see p. 149 *Oil and Gas Journal*, February 11, 1978 "New Finds Heat Appalachian Basin Interest"). Beyond these levels large potential hydrocarbon bearing sediments are believed to exist down to 20,000 feet.

CURRENT INFRASTRUCTURE

The Appalachian gas industry will be analyzed by a dissection that looks first to the participants, then to the pipeline network, and finally to the region's gas markets.

The participants in the Appalachian gas industry are the same as might exist in other gas producing regions, except for the size and distribution (or dominance) of several of the players. The dominant gas producers in Appalachia are intrastate gas distribution companies - the utilities. Also involved are interstate gas transmission companies, independent gas producers, major oil companies and industrial companies. Each of these will be examined below.

Intrastate gas distribution utilities are the corporate inheritors of those who built the gas industry. Natural gas was first utilized in Fredonia, New York back in the 1820's. It was produced from shales to light an Erie, Pennsylvania light house in the mid-19th century. In 1880 the Bradford Gas Company installed the first gas compressor stations and shortly thereafter the Peoples Natural Gas Company was bringing natural gas to Pittsburgh. These companies early established a dominance in gas producing leases and, by the extensive nature of their gathering systems, became the major gas purchasers.

As the gas industry moved toward the Southwest, corporate reorganizations affected the above mentioned early corporate identities. These "interstate" successors also established gas producing interests. At first gas was brought from West Virginia to Ohio, Pennsylvania or New York; ultimately gas was brought from the Southwest. Ongoing corporate organization and reorganization affected, and continues to affect, the character and function of the interstate and intrastate utilities. Thus, Columbia Gas Transmission - an interstate pipeline and part of the Columbia Gas System is an active Pennsylvania gas producer, while Columbia Gas of Pennsylvania - an intrastate utility - is not considered an active producer or purchaser. On the other hand, though the Peoples Natural Gas is a major Pennsylvania gas producer and purchaser, its sister-interstate-company, the Consolidated Natural Gas

Supply Company, is also a major gas producer and purchaser.

Both interstate and intrastate utilities obviously use corporate dollars in their production and development programs, although they will occasionally employ private capital in joint ventures. Along with being producers, these companies are the region's major purchasers. Indeed prior to the early 70's - aside from some historic anomalies - they were the only purchasers of Appalachian produced gas.

Appalachian Basin based interstate utilities annually make a difficult allocation decision which broadly affects the Basin's gas activity levels. I am referring of the deployment of corporate gas development dollars. For example, both the Columbia Gas System and the Consolidated Natural Gas Company were born in Appalachia and recognize the importance to their respective systems of Appalachian gas. Indeed, Columbia's Appalachian purchases and production were 111 Bcf in contract year 1979 (about 8 percent of Columbia Gas Transmission's total available gas of 1,433 Bcf). Consolidated purchased and produced 172 Bcf of Appalachian gas in 1978 (21 percent of its total supply of 838 Bcf). As an aside, if the Appalachian production and purchases of but two more utilities - Equitable Gas and National Fuel Gas - were added to the above, approximately 80% of Appalachian production is accounted for. These production and purchase efforts add up to a lot of wells and considerable dollars but still are a small part of each company's overall supply. Thus, corporate dollars must be spent elsewhere to secure the majority of supply volumes. Corporate investment is spent seeking gas in the Southwest, the Gulf of Mexico, the Rocky Mountains, the Arctic, Algeria . . . However, given that there is always a limited amount of dollars, it might be argued that development in the Appalachian Basin competes with development in the Rockies. The companies have the responsibility to see that corporate dollars are invested in the most productive manner - the most Mcf produced per invested dollar. Yet, whenever their Appalachian activity levels off or is curtailed, the gas drilling activity of the whole Basin is affected.

The third participant in the Appalachian gas industry are the oil companies. They are either integrated regional companies such as Quaker State and Pennzoil who are in the gas business only as a sideline for the search for Penn Grade crude oil; or majors such as Amoco, Cities Service and Exxon which have consciously staked out a role in the Appalachian gas play. The latter companies make more of an impact than the former, for they utilize their vast corporate development programs to push the unconventional into the conventional by exploring the deeper horizons and experimenting with new drilling and/or completion techniques. These companies are the region's true wildcatters. They stake out positions far from the pipeline network such that there exists all over the Basin wells they have drilled but - though average or better-than-average Appalachian wells - are simply too far from the utility system to actually hook into line.

The entrepreneurs or independent producers are, next to the intrastate distribution utilities, the most important participants in the Appalachian gas producing basin. They drill the interstate and intrastate utilities' farmouts, and oil company farmouts as well as their own acreage. Their numbers vary with

their fortunes but have been estimated to average 400 in Pennsylvania, 600 in Ohio and 400 in West Virginia. An individual independent producer may drill from one to one hundred wells a year, depending on the size of his organization, and the availability of rigs, leases, and dollars. One year he might be a gas producer; the next an oil producer; the next a drilling contractor; the next a leaseholder; or if business is bad, even out of the industry for a year or two. These independents are not to be confused with the independents operating in the Southwest. The average size organization is likely to be three to five people. Their emphasis is on leasing land and drilling wells. Indeed, in many cases, this emphasis has caused ongoing well operation not to receive warranted attention. Strong willed individuals running loose organizations, working long and difficult hours, directing all facets of the business - from leasing to right of ways, to fund raising, to making contracts, to sub-contract drilling, to overseeing logging, to directing fracs, to cleaning up drilling sites, to operating wells - characterize the Appalachian independent producer. In a few cases the independent producer is a drilling contractor and has a substantial organization. However, for the majority, the independent has a small office with but three or four people working for him.

The independent's main source of drilling money comes from the promotion of wells among private sources of capital. A simple partnership or complex joint venture might be the structure by which anywhere from a few - two or three - well programs to fifty well programs are structured. An independent's ability to raise money is all important to his business survival. Often that ability results from factors reasonably believed to be under his control: the geologic merit of his acreage, his tract record, reputation, etc. On the other hand, the ability to raise money is also affected by factors beyond the control of producer - most notably, the price to be received for the gas produced. These factors explain why the Appalachian independent does not step out too far from the existing gathering system. The Basin's marginality and the kind of drilling money which is available do not justify true wildcats that might be drilled far from the market and/or pipelines. The independent is forced to develop acreage by stepouts lest he lose his credibility and hence his sources of funds.

Appalachian producers have long felt that they have suffered disproportionately by the maintenance of low gas prices. With Appalachian gas volumes being marginal, higher prices have long been needed to stimulate investor capital. Of course, the pill has been especially bitter for those selling to intrastate utilities which have not been subjected to federal interstate wellhead price regulations - at least before the passage of the NGPA. As of the day that Act became law - November 8, 1978 - the so called high - unregulated - intrastate price in Western Pennsylvania was \$1.45 per Mcf - probably the lowest intrastate price in the nation.

Independent producers thus welcomed, with open arms, the newest Appalachian Basin participant - the industrial customers. In the early to mid 70's as the national natural gas shortage began to become more apparent, the distribution utilities began limiting deliveries to industrial customers. These limitations or curtailments grew to the point that industrial operational levels were threatened. Where an industrial could switch to an alternate fuel, he did so. But a number of industries and/or companies had

processes which required natural gas in order to operate. Those companies fortunate enough to have facilities in the gas fields, either drilled wells in their parking lots, or began to purchase gas from the independents. By offering a premium above either what the intrastate utilities were willing to pay or the interstate companies were able to pay, they quickly attracted many willing sellers. Simultaneously, various regulatory programs were developed by the utilities and/or their jurisdictional agencies allowing for the transportation of privately owned gas.

The independents obviously encouraged this new participant; the intrastate distribution utilities were forced by their respective supply situations to accommodate the new player; while the interstate pipelines benignly tolerated this new force in the Appalachian gas play. And now, with the shortage over - for a while, at least - the new player is not making any signs of rapidly departing the scene either - a fact of vague discomfort for both the intrastate and interstate utilities.

PIPELINE NETWORK

The gas pipeline network existing in the Appalachian Basin is probably similar to that of most gas producing areas. Gathering lines are likely to be interlaced with high pressure transmission lines and/or low pressure distribution lines. Ownership of the various lines follows that of the participants mentioned earlier. The transmission lines might be carrying gas through the Appalachian Basin to East Coast markets or to markets in the Basin itself. The gathering lines might be those of a utility or a private company. Conversely, some utilities have organized themselves as integrated systems with gathering lines, transmission lines, and distribution lines all interconnected; while others may be comprised of only distribution lines with all interconnecting facilities belonging to a separate corporate identity.

Directly in the gas fields, the lines that predominate generally belong to the companies who have been active in the area for the longest time. In Western Pennsylvania, that company is probably an intrastate utility, in Ohio and West Virginia both intrastate and interstate utilities dominate.

Capacity of lines in the gas field is often as much a function of the strength of the immediate gas market (especially if the lines are those of an intrastate utility) as the availability of capital to expand the system. A perennial system bottleneck will sooner or later be broken by pipeline enlargement, looping, etc., but if the system itself is limited by the size of the market, it makes little sense to enlarge a gathering system. Again, if the particular gathering system bottleneck feeds the interstate transmission system, it will be eliminated as the market demand of the interstate system calls for incremental volumes of gas. The important point here is that not all gathering systems (in Devonian Shale, coal mine methane and tight sand areas) feed the interstate system and, indeed, many are effectively blocked by more than miles from the interstate system.

GAS MARKET

Within the Appalachian Basin there exists a more or less normal gas market - except again for those characteristics resulting from age. Residential heating is relatively highly gas saturated.

This is significant, of course, because of the relatively high number of heating degree days in the region. Also within the region are areas of high concentration of industrial activity. Intrastate utilities serving these concentrations have uniquely high load factor annual sales.

It might be argued that 19th century New England and East Coast industrial activity migrated to the Appalachian Basin because of the availability of natural gas. In certain instances - the glass industry - it seems certainly to be the case; in other cases, obviously many factors were involved. Nonetheless, the post World War II industrial expansion in the Appalachian Basin was in a large part fueled by natural gas. The Big Inch and Little Inch pipelines were converted from oil to gas and many plants were built in the area to burn exclusively this cheap wonder fuel.

Indeed, the appropriate emphasis should be placed on both of the just mentioned adjectives - 'cheap' and 'wonder.' Gone was the need for complex and dirty fuel and/or residue handling equipment. And when the environmental consciousness was awakened, its ultimate value was perceived by many. But 'cheap' also continued to characterize natural gas. Few outside the industry took note of the infamous Phillips decision in 1954, for this fuel was far cheaper than any alternative and no one was worried about gas availability back then. The gas market seemed unlimited as the utilities took industrial orders, actively promoted area development projects, and aggressively competed with whatever the competing fuel happened to be.

As the signs of the shortage began to prevail in the early 70's the reaction was one of widespread disbelief. The industrial community could not comprehend how "all-of-a-sudden" there was no gas for current operations let alone growth. The commercial community grudgingly installed propane systems in new buildings, but was unprepared for shortages which forced conversions of heating systems to oil and even the shutdown of buildings. Initially, the residential community was affected by the shortage only insofar as those new homes which could not get gas heat. However, the longer term effect of the shortage on the residential community was more insidious from a gas marketing viewpoint. The constant appeals to conserve energy as well as the growing appreciation of the increasing cost of gas have resulted in a significant market development: appreciably less gas use per dwelling and/or building. Indeed, the utility industry is having to readjust procedures and accounting for the recovery of line extension and hook up charges since normal home usage no longer affords a reasonable pay-out.

In the industrial area, federal policy has evolved to the point wherein industrial gas consumption is viewed as being inherently bad and the industrial gas market openly discouraged. The current vehicle for this policy is a pricing program - incremental pricing - which is specifically designed - say some - to reduce the industrial demand for gas. Yet, incremental pricing is not supposed to immediately cause that demand reduction by forcing industrial conversions to oil. Rather, the program is designed to erode the industrial market over time so that when gas deregulation occurs, industrial demand for gas won't cause the "deregulated" prices to be bid up too far. The gas industry however, appreciates that load loss is just that, load loss, and is afraid that this forced downward trend in industrial consumption when combined

with conservation in the residential and commercial sectors are likely to leave them with plenty of gas and nowhere to sell it. Thus, it is appropriate to discuss a major gas supply improvement effort - the Unconventional Gas Recovery program - in the light of potential major market limitations or constraints.

UNCONVENTIONAL GAS RECOVERY COMMERCIALIZATION CONSTRAINTS

The UGR program can now be seen to potentially be limited by the operation of the Appalachian Basin gas industry infrastructure. Acting as constraints to full UGR exploitation in the Basin are: local and regional, as well as national, gas markets; the extent, capacity and ownership of gathering lines; and the number, organization, talents, and training of the important independent gas producers.

As has been shown in the prior discussion, gas markets have been heretofore primarily a function of price - especially as far as the industrial segment has been concerned. Usage in the residential and commercial sectors of the market, though perhaps initiated and stimulated by price (and perhaps convenience), is in an established market, a function primarily of weather. As stated above, the appeals for energy conservation are having increasing effects as will the various residential conservation programs which are being instituted per the direction of state public utility commissions and federal statute.

Usage in the industrial sector is no longer a function of simply the natural operation of price, but rather to an increasing degree a function of evolving social policy. Whether it is the enforced subsidization of residential and commercial costs imposed by state public utility commission regulation or the implementation of incremental pricing, artificial or non-market influences are affecting the industrial price of gas and hence demand for gas. Beyond such evolving price policies there exist also direct prohibitions on the use of gas in certain applications. The Powerplant and Industrial Fuel Use Act is specifically designed to get new and existing boilers off natural gas.

The premise of these programs is that since gas is a limited finite resource, its market must be limited or discouraged. A premise of UGR is that the finiteness of gas can be extended. These contrasting and conflicting premises are bound to clash from time to time and the Appalachian Basin may provide a battleground.

For example, it is entirely conceivable that this summer Peoples may be forced to shut in its own production and/or limit its local purchases. It may be forced into this action as a result of its gas storage being filled (because of winter weather last year), its industrial market eroded (due to recession and/or the operation of incremental prices), and its ongoing take or pay purchase commitments for gas volumes coming from the Southwest and/or Algeria. If coal mine methane or Devonian shale gas were flowing in the Peoples gathering system during such a cut-back, they too would be shut-in. There would simply be no place for the gas to go. It could not get into the interstate market if Peoples were the normal purchaser and/or developer. Its flow would be entirely dependent on the Peoples gas market and the other sources of gas supply to Peoples. But if the Peoples market has been eroded by national policy,

there simply will be no market for the coal mine methane or Devonian shale. Developers of this high cost gas may be unwilling to risk development when their market is not 'guaranteed.'

On the other hand, some might argue, the NGPA incremental pricing program is not designed to get the industrials off gas - only to insure that they preferentially pay for the higher cost sources of gas. Conventional wisdom is that in order to stimulate UGR we need not only to develop the technology, but also to offer incentive prices for the gas. For tight sands, FERC currently believes an 'incentive price' is one that bears some relationship to oil prices. Peoples then, may someday have to pay oil type prices for tight sand gas and turn around and sell it to its industrial customers at oil type prices plus their own costs. Is it not reasonable to believe that the industrial customer who can burn oil will do so and thus not be in the market for gas at or above oil prices (it may be difficult to keep industrial gas prices below oil prices).

The extent, capacity and ownership of gathering lines can act as an UGR commercialization constraint through the operation of the market as seen above. For a company with a declining market, there will be a natural reluctance to expand or extend gathering systems. An interstate company with an ample gas market may be miles from coal mines or shale wells. Indeed, the relatively small volumes obtained per well or location will make the gathering system investment relatively more expensive. The ability to recover such costs through the constant flow of gas then becomes even more important.

Finally, the important Appalachian Basin independent gas producers can act as a constraint to UGR commercialization. These are the people who will drill most of the shale or tight sand wells. Thus their numbers, organizations, training and talents become crucial to the full exploitation of UGR. Since they are involved in all aspects of the gas producing

business the independent producer is pivotal. If because of a drying up of drilling money and/or low gas prices, independent producers are forced to leave the business (as happened nationally during the 50's and 60's, then the reserve of talents and people to exploit UGR is diminished. A lower rate of conventional drilling activity will not only erode the people resources but also cause an erosion of available equipment (fewer rigs, etc.) and services. Hence this available talent pool is important for UGR programs.

CONCLUSION

Having focused upon constraints to commercialization of unconventional gas recovery, I nonetheless believe that the Appalachian gas industry can meet the challenges of UGR exploitation. However, it is important to see the countervailing impacts of national policy on the Appalachian gas industry infrastructure. The ongoing conventional drilling activity is important to future UGR. Current evolving gas policy should not discourage that activity. Strong regional and national gas markets are crucial to UGR programs. National policies which discourage gas markets - especially regional markets - are going to act as a severe constraint to UGR. Pricing policies to encourage supply will have an impact upon demand and those gas markets.

My fundamental point in addressing you today is to stress that the UGR programs cannot proceed in a vacuum. The market into which all unconventional gas must flow is as important from a policy point of view as is the development of the technology which will allow the gas to be recovered. The infrastructure constraints - once identified - can be overcome. Timing and realistic expectations will be all important. My concern is that once millions of dollars have been spent on technology and, say, the shale has been unlocked, frustrations may develop at the speed of exploitation. Frustrations can then - as they have done in the past - lead to punitive legislation and/or regulations - from which nobody benefits.

ECONOMICS OF DEVONIAN SHALE, COAL SEAM AND SIMILAR SPECIAL APPALACHIAN GAS SOURCES

by Richard M. Miller and Norman E. Mutchler,
Berger Associates

This paper was presented at the 1980 SPE/DOE Symposium on Unconventional Gas Recovery held in Pittsburgh, Pennsylvania, May 18-21, 1980. The material is subject to correction by the author. Permission to copy is restricted to an abstract of not more than 300 words. Write: 6200 N. Central Expwy., Dallas, Texas 75206

ABSTRACT

The natural gas curtailments during the winter of 1976-77 and the threat that gas interruptions would become a permanent way of industrial life sparked widespread interest in the investigation of local, higher-cost gas sources. Analyses of the technical, institutional, legal and economic constraints and opportunities associated with these gas sources located in the Appalachian Region were undertaken for the Appalachian Regional Commission. The economic potentials appeared encouraging providing certain constraints are removed and/or relaxed.

INTRODUCTION

Natural gas is an important fuel throughout the Appalachian Region. Yet only two of the thirteen Appalachian states produces sufficient gas to supply their own needs (Table 1). Understandably, then, industrial gas curtailments resulting from the natural gas crisis during the winter of 1976-77 stirred widespread interest among northeast industry and public officials to secure independent supplies of gas from sources located within the Region.

This paper describes the research and the report done for the Appalachian Regional Commission on the prospects and opportunities of marginal gas sources in Appalachia as they relate to maintaining and increasing economic development in the Region. Three categories of marginal sources were studied -- gas from coalbeds, Devonian Shale and other difficult sources. The latter category included other low permeable gas formations, deep drilling and gas from Lake Erie.

This was primarily an institutional-type study of governmental energy and non-energy programs and activities and the actions of the private sector. Technical, economic and institutional factors were analyzed from the standpoints of the literature, many and varied interviews, and from case histories to try to discover the encouraging and constraining aspects to greater expansion. Based on these factors

estimates of the potentials of the difficult gas sources were made under existing and improved price/cost relationships.

THEORY AND DEFINITIONS

The term marginal gas source is used to describe a 'higher cost' gas. The reasons that a gas source(s) may be high cost are many, varied and often interrelated. Technical, geologic, institutional and attitudinal factors frequently combine in some way to adversely affect the profitability of recovery and the economics of using a marginal gas source. Such are the circumstances with regard to exploiting the relatively abundant Appalachian gas resources from coalbed methane, the Devonian Shales and gas from other difficult Appalachian sources.

GAS FROM COALBEDS

The reasons that this resource has not been utilized are many and varied:

- ° Legal ownership problem
- ° Coal operator attitude toward utilization
- ° Profitability
- ° Other institutional factors including regulatory
- ° Technical
- ° Safety

Profitability has not been established in the minds of many coal operators, even some who have previously cost-shared projects with the Bureau of Mines. This is probably due to the marginal economics and the experimental nature of the few projects underway or completed. Utilization suffers from limited replication of successful demonstration projects.

Technology in general exists for utilization but needs scaling down in most cases for this lower volume, lower gas pressure source. Except for a few pipeline injection projects and a few current experimental projects there are not many examples of utilization.

References and illustrations at end of paper.

GAS FROM DEVONIAN SHALES

Devonian Shale wells are typically low permeable, low productivity, long-lived wells. The main factor appears to be fracture permeability. By some estimates only about four percent of the gas is recovered under present technology in the better Fields.

There are an estimated 9,615 producing wells (P. J. Brown, 1976) in eastern Kentucky (70 percent of state gas production), West Virginia, Ohio and Virginia.

Fifty-five percent of Devonian Shale production is estimated to be by utilities, 40 percent by independents, and less than five percent by producer-consumers.

The main constraints against expansion of this source are:

- Long payback period to recover investment
- Low price of gas
- Rising well completion costs
- Need for improved technology

The total in-place Devonian gas resource has been estimated to range between 500 to 600 tcf in the Eastern United States.² Such an abundance of gas cannot rationally be ignored by the numerous energy deficient eastern industries.

GAS FROM OTHER DIFFICULT SOURCES

Historically, exploration and development of natural gas in Appalachia has been essentially in the areas of known, easily recovered gas fields. Records indicate that over 590,000 oil and gas wells have been drilled into the Basin. Further, the gas wells average 3,700 feet in depth and 84 percent of accumulated natural gas production has come from Pennsylvanian, Mississippian, and Devonian Formations. Correspondingly, 85 percent of known Appalachian gas reserves lie in the same regions as the above formations.

A difficult, low permeable formation is generally defined as one having a permeability less than 1.0 millidarcy and an effective porosity of less than twelve percent. An examination of formations throughout the Basin reveals that such characteristics are common. However, a gas-bearing horizon could be an excellent producer in one field and yet be a relatively impermeable rock as close as a few miles away.

Drilling and completion technology for the low permeable formations is similar to that discussed for Devonian Shales. Of course, the stimulation method design will vary for individual well parameters, while drilling techniques will be more standard.

The deeper Silurian, Ordovician, and Cambrian rocks have not been adequately explored. Deep well drilling does have one additional problem. In 1977, the Hughes Rig Count showed 223 rotary drills in the entire Northeast Region of the United States, but only eleven were capable of drilling beyond 10,000 feet.

Lake Erie offshore drilling is a difficult source (i.e. marginal) because of the various state

legislative and environmental actions, rather than because of any problems with technology. The operational Canadian offshore rig count in the Lake is presently limited to about one-half dozen. Water depth, projected well depth, and rock pressures will not require the larger more powerful and costly operations used in the Gulf or Outer Continental Shelf. Low permeable sources such as the Medina Formation will be the main target.

The initial economic objective was to determine the wellhead prices that would induce significant expansion of production of each of the marginal gasses. Production history data was collected from numerous reports (Reference 3 is illustrative of the documented research) and from other case history data that was gathered by interviews. The economic investigation of the potentials of the three marginal gas sources, however, could not be conducted without considering the critical non-economic factors. The projections that are presented, then, incorporate judgmental assessment of the non-economic factors.

ECONOMIC PROJECTION RESULTSGAS FROM COALBEDSCost

Although Bureau of Mines' investigators are reportedly encouraged by the economic potential of the vent shaft/horizontal borehole production method, it suffers from an extremely limited cost data base, since the Bureau/Eastern Associated Coal Corporation project was experimental. Consequently the costs used for the return on investment analysis were those associated with the vertical borehole, a widely used oil and gas development technique.

The cost range depicted in Table 2 corresponds to variations caused by subsurface and surface conditions and other site specific locational factors including accessibility, and also variable charges for drilling by producer type. Since the data base was so limited it was decided that average costs would be the best indicator throughout the Region and, therefore, a more reasonable measure of potential profitability. A second reason for choosing average costs, as presented in Table 2, was the consideration that future development would appear to have the greatest potential among the larger coal operators whose costs would tend to correspond with high overhead utilities. This result, notwithstanding continuing coal operator reluctance, was the consensus of those interviewed during this study, especially utility representatives. Yet there is an additional modifying condition that would suggest lower cost production. It is generally agreed that the economics will only be improved on a production basis, say field development of 25-50 wells, where economies of scale would result in lower per well costs. Hence, although indications are that the higher overhead coal companies are likely to be the prime developers of methane gas resources, it is also apparent that significant expansion would be on a scale sufficient to affect some cost reduction. The average price condition shown in Table 2 satisfied both conditions.

Production

Production data are presented on the basis of typical high and low yield methane wells (Table 3). The production data pertain solely to removing methane from coalbeds in advance of mining by surface vertical boreholes. The production profiles reflect composite coalbed degasification experience from a group of wells in the Pocahontas No.3 and Pittsburgh Coalbeds.^{4,5} The production profiles represent wells that include stimulation and continuing decline over the 15 year analytical period. It is recognized that in an actual field project individual wells could vary widely from the norm.

Results and Projections

The analytical results of the discounted cash flow - return on investment computations are presented in Table 4. The results show that production from a higher volume production well is economically viable at all prices. Unfortunately, experience is unable to provide assurance of achieving production volumes as presented in this case. The high volume producer represents limited operating experience in the Pittsburgh coalbed where natural fracturing has created unique production circumstances.

For the lower volume production example it would not be economically feasible to develop this resource at the lowest price. At a price of \$2.00/mcf the investment achieves marginal acceptance. At \$3.00/mcf the lower volume producer is an attractive investment.

Although various demonstrations have shown that production is generally improved through stimulation -- too little is known at this time of its potential for increasing methane production (or the effect of stimulation on the mine roof and floor). Many more demonstrations encompassing a broader geological and geographical area are required before definitive results can be reported.

Nevertheless, higher wellhead prices would conceivably improve the economic attractiveness of this marginal source. Assuming that the lower volume example has a higher occurrence probability, then an increased wellhead price could have the effect of expanding the recoverable reserve base for methane gas recovery.

To date, slightly less than three bcf of methane gas has been produced for commercial sale. Approximately one-half has been produced from 23 vertical borehole wells over a 29 year period. And, slightly less than half was produced from two demonstration vent shafts with horizontal boreholes -- one of which produced gas for sale over a 2½ year period while the other was productive for about 1½ years; the approximate remainder has reportedly been produced by several coal companies on a very limited basis.

Since these few examples are insufficient evidence of potential opportunities, the approach to estimating future reserves must otherwise depend on judgmental analysis.

Coal operators will extract methane gas, but they will be reluctant to utilize it. At 1977-78 gas prices the market value of the coal was about 100 times the value of the gas. At \$2.50/mcf it

would still be 60 times greater, and given the same percentage of profits from coal/gas, the increase in profit would be only 1.5 percent.

Furthermore, at higher prices that apply equally to all gas sources, the relative economics are in favor of expansion of conventional sources. A higher price for all natural gases would generally not alter the relative attractiveness of difficult source gas as compared to conventional gas. Understandably, then, deregulation affecting all gas sources, or simply a higher ceiling price for all gas, would in general result in considerable exploration and development of new conventional Appalachian gas and the potentially much larger volume of off-shore gas in the Gulf of Mexico, and similar conventional gas sources.

This probable pattern of natural gas exploration and development is not meant to indicate that no expansion would occur in recovering methane gas. Obviously, a higher natural gas price would improve methane extraction and utilization profitability, and as a result some coal operators might be encouraged to reexamine methane opportunities.

It has been estimated that the cumulative Appalachian Region coal production between 1973 and 1990 may be 14.2 billion tons.⁶

The West Virginia - Pennsylvania area features many characteristics favorable to methane extraction:

- Large coal reserves
- Considerable present and future mining activity
- Extensive pipeline system (especially in the northern sections)
- Large sized coal and utility companies

It is, therefore, the 'best' candidate for the development of methane extraction expansion within the Appalachian states. At present 100 million cubic feet per day (or approximately 36 bcf per year) of methane is wasted to the atmosphere from the Pittsburgh vein alone. If over the next 20 years ten percent of the total 700 bcf of methane were to be recovered for commercial application then 70 bcf of methane would be added to the producible reserves. Considering that a vertical well has about a 20 year life and total producible reserves of 120 mmcf, then the 70 bcf of methane could be recovered with 600 wells. Similarly, a vent shaft - horizontal hole recovery system has about a five year premining life span and 1,000 mmcf producible reserves and, accordingly, 70 vent shafts would recover the 70 bcf producible reserves.

Alternatively, eight groups containing 50 vertical wells spaced at 1,000 feet intervals, and including 22 premining vent shafts with 6,000 lineal feet each of horizontal boreholes would be sufficient to recover this volume of methane (70 bcf). There are at least eight large operators or utilities with mining operations of sufficient size to achieve this minimal recovery rate.

Extrapolating this approach to other major coal seams, such as the Mary Lee Vein (Warrior Basin) in Alabama and relating the methane recovery to the estimated coal production would add considerably

to the methane gas producible reserve base. As noted, Appalachian coal production may total more than 14 billion tons over the next 20 years. Assuming on the average that each ton of coal contains 300 cf of methane gas, then approximately four tcf of methane gas would be contained in the coal. Considering also that ten percent of the methane contained in this coal might be recovered prior to, during and following mining, then approximately 400 bcf of methane could be added to the producible reserve base.

Figure 1 - Projected Appalachian Methane Gas From Coalbeds, illustrates the two prospective outcomes supported by a higher gas price and estimated coal production. Relating methane extraction to the anticipated coal production over a 20 year period can be supported on various fronts. Future coal production will largely be extracted from deeper, gassier seams causing increased ventilation costs and increased risks to the safety of the miner. Mining productivity would also be affected through mining in gassier seams. Coal operators could, therefore, be attracted increasingly to extracting the methane, but it will be a gradual process as they begin to utilize more of the gas, perhaps through further increases in gas prices.

At a price level of, say, \$2.50/mcf the opportunity will be present to induce the necessary experimentation. At this price other constraining factors, especially the gas rights issue, might be resolved through cooperation, especially with succeeding gas price increases. While any estimate of future producible reserves must necessarily be based on factors other than experience -- such as future mining activity -- it would appear that the required technology refinements while numerous, do not need to be major.

GAS FROM DEVONIAN SHALE

Costs

Costs to develop a Devonian Shale well can vary widely due to geologic and topographic conditions, accessibility, labor rates and work rules, overhead, etc. Table 5 presents cost data for Devonian Shale producers based on information contained in the literature and supported by discussions with company officials as covered under the case studies.

Producers of Devonian Shale gas must stimulate their wells. The two most common methods of stimulating a well are by shooting, or normal hydraulic fracturing with primarily water-based fluids. The stimulation method employed would appear to depend principally on the past practices and experiences of the producing company with one particular technique. Stimulation costs range between \$5,000 and \$150,000 per well. The lower costs represent nitroglycerin shots and the \$150,000 is indicative of the cost of a Massive Hydraulic Fracture (MHF). Normal hydraulic fractures are estimated at about \$10,000 to \$20,000 per well.

Annual operating costs, including maintenance, generally fall within the range of \$500 - \$2,000 per well. Again individual circumstances and operational maintenance practices determine these costs, but it would be unlikely that any operation costs

would be outside this range. There is not sharp difference between the operating costs of the three producer types.

Production

Production data have been obtained from the case study data. The figures shown in Table 6 represent a typically good producing well, experiencing peak production normally three to five years following stimulation. The use of a typical good producing well performance profile is not intended to infer that similar production is not geographically constrained. The reported ranges of well life production are 250 to 460/mmcf. In fact, considerable variability of production can and does occur between wells even at the same location. However, since the prime purpose of this analysis is to compare the investment potentials of the various producers, it is convenient to calculate the return-on-investment employing a single production environment. The production data used is taken from the present gas producing areas.

Results and Projections

The analytical results of the discounted cash flow - return on investment computations are presented in Table 7. The columns depict the four price alternatives selected for this analysis. The row entries include the alternative investment costs for normal hydraulic fracturing. The entries in the body of the Table are after-tax returns on investment (ROI in percent) based on a typical production profile, the alternative price levels, and the associated revenue - cost profile.

This analysis considers a profitable investment opportunity for ROI's, after taxes, of ten percent or greater.

The Table clearly illustrates why Devonian Shale gas is a marginal source. At a price of \$1.42/mcf (regulated gas price at the time of the analysis) Devonian Shale development is not economically justified. At a price of \$1.75/mcf it is only a marginally attractive investment for the low cost producer. As the price reaches a level of \$2.00/mcf and above, the return generally is sufficient to warrant the investment.

These analytical results generally conform to the operating experiences occurring at the time of the analysis. The principal producers were those firms -- independent and utility -- whose development costs were generally compatible with that depicted for the low cost investment. Possibly because of the location, the costs of one of the largest single producers from the Devonian Shales -- Kentucky-West Virginia Gas Company -- are generally lower than that reported for other utility companies. Their lower costs for development may also be attributable to the fact that they are quite experienced in developing this source. Smaller independent producers experienced in the Devonian Shales also have costs below the average.

Alternatively, as reported, the higher cost producers, mainly the larger utilities, were not developing this source since the return did not justify the investment at current prices. This result is

borne out by the findings in Table 7 which similarly illustrate that the current price level did not justify the investment for average or high cost producers.

The producer-consumer is a special category of producer type not necessarily guided by price considerations, but rather by assurances of supply. The data base on costs for the producer-consumer type was inconclusive. Consequently, any comparison relative to the cost data used in the rate of return analysis is not possible.

It is also noted that the results of the study conducted by the Office of Technology Assessment (OTA) were comparable to those presented in this report.⁷ In that study, a price level of \$2.00/mcf was the lower limit warranting significant expansion of these resources, essentially the findings of this report. The cost estimates used in both reports are essentially the same.

In the absence of total natural gas deregulation, or deregulation applying only to unconventional sources, Devonian Shale production should, nevertheless, expand due to the recent gas price increases. Such a conclusion was supported by evidence that showed Devonian Shale well development increasing slightly in response to higher prices. However, expansion based on existing price ceilings and technology would be limited to less than one tcf over a 20 year period. The principal constraints limiting further expansion are a low rate of return relative to conventional sources, development difficulties, and higher costs and risks associated with deposits lying outside the already densely developed 'better producing' brown shale areas.

Significant and immediate expansion in the short term would be limited by geological and technological constraints and the available drilling industry capacity. Consequently, the approach in determining the economically recoverable reserve base involves a comparison of alternative scenarios as shown on Figure 2.

Total well drilling in the four state area including West Virginia, Kentucky, Ohio and Pennsylvania had been increasing at an annual rate of about twelve percent per year. Devonian Shale well completions in the same period averaged a little less than three percent of total well drilling. Based on the available data, it is estimated that approximately 5,300 wells were drilled in the four states in 1976. Therefore, an estimate of 1976 Devonian Shale well completions would be on the order of 150 wells.

Expansion of Devonian Shale reserves can be anticipated to occur in two phases. Phase 1 represents the potential expansion under alternative pricing policies. The response from a higher price should be visible within three years. Phase 2 represents a much larger potential increase in reserves based on substantial technological improvements, particularly with improvements in stimulating the less permeable grey shale formation intervals. Department of Energy test drilling and core analysis have already shown that natural gas exists in the full column of the grey shales and not just in the rich brown shales. However, the higher tensile strength makes them harder to fracture than the brown

shales. Major technology improvements on a routine commercial basis likely would not be available until about 1988 -- at which time the current DOE Eastern Gas Shales Project will have been concluded. Both phases are shown on Figure 2 and discussed below. A 20 year period is considered.

Phase 1 (First Ten Year Period)

Three different pricing options are considered in Phase 1. In all three cases, no significant technological changes are anticipated to occur. Hence, any substantial increase in Devonian Shale reserves would result from price increases and other non-technological factors. Development during this phase would be expected to continue largely in the traditional naturally fractured brown shales.

Base Case (Scenario 1)

The base case represents the existing gas production environment, except that a ceiling price for all natural gas is set at \$2.00/mcf. As shown in Table 8 a \$2.00/mcf price ceiling would result in about 14,400 Devonian Shale wells and an increase in the reserve base of approximately four tcf over a 20 year period. The majority of the annual production would occur in the 'better producing' naturally fractured brown shale areas, but some production would be induced in the lesser quality adjacent areas (brown shale with somewhat less natural fracturing). A higher reserve base has not been anticipated since, given a choice of conventional vs. Devonian Shale gas at no price differential, it is most likely that producers would continue to concentrate on conventional gas.

The number of new wells estimated by applying recent growth trends (14,400 wells) have been found to correspond in a different approach with well potentials on an areal basis (14,200). For the base case, then, additional reserves can be added without technological improvements and with present drilling industry capacity.

Deregulation of All Natural Gas (Scenario 2)

The deregulation of all natural gas would not immediately nor substantially improve the opportunities for developing the Devonian Shale deposits, since it would still have a profit disadvantage relative to conventional gas sources. The most likely occurrence, in this case, is that significant Devonian Shale expansion would occur following the 'peaking' of conventional gas resources. In other words, increasing the gas prices will increase gas production for a period of time and then start a downward trend. It is believed under this Scenario, with all gas priced equal, that major Devonian Shale exploitation would occur along with many other difficult sources at the time of the downward slide.

Total deregulation, estimated at about \$2.25/mcf would, however, result in further expansion of Devonian Shale gas as shown on Figure 2 (Scenario 2). The increase shown represents a slight upward shift of the curve corresponding to the base case conditions.

Since deregulation would entail expansion of the entire natural gas industry, the response would

be somewhat delayed for difficult source gas, hence a three year lag represents the time required before the effects of deregulation might be visible.

The 20 year increase in recoverable reserves has been estimated at seven tcf.

Deregulation of Devonian Shale Gas (Scenario 3 and 3A)

Like the base case and total deregulation, the effect of deregulation of Devonian Shale gas only essentially represents a stimulant to development with current technology. In this case the natural gas price is considered to be at a level of \$2.00/mcf while the price of Devonian Shale gas is \$2.50/mcf. Therefore, total gas industry expansion in the Appalachian Region is assumed to grow at the same rate used to calculate reserves in the base case. However, the economic disadvantages pertaining to Devonian Shale gas would be removed and, as a result, added incentive is provided in expanding drilling for Devonian Shale gas relative to conventional sources.

It has already been mentioned that additional production would have to come from areas other than the so-called 'better producing' areas. However, the bulk of the production would continue to come from these areas with more intense well spacing both within the area and nearby. This need not be a subject of probability, because a massive Devonian Shale characterization program is underway involving most of the affected State Geological Surveys and coordinated by the U.S.G.S. Together with improved remote sensing, aerial and ground surveys and other techniques for locating joints and lineaments, expanded promising areas should be known somewhat before the beginning of the second decade. For this reason, this portion of the curve is shown as Scenario 3A on Figure 2.

Known recoverable reserves would increase to 17 tcf between now and 1998.

Technological Improvements (Scenario 3 and 4)

The significant contribution of Devonian Shale gas cannot be achieved without techniques that would either lower costs, increase gas production, or both, along with a higher gas price to increase profit margins. The ARC study compared the geographically limited naturally fractured brown shale areas with the much larger geographically distributed deposits of non-fractured brown and grey shales. These latter shales are variously labelled light grey shales, grey shales, or greenish-grey shales. In order for these less permeable locations of shale to make a significant contribution, it would be necessary that technology be advanced, principally in the area of new or improved techniques to stimulate the grey shales and, of course, non-fractured areas of brown shales. However, it should be pointed out that such a technical breakthrough for economical high productivity stimulation technology is by no means assured. However, the potential warrants the effort. According to DOE, as much as 150 tcf of Devonian Shale gas could possibly be added to the nation's producible reserves.

Figure 2 shows that an economic technology breakthrough in stimulation technique would substantially accelerate the producible reserves beginning about 1988. DOE's \$80 million, eight year research program is directed toward achievement of expanding producible reserves through technological improvements and defining the resource.

GAS FROM OTHER DIFFICULT SOURCES

This category covers all other known marginal gas sources located in the Appalachian Region and includes: (1) other low permeable formations; (2) deep drilling; and (3) offshore drilling in Lake Erie.

Other difficult source wells would involve one or more of the following characteristics:

1. Targeted horizons are below or remote from those normally sought.
2. Stimulation requires special design considerations.
3. Drilling requires non-standard technology.
4. Production volume sold is low compared to investment involved.
5. Statutory or regulatory restrictions prohibit or hamper development.
6. Low success ratio.

Because of the general similarities to Devonian Shale well development -- geophysical, technological and economic -- the potential of broadening the economically recoverable reserve base would be comparable to the potential opportunities for the Devonian Shales.

Accordingly, at a price of \$2.50/mcf with deregulation of difficult source gas only, the potential producing reserves over the next 20 years from 'Other Difficult Sources' may be in the range of 20-30 tcf, or an average of 1 to 1.5 tcf per year. The bottom of the range (20 tcf) essentially corresponds to the potential from Devonian Shale. The similarities between the Devonian Shales and the slightly more attractive low permeable shallow well gas sources permit an order-of-magnitude estimate for "Difficult Sources" that corresponds to the more rigorously derived Devonian Shale estimates. The upper range (30 tcf) is a very tentative estimate reflecting the growing interest and hopefully potentials in deep well development, tight sandstones (and some limestones).

It is noted, however, that the potentials for expanding the recoverable reserve base may be slightly higher in this category (20-30 tcf over 20 years) for the following reasons:

1. 'Other Difficult Sources' encompasses all other marginal gas sources at various depths -- shallow to very deep.
2. Low permeable shallow wells, such as those in the Berea, Clinton, Medina, etc., have 'quick flush' and slightly greater yields.

3. Ohio, a major Appalachian industrial state, is encouraging greater expansion of both low permeable shallow wells and deep wells. In the four years since its inception, the results -- in terms of increased drilling -- are quite noticeable.

4. Deep well drilling, while a high risk venture, may pay off in the discovery of large volume reserves.

A producing reserve of 20-30 tcf over a 20 year period would require the completion of approximately 50,000 successful wells (over 70,000 total drilled wells assuming a 70 percent success ratio). The 50,000 wells are based on the presumption that most of the reserve would be produced from low permeable shallow wells each producing about 400 mmcf over a 20 year life span.

Recoverable reserves from approximately 50,000 wells would range between 20-30 tcf between now and 1998 with deregulation of difficult source gas only and current technology. Again, the higher figure (30 tcf) reflects the potentials primarily in deep drilling.

CONCLUSIONS

Estimates of marginal gas source development in the Appalachian Region must be largely judgmental due to the many non-economic constraints to expansion. Nevertheless, a more favorable gas price should promote expansion since the economic inducement should encourage the elimination of the non-economic barriers. As intended in performing the study for the Appalachian Regional Commission the economic considerations were presented so as to derive appropriate programs.

ACKNOWLEDGEMENTS

This paper is based on work completed as part of the Appalachian Regional Commission Report,

ARC 77-2-CO-5246, "Study on Devonian Shale, Coal Seam and Similar Special Appalachian Gas Energy Prospects and Opportunities".

The work was under the direction of Dr. David R. Maneval, (former) Technical Project Officer and Science Advisor, and Dr. John J. Demchak, Director, Natural Resources Division, Appalachian Regional Commission.

REFERENCES

1. Brown, P.J.: "Energy From Shale - A Little Used Natural Resource", National Academy of Sciences, FE-2271-1, 1976, pp.86-99.
2. Avila, J.: "Devonian Shale as a Source of Gas", Chapter 5, Natural Gas From Unconventional Geologic Sources, National Academy of Sciences, 1976, p.113.
3. TRW Energy Systems Planning Division: Systems Studies of Energy Conservation, "Methane Produced from Coalbeds", 2 Volumes, McLean, Virginia, January, 1977.
4. Cervik, J. and Elder, C.H.: "Removing Methane from Coalbeds in Advance of Mining by Surface Vertical Boreholes", Reprinted from Proceedings Conference on the Underground Mining Environment, University of Missouri - Rolla and Bureau of Mines, October 27-29, 1971.
5. Production profiles of Equitable Gas Company Wells in Wetzel County, West Virginia.
6. Miernyk, W.H.: "Coal and the Future of the Appalachian Economy", Appalachia, October-November, 1975, pp.29-35.
7. Congress of the United States, Office of Technology Assessment, "Status Report on the Gas Potential from Devonian Shales of the Appalachian Basin", November, 1977.

TABLE 1

NATURAL GAS PRODUCTION AND USE
WITHIN
APPALACHIAN REGION - 1976

<u>State</u>	<u>BILLION BTU</u>	
	<u>Natural Gas Production</u>	<u>Natural Gas Use</u>
Alabama	1	161,748
Georgia	0	46,627
Kentucky	63,375	26,910
Maryland	75	9,164
Mississippi	1,619	54,455
New York	752	25,515
North Carolina	0	21,334
Ohio	40,996	104,048
Pennsylvania	89,975	274,583
South Carolina	0	38,795
Tennessee	26	124,661
Virginia	6,937	11,568
West Virginia	146,311	104,276
Totals	350,066	1,003,600

Source: Brookhaven National Laboratory, The Energetics of the United States of America: An Atlas; American Gas Association, Natural Gases of North America, Vol.2; and Berger Associates.

TABLE 2

TOTAL ESTIMATED METHANE RECOVERY COSTS PER WELL
(1977 Dollars)

	<u>Utility</u>	<u>Large Independent Producer/Large Producer-Consumer</u>	<u>Small Independent Producer</u>
<u>Vertical Borehole Method</u>			
Extraction Cost	\$52,000	\$ 52,000	\$33,500
Collection System Cost	\$14,300	\$ 14,300	\$ 6,300
TOTAL, DEVELOPMENT COST	\$66,300	\$ 66,300	\$39,800
Operation and Maintenance (Per Year)	\$ 1,000	\$ 1,000	\$ 1,000
<u>Vent Shaft With Horizontal Borehole Method</u>			
	N/A		N/A
Extraction Cost		\$566,000	
Collection System Cost		\$ 60,000	
TOTAL, DEVELOPMENT COST		\$626,000	
Operation and Maintenance (Per Year)		\$ 2,500	

TABLE 3

PRODUCTION PROFILE FROM COALBED GAS
(mcf per year)

<u>Year</u>	<u>High Yield</u>	<u>Low Yield</u>
1	14,400 (i.e. 40,000 cfd)	7,200 (i.e. 20,000 cfd)
2	13,900	6,800
3	13,300	6,500
4	12,800	6,100
5	12,200	5,800
6	11,700	5,400
7	11,200	5,000
8	10,600	4,700
9	10,100	4,300
10	9,500	4,000
11	9,000	3,600
12	8,500	3,200
13	7,900	2,900
14	7,400	2,500
15	6,800 (i.e. 18,900 cfd)	2,200 (i.e. 6,000 cfd)

TABLE 4

RETURN ON INVESTMENT, AFTER TAXES

(Percent)

METHANE RECOVERY

VERTICAL BOREHOLE METHOD

	<u>WELLHEAD PRICE PER MCF</u>		
	<u>\$1.42</u>	<u>\$2.00</u>	<u>\$3.00</u>
<u>PRODUCTION</u>			
High Volume	22.0	34.2	54.3
Low Volume	*	11.3	22.3

*Resulting return after taxes less than 10 percent

TABLE 5

COMPOSITE REVIEW OF ECONOMIC DATADEVONIAN SHALEPRODUCER TYPES

(1977 Dollars)

TABLE 6

TYPICAL
PRODUCTION PROFILE FROMDEVONIAN SHALE WELL

(mcf per year)

	<u>Utility</u>	<u>Independent Producer</u>	<u>Producer- Consumer</u>	<u>YEAR</u>	<u>PRODUCTION</u>
Development Costs	\$80,000 - 160,000	\$50,000 - 125,000 (Small Independent)	*	1	3,600
				2	12,500
				3	18,600
		\$80,000 - 160,000 (Large Independent)	*	4	18,700
				5	18,400
				6	17,500
Operating Costs	\$1,000 - 2,000	\$500 - 2,000	*	7	16,200
				8	14,300
Price	\$0.295 - 1.42/mcf** (Interstate)	\$1.75 - 1.80/mcf (Intrastate)	*	9	11,800
				10	10,000
		\$0.295 - 1.42/mcf** (Interstate)	*	11	9,500
				12	9,200
				13	9,000
				14	8,800
				15	8,700

*Interest and limited development by producer-consumers is quite recent and generally has not been available.

**Former FERC regulated price (1977).

TABLE 7

RETURN ON INVESTMENT, AFTER TAXES

(Percent)

DEVONIAN SHALE

	<u>WELLHEAD PRICE PER MCF</u>			
	<u>\$1.42</u>	<u>\$1.75</u>	<u>\$2.00</u>	<u>\$3.00</u>
<u>Normal Hydraulic Fracturing</u>				
Low Cost - \$117,500	*	10.5	12.4	21.3
Average Cost - \$140,400	*	*	10.0	17.6
High Cost - \$162,500	*	*	*	14.9

*Resulting return after taxes less than 10 percent.

TEST RESULTS OF STIMULATED WELLS IN DEVONIAN SHALES

by Raj M. Kumar and James H. Hartsock, Gruy Federal, Inc.;
K.H. Frohne, U.S. Dept. of Energy.

This paper was presented at the 1980 SPE/DOE Symposium on Unconventional Gas Recovery held in Pittsburgh, Pennsylvania, May 18-21, 1980. The material is subject to correction by the author. Permission to copy is restricted to an abstract of not more than 300 words. Write: 6200 N. Central Expwy., Dallas, Texas 75206

ABSTRACT

The long test times required to attain radial flow in stimulated Devonian shale gas wells are impractical. However, experience shows that a short test period (about two weeks) is sufficient to evaluate reservoir and fracture properties using conventional techniques followed by mathematical simulation of the observed pressures. History matches, whether unique or not (insufficient production data are available at present to establish uniqueness), give clear insight into reservoir properties, the effectiveness of frac treatment, and well deliverability.

INTRODUCTION

Estimates of recoverable gas reserves in eastern Devonian shales range from a few trillion cubic feet to several hundred trillion cubic feet, depending on whether (1) the bulk of gas is contained within natural fracture system networks and the matrix contributes very little to production (single porosity system), or (2) the bulk of gas is contained in the matrix, and fractures merely provide flow channels to the wellbore (dual porosity system). Each school of thought is supported by production data and history matching of production decline curves. Both have been supported by numerical models and can account for total gas production. In other words, at present the exact mechanism of production from Devonian shales is not fully understood.

In 1978 the U.S. Department of Energy initiated a gas well testing program whose principal objective was to "develop and conduct a program of gas well testing procedures and to analyze the results in support of the Eastern Gas Shales Program. The well tests and analyses are intended to permit evaluation of the relative effectiveness of various hydraulic and explosive stimulation techniques as conducted under this program."

To accomplish this objective, a two-phase project was planned. Phase I consisted of tests on three Devonian shale wells to develop (1) a practical field procedure for testing and (2) a comprehensive analytical technique for evaluating reservoir rock and fracture properties and the results of subsequent stimulation

References and illustrations at end of paper.

treatment. Phase II involves the application of the techniques developed in Phase I to routine testing and analysis of Devonian shale wells for a contract period of about one year. So far, two wells have been tested in Phase II. Of the five wells tested during Phases I and II, four were stimulated by cryogenic frac treatments and the fifth was foam fraced. No well which had been stimulated with a chemical explosive was tested; therefore, the procedure developed may not apply to wells completed by this method.

THEORETICAL BACKGROUND

It has long been recognized that the pressure behavior of a reservoir following a rate change directly reflects the geometry and flow properties of the reservoir fluids. However, when a well is fractured, the pressure behavior can no longer be described by conventional radial flow theory. Instead, pressures exhibit linear flow behavior in the early stages of testing. Later, pressure waves of semielliptical shape move away from the fracture. As the pressure disturbance continues to be propagated away from the fracture, the streamlines approach radial geometry, assuming that boundary effects do not first come into play. The duration of linear flow, which is a function of reservoir and fracture properties, is extremely long in Devonian shale wells, and radial flow does not occur during tests of practical duration. Hence, only the linear flow regime is available for analysis to estimate reservoir rock and fracture properties.

SURFACE FACILITIES

The surface facilities shown in Fig. 1 were designed for testing Devonian shale wells and performed exceptionally well.

Bottomhole pressures were recorded by a quartz crystal Hewlett-Packard gauge with a surface readout. Surface pressures were recorded by an Amerada RPG-6 recorder. However, surface measurements are of little value in the analysis except for those cases where fluid remains in the wellbore and fracture and the fluid level must be computed as it changes with time, or where bottomhole pressures cannot be recorded because of mechanical problems.

TEST PROCEDURES (Phase I)

During Phase I three wells were tested.

Pacific States Gas and Oil Co. L. Bonnett No. 1

The first test well was the Pacific States Gas and Oil Co. L. Bonnett No. 1 in Gilmer County, W. Va. This well was drilled to a total depth of 6,603 and completed through perforations from 6,377 to 6,501 ft. The formation was fractured using a cryogenic fluid containing 50,000 lb. of sand.

The test was initially planned to last for 41 days. The test prognosis specified two 3-day flow periods, each followed by a 6-day shut-in period, and a 7-day flow period followed by a 14-day shut-in period. Two days were allowed for mobilization and demobilization. Approximately seven days into the test it became obvious that the initial bottomhole pressure had been significantly below the static reservoir pressure. Because the wellhead assembly was leaking, it was decided to leave the pressure gauge in the well until static conditions were approached and the wellhead was repaired. This shut-in period lasted for approximately 5 weeks, after which a revised testing program was adopted. The new test sequence included two 4-day flow periods, each followed by a 6-day shut-in period, and a 7-day flow period followed by a 7-day shut-in. Details of the test are discussed elsewhere.¹

COLUMBIA GAS TRANSMISSION CORP. WELL NO. 20336

The second well tested was the Columbia Gas Transmission Corp. Well No. 20336, located in Martin County, Ky. It was drilled to a total depth of 4,000 ft. and completed in the intervals 2,666 to 2,712 ft and 2,968 to 3,122 ft. The upper zone was fractured using 98,924 gal. of cryogenic fluid containing 120,000 lb of sand, the lower zone with 75, 120 gal of cryogenic fluid and 110,000 lb of sand.

For this well the test procedure was altered by flowing the well at only two rates separated by an 11-day shut-in. The first flow lasted for 16 days and the second for 5 days. Details of the test are discussed elsewhere.²

Kentucky-West Virginia Gas Co. Well No. 1627

The last well to be tested in Phase I was the Kentucky-West Virginia Gas Co. Well No. 1627 in Perry County, Ky. This well was drilled to a total depth of 2,856 ft. and completed through perforations in the gross intervals 2,562 to 2,582 ft. and 2,728 to 2,790 ft. The well was stimulated with 28,770 gal. of foamed frac fluid containing 52,000 lb. of sand.

In an effort to reduce testing time, the test prognosis was designed to limit the test to a total on-site time of two weeks. Two 4-day flow periods were separated by a 4-day shut-in period. Allowing one day to rig up and one day to rig down, this prognosis could be followed without difficulty. A detailed discussion of the test operations and analysis of the test results is given in the contract report.³

TEST PROCEDURES (Phase II)

Experience during Phase I indicated that the flow pattern characteristic of quasiradial flow was not detected, even in flow periods of 16 days (Columbia well). This indicated that the test time required to investi-

gate beyond the created fracture system would be excessively long and impractical. Since the Kentucky-West Virginia Gas Co. well yielded as much information in two weeks as the Columbia well yielded in a month, it appeared that a test time of about two weeks would be adequate.

Morgantown Energy Research Center Well No. 1

This well, located in Morgantown, W. Va., was drilled to a total depth of about 7,520 ft and completed through perforations from 7,107 to 7,155 ft. The well was fractured using 120,000 lb of sand carried into the fracture by 62,450 gal of gel and 12,980 gal of CO₂.

The test comprised about 5.5 days of flow followed by 5.5 days of shut-in, followed in turn by about 2 days of flow. Details of the test are found in the contract report.⁴

Combustion Engineering Well No. 1

The Combustion Engineering Power Systems Group Well No. 1, located near the town of Belle Vernon in Allegheny County, Pa., was drilled to a total depth of about 7,500 ft and completed through perforations at 7,020 to 7,080 ft and 7,330 to 7,440 ft in the Burkett and Marcellus shales, respectively. The well was fractured through the two perforated intervals separately. The upper zone was propped with 74,000 lb of sand and the lower zone with 1,760,000 lb of sand.

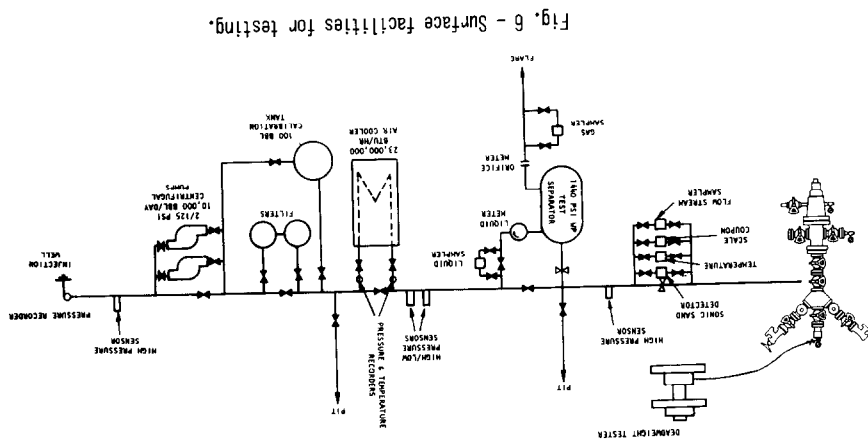
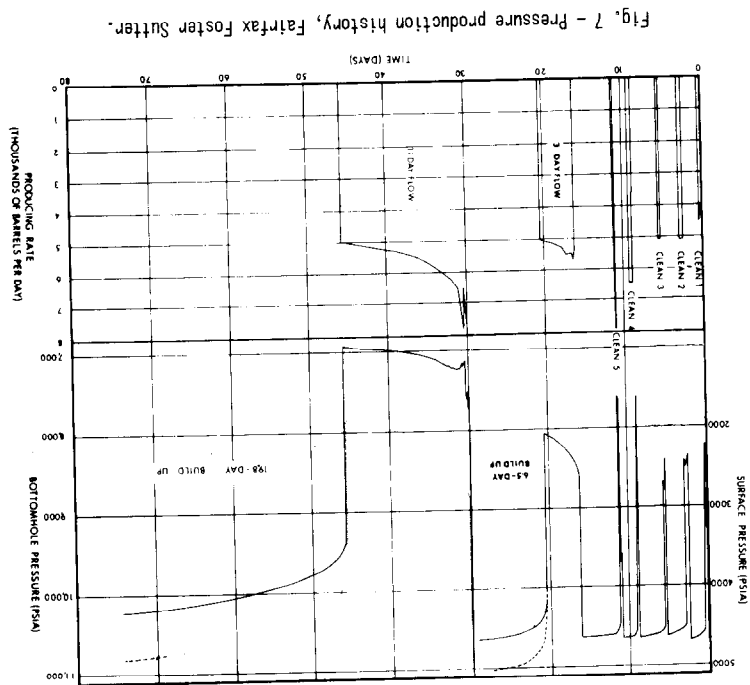
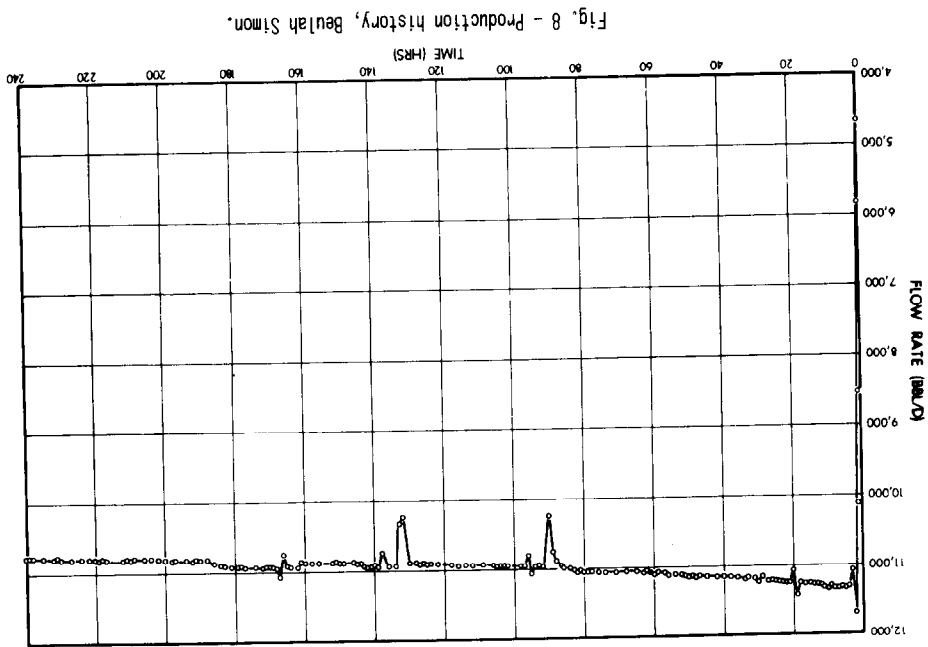
The test consisted of two flow periods of about 4 days and 3 days separated by a 4-day shut-in. Test details are given in the contract report.⁵

DIFFICULTIES WITH TEST PROCEDURES

No major difficulties were encountered with the surface equipment, but a few operating problems did occur. On the first well tested, approximately 12 bbl of frac fluid remained in the wellbore and an unknown amount in the fracture and formation. Since the velocity of the gas in the 4- $\frac{1}{2}$ -in. OD casing was insufficient to lift this fluid to the surface, the depth of the fluid level continually changed during the test, making analysis of the results difficult.

The frac water was contained in the wellbore, the hydraulically created fractures, and possibly the microfractures. As the well was placed on production the water was displaced by gas and migrated to the wellbore. The reservoir simulator could be reprogrammed to incorporate this behavior, but it was necessary to know the relative permeabilities in both the microfractures and the hydraulic fractures, as well as the initial water saturations in each. This information is unavailable. Allowing these parameters to "float" by adjusting them to achieve a history match would merely increase the number of degrees of freedom and decrease the reliability of the results.

Another problem encountered in testing Devonian shale wells is the inability to maintain a constant flow rate. On the first well tested, the gas production was metered and flowed into a 40-psi sales line. No backpressure regulators other than the sales line were used. Although the adjustable choke was set at a very small opening (approximately 1/64 in.), the



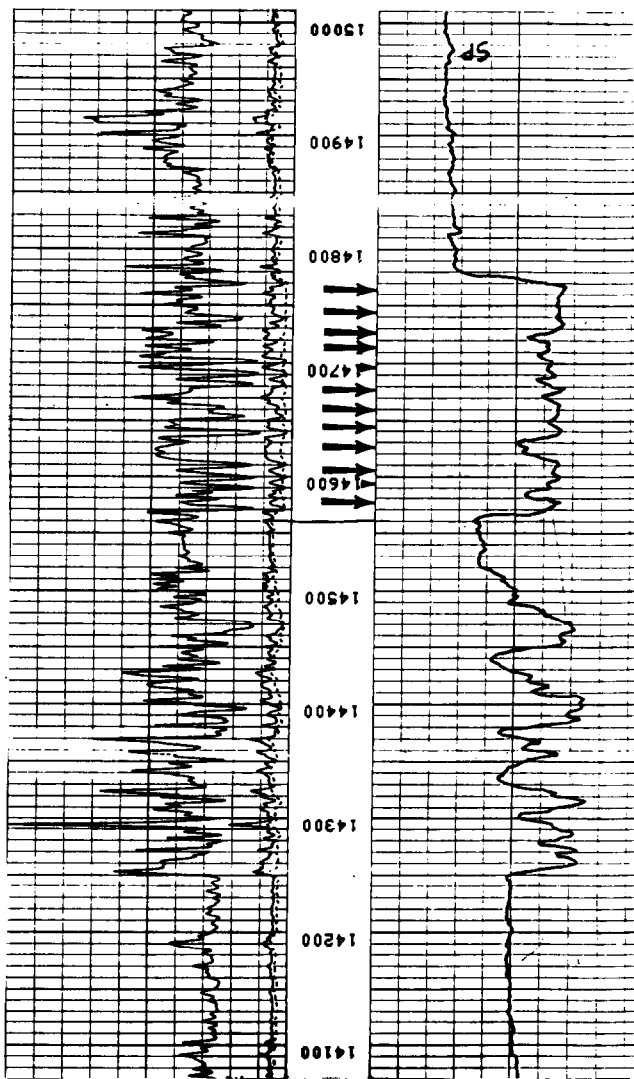


Fig. 5 - Log of B. Simon test section.

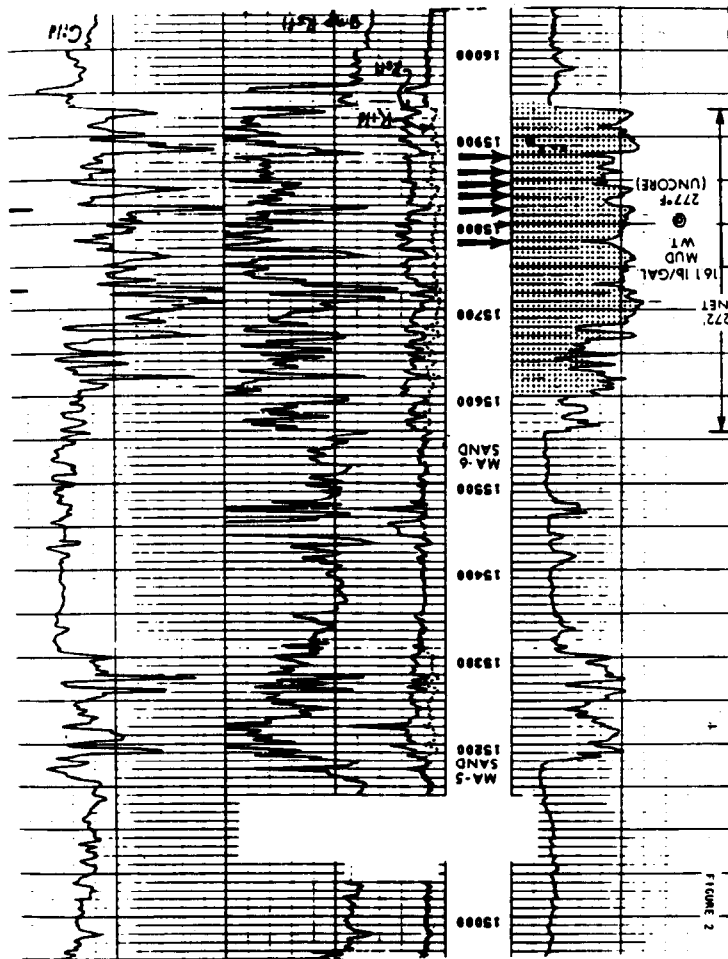


Fig. 4 - Log of Foster Sutter No. 2.

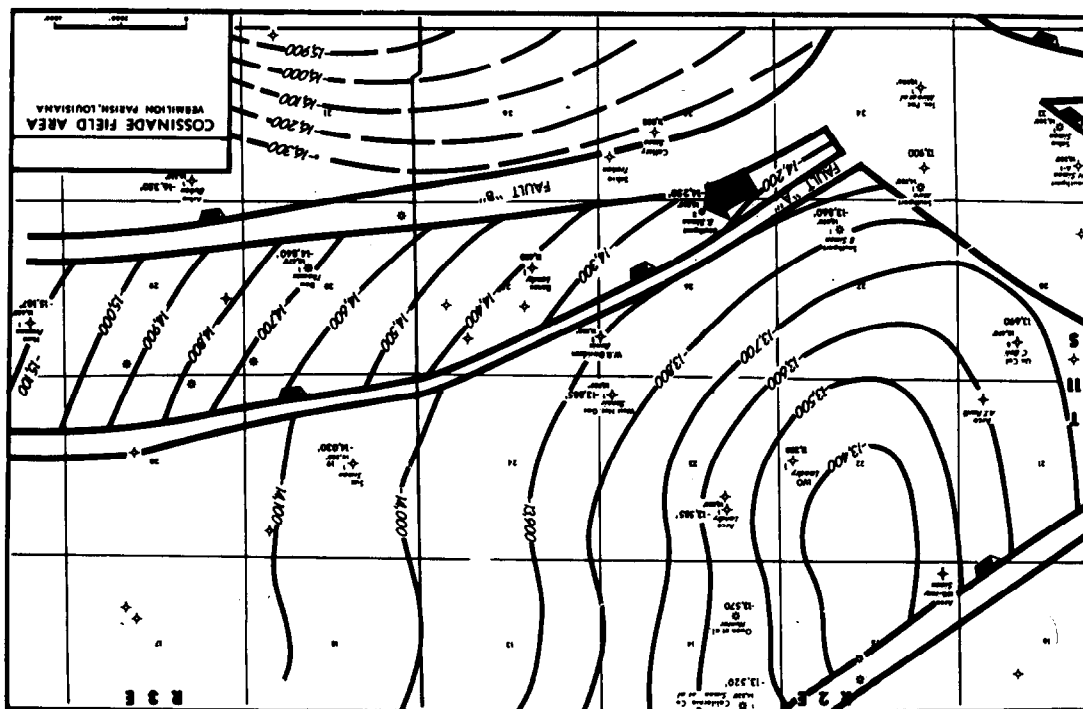


Fig. 3 - Top of Camerina Sand.

TABLE 8

DEVONIAN SHALE
ESTIMATED ECONOMIC RESERVE BASE
 (1978 - 1998)

		<u>Price</u>	<u>Number of Wells</u>	<u>20 Year Reserve Addition</u>
1	Base Case	\$2.00/mcf	14,365	4.0 tcf
2	Deregulate All Gas	\$2.25/mcf	25,565	7.0 tcf
3 & 3A	Deregulate Difficult Sources	\$2.50/mcf	61,200	17.0 tcf
4	Technology Improvement	*	*	*

*Undetermined, but well in excess of Scenario 3; earliest date equals 1988.

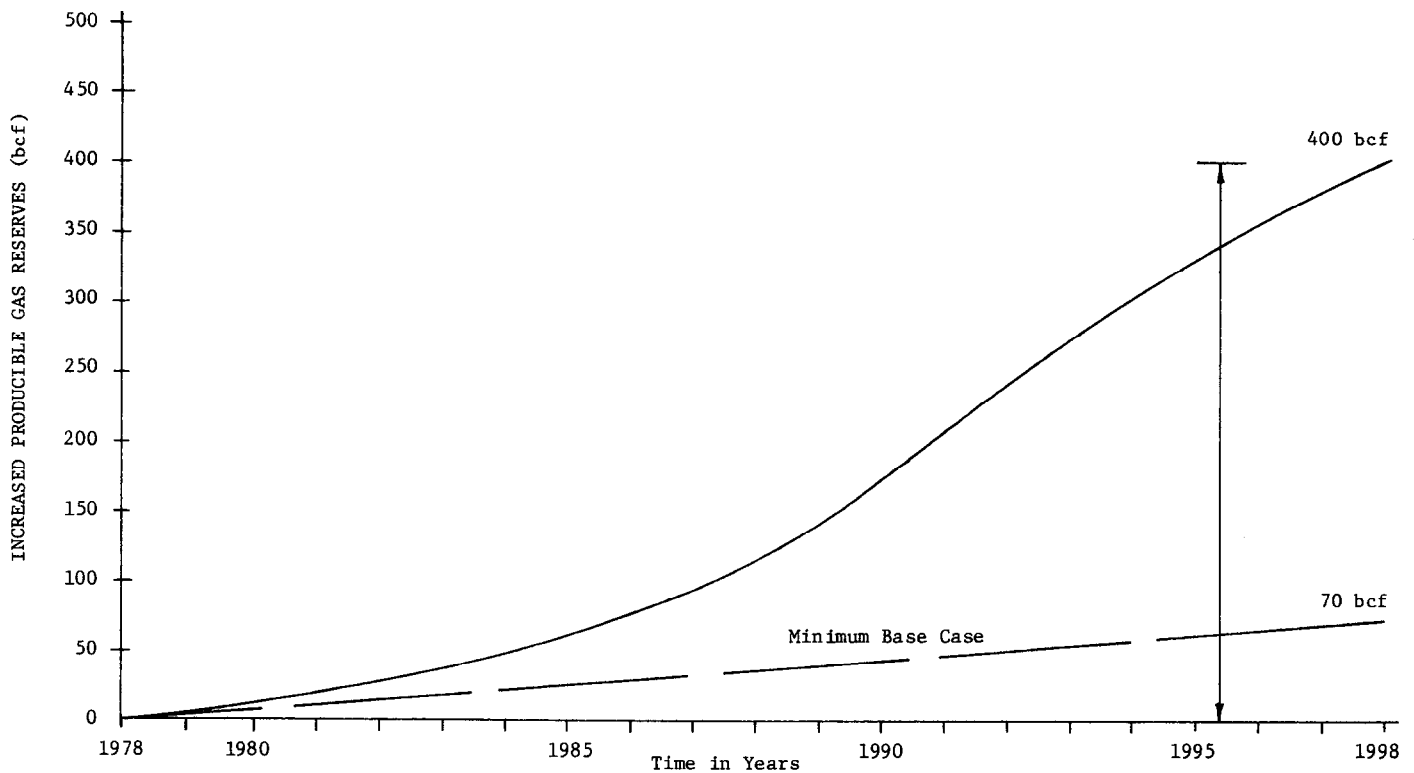


FIGURE 1 - PROJECTED APPALACHIAN METHANE GAS FROM COALBEDS

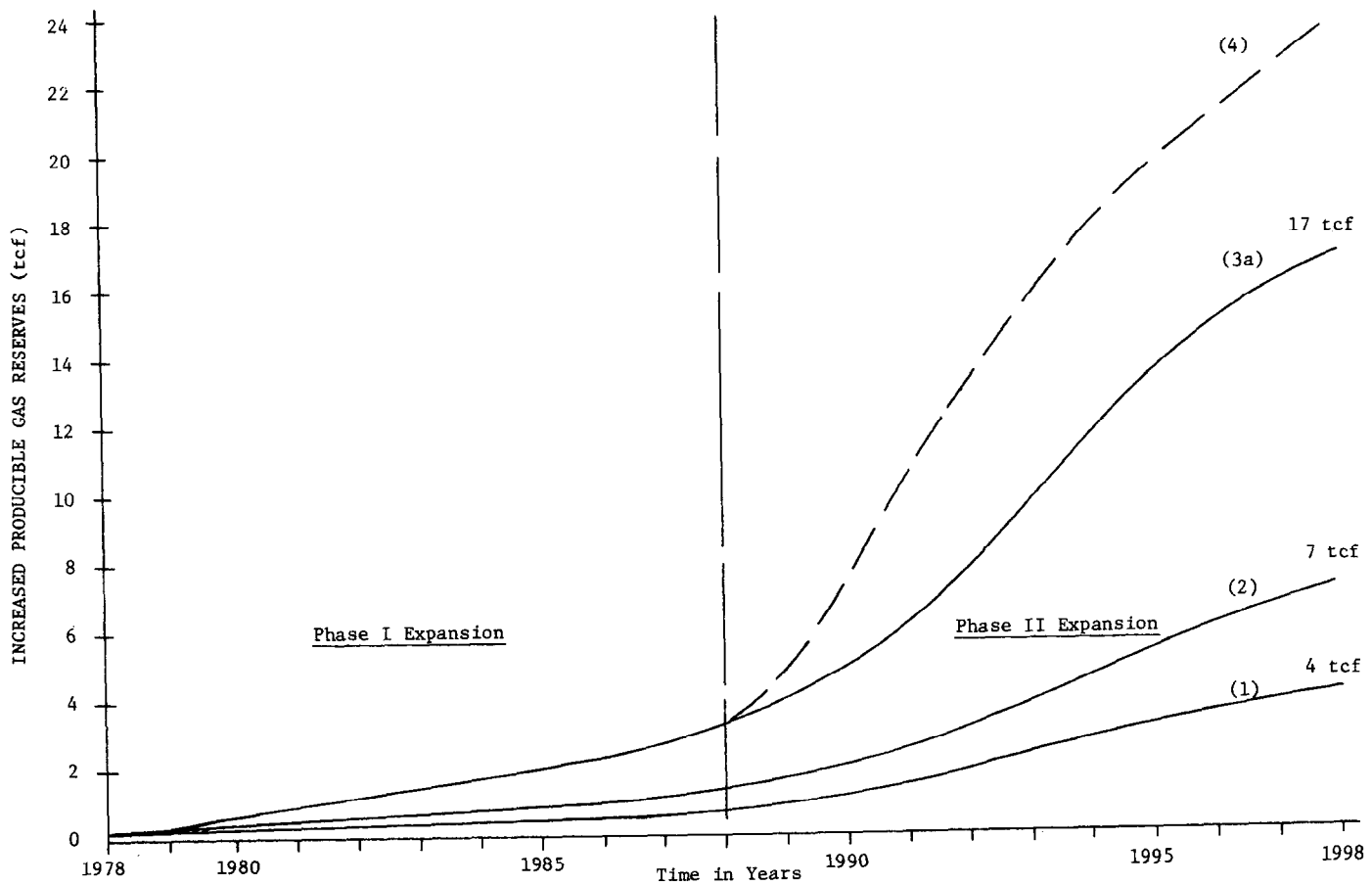


FIGURE 2 - PROJECTED APPALACHIAN DEVONIAN SHALE

UTILIZATION AND RECOVERY ECONOMICS FOR VERTICAL WELLS IN COALBED METHANE

Alexander Gillies, Arnold J. Snygg and
Debra Dickehuth, TRW Energy Systems

This paper was presented at the 1980 SPE/DOE Symposium on Unconventional Gas Recovery held in Pittsburgh, Pennsylvania, May 18-21, 1980. The material is subject to correction by the author. Permission to copy is restricted to an abstract of not more than 300 words. Write: 6200 N. Central Expwy., Dallas, Texas 75206

ABSTRACT

Previous economic studies of the recovery and utilization of methane from coalbeds using vertical wells were based on drainage in advance of mining where a single seam is drained with well spacing designed for rapid predrainage. A production economics study has been conducted which shows that the lower overall investment costs for wider spacing and increased production from multiple seams result in gas recovery at costs well below current prices for new gas imports. When applied to some of the thicker, deeper Western coals, the method also results in a favorable ROI.

INTRODUCTION

A study conducted by TRW¹ in 1977 for the U.S. Department of Energy's Morgantown Energy Technology Center (METC) examined the recovery of the methane contained in coalbeds using various extraction techniques and utilization options. The extraction options considered stimulated vertical wells and horizontal wells drilled into the coalbeds from within the mine or directionally drilled from the surface. The holes drilled from the mine considered both holes drilled immediately in advance of mining and from a shaft sunk into the mine several years in advance of when it was required for mine operations.

The economics of vertical wells to extract methane in advance of mining did not compare favorably with in-mine drilling, principally due to the higher costs of the wells and the close well spacing typical of the short time desirable for drainage for mine safety purposes (approximately 3-5 years). The wells were typically spaced at 20 acres or less and drained only the coalbed associated with the mining. For typical installations associated with mine predrainage the required gas selling price for a favorable return on investment was 2-3 times the price for horizontal wells and was in excess of the market price for the gas by 30 to 100 percent.

This paper extends the earlier work to the economics of multiple vertical wells, each producing from several coalbeds with spacing based solely on economic effectiveness. Several utilization options are also considered to provide a more complete picture of the economics of this widely applicable recovery technique for this marginal resource.

RESOURCE CHARACTERIZATION

The specific methane content of a particular coalbed can generally be related to the type of coal, the depth, the geological structure and the geographical area. While the coal rank and the depth are the major factors, the structure in which the coalbed lies can provide paths of migration which result in loss of the gas through outcrops or along faults. The geographical variance in methane content suggests that the depositional environment may have affected the original formation and retention of the methane. The methane content has been measured directly in many coalbeds in the eastern U.S. and determined from indirect measurements from mine ventilation data. The wide variation in methane content is shown in Figure 1 for selected coalbeds. The primary factors considered in this study are the amount of gas in place in the coalbeds and the depth of vertical wells to extract the gas.

A second resource characteristic to be considered in the effectiveness of vertical wells is the number of coalbeds that occur with a single well. As shown in Figure 2, while the gas in place can be treated as the total for all the coalbeds in a single well, the number of separate zones directly affects the completion and stimulation costs. Similarly, the very thick coalbeds which occur in the West may have to be treated as multiple zones for the purpose of stimulation and completion and their attendant costs. Since the production of the methane is permeability limited, multiple zones could provide a higher flow rate than if all the gas was contained in a single coalbed with high specific gas content.

References and illustrations at end of paper.

WELL PERFORMANCE ASSUMPTIONS

Examination of the production histories of coalbed methane wells indicate several mechanisms are affecting the methane flow rates: (1) the depletion of gas in the fractures near the well bore, (2) the dewatering of the coalbed which increases the relative permeability to methane flow, and (3) the desorption of methane from the coal as reservoir pressure is reduced. These mechanisms can be related to a typical flow history in Figure 3. Also affecting the flow history of coalbed methane reservoirs in some instances is (4) the influx of gas from surrounding formations as the reservoir pressure is lowered.

This economic analysis of single and multiple zones considers only the case where the gas in place is of a sufficient magnitude to warrant development. Total measured gas content (desorbed + lost gas + residual gas) is assumed to vary between 8 and 12.5 cc per gm (256 to 400 cu.ft. per ton). The economic life of each well is assumed to be limited by the extraction of 50 percent of this total measured gas. While the total measured gas content includes gas only recoverable by crushing the coal (residual), production histories of coalbed methane wells show that the total measured value is only indicative of the actual total gas in the reservoir. Gas in the major coal fractures and surrounding formations are not included in the measurement process.

While previous studies¹ related the initial gas flow rates to specific gas content and reservoir pressure, the available data also correlates equally well to the gas in place per unit of reservoir area. The assumed flow rates used in this study are shown in Figure 4 along with data^{2,3} from several wells in the Pittsburgh and Mary Lee coalbeds.

Decline curves for this study are assumed to be logarithmic with the decline starting from initial production time. Experience indicates that the initial flow rate is frequently sustained for several years, making this type of flow rate history somewhat conservative. As previously noted the total recovered gas from each well is assumed to be 50 percent of the total measured gas in place, also a conservative assumption.

The above assumptions can be represented by the following algorithms which relate flow rates, well spacing and production life. The decline curve is shown in equation (1):

$$q = q_o e^{-kT}, \text{ m}^3/\text{h} \quad (1)$$

Based on the assumption of 50 percent recovery, k is 0.07 when T is in years. Integrating the decline curve, equation (1), and setting the integral equal to one-half the gas in place, after clearing terms, the gas in place is shown in equation (2):

$$G = \frac{8766 q_o T}{0.07}, \text{ m}^2 \quad (2)$$

The area drained per well is then defined by equation (3):

$$A = \frac{G}{V}, \text{ m}^2 \quad (3)$$

The gas in place per unit area is derived from Figure 4. The well spacing resulting from these assumptions are shown in Figure 5 for 3, 5, and 10 year drainage times.

WELL AND SITE DEVELOPMENT COSTS

The well and surface equipment and operations costs assumed in this study were developed from existing data and by detailed engineering estimates for several major elements where existing data was not applicable. The costs were categorized by:

- Items basically independent of field size or production rates including site investigations, permits, and an initial exploratory core hole (normally assumed to be an add-on to the initial well).
- Items dependent on well spacing and total site area including site preparation, surveying, roads, fences, mineral leases, land use damages, and gathering systems.
- Items for each well but basically independent of depth including well heads, pumps electrical power equipment, meters, compressor capacity, and the stimulation cost for each zone.
- Items dependent on well depth including drilling, casing, testing, etc.

The cost estimates as related to well depth and number of production zones is shown in Figure 6 for a section size development and 16 wells. The base period for costs is March 1980. All existing data were escalated to this date using the applicable escalation factors.

UTILIZATION OR MARKETING OPTIONS

Variables associated with production rate, distance to existing transmission systems, quality of the gas, rate structure (peak demand applications), and regulatory constraints will dictate the method by which the gas from a field will be utilized. Three methods for bringing the gas to market were considered:

1. Gas cleaned, transported, and injected into an existing pipeline
2. Electricity transmitted to the power grid
3. Gas liquefied and trucked to market.

The analyses of these options are based on the following general production and development assumptions:

1. The gas is received from the field at one to two atmospheres with some water knocked out by a separator.

2. The life of the field is 10 years.
3. Production is sensitive to interruptions in flow rate and the utilization systems are thus operated in a steady state mode.
4. Salvage value is based on a 20 year life for moveable equipment. The other equipment (pipelines, transmission lines, mounting slabs, etc.) have no salvage value.
5. The production rates from representative fields are from 0.5 to 2.0 MMcfd.

OPTION 1 - PIPELINE INJECTION

In order to inject methane gas directly into commercial pipelines, the gas must meet certain specifications established by the pipeline gas companies.

- Gas must be free from dusts, gums, gum-forming constituents, or other liquid or solid matter which might become separated from the gas in the course of transportation through pipelines.
- Gas must not contain more than three-tenths (0.3) of a grain of hydrogen sulfide (H_2S) per one hundred (100) cubic feet.
- Gas must not contain more than thirty (30) grains of total sulfur per one hundred (100) cubic feet.
- Gas must not contain more than four percent (4%) by volume of a combined total of inerts such as carbon dioxide, nitrogen, argon and helium; provided, however, that the total carbon dioxide content shall not exceed three percent (3%) by volume.
- Gas must not contain more than one percent (1%) of oxygen by volume.
- Gas must have at least nine hundred and fifty (950) British Thermal Units per cubic foot calculated as the gross saturated value at 14.73 psia and 60°F.

The costs assumed for this utilization option were built-up from engineering estimates of specific design cases and from reports of existing installations. The costs for this option are shown in Figure 7 for variations in pipeline length and field size. Approximately 25 to 50 percent of this cost can be attributed to a scrubber which in many cases is not required due to the low CO_2 content of coal-bed methane.

OPTION 2 - POWER GENERATION

Since gas turbines are tolerant to variations in gas quality the option of generating electrical power may be preferable to treating gas and piping it to market. Distance to the customer hookup and relative cost of electric power lines and pipelines would also be important if not principal factors.

The sizes of turbine-generators applicable to the production rates under consideration range from 1300 to 6000 kw. Cost estimates of turbine-

generators are based on cost build-up data and recent discussions with representatives of turbine manufacturers. Cost estimates of transmission lines are based on data from recent contract awards. The costs for this option are shown in Figure 8 including the O&M costs for a 10-year period.

OPTION 3 - LNG PRODUCTION

On a direct comparison basis with the other options, liquefying the gas and trucking it to market is a high-cost operation. However it may be feasible for the peak demand market where the supply could negate the need for a utility customer to build a LNG facility. Another market for the liquid product may be automotive fleets equipped to burn LNG. The Atlanta Gas Light Company is currently operating a fleet of 27 trucks and 46 sedans₅ and light trucks on a dual LNG/gasoline system.

The system postulated for this option assumes that the facility will have access to electrical utility hookup and that water pumps, cooling towers, etc., will be powered by low-cost electricity. Cost estimates for a turnkey facility were based on discussions with LNG plant contractors and are dependent to a large extent on the degree of CO_2 scrubbing required. O&M costs are relatively high and essentially independent of plant size, as an operator is required on a round-the-clock basis. O&M requirements are based on discussions with operators of peak shaving plants in the Boston area. Equipment costs and O&M costs are shown in Table 1 for three production rates.

ECONOMIC ANALYSIS

Recovery economics were computed using the TRW ECONOGAS model. This model was developed in 1976 in support of studies conducted for the U.S. Energy Research and Development Administration. Since that time it has been enhanced and used in several studies conducted for the DOE and the Gas Research Institute including the Analysis of Benefits for Research, Development Projects for Unconventional Gas Resources and Analysis of Tight Formations, and the Methane Recovery from Coalbeds Project. ECONOGAS employs a basic discounted cash flow (DCF) algorithm which related the actual DCF to the revenues, expenses, tax retention rate, tax credits and the return. Return on investment (ROI) is determined by solving for the return. The assumptions used in this analysis and model inputs are:

- Royalties and ad valorem taxes are 14.5 percent.
- Tax retention rate is 50 percent.
- 25 percent of original outlays can be depreciated over the life of the field.
- Gas sales are computed on a 1980 basis.
- Investment credits are applicable.
- Gas production declines exponentially until 1/2 of the gas is recovered at the end of field life.

The basic assumptions for all of the variations considered here are:

- Field size is 259 hectares (640 acres).
- Basic well depth is 305 meters (1000 feet).
- Spacing between production zones is 30 meters (100 feet).
- Each zone contains 2.1 meters (7 feet) of coal.
- No utilization systems are included.

CASE I - MINE PREDRAINAGE

This case represents the predrainage ahead of mining where the basic objective is the rapid removal of the methane. The specific gas content is 8 cm³/g. The production well is completed in a single zone. Well life is five years and spacing of the 32 wells is eight hectares (20 acres). The initial cost for this configuration is \$4.75 million. Annual operations and maintenance costs are \$100,000. As shown in Figure 9 the required gas sales price for a 20 percent ROI is \$10.75 per Mcf.

The case where the specific gas content is 12.5 cm³/g is also shown in Figure 9. The required sales price decreases by approximately 30 percent.

CASE II - SINGLE ZONE WELL

This example is similar to the predrainage case (I) except the objective is to decrease the initial investment and extend field life. Well spacing is increased to 32 hectares (80 acres). Each of the eight wells has a single production zone. Well life is 10 years. The initial costs are \$1.75 million with a \$50,000 annual O&M cost.

The required selling price is \$6.38 per Mcf for a specific gas content of 8 cm³/g.

CASES III AND IV - MULTIPLE PRODUCTION ZONES

These cases are identical to the single zone case except for the additional gas production, changes in well depth, and completion costs. Initial costs for the two zone case (III) are \$2.1 million and for the three zone case (IV) are \$2.5 million. Annual operations and maintenance costs are \$75,000 and \$100,000, respectively.

The required gas sales prices are \$3.92 for the two zone example and \$3.17 for the three zone case. The prices drop by 30 percent when the higher specific gas content is assumed.

RESULTS

The required selling prices for the two and three production zone examples and a 20 percent ROI are approximately the same as the January 1980 regulated price for new gas of \$2.358 for the higher value of specific gas content (12.5 cm³/g). Considering the conservative assumptions used in this analysis many existing coal basins contain sites where coal thickness and specific gas content will provide favorable economics even when

competing with new U.S. gas. In competing with LNG and Canadian and Mexican gas imports development of this resource would even be more attractive.

The cost of utilization options can be applied to each of the cases using the data in Figures 7, 8 and in Table 1. The pipeline option applied to the two and three zone cases (lower gas content) will increase the required selling price by approximately \$0.66 per Mcf for a one-mile pipeline and no major gas scrubbing.

CONCLUSIONS

Use of multiple production zone wells can lead to substantial reduced costs for the recovery of coalbed methane and provide the higher return on investment required to develop this resource independent of mining operations. Even where mining is a major factor in the methane recovery, long-term planning and investment can lead to lower overall costs by reducing the number of drainage wells. Where vertical wells are used for predrainage, mine operators should consider the use of the production benefits from multiple zones to offset predrainage costs.

NOMENCLATURE

- A = Well spacing, area, m²
 G = Reservoir Total gas volume, m³
 k = Decline curve constant, 1/a (when used with T)
 q = Flow rate at anytime, m³/h
 q₀ = Initial flow rate, m³/h
 T = Production time, a
 V = Reservoir gas volume per unit area, m³/m²

ACKNOWLEDGEMENTS

This work was funded in part by the TRW effort under U.S. DOE Contract DE-AC21-78MC08089. Dr. Harold B. Shoemaker is the Technical Project Officer for this contract. The sponsoring organization is the Methane Recovery from Coalbeds Project, John R. Duda, Manager.

REFERENCES

1. TRW Energy Systems Group, "Methane Produced from Coalbeds - System Studies of Energy Conservation", USDOE MERC/CR - 77/4, January 1977.
2. Sterdl, Peter F., "Foam Stimulation to Enhance Production from Degassification Wells in the Pittsburgh Coalbed," USBM ROI 8286, 1978.
3. U.S. Steel, "Demonstration of the Degassification of a Portion of the Mary Lee Coal Group, Technical Report Contract No. ET-76-C-01-9027," U.S. Steel Corporation, Monroeville, Pa., February 1977 and subsequent issues.
4. "Pipeline Economics Report: U.S. Pipeline Construction Costs up 18%", Oil and Gas Journal, August 13, 1979.

TABLE 1

ITEM	COSTS (\$000)		
	FIELD PRODUCTION (m ³ /h)		
	590	1150	2380
LNG Plant	2500	4000	6300
Transportation Equipment	200	200	300
Total	2700	4200	6600
O&M*	183	205	250
Transportation (161 km)	36	73	146

*Assumes No Cost for the Gas Used for LNG Production

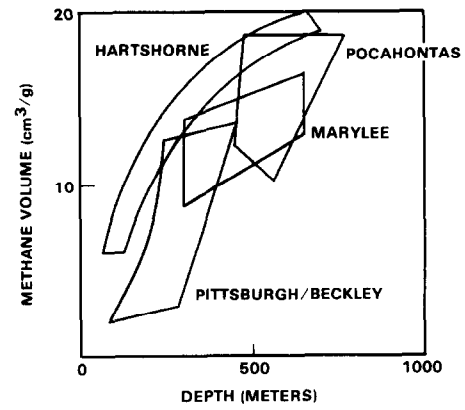


Fig. 1 - Coalbed gas volumes.

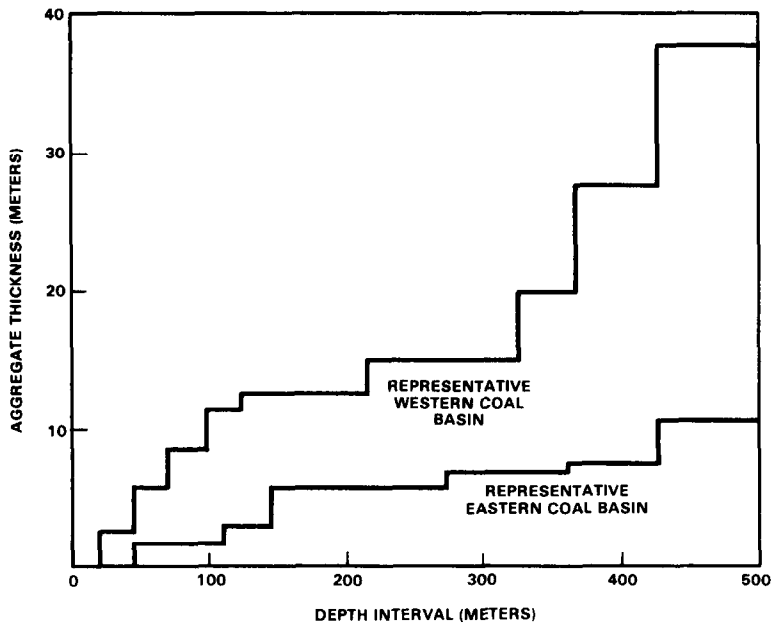


Fig. 2 - Multiple coal seam occurrence.

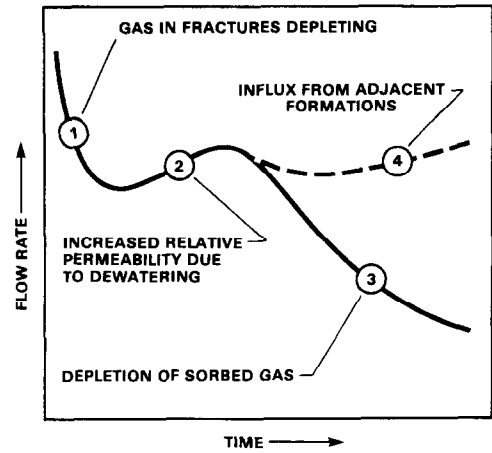


Fig. 3 - Typical decline curve.

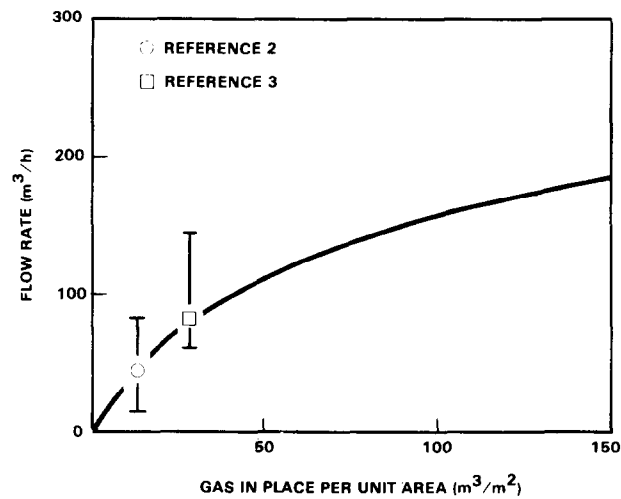


Fig. 4 - Estimated first flow rate.

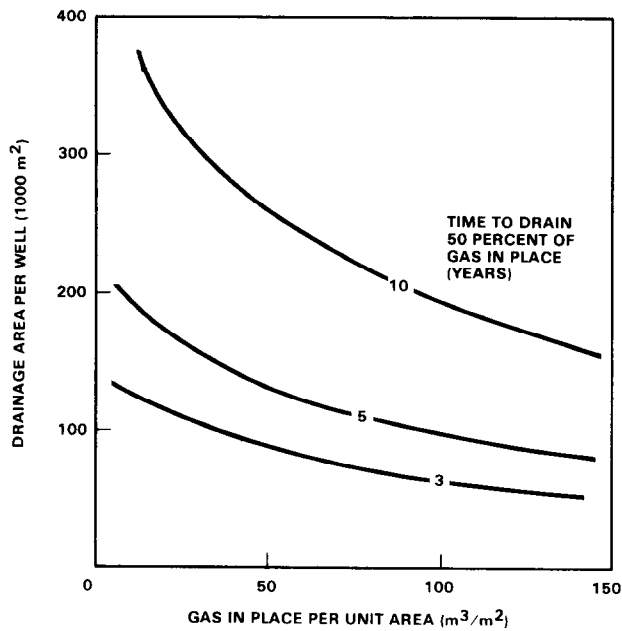


Fig. 5 - Well life and spacing.

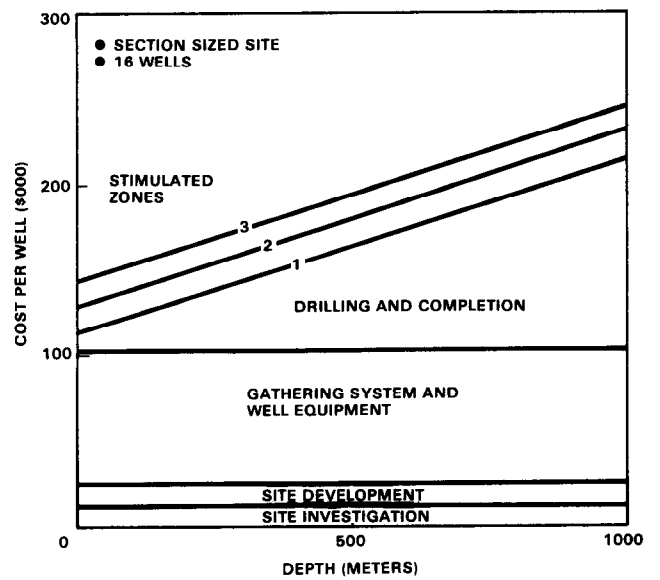


Fig. 6 - Well costs.

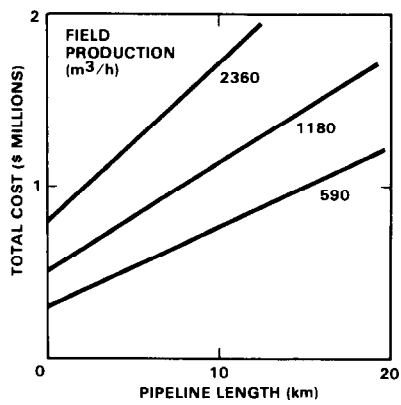


Fig. 7 - Gas processing.

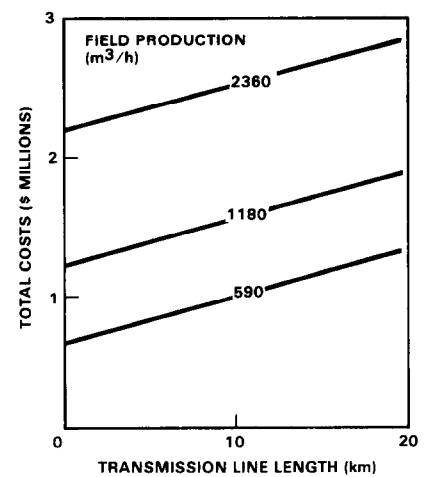


Fig. 8 - Power generation and transmission.

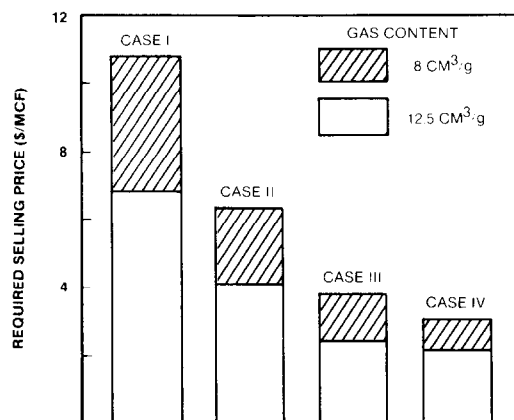


Fig. 9 - Required gas sale price, ROI = 20%.

LEGAL ASPECTS OF GAS FROM COALBEDS

by Norman E. Mutchler, Berger Associates, Inc.;
Harry R. Sachse, Sonosky, Chambers & Sachse

This paper was presented at the 1980 SPE/DOE Symposium on Unconventional Gas Recovery held in Pittsburgh, Pennsylvania, May 18-21, 1980. The material is subject to correction by the author. Permission to copy is restricted to an abstract of not more than 300 words. Write: 6200 N. Central Expwy., Dallas, Texas 75206

ABSTRACT

By far the major institutional problem with respect to gas from coalbeds is the legal question ---- who owns the gas. In this study related judicial decisions are examined in West Virginia along with Federal and state regulations, and a limited overview in Pennsylvania. Resolution of the problem could be by litigation, legislation or cooperation. An outline for a model legislative solution is given. However, it is recognized that cooperation may also be a viable solution for near term development of this unconventional gas source.

INTRODUCTION

Berger Associates, Inc., completed a comprehensive technical, economic and institutional study for the Appalachian Regional Commission on Appalachian unconventional gas sources which included a special legal study of coalbed gas ownership. No judicial decisions exist on the subject, although a case is being litigated now in Greene County, Pennsylvania. Another dormant case was found in Virginia. Hence, research and analysis must rely on related cases.

The legal ownership problem must be solved if this gas source is to make the contribution that many have predicted. The risk of expensive lawsuits is a major deterrent to utilization of the gas.

METHANE GAS - LIABILITY TO ASSET

Traditionally methane gas released in connection with mining of coal has been considered a costly and hazardous liability rather than an asset.

Methane gas is a hydrocarbon gas formed in the process of peat turning into coal. It has roughly the same BTU content and is in the same chemical family as "natural gases" found in connection with petroleum. In this sense it is "a natural gas", but it is not necessarily "natural gas" in the conventional sense of this term.

References at end of paper.

Methane gas released in coal mining may accumulate in mined out areas (gob gas), and may also migrate into coal mines from adjacent areas. If the coal seam does not have a relatively impermeable cap rock methane gas may be present in the overburden as well, and it is believed by many that this gas migrated upwards from the coal seam.

It is now technically and many believe economically feasible in certain coalbeds to produce and market methane gas. Methane drainage (the earlier term) has been practiced in the U.S. since 1920; however, except for certain exceptions, recovery is generally a more recent occurrence. The OPEC oil embargo of 1973 and subsequent shifts in national policies caused utilization to be emphasized in 1974. However, one private recovery effort is known to date from 1931 and a Bureau of Mines cost-shared project recovered methane gas in 1972.

Recovery of methane gas in advance of mining, during mining, and/or after mining (gob gas) may contribute to the safety of the mining process, increase coal mining productivity, reduce ventilation costs and conserve a valuable energy resource. Many coal operators are venting methane gas to the atmosphere, but an insignificant amount is presently being recovered for use.

THE LANDOWNERS'S OWNERSHIP OF MINERALS

It is well established at common law, and under West Virginia law that the landowner begins by owning every resource of value, and even of no current value, on and underneath his land. In West Virginia the breath of this ownership is indicated in the definition of "minerals" mentioned in Horse Creek Land and Mining Co. v. Midkiff¹: "every inorganic substance which can be extracted from the earth for profit, whether it be solid or stone ---- and coal, or liquid, as, for example, salt and other mineral waters and petroleum oil, or gaseous ----."

The theory in some states is that oil and gas unlike solid minerals are fugacious like wild animals and are not susceptible to private ownership

until they are reduced to possession by extraction. Oil and gas in West Virginia, to the contrary, are considered susceptible to absolute ownership in place. See Robinson v. Milam² and Williamson v. Jones.³ There is little practical difference in the two theories. West Virginia considers, as a corollary to ownership in place, that any person may drill on his land and extract such oil and gas as he can, regardless of its origin, unless he has already disposed of that right. Other states accept the exact same conclusion of law, as a feature of non-ownership in place. Both results are now usually limited by pooling arrangements. While the lack of significant difference in most cases blurs the distinction between the two theories, William and Myers⁴ lists states following a non-ownership theory as Alabama, California, Illinois, Indiana, Kentucky, Louisiana, New York, Ohio and Wyoming.

The landowner's ownership of minerals does not mean that he has unlimited control over them even before creating separate estates. For example, a mine owner must obey all safety regulations, although this may limit his mining activities, or prohibit mining certain parts of his coal estate. Similarly the rate of production of gas can be regulated to assure the maximum recovery by all participants in a pool. In determining which of several parties is the owner of methane gas, the limitations on that ownership, wherever placed, must also be considered.

THE CREATION OF SEPARATE MINERAL ESTATES

The question of whether the landowner, the holder of a coal right, or the holder of oil and gas rights owns methane gas in coal arises because West Virginia and other states recognize a right in the landowner to dispose of his minerals separate from the land itself and separate from other mineral interests. In West Virginia title to any mineral or group of minerals can be conveyed in perpetuity by a landowner in any manner that real estate can be conveyed.⁵ Similarly, a landowner may convey his land and reserve to himself a perpetual estate in the minerals. See Horse Creek Land and Mining Company (above).⁶

There is no requirement, federal or otherwise, that a system of law must allow separate and perpetual estates in any or all minerals. The forms of property ownership, except for federal lands, are left by the Constitution for state legislation.

The division of the landowner's estate provides a basic method for obtaining production of minerals. The landowner often does not have the capital or technical knowledge to produce the minerals himself. He thus may sell his mineral rights to a producer. However, as stated, the excessive division of mineral rights in Appalachia has led to the current impasse on coalbed gas ownership. Involved parties may be landowners, owners of coal rights and/or owners of gas rights.

CASES CONCERNING CONVEYANCE AND RESERVATION OF MINERALS

Where there is single ownership by the landholder, i.e. mineral rights have not been sold or leased, no problems exist; however, such locations are few.

In examining related cases in West Virginia there are important arguments from the standpoints of the holder of the gas right and the holder of the coal right.

To begin with, it seems likely that a conveyance of "minerals" or "all minerals", without further description, would include a conveyance of the methane gas found in connection with coal. See for example, Horse Creek Land and Mining Company (above); Sult v. Hochstetter Oil Company⁷; Freudenberger Oil Company v. Simmons⁸; Columbia Gas and Electric Company v. Moore.⁹ Such conveyances include all solid, liquid and gaseous minerals without limitation, and methane gas from coalbeds should be included in this category. A determination of what is included poses a more difficult problem where the conveyance uses the word minerals but then also lists particular minerals, or simply lists particular minerals.

The above interpretation of "minerals" or "all minerals", however, has not produced predictable results. In 1926 in Norman v. Lewis¹⁰, the West Virginia court interpreted a reservation of "all minerals, coal, iron, etc." with necessary mining rights as including a reservation of oil and gas. A contrary ruling in Horse Creek was cryptically distinguished by saying here the use of the words "coal, iron, etc." after the words "all minerals" must have been intended to include oil and gas. In fairness to the court, who knows whether either party intended to reserve oil and gas? Yet the courts were forced to resolve the disputes.

The determination of the intent of the parties is discussed in Rock House Fork Land Company v. Raleigh.¹¹ The question was whether a seam of clay was included in a conveyance of "all the coal and other minerals of every kind and description except gas and oil in and underlying such land." The court first stated that the scientific definition of minerals was not controlling and terms such as "mine and mineral":

"are susceptible of limitation according to the intention with which the parties used them, and in their construction regard must be had, not only to the deed in which they occur, but also to the relative position of the parties interested, and to the substance of the transaction or arrangement which the grant embodies. Consequently, in themselves these terms are incapable of a definition which would be universally applicable."

The Court held that it had no evidence outside of the document itself to show what the parties might have meant in their grant, but that the document's reference to mining and tunnelling (surface mining was not practiced at that time) showed that they meant minerals that had to be extracted in that way. The court ultimately held that clay was not included in the conveyance.

The court, significantly, has relied on the absence of known value of a mineral as an indication that it was not retained. Thus in Murphy v. Van Voorhis¹², the West Virginia court interpreted a reservation of "oil privileges" and the right to bore for "minerals or petroleum (sic)" contained in an 1865 deed as not including natural gas. The court

pointed out that the search for oil near Titusville began in 1859 and that this deed was obviously made with that in mind as the area is near the Pennsylvania border. The court stated:¹³

"It may be observed, further, that while there had been very early discoveries of natural gas in this country, it was not considered of any general commercial value until after the Civil War."

The same argument could be made to show that minerals were not conveyed.

In a somewhat similar holding in Bruen v. Thaxton,¹⁴ the Court held that the reservation of "all the coal and iron minerals found in or upon said lands" did not reserve oil and gas. In a discussion that may have some relevance to the methane gas problem, the court stated:¹⁵

". . . speaking from a clearly legal standpoint, and as understood in this day, coal while a mineral, is clearly distinguishable from the kindred minerals known as oil and gas. That there is a chemical relation between these minerals is undoubted. But we do not think it will be denied that from the time oil came into commercial use in 1859 and natural gas later on, the distinction of oil and gas minerals from coal minerals has been, in a legal sense, clearly marked."

The court was, of course, not considering gases produced in the production of coal, and thus we cannot know if methane gas from coalbeds would have been considered a "coal mineral". However, it is not likely that a landowner would intend to grant separate rights for "coal minerals" and methane gas without specifically saying so since both occupy essentially the same physical space. Hence by this reasoning the methane gas would be granted with the "coal mineral".

CASES CONCERNING MINING RIGHTS AND DUTIES

Perhaps the cases that give the most light on the question of methane gas production are not those distinguishing the ownership of one mineral from another but those describing the mining rights of a person holding a particular mineral. In Cole v. Ross Coal Company,¹⁶ the question was whether the holder of coal rights in a particular stratum had the right to build a tippie on the surface to get the coal up. The argument was that since his mining rights were enumerated, he would have only the enumerated rights and not the implied right to put a tippie on the surface.

The federal court after reviewing the West Virginia cases quoted with approval from Armstrong v. Maryland Coal Company,¹⁷ which in turn quoted approvingly from Barringer and Adams on Mines and Mining (an early legal textbook), as follows:

"It is a general rule of law that, when anything is granted, all the means of attaining it and all the fruits and affects of it are also granted; . . . And this right is so inseparable from a grant of minerals, that not only is it necessarily an implied incident thereof, but it and its derived rights cannot

be restrained or excluded by a special affirmative power to do acts, or by a grant of other privileges necessary or convenient to the working of mines." (emphasis added).

The federal court concluded that it would take an express limitation of implied mining rights, not just a listing of rights, to limit such implied rights. The court stated, relying on another West Virginia case, Squire v. Lafferty,¹⁸ that the test to be applied as to implied rights to use the surface is whether a particular use of the surface would be "fairly necessary to the enjoyment of the mineral".

This same reasoning could, of course, support a conclusion that the holder of a coal right has the right to "all the fruits of it" including methane gas, and has the right to use "all the means of attaining it" (the coal), including production of methane gas. In order to mine the coal he must abide by the legal requirements regarding methane gas "affects of it"; also by law he must control acid mine drainage, again, "affects of it", caused by iron, sulfur, etc., in the coal ---- at the same time enjoying the "fruits of it".

Cases on surface mining also define mining rights. Surface mining was not prevalent in West Virginia before the late 1940's. The West Virginia Supreme Court has thus had to decide whether older coal conveyances and leases permit surface mining. In several cases it had held mining cannot be inferred to give that privilege. West Virginia - Pittsburgh Coal Company v. Strong,¹⁹; Oresta v. Romano Brothers.²⁰ The court to some extent has relied on strict regulation of surface mining by statutes passed after the date of the agreements as a reason to interpret early deeds as not intended to permit surface mining. The court was, of course, seeking to protect surface owners from unexpected destruction of their estates.

PRELIMINARY ANALYSIS OF WEST VIRGINIA CASES

It is our conclusion from a study of the West Virginia cases that they give no secure indication of whether West Virginia courts would hold that the owner of a coal right owns the methane gas associated with the coal. The cases are too conflicting and too limited to the facts before the court to provide a reliable prediction. But there is a strong argument that methane gas is so associated with coal that the right to produce the methane gas is part of the implied mining right of doing what is necessary to produce the coal and to benefit from "all the fruits and affects of it". See Armstrong v. Maryland Coal Company.²¹ On balance this is probably the more likely position. It seems stronger than the argument that the landowner in granting the coal right could not have had in mind a grant of the right to produce methane gas since such production was either unknown or relatively without value at the time of the grant.

But it could also be argued that a landowner, in granting oil and gas rights to a gas company, impliedly grants the right to produce any kind of gas from any strata including a coal seam unless the landowner has expressly stated to the contrary or has already disposed of the coal rights. The issue, thus, is also complicated by the order in which minerals are granted. If the court held that

neither a grant of gas rights nor a grant of coal rights would include the right to methane gas, (see Murphy v. Van Voorhis) that right would be retained by the landowner regardless of timing. Similarly, if the court held that the methane gas was impliedly part of either the coal right or the gas right to the exclusion of the other, the time sequence would not matter. But if the court held that the grant of either a coal right or a gas right could include the methane gas, depending on the intention of the parties, then the methane gas could be granted by the first conveyance, whether to a coal company or to a gas company. For example, if a landowner first granted the coal and that was held to carry with it the methane gas, then a subsequent grant to a gas company clearly would not cover the methane gas, because the landowner had already disposed of that. If on the other hand, the first grant by the landowner was to a gas company, it might be held that the gas grant would cover gas wherever found. The grantee of the coal in a subsequent grant would presumably know this but in any event would acquire rights subordinate to the gas grant.

The uncertainty left by the decisions of the West Virginia court, and they are not substantially different from the decisions of other jurisdictions, requires the examination of Federal and West Virginia statutes and regulations concerning methane gas.

FEDERAL AND WEST VIRGINIA STATUTES AND REGULATIONS CONCERNING METHANE GAS

FEDERAL STATUTES

The Coal Mine Health and Safety Act of 1969,²² provide detailed requirements for removing methane gas from coal mines by ventilation of the mine. These include ventilation of the mine that will "be sufficient to dilute, render harmless, and to carry out flammable, explosive, noxious and harmful gases and dust, and smoke and explosive fumes"; ". . . three hours immediately preceding the beginning of any shift . . . certified persons . . . shall make tests in each such working section for accumulations of methane with means approved by the Secretary for detecting methane"; and, ". . . when any working face approaches within fifty feet of abandoned areas in the mine . . . and which may contain dangerous accumulations of water or gas . . . a bore hole or bore holes shall be drilled to a distance of at least twenty feet in advance of the working face". Methane gas in the working areas must be diluted with air and removed, as may be required, to maintain concentration in the air at less than 1 percent during mining operations. Except for the three hour limitation, there is no requirement for methane gas being removed from the coal prior to mining, or from the mine when mining operations are not going on.

The federal regulations provide more detail, but similarly do not specifically require or prohibit production of methane gas by the coal mine operator. See 30 CFR 22.0 to 22.11; and 30 CFR 27.1 to 27.41 concerning methane monitoring systems. 30 CFR 75.1700 addresses the dangers of the possible sudden release of gas in large quantities to a mine if a gas well were to be mined through. Reasonable care is required in locating gas wells, and a coal barrier must be maintained around such wells in

accordance with State laws and regulations (but not less than 300 feet in diameter).

The federal regulations for mining on federal land are in 30 CFR 200 et seq. There are several provisions there that could provide some guidance, though clearly not a solution in themselves, in the problem of obtaining methane gas production. For instance, 30 CFR 211.11 requires that where mining is in a known area of oil and gas, or other wells or bore holes, the mining company must submit a plan "to protect wells or bore holes, and obtain maximum recovery of the coal resource". This provision is directed towards two goals": coordination of mineral extraction and maximization of recovery of minerals. Similarly, 30 CFR 211.30 provides "underground mining operations shall be conducted so as to yield the maximum recovery of coal deposits consistent with the protection and use of other natural resources, sound economic practice, and the protection of the environment--land, water and air". (emphasis added). In pursuit of the same goals 30 CFR 221.9 provides that the appropriate federal supervisor "shall require correction . . . of any condition which is causing or is likely to cause damage to any formation containing oil, gas or water or to coal measures . . . or which is dangerous to life or property or wasteful of oil, gas or water . . ."

WEST VIRGINIA STATUTES

West Virginia has extensive legislation on mines and minerals, oil and gas. Chapter 22 of the West Virginia Code Annotated is devoted to mines and minerals. Article I (22-11 to 22-135) sets up the State Department of Mines to enforce health and safety standards.

Article II required that a plan of ventilation be approved by the Director of the Department of Mines (22-2-2), sets standards for ventilation (22-2-3) including the general standard that the ventilation must be adequate "to dilute and render harmless and carry away flammable and harmful gases" (22-2-4). As with the federal regulations, these state statutory requirements neither require nor prohibit commercial production of methane gas with, in advance of, or after mining.

Article IV is concerned with regulation of oil and gas wells.

These provisions requiring coordination between gas operators and coal operators, and advanced planning and notification by each, provide a system for arriving at an agreement and an administrative resolution with judicial review if no agreement can be had. They are designed for the extraction of natural gas in the vicinity of coal mines, not from coalbeds. They could perhaps be adapted to provide the framework for resolution of some of the problems of methane gas production if the methane gas rights are not recognized as part of the coal right.

Another set of statutes dealing with production of gas, without reference to coordination with coal production, are also important in the methane gas study. Section 22-4-14 prohibits waste of natural gas "when it is reasonably possible to prevent such waste, . . ." The Section, however, allows a number of specific exceptions, including waste of gas necessary in the production of oil. But a lessee of

a mineral interest under the terms of the lease usually does have a duty to produce. Thus a coal lease usually requires the lessee to mine all "merchantable" "available" or "mineable" coal or words to that effect. The West Virginia courts have defined these words in terms of coal that ordinarily can be produced at a profit. Tressler Coal Mining Co. v. Klefeld.²³ It is at least arguable that if methane gas is a part of the coal, the lessee has a duty to produce if it is economically feasible to do so.²⁴

In these Federal and West Virginia statutes and in Tressler Coal Mining Co. (above), methane gas is not specifically mentioned. Even so they provide a declared principle against unnecessary waste which can be used as a precedent for legislation against unnecessary waste of methane gas in the mining of coal.

CONCLUSIONS AS TO EFFECT OF STATUTES ON OWNERSHIP

The extensive regulation of methane gas as a part of coal mine safety is perhaps the strongest argument that the law considers methane gas as a part of the coal right, along with "all the fruits of it". It can be argued with some conviction, that since the coal owner, if he mines his coal, has the duty to deal with the methane gas, and is therefore free to deal with it in the best manner he can; if that is extraction and sale or other use rather than removal from the mine by ventilation, the law permits that also. Currently, production from conventional ventilation is not considered to be economical. However, it is not inconceivable technology that would make it economical may be developed in the future.

A question of lease interpretation would remain. A company producing coal under a lease would probably find that the royalty terms of the lease do not provide a basis for paying a royalty on methane gas to the coal owner or landowner. There would then be uncertainty as to whether the company could produce methane gas without paying a royalty. Some new negotiation with the coal or landowner would probably be necessary.

OVERVIEW OF THE LEGAL PROBLEM IN PENNSYLVANIA WITH COMPARISONS TO WEST VIRGINIA

The law in Pennsylvania concerning the right to methane gas in coalbeds is not substantially different from that of West Virginia. The basic mining and oil and gas law is far more similar than different. Pennsylvania cases are frequently referred to by West Virginia courts. The leading treatise on oil and gas law, Williams and Myers, Oil and Gas Law, classified both West Virginia and Pennsylvania as states adhering to the "ownership in place" theory of oil and gas rights,²⁵ rather than the non-ownership theory, and shows neither of these two states (in comparison with Kentucky, Illinois and Kansas) as accepting an ownership of strata theory.²⁶ The Pennsylvania cases clearly support this view. In Hamilton v. Foster,²⁷ the Pennsylvania Supreme Court held that despite earlier cases to the contrary, it is now firmly established in Pennsylvania that oil and gas are capable of ownership even when in place, and may be the subject of a grant just as in the case of other minerals.²⁸ Compare the opinion of the Pennsylvania Attorney General, discussed below.

In determining coal mining rights, West Virginia and Pennsylvania courts cite one another. Decisions in both jurisdictions are used extensively for the same propositions in the leading text on the law of mining in the United States, The American Law of Mining (Matthew Bender & Company, 1960). See, for example, Volume 3, Section 1628 "Mining Rights and Privileges Granted or Implied" in which the decisions in the two states are used to illustrate various points in mining law in a complementary rather than conflicting fashion.

Pennsylvania is, of course, subject to the same federal regulation as any other state. Thus the essentials of coal mine safety and of mine ventilation will be the same in both states because of the comprehensive federal legislation on that subject. Pennsylvania's own statutory provisions on mining and on oil and gas also resemble those of West Virginia. However, on the whole, the Pennsylvania statutes on coal mining seem less detailed than those of West Virginia.

The Pennsylvania statutes on gas operations in the vicinity of coal mines (Pennsylvania Gas Operations, Well Drilling, Petroleum and Coal Mining Act of 1955 as amended; Purdon's Pennsylvania Statutes Annotated 52-210k, et seq.) are more detailed than those of West Virginia, but the basic requirements are the same: notification if an oil and gas well is to be drilled in the vicinity of a coal mine, objection by the coal company if it disapproves of the plan, administrative hearing in which agreement is sought, a decision by the administrative body if there is no agreement.

Pennsylvania also has an oil and gas conservation law somewhat more complete, but much like that of West Virginia. As with West Virginia, the law applies only to wells in formations generally beneath the level of common coal mining.

In Pennsylvania gas is defined²⁹ as "all natural gas and all other volatile hydrocarbons not herein defined as oil, including condensate because it originally was in a gaseous phase in the reservoir". The act broadly prohibits waste in a statement³⁰: "Waste of Oil and Gas is Prohibited".

Waste is defined³¹ as follows (a similar definition exists in the West Virginia Code):

"(i) Physical waste, as the term is generally understood in the oil and gas industry, which includes - A. Permitting the migration of oil, gas or water from the stratum in which it is found to other strata, if such migration would result in the loss of recoverable oil or gas, or both; . . . C. The unnecessary or excessive surface loss or destruction of oil or gas, and D. The inefficient or improper use, or unnecessary dissipation of reservoir energy".

Thus both the common law legal framework and the regulatory control of methane gas and natural gas leave the question of the ownership of methane gas precisely as open in Pennsylvania as in West Virginia.

It has been reported that a case is currently being litigated in Greene County, Pennsylvania, i.e., U.S. Steel Corporation v. Mary Cunningham, et al.

ATTORNEY GENERAL
OF PENNSYLVANIA'S OPINION

There is one substantially different development in Pennsylvania. The Attorney General of Pennsylvania on October 31, 1974, issued an opinion to the Director of State Planning and Development which has been widely circulated. It states among other things, "It is our opinion, and you are so advised, that methane gas is a natural gas and, therefore, the owner or grantee of the gas rights has the right to assert legal title thereto". The opinion has no binding effect on the rights of private individuals. It does, however, speak the official state position on the subject until it is revoked.

Attorney Generals' opinions often carry considerable weight by the force of their reasoning. The Pennsylvania Attorney General's opinion however does not warrant this respect. The Attorney General relies extensively on the proposition stated in the 1899 Pennsylvania case of Westmoreland and Cambria Natural Gas Company v. Dewitt,³² to the effect that gas, like a wild animal, is not subject to ownership. Of the four-page opinion, quotation from that case occupies nearly a page and a half. But Westmoreland was long ago overruled in Pennsylvania by Hamilton v. Foster, (above),³³ which brought Pennsylvania into the ownership in place theory and rejected the prior ferae naturae theory used in the Westmoreland case.

The attorney General also relied on a statement in an 1893 Pennsylvania case, Chartiers Block Coal Co. v. Mellon,³⁴ to the effect that the "grantee of coal owns the coal but nothing else, save the right of access to it and the right to take it away". This case, of course, did not consider at all the question of the production of methane gas from coalbeds which was not at that time considered more than a detriment. The Attorney General concludes that the coal owner has the right to vent methane gas without liability as part of production of the coal, but "any attempt by the owners or grantees of coal rights to convert methane to profitable use could be challenged by those individuals who have acquired the gas rights". The Attorney General's opinion would thus solidify a pattern that permits without exception the waste of methane gas by the coal owners, but limits utilization of it to the holder of the gas rights or his grantee. This result seems counterproductive and not required by Pennsylvania law.

PROPOSED REFORMS

We suggest that there should be three objectives in legal reform concerning the production of methane gas. One should be to clarify the ownership of methane gas. This permits private parties to arrange for its utilization without being hampered by uncertainty caused by the law itself. A second goal is to maintain or to improve mine safety while putting methane gas to use. Changes in the law facilitating methane gas production should as a minimum maintain present mine safety standards and if possible should encourage higher standards of mine safety through degasification. The third objective is maximum utilization of energy sources. One energy source, methane gas, should not be wasted unnecessarily in the production of another, coal. In both safety and conservation

the state of technology and the economics of coal and methane gas production will, of course, be major parameters. There are three methods of reform.

LITIGATION

The traditional common law method of resolving disputed ownership is litigation. To a great extent litigation has determined ownership of coal and natural gas, and if nothing else is done, judicial resolution of disputes between oil and gas interests, coal interest, and landowners will eventually shed some light on ownership of methane gas. The disputes are becoming public now, as shown by the renewed interest in ownership of methane gas. As the value of natural gas increases and the technology of methane recovery improves, litigation can be expected. The problem with litigation as a problem-solving technique is that it is geared to an individual problem and fact situation, not a general one. Litigation thus might well follow the pattern of the former litigation on coal rights. Individual problems will be resolved but it could take perhaps ten years or more, and much expense to arrive at predictable results for the industries as a whole.

The above will be true of the case being litigated in Greene County, Pennsylvania. While it will begin the process of assembling a body of case law, and it will be helpful in eventually resolving the issue, the results tend to bear on the unique features of the particular situation which may not be applicable elsewhere. And, a case brought in the future in a neighboring state could result in an opposite view since these are matters of state law.

If the public needs the gas as soon as possible, this method of reform will not assure an early industry-wide resolution of the issue.

COOPERATION

An alternative to litigation is cooperation. With the increased allowance as a "higher cost gas" under FERC and as the price of gas increases, the prospects for private solutions may become more promising. Mr. Maurice Deul, the leading authority on the subject with the U.S. Department of Interior, Bureau of Mines, has stated that -- "Where there is money to be made by both parties, reasonable people will reason together". He has also recognized a practical aspect of the problem. Coal operators are chiefly interested in mining coal. But as mines go deeper, provision of sufficient outside air is taxing the ability to provide the increasing amounts of such air at the coal face. Therefore, when coal operators are forced by circumstances to degasify, they will be looking for ways to offset this cost.

One cooperative method was suggested by a representative of a trade association in West Virginia which avoids an impasse on the ownership problem.

By means of a contract the holder of the oil and gas rights grants the owner of the coal rights to remove the methane gas from the seam for a nominal fee (say one dollar per year). At the same time the coal company agrees to deliver the methane gas to a utility company for purchase. The purchase price can be divided between the gas and coal interests according to a formula set up in the agreement along with the details of production and expense.

A problem with cooperative solutions is that the uncertainty of ownership of either party may lead the other to litigate rather than to agree to a division of profits. Almost any dispute can be solved by cooperation but the volume of litigation in the courts, even between rational business interests with profits to make, shows that cooperation often breaks down. Cooperation also does not bring into play (for better or worse) the power of government to encourage safety and production. Nevertheless, cooperation can be a viable solution to the problem.

LEGISLATION

In our view, legislation, if it can be enacted, provides the fullest solution to the ownership of methane gas, to removing legal impediments to its utilization, and to providing incentives for its production (and not waste) of this valuable resource.

It is well within the realm of legislative action to clarify principals of ownership that may be left in doubt by the courts. Codification (systematic legislation to solve a problem) is a well accepted procedure in the United States and is the very basis of private law in most European countries. As examples of successful codification in the United States, we need only mention the Uniform Commercial Code and the wide range of model codes created by the American Bar Association and the American Law Institute, which have been adopted in numerous states. These are, of course, examples of state codification. Since ownership of minerals and other property is essentially a question of state law under the Constitution, the most unobjectional codification, from the constitutional viewpoint, would be by the states, with, perhaps, a model code to promote uniformity between the states.

Federal codification is also possible, but it would run into the need to justify such legislation as part of the regulation of interstate commerce or some other basis of federal legislative authority. Such grounds could be found as an adjunct to the extensive federal regulation of coal mine safety and the increasing federal regulation of energy production, already based on constitutional grounds. Congress, however, would probably be reluctant to legislate on the ownership of private property within a state.

AN OUTLINE OF A MODEL LEGISLATIVE SOLUTION

It is beyond the scope of this legal study to draft legislation -- a painstaking task with political and technological considerations as well as legal. Secondly, any of a number of legal solutions are possible, favoring landowners, oil and gas interests, coal interests, maximizing safety, maximizing production (and not waste), and with greater or lesser governmental participation.

What we have outlined is a model legislative approach based on what we see as a tendency of West Virginia and Federal law to consider the production of methane gas as an integral part of coal mining. And, especially in higher court decisions where there is conflicting related case law, there is a tendency to find a practical solution for the public good. In this case the solution would provide for the extraction and use (rather than waste)

of energy, increased coal mining productivity, and the protection of miners through increased safety. We thus partially base our solution to the ownership problem on whether the gas is in a mineable seam of coal. We now present our outline of a model legislative solution.

A LAW TO DETERMINE OWNERSHIP OF METHANE GAS IN COALBEDS AND TO ENCOURAGE ITS PRODUCTION AND UTILIZATION

- Article I "Methane gas in coalbeds" should be defined so as to include all the hydrocarbon gases ordinarily found in coal.
- Article II "Mineable coalbeds" in terms of methane gas production should be broadly defined, probably in terms of depth of burial of coalbed, thickness and, where appropriate, aerial extent. The final determination on a case by case basis should be by an administrative body which represents the public, including the involved industries.
- Article III The operative article on ownership of methane gas in mineable coalbeds should state essentially that any lease, conveyance or reservation of a right to mine coal carries with it, in the absence of an express provision to the contrary, the right to extract and utilize the methane gas in all mineable coalbeds. It should also make clear that this right covers pre-drainage, during mining and post mining rights, and includes gob gas and methane gas in the overburden.
- Article IV The operative article on unmineable coalbeds with methane gas should state essentially that a conveyance, etc. of oil and gas, or gas alone, in the absence of an express statement to the contrary, carries with it the right to produce methane gas from any strata except a mineable coalbed -- including unmineable coal seams as defined in Article II, above.
- Article V An article on waste, like the provisions against waste of natural gas, or coordination of production in federal leases, should make it illegal unnecessarily to waste methane gas which is economically and technically susceptible to production. It should refer to regulations on this subject to be administered by the State Department of Mines, or some other appropriate state administrative agency. It should link the right to produce methane gas with a duty to do so where economically and technically feasible, and should cover pre-drainage, production during mining and post mining recovery.
- Article VI The degree to which the articles are prospective and the degree to which they are retroactive should be stated.

Essentially, to be useful, the legislation must be retroactive -- that is, it must apply to coal and gas rights already conveyed or reserved. Otherwise, few problems would be solved, because most coal and gas rights have already been conveyed or reserved. However, it may be advisable to save from operation of the article methane gas already in production and cases already in litigation.

Article VII This article could state that all production of methane gas must be approved by the safety division of the state, Department of mines, or the appropriate state administrative agency. Clearly production of methane gas must meet state and federal safety requirements. Whether prior approval is desirable is debatable.

CONCLUSIONS

We suggest a model legislative solution rather than either a solution through litigation or through private bargaining for reasons that we have already explained. Litigation tends to deal with the particulars of a given situation. While there is always the possibility that legislation will be challenged in the courts, at least the results of the litigation may be definitive.

Similarly, as long as there is no legislative guidance, the threshold at which it becomes practical for mining companies, gas companies, and landowners, etc. to arrive at a solution through negotiation is elevated. Negotiations may be necessary even when ownership is clear, they should not needlessly be freighted with uncertainties about the basic premises from which the parties negotiate.

The division of ownership based on mineability of the seam is based to some extent on the probable intent of the parties in a coal mining state. We, of course, bear in mind that the parties may never have considered methane gas except as a detriment in mining, but this absence of expressed will as to its exploitation makes a legislative determination of probable or implied intent particularly appropriate. The division we propose is also based on the assumption that joining the coal right and methane gas right as to mineable seams will facilitate methane gas production by minimizing problems of coordination. An excessive division of mineral ownership is part of the problem in present West Virginia law and is minimized by joining coal and methane production rights in mineable seams.

Also the relative value of the gas contained in coal is about two percent of the value of the coal. If methane gas from coalbeds is to be recovered for use, the coal operator must be the prime party in the negotiation to protect his valuable estate.

The principle that minerals should be produced rather than wasted is an old one. It is reflected in both the West Virginia and Pennsylvania statutes against waste of natural gas. It is also part of the general theory of compulsory pooling in the production of natural gas required by most gas producing states. See Williams and Myers (above).³⁵

Compulsory pooling amounts to a limitation on private ownership in the sense that it may require a particular owner not to produce his gas or to produce it only at a certain rate so that the maximum recovery may be made from the entire pool. The states' interests in passing such legislation is to prevent economic waste in the drilling of unnecessary wells, and to prevent physical waste by assuring that the pressure in the pool is used to produce the maximum quantity of gas. Such legislation has routinely survived constitutional attack as a valid exercise of police power. See Village of Euclid v. Ambler Realty Co.³⁶

Compulsory pooling also provides an administrative model for preventing excessive waste of methane gas in the process of mining coal. Questions of practicality and economic feasibility are routinely handled by administrative bodies in that context. Similarly, a conservation statute which requires maximum economically feasible production of methane gas in connection with the production of coal can be administered by an administrative body.

The relationship between the removal of methane gas and mine safety is discussed elsewhere in this legal study. There are numerous burdens already placed by law on mine operators for the benefit of their employees. We cannot suggest the exact safety provisions that should be enacted as to methane gas utilization. There are too many technical questions for this to be solved in a study of this type. Clearly, however, in feasible coalbeds some requirement for production of methane gas in advance of mining, during mining, and recovery of gob gas, could be established (on a state or federal level) for methane gas extraction/utilization at or before the time of submission of plans for mining.

ACKNOWLEDGEMENT

This paper is based on work completed as part of the Appalachian Regional Commission Report, ARC 77-2-CO-5246, "Study on Devonian Shale, Coal Seam and Similar Special Appalachian Gas Energy Prospects and Opportunities."

The work was under the direction of Dr. David R. Maneval, (former) Technical Project Officer and Science Advisor, and Dr. John J. Demchak, Director, Natural Resources Division, Appalachian Regional Commission.

REFERENCES

1. 95 S.E. 26, 27 (1918).
2. 24 S.E. 2d 236 (1942).
3. 19 S.E. 436 (1894).
4. Oil and Gas Law, pp. 17-167.
5. See generally Donnelly, The Law of Coal, Oil and Gas in West Virginia and Virginia, pp. 28-40.
6. Supra Ref. 1 at 26.
7. 61 S.E. 307 (1908).
8. 83 S.E. 995 (1914).

9. 93 S.E. 1051 (1917).	23. 24 S.E. 2d 98 (1943).
10. 130 S.E. 913 (1926).	24. Supra Ref. 5 at pp. 135-136.
11. 97 S.E. 684 (W.Va. 1919).	25. Volume 1, Section 203.3.
12. 119 S.E. 297 (1923).	26. Id. at Section 203.4.
13. Id. at 298.	27. 116 Atl. 50 (1922).
14. 28 S.E. 2d 59 (1943).	28. Id. at 53.
15. Id. at 67.	29. 58: 402(3).
16. 150 F Supp. 808 (S.D., W.Va. 1957).	30. 58: 404
17. 69 S.E. 195, 203 (1910).	31. 58: 402(12).
18. 121 S.E. 90 (1924).	32. 130 Pa. 235 (1889).
19. 42 S.E. 2d 46 (1957).	33. Supra Ref. 27.
20. 73 S.E. 2d 622 (1952).	34. 152 Pa. 286, 296.
21. Supra Ref. 17.	35. Supra Ref. 4, pp. 13-75.
22. 30 U.S.C. 801 <u>et seq.</u>	36. 272 U.S. 365 (1926).

AN EVALUATION OF THE GEOPRESSURED ENERGY RESOURCE OF LOUISIANA AND TEXAS

by Garland Samuels, Union Carbide Corp.

This paper was presented at the 1980 SPE/DOE Symposium on Unconventional Gas Recovery held in Pittsburgh, Pennsylvania, May 18-21, 1980. The material is subject to correction by the author. Permission to copy is restricted to an abstract of not more than 300 words. Write: 6200 N. Central Expwy., Dallas, Texas 75206

ABSTRACT

The economics of extracting either the geothermal energy or natural gas from geopressured aquifers does not look promising. The combined requirements of high well flow rates, long life, and the necessity for close well spacing to minimize the cost of the collection system may be incompatible with the actual characteristics of the reservoirs. These factors place such stringent requirements on the reservoir size, permeability and compressibility that the number of promising production areas may be severely limited.

INTRODUCTION

Two of the many energy resources receiving increasing study today are geothermal energy and unconventional sources of natural gas. The purpose of this paper is to discuss one, perhaps the largest, potential source of geothermal energy and natural gas - the geopressured aquifers along the northern Gulf of Mexico (Fig. 1)¹. These high pressure aquifers are characterized by higher than normal temperatures and are believed to be saturated with natural gas. Thus, these formations offer the potential for recovery of three forms of energy - thermal, chemical, and hydraulic. Although the potential exists to extract all three forms of energy, the potential for recovering large quantities of methane is of most importance and is responsible for the increasing interest in these aquifers.

The following sections of this paper discuss the potential magnitude of the resource, the economics of exploiting these aquifers, and the reservoir properties and their effect on production rates and resource recoverability.

RESOURCE AND RECOVERY ESTIMATES

Estimates of both the magnitude of the geopressured aquifers and the energy that may be recovered from them vary widely. Much of the initial interest concerning the potential energy of the geopressured

aquifers was generated by a U.S. Geological Survey (USGS) report by Papadopoulos et al. in 1975.² In this report, the authors divided the onshore area of Texas and Louisiana into 21 subareas corresponding to faulting patterns and evaluated each subarea separately. They estimated the sandstone and shale thickness and porosity and the pressure and temperature of the brine in each subarea. From this information they derived a value of the potential resource base of all three forms of energy - thermal (46,000 EJ), methane (25,000 EJ) and mechanical (2300 EJ).

Papadopoulos et al. also estimated the potential recovery of energy using three different production plans. The percentage recovered varied from about 0.5 to 3.3%. The authors note that their assessment does not include the total geopressured resource. They predict the offshore and other onshore sediments in Texas and Louisiana not included in their analysis to be 1-1/2 to 2-1/2 times those estimated in their study. A later USGS Circular³ estimates the total resource base of this basin to be about 2-1/2 times the values listed above.

Jones⁴, building on the initial USGS report, estimated the methane content of the total basin sandstone formations to be 49,000 Tcf (51,000 EJ), of which, 17,000 Tcf (18,000 EJ) was offshore. He also stated that the methane resource base, including that in shale formations, was 100,000 Tcf (105,000 EJ) and that 246 to 1145 Tcf (260 to 1200 EJ) could be recovered.

The optimistic projections made by Jones and Papadopoulos were apparently the source of other statements implying enormous natural gas resources. In reference to the geopressured zones, Brown⁵ states that the total resource base "has been estimated by two competent sources to lie between 60,000 and 105,000 quads for the natural gas alone." He notes that the eventual recoverability is highly uncertain "but probably lies in the range of 4 to 50 percent of the methane within the reservoirs which are eventually developed."

References and illustrations at end of paper.

*Newsweek*⁶ also reported the 100,000-quad (105,000 EJ) value but noted that no solid research backs the claim. In this article it was also stated that Henry Linden, President of Gas Research Institute, speculated that as much as 160 quads of natural gas might be available at less than \$4/Mcf³ (\$0.14/m³). This value is similar to projections of the recoverable resource made in the Energy Research and Development Administration's (ERDA's) [now the Department of Energy (DOE)] *Market Oriented Program Planning Study (MOPPS)*,⁷ which gave a total range of 150 to 2000 quads.

Hise⁸ and Dorfman,⁹ speaking to a special National Resource Council Board, as was Jones, projected much smaller values. Hise estimated the total area of the aquifers, both onshore and off, for Louisiana and Texas to be about 100,000 sq miles (260,000 sq km). He assumed an average thickness of 10,000 ft (3050 m) of sediment, of which 10% was sandstone and the remainder shale. Using a value of 20% for the sand porosity and a value of 30 scf/bbl (5.34 m³/m³) for the natural gas content of the brine, he estimated the total gas in place in the geopressured aquifers to be 3000 Tcf (3100 EJ). He states that "preliminary and unfounded estimates of the number of geopressured aquifers that exist of commercial size vary from 0 to 1000." Using a value of 1000, he estimated a total recovery over a 30-year period of 27.4 Tcf (28 EJ). The United States currently uses about 20 EJ of natural gas each year.

Dorfman made no estimates of reserves. He does state that if the price for natural gas were high enough to make such ventures attractive, about 0.33 Tcf (0.35 EJ) could be produced per year by the year 2000. This represents less than 2% of our current annual use.

More recent studies published by Swanson and Osoba¹⁰, and Doscher et al.¹¹ are not encouraging. Swanson and Osoba estimates the upper limit of producible methane from known geopressure fairways to be about 7 Tcf (7.4 EJ). Their estimate of wellhead cost from one of the most promising fairway was \$7.50/Mcf (\$0.26/m³). Doscher et al. estimated production costs of from \$4 to \$15/Mcf (\$0.14 to \$0.53/m³). These latter two reports contain caveats that imply that the quantities or costs projected may be less favorable. They also assumed that 40 scf (1.13 m³) of methane could be recovered from each barrel (.159 m³) of brine.

RESOURCE RECOVERY COSTS

Although estimating the cost of any emerging technology or new resource is speculative, it is necessary in order to provide insight into the effects of the key parameters on its economic potential. For this purpose, results of earlier cost studies will be used to understand the importance of the key geopressure parameters - the size, compressibility and permeability of the reservoirs and the gas content, pressure and temperature of the brine.

One of the most detailed and best documented studies of the economics of using the energy from geopressured aquifers is by Wilson et al.¹² In this study of a 25-MW(e) plant, the system was separated into a fuel plant and a power plant. The fuel plant consisted of production wells, a methane removal system, reinjection wells, and a piping system to collect and dispose of the brine. The power plant

consisted of a hydraulic turbine to convert the excess wellhead pressure into electrical power, a separation system for further gas recovery, a steam flash system, and a steam turbine-generator with the electrical gear, condensers, and other equipment necessary for a complete power plant. Both a single- and a double-flash system were analyzed in the study.

The assumptions used for the Wilson et al. study and a summary of the costs are listed in Tables 1 and 2. In addition to the assumptions listed in Table 1, other ground rules adopted for the study were: the production wells were located at 1/2-mile (0.8-km) intervals, two reinjection wells were required for each production well, and the reinjection pressure required at the processing plant was 300 psi (2.1 MPa). Also, the costs shown in Table 2 do not include any costs for land, royalties, architect-engineering, interest during construction, or contingency.

The data of Table 2, without any changes, were used to calculate the power cost as a function of the methane value in the brine - shown by the lower set of lines in Fig. 2. The lower-right end points of these lines represents the methane value for which the hot brine can be delivered to the power plant without cost. For example, if the brine contains 40 scf/bbl (7.1 m³/m³), the methane would have to be priced at \$2.80 to \$2.90/MCF (\$0.097 to \$0.102/m³) and the resulting power cost would be 22 to 26 mills/kWh.

In order to bring these costs up to date and to include an allowance for some of the omissions, the costs of Table 2 were increased by 75%. The result of applying this factor is shown as the middle lines of Fig. 2. The lower-right end of the lines again represent the methane value for which the hot brine can be delivered to the power plant without cost. For this case, with 40 scf of methane per barrel of brine (7.1 m³/m³) the methane price must be \$5/Mcf (\$0.18/m³), or with only 20 scf/bbl (3.6 m³/m³) the price must be \$10/Mcf (\$0.35/m³). Even at these methane values, the power costs would be 40 to 50 mills/kWh.

The ground rule that 20,000 B/D (0.037 m³/s) could be reinjected by each disposal well at a pressure of 300 psi (2.1 MPa) at the processing plant is very optimistic. Doscher et al.,¹¹ in an analysis of brine reinjection to shallow aquifers (1800 m), determined the reinjection rate vs injection pressure for 1000 ft (305 m) thick aquifers with a porosity of 30% and a permeability in excess of 100 md (1 x 10⁻¹³ m²) - their definition of a "best case" aquifer. For one disposal well per sq. mile (2.56 sq. km), they found that the injection rate varied from 2800 to 5500 B/D (0.005 to 0.010 m³/s) for injection pressures of 1000 to 2000 psi (7 to 14 MPa). These conditions would require 4 times the number of reinjection wells and several times the reinjection pressure assumed for the Wilson et al. study.

The effect of increasing the reinjection pressure by 1000 psi (7 MPa), which reduces the net power output of the plant, is illustrated by the upper set of lines in Fig. 2. No attempt is made to adjust the costs for additional reinjection wells and additional piping. However, if reinjection wells were limited to a flow of 5000 B/D (0.009 m³/sec), the additional cost would shift the upper lines of Fig. 2 to the right by about 50%.

The cost of producing methane would be even higher without the power plant. For this case, the pump-

ing power for reinjection would have to be purchased or supplied by the methane. If supplied by a methane-fueled engine-driven compressor, 3.5 ft³ (0.1 m³) of methane would be required for each barrel of brine reinjected at a pressure of 1000 psi (7 MPa).

The assumption that the production wells, located at 1/2-mile (0.8 km) intervals, could produce 40,000 B/D (0.074 m³/s) for 20 years is also far too optimistic. As will be discussed later, the required spacing between wells for this sustained production rate will probably be a few miles.

The importance of well spacing on economics is illustrated in a report by Bloomster and Knutsen¹³ on the cost of using the thermal and hydraulic energy of geopressure brine for electricity. They analysed three power conversion systems: a flash steam system, an isobutane Rankine-cycle system, and a "total flow" system. The power costs from the flash steam and the isobutane systems were about the same; the isobutane was slightly lower. The total flow system gave costs 15 to 30% higher than those of the other cases considered. The authors emphasize that the exploitation of geopressured energy is highly dependent on the methane value and start with the assumption that the value of the methane is sufficient to offset the capital and operation and maintenance costs of the wells and the methane recovery system. However, they do include the cost of the collection piping system in the cost of the power plant.

A summary of their results is shown in Fig. 3. These results are based on December 1975 costs, a well spacing of about 1.85 miles (3.0 km), and a well flow rate of 81,500 B/D (0.15 m³/s). The high cost of the collection system offsets the savings from larger power plants and leads to the flat curves of power vs plant size. Figure 4 shows the effect of well spacing on power cost for a 55-MW(e) plant and a 327°F (164°C) brine temperature. The cost of the fluid transmission system equals the cost of the power plant for a well spacing of about 1-1/4 miles (2.0 km).

The study by Bloomster and Knutsen also emphasizes the importance of the brine temperature on power costs. Although temperatures in the geopressured formations range well above 300°F (150°C), the temperature from the Department of Energy test wells has been from 220 to 300°F (105 to 150°C).

METHANE CONTENT

Most studies of these reservoirs have assumed a methane content of 40 scf/bbl (7.1 m³/m³) - a reasonable value if the brine is saturated with methane and if the salinity of the brine is low. The data of Culberson and McKetta¹⁴ (Fig. 5) shows the solubility of methane in pure water. However, the solubility of methane varies inversely with water salinity; at a temperature of 250°F (121°C), the solubility decreases at a rate of 3 to 4% for each 10,000 ppm dissolved solids.^{15,16} Data from the first geopressured test well in Louisiana showed the solubility of the gas (which contained 93 to 96% methane) to be reduced by 35 to 50% for total dissolved solids at 110,000 to 140,000 ppm at a temperature of 240°F (115°C).¹⁷ These data also indicated that other gases (N₂, CO₂, and higher hydrocarbons) tend to decrease the solubility of methane in water. Results from recent test wells have shown dissolved solids ranging from 100,000 to 200,000 ppm and a methane content of about 20 scf/

bbl (3.6 m³/m³). If these low methane values are typical of the geopressured formations, then most earlier projections of the required price of the methane are too low by at least a factor of two.

RESERVOIR DRIVE

The primary driving force of a reservoir is its compressibility, which is a function of the compressibility of the liquid, C_e ; the compressibility of the rock matrix (the particles forming the structure), C_s ; and the pore compressibility, C_p . For a reservoir not containing free gas, the fluid compressibility is that of water, which, for the temperature and pressure range of interest, is $3.3 \times 10^{-6} \text{ psi}^{-1}$ ($4.8 \times 10^{-4} \text{ MPa}^{-1}$). Considering that the maximum pressure drawdown expected in a reservoir is about 5000 to 6000 psi (34 to 41 MPa), the maximum recovery from the depressurization of the brine would be 1.65 to 1.98% of the initial reservoir inventory.

As the fluid pressure in a reservoir is reduced, the weight of the overburden applies an increasing compressive load to the rock structure, which reduces its porosity and forces brine from the structure. The compressibility of the structure can vary widely depending on its degree of consolidation and cementation. Unfortunately, there are few data available on the compressibility of the geopressured reservoirs.

Van der Knaap¹⁸ found the rock matrix compressibility to be in the range of 2.97 to $3.44 \times 10^{-5} \text{ MPa}^{-1}$ (2 to $2.4 \times 10^{-7} \text{ psi}^{-1}$). Geertsma¹⁹ recommends using the compressibility of quartz for sandstone, about $1.9 \times 10^{-7} \text{ psi}^{-1}$ ($2.8 \times 10^{-5} \text{ MPa}^{-1}$).²⁰ For this paper a value of $2 \times 10^{-7} \text{ psi}^{-1}$ will be used.

Swanson and Osoba¹⁰ report a bulk compressibility value of 1.62×10^{-6} to $2.2 \times 10^{-6} \text{ psi}^{-1}$ (2.35×10^{-4} to $3.19 \times 10^{-4} \text{ MPa}^{-1}$) for geopressured core samples taken from a depth of 10,200 ft (3100 m) in a Brazoria County, Texas well. For a typical porosity value of 20%, these values correspond to a pore compressibility of 8×10^{-6} to $11 \times 10^{-6} \text{ psi}^{-1}$ (1.2×10^{-3} to $1.6 \times 10^{-3} \text{ MPa}^{-1}$). For consolidated and cemented sandstone from normally pressured reservoirs, a pore compressibility (measured by conventional laboratory hydrostatic tests) in the range of 3×10^{-6} to $10 \times 10^{-6} \text{ psi}^{-1}$ (4.4×10^{-4} to $15 \times 10^{-4} \text{ MPa}^{-1}$) is typical.^{18,21,22} However, hydrostatically determined values of C_p are not directly applicable to a reservoir. During the pressure drawdown of a reservoir, the weight of the overburden applies a uniaxial compaction load on the reservoir, whereas the hydrostatic tests subject the sample to a uniform load over the entire surface. Van der Knaap¹⁸ and Geertsma²³ recommend using an effective reservoir compressibility of $C_p/2 - C_s$ where C_p is the hydrostatically measured value of the pore compressibility.

Reservoir compressibility can also be estimated from the uniaxial compaction coefficient, C_m , which is defined as the fractional change in the height of the reservoir (or sample) per unit load applied. By assuming that the volume change results only from the change in pore volume, C_m can be related to the pore volume compressibility by the expression $C_m = \phi C_p/2$. Geertsma¹⁹ reports values of C_m for sandstone of various degrees of consolidation and different porosities for preloading conditions that correspond to burial depths of 1000 and 3000 m. For well-consolidated samples that have a porosity of 20% and are loaded to correspond to a burial depth of 3000 m, he

reports values of C_m ranging from $4 \times 10^{-5} \text{ MPa}^{-1}$ to $11 \times 10^{-5} \text{ MPa}^{-1}$ with an average value of about $7 \times 10^{-5} \text{ MPa}^{-1}$ ($4.8 \times 10^{-7} \text{ psi}^{-1}$). For similar samples loaded to correspond to a depth of only 1000 m, an average value of C_m of $9 \times 10^{-5} \text{ MPa}^{-1}$ ($6.3 \times 10^{-7} \text{ psi}^{-1}$) is obtained. These average values correspond to pore compressibilities of $7 \times 10^{-4} \text{ MPa}^{-1}$ ($4.8 \times 10^{-6} \text{ psi}^{-1}$) and $9 \times 10^{-4} \text{ MPa}^{-1}$ ($6.3 \times 10^{-6} \text{ psi}^{-1}$). Geertsma also gives data for semiconsolidated rock; these data show greater scatter and, for a porosity of 20%, indicate a compressibility about twice that of well-consolidated.

For this paper a pore compressibility of $7 \times 10^{-6} \text{ psi}^{-1}$ ($1 \times 10^{-3} \text{ MPa}^{-1}$) will be used. The effective reservoir compressibility, $C_e + C_p/2 - C_s$, is then $6.6 \times 10^{-6} \text{ psi}^{-1}$ ($9.6 \times 10^{-4} \text{ MPa}^{-1}$). The effect of the pore compressibility on the reservoir porosity and the maximum amount for brine that can be recovered from a reservoir is shown in Fig. 6 for an average reservoir pressure change of 6000 psi (41 MPa). Note that the recovery percent shown in Fig. 6 is the maximum that can be recovered regardless of flow rates or time required to reach the pressure drawdown. For the reference values used here, the maximum recovery is about 4%.

Some perspective can be given to these values by noting that the total brine required from a well producing 40,000 B/D ($0.074 \text{ m}^3/\text{s}$) for 20 years is 1.6 Bcf ($4.5 \times 10^7 \text{ m}^3$). For a porosity of 20% and a maximum recovery of 4%, the reservoir volume required to supply a single well is about 1.4 cu mile (5.8 km^3). This is illustrated in Fig. 7, which shows the reservoir thickness required as a function of well spacing for well flow rates of 40,000 and 80,000 B/D ($.074$ and $.146 \text{ m}^3/\text{s}$). Large reservoirs with a sandstone thickness sufficient to support wells on less than 2 to 3 miles (3.2 to 4.8 km) will probably be rare finds.

Unless these formations exhibit unusual compressibility characteristics, only very large reservoirs can support even a single well and the cost of a collection piping system would make multiwell processing plants very costly. Free gas within a reservoir would increase its compressibility and prolong its production life. Shale water influx could also act as a driving force. However, unless the permeability and compressibility of the shale in these reservoirs is one or two orders of magnitudes greater than normally pressured shale, the effect of shale water influx will be small.²⁴

PERMEABILITY

Generally, the permeability of the geopressured zone is very low along the lower Texas coast and increases toward the northern and eastern areas. Swanson et al. studied the permeability of geopressured gas fields in six counties (Cameron, Hidalgo, Willacy, Kenedy, Brooks, and Live Oak) of southern Texas. They found permeability values to range from less than 0.03 md ($3 \times 10^{-17} \text{ m}^2$) to more than 8 md; the average over all of the fields was about 1 md. Although there has been considerable speculation that the undercompaction of the geopressured zone would lead to an increase in permeability, this study did not find this to be true. They found that over the entire study area the permeability continued to decrease with increasing depth; the change was about one order of magnitude for each 2000 ft (610 m) of depth between 6000 (1830 m) and 14,000 ft (4270 m).

Even along the northern geopressured areas, permeabilities vary widely. Results from Department of Energy geopressure test wells indicate permeability values ranging from 10 to 15 md (10 to $15 \times 10^{-15} \text{ m}^2$) to over 300 md.

Figure 8 shows the life of a single well as a function of the reservoir permeability and size for constant well flow rates of 20,000, 40,000, and 80,000 B/D (0.037, 0.074, $0.147 \text{ m}^3/\text{s}$). For this case, the depth of the production interval is 14,000 ft (4300 m), the production interval is 200 ft (61 m), the initial pressure is 12,000 psi (83 MPa), the well diameter is 6 in. (15.2 cm), the effective reservoir compressibility (water plus rock structure) is $6.6 \times 10^{-6} \text{ psi}^{-1}$ ($9.6 \times 10^{-4} \text{ MPa}^{-1}$), the porosity is 20% and only single-phase flow is considered. The end-of-life wellhead pressure is assumed to be 250 psi (1.7 MPa), the pressure needed to suppress boiling of the water and allow sufficient pressure to deliver the brine to a central plant. However, after the wellhead pressure drops to 250 psi, the flow rate could be reduced and production continued at a lower flow rate.

During the early production period the reservoir acts as an infinite area system until the drawdown reaches the outer perimeter of the reservoir. After this time the pressure gradient in the reservoir goes through a transition period, and a new gradient is established that remains approximately constant with time. For the 80,000 B/D ($0.147 \text{ m}^3/\text{s}$) case, a reservoir of infinite size would require a permeability of about 30 md ($30 \times 10^{-15} \text{ m}^2$) for a 20-year life. A reservoir with a radius of 8 miles (12.9 km) would require a permeability of about 50 md for a 20-year life, whereas a 4-mile (6.4 km) radius would be too small regardless of the value of permeability. A 20-year life at 40,000 B/D ($0.074 \text{ m}^3/\text{s}$) requires a reservoir radius of about 4 to 8 miles and a permeability of 15 to 20 md. The 4-mile (6.4-km) radius corresponds to a well drainage volume of 1.9 cu mile (7.9 km^3).

RESERVOIR SIZE

The University of Texas and Louisiana State University have made extensive studies of the geopressured formations. The most promising area located by the University of Texas is the Brazoria Fairway.²⁶ This fairway has sandstone intervals totaling 800 to 900 ft (245 to 275 m) between the depth of 13,500 and 16,500 ft (4100 and 5000 m). The total area is about 60 sq miles (155 km^2). These values give a total sandstone volume of about 10 cu mile (42 km^3). However, the size of individual reservoirs will be much smaller.

The LSU study²⁷ included all of the known onshore geopressured areas of Louisiana and those offshore areas under state jurisdiction. They studied logs of about 6000 wells ranging in depth from 7500 to 25,600 ft (2290 to 6890 m) and averaging 12,980 ft (3950 m). Although the maximum sandstone thickness in one well was 2955 ft (900 m) the average was 434 ft (132 m).

Doscher¹¹ in an analysis of the Texas and Louisiana geopressured areas concluded that "it is optimistic to assume that a single geopressured reservoir having a volume of 3 cu miles will be found. Further, the geopressured aquifer volumes probably will not exceed 1 cu mile in volume, and the mode of the distribution may well be a minor fraction of 1 cu mile."

CONCLUSIONS

The geopressured aquifers of the northern Gulf of Mexico undoubtedly contain an enormous quantity of thermal and chemical energy. Much more information is needed to make accurate projections of the contributions of these aquifers to national energy needs; it will, however, probably be small, at least in the foreseeable future.

The expectation that the multiple energy aspects of the aquifers will enhance their economic potential is questionable unless improvements are made in low temperature power systems, or uses other than power generation is found for the low temperature energy.

Methane costs will be highly dependent on the reservoir size and characteristics. Costs of \$5 to \$10/Mcf (\$0.18 to \$0.35/m³) appear to be the best that can be expected for the most favorable reservoirs. However, if recent findings of only 20 scf (0.57 m³) of methane per barrel (0.16 m³) of brine are typical of these aquifers, then methane costs will probably be well above \$10/Mcf (\$0.35/m³).

NOMENCLATURE

Ce = brine compressibility - psi⁻¹ (MPa⁻¹)
 Cm = uniaxial compaction coefficient - psi⁻¹ (MPa⁻¹)
 Cp = pore compressibility - psi⁻¹ (MPa⁻¹)
 Cs = rock matrix compressibility - psi⁻¹ (MPa⁻¹)
 Ø = porosity

ACKNOWLEDGEMENT

This work was performed through the Energy Division of the Oak Ridge National Laboratory - operated by Union Carbide Corporation - under contract W-7405-eng-26 with the U.S. Department of Energy.

REFERENCES

1. Dorfman, M. H., and Deller, R. W., *Summary and Future Projections*, vol. 1 of *Proceedings, Second Geopressured Geothermal Energy Conference*, Center for Energy Studies, University of Texas, Austin, Feb. 23-25, 1976.
2. Papadopoulos, S. S., et al., "Assessment of Onshore Geopressured-Geothermal Resources in the Northern Gulf of Mexico Basin," pp. 125-46 in *Assessment of Geothermal Resources of the United States - 1975*, D. E. White and D. L. Williams, eds., U.S. Geological Survey Circular 726, 1975.
3. Wallace, R. H., et al., "Assessment of Geopressured-Geothermal Resources in the Northern Gulf of Mexico Basin," pp. 132-55 in *Assessment of Geothermal Resources of the United States - 1978*, L. J. P. Muffler, ed., U.S. Geological Survey Circular 790, 1979.
4. Jones, P. H., "Natural Gas Resources of the Geopressured Zones in the Northern Gulf of Mexico Basin," pp. 17-33 in *Natural Gas from Unconventional Geologic Sources*, National Academy of Sciences, Washington, D.C., 1976.
5. Brown, W. M., *100,000 Quads of Natural Gas?*, Research Memorandum #31, Report HI-2415/2-P, Hudson Institute, Inc., Croton-on-Hudson, N.Y., July 1976.

6. "The New Gas Bonanza," *Newsweek*, October 30, 1978, p. 64.
7. *Market Oriented Program Planning Study (MOPPS)*, U.S. Energy Research and Development Administration, Draft Report, May 1977.
8. Hise, B. R., "Natural Gas from Geopressured Aquifers," pp. 41-63 in *Natural Gas from Unconventional Geologic Sources*, National Academy of Sciences, Washington, D.C., 1976.
9. Dorfman, M. H., "Potential Reserves of Natural Gas in the United States Gulf Coast Geopressured Zones," pp. 34-40 in *Natural Gas from Unconventional Geologic Sources*, National Academy of Sciences, Washington, D.C., 1976.
10. Swanson, R. K., and Osoba, J. S., "Production Behavior and Economic Assessment of Geopressured Reservoirs in the Texas and Louisiana Gulf Coast", in *Proceedings of the Third Geothermal Conference and Workshop*, EPRI-WS-79-166 to be published.
11. Doscher, T. M., et al., "The Technology and Economics of Methane Production From Geopressured Aquifers", *J. Pet. Technol.* 31: 1502-14 (December 1979).
12. Wilson, J. S. et al., *A Study of a Phase "O" Plant for the Production of Electrical Power from U.S. Gulf Coast Geopressured Geothermal Waters*, Dow Chemical Company, February 1976.
13. Bloomster, C. H., and Knutsen, C. A., *An Analysis of Electricity Production Costs from the Geopressured Geothermal Resource*, BNWL-2192, Battelle Pacific Northwest Laboratories, Richland, Wash., February 1976.
14. Culberson, O. L., and McKetta, J. J., "Phase Equilibria in Hydrocarbon Water Systems III - the Solubility of Methane in Water at Pressures to 10,000 psia," *Trans. Am. Inst. Min. Metall. Pet. Eng.* 192: 223-26 (1951).
15. Silberberg, I. H., "Reservoir Fluid Sampling and Analysis for a Geopressured Geothermal Well," pp. 59-82 in *Reservoir Research and Technology*, vol. 3 of *Proceedings, Second Geopressured Geothermal Energy Conference*, Center for Energy Studies, University of Texas, Austin, Feb. 23-25, 1976.
16. Knaap, R. M., and Isokrari, O. F., "Aspects of Numerical Simulation of Future Performance of Geopressured Geothermal Reservoirs," pp. 103-61 in *Reservoir Research and Technology*, vol. 3 of *Proceedings, Second Geopressured Geothermal Energy Conference*, Center for Energy Studies, University of Texas, Austin, Feb. 23-25, 1976.
17. Karkalitis, O. C. and Hankins, B. E., "Chemical Analysis of Gas Dissolved in Geothermal Waters in a South Louisiana Well," pp. ED-41-ED-66 in vol. 2 of *Proceedings, Third Geopressured Geothermal Energy Conference*, Center for Energy Studies, The University of Southwestern Louisiana, Lafayette, Nov. 16-18, 1977.

AN EVALUATION OF THE GEOPRESSURED ENERGY RESOURCE OF LOUISIANA AND TEXAS

18. Van der Knapp, W., "Nonlinear Behavior of Elastic Porous Media," *Trans. Am. Inst. Min. Metall. Pet. Eng.* 216: 179-87 (1959).
19. Geertsma, J., "Land Subsidence Above Compacting Oil and Gas Reservoirs," *J. Pet. Technol.* 25: 734-44 (June 1973).
20. Kaye, G. W. C., and Laby, T. H., *Tables of Physical and Chemical Constants*, Wiley, New York, 1966, p. 34.
21. McLatchie, A. S., et al., "The Effective Compressibility of Reservoir Rock and its Effects on Permeability," *Trans. Am. Inst. Min. Metall. Pet. Eng.* 213: 386-88 (1958).
22. Hall, H. N., "Compressibility of Reservoir Rocks," *Trans. Am. Inst. Min. Metall. Pet. Eng.* 198: 309-11 (1953).
23. Geertsma, "The Effect of Fluid Pressure on Volumetric Changes of Porous Rock," *Trans. Am. Inst. Min. Metall. Pet. Eng.* 210: 331-340 (1957).
24. Samuels, G., *Geopressure Energy Resource Evaluation*, ORNL/PPA-79-2, Oak Ridge National Laboratory, Oak Ridge, Tennessee, May 1979.
25. Swanson, R. K., et al., *Development of an Assessment Methodology for Geopressured Zones of the Upper Gulf Coast Based on a Study of Abnormally Pressured Gas Fields in South Texas*, C00-2687-6, Southwest Research Institute, San Antonio, Texas, August 1976.
26. Bebout, D. G., Loucks, R. G., and Gregory, A. R., *Frio Sandstone Reservoirs in the Deep Subsurface Along the Texas Gulf Coast - Their Potential for the Production of Geopressured Geothermal Energy*, Bureau of Economic Geology Investigation Report No. 91, University of Texas, Austin, 1978.
27. Bernard, W. J., "Geopressure Resource Assessment - Southern Louisiana," pp. GI-109-GI-119 in vol. 1 of *Proceedings, Third Geopressured Geothermal Energy Conference*, Center for Energy Studies, The University of Southwestern Louisiana, Lafayette, Nov. 16-18, 1977.

Table 2

Cost summary for 25-NW(e) single- and double-stage flash plants

Table 1

Assumptions for Plant of Ref. 12

Date of costs = January 1976,

Brine production rate per well = 40,000 B/D ($0.074 \text{ m}^3/\text{s}$),

Brine temperature = 325° (163°C),

Plant operating factor = 90%,

Brine pressure to the hydraulic turbine = 2000 psia (13.8 MPa),

Return on investment = 12.8%,

Depreciation = 5% of capital cost,

Taxes, insurance, general and administrative costs, overhead = 4% of capital cost,

Operating costs = 8% of capital cost.

	Single-stage flash	Double-stage flash
Production wells		
Number required	10.8	8.5
Number provided	12	10
Brine production rate, $10^3 \text{ B/D } (\text{m}^3/\text{s})$	432 (0.80)	340 (0.63)
Fuel plant		
Capital cost, $\$10^6$	53.07	43.55
Annual capital and operating cost, $\$10^6/\text{year}$	15.81	12.96
Cost of brine, $\text{¢/bbl } (\text{¢/m}^3)$	11.1 (70)	11.6 (73)
Power plant		
Capital cost, $\$10^6$	14.49	16.95
Annual capital and operating cost, $\$10^6/\text{year}$	4.32	5.05
Annual power output, 10^6 kWh/year	197	197

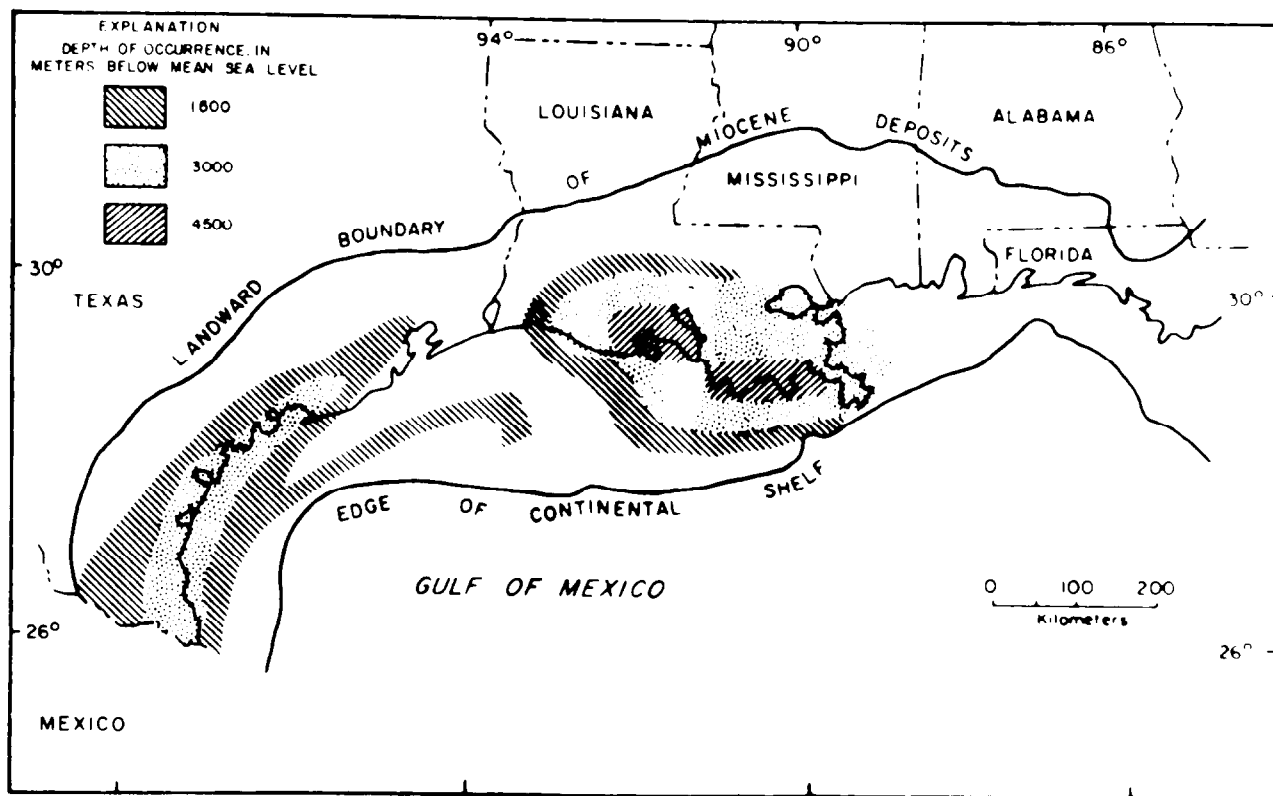


Fig. 1 - Areas of potential geopressure resources in the northern Gulf of Mexico Basin.
(From Ref. 1).

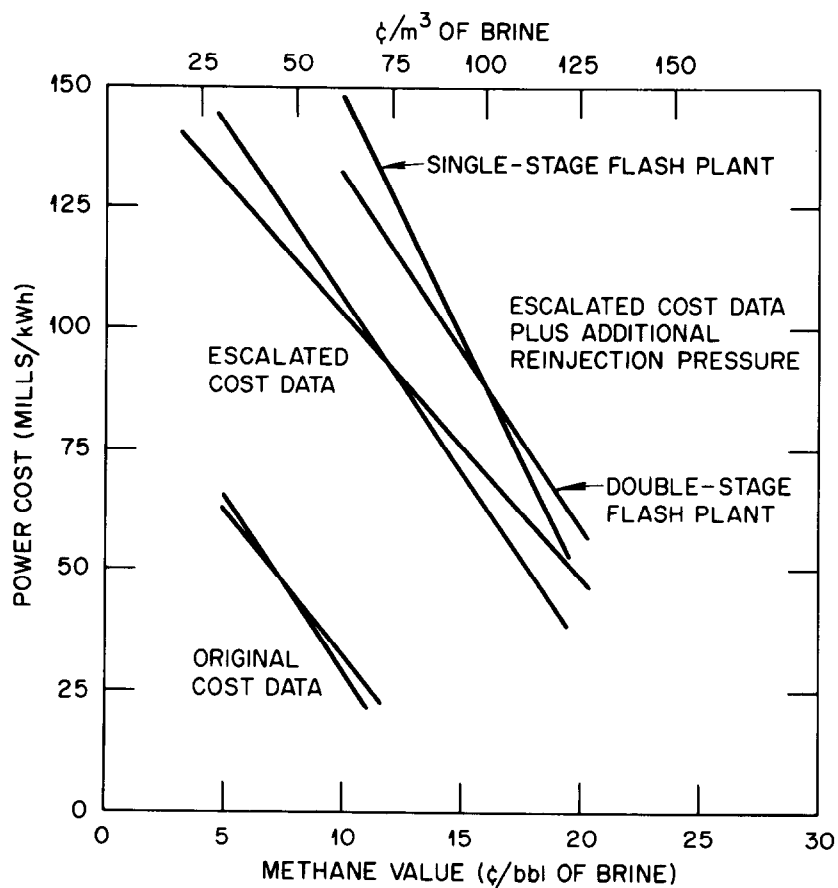


Fig. 2 - Cost of electrical power from a geopressure geothermal plant as a function of the methane value.

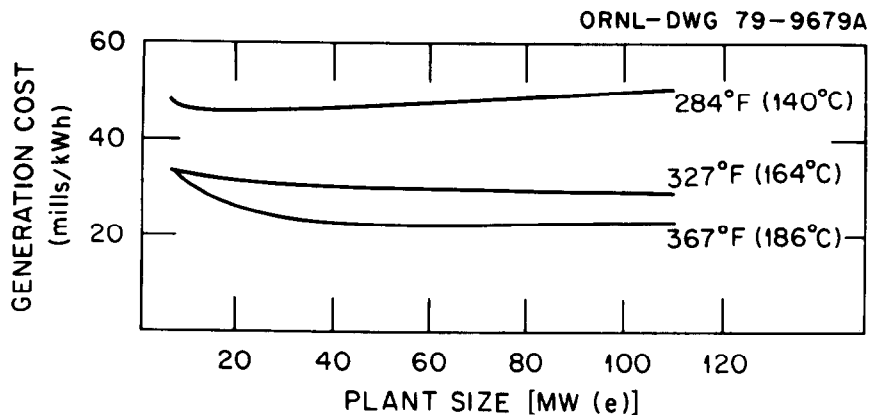


Fig. 3 - Impact of plant size on generation cost (From Ref. 13).

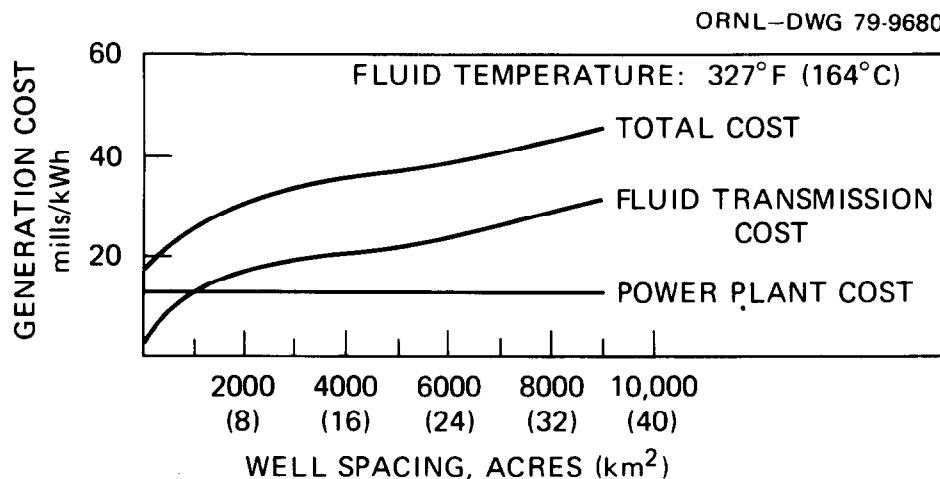


Fig. 4 - Impact of well spacing on generation cost distribution (From Ref. 13).

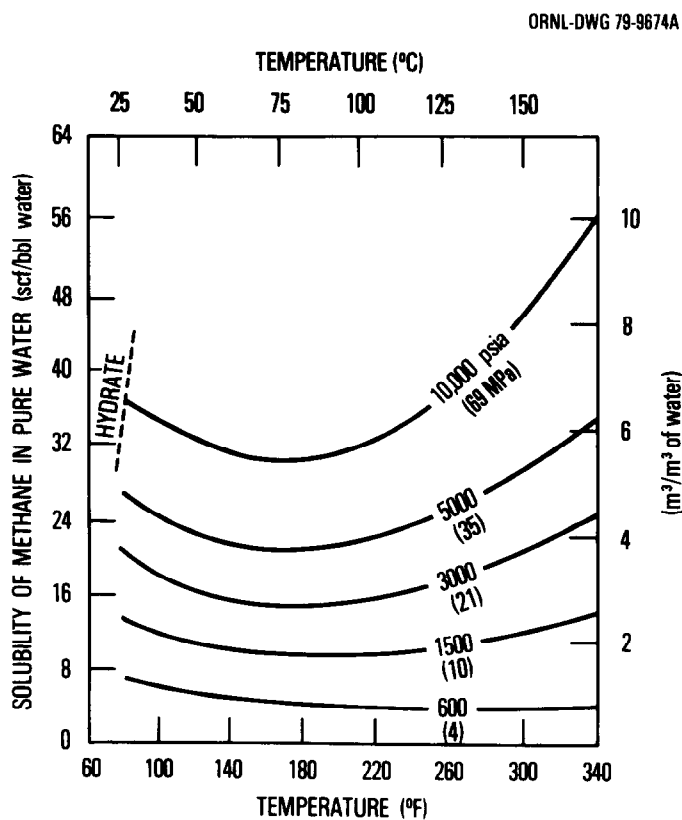


Fig. 5 - Solubility of methane in pure water (From Ref. 14).

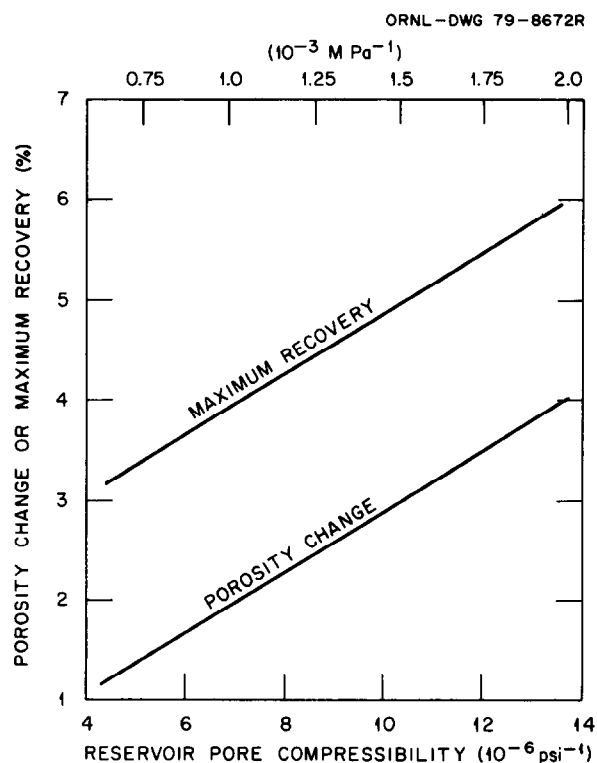


Fig. 6 - Effect of reservoir pore compressibility on the porosity change and maximum recovery for a 6000-psi (41-MPa) change in reservoir pressure.

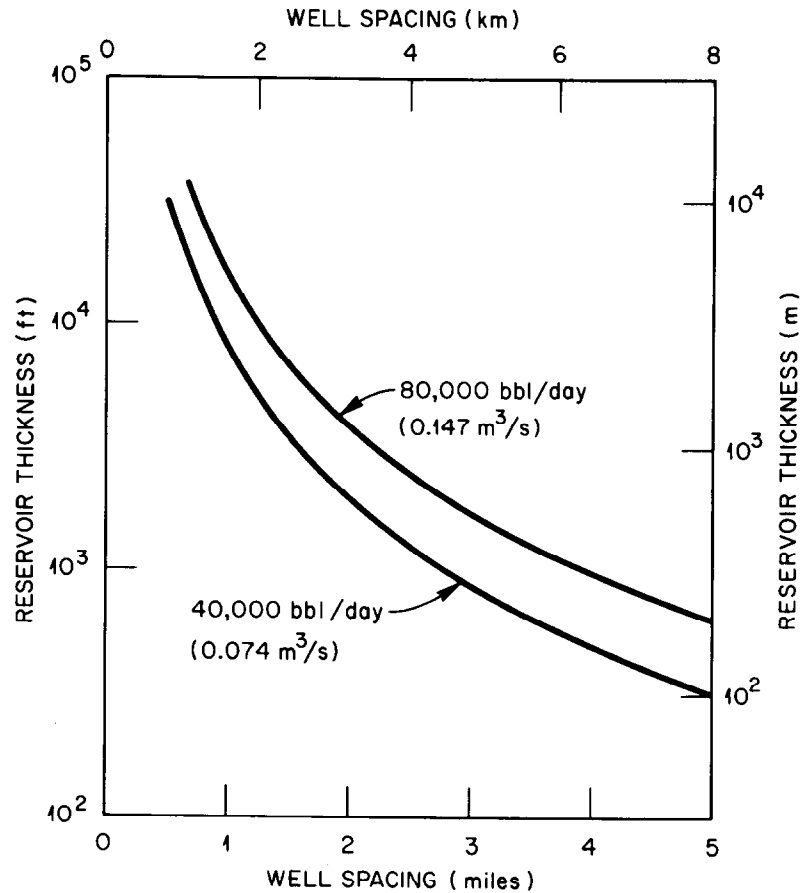


Fig. 7 - Required reservoir thickness as a function of well spacing for well flow rates of 40,000 B/D ($0.074 \text{ m}^3/\text{s}$) and 80,000 B/D ($0.147 \text{ m}^3/\text{s}$) and a well life of 20 years.

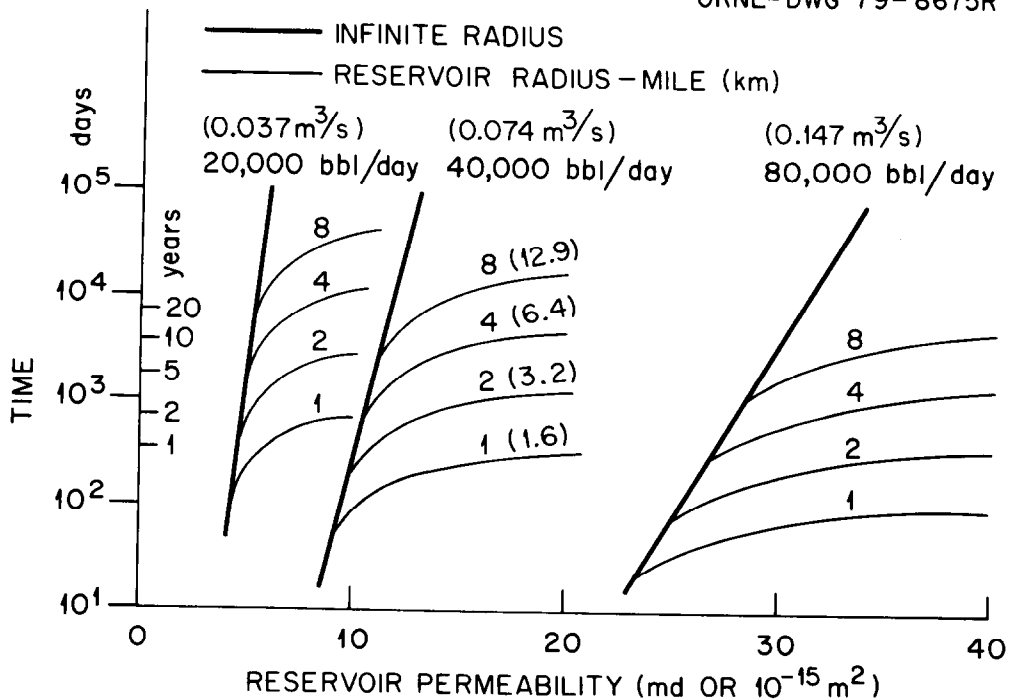


Fig. 8 - Well life as a function of permeability, flow rate, and reservoir radius.

SECOND GENERATION TECHNOLOGY FOR THE PRODUCTION OF PIPELINE QUALITY GAS FROM SANITARY LANDFILLS

by Frederick C. Rice, Getty Synthetic Fuels, Inc.

© Copyright 1980, Society of Petroleum Engineers

This paper was presented at the 1980 SPE/DOE Symposium on Unconventional Gas Recovery held in Pittsburgh, Pennsylvania, May 18-21, 1980. The material is subject to correction by the author. Permission to copy is restricted to an abstract of not more than 300 words. Write: 6200 N. Central Expwy., Dallas, Texas 75206

ABSTRACT

With the advent of replacement energy cost pricing for natural gas, the recovery and treatment of methane generated by sanitary landfills has become a commercial reality. The first landfill methane recovery plant, owned and operated by Getty Synthetic Fuels, Inc., has been in operation at Palos Verdes, California since 1975. Getty has built a second plant, which has been in operation in the city of Monterey Park, California since August 15, 1979. These two facilities are the only plants in the United States which produce pipeline quality gas from landfills.

Although similar to the Palos Verdes facility in some respects, the Monterey Park methane recovery facility is four times as large, and represents a significant advance in the State of the Art of landfill methane recovery and purification. This paper will discuss the similarities between these two operations, but, more importantly, will point out the significant technological advances made over the past four years, which have advanced landfill methane recovery from the demonstration project phase to the large scale, economically viable operation that it is today.

BACKGROUND

Historically, the generation of methane from the natural decomposition of refuse in sanitary landfills has long been known, but was considered for years to be more of a liability than an asset because of its potential for underground migration into nearby areas. Many landfills have controlled this migration by the use of venting systems or peripheral wells from which the gas was withdrawn under vacuum and pumped to flares.

Although the energy value of this gas began to be realized in the early 1970's, there was not sufficient economic incentive to develop it on a commercial scale. The very creation of the natural gas industry itself, and the explosive growth in the transmission and consumption of natural gas was brought about, in part, by an extremely low pricing structure. This continued, artificially set, low gas price discouraged the development of alternative energy sources for a number of years. With the natural gas shortage of 1973, and the rapid increases in the price of natural gas which followed, the possibility of developing landfill methane recovery on a commercially viable scale began to come into focus.

The world's first landfill methane recovery facility at Palos Verdes, California, was built entirely with private capital by Reserve Synthetic Fuels, the predecessor of Getty Synthetic Fuels, Inc., and began operations in June, 1975. This was a pilot plant, designed primarily to prove the technical feasibility of methane recovery and processing on a commercial scale. Since low pressure and volumes would be encountered, a molecular sieve, pressure swing adsorption system was used for carbon dioxide removal, with activated carbon pretreaters to remove other components of the gas stream. Severe technical difficulties were encountered during the first year of plant operation, requiring over \$1,000,000 in major plant modifications to correct. Since returning to operation in January, 1977, the Palos Verdes facility has enjoyed a 90%-plus on-stream time for the past three years. The lessons learned in the development of this pilot facility proved invaluable in the design of a second, larger facility at the Operating Industries landfill in Monterey Park, California. The detailed knowledge gained about both the nature of landfill gas and the unique steps required

SECOND GENERATION TECHNOLOGY
FOR THE PRODUCTION OF PIPELINE QUALITY GAS FROM SANITARY LANDFILLS

for its handling have enabled Getty Synthetic Fuels, Inc., a wholly-owned subsidiary of Getty Oil Company, to design and build a facility which is technologically and economically superior to its pioneering effort at Palos Verdes.

DESCRIPTION OF SYSTEM

The Monterey Park system consists of four major phases: (1) Gas Collection System; (2) Compression; (3) Pretreating; and (4) CO₂ Removal. In addition to these four phases, the Palos Verdes facility included a fifth phase, Delivery Compression, which is unnecessary at Monterey Park.

GAS COLLECTION SYSTEM

The Operating Industries landfill is one of the largest in the United States. It covers approximately 60 hectares and contains approximately 18,144 kg of refuse piled to an average depth of over 90 meters, with some sections over 105 meters. Because of the size and configuration of the landfill, the gas collection system is far more complex than the one at Palos Verdes, which consists of only ten wells over an area of approximately 20 hectares. At Monterey Park there are presently 51 operational wells, half of which recover gas from the upper portion of the landfill, with the other half pulling gas from the deeper sections. Gas is withdrawn from the wells through a network of over 4.5 kilometers of laterals and header pipes which route the gas to the plant inlet.

Heavy wall polyethylene pipe is used at Monterey Park, as at Palos Verdes, but newer, more sophisticated, wellhead control systems have been developed to facilitate balancing the entire collection system to ensure uniform gas flow.

COMPRESSION

Collection system vacuum and process pressure is provided by two 820 KW gas fueled, four-stage reciprocating compressors, which are capable of withdrawing over 225,000 cubic meters of raw gas per day from the landfill. This is a significant increase in size over the two-stage 300 KW compressor used at Palos Verdes, which was only capable of withdrawing approximately 37,000 cubic meters of raw gas per day. The Palos Verdes inlet volume was increased to nearly 56,000 cubic meters per day in May, 1979, by the installation of auxiliary equipment, so that this plant can now also be considered to be of commercial size.

Process pressure at Monterey Park is approximately 3450 kilopascals as compared to less than 345 kilopascals at Palos Verdes. This higher pressure eliminates the need for another stage of compression prior to delivering product gas.

PRETREATING

Whereas the Palos Verdes facility used various combinations of activated carbon, molecular sieve, and triethylene glycol to remove moisture, heavy hydrocarbons, and other trace contaminants, the Monterey Park facility uses a more straightforward, but sophisticated, approach to the problem through the use of chilling and a specially-designed pretreatment step whose design was based on the knowledge of landfill gas composition learned at Palos Verdes. The main key to the processing of raw landfill gas lies in this unique pretreatment step, which removes contaminants from the raw gas, making it compatible for use with conventional CO₂ removal processes.

CARBON DIOXIDE REMOVAL

Carbon dioxide removal is accomplished by a commercially licensed physical solvent-type process, which was selected for use at Monterey Park over a molecular sieve process because of the higher gas volumes and delivery pressures involved. Two absorber columns are used due to aesthetic and environmental restrictions to having a taller, single column. The solvent is regenerated in a three-stage flash system, with the CO₂ being vented to the atmosphere. Discussions are presently underway for the sale of this CO₂ by-product to a commercial user. Following carbon dioxide removal, gas is delivered directly to a Southern California Gas Company metering station which measures volume, heating value, and specific gravity. An odorant is also added to the gas before it is delivered into the SoCal distribution system.

The facility is fully automated, and has an extensive process monitoring system which would shut the plant down and notify operators, police or fire departments, as appropriate, in the event of malfunction, fire, or intrusion.

OPERATIONAL STATUS

The Monterey Park facility began operations on August, 1979. Mechanically, the plant has encountered only one problem of any significance. Due to vendor error, one of the compression cylinder liners cracked on start up and required nearly two months to replace. From a process standpoint, the plant has operated entirely up to expectations, with a 90% on-stream factor during the first month of operation, and as high as 99% during some subsequent months.

The major problem encountered thus far at the Monterey Park facility was in the tuning of the gas collection system. Due to the immense size of the landfill itself, its non-homogeneity, and the complexity of the collection system, an initial over-pulling of some of the wells caused air to be drawn

SECOND GENERATION TECHNOLOGY
FOR THE PRODUCTION OF PIPELINE QUALITY GAS FROM SANITARY LANDFILLS

in through poor cover and previously undetected cracks in the landfill cover. The resulting air intrusion has temporarily reduced the methane production rate along the periphery of the landfill. These wells are being brought back into production at a lower wellhead pressure and at a lower gas flow. The remaining wells in the center of the landfill have produced at a fairly high rate on a continuous basis but, for reasons of caution, the plant inlet rate is presently at less than rated capacity. This rate is being steadily increased as methane production returns to normal.

ECONOMICS

Although specific economic details of the Monterey Park operation cannot be divulged, it is significant to note that the contract for sale of the gas to Southern California Gas Company, and a renegotiated contract at the Palos Verdes facility, have succeeded in identifying pipeline quality product gas processed from sanitary landfills as a separate energy entity, such as SNG or LNG. No longer are attempts made to equate the price of processed landfill gas to the artificially regulated price paid to traditional suppliers.

Landfill gas is now uniquely identified as having its own quality standards, which incidentally, are the same as the standards for traditional natural gas supplies. Landfill gas was specifically exempted from federal price controls with the passage of the Federal Energy Bill in 1978. Getty Synthetic Fuels, Inc., is taking a strong stand against government involvement in this free enterprise area so that landfill gas can continue to compete favorably with other alternate energy sources.

OTHER TECHNOLOGICAL ADVANCES

In addition to the advances made in process technology and collection system design, Getty Synthetic Fuels, Inc., has also made significant strides in the development of sophisticated testing techniques to determine the gas production potential and longevity of a given landfill. In addition

to the two full months of round-the-clock field testing currently performed on every landfill considered for development, both aerobic and anaerobic refuse samples are subjected to a variety of laboratory tests to confirm field test data. Evaluation of alternate gas processing technologies is also continuing and investigation is currently underway to find methods for improving landfill gas collection system efficiencies.

RELATED DEVELOPMENTS

Although Palos Verdes and Monterey Park are the only facilities which produce pipeline quality gas with a heating value of 9550 kilocalories per cubic meter from landfills, other developers, primarily engineering consulting firms, have brought six other facilities on line which produce an intermediate, level fuel gas for direct use by nearby industrial consumers. Processing at these facilities varies from simple dehydration to removal of heavy hydrocarbons by chilling, resulting in a product gas with a heating value of approximately 5400 kilocalories per cubic meter. Another facility uses a molecular sieve process to produce an intermediate level product gas with a heating value of approximately 6700 to 8600 kilocalories per cubic meter, which is injected into a high volume natural gas pipeline.

Getty Synthetic Fuels' operations for the immediate future include construction of pipeline quality gas facilities in Chicago and Staten Island, New York. Two intermediate-value fuel gas facilities in Northern California are scheduled to go on stream in late 1980.

In summary, while landfill gas will never represent a major portion of the overall energy picture in this country, it is nonetheless, a significant contribution to the country's continuing search for alternate energy sources. It is likely that, as future development occurs, the present second generation technology will continue to give way to even more advanced techniques for turning the nation's refuse into a useable resource.

AN ECONOMIC NATURAL GAS RECOVERY METHOD FOR WELLS WITH NO PIPELINE CONNECTION

by Jack M. Burns, Texas Gas Transport Co.
and Pressure Transport Inc.

© Copyright 1980, Society of Petroleum Engineers

This paper was presented at the 1980 SPE/DOE Symposium on Unconventional Gas Recovery held in Pittsburgh, Pennsylvania, May 18-21, 1980. The material is subject to correction by the author. Permission to copy is restricted to an abstract of not more than 300 words. Write: 6200 N. Central Expwy., Dallas, Texas 75206

ABSTRACT

Marginal gas fields located remote from gas transmission lines represent a serious challenge in gas management. Often the net revenue from the estimated reserves of such fields will not justify the cost of pipeline construction and as a result many wells with substantial flow rates are never commercially produced. This paper describes the process of transporting Compressed Natural Gas (CNG) by truck as an alternative to pipeline construction. It can be used to transport gas to commercial markets until either the reserve estimates are amended upward, thus allowing pipeline construction, or until the field is depleted. It is also an economically feasible alternative to the flaring of natural gas associated with oil production.

INTRODUCTION

When natural gas and other energy prices rose precipitously after the oil embargo of 1973, it became economically feasible to lay gathering and transmission pipelines to many gas wells and fields previously deemed non-commercial because of limited or unknown reserves. Higher gas prices increased the total revenue expected from those wells to a point commensurate with the risk of installing the gathering pipeline systems. Many other wells, however, are still not connected because of the unacceptable financial risks. Usually these wells are small or remotely located such that the value of gas believed to exist is insufficient to pay for the cost of installation and operation of the pipeline. Recognition of the existence of these unconnected wells has brought about investigations of numerous production schemes including gas liquification, chemical conversion, and well site electricity generation, all of which strive to find a means to produce the wells at lower overall cost, so that the total cost to produce each well falls below that value deemed recoverable based on the best reservoir size estimates.

Illustrations at end of paper.

One production technique that has been proven to be economically feasible is the transportation of Compressed Natural Gas (CNG) at ambient temperature in high pressure cylinders mounted on appropriate transport vehicles. This process, which was pioneered and patented by Texas Gas Transport Company, has been used since 1975 to transport over 4000 loads of natural gas from 12 wells in four states. It is a simple system applicable to either onshore truck and rail transportation or to offshore barge transportation of natural gas with a wide range of compositions. CNG transportation has relatively low capital and relatively high operating costs, which makes it competitive with pipelines in those specific circumstances where high capital costs cannot be justified. It is believed to be more commercially adaptable than any of the alternative gas production techniques both because of its cost and because the gas is not converted to a less desirable product or form.

It is the purpose of this paper to describe onshore CNG transportation systems as they now exist and to compare their costs to those of a pipeline for a range of operating conditions.

CNG TRANSPORTATION SYSTEM DESCRIPTION

Compressed natural gas is transported in specially designed jumbo tube trailers, each containing ten horizontal, cylindrical, forged pressure vessels 22 inches (0.56 m) in diameter and 34 feet (10.4 m) long with an interior volume of about 77 cubic feet (2.2 m³) and with a rated pressure of at least 2400 psi (16.5 MPa), but seldom exceeding 2800 psi (19.3 MPa). These vessels are made by United States Steel Corporation. Several different system operating configurations exist, but they all follow the same basic steps. In each system, gas at the wellhead is treated as necessary, compressed and loaded into trailers. It is then hauled to an appropriate discharge site and unloaded through a metering system into a discharge line using pressure differential between trailer and line. A discharge compressor may be employed to evacuate the cylinders to a pressure below the pipeline pressure, or the

trailers may return to the load site with a residual pressure equal to the pipeline pressure. At no time is the trailer pressure allowed to drop below ambient pressure. Figure 1 shows a schematic for a typical loading site.

Since most pipeline companies want to independently measure all gas entering their pipelines, they frequently require the installation of orifice or turbine metering stations at the unload sites. However, the most accurate metering system is the known, fixed volume and easily measured temperature and pressure of a trailer. Each load of gas has its temperature and pressure measured four times: before and after both loading and unloading. These four measurements, coupled with the gas analysis, provide stable readings for the determination of the net delivered gas volume with a much greater degree of accuracy than is possible with either orifice or turbine meters.

Each transport system consists of one or more trailers transporting gas from one or more wells or load sites to a single unload site. The maximum capacity of each trailer depends on the measured interior volume of the cylinders, the pressure and temperature at which the gas is hauled, and the gas composition, but generally lies between 150 MCF ($4.3 \times 10^3 \text{ m}^3$) and 175 MCF ($5.0 \times 10^3 \text{ m}^3$). Numerous loads may be required to transport the daily output of any given well or set of wells and for this reason, most systems operate 24 hours a day 7 days a week.

The most common system in operation consists of two trailers and one tractor transporting gas from one load site serving several wells to one unload site at a pipeline. In such a system, one trailer is always at the load site being filled, while the other trailer is driven to the unload site, discharged, and returned to the load site. When the first trailer is full, the empty trailer is started loading and the process repeated. In this system, one trailer is always at the well site loading, so the wells can be kept in continuous production.

When the trailer unload time plus the two way driving time is greater than the usual time required to fill a trailer, a third trailer can be added so that one trailer is always loading, one is always unloading, and the third is always in transit, thus shortening the time between trailer changes and increasing the volume hauled. In another system where there are several wells in different locations, each producing only one or two loads per day, all within a reasonable distance of the unload site, a system may be established in which one trailer is placed at each load site, with a common trailer always in transit. In this operating system, the common trailer is taken and discharged. That empty trailer is then taken to another well site where it is left and the process is repeated.

Other systems using permanent on-site gas storage could be devised, but in general loading directly into the trailers is more cost effective because on-site storage must either be at considerably higher pressure or must be of considerably larger volume than the trailers in order for the equalized loaded trailer pressure to be near the trailer's maximum pressure. Filling trailers through a compressor from on-site storage is inefficient because the trailers are out

of service while filling just as if they were filling directly from the wells. It is also not clear that on-site storage facilities are any less expensive than the trailers themselves because the possibility exists that any permanent storage facility would need to be buried to meet all federal regulations.

CNG TRANSPORTATION SYSTEM APPLICATIONS

Truck transportation of CNG is a process that can produce significant volumes of natural gas that have previously been too remote to be considered marketable. In the past, numerous hydrocarbon wells have encountered natural gas but have never been produced. Over 3000 shut-in or plugged and abandoned natural gas wells have been identified in the state of Texas alone and many others are believed to exist throughout the country. These wells were not deemed marketable at the time of drilling because estimated gas reserves at then current prices was not sufficient to justify a pipeline. Even today many of these wells can not justify pipeline construction because of unknown reserve size. It is only through extensive drilling programs or through production history that reservoir sizes can be determined with any degree of accuracy. For these wells, the drilling programs failed to confirm adequate reserves and therefore pipelines have not been built and no gas production history established. Herein lies one of the great advantages of CNG truck transportation. With very little capital risked, those wells and fields can now be produced for a sufficient time to establish a production history and a "proven" reservoir size. Once that reservoir size is proven, one of two events will occur: either a pipeline will be built and the trucks removed, or the reserves will be of insufficient size and the trucks will remain until the field is depleted. In either event, gas is brought to market that would have otherwise remained in the ground.

CNG transportation removes the capital investment risks that keep the pipelines away. For the same reason, CNG transportation could be used on any gas field where some risk is involved even if estimated reserves do justify the pipeline. Estimated reserves are never assured, and CNG transportation can add the certainty needed to bolster the economics of a questionable project. Of course there are also CNG projects in which it is known in advance that no pipeline can ever be justified.

Other applications for CNG transportation include the following:

1. Lease saving - truck transportation can be used temporarily where tight deadlines otherwise prevent "commercial" production before oil and mineral leases expire.
2. Flared gas - truck transportation of small quantities of gas can allow oil production where flaring is not allowed.
3. Emergency supply - truck transportation can replace disrupted primary gas supply systems at hospitals, factories, schools or even whole cities.
4. Right-of-way problems - truck transportation can produce gas where pipeline right-of-way acquisition is impossible or delayed due to

environmental, safety or other considerations.

5. Well testing - truck transportation can allow wells to be tested without wasting gas by flaring or venting.
6. Cash flow generation - truck transportation can be used as soon as wells are completed, thus generating early cash flow for other drilling or for pipeline construction.

CNG TRANSPORTATION SYSTEM LIMITATIONS

Limitations on truck transportation of CNG are of three types: capacity, cost, and gas quality. Capacity limitations relate to the physical limits on time required to load and unload each trailer and the time required to transport the trailers between load and unload sites. The trailers are very heavy and travel speeds are limited by road conditions. Only on reasonably long runs of 30 miles (48 km) or more are speeds able to approach 50 mph (80 km/h) and only then if the entire distance is on paved highway. Average speeds tend to be more nearly 15 to 20 mph (24 km/h to 40 km/h) during the travel time. The time required for loading is related to the output of the wells being serviced, but it is unlikely that a load time of less than 1/2 hour could be achieved. Similarly, unload times are determined by the rate at which gas can be accepted by the unload facility, but unloading in less than 1/2 hour is not desirable. One and one-half hours is the minimum possible time per load if we assume these minimum load and unload times along with some minimum transport distance of say 2 miles (3.2 km) or 10 travel minutes each direction with 10 minutes total to connect and disconnect at each end. Twenty-four hours divided by 1½ hours gives 16 loads per trailer per day. Sixteen loads times 175 MCF ($5.0 \times 10^3 \text{ m}^3$) per load gives 2800 MCF ($80 \times 10^3 \text{ m}^3$) per trailer per day as an absolute maximum delivery rate. As will be described later, the delivery of that volume of gas a distance of 2 miles (3.2 km) can be accomplished much more cheaply by pipeline unless some extraordinary circumstances exist. Table 1 shows the maximum daily delivery volume for several one way distances, assuming a two trailer system hauling 175 MCF ($5.0 \times 10^3 \text{ m}^3$) per load on paved roads with a minimum 30 minute unload time.

Cost limitations on truck transportation of CNG will be discussed in greater detail later, but suffice it to say that standard one trailer CNG transport system equipment costs may be as much as \$200 000 and must generate about \$3200 per month just to pay for itself. If that system is dedicated to a given gas well, that well must flow 53 MCF/D ($1.5 \times 10^3 \text{ m}^3/\text{d}$) for 30 days at \$2.00/MCF (\$70.00 m^3) just to get enough gas to cover equipment costs with nothing left for the producer or royalty owner, or to cover operating costs. The transport cost per unit of gas at low delivery rates is generally high when compared to the cost of the gas. The exact minimum delivery limitation is an economic judgement, but the limitation does exist.

Gas quality limitations are very clearly defined by the Department of Transportation for CNG transportation on public roads and highways or in any interstate commerce. At the present time NO SOUR GAS CAN BE TRANSPORTED. Each well must be tested using specified procedures, and total H_2S in the gas after

treatment must be less than .1 grain per 100 SCF (2.29 mg/m^3). Normal pipeline quality is .25 grains per 100 SCF (5.73 mg/m^3). In addition, moisture content of the gas must be less than 1/2 pound water per 1000 MCF (8.0 g/m^3) after treatment, where normal pipeline quality is 7 pounds water per 1000 MCF (112 g/m^3). Non-hydrocarbon gases such as carbon dioxide and oxygen also have specified maximum allowable levels, but the levels are very nearly standard pipeline quality and therefore pose little, if any, limitations on the system.

PHYSICAL PROPERTIES OF CNG

Natural gas is an ill-defined term relating to any of a wide range of primarily hydrocarbon gases occurring in natural earth formations. Methane is usually the most abundant constituent and may account for up to 99% of the gas but heavier hydrocarbons, including ethane, propane, butanes, pentanes, etc., as well as non-hydrocarbon gases such as carbon dioxide and nitrogen are usually present. Hydrogen Sulfide may also be present but gases containing H_2S in concentrations greater than limits specified cannot be transported as CNG and therefore are not considered here.

The various mixtures of gas have an extremely wide range of properties some of which cannot be clearly defined without laboratory tests on actual gas samples. Some properties are defined however, and these relate to both the state of the gas at pressure and to the supercompressibility of the gas.

The primary economic advantage of the high pressure method of transporting natural gas in contrast to techniques requiring refrigeration, is based on the fundamental laws of physical science, namely that the high pressure method of transporting natural gas minimizes the total change in the thermodynamic state (characterized by the property of entropy) of natural gas between the load site and the unloading site and that such thermodynamic changes are directly related to the cost of mechanical equipment required to perform such changes of state.

Although there is no theoretical upper limit on the pressure at which natural gas can be transported at ambient temperatures, practical limitations and economic factors suggest pressure near 2400 psi (16.5 MPa) as optimal for several reasons. Perhaps the most important of which is the availability of pressure vessels approved by the Department of Transportation for highway use. These vessels are available in large sizes for the specialty gas industry with pressure ratings of 2400 to 2800 psi (16.5 to 19.3 MPa) depending on individual vessel pressure tests. This pressure rating could not have been more appropriately chosen from a thermodynamic standpoint, as the maximum supercompressibility of natural gas at ambient temperatures occurs at pressures between 1500 and 2200 psi (10.3 to 15.2 MPa) depending on the gas composition (see Figure 2). At higher pressures, supercompressibility is reduced until it has almost no effect at 5000 psi (34.5 MPa). Also from a thermodynamic standpoint, virtually all naturally occurring multi-component hydrocarbon gases are above both the critical point and the cricondenbar at pressures in excess of 2000 psi (13.8 MPa), thus only a single phase fluid exists in the trailers during transport and at those times when initial volume determinations

are made. The availability of standard loading compressors and oil field type equipment also suggest 2400 psi (16.5 MPa) as a good hauling pressure. Higher pressure compressors are available but only at inordinately higher capital and maintenance costs.

CNG TRANSPORTATION COSTS

The transportation of CNG by truck, though relatively simple from a technical standpoint, is somewhat complicated in financial terms. The value at wellhead prices of one load of gas ranges from only \$350.00 to \$550.00 but requires personnel and equipment similar to cross-country truck transportation of merchandise where the cargo value may easily be greater than \$100 000. Obviously, CNG transportation requires diligent effort to get as many loads of gas per unit of equipment as possible and to make appropriate trade-offs between equipment and personnel costs and operating efficiency.

Equipment utilization is dependent on several factors, all related to the time required to transport a load of gas including load time, round trip travel time, unload time and maintenance downtime.

Generally, load time is determined by the output rate of the well or wells and is independent of other factors except the net delivery capacity of the trailer. For a given well, the output rate of gas can be determined by test prior to the transport system installation but the initial rate may decline with time as the reservoir is depleted. Additional wells may be connected to a central loading station in order to maintain the initial flow rate, or the system may be changed to maintain efficiency as the wells decline. If load compression or other load site equipment is required, it is sized to match the well output rate so there are no equipment limitations on load time.

Round trip travel time is a function of road conditions, total travel distance, and weather. Vehicle speeds are seldom more than 15 mph (24 km/h), on unpaved roads, and are limited to standard speed limits on highways. In the best of circumstances, 40 mph (64 km/h) is the maximum average speed over fairly short distances and some time to turn around and park, and to hook or unhook the load or unload station is required. Additional time to "dolly-down" the trailer and switch the tractor may also be necessary.

Unload time depends on the maximum rate of acceptance of the gas by the recipient or on the maximum rate at which it can be discharged from the trailer. Pipeline unload sites are chosen to minimize problems relating to acceptance rate, but if the gas is delivered to an industrial end user, his consumption may be relatively slow. Also, unload rates may need to be controlled to facilitate orifice or turbine meters, if used.

Maintenance downtime is less definable than any other equipment utilization factor. Simple steps such as careful preventive maintenance help minimize downtime, but additional steps are also needed. A good supply of spare parts is necessary and for high maintenance items such as diesel tractors, a complete spare unit may be kept waiting. Not surprisingly, road conditions are a major factor in vehicle downtime, and effort spent to keep unpaved roads in top

condition is worthwhile.

In evaluating any given project, the first step is to determine the load time and the travel plus unload time so the system equipment can be sized and personnel requirements determined. From that, and from historical operating data, monthly operating costs including equipment carrying costs and overhead costs are estimated. Since all of the equipment is skid mounted, and can be moved from project to project, its cost can be amortized over a life span greater than the project itself. For this reason, monthly equipment costs are kept fairly low. Equipment set-up costs however must be amortized over the life of the project. These costs vary but typically are less than \$30 000.

As an example case, consider an isolated well, 20 miles (32 km) by road from a low pressure, 100 psi (0.69 MPa) pipeline, with a flow rate of 1000 MCF/D ($28 \times 10^3 \text{ m}^3/\text{d}$) at 1000 psi (6.9 MPa). Also assume the gas analysis shows 1100 BTU/CF (40.9 MJ/m³) and that the cost of one spare tractor can be shared with four similar systems. Since the round trip travel time plus unload time is less than 3 hours, 8 loads per day could be hauled with a two trailer system. However, only 7 loads at 142 MCF ($4.1 \times 10^3 \text{ m}^3$) per load is available, so there will be some waiting time at the well site. A single stage compressor of about 50 horsepower (37 kW) is required at the load site, but no compressor is deemed necessary at the unload site. The equipment required for the operation and its cost is as follows:

2 ea. CNG Trailers @ \$100 000.....	\$200 000
1.25 Tractors @ \$55 000.....	\$ 68 750
1 ea. Dehydrator.....	\$ 35 000
1 ea. Load Compressor.....	\$ 60 000
2 ea. Stations (1-Load, 1-Unload) @ \$15 000.....	\$ 30 000
1 ea. Field Office & Communications....	\$ 17 000
1 ea. Foreman's Vehicle.....	\$ 10 000
TOTAL.....	\$420 750

Book life on this equipment varies from 3 years to 11 years, but the weighted average total cost is about 1.6% per month or \$6700. Total monthly project costs are as follows:

Equipment Cost.....	\$ 6 700
Labor Cost (Drivers & Foremen).....	\$ 9 600
Maintenance, Tires, Fuel & Oil.....	\$ 4 800
General & Administrative, Insurance, Taxes and Return on Equity.....	\$ 8 700
TOTAL MONTHLY PROJECT COST.....	\$29 800

This value can be related back to a unit cost for the gas if we assume we get a constant 1000 MCF/D ($28 \times 10^3 \text{ m}^3/\text{d}$) flow rate at 1100 BTU/CF (40.9 MJ/m³) for an average month of 30.4 days:

$$\frac{(29\ 800)(1000)}{(1000)(30.4)(1100)} = \$0.89/\text{MMBTU} (\$0.84/\text{GJ})$$

If the project lasts for one year, another 7.5 cents should be added for start-up cost amortization.

As shown previously (Table 1), this same set of personnel and equipment (except for the compressor)

can be used to haul much larger volumes of gas and the prices would be correspondingly lower. The net transportation cost if the well were to deliver 2000 MCF/D ($57.2 \times 10^3 \text{ m}^3/\text{d}$) is only \$0.64 per MMBTU (\$0.61/GJ). With the addition of another trailer, the volume can go up to about 3000 MCF/D ($85.8 \times 10^3 \text{ m}^3/\text{d}$) and the price down to only \$0.48 per MMBTU (\$0.45/GJ). Figure 3 gives the approximate cost for delivery of gas as specified in the example case for a variety of flow rates and distances. It shows that the cost per unit of gas increases very rapidly at the lower volumes. This rise in cost can be partially offset by the deletion of some equipment and personnel, but operating procedures for such reduced systems are not well defined and actual costs are still unknown. Several alternative operating systems could be used for low flow rate isolated wells with the optimum system probably including one or more of the following:

1. Smaller trailers
2. Reduced operations at night with temporary gas storage
3. Fewer trailers with temporary gas storage
4. Lower pressure trailers

The dotted line on Figure 3 gives the current best estimate of reduced costs on low flow isolated systems. Further research may significantly reduce these values, opening up even more economic opportunities for truck transport of CNG, and it should be remembered that several small systems in one locale can benefit from sharing personnel, tractor, unload station, and some other equipment. These shared systems have even lower costs than those using the operating system outlined above.

CNG AND PIPELINES COST COMPARISON

Cost comparisons between CNG transportation by truck and transportation of gas by pipeline is difficult because of the differing factors that influence the cost of each. The cost of small gathering pipeline systems must be justified solely on the basis of reserve estimates for the fields being served. Those reserves may last a few months with high flow rates or many years with low flow rates, but if the reserves are sufficient the cost of the pipeline can be recovered in either event. On the other hand, the cost of CNG transportation, with its much lower non-recoverable investment but with higher operating cost, is dependent on the flow rate of a gas field instead of the total reserves. Therefore, it is only by giving both a flow rate and a total reserve estimate for a field that the two transportation methods can be compared. In those instances where flow tests are not yet available, a rule of thumb for formations with moderate permeability might be to estimate average daily flow at 0.1% of the estimated reserves. On that basis, a reservoir with 1 BCF ($28.6 \times 10^6 \text{ m}^3$) reserves might flow 1000 MCF/D ($28.6 \times 10^3 \text{ m}^3/\text{d}$) per well.

Another factor adversely affecting cost comparisons between truck and pipeline transportation of natural gas is the accounting procedures frequently used. Large pipeline companies amortize pipeline costs over a 22 year life even though the reservoir they serve may be depleted in only one or two years.

That may be a good policy for transmission pipelines, but if a small line is abandoned after only 2 years, its actual cost and benefit are greatly distorted by the accounting procedure.

These difficulties in cost comparison can be overcome however, if appropriate assumptions are made. For the purpose of the comparison, only first transporter operations are considered: both in-field gathering and cross-country transmission lines are beyond the scope of this comparison.

Assumptions:

1. Rate base accounting is applied to both pipeline and truck transport operations.
2. Pipelines are not recoverable.
3. Pipelines are amortized over the life of the reserves, no matter how short.
4. Truck transport systems are moveable from one field to another and are amortized over the life of the equipment except for start-up costs.
5. Both transport methods are financed in a similar fashion at the same rates with a constant 3 to 1 debt to equity ratio.
6. The minimum pipeline is a 4" (0.1 m) nominal size steel line, coated and wrapped.
7. Straight line depreciation is used.

Although pipeline capital costs vary throughout the country, typical cost per mile (per 1600 m) of 4" (0.1 m) line are estimated as follows:

Right-of-way & Damages	
@ \$50/rod (\$10/m).....	\$16 000
Engineering & Surveying.....	\$ 8 000
Pipe @ \$1.81/foot (\$5.94/m).....	\$ 9 500
Coating & Wrapping @ \$0.53/foot	
(\$1.74/m).....	\$ 2 800
Clearing, Ditching & Backfill	
@ \$2.60/foot (\$8.53/m).....	\$13 700
TOTAL COST PER MILE (per 1600 m).....	<u>\$50 000</u>

Operating costs for small pipelines are estimated at 6% of capital cost per year which is \$3000 per year per mile (1600 m) for the line described above.

For a line 20 miles (32 km) long to a gas field with average flow rate of 1000 MCF/D ($28.6 \times 10^3 \text{ m}^3/\text{d}$) (see example under CNG Transportation Cost) and with an assumed reservoir size of 1 BCF ($28.6 \times 10^6 \text{ m}^3$) of gas, the project life would be 33 months and the monthly project costs would be as follows:

Pipeline Cost	
Depreciation (\$1 000 000 ÷ 33).....	\$30 300
Interest.....	\$ 3 360
Operation & Maintenance	
(including insurance).....	\$ 5 000
Taxes & Return on Equity.....	\$ 2 700
TOTAL.....	<u>\$41 360</u>

Relating this cost back to a unit cost for the gas as we did in the trucking cost example we get:

$$\frac{(41\ 360)(1000)}{(1000)(30.4)(1100)} = \$1.23/\text{MMBTU} (\$1.17/\text{GJ})$$

This cost is clearly higher than the equivalent cost for CNG truck transportation. However, if the discharge point were only 10 miles (16 km) from the field, the pipeline costs would be almost halved, while the CNG cost would remain about the same. On the other hand if the field reserves were only half of the original estimate, the pipeline costs would almost double because the project life would be halved, and CNG cost would still remain unchanged. Figure 4 shows approximate pipeline costs for several reservoir sizes and distance to markets assuming the line size given in the previous example.

For any given field for which both available flow and "proven" reserves are available, a cost comparison of trucked CNG and pipeline systems can be made by referring to Figures 3 and 4. If the relationship between reserve size and flow rate is known, the two figures can be combined and the locus of points of equal cost can be drawn to divide the chart into areas where each transportation system is more economical. A typical undimensioned graph showing the line of equal cost on a plot of distance versus flowrate (or reservoir size) is shown in

Figure 5. In actuality, since reserves are not "proven", no clear delineation between the cost of the two transportation methods exists, and there is actually a zone where the more economical method is undefined. This is shown as a shaded area on Figure 5. In this area, CNG transportation may be used to define and eliminate the financial risks before a pipeline is constructed.

CONCLUSIONS

The transportation of compressed natural gas (CNG) by truck is shown to be a simple process using trailer mounted pressure vessels and readily available oil field type equipment. It is an economically feasible gas production technique that can offer significant cost advantages over pipeline systems for many small or remotely located natural gas sources. Financial risk can be reduced by first using truck transportation even in areas where pipelines are justified based on gas reservoir size estimates.

Costs for truck transportation of natural gas are related to the daily volumes available, the distance hauled, gas quality, and numerous other factors some of which affect the equipment utilization. Not all natural gas can be hauled by truck because of various system limitations, including gas quality, but where truck transportation has been used appropriately, it has been remarkably safe and reliable.

TABLE 1
MAXIMUM TRANSPORT CAPACITY
FOR 2 TRAILER SYSTEM

DISTANCE	MAXIMUM CAPACITY
10 miles (16 km)	2,800 MCF/D ($80.2 \times 10^3 \text{ m}^3/\text{d}$)
20 miles (32 km)	2,290 MCF/D ($65.6 \times 10^3 \text{ m}^3/\text{d}$)
30 miles (48 km)	2,050 MCF/D ($58.7 \times 10^3 \text{ m}^3/\text{d}$)
40 miles (64 km)	1,720 MCF/D ($49.2 \times 10^3 \text{ m}^3/\text{d}$)
60 miles (97 km)	1,300 MCF/D ($37.2 \times 10^3 \text{ m}^3/\text{d}$)
100 miles (161 km)	880 MCF/D ($25.0 \times 10^3 \text{ m}^3/\text{d}$)

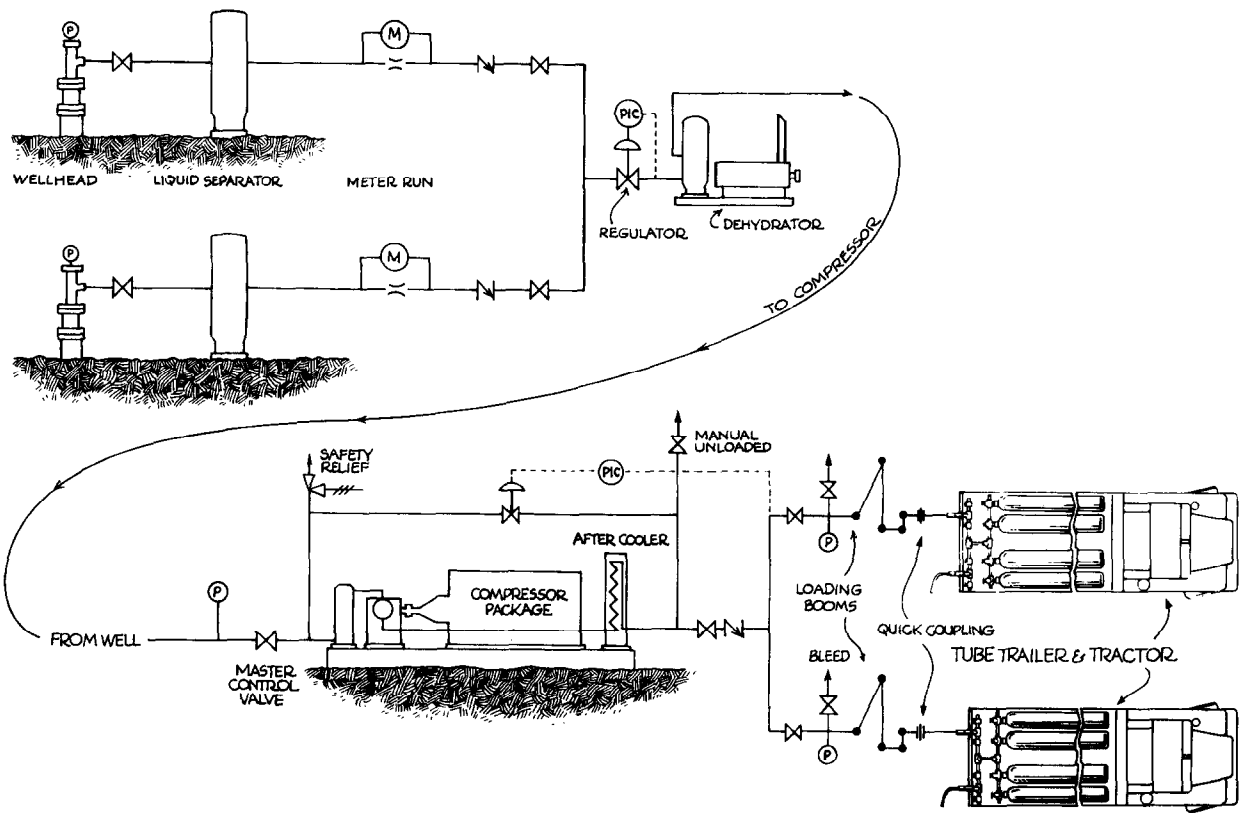


Fig. 1 - Loading equipment schematic.

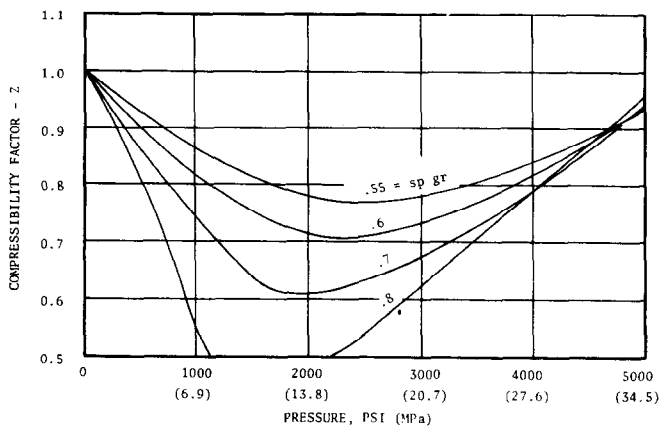


Fig. 2 - Natural gas supercompressibility at 50 F (10 C).

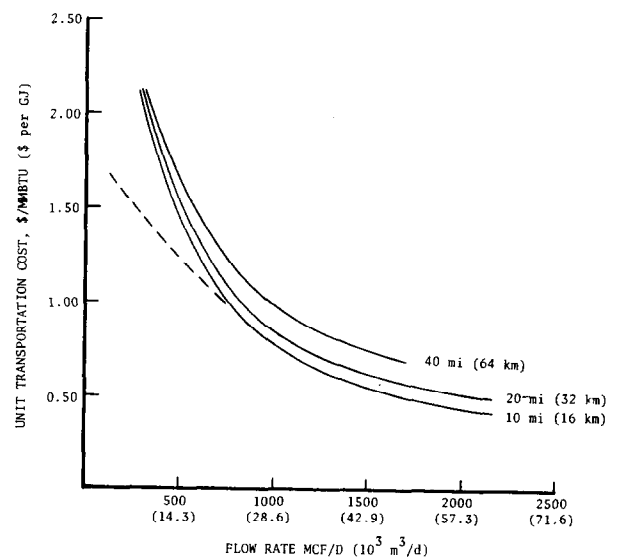


Fig. 3 - Truck transportation cost for two trailer CNG system.

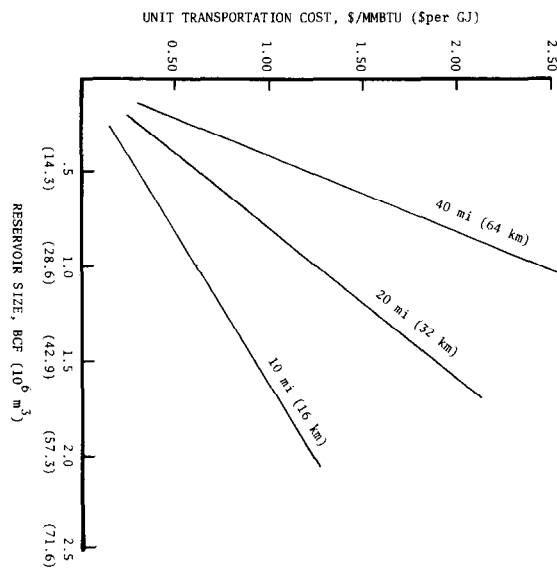


Fig. 4 - Pipeline transportation cost for 4" (0.1 m) diameter line.

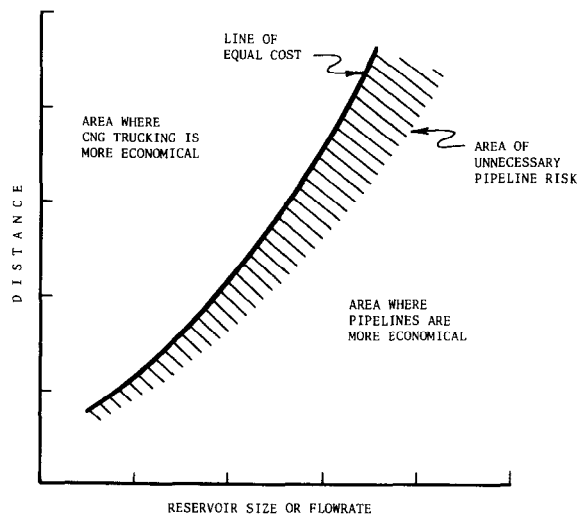


Fig. 5 - Relative cost areas for pipelines and CNG trucking.

PERSPECTIVE ON DEVONIAN SHALE GAS EXPLORATION

by Claude S. Dean, U.S. Doe (METC)

This paper was presented at the 1980 SPE/DOE Symposium on Unconventional Gas Recovery held in Pittsburgh, Pennsylvania, May 18-21, 1980. The material is subject to correction by the author. Permission to copy is restricted to an abstract of not more than 300 words. Write: 6200 N. Central Expwy., Dallas, Texas 75206

ABSTRACT

Since fractured reservoirs are essential to production, exploration rationales specific to the Devonian shale unconventional gas resource are characterized by a geologic fracture creating mechanism. One such predicts intense fracturing in the shale wherever proximally associated with the major thrust faults of the Appalachian overthrust belt. Gruy Federal No. 1 Grainger Co. (DOE EGSP-TN9), a U.S. Department of Energy (DOE)-funded rank wildcat located in Grainger County, TN, successfully tested that rationale. The well penetrated the Saltville Thrust Fault (stratigraphic throw: over 10,000 feet) and encountered the Devonian-Mississippian Chattanooga Shale in the lower plate. The shale proved to be 720 feet thick, of which 480 feet or 67% was anomalously radioactive (25 API above shale base line). Two hundred twenty (220) feet of core was recovered from the most highly radioactive (organic rich) intervals and a full suite of wireline logs was run. Widespread and locally intense fracturing in the shale, especially in the organic sections, observed in the core and evidenced by the logs vindicates the exploration rationale. The well will be hydraulically fractured and tested to evaluate production potential.

INTRODUCTION

The classical trinity of essential factors in natural gas exploration, source, reservoir, and trap, is as relevant to unconventional resources as it is to conventional. In the unconventional resource the three are merely manifested in an unusual way and/or bear an unusual relationship to each other. The nature of the resource must be taken into account when charting exploration strategy, i.e., both exploration rationales and exploration techniques must be tailored to the specific resource. A conventional rationale is typically based on and characterized by some trapping mechanism. Exploration rationales for the unconventional

Devonian shale resource, however, are distinguished by their fracture creating mechanism, which for the ultra-tight shale is equivalent to the reservoir creating mechanism. Inasmuch as fracture systems are necessary, but not alone sufficient, ancillary factors, especially those relating to source potential, become important in evaluating Devonian shale rationales. A number of exploration rationales and techniques have been identified as holding promise for the Devonian shale. The Eastern Gas Shales Project's (EGSP) development of prospects in eastern Tennessee through the application of some of the techniques to one of the rationales and subsequent testing of one of them serves as a case study.

From January 3 to 21, 1980, U.S. Department of Energy (DOE), through its contractor Gruy Federal, Inc., drilled a Devonian shale wildcat well in Grainger County, TN. The geographic coordinates of Gruy Federal No. 1 Grainger Co. (DOE EGSP-TN9) are 30°18'56"N latitude by 83°24'33"W longitude (Tennessee coordinates 710,300N by 2,762,000E). The ground elevation of the well is 1140 feet above mean sea level. All depths were measured from the kelly bushing, which stood 10 feet higher at 1150 feet. The site is on lot A-8 of the Grainger County Industrial Park, public land belonging to the county situated along U.S. Highway 11-W midway between Rutledge and Bean Station (Figure 1). Gruy Federal, Inc., operated the well under an agreement with Grainger County whereby the former received permission to drill, core, log, and test the well, while the latter retained the mineral rights and hence ownership of any producible hydrocarbons. The primary targets were the dark, organic rich intervals within the Devonian-Mississippian Chattanooga Shale.

EXPLORATION RATIONALE

The drilling and testing of this wildcat well in Grainger County, TN, is a field demonstration project of the DOE's Eastern Gas Shales Project under the Unconventional Gas Recovery (UGR) Program. The EGSP seeks to encourage

References and illustrations at end of paper.

commercial development of the natural gas producing potential of the organic rich Devonian shales that underlie some 200,000 square miles of the eastern United States (Figure 2). Devonian shales are an unconventional natural gas resource in that, although they contain vast volumes of gas, they usually lack sufficient natural permeability to permit the gas to migrate to the wellbore. Historical natural gas production at commercial rates from the shales has occurred in isolated areas of the Appalachian, Illinois, and Michigan Basins. Most of this production can be attributed to extensive natural fracture systems that act as interconnected conduits feeding gas desorbed from the shale matrix to the wellbore. One of the primary goals of the EGSP is to develop the capability of creating artificial fractures in the shale in order to create a permeable link between the wellbore and such natural fractures as may exist in the vicinity. Fracture stimulation technology is not alone sufficient to induce gas production from the Devonian shales; natural fracture permeability must be present. Hence, another primary goal of the EGSP is the formulation of shale specific exploration rationales characterized by some geological fracture producing mechanism and identification of the areas to which these rationales apply.

Gruy Federal No. 1 Grainger Co. tested an exploration rationale that predicts intense and intricate natural fracturing in the Devonian shale wherever proximally associated with the major thrust faults of the Appalachian overthrust belt. In eastern Tennessee the Devonian shale is represented by the Chattanooga Shale, a formal stratigraphic unit, the bulk of which is Upper Devonian, but the uppermost portion, is Lower Mississippian. Within the Valley and Ridge Province it crops out along the northwestern flanks of two isolated northeast trending synclines, the Newman Ridge and Greendale Synclines (Figure 3). Both synclines are bounded to the southeast by major thrust faults of regional extent, the Clinchport and Saltville Thrust Faults, respectively. The Chattanooga Shale passes into the subsurface beneath these southeast dipping thrusts. The above stated exploration rationale is based on USGS Professional Paper 1018 (Harris & Milici, 1977). The authors observe at those few localities in the Southern Appalachians where major bedding plane faults, termed "decollements", are exposed that the overlying rocks are very highly fractured. The most intensely fractured rocks occur in their "broken formation zone" immediately above a decollement. The rocks in their overlying "fractured zone" are still pervasively fractured, but less intricately so. That the Chattanooga Shale in the Newman Ridge and Greendale Synclines occurs beneath the associated major thrust faults does not invalidate the exploration rationale if one supposes the existence of bedding plane faults in the shale induced by activity on the overlying master thrust. This is a reasonable supposition for which there is at least indirect evidence. In the general vicinity of Evanston, TN, (Figure 4) Chattanooga Shale passes under the entire length of a portion of the upper plate of the Hunter Valley Thrust isolated by erosion and the more steeply dipping Clinchport Thrust. Where it emerges to the northeast it may be observed in a roadside borrow

pit to be intensely fractured (Milici & Statler, in press), clearly reflecting historic activity on the overlying Hunter Valley Thrust, now eroded away to reveal the shale.

PROSPECT DEVELOPMENT

In 1967 U.S. Energy Research & Development Administration (ERDA) (now DOE) let a three-year contract (DE-AC21-76MC05196) to the Tennessee Division of Geology (TDG) to characterize the Chattanooga Shale in the Valley and Ridge Province of eastern Tennessee and to evaluate its natural gas producing potential. The TDG conducted a double thrust research program designed to define two separate aspects of the resource:

1. To learn the true thickness of the shale, its internal stratigraphy, and especially the relative proportion of organic rich to organic lean material, they sponsored an NX core drilling program along the major outcrop belts of Chattanooga Shale. Eight holes were cored, three in the Newman Ridge Syncline and five in the Greendale Syncline.
2. To reveal the subsurface extent of the Chattanooga Shale beneath the Hunter Valley, Clinchport, and Saltville Thrust Faults they arranged for seismic surveys to be conducted along two lines, KIS-TC1 and TC2 (Figure 3).

The salient results may be summarized as follows:

1. The total stratigraphic thickness of the Chattanooga Shale varies from several hundred feet to well over a thousand feet, a very substantial proportion of which is organic rich.
2. The Chattanooga Shale extends at least several miles back beneath the thrusts before being truncated and is accessible to exploratory drilling at surprisingly shallow depths, less than 4,000 feet.

In a memo to DOE EGSP management dated May 18, 1979, this author summarized progress under the TDG contract, expounded the exploration rationale at length, and identified seven Devonian shale prospects for exploratory drilling. These are shown on Figure 3. Gruy Federal No. 1 Grainger Co. (EGSP-TN9) was drilled to test prospect P3. Criteria for site selection in order of priority were the following:

1. Location within the P3 area as defined on Figure 3.
2. Proximity to seismic line TCL.
3. Availability of public land.
4. Potential local consumer of natural gas.
5. Proximity to an all-weather road.

Hence, the Grainger County Industrial Park was the natural choice. At this location the well was spudded in the Cambrian Conasauga Group in the upper plate of the Saltville Thrust Fault. It

penetrated the gently dipping fault and encountered the Chattanooga Shale in the lower plate. Thrusting Lower Cambrian over Lower Mississippian, the fault has a stratigraphic throw of over 10,000 feet.

DRILLING AND CORING

Drilling predominantly on air, the well was spudded in the Rogersville Shale and passed through two other formations belonging to the Cambrian Conasauga Group, the Rutledge Limestone and the Pumpkin Valley Shale, before entering the Cambrian Rome Formation (Figure 5). Surface casing was set at 200 feet. Water entry into the wellbore was first noticed at 400 feet. The volume of water increased markedly at approximately 600 feet and a strong hydrogen sulfide odor was emitted. (Richland Valley, in which the industrial park is situated, is noted for its mineral springs, associated with which were several health spas.)

Penetration of the Saltville Thrust Fault occurred at 667 feet. Surprisingly, this event was readily recognized in the samples. The 650-60 sample contained slightly dolomitic, medium grained sandstone similar to the preceding five samples of Rome sandstones, some of which are notably micaceous. The 660-70 was lithologically similar to the above, but contained abundant slickensided cuttings and what the author interprets to be mylonite. The 670-80 was gray fossiliferous siltstone containing an identifiable brachiopod and crinoid columnal. Further along, abundant glauconite appeared in samples 710-20 and 720-30, by which the "glauconite zone" of Hasson (1967) was recognized. The measured outcrop sections of the Mississippian Grainger Formation in Kenneth Hasson's (1967) Ph.D. thesis indicate a prominent glauconite zone near the top of the "middle shale-siltstone member". Recognition of the "glauconite zone" in the cuttings enabled the accurate prediction of the top of the Chattanooga Shale, which subsequently was encountered at 1136 feet. A possibly significant aside, the position of the glauconite zone relative to the Saltville Fault in the well indicates approximately 90 feet of migration of the fault downward through the Grainger Formation from the outcrop to the well, a distance of about 3/4 of a mile. That is equivalent to a down-dip loss of section of 120 feet per mile.

Before proceeding into the Chattanooga Shale an intermediate string of casing was set to shut off the flow of water, which was substantial. This was done to protect any fractured reservoirs that might be encountered in the shale, inasmuch as it was suspected that they might be underpressured. From this casing point to T.D. hole was made by alternately drilling and coring. Cored intervals are indicated on Figure 5, as also are the major lithostratigraphic units within the Chattanooga Shale and their probable regional correlation. Primary coring targets were the most richly organic intervals within the shale, as previously determined from two nearby NX holes cored and logged under the TDG contract. Core points were accurately picked on the basis of samples taken at five-foot intervals, and additionally in the case of the Lower Huron, a gamma ray log run for correlation. Fifty feet of core was recovered from the Sunbury-Cleveland interval; 132 feet, from the Lower Huron; and 48 feet, from the Rhinestreet, of which the last ten feet is actually Wildcat Valley Sandstone.

Ten-foot samples were taken and logged as usual throughout the drilled intervals. An unexpected water bearing zone was encountered at 1410 feet while drilling through the lower part of the Chagrin interval. Initial water production was a 2-inch stream; with time that eventually diminished to less than 1/2-inch. Sample 1410-20 is siltstone containing anomalous quantities of slickensided cuttings and coarse crystalline dolomite, indicative of slickensided and mineralized fractures. The author noted possible *Foerstia*, a unique marker fossil, between 1600 and 1610, and identified bentonite, probably the Center Hill Bentonite, in sample 1760-70. Following the extraction of the last core, a 53-foot rat hole was drilled through the remainder of the Devonian Wildcat Valley Sandstone and into the Silurian Clinch Sandstone. The last 20 feet of Clinch is brownish shale of Rockwood aspect. The base of the Chattanooga Shale stands at 1856 feet. Thus, the total thickness of the Chattanooga proved to be 720 feet. The aggregate thickness of abnormally radioactive shale (an indicator of organic content) as revealed on the gamma ray log (25 API units above the shale base line) is 480 feet (67% of the total), of which 220 feet was cored.

Indications of hydrocarbons during drilling and coring operations were meager. No gas detector was stationed on the well. After coring the Lower Huron, the most prospective interval in the Chattanooga Shale, the rig compressors were shut down and a futile attempt was made to ignite whatever gases might be flowing from the well. No natural flow of any kind was detected. Only when the compressors were restarted was a flash observed, indicating the presence of a small amount of gas. Gas bled out of a few fractures in the core extracted from the Lower Huron and Rhinestreet intervals. More impressive natural gas shows in the Chattanooga Shale may have been precluded by near-wellbore formation damage (skin effect) arising from water production at 1410 feet. Light gravity, straw colored oil was observed in the core and cuttings of the Wildcat Valley Sandstone. The sandstone appears to be tight, the oil being contained in fractures.

FORMATION EVALUATION

Virtually all the shale core recovered from the well is naturally fractured, some of it intensely so. In fact, the core from Gruy Federal No. 1 Grainger Co. (EGSP-TN9) is more highly fractured by far than any of the 46 other cores recovered under the EGSP to date. The greatest degree of fracturing occurs in the lower part of the Lower Huron and in the Rhinestreet (Figure 5). Most of the rest of the core is at least moderately fractured; only 23% is unfractured. Moderate to low angle slickensided fractures predominate; sub-vertical extensile fractures are moderately abundant. The vertical fractures are mineralized with dolomite. Some of the moderate to low angle fractures are also mineralized with dolomite; most are simply slickensided. A few fractures are related to the growth of septarian concretions, which are not abundant, and hence are non-tectonic. A distinct vertical progression of fracture intensity and style occurs at least twice, once in the Lower Huron and once in the Rhinestreet. Proceeding downward, it first manifests itself as several sub-vertical, mineralized

fractures. These rather abruptly give way to moderate and low angle slickensided fractures, which increase in abundance until the core is reduced to slickensided rubble. The bottom of this rubble zone is fairly well defined. This progression is reminiscent of the "zone of fracture" and "broken formation zone" observed above decollements by Harris and Milici (1977).

A full suite of wireline logs* was run through the Chattanooga Shale. They are the following:

1. Caliper
2. Gamma Ray
3. Density, Borehole Compensated (Porosity on a 2.68 matrix) (dry hole)
4. Temperature
5. Sibilation
6. Simultaneous Compensated Neutron-Formation Density (wet hole)
7. Spontaneous Potential
8. Dual Induction - Laterolog
9. Fracture Identification
10. Borehole Compensated Sonic
11. Open Hole Amplitude - Variable Density

Copies of the logs rest in the UGR Open File at the Morgantown Energy Technology Center (METC), Morgantown, WV, and are available for public inspection.

The gamma ray log reveals substantial thicknesses of highly radioactive shale, 250 API units or greater, within the Sunbury-Cleveland, Upper Huron, Lower Huron, and Rhinestreet intervals (Figure 5). As rule of thumb, shale radioactivity is directly correlated with organic content. The bulk density curve, however, indicates that the highly radioactive intervals are not nearly as organic rich as the gamma ray readings imply. The various nuclear porosity logs faintly suggest some gas filled porosity development in all of the above named shale intervals. They somewhat more strongly imply such development in the siltstones in the lower part of the Chagrin between 1350 and 1420. The clay content in the siltstones makes it difficult to estimate porosity; however, it does not exceed a few percent. At 1408 near the base of the Chagrin the nuclear logs indicate a narrow zone of liquid (water) filled porosity that can only be interpreted as a highly porous fracture zone. The resistivity measuring logs are enigmatic. It should be here cautioned that porosity and resistivity logs were intended to evaluate shale-free formations (sandstones and carbonates) and their interpretation in shales is a qualitative art at best.

Two of the logs, Temperature and Sibilation, directly indicate gas entry into the wellbore, in shale presumably from fractures. Two other logs, Fracture Identification and Open Hole Amplitude - Variable Density, were run as fracture finders. There is a reliable sibilation anomaly and an associated temperature anomaly in the lower Chagrin at 1363 feet opposite a four-foot shale break within a 25-foot potentially

gas bearing siltstone interval. A second sibilation anomaly at 1786 feet without associated temperature anomaly is dubious due to the close proximity of fluid in the hole. A broad, shallow temperature anomaly stretching from 1660 to 1740 across most of the Lower Huron interval is one of the more hopeful indications of producible shale gas in the well. Activity on the Fracture Identification Log (FIL) is considerably less than one would anticipate from the core and correlates only modestly with core observed natural fracturing. The correlation with fracture indications on the Open Hole Amplitude - Variable Density log (VDL) is much better. Perhaps by virtue of tool design and operating principle, the FIL is better able to detect sub-vertical fractures than the VDL, while the VDL is better able to detect sub-horizontal fracturing than the FIL. Both logs, however, concur in drawing the following general conclusions:

1. The water bearing zone at 1410 feet is massively fractured. The remainder of the lower part of the Chagrin from 1310 to 1420 feet is heavily fractured, especially opposite the sibilation-temperature anomaly at 1363 feet.
2. The upper part of the Chagrin appears to be fracture free. This section is useful for calibration and comparison with variably fractured sections.
3. The interval from the top of the Lower Huron to the base of the Chattanooga Shale is nearly continuously fractured, at least to a moderate degree.
4. The Sunbury-Cleveland interval is only lightly fractured.

STIMULATION AND TESTING

Widespread and locally intense fracturing within the Chattanooga Shale, especially within the organic rich intervals, observed in the core and evidenced in the logs vindicates the exploration rationale used in siting a Devonian shale wildcat well in the P3 prospect area (Figure 3), Grainger County, TN. Whether the shale will produce natural gas at a useful rate remains to be proven through a planned hydraulic fracture stimulation and subsequent well test. Very few Devonian shale wells produce without any stimulation; some good producers had no measurable natural flow of gas prior to stimulation.

Following drilling operations a production string of 4.5 inch casing was set at 1895 feet and cemented back to surface. In April 1980 U.S. DOE through its contractor Gruy Federal, Inc., intends to run a cement bond log and perforate the casing from 1630 to 1850 feet. After formation breakdown with 1500 gallons of acid and nitrogen gas to generate 6,000 gallons of foam, the well will be hydraulically fractured with 50,000 gallons of 75 quality foam and 50,000 pounds of 20/40 mesh sand pumped at a rate of 25 barrels foam per minute. After flow back the well will be tested to measure its deliverability, evaluate fracture geometry, and compare well performance with other Devonian shale wells tested under the EGSP well testing program. This should result in an accurate evaluation of the gas producing potential

* The occasional use of trade names rather than generic names for various products and services reflects field usage and does not imply U.S. Government endorsement of any company, product, or service.

of the Lower Huron, Olentangy, and Rhinestreet intervals in Gruy Federal No. 1 Grainger Co. (EGSP-TN9). Depending on the results, the Sunbury-Cleveland, Upper Huron, and possibly the Chagrin intervals may be tested at a later time.

Hydraulic fracturing will overcome the near-wellbore formation damage that occurred during drilling and coring operations. This may well explain the lack of a substantial natural gas show despite the highly fractured nature of the Chattanooga Shale. On the negative side, the slickensided and mineralized fractures encountered may be insufficiently permeable to create a proper matrix rechargeable reservoir. Alternatively, reservoir pressure may be depleted through gas leakage to the surface; the shale outcrops only 1.5 miles away from the well.

REFERENCES

1. Harris, L.D., and Milici, R.C.: "Characteristics of Thin-Skinned Style of Deformation in the Southern Appalachians, and Potential Hydrocarbon Traps", U.S. Geological Survey Profes-

sional Paper 1018, 1977, 40 p.

2. Hasson, K.O.: "Lithostratigraphy of the Grainger Formation (Mississippian) in Northeast Tennessee", unpublished Ph.D. dissertation, University of Tennessee, Knoxville (1972).
3. Milici, R.C., and Statler, A.T.: "Fractures Related to Major Thrusts--Possible Analogues to Tectonically Fractured Chattanooga Shale in Tennessee", Abstracts with Programs, S.E. Geological Society of America Meeting, v. 10, no. 4, 1978, p. 176 (in press).
4. Milici, R.C., Harris, L.D., Statler, A.T.: "An Interpretation of Seismic Cross Sections in the Valley and Ridge of Eastern Tennessee", Tennessee Division of Geology, Oil and Gas Chart 6, Sheet 2 (in press).
5. Tegland, E.R.: "Seismic Investigations in Eastern Tennessee", Bull. 78, Tennessee Division of Geology, Knoxville (1978).

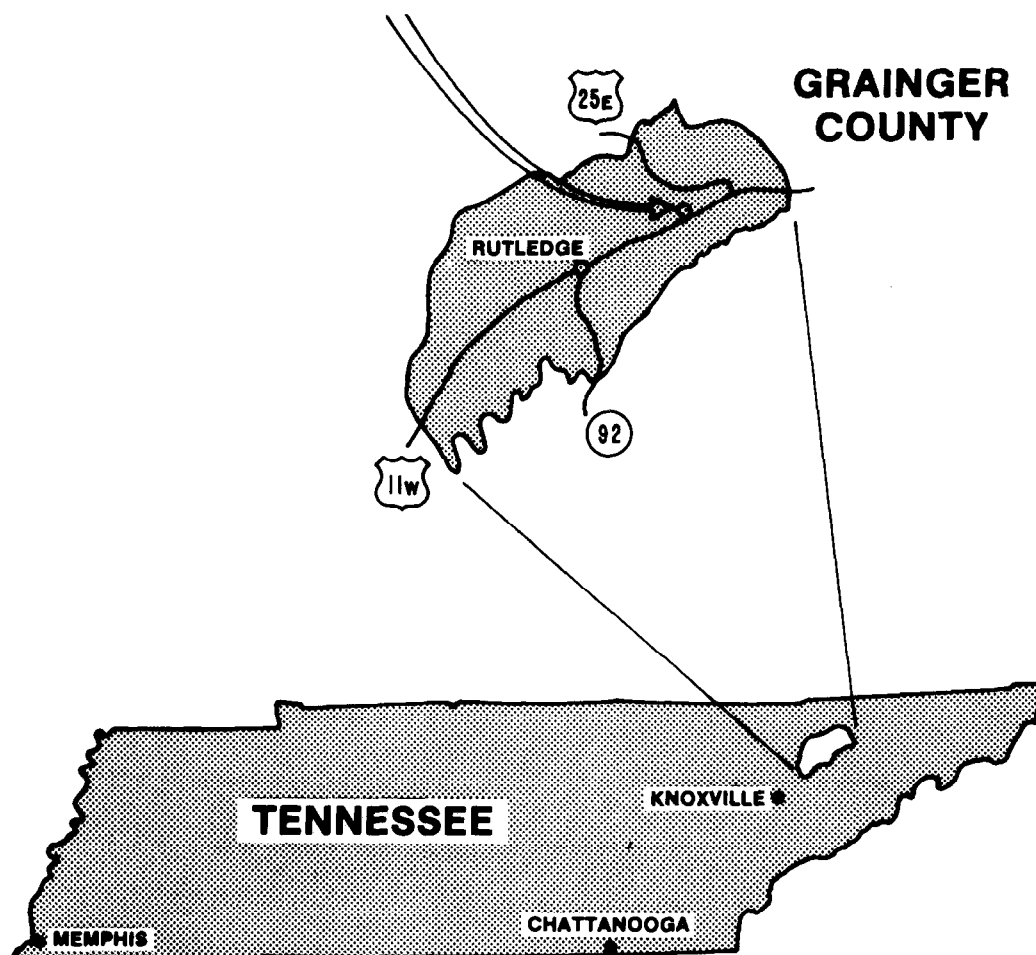


Fig. 1 - Location map.

Known Gas Shale Deposits Located in the United States

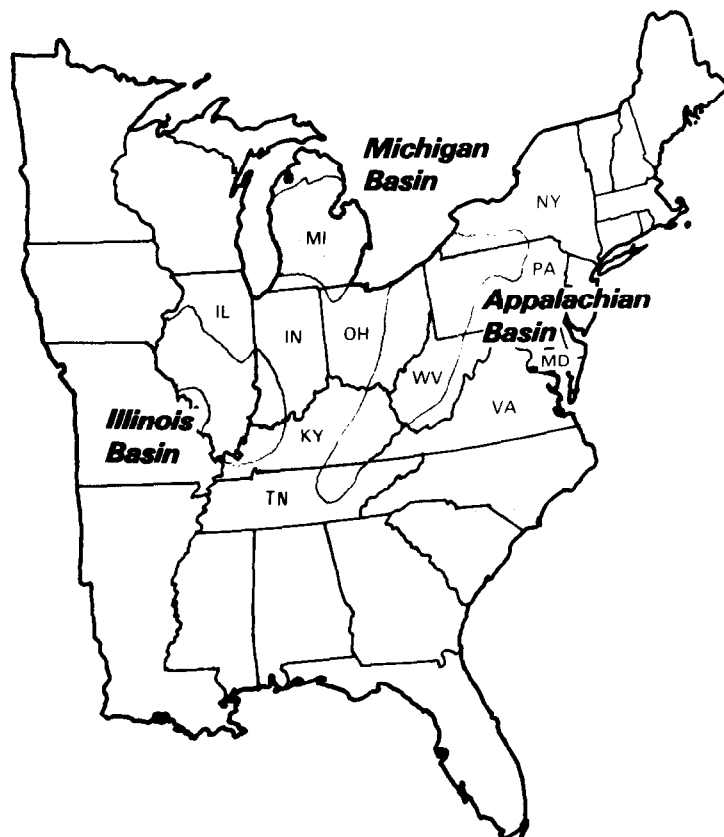


Fig. 2 - Eastern gas shale deposits.

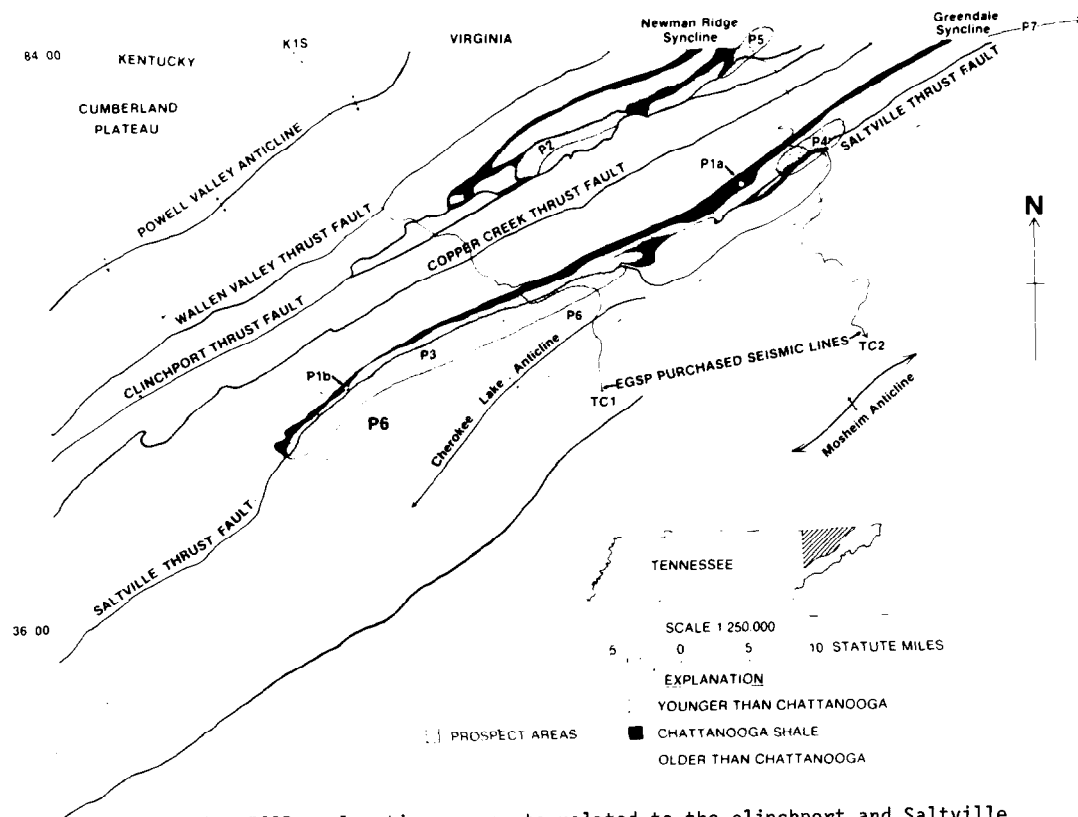


Fig. 3 - EGSP exploration prospects related to the Clinchport and Saltville Thrust Faults, Eastern Tennessee and Southwestern Virginia.

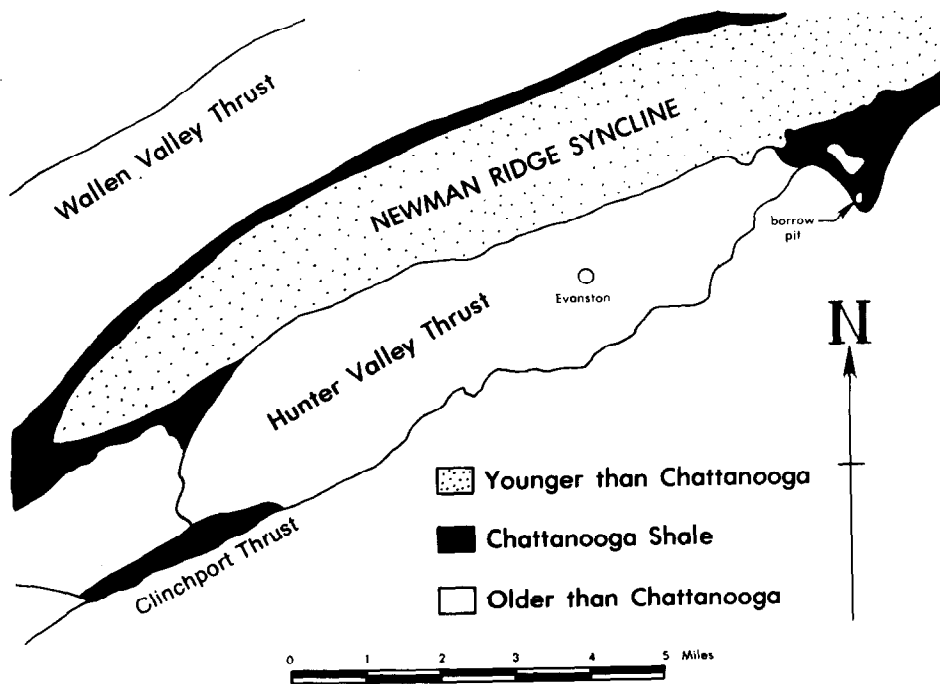


Fig. 4 - Geologic map of the Evanston Area, Tenn.

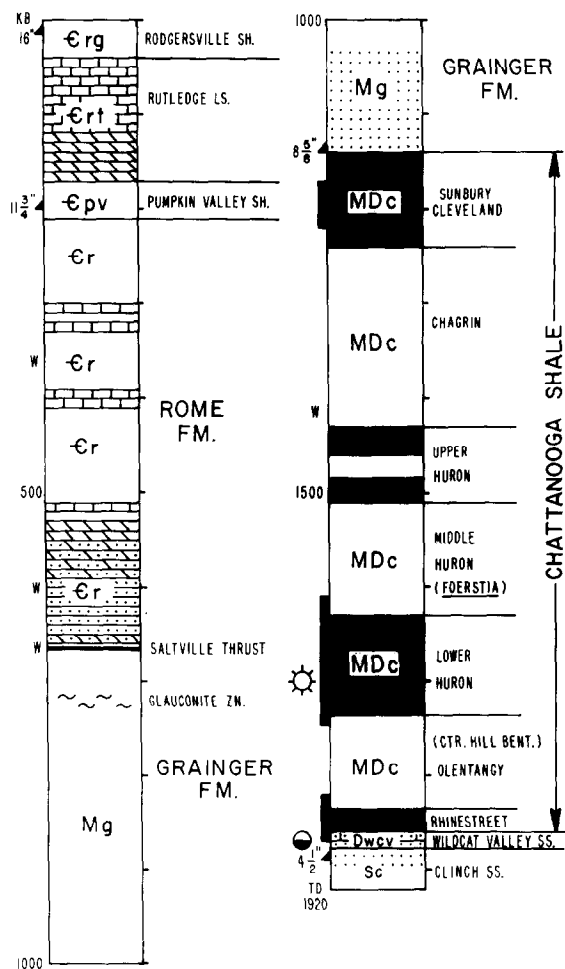


Fig. 5 - Summary: Grainger County, Tenn.

NATURAL GAS FROM TIGHT SILTSTONES IN THE CATSKILL CLASTIC WEDGE IN WEST VIRGINIA

by Joseph F. Schwietering, West Virginia
Geological & Economic Survey

This paper was presented at the 1980 SPE/DOE Symposium on Unconventional Gas Recovery held in Pittsburgh, Pennsylvania, May 18-21, 1980. The material is subject to correction by the author. Permission to copy is restricted to an abstract of not more than 300 words. Write: 6200 N. Central Expwy., Dallas, Texas 75206

ABSTRACT

Stratigraphic studies of Middle and Upper Devonian rocks in West Virginia suggest that thick zones of interbedded siltstone and shale present between the Devonian Shale gas fields in southwestern West Virginia, and the gas fields in Upper Devonian sandstones and siltstones in central and eastern West Virginia may contain important reserves of natural gas. Wells drilled into these zones of interbedded siltstone and shale should be completed in the same way as wells drilled into the black shales; i.e., the entire zone should be fractured, not selected siltstones.

INTRODUCTION

During much of Middle and Late Devonian time, the Appalachian Basin was covered by a shallow epicontinental sea. This sea was bordered on the east by a land area that supplied the large amount of clastic sediments that formed the Catskill clastic wedge in the eastern part of the sea. To the west, north, and south, the sea encroached upon low-lying parts of the interior of the continent. Figure 1 shows the location of the Appalachian Basin and some of the structural elements associated with it.

For the purpose of this paper, rocks in the Catskill clastic wedge are divided into three facies: (1) red beds; (2) gray shale and sandstone; and (3) dark-gray shale and siltstone. Facies 1 contains red, gray, and green shale, siltstone, sandstone, and conglomerate deposited in terrestrial and near-shore marine environments. This facies forms the Hampshire Formation and the uppermost part of the Greenland Gap Group. The facies is present in the eastern and upper part of the clastic wedge (Fig. 2).

References and illustrations at end of paper.
Published with permission of the Director and State Geologist, West Virginia Geological and Economic Survey. Funded under U.S.D.O.E. Contract No. DE-AC21-76MC05199.

¹West Virginia Geological and Economic Survey, P.O. Box 879, Morgantown, WV 26505.

The Fifth, Bayard, Gantz, Fifty-foot, and Gordon are some of the sandstones in this facies. They have produced significant amounts of oil and gas in northern West Virginia.

Facies 2 contains gray shale, sandstone, and some siltstone. These rocks were deposited in a shallow to moderately deep marine environment west of facies 1. This facies roughly corresponds to the "Chemung facies" of older usage. Most of the Greenland Gap Group belong to this facies. The Speechley, Balltown, Warren, Bradford, Riley, and Benson are some of the sandstones and siltstones present in this facies. They have produced significant amounts of gas throughout the "Benson trend" in Barbour, Upshur, and adjacent counties in West Virginia. Many of the sandstones and siltstones within this facies appear to be turbidites deposited from turbidity currents that flowed west into the shallow epicontinental sea ^{1, 2}.

Facies 3 contains dark-gray shale and siltstone deposited in the deepest part of the epicontinental sea, and west of facies 2. The siltstones in this facies appear to be turbidites deposited from turbidity currents that reached the deepest part of the basin. In outcrops in eastern West Virginia, this facies is characterized by the Brallier Formation. Intervals of interbedded siltstone and shale within this facies make up the tight siltstones that may be important sources of natural gas.

Facies 3 intertongues westward into a black shale facies. The black shale facies contains organic-rich black shale, greenish-gray shale, gray shale, and minor amounts of limestone deposited in the shallow to moderately deep marine environment present on the western side of the epicontinental sea. The Ohio Shale and the Chattanooga Shale are examples of the black shale facies. The Devonian Shale gas production of southwestern West Virginia is from these rocks. Figure 2 shows an idealized interpretation of the relations between these facies.

The Upper Devonian rocks in the Appalachian Basin were deposited in a rising sea that transgressed westward onto the interior of the continent. As a result

of the westward transgression of the sea, and the concurrent westward building of the Catskill clastic wedge, all of the facies migrate westward and upward in the section as shown in Figure 2.

SOURCE OF THE NATURAL GAS

The thermochemical conversion of the organic matter in the Devonian rocks in the Appalachian Basin is in an early stage of development in the western part of the basin, and approaches completion in the eastern part of the basin.³ This eastward increase in the thermal rank of the organic matter in the Devonian rocks, and the eastward dip of the organic-rich shales from the Cincinnati Arch into the Appalachian Basin suggest that the western organic-rich shales are not the source of the natural gas in the siltstones and sandstones in central and eastern West Virginia.

The probable source for the natural gas in the Upper Devonian siltstones and sandstones in central and eastern West Virginia is the organic matter present in the dark-gray shale and siltstone facies (facies 3). Facies 3 was deposited in the deeper parts of the epicontinental sea. Rocks in this facies were more deeply buried than rocks age to the west. As the folds in the eastern part of the Appalachian Basin developed, some of the rocks in the east were raised higher than their lateral equivalents in the central part of the basin. During diagenesis, compaction, lithification, and folding, fluids and gases expelled from the sediments in the central part of the basin either migrated up dip (east or west), or vertically through the overlying rocks. Some of the gas generated in the rocks of facies 3 may have been trapped in the pores and fractures of the interbedded siltstone and shale in facies 3. Thus, thick intervals of fractured siltstone and shale in facies 3 may contain important deposits of natural gas.

STRATIGRAPHY

A brief review of the Middle and Upper Devonian stratigraphy and geologic history will show why the prospect area shown on Figure 1 might contain thick intervals of gas-bearing siltstones. The chart in Figure 3 shows the correlation of the major Devonian formations in West Virginia.

The Hamilton Group contains dark-gray to black shale, siltstone, and minor amounts of limestone. The dark-gray shale and siltstone make up the Mahantango Formation. The siltstones in the Mahantango are in the northeastern part of West Virginia⁴. The dark-gray shale of the Mahantango is present in northeastern and central West Virginia. The Mahantango is recognized on gamma-ray logs by relatively low gamma-ray readings. The black shale in the Hamilton makes up the Marcellus Shale. It underlies the Mahantango, and overlies the Onondaga Limestone. The Marcellus is recognized on gamma-ray logs by relatively high gamma-ray readings.

The isopach map of the Hamilton (Fig. 4) shows a broad shelf in the western part of the state that is covered by a thin (0 to 30 meters) layer of Hamilton rocks. East of the shelf, the Hamilton thickens rapidly to the east. The western limits of this shelf shown on Figure 4 is supported by the conodonts

of possible Hamilton age collected by Clarkson⁵ from a core collected in Mason County, West Virginia.

On the shelf, an unconformity separates the Hamilton from overlying Upper Devonian rocks. East of the shelf, the Tully Limestone rests conformably on the Hamilton. The Tully is not present on the shelf. On the isopach map, the 10 meter contour outlines the Warfield Anticline. This suggests that the anticline was in existence during Middle Devonian time.

At present, gas is being produced from the Hamilton (Marcellus) in eastern Gilmer County in the central part of the state. Here the Marcellus is unconformably overlain by the Genesee Formation. This area is along the eastern flank of the Rome Trough. The gas is probably being produced from fractures in the shale. However, because of the thinness of the unit, and the depth (1800-2400 meters; 6000-8000 feet) of the Hamilton in this area, it is not a primary target for gas production.

Early in the Late Devonian, the epicontinental sea began to transgress westward onto the interior of the continent. The Genesee Formation, and then the Sonyea Formation were deposited during the early part of this transgression. As the sea transgressed westward onto the shelf bordering the eastern flank of the Cincinnati Arch, siltstones (turbidites) were deposited in deeper water to the east. The turbidites were deposited from turbidity currents that flowed down the shelf and slope in the eastern part of the sea^{1, 2}. While a few relatively clean siltstones (units identified by low gamma-ray values on the gamma-ray log) were identified in the eastern part of the state, no thick intervals of interbedded siltstone and shale were identified in the Genesee-Sonyea interval. Figure 5 is an isopach of the Genesee-Sonyea interval.

Gas is being produced from the highly radioactive, organic-rich black shale in the Genesee Formation in eastern Gilmer County along with the gas from the Hamilton Group discussed above. A minor amount of gas has been produced from the Burket Shale (an equivalent to part of the Genesee Formation) from the test well drilled by the U.S. Department of Energy at the Morgantown Energy Technology Center in Morgantown. However, because of the thinness of the organic-rich black shale, the small amount of siltstone, and the depth of the formations (1500-2100 meters; 5000-7000 feet), rocks in these formations are not primary targets for gas production.

The sea continued to transgress westward during the deposition of the West Falls and Java Formations. Moderately to highly radioactive, organic-rich black shale, dark-gray shale, and gray shale were deposited in southwestern West Virginia. Dark-gray shale and siltstone of facies 3, and gray shale, siltstone, and sandstone of facies 2 were deposited in the central and eastern parts of the state. The Rhinestreet Member of the West Falls Formation is composed of organic-rich black shale with interbedded dark-gray shale. In parts of southwestern West Virginia, there are more than 30 meters (100 feet) of organic-rich black shale in the Rhinestreet. The Rhinestreet produces natural gas in southwestern West Virginia^{6, 7}.

The 200 and 300 meter contour lines on Figure 6 are the approximate boundaries of the zone where the basinal dark-gray shale and siltstone facies inter-

tongues with the moderately deep to shallow water black shale facies. In this area, siltstones (turbidites) can be interbedded with black shales. In the West Falls-Java interval, relatively "clean" siltstones (Sycamore, Elk, and Alexander) extend westward into the central part of the state (Fig. 6).

In central West Virginia, thick zones of interbedded siltstone and shale occur in the West Falls-Java interval. Where these zones of interbedded siltstones and shale are fractured, they are potential reservoirs for natural gas. The area in which to search for these zones of interbedded siltstone and shale is between the 200 and 400 meter contour lines on Figure 6. These zones of interbedded siltstone and shale occur at depths between 1000 and 1600 meters (3500-5500 feet).

Sea level continued to rise during the deposition of the Ohio Shale and its equivalents. The Ohio Shale contains two organic-rich black shales that are moderately to highly radioactive. The lower black shale is the Huron Member. It is thicker and more widespread than the upper black shale, the Cleveland Member. These black shales intertongue eastward into dark-gray shales and siltstones of facies 3. Farther east, equivalents of the Ohio Shale consist of gray shales, siltstones, and sandstones of facies 2, and red beds of facies 1. During the latest part of the Devonian, the Catskill clastic wedge was built westward into central West Virginia (Figures 1, 7).

In parts of southwestern West Virginia, there are more than 100 meters (300 feet) of organic-rich black shale in the Huron Member. Here, the Huron produces natural gas^{6, 7}. To the east, in central and eastern West Virginia, the Benson, Riley, Balltown, Speechley, Bayard, Fifth, and other sandstones that produce natural gas occur in this interval. The 500 and 700 meter contour lines on Figure 7 are the approximate boundaries between gas production from black shale in southwestern West Virginia, and gas production from siltstones and sandstones in central and eastern West Virginia. It is in the area between the 500 and 700 meter contours where thick zones of interbedded siltstone and shale belonging facies 3 may occur. Where these zones of interbedded siltstone and shale are fractured, they are potential reservoirs for natural gas.

SUGGESTED EXPLORATION AND DEVELOPMENT TECHNIQUES

It is suggested that stratigraphic studies be made to locate thick intervals of interbedded siltstone and shale in eastern equivalents of the Ohio Shale and the West Falls Formation in west-central West Virginia. Studies should also be made to locate areas where these zones of interbedded siltstone and shale are naturally fractured. If a thick zone of interbedded siltstone and shale is located and drilled, then the entire zone should be hydraulically

fractured, not just selected siltstones.

Figure 8 shows parts of two logs of wells drilled through the Upper Devonian in West Virginia. The section shown on the log for the well Fayette 241 is an eastern equivalent of the Ohio Shale. On the Fayette 241 log, the zone of interbedded siltstone and shale is between 3520 and 3710. The section shown on the log for well Gilmer 1978 is an eastern equivalent of the West Falls Formation. On the Gilmer 1978 log, the zone of interbedded siltstone and shale is between 4890 and 5120.

REFERENCES

1. Cheema, M.R.: "Sedimentation and Gas Production of the Upper Devonian Benson Sand in North-central West Virginia - a Model for Exogeosynclinal Mid-fan Turbidities off a Delta Complex", West Virginia University, Ph.D. Dissertation, 1977, (unpublished).
2. Lundegard, P.D., Samuels, N.D., and Pryor, W.A.: "The Brallier Formation - Upper Devonian Turbidite Slope Facies of the Central and Southern Appalachians", in Preprints for Second Eastern Gas Shales Symposium, Volume 1, U.S. Department of Energy, Morgantown Energy Technology Center, Morgantown, West Virginia, 1978, pp. 4-23.
3. Claypool, G.E., Threlkeld, C.N., and Bostick, N.H.: "Natural Gas Occurrence Related to Regional Thermal Rank of Organic Matter (Maturity) in Devonian Rocks of the Appalachian Basin", in Preprints for Second Eastern Gas Shales Symposium, Volume 1, U.S. Department of Energy, Morgantown Energy Technology Center, Morgantown, West Virginia, 1978, pp. 54-65.
4. Dennison, J.M., and Naegle, O.D.: "Structure of Devonian Strata Along Allegheny Front from Corriganville, Maryland, to Spruce Knob, West Virginia", West Virginia Geological and Economic Survey, Bulletin 24, 1963.
5. Clarkson, G.R.: "Devonian Conodont Biostratigraphy and Paleoecology of Mason County, West Virginia", West Virginia University, M.S. Thesis, (in preparation).
6. Dowse, M.E.: "The Subsurface Stratigraphy of the Middle and Upper Devonian Clastic Sequence in Northwestern West Virginia", West Virginia University, Ph.D. Dissertation, (in preparation).
7. Neal, D.W.: "Subsurface Stratigraphy of the Middle and Upper Devonian Clastic Sequence in Southern West Virginia and its Relation to Gas Production", West Virginia University, Ph.D. Dissertation, 1980, (unpublished).

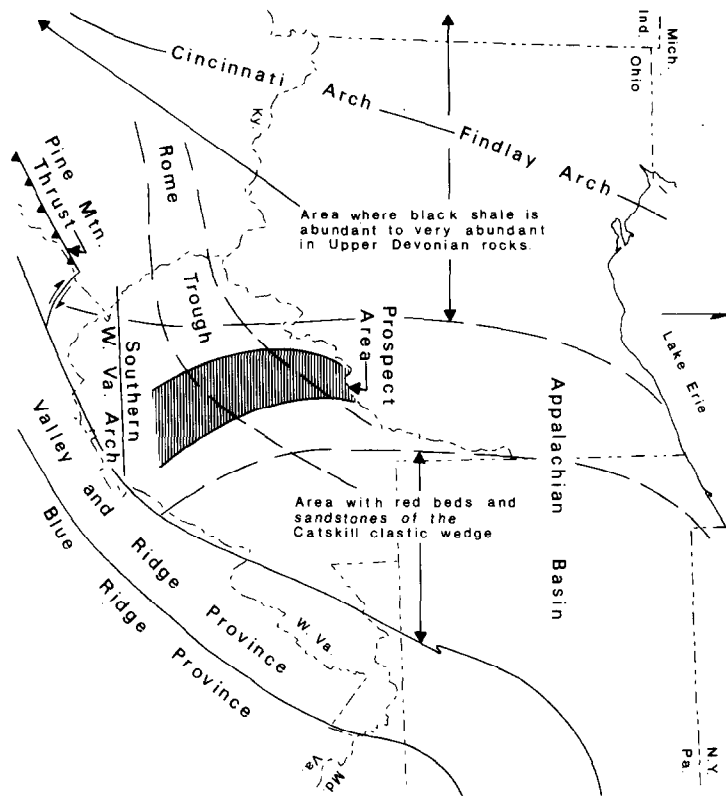
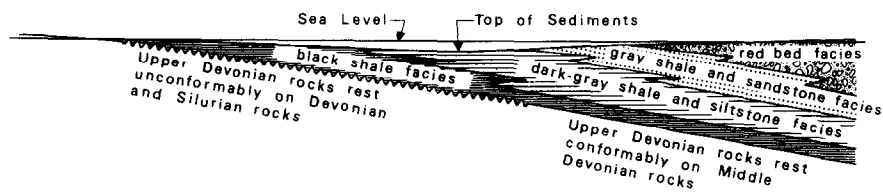


Fig. 1 - Index map.

Interior of
Continent

Shallow Epicontinental Sea

Clastic Wedge -
sediment from
eastern source



Idealized Cross Section

Fig. 2 - Idealized East-West cross section showing relation of facies.

Middle and Upper Devonian Formation in West Virginia

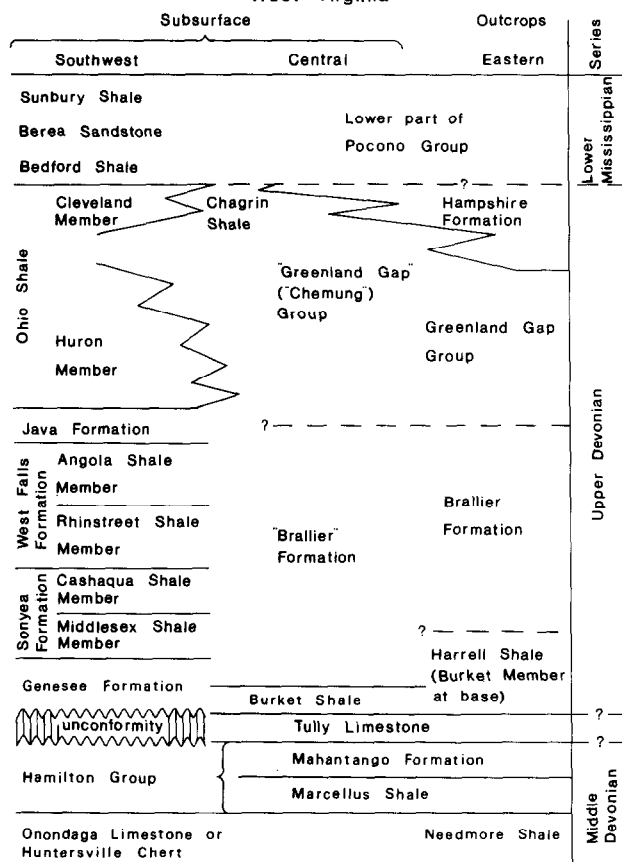


Fig. 3 - Correlation chart.

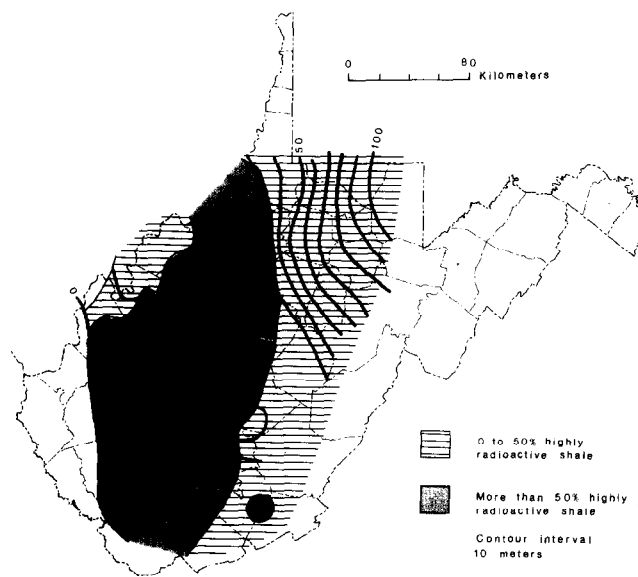


Fig. 4 - Isopach map of Hamilton Group.

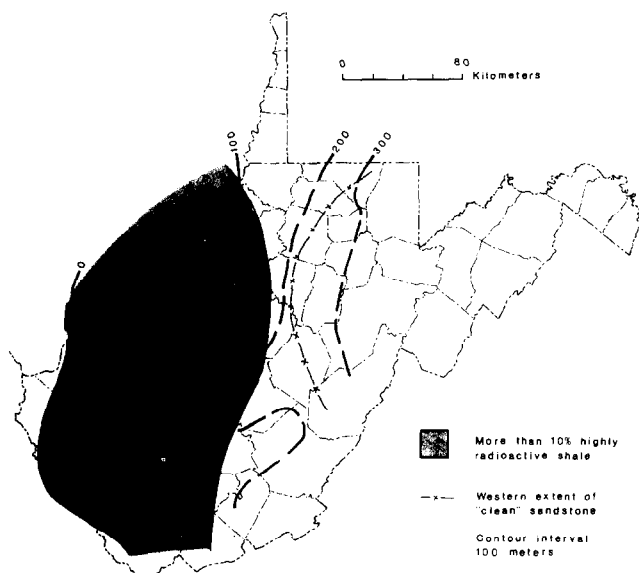


Fig. 5 - Isopach map of Genesee-Sonyea interval.

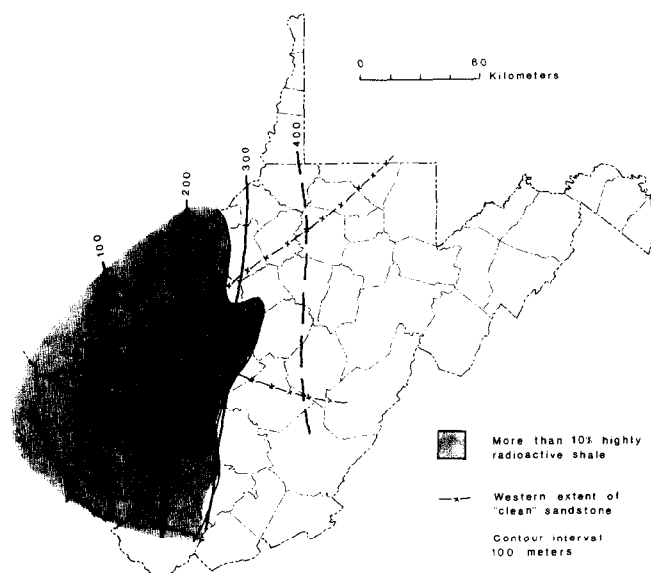


Fig. 6 - Isopach map of Java-West Falls interval.

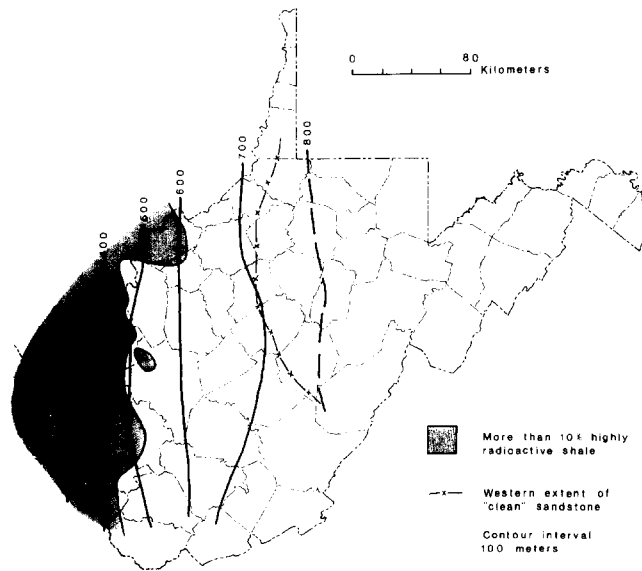


Fig. 7 - Isopach map of base of Berea-top of Java interval.

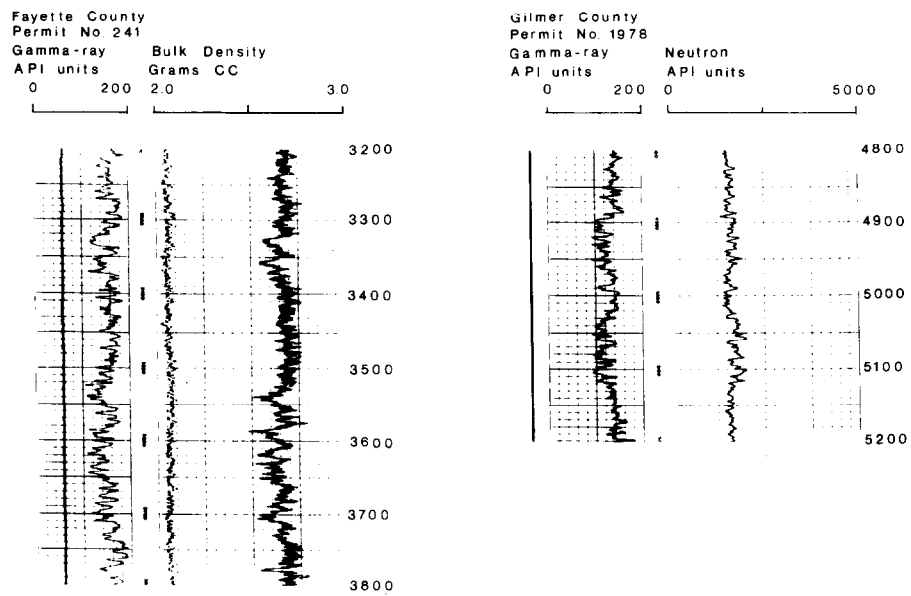


Fig. 8 - Wire-line logs showing zones of interbedded siltstone and shale.

PREDICTING THE IN-SITU STRESS FOR DEEP WELLS USING DIFFERENTIAL STRAIN CURVE ANALYSIS

by Frank G. Strickland and Nae-Kan Ren, Dow Chemical

© Copyright 1980, Society of Petroleum Engineers

This paper was presented at the 1980 SPE/DOE Symposium on Unconventional Gas Recovery held in Pittsburgh, Pennsylvania, May 18-21, 1980. The material is subject to correction by the author. Permission to copy is restricted to an abstract of not more than 300 words. Write: 6200 N. Central Expwy., Dallas, Texas 75206

ABSTRACT

Recent developments in energy exploration at depths of 5000 to 25,000 feet have made it necessary to quickly and reliably determine the in-situ stresses acting on the wellbore.

Differential Strain Analysis (DSA) is being investigated as a technique applied to core samples to indirectly determine the in-situ stress state.

Testing is being pursued in three steps. First, field measurements of strain are made in-situ as the core is pulled out of the well. Second, the cores are brought to the lab and DSA is performed under in-situ hydrostatic conditions. Third, the rock is examined microscopically.

These tests have been performed on both oriented and non-oriented cores from Texas, Louisiana and Pennsylvania.

At this point in the investigation, it appears very favorable that a reasonably accurate estimate of the 3-dimensional stress state can be obtained using the strain curve analysis method. It has been demonstrated mathematically that not only the ratio of the stresses can be derived but also the orientation of the stresses in free space. The application of these equations to the data from the latest high quality runs yields results well within the reproducible tolerance of other methods.

INTRODUCTION

Recent trends in the oil and gas industry have been toward developing reservoirs that were previously passed over due to one reason or another. One type of these reservoirs is the "tight" gas or oil formations. The development of advanced fracturing techniques has allowed commercially viable production rates from these formerly low producers. However, even with these fracturing techniques, much of the reservoir may be left unrecovered because of the unique drainage pattern in low permeability reservoirs. Smith¹ (1979) has demonstrated that the drainage around a fracture-stimulated well is elliptical rather than radial. This is even

more pronounced as the fractures increase in length, as in massive hydraulic fracturing. Consequently, well spacing based on radial drainage may provide inefficient recovery due to overlapping drainage at fracture tips and "dead" areas between fracture flanks. If there was a way of predicting the fracture orientation when planning the spacing of wells in a developing field, recoveries could be increased to recover an additional 30% of the total reserve (Smith¹, 1979). That would greatly increase the realized potential from many of the giant gas fields.

Considerable research has been devoted to measuring fracture propagation during the fracturing process. The various methods used include: tiltmeter surveys, acoustic emission surveys (both surface and well-bore), resistivity surveys, etc. The major restriction on the fracture propagation surveys is depth. Resolution drops off rapidly as depth (and therefore, distance from sensors) increases. Another attempt at predicting fracture orientation has been to measure directly the in-situ stress field, since this is the primary factor influencing the control of fracture orientation (Warpinski, et al.², 1980; Hubbert and Willis³, 1956). The traditional method of determining stress in rock masses has been by the overcoring process (Obert and Duval⁴, 1967). Strain gages are attached to the bottom of a core hole and the differential expansion of the rock is measured as the rock is released from the in-situ stresses by overcoring. The method is relatively accurate but limited to shallow depths (a few hundred feet) and to only one plane of measurement (i.e., 2-dimensional). Another method employed at greater depths is the mini frac-impression packer method (Haimson⁵, 1978). This method isolates a zone by openhole packers and induces a small fracture by pressurizing the interval. An impression packer is then inflated over the fractured interval and the imprint of the fracture opening on the packer can then be oriented. This method's shortcomings are: 1) borehole stresses and skin damage may interfere with the fracture initiation and since the packer only measures the inside surface, any re-orienting of the fracture as the fracture penetrates away from the well bore is not measured, 2) only one plane (that of the fracture plane) is being measured, 3) physical problems are often encountered (packer damage, hole collapse, trip time for impression packer, fractures in certain formations not leaving discernable impression,

References and illustrations at end of paper.

etc.). In addition, there has been reluctance in industry to use this method because a fracture is being produced in an uncased, open hole with attendant zone isolation and well control problems.

Ideally, a method is needed that can give an idea of the 3-dimensional stress state, as to both the stress directions in space, uninfluenced by the well-bore, and to the relative and/or absolute magnitude of each of the 3 principle directions. This is something no method to date can do at the typical depths encountered in the energy industry.

In this study, a variation of Differential Strain Analysis (DSA) is being investigated as a method that might be used to get such a 3-dimensional stress measurement. High precision measurements ($\pm 3 \times 10^{-6}$) of strain as a function of hydrostatic pressure to 124,107 kPa were performed on cored samples (oriented and unoriented) from depths of 820 meters to 3642 meters.

EXPERIMENTAL DETAILS

Samples

Three cores were used in this study. The first was a 12.8 m long section of four-inch (10.16 cm) diameter core from the Schuler Formation (Cotton Valley group) in Panola County, Texas. The second core, also from the Cotton Valley group, was a 3-inch core from Jackson Parish, Louisiana. The third was a set consisting of 10.16 cm cores taken from intervals in the Warren, Tiona and Bradford Formations (Devonian) in Indiana Co., Pennsylvania. The depths from which the cores were taken are: Panola Co. 2789-3018 meters; Jackson Parish, 3612-3632 meters; and Indiana Co. 829-844 meters (Warren Formation), 938-970 meters (Tiona Formation), and 1084-1094 meters (Bradford Formation).

Although the overall composition of the cores varied greatly, the samples chosen for the study were selected for, 1) homogeneity 2) structural soundness (no obvious cracks) and 3) whether the interval selected was in the pay zone or in a barrier. Most samples were fine-grained sandstones, although some shales and conglomerates were used. Table 1 lists the samples selected, their depth, rock type and orientation information.

The Panola cores are totally non-oriented. The Jackson Parish cores are oriented relative to each other, but their absolute orientation is not known. The Indiana County cores were collected using an oriented core barrel to a depth of 941 meters, at which point abnormal circulating pressure made it necessary to remove the oriented barrel. The remainder of the cores were only oriented relative to each other.

PREVIOUS RESEARCH

Earlier research was conducted by the authors (Strickland, et al.⁶, 1979) into the generation and amount of crack damage caused by the coring process. Differential Strain Analysis (DSA) was used in that study because it could determine, 1) the linear and volumetric compressibility as a function of pressure, 2) the strain associated with cracks of a particular closure pressure, and 3) the orientation of cracks with particular closure pressures. For details of sample preparation, data analysis and DSA theory, the reader is referred to the original article (Strickland, et al.⁶, 1979), and to the works of Simmons et al.⁷, (1974) and Seigfried and Simmons (1978).

During the course of the earlier study, it became apparent that there might be a strong and direct correlation between the amount and direction of crack generation in the rock matrix and the original in-situ stress field. In order to modify DSA to be able to predict in-situ stress, four assumptions needed to be tested. The assumptions are: 1) microcracks are induced in the core matrix as the rock expands in response to release from in-situ stresses, 2) these cracks are aligned primarily by the direction of the original stress forces, 3) the cracks are proportional volumetrically to the corresponding in-situ stress magnitudes, as modified by the rock matrix and, 4) by reversing the expansion of the sample by subjecting it to hydrostatic pressure, the contraction of the rock in any specific direction will be analogous to the original strain in that direction.

Assumption #1 was demonstrated in an earlier paper (Strickland, et al.⁶, 1979) and by the work of Simmons and Richter (1974)*. A program of field core relaxation, lab compression and microscopic examination was initiated to test the other assumptions.

*(The Simmons, et al.⁶ (1974) study also demonstrated direct correlation between the type and slope of the strain curve and the source of the microcracks. This represents a kind of "fingerprint" imparted by each event in the rock's history.)

DIFFERENTIAL STRAIN CURVE ANALYSIS - PRINCIPLE AND CALCULATION

A step-by-step procedure from the one-dimensional case through to the 3-dimensional case showing how the strain analysis method works will now be presented.

It was discovered in earlier work (Simmons et al.⁶, 1974), and confirmed in this work, that for most rocks under compression the strain vs. pressure curve consisted of linear segments separated by distinct slope discontinuities. For a gage representing one direction this generally takes the form shown in Figure 1, where there are two distinct linear segments separated by a zone where the slope is continuously changing.

The position of the transition zone on the strain curve between the linear portions of the strain curve is related to the in-situ pressures. This is a result of the curve passing at that point from a matrix with induced crack damage to a matrix approximating the in-situ state. The sharpness with which this transition takes place is apparently a function of the mineralogy of the rock. Crystalline rocks, as used in the Simmons study, generally produced very sharp breakovers, whereas the sedimentary rocks used in this study produced longer transition zones. The deeper samples produced sharper transitions, probably due to the better lithification of the sediments. In the case of sharp breakovers, the strain at that point may be used to directly ascertain the in-situ stress. It is worth noting that the transition does shift position in curves representing different directions on the same rock. This would be expected, with the curve going into transition earlier in curves representing smaller in-situ stresses.

The last linear portion (part 2) represents the intrinsic compressibility of the constituent minerals in the rock matrix after all the cracks and most of the pore space is closed.

The first linear portion has a steep slope

because the cracks are only partially closed. Consequently, a corresponding increase in pressure yields a larger strain than in the latter portion where the cracks are closed.

Consider Figure 2. The last linear portion of the strain curve represents the intrinsic compressibility of the sample in that particular direction. It can be expressed either as the ratio of $\Delta\epsilon$ to ΔP or as the slope (β) of the linear portion of the curve.

Points X and Y lie on the first linear portion of the strain curve and are represented by the values (P_x, ϵ'_x) and (P_y, ϵ'_y) . The values ϵ'_x and ϵ'_y are the zero pressure intercepts obtained by projecting lines parallel to the intrinsic compressibility slope through points x and y.

The quantity $(\epsilon'_y - \epsilon'_x)$ is the strain change that occurs over the pressure range $(P_y - P_x)$ caused by the complete or partial closing of all cracks that were open at $P < P_x$ (see Simmons et al., 1974).

$$\text{So: } \epsilon'_y = \epsilon'_x + \beta P_y \quad (1) \quad [\text{See Figure 2}]$$

$$\epsilon'_x = \epsilon'_x + \beta P_x \quad (2)$$

$$\beta = \frac{\Delta\epsilon}{\Delta P} \quad [\text{As in Figure 2}]$$

If the curve between ϵ_x and ϵ_y is linear; then

$$\frac{\epsilon'_y - \epsilon'_x}{P_y - P_x} = \frac{\epsilon_y - \epsilon_x}{P_y - P_x} - \beta \frac{P_y - P_x}{P_y - P_x} \quad (3)$$

$$\text{set } \frac{\epsilon_y - \epsilon_x}{P_y - P_x} = \theta = \text{slope}$$

$$\text{so } \frac{\epsilon'_y - \epsilon'_x}{P_y - P_x} = \theta - \beta = \epsilon' \quad (4)$$

This gives the value of strain change caused by the complete or partial closing of all cracks over a unit pressure range on this linear strain region. This is defined as ϵ' .

Next, for the two-dimensional case, refer back to the four assumptions stated earlier concerning crack genesis in relation to the original stress state. The following is a simple example to help illustrate the principles being assumed. In Figure 3 (a) we have a rock under in-situ stress in 2 directions, X and Y.

$$P_{\max} = 12 \text{ MPa in X direction}$$

$$P_{\min} = 6 \text{ MPa in Y direction}$$

Upon coring, the in-situ stresses are released and the rock is allowed to expand in all directions (it is at this point the overcoring method is used to measure the relative expansion of the rock). Since the X direction has the greatest stress release, it will expand the most by crack genesis and direction Y will be the least cracked since it has the least amount of stress release. This is shown schematically in Figure 3(b). In Figure 3(c) the rock is subjected to 3 MPa hydrostatic reloading in a pressure vessel. Since the X direction had the most cracks, it will be the most easily compressed and will, therefore, have the highest ϵ' (see Figure 3) value at P_{3MPa} . For the same reason Y will have the lowest ϵ' value.

From this it can be predicted that the direction of the original maximum in-situ stress was X and the direction of the minimum in-situ stress was Y.

Now, let's see how this works on a sample. A three strain gage rosette will give 3 strain curves as shown in Figure 4 (compare with Figure 1). In a homogenous rock $\beta_1 = \beta_2 = \beta_3$, or in other words, the intrinsic compressibility will be approximately the same. Because the strain curves have an early linear portion, equation (4) can be applied.

$$\epsilon'_1 = \theta_1 - \beta_1 \quad \epsilon'_2 = \theta_2 - \beta_2 \quad \epsilon'_3 = \theta_3 - \beta_3 \quad (5)$$

ϵ' is the strain due to crack closure per unit of pressure change.

Set

$$\begin{aligned} \epsilon'_1 &\rightarrow \epsilon_x & \epsilon'_2 &\rightarrow \epsilon_{xy} \\ \epsilon'_3 &\rightarrow \epsilon_y & (\epsilon'_4 &\rightarrow \epsilon_{xy}) \end{aligned} \quad (\text{See Figure 5})$$

The strain ϵ in the direction inclined at some angle θ to ox is given by

$$\epsilon = \epsilon_x \cos^2 \theta + \epsilon_y \sin^2 \theta + 2\Gamma_{xy} \sin \theta \cos \theta \quad (6)$$

(Jaeger & Cook¹⁰, 1976)

where $\Gamma = 1/2 \bar{\gamma}_{xy}$, $\bar{\gamma}$ = shear strain

Then the principal axes are inclined at

$$1/2 \tan^{-1} \frac{2\Gamma_{xy}}{\epsilon_x - \epsilon_y} \quad (7) \quad (\text{Jaeger & Cook}^{10}, 1976)$$

to ox , and ϵ_{\max} and ϵ_{\min} are

$$1/2(\epsilon_x + \epsilon_y) \pm [\Gamma_{xy}^2 + 1/4(\epsilon_x - \epsilon_y)^2]^{1/2} \quad (8)$$

Finally, consider the 3-dimensional case (Figure 6). The same type of forms can be defined as in equation (5):

$$\epsilon'_1 = \theta_1 - \beta_1 \quad \epsilon'_2 = \theta_2 - \beta_2$$

$$\epsilon'_3 = \theta_3 - \beta_3 \quad \epsilon'_4 = \theta_4 - \beta_4$$

$$\epsilon'_5 = \theta_5 - \beta_5 \quad \epsilon'_6 = \theta_6 - \beta_6$$

$$\epsilon'_7 = \theta_7 - \beta_7 \quad \epsilon'_8 = \theta_8 - \beta_8$$

$$\epsilon'_9 = \theta_9 - \beta_9 \quad (9)$$

Three pairs are parallel in direction and can be averaged so:

$$\epsilon'_1 \approx \epsilon'_9 \quad \epsilon'_3 \approx \epsilon'_4 \quad \epsilon'_6 \approx \epsilon'_7$$

This reduces to six knowns as follows:

$$\text{Set: } 1/2(\epsilon'_1 + \epsilon'_9) \rightarrow \epsilon_x, \quad 1/2(\epsilon'_6 + \epsilon'_7) \rightarrow \epsilon_z,$$

$$\epsilon'_5 \rightarrow \epsilon_{xy}, \quad 1/2(\epsilon'_3 + \epsilon'_4) \rightarrow \epsilon_y, \quad \epsilon'_2 \rightarrow \epsilon_{yz},$$

$$\epsilon'_8 \rightarrow \epsilon_{xz} \quad (10)$$

In three dimensions, strain ϵ may be described using, direction cosines (l, m, n) with angles (α, β, γ) with respect to the three perpendicular axis (ox, oy, oz), by the following equation:

$$\epsilon = l^2 \epsilon_x + m^2 \epsilon_y + n^2 \epsilon_z + 2mn \Gamma_{yz} + 2nl \Gamma_{xz} + 2lm \Gamma_{xy}$$

(Jaeger & Cook, 1976) (11)

From the definition of the three principal strains the following three equations can be established.

$$l(\epsilon_x - \epsilon) + m\Gamma_{xy} + n\Gamma_{xz} = 0 \quad (12)$$

$$l\Gamma_{xy} + m(\epsilon_y - \epsilon) + n\Gamma_{zx} = 0 \quad (13)$$

$$l\Gamma_{xz} + m\Gamma_{yz} + n(\epsilon_z - \epsilon) = 0 \quad (14)$$

The three real roots of ϵ will be three principal strains ($\epsilon_{p1}, \epsilon_{p2}, \epsilon_{p3}$)

By displacing ϵ_{p1} into equations (12) (13) and (14), one set of (l, m, n) can be solved. The same applies to solving ϵ_{p2} for (l₂, m₂, n₂) and ϵ_{p3} for (l₃, m₃, n₃) and three corresponding sets of angle can be obtained as ($\alpha_1, \beta_1, \gamma_1$); ($\alpha_2, \beta_2, \gamma_2$) and ($\alpha_3, \beta_3, \gamma_3$), respectively.

Two computer programs were written to calculate the two-dimensional and three-dimensional case. By knowing the (ox, oy, oz) orientation and the three sets of principal strain cosine angles, the true orientation of the three principal directions can be plotted using the "Stereographic Projection Method" (Goodman¹¹, 1976). The ratio between the three principle stresses can be relatively determined by the ratio between ϵ_{p1} , ϵ_{p2} , and ϵ_{p3} . Specific values can be assigned by using the instantaneous shut-in pressure (ISIP) during a fracture treatment as the minimum stress and using the ratios to calculate the other 2 stress values.

PROCEDURE

The sample preparation has been standardized after investigating different strain gage configurations. First, the cube is carefully cut (to avoid further crack generations) and hand lapped into a cube approximately 1-1/2" on each side, being careful to preserve the orientation references. It is important that all faces are at right angles to simplify data analysis. Then on each of three faces surrounding a common corner(o), a foil strain gage rosette comprised of 3 gages at 45° apart and a single gage were mounted as shown in Figure 6. The single gage is mounted perpendicular to the middle gage on the rosette. The four-gage configuration allows the selection of 2 or more rosette displays for calculating the stress field in that plane. This increases the accuracy and provides a backup in case one of the gages fail. The rosettes are aligned parallel to the edges of the cube. In order to get point strain, the rosettes were mounted as close as possible to point o, but no closer than 1/8" to the edge of the cube to avoid edge effects. After wiring, the sample was vacuum dried and potted in a clear, flexible and impermeable jacket to exclude the pressure medium from the cracks in the sample. The sample was then cured overnight at 120°F with a slow heating and cooling rate. The cube, along with a fused silica standard, were then loaded into the pressure vessel and subjected to a total hydrostatic pressure of 100 to 140 MPa (depending on the depth of the core). The total hydrostatic pressure was achieved by small initial increments of 1-3 MPa

and then by larger increments of 5-10 MPa. The recorded stress-strain curves are compared with the fused silica sample and any deviations were removed. Finally, the curves were plotted, numbering 1 to 12.

FIELD RELAXATION DATA

An on-site field program was initiated in an attempt to get measurements of the original rock expansion and crack genesis after the rock is released from the in-situ stresses. As soon as possible after the cores were received at the surface, strain gages were applied to the cores (Figure 7) and placed in an oven preheated to in-situ temperatures to reduce thermal effects. The resulting strain data was plotted and compared with the lab compression curves to see if there was a correlation.

RESULTS

Differential Strain Analysis

Table 2 contains the calculations for a typical sample (#2865.5) from the Pennsylvania well. True compass orientation is known for this sample, but to simplify the example, assume that the X axis = 0°N; Y axis = 0°W and Z axis = 0° vertical (it is easier to apply a single correction to the final stress direction determination than carry the true axis directions through the calculations).

In Table 2, strain curves from each of the twelve strain gages shown in Figure 6 are resolved for β , θ , and ϵ' . Then using the four gages on each face to form 2 sets of 3 gage rosettes (by interchanging the intermediate gages) two sets of values are obtained for the maximum and minimum stress values. As can be seen, the ratios are very consistent but the directions differ by 8.5° to 16°.

To extend the data to the 3-dimensional case, first the ϵ' values for the 3 duplicate direction pairs are averaged to give the 6 directions of ϵ' values (Table III). Again, by interchanging the intermediate gages in the rosettes, two sets of ratios and stress directions are calculated (Table IV). The ratios between the maximum, intermediate and minimum stress values for the two rosette patterns are identical. The direction of the maximum principal stress direction varies by 14° azimuth and 10° dip.

In all but one sample, the vertical strain was greatest in the Texas and Louisiana cores and in the Warren and Bradford Formations in Pennsylvania. Samples from the Tiona Formation revealed that in 4 of the 6 samples the maximum and minimum strains were in the horizontal plane and the intermediate was vertical.

Field Data

Technical problems prevented getting useful data for most of the Louisiana and Pennsylvania cores. Once the technical problems were solved, curves similar to Figure 8 were normal. The steep initial slope was due to warming the cores back to downhole temperature after cooling off during gaging the sample. Then a steady decrease was observed, tapering off to essentially no slope after about 12 hours. The trip time to bring cores out of the Louisiana well averaged about 5 hours and in the Pennsylvania well it was between 2-3 hours. By this time most of the relaxation had occurred and we were measuring only the very tail end of the strain curve. When compared to the lab DSA curves, there was

generally good agreement, although the field curves were somewhat erratic in nature.

DISCUSSION

From earlier work, it appears that the stress field becomes uniform over larger areas with increasing depth (Haimson¹², 1977). This makes it necessary to sample only a few wells in a field to predict the stresses over the entire area. For most sedimentary rocks encountered in the oil field, the solving for the primary horizontal stress vectors (two-dimensional case) would be adequate. This assumes the stresses are not inclined by tectonics or bedding planes and the depth is sufficient so the fracture will be vertical. In all the samples tested, without exception, the minimum strain was horizontal, tending to confirm the vertical fracture assumption in the formations examined.

The reversal of strain observed in the Tiona Formation curve may be due to mineralogy, but at the time of this writing, this was not conclusive. Another explanation may be that there is an actual reversal of stress directions in that formation. This would be difficult to determine by any previous method involving fracture mechanics because the fracture would still be vertical and the minimum stress is still horizontal. Consequently, changes in the other two stress directions would be undetectable. The main affect if the maximum and minimum stress directions were both in the horizontal plane would be an even stronger resolution of the fracture direction due to the larger contrast in values.

CONCLUSIONS

At this point in the investigation, it appears very favorable that a reasonably accurate estimate of the 3-dimensional stress state can be obtained using the strain curve analysis method. It has been demonstrated mathematically that not only the ratio of the stresses can be derived but also the orientation of the stresses in free space. The application of these equations to the data from the latest high quality runs yields results well within the reproducible tolerance of other methods.

Comparison with the relaxation curves obtained in the field experiments has tended to confirm the reliability of the lab measurements, although the quality of the field data was not what we had anticipated.

FUTURE WORK

The next step planned in evaluating this method is to perform fracture treatments, such as on the Pennsylvania well, in the next few months and make measurements with other methods and compare the results. Also, samples where the stress field is already known are being tested and the results compared.

ACKNOWLEDGEMENTS

The authors would like to express their gratitude to Anadarko Production and Delta Drilling Company for supplying the cores used in this study and allowing access to their well sites to make the field measurements. The author also gratefully acknowledges Carl Montgomery and Jim Wallace for their suggestions, encouragement and help during the course of this work.

Thanks are also extended to the management of Dowell Division of Dow Chemical for permission to publish this paper.

REFERENCES

1. Smith, M. B., 1979, "Effect of Fracture Azimuth on Production with Application to the Wattenburg Gas Field," Proceedings 54th Ann. SPE Tech. Conf. and Exhib., SPE #8298, Las Vegas, Nev.
2. Warpinski, N. R., Schmidt, R. A. and Northrop, D. A., 1980, "In-Situ Stresses: The Predominant Influence on Hydraulic Fracture Containment," in Proceedings, SPE-DOE Symposium on Unconventional Gas Recovery, May 18-21, Pittsburg, Pa., SPE#8932.
3. Hubbert, M. K. and Willis, D. G., 1956, "Mechanics of Hydraulic Fracturing," 31st Annual Fall Meeting, Petrol, Branch AIME, Los Angeles, Oct 14-17, paper No. 686-G.
4. Obert, L., and Duvall, W. E., 1967, Rock Mechanics and the Design of Structures in Rock; Wiley, New York, New York, pp 409-419.
5. Haimson, B. C., 1978, "The Hydrofracturing Stress Measuring Method and Recent Field Results," Int. J. Rock Mech. Min. Sci. & Geomech. Abstr., Vol 15, pp 167-178.
6. Strickland, F. G., Feves, M. L. and Sorrells, D., 1979, "Microstructural Damage in Cotton Valley Cores," SPE #8303 in Proceedings SPE 54th Annual Tech. Conf. and Exhib., Sept 23-26, Las Vegas, Nev.
7. Simmons, G., Siegfried, R. W., and Feves, M., 1974, "Differential Strain Analysis: A New Method for Examining Cracks in Rocks," J. Geophys. Res., Vol 79, 4383-4385.
8. Siegfried, R., and Simmons, G., 1978, "Characterization of Oriented Cracks With Differential Strain Analysis," J. Geophys. Res. 83, pp 1269-1278.
9. Simmons, G., and Richter, D. A., 1974, "Microcracks in Rocks: A New Petrographic Tool (abstract), EOS Trans. AGN, 55, 478.
10. Jaeger, J. C. and Cook, N. G., 1974, Fundamental of Rock Mechanics, Chapman and Hall Lts., London, pp 9-52.
11. Goodman, R. E., 1976, "Methods of Geological Engineering in Discontinuous Rock," West Publishing Co., New York, New York, pp 209-276.
12. Haimson, B. C., 1977, "Crystal Stress in the Continental United States as Derived From Hydrofracturing Tests," The Earth's Crust. Geophy. Monogr. Ser., Vol 20, edited by J. C. Heacock, pp 576-592, AGU, Washington, D. C.

NOMENCLATURE

β = Intrinsic compressibility - $\mu\epsilon/\text{MPa}$
 θ = Compressibility at local - $\mu\epsilon/\text{MPa}$
 γ = Shear strain
 Γ = One half of shear strain
 (l, m, n) = Direction cosine
 (α, β, γ) = Angle of direction cosine - degrees
 ϵ = Axial strain
 P = Pressure - MPa

TABLE 1

Sample # (ft/depth)	Rock Type	Orientation	Field Gauges
9184	Fine grained sandstone	none	No
9187	Fine grained sandstone	none	No
9189	Fine grained sandstone	none	No
9191	Medium grained sandstone	none	No
9198	Medium grained sandstone	none	No
9200	Medium grained sandstone	none	No
9203	Medium grained sandstone	none	No
9207	Medium grained sandstone	none	No
<u>Texas</u>			
11010	Fossiliferous Calc-arenite	none	Yes
11029	Shale	none	Yes
11042(1)	Medium grained sandstone	relative	Yes
11042(2)	Medium grained sandstone	relative	Yes
11044	Medium grained sandstone w/shale stringers	relative	Yes
11046	Medium grained sandstone w/shale stringers	relative	Yes
11048	Fine grained sandstone w/shale stringers	relative	Yes
<u>Pennsylvania</u>			
2551.5	Fine grained sandstone	absolute	Yes
2564.5	Fine grained sandstone	absolute	Yes
2571.0	Verigated sandstone & shale	absolute	Yes
2865.5(1)	Fine grained sandstone	absolute	Yes
2865.5(2)	Fine grained sandstone	absolute	Yes
2865.0(1)	Fine grained sandstone	absolute	Yes
2865.0(2)	Fine grained sandstone	absolute	Yes
2929.5(1)	Fine grained sandstone	relative	Yes
2929.5(2)	Fine grained sandstone	relative	Yes
3311.0	Qtz conglomerate	none	Yes

TABLE 2

Two Dimensional Solution
(Sample #2865.5)

	xy Plane				xz Plane				yz Plane			
	ϵ_x	ϵ_{xy}	ϵ_y	$\overline{\epsilon_{xy}}$	ϵ_x	ϵ_{xz}	ϵ_z	$\overline{\epsilon_{xz}}$	ϵ_y	ϵ_{yz}	ϵ_z	$\overline{\epsilon_{yz}}$
β	0.1036	0.0904	0.0737	0.0741	0.0866	0.0842	0.0724	0.0825	0.0570	0.0689	0.0670	0.0802
θ	0.2522	0.2212	0.1501	0.1805	0.2215	0.2206	0.1788	0.1991	0.1506	0.1770	0.1909	0.1960
$\epsilon' = \theta - \beta$	0.1487	0.1308	0.0762	0.1064	0.1349	0.1364	0.1064	0.1166	0.0936	0.1081	0.1220	0.1137
Rosette Using xy ϵ_{max}	13.5° to OX Ratio = 2.1				24° to OX Ratio = 1.4				0° to OZ Ratio = 1.3			
Rosette Using xy ϵ_{max}	5° to OX R = 2.0				8° to OX R = 1.3				11° to OZ R = 1.3			

TABLE 3

Three Dimension Data (Sample #2865.5)

ϵ_x	ϵ_y	ϵ_z	ϵ_{xy}	ϵ_{xz}	ϵ_{yz}	$\overline{\epsilon_{xy}}$	$\overline{\epsilon_{xz}}$	$\overline{\epsilon_{yz}}$
0.1487	0.0936	0.1220	0.1308	0.1364	0.1081	0.1064	0.1166	0.1137
0.1349	0.0762	0.1064						
(0.1418)	(0.0850)	(0.1142)						

TABLE IV
Three Dimension Solution (Sample #2865.5)

Results Using xy, yz, xz Rosettes	Ratios	Direction Cosines			Angles			Stereographic Projection	
		l	m	n	1	m	n	ϵ_{max}	
Results Using yx, yz, xz Rosettes	1.9:1.4:1	0.92	0.28	0.29	24°	71°	76°	E76°S	
		0.32	-0.10	-0.90	74°	95°	163°	dip 15°	
		0.24	-0.96	0.17	73°	161°	80°		
		Direction Cosines			Angles			ϵ_{max}	
		l	m	n	1	m	n		
	1.9:1.4:1	0.88	0.23	0.16	28°	76°	81°	E90°S	
		-0.01	0.47	-0.93	90°	62°	159°	dip 25°	
		0.47	-0.85	-0.32	62°	148°	109°		

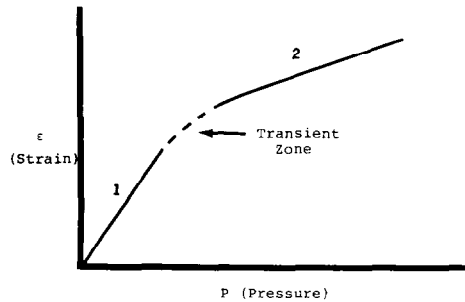


Fig. 1 - Typical strain curve.

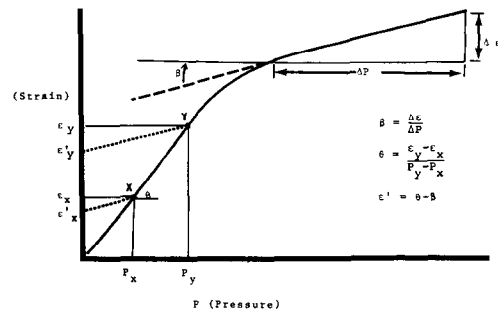


Fig. 2 - Strain curve analysis.

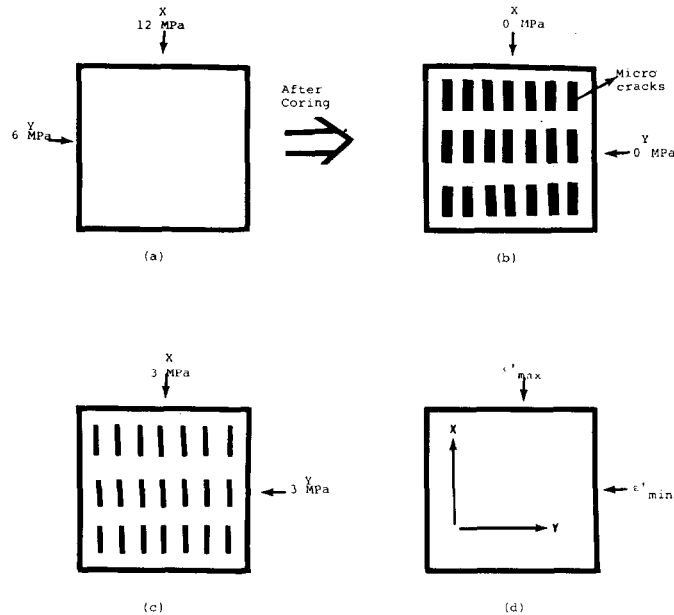


Fig. 3 - Cracks vs pressure schematic.

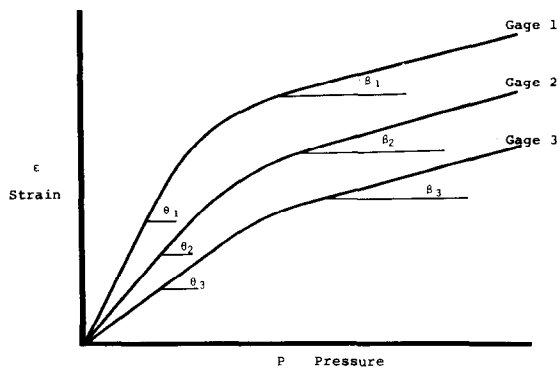


Fig. 4 - Strain gage Rosette curves.

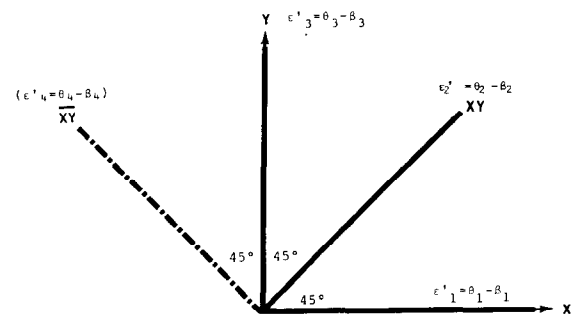


Fig. 5 - Two dimensional case.

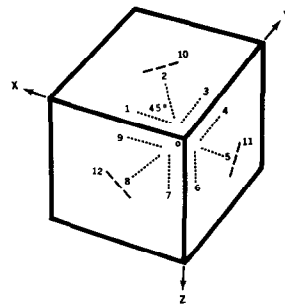


Fig. 6 - Cube gage pattern.



Fig. 7 - Field sample preparation.

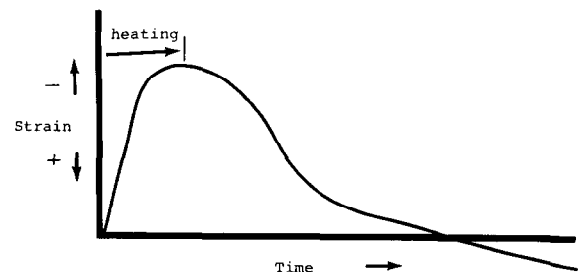


Fig. 8 - Field data plot.

EARTH STRESS RELATIONSHIPS IN THE APPLACHIAN BASIN

by Steven F. McKetta, Columbia Gas System Service Corp.

© Copyright 1980, Society of Petroleum Engineers

This paper was presented at the 1980 SPE/DOE Symposium on Unconventional Gas Recovery held in Pittsburgh, Pennsylvania, May 18-21, 1980. The material is subject to correction by the author. Permission to copy is restricted to an abstract of not more than 300 words. Write: 6200 N. Central Expwy., Dallas, Texas 75206

ABSTRACT

This paper presents a derived stress ratio which permits the identification of the extent of the regional tectonic forces acting upon a formation. Once identified, these tectonic forces allow certain inferences to be made about the maximum potential of natural fracturing present in a formation. Investigation of three gas producing formations in the Appalachian Basin shows that the Berea sandstone, the Clinton sandstone and the Devonian Shale all display a similar tectonic relationship. This leads to the conclusion that much of the Basin can be categorized into different stress regions with each region relating the degree of natural fracturing present.

INTRODUCTION

The in-situ stress field acting upon a particular formation can be defined if the three principle stresses can be calculated (Figure 1). Hubbert,¹ Kehle,² Haimson and Fairhurst,³ and others have shown that the pressures obtained during hydraulic fracturing operations can be related to the magnitude of these in-situ earth stresses. This work provides a basis whereby selected dynamic and static treatment pressures are used to determine the principal stresses acting upon an induced vertical crack.

Once determined, these principal stresses can then be used to develop a regional stress ratio (or fracturing gradient). This stress ratio, in turn, provides a means of defining the degree of natural fracturing that exists in a formation by defining the degree of tensional relief present.

CONCEPT

If the formation being hydraulically stimulated is an isotropic, elastic medium, a pressure-created vertical crack will propagate in a plane perpendicular to the minimum compressive in-situ principal stress.⁴ The pressure required to hold this vertical crack open will be a measure of the minimum horizontal stress acting normal to it. According to the solution for an elastic medium for a pressurized cylindrical cavity

proposed by Hubbert¹ and Haimson and Fairhurst,³ the entire stress field can be calculated as follows:

$$\sigma_{HMAX} = T_o + P_s - P_b - P_o \dots\dots\dots(1)$$

$$\sigma_v = \rho H \dots\dots\dots(2)$$

$$\sigma_{HMIN} = P_s \dots\dots\dots(3)$$

where σ_{HMAX} is the maximum compressive stress in the horizontal plane, σ_{HMIN} is the minimum compressive stress in the horizontal plane and σ_v is the total overburden stress. The empirically derived values acquired from the hydraulic fracturing treatment to satisfy the equations are: the breakdown pressure (P_b) obtained early in the treatment after the initiation of the induced fracture, and the instantaneous shut-in pressure (P_s), obtained immediately at the termination of treatment when pumping ceases. The tensile strength (T_o), bulk density (ρ), formation thickness (H), and pore pressure (P_o) are formation-specific properties and are readily available through standard techniques.

It should be noted that Equations (1) and (3) are valid only for instances where the fracturing fluid used does not penetrate the matrix of the formation to any significant degree. Also, Equations (1), (2), and (3) are not applicable if the vertical overburden stress (σ_v) is less than the minimum horizontal stress (σ_{HMIN}), in which case the induced fracturing will be in a horizontal direction.

DERIVATION OF STRESS RATIO

Utilizing the above concept, a stress ratio can be determined for any formation or for any region, based on pressure data from hydraulic fracturing treatments. The basic conditions under which this analysis applies are that the fracture created:

1. is essentially vertical and of constant height during propagation
2. is in a quasi-elastic formation
3. extends continuously when fluid is being pumped and stops growing when pumping stops

References and illustrations at end of paper.

4. closes quickly without significant interference from the proppant injected

The instantaneous pressure (P_g) obtained directly after the hydraulic fracturing treatment is related to the minimum horizontal stress (σ_v) by Equation (3). The overburden stress (σ_v) is determined from a density log by integrating individual densities of the overlying rock sections. A value of 1.0 p.s.i./ft. of overburden can be used as representative if density logs are not available.

When two of the three principal stresses are known, the stress ratio (SR), sometimes referred to as the fracturing gradient (FG), can be derived:

$$SR = \frac{\sigma_{HMIN}}{\sigma_v} = \frac{P_s + P_h}{D} \dots \dots \dots (4)$$

where P_h is the hydrostatic head of the fluid remaining in the treating string when pumping stops and D is the average depth of the treated formation.

Traditionally, this stress ratio has been used as a measure of the ease of inducing an hydraulic fracture in a particular formation. Its values range typically from slightly less than 0.43 psi/ft to greater than 1.0 psi/ft. Ratio values less than 0.43 psi/ft indicate the formation cannot sustain an hydraulic head of water upon it. Values equal to or greater than 1.0 imply that the overburden is being lifted and presumably a horizontal fracture is being produced. Intermediate gradient values near 0.43 indicate the formation is accepting the hydraulic fluid readily while higher values indicate less ready acceptance of the treating fluid.

For this study, the stress ratio will be viewed as a measure of the minimum horizontal stress (σ_{HMIN}) acting upon a particular formation at a certain depth. Considering the ratio as such, a comparison of the horizontal stress acting at various depths can be made to ascertain the extent of natural fracturing present.

For the case of the stress ratio to increase with an increase in depth, the minimum horizontal stress would have to increase to satisfy Equation (4). Accordingly, this increase in minimum horizontal stress with depth signifies a state of compression acting upon the formation as it deepens. On the other hand, if the ratio decreases with increasing depth, the minimum horizontal stress would have to remain the same, or decrease, signifying a state of relief (tension) as the formation deepens. In any case, this ratio becomes a relative measure of the tectonic forces acting upon a formation at a given depth. The implication is that a maximum state of relief (compared to compression) will give rise to the greatest potential for the presence of natural fractures.

A REGIONAL STRESS RELATIONSHIP

The stress ratio described by Equation (4) has been calculated from data obtained on individual fracturing treatments for three gas-bearing formations in the Appalachian Basin in the Eastern U.S. The formations investigated were the lower Mississippian Berea Sandstone, the Upper Devonian Shale, and the Middle Silurian Clinton Sandstone. Figure 2 shows the geographical locations of the wells studied in each formation. Efforts were made to obtain as wide a range of depths as possible.

Tabulation of all the individual ratios for each particular formation yielded the regional picture depicted in Figure 3 for the Berea Sandstone, in Figure 4 for the Devonian Shale, and in Figure 5 for the Clinton Sandstone. A second-order polynomial regression curve was fitted to the stress ratios and average treatment depths. The statistics associated with these relationships are shown on the respective figures.

These regional relationships clearly indicate that the three formations tell the same story. In each case there is a trend to a minimum value of the stress ratio (maximum tensional relief) toward the center of the Basin and then an increase in the ratio (compression) as the formations near the fold belt near the eastern Appalachian front (Figure 6).

The findings from this analysis accord with current plate tectonic theory which suggests that the eastern edge of the North American continent and the western edge of the African continent collided under compressional forces and subsequently pulled apart under tensional forces to their current positions.⁵ This places the Rome Trough (tensional feature) in the central portion of the Basin and the Fold Belt (compressional feature) in the eastern portion of the Basin.

APPLICATION

The similarity of the stress ratios in all three formations investigated implies there are "optimum" conditions prevailing where natural fracturing could occur to an extensive degree in each formation. The analysis of the Berea Sandstone indicates that its greatest degree of tensional relief occurs at depths of 4,000 to 4,500 feet (Figure 3). As shown in Figure 4, the greatest relief for the underlying Devonian Shale occurs at 3,500 to 4,000 feet. From Figure 5 it is difficult to assess where the Clinton Sandstone's greatest degree of relief occurs, but the trend indicates it may be beyond 6,000 feet of depth.

Given these conditions, one could devise stress maps for each formation based on its depth. These stress maps could then be used to portray the probable regions of extensive natural fracturing (regions with stress ratios near 0.4 psi/ft) and regions of a lesser degree of natural fracturing (regions with ratios near 1.0 psi/ft) throughout the Basin. The assumption here is that the accumulation of hydrocarbons will be more abundant in areas of greater natural fracturing for each formation. This assumption is currently being investigated for validity.

It should be noted that much data has been used to generate the relationships described. However, it has been concentrated in only a portion of the Appalachian Basin. As Figure 2 shows, the only data presently available for the Devonian Shale and the Berea Sandstone occurs in the Big Sandy area (eastern Kentucky and western West Virginia). It is a well known fact that glacial unloading, and hence, "unloading," occurred in much of the northern part of the Basin. Accordingly, these shallow formations could have "readjusted" to tectonics in this part of the Basin could be expected to exhibit a different stress relationship. However, it is postulated the general relationships described above will still hold but the curves presented will be shifted according to the glacial unloading.

CONCLUSIONS

This paper has demonstrated that three targeted formations in the Appalachian Basin are undergoing a similar stress phenomena which can be broadly defined by a stress ratio (fracturing gradient). In each formation studied, it is relatively easy to induce artificial fractures down to a certain depth. At deeper levels the situation is reversed and hydraulic fracturing becomes more difficult. In other words, all three formations are undergoing less horizontal stresses as they deepen under tension to a certain point; where the horizontal stresses increase again under compression.

The implications of these tensional and compressional indicators can be used as an index for natural fracturing. Maximum natural fracturing should occur in the areas of maximum tensional relief, depicted by a low fracturing gradient.

REFERENCES

1. Hubbert, M.K., and Willis, D.G., "Mechanics of Hydraulic Fracturing," Trans. A.I.M.E., Volume 210, 1957, p. 153.
2. Kehle, P.O., "Determination of Tectonic Stresses Through Analysis of Hydraulic Well Fracturing," Journal of Geophysical Research, Vol. 69, January 1964, p. 259.
3. Haimson, B., and Fairhurst, C., "In-Situ Stress Determination at Great Depth by Means of Hydraulic Fracturing," Proc. Eleventh Symposium on Rock Mechanics, University of California, June 1969, p. 559.
4. Abou-Sayed, A.S., Brechtel, C.E., and Clifton, R.J., "In Situ Stress Determination in the Devonian Shale," Report Submitted by Contract to Columbia Gas, October 1977.
5. Rodgers, J., The Tectonics of the Appalachians, N.Y. Wiley Interscience, 1970.

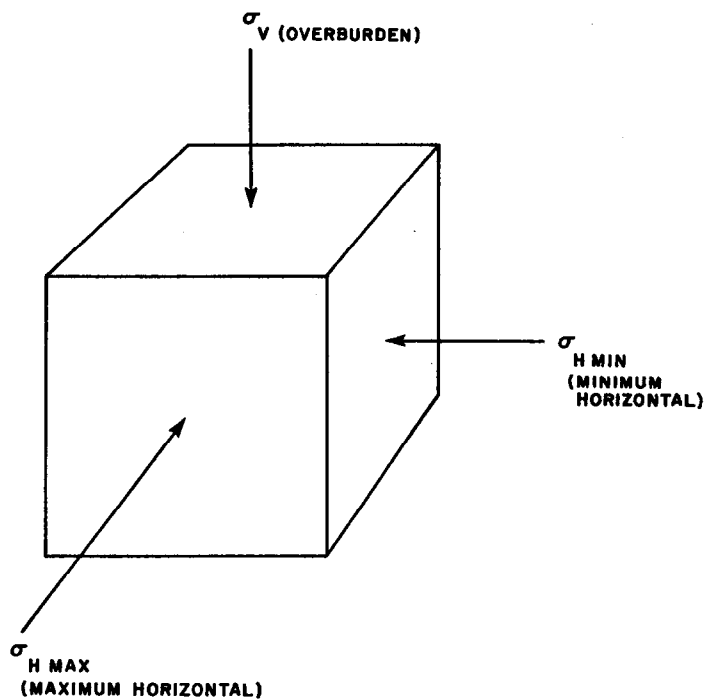


Fig. 1 - Principal earth stresses acting upon a formation.

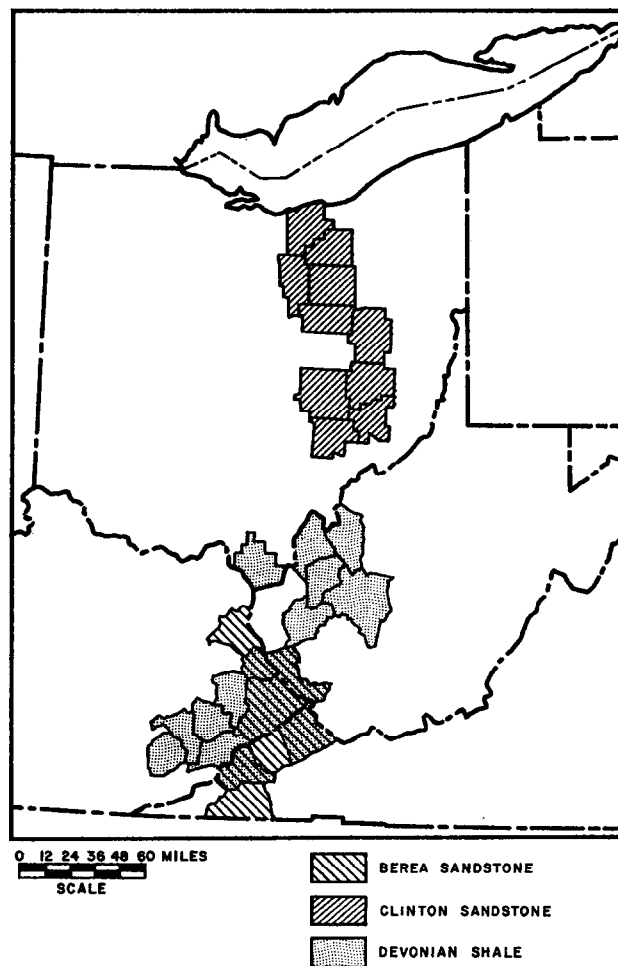


Fig. 2 - Counties investigated in this study.

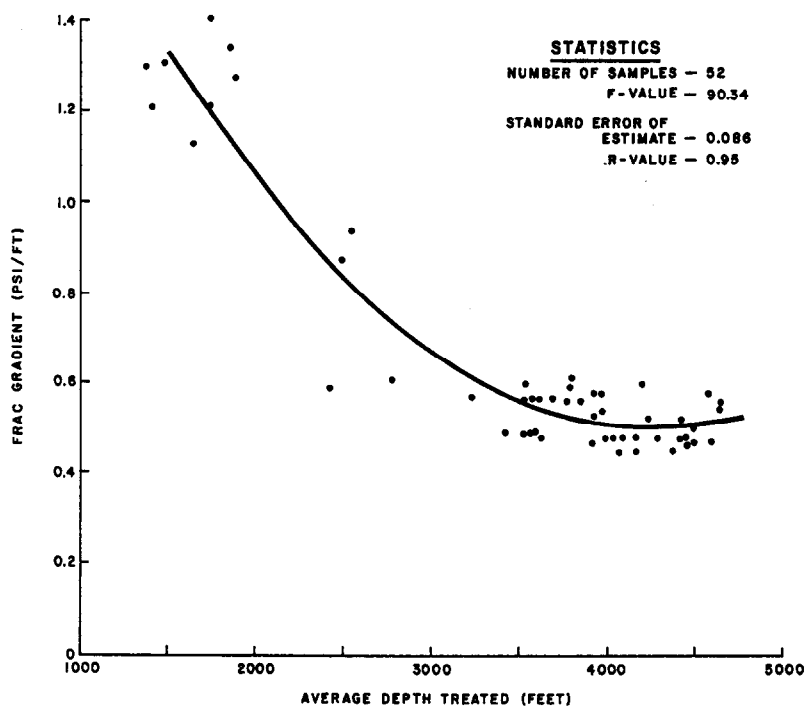


Fig. 3 - Frac gradient vs. average depth treated for Berea Sandstone.

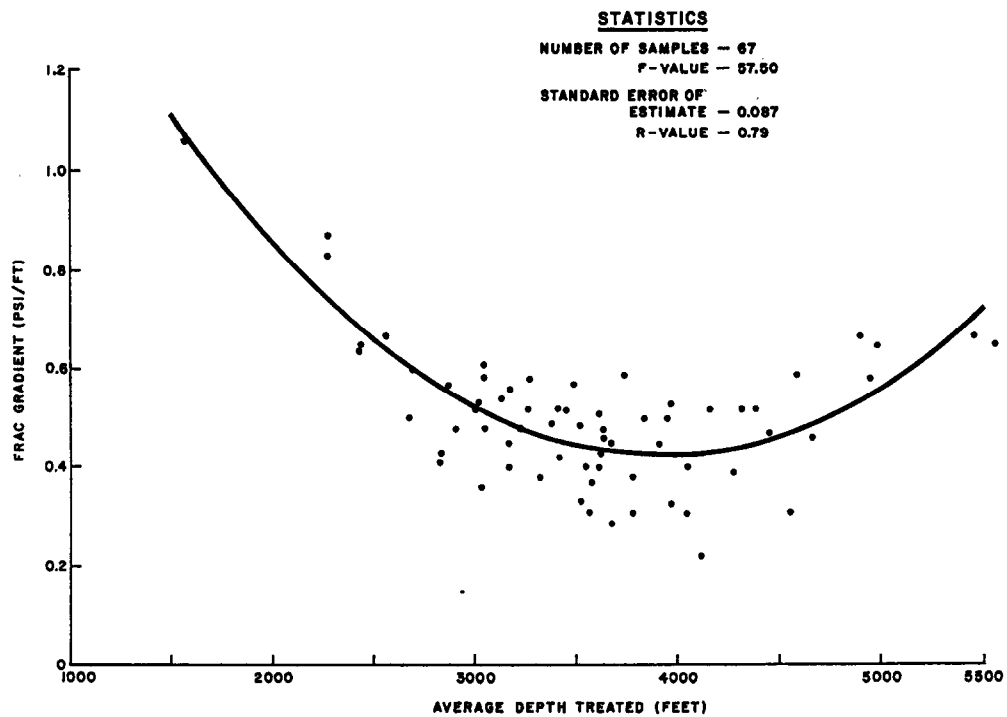


Fig. 4 - Frac gradient vs. average depth treated for Devonian Shale.

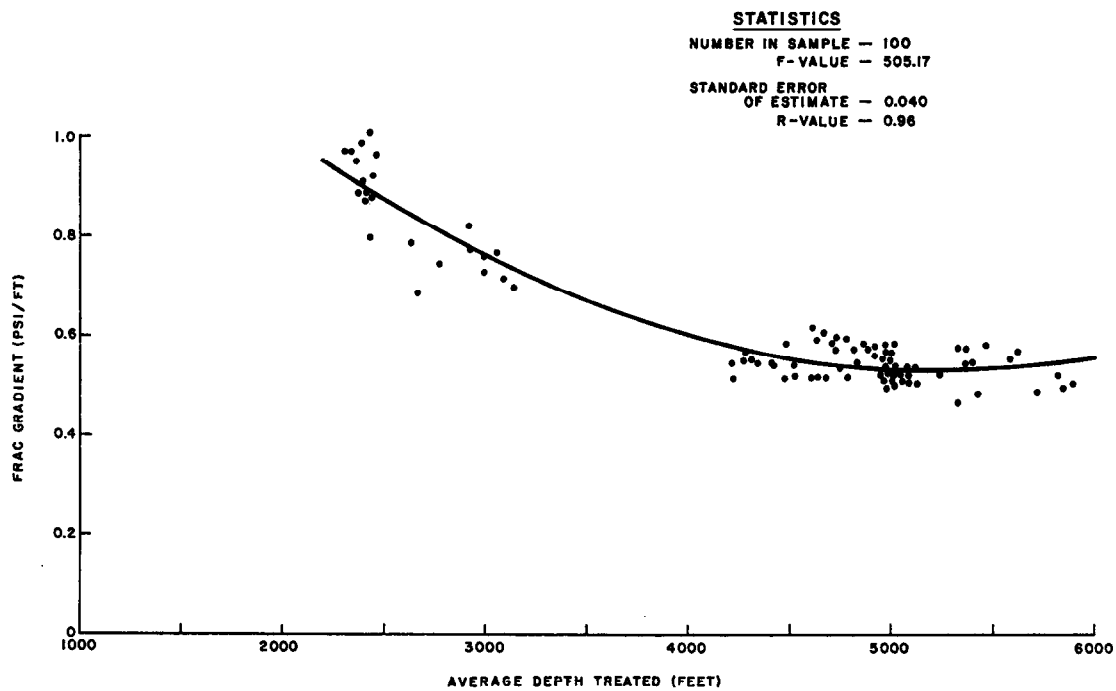


Fig. 5 - Frac gradient vs. average depth treated for Clinton Sandstone.

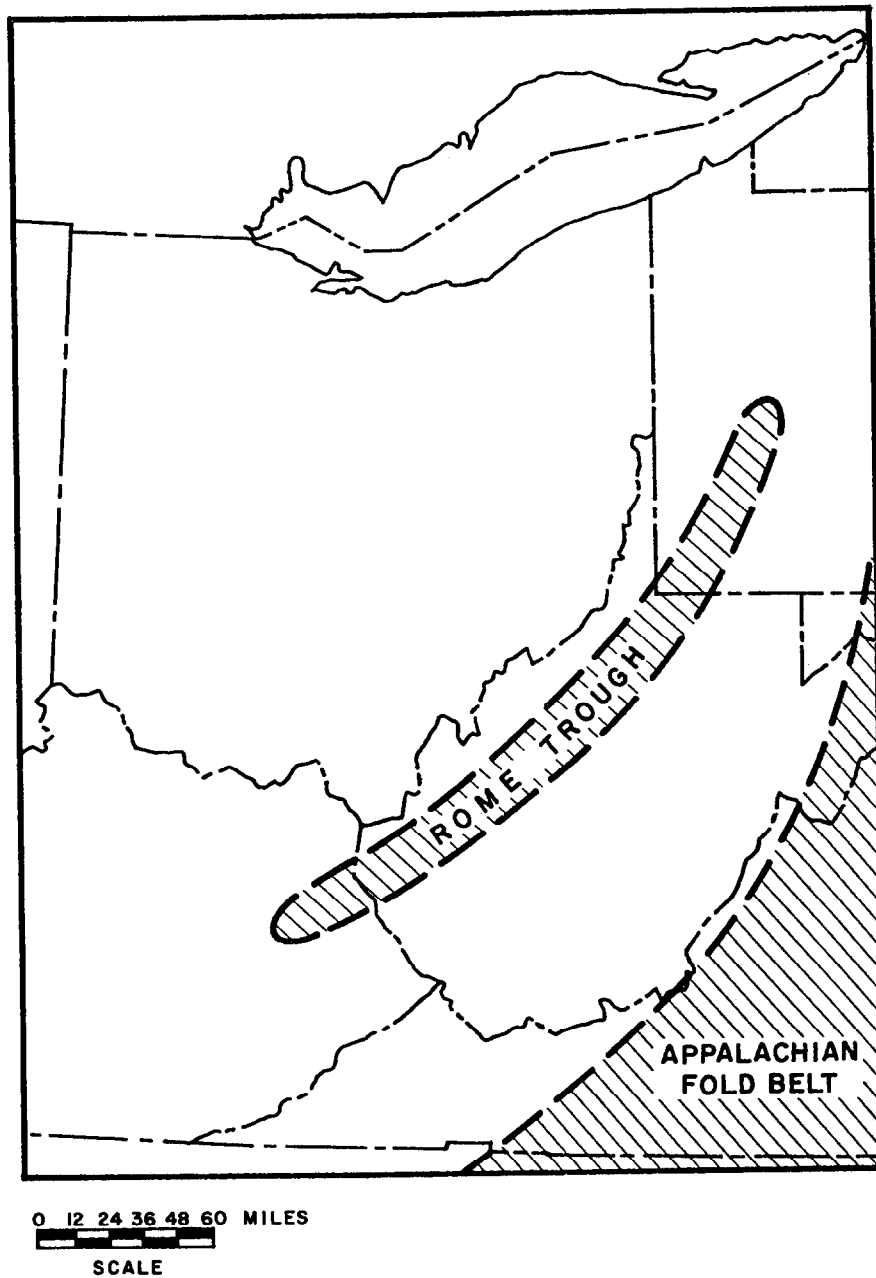


Fig. 6 - Map showing major tectonic features existing in the Appalachian Basin.

UNCONVENTIONAL EXPLORATION FOR NATURAL FRACTURES

by W. M. Hennington, Mitchell Energy & Development Corp.

This paper was presented at the 1980 SPE/DOE Symposium on Unconventional Gas Recovery held in Pittsburgh, Pennsylvania, May 18-21, 1980. The material is subject to correction by the author. Permission to copy is restricted to an abstract of not more than 300 words. Write: 6200 N. Central Expwy., Dallas, Texas 75206

ABSTRACT

This is a progress report on the evaluation of a new unconventional exploration technique for locating the natural fracture reservoirs in the Devonian - Ohio Shale. Five PHASE I tests have been drilled, cored, logged, cased and are currently being tested. Findings to date indicate that the technique has been successful in predicting the presence of natural fractures. In the six well PHASE II program, scheduled for later this year, the technique will be used to define the limits of these fracture systems. If PHASE II is successful, the project will have demonstrated that natural fracture reservoirs can be selectively located with a high degree of certainty.

INTRODUCTION

The natural fracture reservoirs in the Devonian - Ohio Shale represent one of the largest potential undeveloped sources for near future and long-term gas supply. This is a progress report on a joint venture industry/government research project which includes the U.S. Department of Energy (USDOE) and the Columbia Gas System (Columbia Gas) with Mitchell Energy Corporation (Mitchell Energy) as operator. The project is partially funded by USDOE Contract No. DE-AC21-78MC08387.

The project area is located in Gallia County, Ohio, Figure 1, and is designed to evaluate an unconventional exploration technique for economical development of Devonian - Ohio Shale gas. A series of five tests (PHASE I) were selectively located, drilled, cored, logged and are currently being tested. Additional testing and evaluation along with a six well (PHASE II) program is intended to demonstrate the cost effectiveness of the technique for immediate large-scale economical development.

The preliminary observations and opinions presented in this paper are those of the author and do not necessarily represent those of others involved in the research project.

References and illustrations at end of paper.

THEORY

The unconventional exploration theory being evaluated proposes that the location of natural fracture reservoirs is related to the depositional structure.¹ During deposition, sediment sorting results in coarser less compactible material on the depositional highs with finer more compactible muds and organic debris being washed onto the flanks and into the lows, Figure 2. Differential compaction will create "natural compaction fractures" along the flanks of the depositional highs, Figure 3.

Depositional structure can be approximated by using nearby well control to establish a relationship between present day structure and the depositional structure. This relationship can then be projected into the project area, the structure reconstructed to approximate the depositional surface and the favorable flank locations selectively located.

The basic assumptions for this project are: (1) there are tremendous undeveloped gas reserves in the Devonian shale, (2) the natural fracture reservoirs are the primary factor controlling gas movement and (3) these natural fracture reservoirs can be selectively located for more economical development of the reserves.

For purposes of evaluating approximately 1100' of Devonian - Ohio Shale in the project area, the section was divided stratigraphically into eight units and assigned alphabetical designations. Zone "A" is at the top of the shale, below the Berea Sand, and Zone "H" is at the bottom of the shale, above the Ohio Big Lime, Figure 4.

PROJECT PROGRESS

PHASE I WELL LOCATION

The project area was selected near established Devonian shale production on a favorable subsurface anomaly, Figure 5. The project area covers approximately 22,000 acres, of which about 18,000 acres are jointly held by Mitchell Energy Corporation and the Columbia Gas System.

EXPLORATION TECHNIQUE

Only a limited amount of old well data was available for this project area, so the exploration technique being investigated in this program utilized the top of the Ohio Big Lime as the critical control surface. This structural surface was used to reconstruct the depositional structure because it was thought to be the most reliable information available from old well data and spot correlation seismic. Enough data was collected to conduct a fairly detailed study of the Cottageville Field in Jackson and Mason Counties, West Virginia (15 miles east of the project area). This study, which was used as a model for the Gallia County, Ohio project study, was presented at the Third Annual Eastern Gas Shales Symposium in Morgantown, West Virginia, October 1-3, 1979.²

Using the Cottageville Field Study as a model, the approximate depositional structure of the Devonian shale in the project area was reconstructed from the present day structure on top of the Ohio Big Lime (as interpreted from the above seismic data). According to the compaction fracture theory, natural fracture reservoirs are located on the flanks of depositional highs.

SEISMIC DATA

The depositional approximation is dependent upon accurate structural interpretations, therefore, a series of 65 spot correlation seismic points were obtained to verify the present day structure.

ENVIRONMENTAL AND ARCHAEOLOGICAL APPROVALS

Environmental approval was obtained for the entire project area.

Five PHASE I locations along with alternates were made for archaeological evaluation and approval. The archaeological approvals proved to be very time consuming. Twenty-one locations were submitted in order to obtain approval for five which would test various depositional structural positions. The locations were given final approval by the Ohio Historical Preservation Officer, the USDOE Technical Project Officer and the Ohio Division of Oil & Gas.

REMOTE SENSED IMAGERY

All available remotely sensed imagery including Landsat, SLAR and Aerial Mapping Photography were analyzed and mapped. Ground truth field checks for fractures in outcrops were made. Based on this interpretation by Columbia Gas Research, predictions of fracture development were made prior to drilling the tests. Results indicated that the #1-5 Carpenter, #1-7 White-Price-Newberry Unit and #1-9 Carter should have more natural fractures than either the #1-8 Straight-Wisemandle Unit or the #1-6 McCombs.

LOCATIONS OBJECTIVES

In order to test this theory, the five PHASE I wells were located to test the various depositional structural positions, Figure 6. The #1-5 Carpenter, #1-8 Straight-Wisemandle Unit and #1-9 Carter were proposed to test the flanks of a depositional high (where natural fractures should be encountered); while the #1-7 White-Price-Newberry Unit was proposed

to test the depositional low and the #1-6 McCombs was proposed to test the depositional high (where natural fractures should be minimal). The locations may be reviewed in the "Site Selection Report" submitted to USDOE.³

DRILLING

Drilling started September 15, 1979 and all five PHASE I tests had been drilled, selectively cored, logged and cased by December 8, 1979.

PHASE I of the program was designed to prove that natural fracture reservoirs could be selectively located both by site selection and in the borehole. Every effort to acquire maximum information on the Devonian - Ohio Shale was made. The tests were drilled with fluid for mobile gas analysis of the mud system, for adequate sample cuttings every ten feet, for a special residual hydrocarbon cuttings analysis, for coring and for openhole logging.

Drilling operations were normal except for lost circulation in the "F" Zone of #1-6 McCombs at 2581' and in the "E" and "F" Zones of #1-8 Straight-Wisemandle Unit at 2523'. The lost circulation in both cases was significant enough to stop coring operations in the two tests.

A total of 5611' of Devonian - Ohio Shale was drilled, sampled, logged and selectively cored.

CORING

Oriented cores were taken in each test hole in an effort to confirm the presence, type and orientation of the natural fractures. One core in each hole was targeted to be a stratigraphically equivalent unit for evaluation of lateral variations in the shale. The other cores were targeted to evaluate the natural fracture reservoir. The core points on the first test were selected on the basis of available data from old tests in the area, Figure 4. In subsequent tests, core selections were based on the logging results obtained in the previous wells.

Our original objective was to take 1870' of oriented core in PHASE I of the research project. A total of 1525' was cored by Christensen and 1521.8' of 3" core was recovered for a recovery of 99.8%. There were a few mechanical problems and lost circulation in the #1-6 McCombs and #1-8 Straight-Wisemandle which prevented additional coring.

A total of 5611' of Devonian - Ohio Shale was penetrated in the five PHASE I tests; 1490.8' (26.6%) of the shale was cored. Preliminary analysis indicated 198.7' of primarily vertical fractures were recovered. About 13.3% of the cored section had natural fractures reported.

Some zones within the shale were originally considered to be more susceptible to natural fracturing than others as indicated on the type log, Figure 4, in the column indicated Approximate Fracture Frequency. The Approximate Fracture Frequency ranged from a low of zero (poor) to 9 (very good).

Table 1, Cored Interval and Recovery, shows the amount of section cored, the amount recovered and the fractures recovered from each test. This raw data is

somewhat deceiving for fracture evaluation since some cores were for stratigraphic rather than fracture information. In addition, #1-6 and #1-8 stopped coring due to lost circulation in the fracture reservoir.

Table 2, Core Intervals by Zones, shows the amount of core and related fractures recovered by zone from each test. The cores represent only 26.6% of the penetrated shale section, however, the better zones of fracturing are "F" and "E", as predicted.

Table 3, Cored Fractures by Zones, shows 30% of the cores from Zone "F" to be fractured. About 198.7' (13.3%) of the cored shale section had fractures. In contrast, 316.7' of core was taken from the stratigraphic Zone "B" with only 0.6' (.2%) of fractured sections indicated.

Core samples for analysis were obtained for Mitchell Energy Corporation, the Columbia Gas System, U.S.G.S., Mound Laboratories, Juniata College, and others. Table 4, Core Distribution, shows a breakdown of the distributed core samples. All remaining core was to be oriented, described, photographed and stored by Cliffs Minerals.

OPENHOLE LOGS

Electric Logs

The objectives of the open hole electric logging program were:

1. Determine what, if any, open hole log or combination of logs would best indicate the natural fracture reservoir both at the borehole and at a distance from the borehole.
2. Determine if the type of fracture, vertical or horizontal, could be detected.
3. Determine if the orientation of the fractures could be found.
4. Determine the hydrocarbon content of the shale, both fixed and mobile.
5. Evaluate the fracture reservoir potential.

Two electric logging companies, Schlumberger and Birdwell, were requested to run their best current set of logs for interpretative analysis of the fractured shale. Table 5 shows the open hole logs that were run in each hole. Test hole #1-8 Straight-Wisemandle Unit was designated the maximum information test hole for the project.

Most of the electric logs were taped for processing and re-evaluation. Logs were run to locate natural fractures that cut the borehole, were close to the borehole and fractures that might exist at a distance from the borehole but did not intersect the borehole. The data and comments presented in this paper are preliminary observations and are subject to modification as the mass of data is further evaluated and studied.

A preliminary comparison of the cored interval fractures to the Schlumberger Fracture Identification Log indications, Table 6, shows very favorable relationships. A total of 198.7' of fractured core was indicated as compared to 455.9' of log fracture indication (FIL) for the same intervals. The log shows 2.2 times more fractures than the cores. This optimism is to be expected since the comparison is between a 3" core and a 7-7/8" hole, where the area of investigation is 2.6 times greater.

Table 7 shows the preliminary evaluation of fractures from the Fracture Identification Logs by zones with the zone thickness and the percent of the shale that is indicated as fractured in each test well. The percentage of fracturing ranged from 12.8% in well #1-7 to 37.7% in well #1-8. A total of 5611' of shale was penetrated with a total of 1448' (25.8%) indicated as being fractured. Zone "F" was indicated as having the most fractures and averaged being 50.9% fractured. Zone "E" ranked second and averaged being 29% fractured.

Baroid - Mud Analysis

A Baroid mud logging unit was used on each of the five tests. Continuous monitoring of the drilling mud was recorded and plotted. Table 8, shows the average reading per foot for the stratigraphic zones for comparison.

The average gas detector reading for the Devonian-Ohio Shale in the five test wells is 21.4 units per foot. The gas detector units reported for the lower zones in the #1-6 and the #1-8 are questionable due to the lost circulation problems encountered in these two tests.

The gas detector readings from the mud system are thought to be a partial measure of the mobile hydrocarbons in the shale.

Drilling time was plotted and the lithology described on the Baroid Litholog.

Mitchell Energy - Sample Log

A detail graphic lithologic description was plotted along with drilling time, shows, textures, porosity, cores, formation tops and remarks. An effort was made to catch and preserve 10' samples from zero to total depth on the project test wells.

In addition to the normal sample log analysis, a special descriptive core record was plotted. This descriptive core record was made prior to samples being extracted for as complete a graphic record of fracture types as possible.

Mitchell Energy - Residual Hydrocarbon Analysis

An effort was made to catch a sample every 10 feet for residual hydrocarbon analysis. For this purpose, well cuttings were caught, washed, sealed in jars, labeled and transported to the laboratory for analysis.

The residual hydrocarbon analysis was accomplished by utilizing a Baroid portable cuttings analyzer, which measures total gas, wet gas (total gas minus methane and ethane) and liquid hydrocarbons. A measured quantity of cuttings and water were placed in a grinder and blended for a specific period of time. The gas released from the shale was analyzed and recorded on a continuous recording chart until the reading stabilized. These stabilized readings were plotted for a cuttings gas analysis log. The average total gas readings for each test by zone are tabulated in Table 9. The average residual hydrocarbon per foot of shale is 67.7 units. The highest average residual hydrocarbon is in Zone "H" with 111.8 units of gas per foot, followed by Zone "F" with 103.1 units. Cuttings

from test #1-8 were limited due to the extensive coring and lost circulation.

More detailed residual hydrocarbon analyses will be obtained through the cored intervals after 1" discs from each foot of core (1226 samples) have been obtained.

SEISMIC INTERPRETATION

Problems have been found with the seismic interpretation of the present day Ohio Big Lime structure. Logs run on the 5 PHASE I wells have revealed significant discrepancies between the top of the Ohio Big Lime interpreted from seismic and that actually encountered. Figure 7 represents the revised Geological - Geophysical Structure on top of the Ohio Big Lime. The structural interpretation discrepancies are as follows:

WELL NAME	DISCREPANCY	
	SEISMIC TO ACTUAL	
#1-5 Carpenter	2'	High
#1-6 McCombs	123'	High
#1-7 White-Price-Newberry	107'	Low
#1-8 Straight-Wisemandle	3'	Low
#1-9 Carter	21'	Low

Since this present day seismic based structure on top of the Ohio Big Lime is a key element in the reconstruction process, the depositional structure resulting from the exploration technique was also affected. Correcting the present day seismic structure resulted in the following revisions to the depositional interpretation and a revised Depositional Structure, Figure 8:

WELL NO.	DEPOSITIONAL DATUM		DEPOSITIONAL POSITION	
	ORIGINAL	REVISED	ORIGINAL	REVISED
#1-5	560	560	Flank	Flank
#1-6	450	565	High	Flank
#1-7	655	588	Low	Flank
#1-8	570	565	Flank	Flank
#1-9	575	565	Flank	Flank

Thus, all 5 PHASE I wells were drilled into the flank of a depositional high, where the compaction fracture theory predicts the presence of natural fracture reservoirs. Evidence collected to date from drilling, coring, sampling and logging data supports the theory, since natural fractures and gas shows were present in all 5 wells. These relationships are indicated in Figure 6.

COMPLETION PROGRESS SUMMARY

Casing (4½") was run in all five test holes and was cemented through the Devonian shale section, Table 10. Cementing problems were encountered in the #1-6 McCombs and the #1-8 Straight-Wisemandle. Both of these tests had to be squeeze cemented. These two tests also had encountered lost circulation when they were drilled.

Two zones in each well are scheduled for completions. All five tests have had cased hole logs run and have been perforated in the Lower Zone.⁴ The original intention was to perforate each zone with 21 holes, breakdown, ballout and pick the best zone for extended pre-frac testing. Stimulation was to be the

same in all five tests. The cementing problems and squeeze operations necessitated modification of the program for the #1-6 and #1-8. In these two tests, the number of perforations in the lower zone was reduced to 10 since the zone will be stimulated thru 2" tubing.

Since this is a progress report, Table 10 shows the testing status on March 11, 1980. All five tests have been perforated and three have been broken down and balled out. Two tests had shows reported after perforation. The #1-7 White-Price-Newberry Unit reported slight gas shows and the #1-9 Carter reported a slight gas blow prior to breakdown.

Three of the tests have been broken down and balled out. After treatment, the #1-5 Carpenter and the #1-7 White-Price-Newberry Unit were cleaning up with shows of gas too small to measure (TSTM). The #1-6 McCombs had just been broken down and was flowing thru the separator in the initial stage of clean up.

PERFORATION SELECTION

One of the original project objectives was to demonstrate that tests could be selectively located in areas with good natural fracture reservoirs. Another objective was to demonstrate that these natural fracture reservoirs could be identified in the borehole. Perforations for the Lower Stage I were selected on the basis of the best indications from cores and electric logs. The Schlumberger Fracture Identification Log (FIL) was the principal log used in perforation selection.

CASED HOLE LOGS

Table 11 shows the cased hole logs that have been received to date.

Another objective of this project was to run a series of cased hole logs in each test hole for maximum through casing evaluation of borehole conditions and cased hole log potential for fracture reservoir potential.

Two sets of cased hole logs are planned for evaluation of both the natural fracture reservoir and the stimulation treatment. The pre-frac set has been run in all test holes. Another set of cased hole logs will be run after stimulation to determine if the effects of stimulation can be detected.

TEMPORARY TEST LINE

Included in this project is a temporary test line system for gathering, metering and utilizing the gas produced during the extensive, long-term testing program. The 4" temporary test line and 2" well line system has been planned and surveyed. Regulations have been checked and right-of-way has been obtained along with archaeological approval. Work on the temporary test line was originally planned for late fall - early winter 1979. Extreme and unusually wet ground conditions, the resulting large backlog of work for pipeline contractors and unfavorable weather conditions were mainly responsible for the apparent high bids received for this work. In order to minimize the effects of these problems and therefore increase the possibility for substantially lowering costs, this construction work was delayed until spring 1980. Work has begun on clearing right-of-way.

PROJECTED OPERATIONS

Throughout the program, the unconventional exploration and remote sensing studies will be updated as reliable new data becomes available. The maps issued July 12, 1979 in the PHASE I Site Selection Report³ have been updated and revised for reissue.

The Stage I Lower Zone in all five PHASE I test holes should have completed breakdown, ballout, clean up and pre-stimulation evaluation.

The test hole with the best pre-stimulation show will be selected for long-term pre-stimulation testing for reservoir evaluation. The other four test holes will proceed with stimulation, clean up, post-frac logging and testing of the Stage I Lower Zone.

Mitchell Energy cuttings gas analysis should be completed along with the detailed residual hydrocarbon analyses of the core samples.

Columbia Gas core analyses should be completed for evaluation.

Core analyses by the other USDOE subcontractors should also be available for evaluation.

Evaluation of the tremendous volume of accumulated data will continue and all new potential ideas will be studied.

The PHASE I Report Draft which was originally schedule for the end of February, 1980 has been delayed and a 6 month extension has been requested. Uncontrollable delays resulting from regulations, data deficiencies, subcontractor scheduling conflicts, poor weather conditions and archaeological problems along with lost circulation zones and cementing problems have caused an estimated 5 month setback in the program as originally presented.

The six well PHASE II verification project will be slightly modified from the original proposal. One of the test holes will be drilled on the crest of a depositional high and one will be drilled in a depositional low, since the tests in PHASE I which were targeted for these positions were actually drilled on the flanks of the depositional high because of significant discrepancies in seismic interpretation. Geological, geophysical and depositional adjustments have been made.

Early approval to proceed with PHASE II, ahead of schedule, would allow the overall project to be completed more nearly on schedule.

PRELIMINARY OBSERVATIONS

This is a progress report on a new unconventional exploration technique. A very large volume of new data is being organized and evaluated. Prior to stimulation and testing, it is impossible to make positive evaluations and conclusions. However, several preliminary observations, which are subject to revision as additional data becomes available, can be made.

The five PHASE I test wells, which all appear to have been drilled on the flanks of a depositional high (Figures 8 and 6), have natural fractures as verified by 198.7' of fractured oriented core. Both near horizontal and vertical fractures were recovered.

These cored oriented fractures seem to be well indicated on the Schlumberger Fracture Identification Log, Table 6.

Both regional and local subsurface conditions effect the natural fracture development. This project demonstrates that over a short distance there can be measureable differences in natural fracture development, residual hydrocarbons and radioactivity as measured by the gamma ray logs.

It was originally predicted that certain stratigraphic zones within the Devonian - Ohio Shale were more susceptible to natural compaction fractures, Figure 4 (F.F. Column: Poor 0 to 9 Good). The second and third cores in the first test, #1-5, were targeted to core Zones "E" and "F" which were thought to have a good fracture frequency. Of the 113.8' of core recovered, 35.1' or 30.8% was fractured.

Table 3 shows that 13.3% of the core recovered from all five test holes was fractured. 30% of the cores from Zone "F" and 22% of the cores from Zone "E" were fractured.

Table 7 shows preliminary fracture identification (FIL) for all zones in the Devonian - Ohio Shale. The average for all five tests was 25.8% fractured. Zone "F" had the best fracture indications with 50.9% of the zone being fractured. Zone "E" was second with 29% of the zone being fractured.

The mobile hydrocarbon indications, Table 8, from the Baroid mud analysis generally indicates the highest average hydrocarbon reading per foot to be related to the zones with the best fractures. The test wells with the most fractures have the highest average mobile hydrocarbons with the exception of the #1-8 which had considerable lost circulation problems.

The residual hydrocarbon indications, Table 9, from Mitchell Energy's cuttings analysis are variable from well to well and zone to zone. Further study may show some unique relationships to log data and may lend considerable knowledge on hydrocarbon movement into the natural fracture system. Additional study seems to be warranted.

Table 10 shows substantial differences in the three tests that have been broken down and balled out. The breakdown pressure, initial shut-in pressure and estimated fracture gradient are quite variable. There seems to be an indirect relationship in test #1-6 between the lowest fracture gradient, lowest breakdown pressure, lowest initial shut-in pressure and the highest percentage of fracturing, Table 7. Test #1-7 has the highest breakdown pressure, highest shut-in pressure, highest fracture gradient and lowest percentage of fracturing. This relationship will be checked in tests #1-8 and #1-9 when they are broken down.

The observation has been made that current data indicates that we may be able to refine our depositional interpretation within the project area with the new control. Further evaluation and refinement will be investigated.

There is some indication that natural fractures can be detected in the borehole by electric logs. An approximation of the type of fracture, horizontal or vertical, may be possible. Some logs read further

away from the borehole and may have significant potential in locating natural fractures outside of the borehole.

CONCLUSIONS

The operations to this point in the new unconventional exploration technique to locate natural fracture reservoirs in the Devonian - Ohio Shale have been slower and more difficult than expected. With the exception of the seismic problem, which caused two of the test wells to be drilled in the wrong depositional positions, all other operations seem to have positive results and are considered successful.

To this point in the project it appears that test wells can be selectively located in areas with favorable natural fracture reservoirs. Zones favorable to natural fracturing can be selected. Certain electric logs can indicate the natural fractures. There are significant local as well as regional variations that are critical to exploration for natural fractures.

Information acquired has added significant data and a better understanding of the natural fractured reservoir in the Devonian - Ohio Shale.

Early USDOE approval of verification PHASE II would substantially accelerate the overall objective of a maximum benefit program at minimum expense for immediate large-scale economical development of the primary gas reserves from the Devonian - Ohio Shale.

NOMENCLATURE

OPEN HOLE LOGS

SCHLUMBERGER LOG ABBREVIATIONS

CNL/FDC/GR	- Compensated Neutron/Formation Density/Gamma Ray
BHC/GR	- Borehole Compensated Sonic/Gamma Ray
DIL/SFL/GR	- Dual Induction/Spherically Focused/Gamma Ray
SDLL/MLL/GR	- Simultaneous Dual Laterolog/Microlaterolog/Gamma Ray
MLL/GR	- Microlaterolog/Gamma Ray
FIL	- Fracture Identification Log
NGT/GR	- Natural Gamma Ray Spectroscopy/Gamma Ray
CMS/GR	- Circumferential Microsonic/Gamma Ray
COMP. PROC. L.	- Computer Processed Log
CORIBAND	- Coriband - Kerogen Analysis
MECH. PROP.	- Mechanical Properties
CMS LIKENESS	- Circumferential Microsonic Likeness

BIRDWELL LOG ABBREVIATIONS

DBC/NBC/GRS	- Density & Neutron Borehole Compensated
IES	- Induction
V3-D-1'	- 3-D Velocity - 1 Foot Spacing
V3-D-3'	- 3-D Velocity - 3 Foot Spacing
V3-D-6'	- 3-D Velocity - 6 Foot Spacing
COM-PRO (K&PI)	- Computer Processed Log/Kerogen & Production Index
COM-PRO (S&P)	- Computer Processed Log/Shear & Pressure Time

COM-PRO (HS&P)	- Computer Processed Log/Hydrocarbon Saturation & Porosity
ELAS. PROP.	- Elastic Properties Log
GDS/GRS	- Gamma - Guard Log

CASED HOLE LOGS

BIRDWELL LOG ABBREVIATIONS

CBL/CCL	- Cement Bond Log/Casing Collar Log
---------	-------------------------------------

SCHLUMBERGER LOG ABBREVIATIONS

HRT	- High Resolution Thermometer
TDT	- Dual Spaced Thermal Decay Time
CCL/PERF	- Casing Collar Log/Perforating Record
CBL/VDL	- Cement Bond Log/Variable Density
WAVE T.P.	- Wave Train Photos

ACKNOWLEDGEMENTS

I wish to thank Mitchell Energy Corporation for allowing participation in this research project. Also a special thanks to Herb Magley, Geological Coordinator for the project, and Dave Ashbrook, Operations Manager for the project, along with their staffs for their assistance.

REFERENCES

1. Hennington, W. M.: "Devonian - Ohio Shale Productive Potential," Third Annual University of Missouri - Rolla & Missouri Energy Council Conference on Energy, October, 1976, pages 31-39.
2. Hennington, W. M.: "Unconventional Evaluation of the Cottageville Field: Jackson and Mason Counties, West Virginia," Proceedings Third Eastern Gas Shales Symposium, October, 1979; METC/SP - 79/6, USDOE, pages 371-384.
3. "PHASE I Wellsite Selection Report." Mitchell Energy - USDOE Devonian - Ohio Shale Exploration Project, Gallia County, Ohio. USDOE Contract No. DE-AC21-78MC08387, July 12, 1979.
4. Magley, H. L.: "Technical Progress Report - March 1, 1980," Devonian - Ohio Shale Exploration Program, USDOE Contract No. DE-AC21-78MC08387.

TABLE 1
CORED INTERVAL AND RECOVERY

TEST	#1-5	#1-6	#1-7	#1-8	#1-9
CORED	170.0'	74.0'	174.0'	933.0'	174.0'
RECOVERED	169.3'	69.7'	175.5'	932.7'	174.6'
FRACTURE	36.4'	.3'	32.8'	133.4'	.7'

TABLE 2
CORE INTERVALS BY ZONES

SHALE THICKNESS	#1-5		#1-6		#1-7		#1-8		#1-9	
	RC'	CF'	RC'	CF'	RC'	CF'	RC'	CF'	RC'	CF'
BEREA							31.0	4.9		
A			14.0	0.0	29.0	0.0	101.0	4.0	16.0	0.0
B	55.6	0.6	44.2	0.0	29.2	0.0	146.0	0.0	41.7	0.0
C							80.0	1.0		
D							190.0	15.0	58.6	0.0
E	8.0	0.7					146.0	33.5		
F	105.7	35.1	11.5	0.3	117.3	31.9	238.7	74.1	4.0	0.7
G									54.3	0.0
H										
TOTAL	169.3	36.4	69.7	0.3	175.5	32.8	932.7	133.4	174.6	0.7

NOTE: RC = RECOVERED CORE; F = FRACTURE FEET.

TABLE 3
CORED FRACTURE IN SHALE BY ZONE

ZONE	CORE FT.	FRAC FT.	%
A	160.0	4.9	3
B	316.7	0.6	0
C	80.0	1.0	1
D	248.6	15.9	6
E	154.0	34.2	22
F	477.2	142.1	30
G	54.3	0.0	0
H	0.0	0.0	0
TOTAL	1490.8	198.7	13.3

TABLE 4
CORE DISTRIBUTION

ORGANIZATION	AMOUNT	INTERVAL	NO. SAMPLES
MITCHELL ENERGY (INITIALLY)	2"	5'	295
MITCHELL ENERGY (DETAILED)	2"	1'	1226
COLUMBIA GAS	6"	10'	158
U.S.G.S.			30
MOUND LAB.			30
JUNIATA COLLEGE			146
OTHERS			?
TOTAL			1885

TABLE 5
OPEN HOLE LOGS

SCHLUMBERGER	#1-5	#1-6	#1-7	#1-8	#1-9
CNL/FDC/GR	*	*	*	*	*
BHC/GR	*	*	*	*	*
DIL/SFL/GR	*	*	*	*	*
SDLL/MLL/GR	*	*	*	*	*
MLL/GR	*	*	*	*	*
FIL	*	*	*	*	*
NGT/GR	*	*	*	*	*
CMS/GR	*	*	*	*	*
COMP. PROC. L.	*	*	*	*	*
CORIBAND	*	*	*	*	*
MECH. PROP.	*	*	*	*	*
CMS LIKENESS	*	*	*	*	*

BIRDMELL	#1-5	#1-6	#1-7	#1-8	#1-9
DBC/NBC/GRS	*	*	*	*	*
IES	*	*	*	*	*
V3-D-1'	*	*	*	*	*
V3-D-3'	*	*	*	*	*
V3-D-6'	*	*	*	*	*
COM-PRO (K&P)	*	*	*	*	*
COM-PRO (S&P)	*	*	*	*	*
COM-PRO (HS&P)	*	*	*	*	*
ELAS. PROP.	*	*	*	*	*
GDS/GRS	*	*	*	*	*

BAROID	#1-5	#1-6	#1-7	#1-8	#1-9
LITHO-LOG	*	*	*	*	*
DENSITY PLOT	*	*	*	*	*

MITCHELL	#1-5	#1-6	#1-7	#1-8	#1-9
SAMPLE	*	*	*	*	*
CUTTINGS GAS	*	*	*	*	*

TABLE 6
PRELIMINARY

FRACTURE COMPARISON - CORE TO LOG (FIL)

ZONE	#1-5		#1-6		#1-7		#1-8		#1-9	
	CF'	LF'	CF'	LF'	CF'	LF'	CF'	LF'	CF'	LF'
A			0.0	0.2	0.9	0.9	4.0	4.6	0.0	2.6
B	0.6	1.8	0.0	1.6	0.0	0.0	0.0	1.1	0.0	8.0
C							1.0	2.2		
D							15.9	19.0	0.0	13.4
E	0.7						33.5	80.8		
F	35.1	58.6	0.3	11.7	31.9	55.0	74.1	183.9	0.7	0.4
G									0.0	10.1
H										
TOTALS										
CORE	36.4		0.3		32.8		128.5		0.7	
LOG		60.4		13.5		55.9		291.6		34.5

LOG 455.9' / CORE 198.7' = 2.2
HOLE 7.84" / CORE 3" = 2.61

CF = CORED FRACTURE
LF = LOG FRACTURE INDICATIONS

TABLE 7
FRACTURE IDENTIFICATION LOG DATA - BY ZONES

ZONE	#1-5		#1-6		#1-7		#1-8		#1-9		ZONE
	F. FT	% F	F. FT	% F	F. FT	% F	F. FT	% F	F. FT	% F	
A	65.0	56.0	31.0	27.7	15.9	14.6	4.6	4.6	30.3	28.1	26.9
B	6.5	4.6	7.8	5.5	1.4	1.0	1.1	0.8	45.7	32.4	8.8
C	1.2	1.5	2.5	2.8	1.2	1.4	2.2	2.8	27.8	33.9	8.4
D	10.4	5.7	10.7	6.1	5.0	2.8	19.0	10.1	53.7	30.0	10.9
E	4.0	2.9	39.7	28.8	2.9	2.2	80.8	55.4	70.4	54.6	29.0
F	117.1	48.0	159.8	66.0	88.0	38.0	183.9	75.4	61.7	26.0	50.9
G	24.9	17.5	48.5	34.2	9.4	6.8	70.3	48.2	23.3	16.8	24.9
H	6.5	7.5	21.8	24.8	16.3	19.2	69.9	75.8	4.7	5.5	27.3
TOTAL FIL	235.6'		321.8'		141.0'		431.8'		317.6'		1447.8'
% F		20.8		28.5		12.8		37.7		28.9	25.8

F. FT = FRACTURED FEET % F = PERCENT FRACTURED

TABLE 8
MOBILE HYDROCARBON - BAROID MUD ANALYSIS

ZONE	#1-5 AVE/FT	#1-6 AVE/FT	#1-7 AVE/FT	#1-8 AVE/FT	#1-9 AVE/FT	AVE/FT
A	5.1	5.5	11.0	10.1	1.3	6.5
B	5.4	10.7	10.8	11.7	5.6	12.8
C	4.0	4.7	17.0	5.9	4.9	7.3
D	4.0	5.5	50.4	10.4	17.5	17.4
E	4.9	10.4	50.9	14.0*	17.6	19.1
F	16.1	18.8*	53.7	11.2*	16.3	23.0
G	14.3	6.3*	21.8	18.8*	71.3	26.3
H	23.9	6.9*	56.7	16.4*	88.4	37.8
AVE/HC/ FT/TEST	9.8	9.8	39.1	12.4	25.5	21.4

AVERAGE MOBILE HYDROCARBON/FOOT 21.4

* QUESTIONABLE DATA DUE TO LOST CIRCULATION PROBLEMS

TABLE 9
RESIDUAL HYDROCARBONS - MEC CUTTINGS ANALYSIS

ZONE	#1-5 AVE/FT	#1-6 AVE/FT	#1-7 AVE/FT	#1-8 AVE/FT	#1-9 AVE/FT	AVE/FT
A	10.1	10.6	9.2	17.5	6.8	19.8
B	44.1	34.8	57.2	23.9	26.5	37.8
C	16.0	25.9	15.9	8.8	18.5	17.7
D	93.0	84.7	62.0	15.4*	69.3	76.3
E	56.9	134.6	84.1	40.4*	132.8	94.1
F	67.9	122.4	132.1	112.8*	89.8	103.1
G	21.3	59.7	77.5	49.5	81.3	58.1
H	84.0	124.4	104.0	49.0*	137.9	111.8
AVE/TEST	53.2	79.5	78.5	43.2*	73.4	

AVERAGE RESIDUAL HYDROCARBON/FOOT 67.7

* POOR SAMPLE VOLUMES

TABLE 10
COMPLETION SUMMARY

	#1-5	#1-6	#1-7	#1-8	#1-9
TOP CEMENT	1842'	1578'	1708'	1770'	1320'
TOTAL DEPTH	2845'	3071'	2770'	3062'	2720'
4 1/2" CASING	2843'	3056'	2756'	3055'	2711'
LOWER STAGE					
NO. PERFS.	21	10	21	10	21
INTERVAL	2322'-2565' (243')	2578'-2820' (242')	2304'-2498' (194')	2512'-2752' (240')	2231'-2446' (215')
NAT. SHOWS	0	0	SI GAS VAPORS	0	SI GAS BLOW
VOLUME (GALS.)	10,000	10,000	10,000		
BREAK DOWN P.	1,700	1,450	2,900		
ISIP	975	300	1,310		
FRAC/GRAD. (EST)	.619	.541	.760		
GAUGE	TSTM	TSTM	TSTM		
STATUS					
MARCH 11	CLEAN UP	CLEAN UP	CLEAN UP	PREP TO	WAITING TO
GAS VOL.	TSTM	FLOW TRNG SEP.	TSTM	BREAKDOWN	BREAKDOWN

TABLE 11

CASED HOLE LOGS

SCHLUMBERGER	#1-5	#1-6	#1-7	#1-8	#1-9
HRT	*	*	*	*	*
TDT	*	*	*	*	*
CCL/ PERF	*	*	*	*	*
CBL/VOL	*	*	*	*	*
WAVE T.P.	*	*	*	*	*
BIRDWELL					
CBL/CCL	*	*	*	*	*
V3-D-3'	*	*	*	*	*
V3-D-6'	*	*	*	*	*

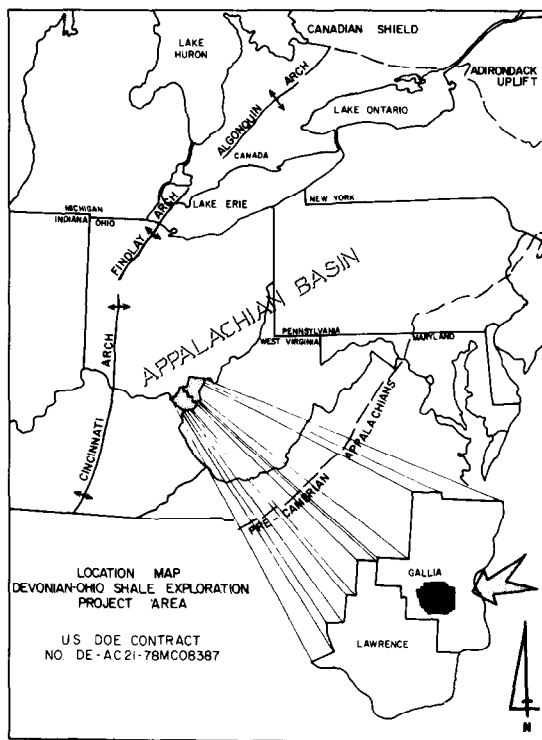


Fig. 1 - Location plat.

DEPOSITIONAL RELATIONS

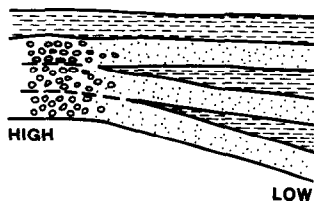


Fig. 2 - Depositional profile.

COMPACTION RELATIONS

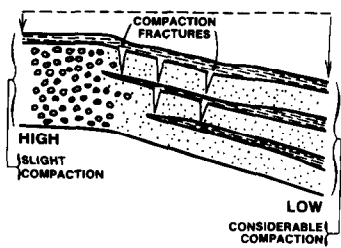


Fig. 3 - Compaction fracture profile.

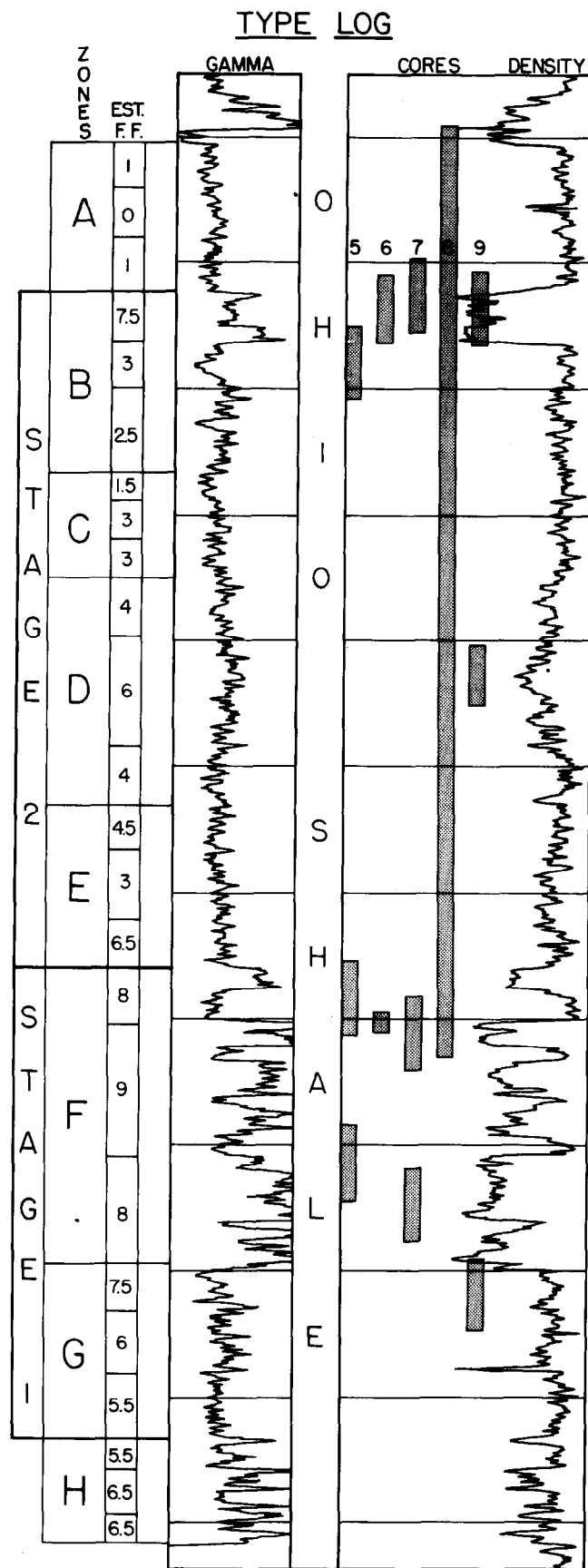


Fig. 4 - Type section.

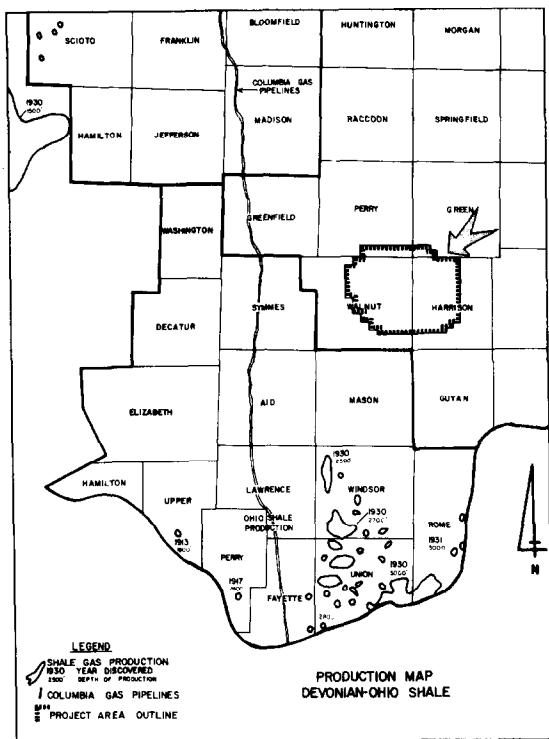
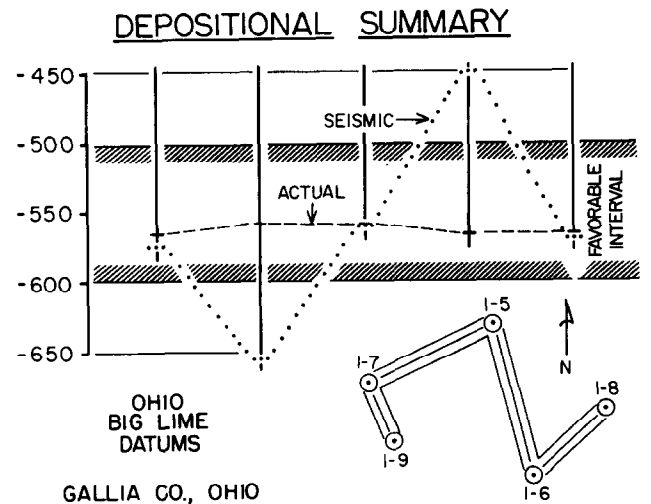
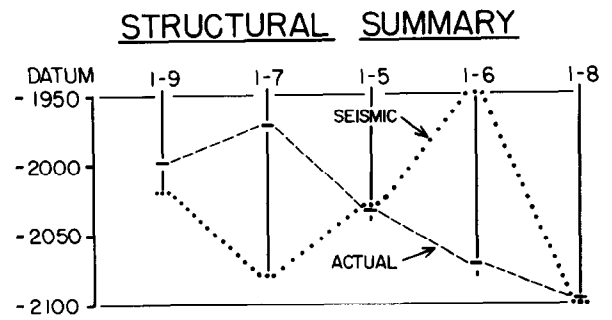


Fig. 5 - Project area.



GALLIA CO., OHIO

Fig. 6 - Depositional Relationships.

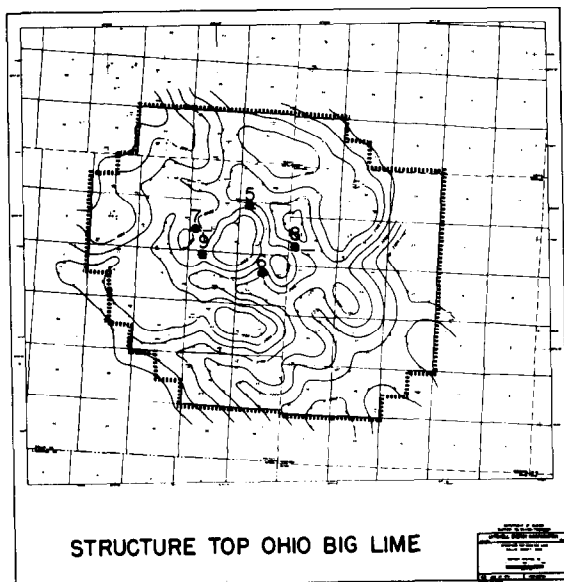


Fig. 7 - Revised structure.

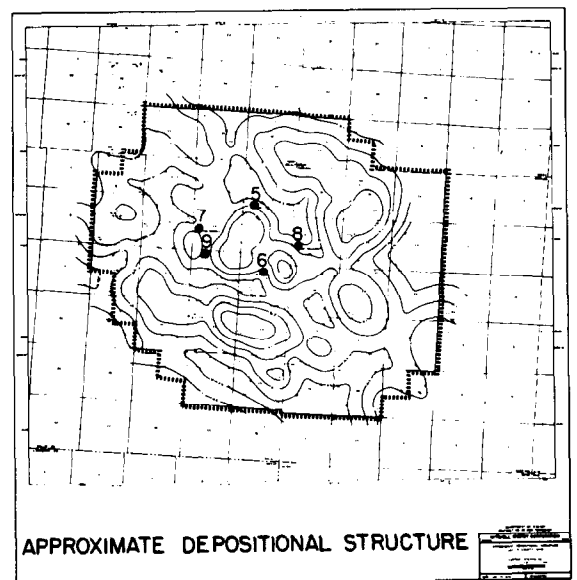


Fig. 8 - Revised depositional structure.

THE UNIQUE METHANE GAS DEPOSIT IN LAKE KIVU (CENTRAL AFRICA) - STRATIFICATION, DYNAMICS, GENESIS AND DEVELOPMENT

by Klaus Tietze, Institute for Geosciences and Natural Resources

© Copyright 1980, Society of Petroleum Engineers

This paper was presented at the 1980 SPE/DOE Symposium on Unconventional Gas Recovery held in Pittsburgh, Pennsylvania, May 18-21, 1980. The material is subject to correction by the author. Permission to copy is restricted to an abstract of not more than 300 words. Write: 6200 N. Central Expwy., Dallas, Texas 75206

ABSTRACT

Lake Kivu, situated in Central Africa, contains a scientific and economic peculiarity: $63 \cdot 10^9 \text{ m}^3$ of methane at STP are dissolved in the deep part of this lake. The gas is held in the water by a special density stratification. The lake has recently been systematically explored during a German research expedition. With help of the results of the expedition and theoretical exploitation models the basis for development of this unique methane deposit has been created.

INTRODUCTION

Lake Kivu is situated in the western branch of the East African rift zone within a volcanic landscape. It contains a methane gas deposit which is of great interest from both the scientific and economic point of view. Since the gas is physically dissolved in the water, this deposit is significantly different from usual gas fields, where gas is present within the pores of rock. In Lake Kivu, however, the gas is held in the water by a stable density stratification.

The lake consists of a main basin and four smaller basins. The latter ones are separated from the main basin by rises in the lake floor. They are Kabuno Bay and the basins near Bukavu, Ishungu and, Kalehe (see Fig.1). The total water surface is ca. 2400 km^2 , the max. water depth 485 m and the total water volume app. 580 km^3 (calc. from. top. map comp. by IRSAC¹ in 1959).

The deposit was discovered by DAMAS² in 1935. Af-

terwards some studies were carried out in the lake by SCHMITZ & KUFFERATH³ 1955, DEGENS⁴ et al. 1973 and others. The quantity of the methane in Lake Kivu was estimated then³ to app. $45 \cdot 10^9 \text{ m}^3$ at STP. However, most of the data obtained, refer to the bottom of the lake, whereas the "water and gas body" of Lake Kivu was only inadequately investigated.

The deposit could be used for energy production or for other industrial uses. In either case this resource is of first importance for the whole of this region in Central Africa.

For this reason an investigational program for their economical development was carried out due to proposals of the states Zaire and Rwanda (see TIETZE^{5, 6, 7, 8}, 1974, 1978, 1980). The objective was to study the feasibility for extraction of up to 10^9 m^3 of methane at STP each year.

NEW DATA

At the end of 1974 and beginning of 1975, a measuring campaign was carried out on Lake Kivu. Various parameters of the lake water were systematically measured in-situ at 30 locations (41 profile measurements) distributed over the entire lake (see Fig.1). Additionally 185 water and gas samples as well as 12 sediment samples were taken from profiles, which were later analysed in the laboratory (see Fig.2).

The investigations are listed in table 1. Selected data are presented in Fig.3-7 and some rounded values are given also in the paragraph "discussion".

References and illustrations at end of paper.

DISCUSSION

Because the gas body is closely connected with the stratification and dynamics of the water in the lake, it will be necessary to devote a large part of this paper on the hydrodynamics of the lake.

GAS CONTENT

In Fig.3 the depth distribution of the major components of the gases physically dissolved in the main basin are shown. The distributions of methane and carbon dioxide are distributed in the stratification in a steplike fashion, whereas the distribution of nitrogen is constant. At the deepest places of the lake, app. 0.35 m^3 of methane, 2 m^3 of carbon dioxide and 0.01 m^3 of nitrogen, all at STP, are dissolved.

The distribution of ethane, propane, and butane was also measured. The concentrations of these gases amount to only 0.03 ‰ to 1 ‰ of the methane. Their depth distribution corresponds to that of the methane⁶. Hydrogen was only found in even smaller traces.

In the separate basins Ishungu, Kalehe and Bukavu Bay the methane content is small; in the Bukavu basin no gas was found. Therefore methane recovery is only viable in the main basin.

In Fig.4 the amount of methane present in each meter water layer is plotted as function of depth. In Fig.5 the total methane quantity integrated down from the surface as function of depths is shown. The total amount of methane dissolved in the whole lake is app. $63 \cdot 10^9 \text{ m}^3$ at STP. From the newly found $18 \cdot 10^9 \text{ m}^3$, possibly about $5 \cdot 10^9 \text{ m}^3$ could be recovered additionally to the $45 \cdot 10^9 \text{ m}^3$ from the deeper water, when the optimal production method recommended at the end of this paper is used.

The total amount of the other gases dissolved in the lake are at STP: $300 \cdot 10^9 \text{ m}^3$ for carbon dioxide, $5 \cdot 10^9 \text{ m}^3$ for nitrogen, $50 \cdot 10^6 \text{ m}^3$ of ethane, $6 \cdot 10^6 \text{ m}^3$ of propane and $1.5 \cdot 10^6 \text{ m}^3$ of butane⁶.

The gases are held in the lake water by a stable density stratification described in the subsequent chapter. This prevents a so-called "turn over" of the lake which would lead to a total loss of the gas content of the water by degasification. By the stratification, additionally the eddy diffusion is weakened.

Therefore the loss of gases from the deposit, by transportation through the stratification from the deep water to the surface is limited. The loss of methane is compensated by the rate of newly formed methane in the sediment (see below).

STRATIFICATION

In Fig.6 the average of 23 profiles from the main basin, measured under comparable conditions, are shown.

Layers possessing an exceptional constancy of the measured parameters alternate with other layers with very marked variations within a small interval of depth. The former are called "mixed layers" and the latter "gradient layers". Now it is possible to classify the waters of Lake Kivu in a number of separate water layers. It consists of 7 well mixed layers and 6 gradient layers.

A normal situation exists in the lake down to a depth of 50 m. Within this range the temperature decreases with depth. The temperature gradient layer shown at 35 m depth, the metalimnion, can shift to a depth as deep as 50 m and vary in structure. The lake has epilimnion, metalimnion and hypolimnion. The water of the lake is mixed down to this depth as can be seen from the conductivity curve, which shows homogeneous conditions up to this depth. Below 50 m, however, there exist a stable stratification which remains constant except for time and place dependent fine-structure variations.

The density increases down to about 50 m due to the decrease of temperature. Below that, it increases due to increasing salt content. This is somewhat reduced since the temperature increases too.

In Fig.7 the stability (density gradient/density), together with the temperature and the conductivity gradients is shown. Because the resolution of this graph is 10 times greater than those of the previous graph, the extreme constancy of the parameter values within the mixed layers is even clearer. Here the variations are smaller than the resolution of the probe ($\pm 5 \cdot 10^{-6} \text{ g/cm}^3$ for the density, $\pm 1 \mu\text{S/cm}$ for the conductivity and $\pm 10^{-3} \text{ }^\circ\text{C}$ for the temperature). It appears that there are convective and other currents within the mixed layers which cause eddy mixing of the water to take place.

In the separate basins of Ishungu and Kalehe the behavior of the water up to the corresponding depths is similar to that in the main basin. In contrast the distribution of the physical parameters in the separate basins of Bukavu and Kabuno Bay differs from that in the main basin⁶. The water of the Bukavu basin is mixed down to the bottom at about 100 m depth. In Kabuno Bay, however, the density gradient is around 15 times greater than in the main basin. Here, the mixed surface layer reaches down to a depth of only 12 m. This is confirmed also by measurements of the tritium concentration as a function of depth.

Anaerobic conditions prevail at different depths in the various basins corresponding to the stratification (biozone = mixed layer 1); that means the biozones reaches

- 50 m in the main basin and in the Ishungu and Kalehe basins;
- 100 m (bottom) in the Bukavu basin and
- 12 m in Kabuno Bay.

EQUATION OF STATE

Using the measured distribution of the physical parameters and the method of multiple regression analysis, it was possible to calculate the equation of state for the lake water. The calculations were continued up to the 5th order, although a quadratic equation appears to be the most suitable approximation. The equation⁶ indicates the influence on density of each of the various parameters; the obvious indication is that the greatest influence is caused by the chemically dissolved materials, and in particular by the salts.

HYDROTHERMAL ACTIVITY

Measurements of δD - and $\delta^{18}O$ -values indicate that water containing light isotopes has infiltrated from the bottom of the lake or is still doing so^{6,7}. That means that Lake Kivu is still hydrothermally active. At its surface, the water shows enrichments of heavy isotopes due to evaporation fractionation. In between is a transition zone which is similar to the main density gradient layer. Despite the complicated density distribution the lake is made up of only three main layers.

Plotting the values of δD and $\delta^{18}O$ for the main basin against temperature and conductivity, these parameters of the hydrothermal waters can be estimated by extrapolation. The temperature is around 30°C and the conductivity around 10 mS/cm. This corresponds to a salt content of ca. 6 ‰. Using the flow data of the river Ruzizi, one can estimate the quantity of inflowing meteoric water to be app. 0.35 km³ per year.

The hydrothermal activity is also indicated by fine structure variations of the stratification (see below).

DYNAMICS

The physical parameter distribution measured in-situ shows in the main basin from the surface down to 50 m depth different variations due to mixing, internal waves and alterations in position and characteristics of the metalimnion.

Below 50 m depth the stratification is stable, but numerous fine structure variations were measured.

The fine structures show typical temperature and conductivity peaks. They can be interpreted as ascending waters which form layers directly below the gradient strata, which they evidently cannot penetrate due to the prevailing density conditions. The peaks vary with time and position.

Other typical variations are step like structures; these were recorded more frequently than peaks. They vary also in time and position. They are a consequence of double-diffusive convection, which takes place in a stratified water body, when heated from below. This is due to the fact, that heat diffuses 100 times faster than dissolved salt. Small convection cells are formed by this mechanism, which are turbulently mixed and have distinct gradient boundary layers⁹. For this reason, the transport of dissolved matter in comparison to molecular diffusion is considerably faster.

Because Lake Kivu is stratified, it reacts to disturbances in a unique way. Such disturbances could originate on the surface by currents and waves, caused by wind action, by temperature and pressure variations, and by evaporation and radiation. On the sea bed disturbances might be caused by the heat flux and by in-

filtration of hydrothermal waters. The lake reacts to all these natural influences

- by mixing the surface layer down to a depth of 50 m (main basin),
- by eddy currents in the various mixed layers,
- by both, double-diffusive and normal convection and
- by oscillations and internal waves in the gradient layers.

This leads to a preferential transport for substances dissolved in the deeper waters up to the surface.

RESIDENCE TIME

When normal diffusion was the only mechanism in play, the quantity of heat present below 250 m would have to be renewed every 1 000 years, the amount of salt in app. 100 000 years and the amount of gas in app. 70 000 years. With the measured data of the fine structure variations caused by the effects of eddy diffusion and double diffusive convection and by comparison with data from JANNASCH¹⁰ (1975) it can be estimated that dissolved materials remain in the deeper layers for a considerably shorter time, in the order of 200 - 400 years.

GENESIS OF THE STRATIFICATION

The stratification is caused most likely by hydrothermal waters that have been infiltrated from the bottom of the lake. At various times these waters have possessed various different temperatures and salt contents, and, while flowing into the lake, they formed layers according to the relative densities involved. The initial form of this stratification would have become modified by the double-diffusive convection phenomenon, which is caused by the flow of heat through the lake bottom.

This lead to the modification of mixed and gradient layers, and to the formation of newly mixed and additional gradient layers. At the same time the overall structure becomes rather less sharply defined due to the eddy exchange, which in its turn is mainly caused by water movements in the mixed layer 1 and by water movements of hydrothermal origin. These phenomena continue to cause modification to the stratification.

To this dynamic water layers the quantities of gases are very closely connected. They participate in all movements in the water body.

As established from the presented data the stratification of density in the lake provides both the cause and the continued existence for the methane deposit. Without the stratification the methane could not have accumulated in the deep waters of Lake Kivu.

GENESIS OF THE METHANE

The carbon dioxide in Lake Kivu is presumably of magmatic origin with admixtures of carbonatic and atmospheric carbon, whereas the nitrogen may be of atmospheric origin⁶. There is no dispute about the source of the carbon dioxide, but previously published opinions on the formation of the methane are contradictory. They are based on too little and partly too inaccurate data.

In 1955 SCHMITZ & KUFFERATH³ explained the origin of the methane by bacterial generation from the organic carbon in the sediment. In 1963, BURKE & MOLLER¹¹ assumed the source of the methane to be magmatic.

In 1973 DEUSER¹² et al. wrote that 80% of the methane was generated bacterially directly from magmatic carbon dioxide and hydrogen, and the remaining 20% from organic carbon in the sediment. They concluded this in essence from their measurements of the $\delta^{13}\text{C}$ -value -45 ‰ from some samples of Kivu methane. In 1975, STAHL¹³ concluded from these measurements, the origin of the methane might be thermocatalytic.

The new data obtained by the measurements listed in table 1 allow, to further develop some of the old concepts to a new model (TIETZE et al.¹⁴ 1980).

The conventional ^{14}C -ages of the methane samples exceed the time span of 17 000 years B.P. The organic portions of samples from the upper sediment in the main basin yielded conventional ^{14}C -ages of app. 11 000 years B.P. Analyses of the pollen in the same samples, however, yielded a "historical" age of about 1000 years. At the first view these data seem contradictory.

The mean $\delta^{13}\text{C}$ -values for the methane were measured by us to -58 ‰ and not to -45 ‰ as measured by DEUSER et al.¹² (1973). The mean $\delta^{13}\text{C}$ -value

for the organic carbon in the upper sediment is ca. -21 ‰ . This value is normal for most sediments as is $\delta^{13}\text{C} = -58\text{ ‰}$ normal for methane generated bacterially in sediments.

But if the methane is generated bacterially in the sediment, how can the high ^{14}C -age and the differing ^{14}C -ages for the methane and for the sediment be explained?

The apparent contradictions are solved when one takes into account the dynamics within the lake and the related transport processes. The following model agrees with all the observations (see Fig.8).

It can be assumed, that about $600 \cdot 10^6\text{ m}^3/\text{year}$ from the mainly magmatic carbon dioxide dissolved physically in the deep waters are transported by eddy diffusion and double-diffusive convection through the stratification into the biozone⁶. This amounts to about a third of the total quantities of carbon dioxide physically dissolved in the biozone. Apart from this, about $120 \cdot 10^6\text{ m}^3$ of methane are transported up into the biozone by the same mechanism, where it becomes oxidized to carbon dioxide and water¹⁰.

The carbon of the mainly magmatic carbon dioxide that reaches the biozone from below is rather old from the point of view of its ^{14}C age. On the other side carbon derived from carbon dioxide originating in the atmosphere, now dissolved in the waters of the biozone is of recent ^{14}C -age. Therefore it is clear that organisms present in the biozone would assimilate a mixture of both "old" and "young" carbon dioxide, such that the bodies of these organisms end up with an apparent ^{14}C -age between the two extremes.

The organisms die and built up the sediment, where methane and carbon dioxide are produced bacterially. The upper parts of the sediment contain about 70% old and 30% young carbon¹⁴.

Due to the difference between the ^{14}C -ages of the upper sediment and the methane it is assumed that the methane comes not only from the upper part of the sediment but also from deeper parts. Therefore, the ^{14}C content of the methane is not 30% modern, but only ca. 10% modern.

So the methane dissolved in Lake Kivu today contains a mixture of carbon which originated from mag-

matic, carbonatic and atmospheric carbon. Part of this just has been recycled in the lake. Important to note, that the carbon of the methane has already passed a biologic cycle.

Probably there is a small admixture of methane of thermocatalytic origin from sediments, if the higher hydrocarbons which are present within levels up to 200 ppm are generated thermocatalytically. Conceivably on the other side, they are generated bacterially. This question still remains open.

According to the model developed above, the lake is, with the exception of minor disturbances, in a quasi-stationary stage. Probably as much methane escapes through eddy diffusion and double-diffusive convection into the biozone as passes from the sediment into the water.

DEVELOPMENT OF THE DEPOSIT

The deposit, which contains around $63 \cdot 10^9\text{ m}^3$ of methane at STP, represents a value of about 15 000 million DM at present natural gas prices, and, therefore, its development would be of considerable importance for the economic development of this region in Central Africa. However, a corresponding large scale production of methane, if carried out incorrectly, could disturb or even destroy the density stratification of the lake, which is the cause for the existence of the gas deposit.

For cost reasons, the production must take place in the following way:

Deep water is pumped up, degassed and then fed back into the lake close to the production station in a controlled fashion. For the production stations the planned size will correspond to a production of $25 - 100 \cdot 10^6\text{ m}^3$ of methane per year. We have been commissioned to investigate the situation with a number of stations having a total production of up to 10^9 m^3 of methane¹⁴ at STP, which corresponds to app. $3 \cdot 10^9\text{ m}^3$ of water being pumped round each year.

To avoid the destruction of the deposit by an illconceived recovery method and to find the most favourable method of production, various different types of production methods were simulated using a digital computer¹⁴.

Three models were devised: a radial model, a three-dimensional partial model and a three-dimensional complete model encompassing the whole lake.

With the radial model the topography was not taken into account. The situation in the water around the production station was assumed to be radially symmetric. Using this model, the processes in the vicinity of the station were calculated to a maximum distance of a few kilometers away, and with high resolution. By simulating a large number of possible production variables, the optimum production method was arrived at¹⁴. Additionally a catalogue of necessary safety precautions was defined¹⁴. The results from this type of model have direct consequences for the construction and design of the production stations.

After this effort two three-dimensional partial models, which take the topography of the lake bottom into account have been computed assuming the use of this optimised production method (1 station for Rwanda and 1 station for Zaire).

Using the optimum production method outlined above, the reaction of the complete lake was calculated over a period of 5 years assuming 20 production stations and a total delivery rate of $1 \cdot 10^9 \text{ m}^3$ methane per year at STP¹⁴. The evolution of the lake up to exhaustion of the deposit after a production period of 50 years has been extrapolated¹⁴.

Up to now there is no permission to publish the optimum production method¹⁴ interpreted from the computations and measurements. But it can be said, that the degasified deep water must be mixed in the stations with surface water and then rejected horizontally back at a special depth, with predefined density and velocity.

The production must under all circumstances be monitored and controlled with help of the underwater probe and, if necessary with the existing computational models (see development plan). The production strategy will have to be changed in time due to alternating stratification conditions. Parallel to the production of the deep gascontaining waters, a new stratification must be built up in the lake.

CONCLUSIONS

Various important parameters of the lake water have been determined over the entire lake area. Their interpretation did lead to the following results:

- $18 \cdot 10^9 \text{ m}^3$ of methane at STP were newly found in the lake (total amount: $63 \cdot 10^9 \text{ m}^3$ at STP);
- the coarse and fine structure of the water stratification was established;
- the equation of state for the lake water was determined;
- the assumption of hydrothermal activity in Lake Kivu, which was deduced from sediment studies, was now confirmed by in-situ and laboratory analyses of the water. Furthermore the temperature, salt content and annual infiltration rate of the hydrothermal waters leaking through the lake bottom was assessed.

The measurements allow:

- to assess the dynamics of the lake;
- to estimate the transport rate of heat, salt and gas passing through the stratification due to exchange processes;
- to discuss the formation and the stability of the stratification, and
- to develop a model of the methane genesis.

The data presented here also serve as a basis for the development of this unique methane gas deposit. The recovery of the methane must be monitored and controlled with the help of the underwater probe system and the existing computer models, both developed especially for this project.

NOMENCLATURE

δ -values; example for carbon:

$$\delta^{13}\text{C} = \frac{R_{\text{(sample)}} - R_{\text{(standard)}}}{R_{\text{(standard)}}} \cdot 1000 \text{ ‰},$$

where R is the isotope ratio $^{13}\text{C}/^{12}\text{C}$.

ACKNOWLEDGEMENT

I would like to thank Mr. W. KROLL, Mrs. G. REHWINKEL and, Mr. P. SCHULZE for their assistance.

REFERENCES

1. IRSAC: "Topographic map of Lake Kivu" (measurements carried out by CAPART (1952,53)). - Institut pour la Recherche Scientifique en Afrique Centrale, (near) Bukavu (1959).
2. DAMAS,H.: "La stratification thermique et chimique des lacs Kivu, Edouard et Ndalager (Congo Belge)". - Verh. Int. Ver. theor. u. angew. Limnol., 8: 51 - 68 (1937).
2. SCHMITZ,D.M. & KUFFERATH,J.: "Problèmes posés par la présence de gaz dissous dans les eaux profondes du lac Kivu". - Académie Royales des Sciences Coloniales, Bulletin des séances, nouvelle série 1: 326 - 356 (1955).
4. DEGENS,E.T. , VON HERZEN,R.P. , HOW-KIN WONG , DEUSER,W.G. & JANNASCH,H.W.: "Structure, Chemistry and Biology of an East African Rift Lake". - Geol. Rdsch., 62: 245 - 277 (1973).
5. TIETZE,K.: "The Lake Kivu Methane-Problems of Extraction and their Mathematical-Physical Study". - UN-ECA, Regional Conference on Petroleum Industry and Manpower Requirements in the Field of Hydrocarbons. E/CN. 14/EP/INF/13, Tripoli 1974.
6. TIETZE,K.: "Geophysikalische Untersuchung des Kivusees und seiner ungewöhnlichen Methangaslagerstätte - Schichtung, Dynamik und Gasgehalt des Seewassers". - 149 S., 90 Abb., 5 Tab., Dissertation Universität Kiel, Kiel 1978.
7. TIETZE,K.: "Hydrothermal Activity in Lake Kivu (Central Afrika)". - Earth and Plan. Sc. Letters (1980), in preparation.
8. TIETZE,K.: "Geophysical Investigations for the Development of the Unique Methane Gas Deposit in Lake Kivu (Central Africa)." - Geologisches Jahrbuch E 20, Hannover 1980, in preparation.
9. TURNER,J.S.: "The coupled turbulent transport of salt and heat across a sharp density interface". - Int. J. Heat Mass Transfer, 8: 759 - 767 (1965).
10. JANNASCH,H.W.: "Methane oxidation in Lake Kivu (Central Africa)". - Limnology and Oceanography, 20: 860 - 864 (1975).
11. BURKE,K. & MUELLER,G.: "Dissolved Gases in East African Lakes".- Nature, 198: 568 - 569 (1963).
12. DEUSER,W.G. , DEGENS,E.T. , HARWEY,G.R. & RUBIN,M.: "Methane in Lake Kivu: New Data Bearing on Its Origin. - Science, 181: 51 - 53 (1973).
13. STAHL,W.: "Kohlenstoff-Isotopenverhältnisse von Erdgasen". - Erdöl und Kohle, 28: 188 - 191 (1975).
14. TIETZE,K. & GEYH,M. , MÖLLER,H. , SCHRÖDER,L. , STAHL,W. , WEHNER,H.: "The Genesis of the Methane in Lake Kivu (Central Africa)". - Geol. Rdsch. 69,2, (1980), in press.
15. TIETZE,K. & MAIER-REIMER,E.: "Mathematisch-physikalische Untersuchungen zur Erschließung der Methangaslagerstätte im Kivusee - Zaire/Rwanda". - 175 S., 85 Abb., 5 Tab., Bundesanstalt für Geowissenschaften und Rohstoffe, Archiv-Nr.76002, Hannover 1977, unpublished report.

TABLE 1
INVESTIGATIONS AT LAKE KIVU

measurements of	applied to
in-situ density, temperature, electrical conductivity and pressure;	lake water containing dissolved gas;
compressibility, stepwise degasification function;	water samples containing dissolved gas under in-situ pressure;
tritium concentration, $\delta^{18}\text{O}$ -values, density, chemical composition and compressibility;	degasified water samples;
gas composition and quantities;	gas from degassed water samples;
$\delta^{13}\text{C}$ -values;	methane, ethane, carbon dioxide, organic carbon in sediment;
^{14}C -age;	methane, organic carbon in sediment;
palynological and organic geochemical data.	sediment.

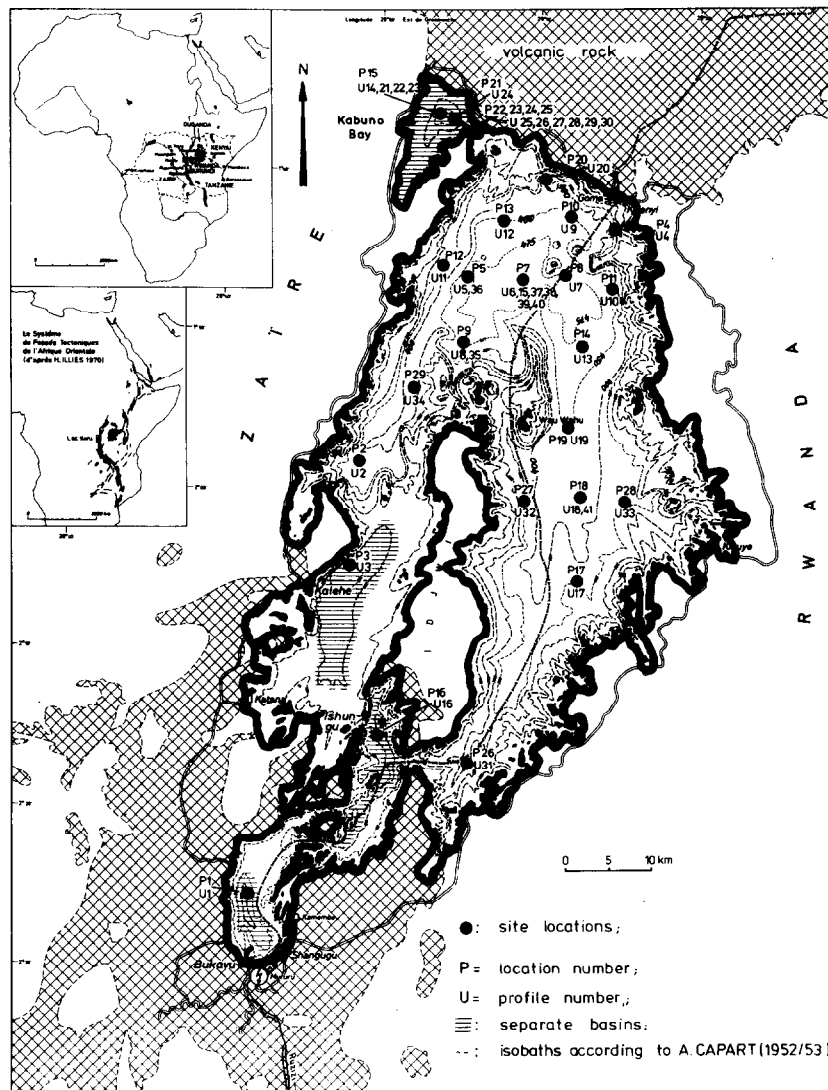


Fig. 1 : Lake Kivu with locations of sites where profiles were measured with the underwater probe from 14 November 1974 to 28 January 1975.

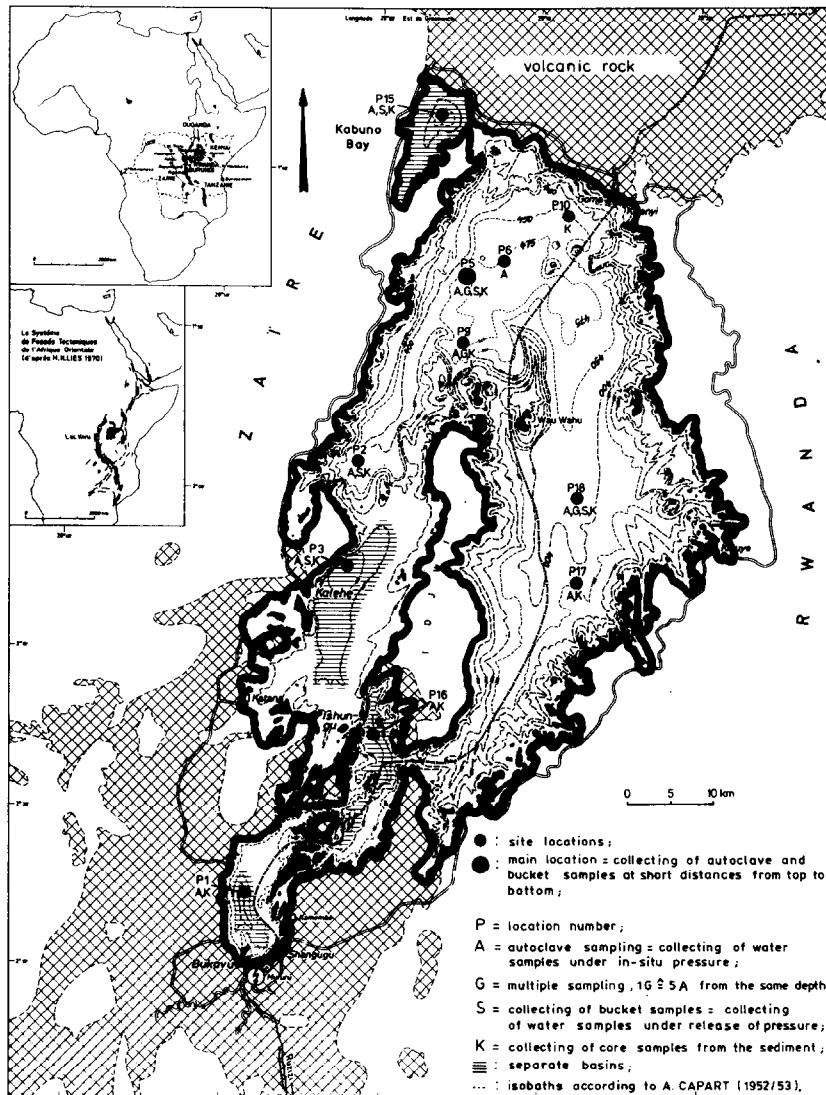


Fig. 2 : Lake Kivu with locations of sites where samples were collected from 14 November 1974 to 28 January 1975.

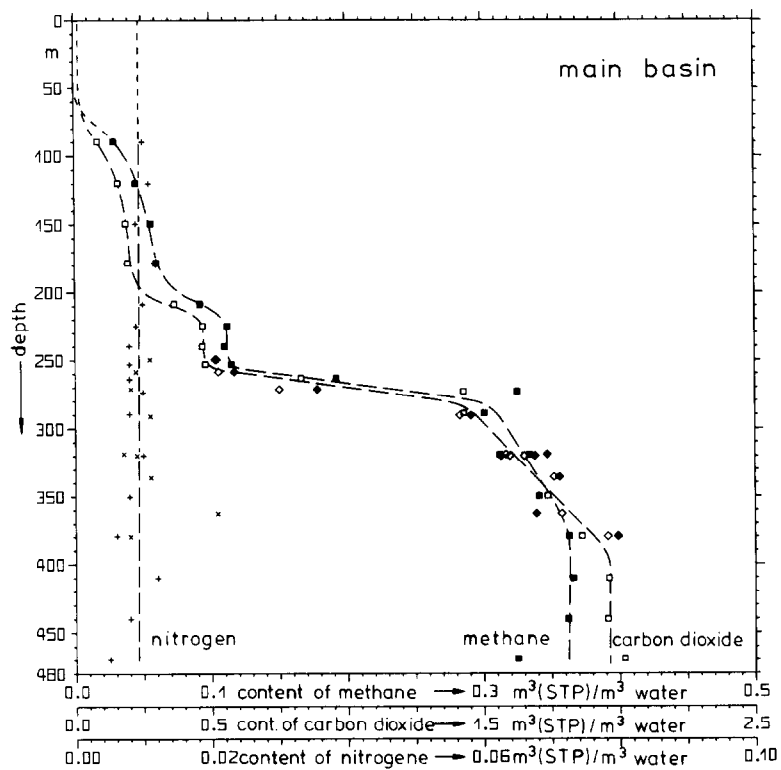


Fig. 3 : Quantities of methane [■♦], carbon dioxide [□◇], and nitrogen [××] contained in physically dissolved gas versus depth in the main basin (location 5 ■♦+, other locations ♦◇×, — — best-fit curve, — — — extrapolation of best-fit curve).

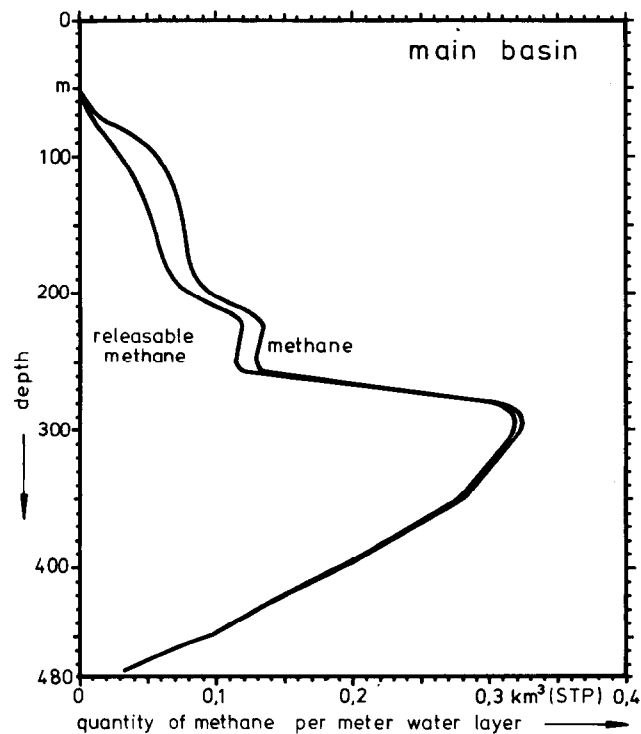


Fig. 4 : Physically dissolved and releasable (at 853 mbar and 25°C) quantity of methane per meter of water layer as a function of depth in the main basin.

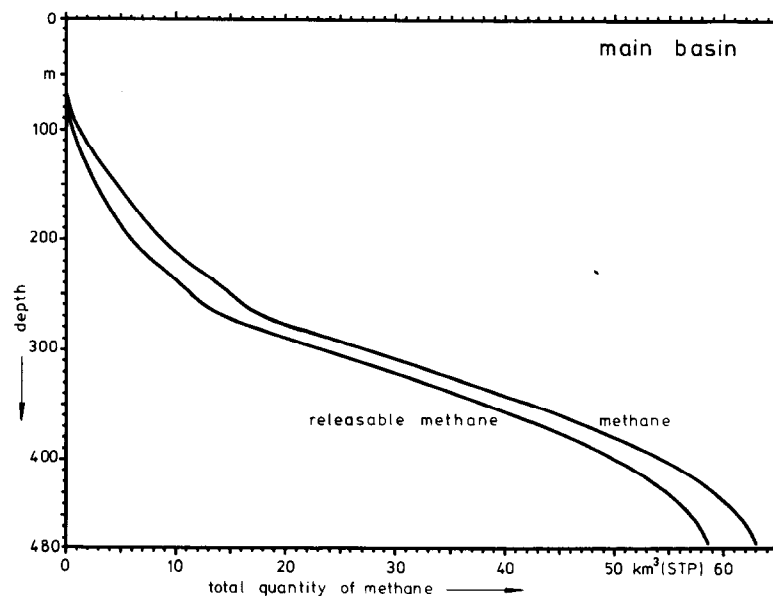


Fig. 5 : Total and releasable (at 853 mbar and 25°C) quantity of methane as a function of depth in the main basin.

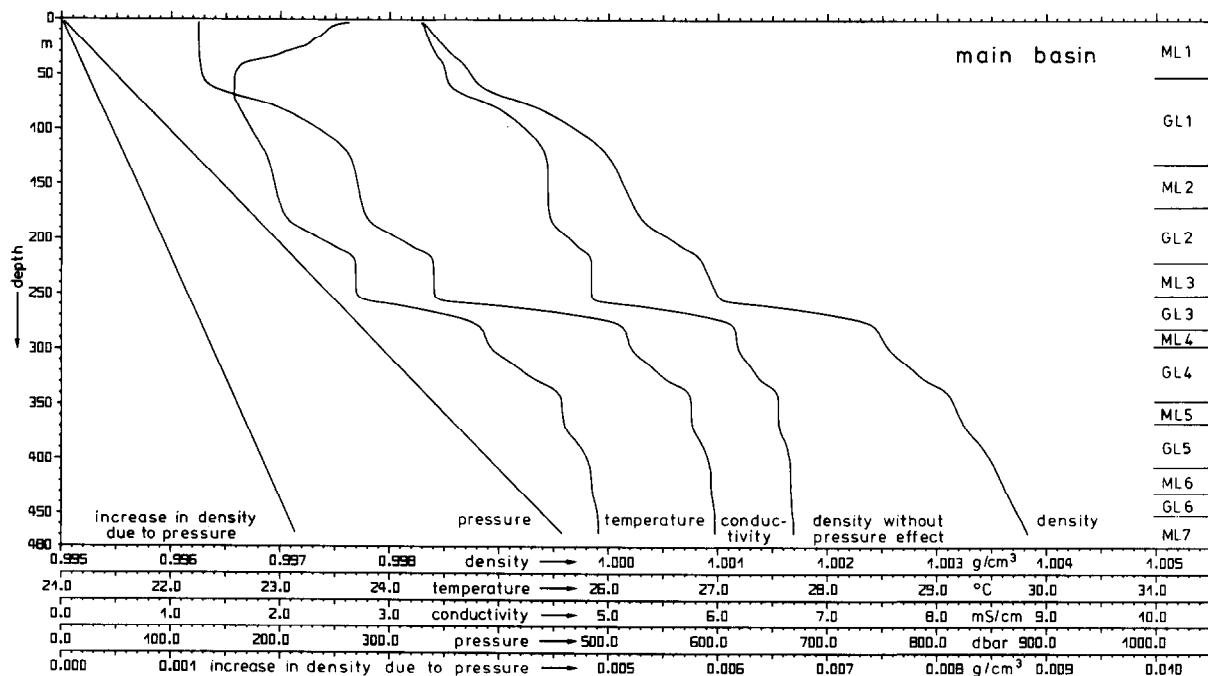


Fig. 6 : Average values of the in-situ density, temperature, conductivity, and pressure obtained from 23 vertical profiles in the main basin. Also plotted are the in-situ density minus the density increase due to pressure and the density increase due to the pressure effect alone.

ML = mixed layer, GL = gradient layer

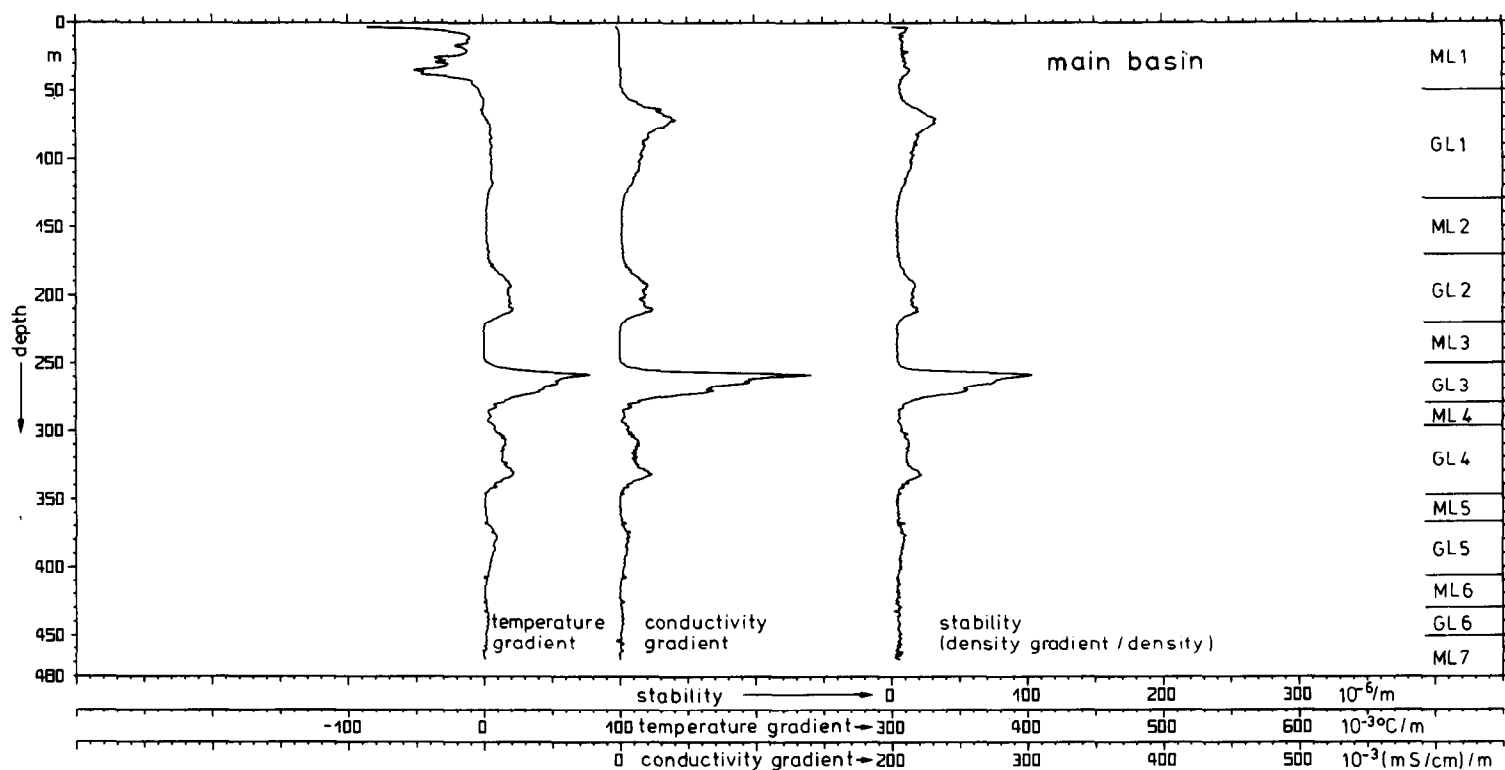


Fig.7 : Average values of the stability (density gradient / density), the temperature, and the conductivity gradient from 23 vertical profiles in the main basin. The resolution is greater than in Fig.6 by a factor of 10.

ML = mixed layer , GL = gradient layer.

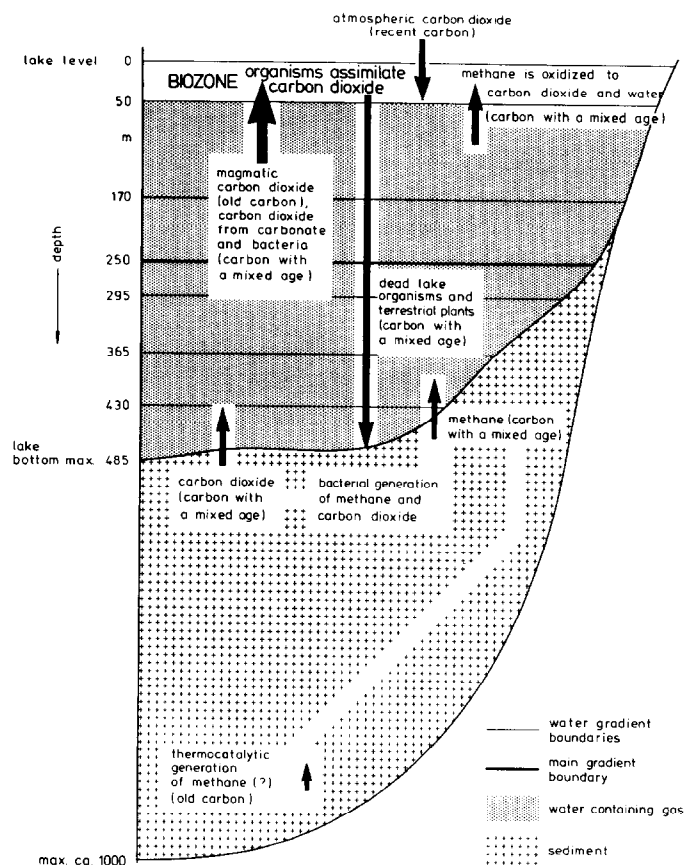
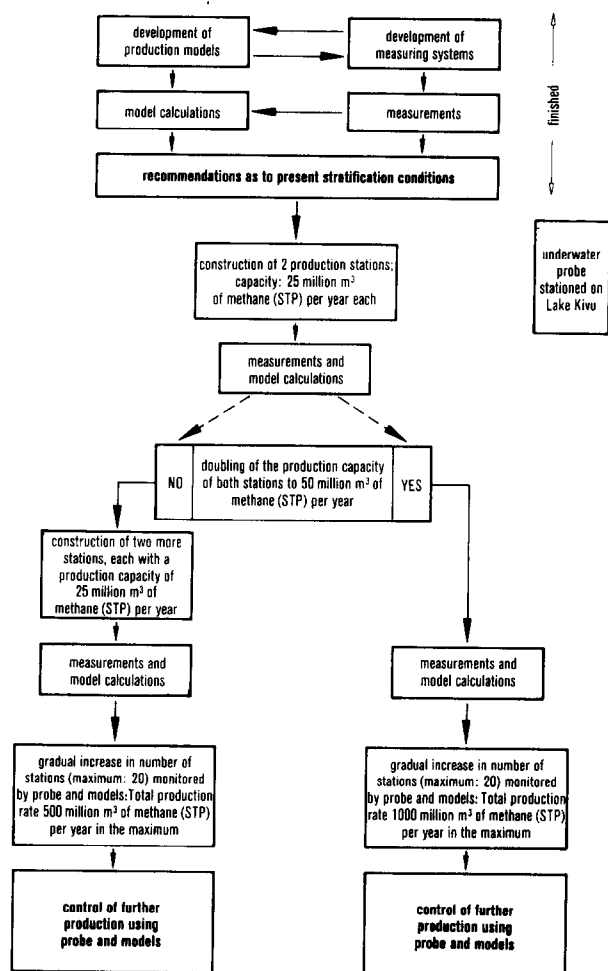


Fig.8 : Model for methane generation in Lake Kivu

Scheme for the development of the deposit



PRELIMINARY RESULTS OF THE WELLS-OF-OPPORTUNITY GEOPRESSURED-GEOTHERMAL TESTING PROGRAM

by Rayford L. McCoy, James H. Hartsock and Richard J. Dobson, Gruy Federal, Inc.

This paper was presented at the 1980 SPE/DOE Symposium on Unconventional Gas Recovery held in Pittsburgh, Pennsylvania, May 18-21, 1980. The material is subject to correction by the author. Permission to copy is restricted to an abstract of not more than 300 words. Write: 6200 N. Central Expwy., Dallas, Texas 75206

ABSTRACT

The Fairfax Foster Sutter No. 2 well located in the East Franklin area of St. Mary Parish and the Beulah Simon No. 2 well located in the Kaplan area of Vermilion Parish, Louisiana were the first successful tests of geopressured-geothermal (Geo²) aquifers under the Well of Opportunity (WOO) program. Gruy Federal assumed the Fairfax Foster Sutter operation on March 8, 1979 when the operator abandoned attempts to discover conventional hydrocarbons at a total depth of 16,340 ft. The Simon No. 2 well was acquired under similar circumstances approximately one month later at a total depth of 15,265 ft.

In both tests, the objectives were all accomplished and data were obtained which will contribute to the overall assessment of the geopressured-geothermal resource of the upper Gulf of Mexico basin. In both instances, the gas solubilities (22.8 and 24.0 scf/bbl) indicated that the waters were saturated with gas at reservoir conditions. The produced water was more saline than expected (190,000 mg/l in one instance, 104,000 mg/l in the other). {The high concentrations of dissolved solids in these waters created a scaling problem that required significant attention and will have to be addressed in future tests.¹}

TEST OBJECTIVES

The Well of Opportunity program was intended to take advantage of non-productive oil and/or gas wells for geothermal-geopressured testing at a much lower cost than the alternative of drilling a well. Utilization of the Geo² resource requires a reasonably extensive reservoir with petrophysical properties capable of sustaining production at high rates (40,000 bbl/day).² The test objectives for the WOO wells were essentially as follows:

- 1) Determine the reservoir geometry and extent.
- 2) Assess the petrophysical properties of the Geo² test horizon, in particular permeability, porosity and formation damage resulting from the drilling and completion operations.
- 3) Obtain chemical analyses of the gas and brine produced. Since the solution gas is expected

to comprise a significant portion of the resource, measurements of the solubility of the gas in the brines was deemed essential.³ The constituents and caloric value of the dissolved gas, as well as the thermal content of the brine was also of interest.

- 4) Assess the disposal problems to be expected in the development of the resource. The range of potential problems varied from fluid incompatibility to aquifer charging.⁴

GEOGRAPHY AND GEOLOGY⁵

This general area occupies a portion of the Gulf Coast geosyncline, a large arcuate depositional geosyncline extending from Florida westward to Mexico (Figure 1).

Sediments of recent to Cretaceous age have been encountered as well as diapiric salt of Jurassic age. The Tertiary, from which most oil and gas is produced, consists almost exclusively of a regressive sequence of sands and shales. Oil and gas accumulations are found most often in sand reservoirs deposited in an inner to middle neritic environment, ranging in age from Miocene to Oligocene.

The area is a south dipping monocline with regional dips of about 150 feet per mile at 10,000 to 12,000 ft. Interruptions of this dip are caused either through vertical uplift by flowage (salt or shale), by gravity slumping along normal faults, by differential compaction between sand and shale bodies, or by a combination of the three.

Salt domes are formed by the movement of salt from its "mother" layer, the Louann Salt, which underlies the area at an estimated depth of at least 40,000 feet. Shale also acts diapirically, and many salt domes are complicated by shale flowage. Faulting associated with salt domes is generally complex. On piercement domes in which the salt has intruded most of the sediments, radial faulting predominates. On deep seated domes, "graben" faulting is a more common feature.

References and illustrations at end of paper.

PRELIMINARY RESULTS OF THE WELLS OF OPPORTUNITY
GEOPRESSURED GEOTHERMAL TESTING PROGRAM

Faults also originate in response to depositional sedimentary loading. These faults are generally developed regionally and are characterized by an expanded sedimentary section in the downthrown block. These are commonly referred to as "growth" or "contemporary" faults.

All faults in the area are normal faults with dips ranging between 30° and 70°, steeper at shallow depth and tending to flatten with increasing depth. Most faults encountered at production depths have a dip of 45° to 55° with displacement on many growth faults exceeding 3000 ft.

Fairfax-Foster-Sutter - St. Mary Parish

This well was tested in the Marginulina ascensionensis (MA) 6 zone of lower Miocene age. The MA section has been differentiated through the MA-6 in the Franklin area, but in the Garden City field five miles south it is further differentiated through the MA-12, where gas production is established. The aquifer tested is a domal structure, bounded to the north by a large regional fault and to the south by a relief fault. In addition, it is separated from the Garden City area by an extensive saddle⁶ (Figure 2).

Beulah Simon No. 2, Vermilion Parish

This test site is in the Cossinade area in the synclinal area between the Abbeyville field to the southeast, the Leroy field to the east, the Perry Point and Leleux fields to the north, the Gueydon field to the west and Kaplan field to the southwest.

The tested aquifer consists of a thick development of Camerina "A" sand of upper Frio age. This was the first significant sand development below a thick Discorbis-Marginulina shale section.

Figure 3 is a structural interpretation at the top of the Camerina "A" sand. This interpretation is based on limited deep well control and seismic interpretation made available by the original operator.

PETROPHYSICS

Data were limited on both test wells because of the lack of appropriate well logs. Core data were unavailable and consequently effective porosity, fluid salinity, and net thickness were calculated from well log data.

The Fairfax Foster Sutter No. 2 well was tested in a zone (15,781-15,878 feet) consisting of 58 net feet of sand with a mean effective porosity of 19.3 percent (Figure 4). The porosity was computed with crossplot techniques utilizing compensated density and neutron data. Fluid salinities were calculated by the Rwa and SP methods and indicated 84,200 mg/l and 92,800 mg/l respectively.⁷ The chemical analysis of the produced brines were approximately twice that anticipated, suggesting a "dual water" model with bound fluids of lower salinity would be more appropriate for analytical purposes.

The observed temperature for this aquifer was 270°F (132°C) and the measured pressure gradient was 0.77 psi/ft.

The disposal section selected was encountered from 3609 feet to 3669 feet and had a mean sonic porosity of 33.7 percent (corrected for shale and compac-

tion).

The log data for the tested interval in the Simon well was limited to an ISF-Sonic analysis and correlation with offset well data. The gross section was encountered from 14,254 feet to 14,762 feet (Figure 5). The net sand thickness in the lower (tested) interval was 186 net feet which had an average porosity of 18.7 percent. The static bottomhole pressure at 14,722 feet was 13,015 psia or .884 psi/ft. and the bottomhole temperature was 266°F (130°C).

The disposal section was perforated from 2600 feet to 2660 feet in an unconsolidated sand body with a mean porosity of 41 percent.

TESTING EQUIPMENT

Fairfax Foster Sutter No. 2

The surface testing facilities were designed to accommodate hot brines at rates of up to 10,000 bbl/day and temperatures as high as 350°F (177°C). A generalized schematic of the surface equipment is shown in Figure 6. The surface equipment was constructed for operating pressures up to 500 psi.

Gas-water separation was accomplished in a conventional three phase 42 inch x 10 feet horizontal separator in which the standard 2 inch dump valves were replaced with 3 inch valves. Although operating pressures never exceeded 280 psi, the vessel was rated to 1440 psi. The fluid retention time was approximately 30 seconds at the maximum design throughput of 10,000 bbls/day.

Liquid volumes were metered by two 10,000 bbl/day HOWCO turbine meters with digital readout capability. A 100 bbl calibration tank was provided in order to periodically calibrate each meter. Gas production was measured using a three inch, flange type orifice meter with a 1/2 inch plate and BartonTM recorder.

A fan-type air-cooled heat exchanger capable of transferring heat at a rate of 23,000,000 Btu/hr. was installed in the system. This was considered necessary to prevent flashing of the liquid while using the calibration tank as well as to cool the fluids, if necessary, prior to injection.

Prior to disposal the produced brine was filtered through a dual tower, replaceable cartridge filter rated to retain 75 micron particulates.

Injection pumps were diesel driven centrifugal models capable of delivering 10,000 bbl/day at a pressure of 125 psi above suction pressure. They were intended for injecting brine into the disposal well and transferring water from the calibration tank to the disposal well.

A 10,000 psi deadweight pressure gauge was installed at the wellhead and a continuous pressure recorder was attached to the injection well.

Early in the test the build-up of scale in most of the surface equipment became excessive and a scale inhibitor (NTC-S621TM, a phosphonate compound) was injected into the system upstream from the positive choke at an average rate of ten gallons per day. This treatment was successful in preventing additional scale buildup but did not eliminate the scale already deposited.

The injection well took fluid at pressures equal to or less than the output pressure of the filters and the booster pumps were never required for injection.

Beulah Simon No. 2

The surface test facilities were essentially the same as for the Sutter operation. The most significant variations were:

1. The cooler although present, was never utilized to cool the brine prior to injection, i.e. the system pressure was maintained above the vapor pressure of the water at that temperature.
2. An additional 10,000 psi deadweight pressure gauge was installed at the wellhead to record the annular pressure.
3. The separator was operated at approximately 500 psi.
4. The dual tower cartridge filters were replaced by HalliburtonTM filters of similar design, but rated a higher pressure.

The completion of this well was different in that the tubing was hung without a packer so that an inhibited fluid could be injected down the annulus and commingled with the produced fluids. This technique controlled the scale and permitted the recording of the static annular pressures during flow periods.

The disposal operation presented some difficulty as a result of the unconsolidated nature of the aquifer selected. The disposal well sanded off initially but after an extensive nitrogen foam lift with a coiled tubing unit, the problem was corrected and the surface injection pressure never exceeded 150 psi.

TESTING PROCEDURE

The test procedure for the Sutter well included several preliminary flow periods to clean the well, test the surface facilities, and evaluate the injectivity potential of the disposal well. Following these preliminary tests, a sequence of flow and buildup tests was made to evaluate the reservoir parameters and flow characteristics of the well. The tests included a 3-day drawdown followed by a 6.5-day buildup, an 11-day drawdown, and finally a 19.8-day buildup. Figure 7 is a representation of the test history of the well showing the pressure and production behavior during the clean-up and test periods. The bottom-hole pressures during the longest flow period and buildup were recorded using a Hewlett PackardTM surface recording gauge.

In an attempt to expediate operations, the test of the Beulah Simon well consisted of a 10-day drawdown followed by a 20-day buildup. Figure 8 presents a graphic history of the testing operation. Bottom-hole pressures were not recorded during the drawdown period and therefore, only surface tubing and annular casing pressures were available for analyses. Bottom-hole flowing pressures were, however, calculated from annular casing pressures.

ANALYSES OF DATA

Sutter No. 2

The variable flow rates during the early tests, the variable rates during the 3-day and 11-day flow tests (approximately 5,000 to 8,000 bbl/day) and the failure of the reservoir to reach static pressure during any shut-in period indicated that multiple rate analyses would be necessary to interpret the data properly.⁸

The results of the conventional superposition solution were then compared to the computed pressure/time output of several analytical models of reservoir geometry.⁹ The history match obtained indicated the interpretations of the various drawdown and buildup data were consistent with the earlier interpretations of the geology. Table 1 is a summary of the significant findings of the reservoir analyses. The permeability was indicated to be approximately 14.5 md and the skin effects indicated to be -1.97. The calculated distances to the parallel linear barriers were 839 and 931 feet. This agrees very well with geological data filed in unitization proceedings (Docket No. 79-298) with the Louisiana Department of Conservation.

The chemical analyses of the brines are shown in Table 2. These waters were characterized by large concentrations of total dissolved solids. Moreover the concentrations of CaCO_3 and MgCO_3 are high enough to cause significant scaling unless inhibited, preferably downhole. The concentration of materials other than sodium chloride and the carbonates are not as consequential.

The composition of the dissolved gas from the two wells is given in Table 3. In both cases the gas is predominately methane with nearly eight percent carbon dioxide. The presence of the CO_2 reduces the BTU content of the gas to below 1000 BTU/SCF.

Simon No. 2

The flow rate history during the 10-day flow period is depicted in Figure 8. The average flow rate was 11,000 ddb/day and the total change in flow rate during the test period was only about 5 percent. This variation was not large enough to warrant the more complex superposition technique and a constant rate solution was utilized. The results of the analyses are presented in Table 1. The permeability was indicated to be approximately 12 md, while the distance to the linear barriers was indicated to be 556 feet and 731 feet (from the analytical model). The skin effect was not calculated because the bottomhole flowing pressure at the time of shut-in was uncertain. (The thermal effects on the fluid density could only be approximated until the fluid column achieved some thermal equilibrium).

Fluid and gas analyses are presented in Table 2 and Table 3. Although the static pressure in this well is 1000 psi higher and the salinity only 50 percent of the Sutter, the gas solubility (24 cubic feet per barrel) was only slightly higher. Recombination studies of the separator samples indicate that the water is saturated with gas at reservoir conditions.

PRELIMINARY RESULTS OF THE WELLS OF OPPORTUNITY
GEOPRESSURED GEOTHERMAL TESTING PROGRAM

CONCLUSIONS

1. In both test operations scale buildup was potentially a serious problem. In future wells a subsurface scale inhibitor system will be required to protect downhole equipment and tubulars.
2. Disposal of large quantities of relatively saline Geo² fluids is not a significant problem, provided a competent disposal aquifer is selected and the disposal well is properly completed and cleaned.
3. It is not necessary to cool Geo² fluids prior to disposal. The hot brines do not appear to affect the clays in the disposal sands adversely. Because of reduced density, hot brines require slightly greater surface injection pressure than do cooled brines.
4. In both tests, multiple linear barriers were encountered less than 1,000 feet from the wellbore. In neither case, however, did the pressure data suggest that all the aquifer boundaries had been reached.
5. The results of the recombination studies of separator gas and water indicate that the waters are saturated with gas. Laboratory measured bubble-point pressures in both cases were within 700 psi of static aquifer pressure.
6. The chemical analyses were consistent throughout the individual tests. The two brines were, however, vastly different in their salinities. Carbonates formation poses the most significant problems when handling these fluids. In both cases the gas was primarily methane with approximately eight percent CO₂ resulting in B.T.U. contents less than 1000 BTU/SCF on both tests.
7. The effective permeabilities in both tests were approximately 15 md. It appears that "skin effect" was not a problem on either of these wells, possibly due to the completion and clean up techniques used.
8. The Hewlett PackardTM downhole quartz crystal gauge does provide excellent data for reser-

voir analyses. The utilization of this device is, however, not without significant risk. For these reasons, the wireline methods and equipment used should be planned carefully.

ACKNOWLEDGEMENTS

The Authors wish to thank Mr. H. J. Gruy and the Department of Energy for their permission to use and publish the data in this paper. We also acknowledge the Gruy Staff for their assistance in the preparation of the manuscript and exhibits.

REFERENCES

1. "Corrosion and Scale-Formation Properties of Geothermal Waters From The Northern Gulf of Mexico Basin," Kharaka, Y.K. et al SPE 7866 presented at SPE Symposium, January 22-24, 1979, Houston
2. "Deep, Geopressured Aquifers: A New Energy Source?," Bernard, W.J. Petroleum Engineer International, March 1978 pp. 84-90
3. "Methane From Geopressured Aquifers Studied," Doscher, T.M. et al The Oil and Gas Journal, April 9, 1979 pp. 178-183
4. "Subsurface Disposal of Brines from Geopressured Reservoirs," Donaldson, E.C., U.S. Department of Energy, Bartlesville Energy Technology Center
5. "Typical Oil and Gas Fields of Southwestern Louisiana," Dobie, C.W., Lafayette Geological Society, Vol. II
6. "Fairfax Foster Sutter No. 2 Well, St. Mary Parish, Louisiana - Volume I: Completion and Testing," Willits, M.H. et al pp. 6-13 DOE/ET/28460-1 Vol. I.
7. "Log Interpretation Charts," Dresser Atlas, 1979 Edition, Sections 1-4 through 2.3
8. "Flow Test Analyses," ODEH, A.S. Lecture Notes for S.P.E. Short Course, (1978 Edition) pp. 7-9
9. "Pressure Transient Analysis in the Presence of Two Intersecting Boundaries," Prasad, R.K., Journal of Petroleum Technology, Jan. 1975, pp. 89-96

TABLE 1
SUMMARY OF RESERVOIR TEST ANALYSES

	Fairfax Foster Sutter	Beulah Simon*
Permeability (Md.)		
(Drawdown)	14.7	13.92
(Build-Up)	14.3	12.35
(Analytical Model)	14.3	11.62
Distance to First Barrier		
(Drawdown)	--	476 ft.
(Build-Up)	881 ft.	727 ft.
(Analytical Model)	839 ft.	556 ft.
Distance to Second Barrier		
(Drawdown)	--	--
(Build-Up)	--	--
(Analytical Model)	931 ft.	731 ft.
Skin Effect	-1.97	--
Initial Pressure	12,080 psi	13,015 psi
Thickness	58 ft.	186
Porosity	.13	.19
Viscosity	.41 cp	.4 cp
System Compressibility	4×10^{-6} vol/vol/psi	6×10^{-6} vol/vol/ps

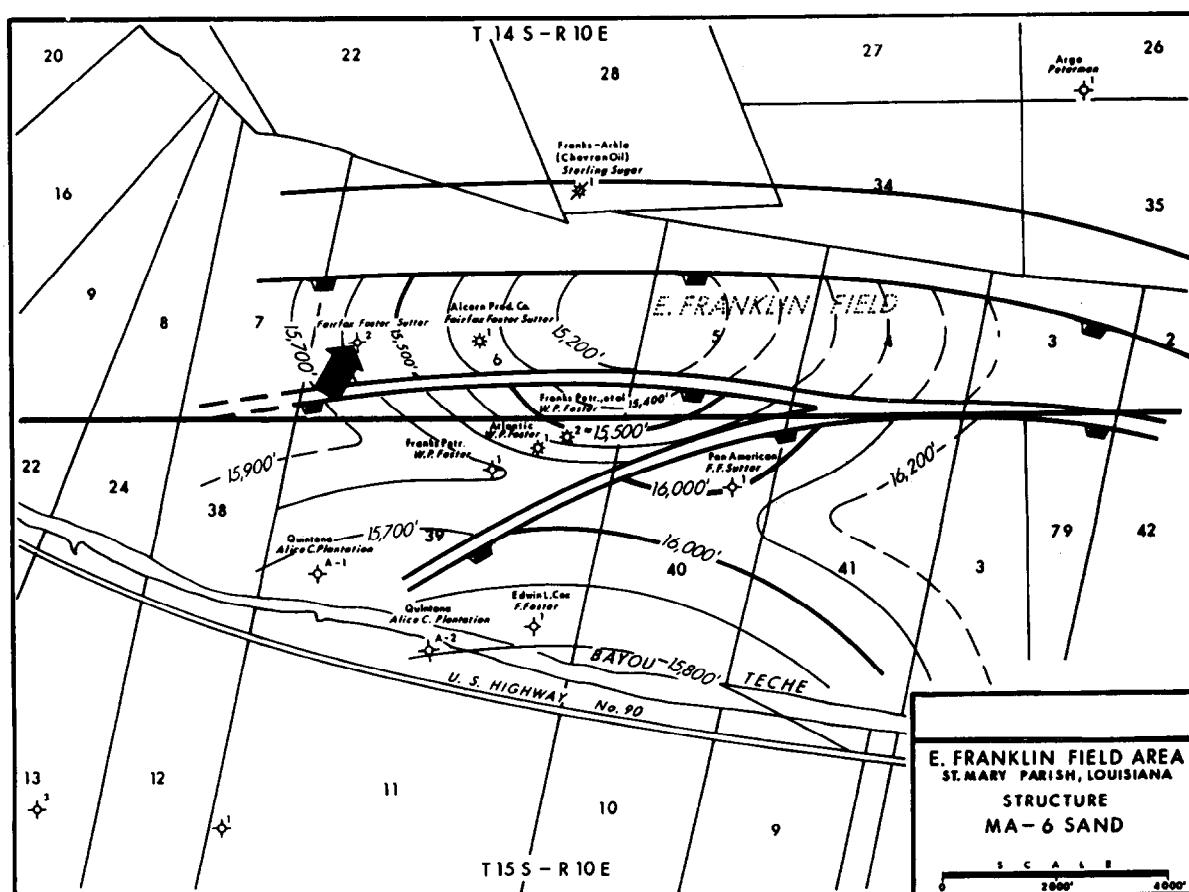
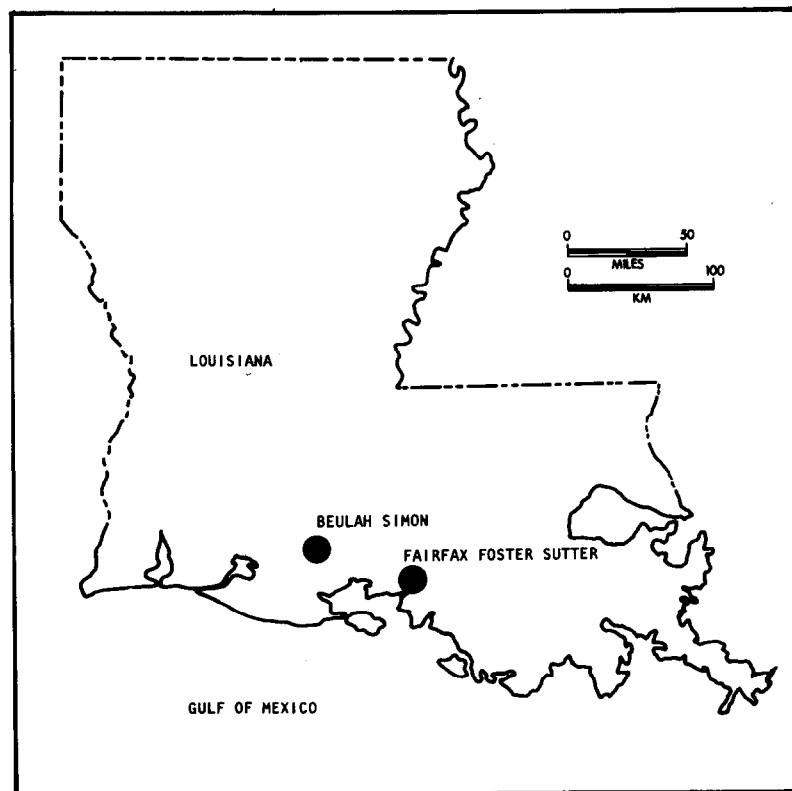
*Results of Analyses of BHP obtained from surface casing measurements

TABLE 2
CHEMICAL ANALYSIS OF PRODUCED WATER
(MILLIGRAMS PER LITER)

Constituent	Fairfax Foster Sutter No. 2	Beulah Simon No. 2
Total dissolved solids	190,904	103,925
Total solids	203,475	104,947
Calcium (CaCO ₃)	18,305	7,870
Magnesium (MgCO ₃)	2,320	910
Bicarbonate (HCO ₃)	208	606
Carbonate	0	1
Chloride (Cl)	91,387	50,300
Total iron (Fe)	56	33
Sulfate (SO ₄)	< 1	444
Dissolved silicate (Si)	60	92
Copper (Cu)	0.33	.152
Zinc (Zn)	2.11	.136
Boron (B)	68.5	89.6
Arsenic (As)	-	.002
Chromium (Cr)	0.16	.086
Mercury (Hg)	< 0.0005	.005
Lead (Pb)	-	7.73
Cadmium (Cd)	0.77	.269
Sodium (Na)	48,281	32,190
Potassium (K)	988	454
Density	1.0932 g/ml	1.066 g/ml
pH	6.18	6.61
Sus viscosity	31.3	28.55

TABLE 3
CHEMICAL ANALYSIS OF GAS
(MOL PERCENT)

Constituent	Fairfax Foster Sutter No. 2	Beulah Simon No. 2
Nitrogen (N ₂)	0.518	.271
Carbon dioxide (CO ₂)	7.85	7.73
Methane (CH ₄)	89.57	88.87
Ethane (C ₂ H ₆)	1.78	2.20
Propane (C ₃ H ₈)	0.20	.60
Isobutane (C ₄ H ₁₀)	0.061	.18
n-Butane (C ₄ H ₁₀)	0.014	.07
BTU content (BTU/Ft. ³)		
Dry:	950	987
Wet:	933	970



production rate did not remain constant. At larger choke sizes the rate of productivity decline became more pronounced. On the remaining four wells, a back-pressure regulator and a differential controller were installed downstream from the orifice meter. With a constant backpressure maintained on the choke, a constant differential pressure across the orifice meter could be achieved by periodic adjustment of the choke. This procedure helped to maintain control of the gas flow rates on some wells, but not on all. Since most wells had variable flow rates during drawdown and shut in periods were short, type curve techniques could not be used.

ANALYTICAL SCHEME

Fundamentally, the following reservoir rock and fracture properties are to be determined from pressure transient tests: permeability, porosity, fracture half-length, fracture height, formation damage, turbulence, fracture width, and fracture permeability. However, experience with the reservoir simulator indicated that gas wells in Devonian shales show negligible turbulence, and formation damage, within limits, has a negligible effect on well performance. On the other hand, changes in fracture width and fracture permeability do not, within limits, significantly affect the computed pressures. No attempt was made to estimate fracture width and fracture permeability from conventional techniques.

Conventional techniques were used first to compute approximations for various reservoir and fracture properties. These values were used as starting points for the reservoir simulator, and were gradually adjusted until a history match of the observed pressures was obtained. The mathematical simulator was used only to "fine tune" these values and arrive at final estimates of the parameters. The analytical scheme is discussed briefly here, using the Morgantown Energy Research Center Well No. 1 as an example for discussion.

1. Flow Regimes

According to transient pressure theory, if a gas well produces at a constant rate into a fracture of infinite capacity, a plot of $\log \Delta m(p)$ against \log time should show three patterns: an early straight-line portion with a slope of 1, a second straight-line portion with a slope of 0.5, and a line convex downward during the late stages of flow. These patterns correspond to (1) wellbore storage effects, (2) linear flow into an infinite capacity fracture, and (3) radial or quasiradial flow. From material balance considerations, however, if the well is not producing at a constant rate, a plot of $\log \Delta m(p)$ against $\log \Sigma q_n t_n$ should exhibit similar characteristics. Similar patterns are observed for shut-in, if $\log \Delta m(p)$ is plotted against $\log \Delta t$.

These plots are constructed in order to identify the linear-flow region, which will subsequently be analyzed to obtain estimates of reservoir/fracture properties. Radial flow was never detected during the test period in any of the five wells tested to date. On the Morgantown well, mechanical problems prevented recording of bottomhole pressures; surface pressures were converted to bottomhole pressures using the Cullender and Smith⁶ method. Fig. 2 shows that wellbore storage effects during drawdown lasted for $\Sigma q_n t_n$ approximately equal to 2000, which corresponds to a flowing time of about 11 hours. Fig. 3 depicts much

longer storage effects (about 70 hours) during the buildup. Storage for the second drawdown was minimal.

2. Estimation of Fracture Length from Frac Data

The initial estimate for the fracture half-length was computed from the weight of the sand injected during the stimulation treatment, based on the following assumptions:

- (1) 10 percent flowback of sand during cleanup operations;
- (2) A fracture porosity of 33 percent;
- (3) A grain density of 2.66 gm/cc;
- (4) A fracture width of 0.1 to 0.2 in.

This computation is oversimplified, but it provides a rough estimate of designed fracture half-lengths.

The Morgantown well was fractured using 120,000 lb of sand. The above assumptions yield an estimate of 971,14 cu ft for the fracture volume. If the fracture width is assumed to be 0.2 in., the half-length is estimated to be 607 ft. However, most of the sand in this well appears to have gone out of the gas-producing interval, and the effective fracture was very small.

3. Estimation of Matrix Permeability

Reservoir permeability can be estimated by using conventional analysis. However, as mentioned earlier, experience indicates that for a tight gas well with a vertical fracture, radial flow does not occur during short test periods. Hence reservoir permeability values obtained by such techniques are overestimated, for two reasons: (1) radial flow toward the wellbore never existed; (2) the computed flow capacity would be an integrated average of the formation and fracture flow capacities dependent upon the volume of the reservoir perturbed by the test. Nevertheless, these permeability estimates define the upper limits and are used to initialize the reservoir simulator. The longer the test time, the nearer the calculated permeability approaches the matrix permeability.

According to Odeh and Jones⁷, for a drawdown with variable flow rate, a plot of $m(p_n)/q_n$ against superimposed time rate $(X_n)/q_n$ should give a straight line with a slope (m) inversely proportional to formation flow capacity. For a buildup with radial flow, a plot of $m(p)$ against superimposed time rate should yield a similar curve, i.e.,

$$k_g h = \frac{1638 T_f}{m} \dots \dots \dots (1)$$

For the Morgantown well, the buildup gave a matrix permeability value of 0.0021 md (Fig. 4), whereas the values obtained from the first and second drawdowns were 0.0034 and 0.0055 md, respectively, averaging 0.0037 md.

4. Estimation of Fracture Half-Length from the Pressure Data

It has been established by pressure transient

theory that for linear flow with constant flow rate q , a plot of $m(p)$ against the square root of time should give a straight line with a slope (m') related to fracture and formation properties:

$$m' = \frac{40.85qT_f}{X_f h_f} \sqrt{\frac{1}{k_g \phi_g \mu_g C_t}} \dots \dots \dots (2)$$

It must be pointed out, however, that this analysis assumes the flow capacity of the fracture to be infinite, which tends to give conservative fracture half-length for finite capacity fractures. The calculated fracture lengths will deviate from actual lengths in proportion to the fracture conductivity. However, for multiple fractures, only $\Sigma X_f^2 h_f^2$ can be estimated.

For estimation of fracture half-lengths for the Morgantown well, plots similar to those used for estimating matrix permeability were constructed, the only difference being that the superimposed time rate (X_n) used with these plots is for linear flow (Fig. 5). The gas properties were obtained from empirical correlations based on chemical analysis of the gas (Table 1).

The fracture half-lengths calculated from the first and second drawdowns were 36 and 29 ft. The buildup gave an estimate of 20 ft. The average of all calculated half-length values was 28 ft.

5. Estimation of Fracture Height

Fracture height could not be estimated from either the logs, the pressure data, or the fracture treatment. Further complicating this estimation is the method used to perforate these wells preparatory to stimulation. They were selectively perforated in an interval that might cover several hundred feet of shale, and the well was stimulated using ball sealants. Lacking a tracer in the frac fluid or proppant, in most wells the fracture height was taken to be the length of the perforated interval within each gas-bearing member of the shale, determined from the perforating record and the gamma ray and density logs.

6. Estimation of Porosity

Effective porosity of the shale to gas was not determinable either from the logs or pressure tests. Effective porosity based on past experience and published information was taken as 1 percent as the starting value for the simulator.

7. History Match Using Reservoir Simulator

Pressure-production history was recreated by a three-dimensional, single-phase, single-well gas reservoir simulator with the following features:

1. Radial coordinates
2. Horizontal or vertical fractures
3. Turbulent flow effects
4. Storage effects of wellbore and fractures
5. Real gas pseudopressure
6. Skin effects
7. Automatic gas property correlations

As mentioned earlier, matrix permeability estimates from conventional techniques are mostly optimistic, whereas fracture half-length calculations are mostly conservative. Therefore, the scheme adopted to obtain a history match of the measured pressure is

to reduce the matrix permeability, increase the fracture half-length, and adjust the porosity of the shale to gas until the best fit is obtained. It must be realized that the determination of best fit was not based upon minimizing some norm, but rather on the judgment of the analyst. The best match of the measured data on the Morgantown well is shown in Fig. 6.

8. Log Analysis

The fracture half-length for the Morgantown well, estimated from pressure data and obtained from the reservoir simulator, is a small percent of the designed half-length. In order to ascertain why such a small fracture was created, detailed log analysis was performed. The radioactive tracer log indicated that bulk of the sand was placed above the perforations (7,107 to 7,155 ft) in the interval from approximately 7,082 to 7,098 ft (Fig. 7). The radioactive streaks at 7,113, 7,118, 7,133, 7,143, 7,147, and 7,149 to 7,158 ft correlate well with the existing natural fracture networks indicated on the fracture identification log.

Examination of the resistivity log indicates higher resistivities (exceeding 100 ohm-m) in the areas of natural fractures where gas is present, i.e., 7,104 to 7,110, 7,115 to 7,123, and 7,141 to 7,158 ft. It is significant that the interval 7,082 to 7,098 ft. which appears to have taken the bulk of the frac sand, does not exhibit the higher resistivity apparent in the fractured zones below 7,100 ft. This interval is, however, indicated to be highly fractured from the top down to 7,091 ft. The low resistivities in this highly fractured (naturally) interval, combines with the moderate resistivity of the less fractured (naturally) zone from 7,091 to 7,100 ft., suggest that although the bulk of the frac sand was placed from 7,082 to 7,099 ft, this interval contributes very little to the total gas production.

9. Sensitivity Analysis

To establish the uniqueness of the results, sensitivity runs were conducted on each of the models.

For the Morgantown well, sensitivity runs were made by holding the product $x_f h_f \sqrt{k_g \phi_g}$ constant. In one run, x_f was halved while the permeability was quadrupled; in the second, porosity was multiplied by a factor of 0.8 and permeability divided by the same factor. One additional run, where the fracture half-length was increased by only 5 ft., is shown in Fig. 8. It is obvious that the computed pressures do not agree with the measured pressures, and the ability to history-match the actual data is sensitive to changes in these properties.

Table 2 is a summary of test results obtained for the five wells tested so far.

DELIVERABILITY PROJECTION

Using the model obtained by history-matching, deliverability projections were made assuming that the well flows into a 40-psig gathering system. Since the drainage area of these wells is unknown, the projections are limited to 5 years using 160-acre spacing. Fig. 9 shows projections for the Morgantown well.

CONCLUSIONS

The results of the analyses of the test data lead to the following conclusions:

1. In some cases, the stimulation treatments were successful in creating high-conductivity fractures with large surface areas.
2. For most wells wellbore storage effects during drawdown were negligible. Wellbore effects were more dominant during buildups.
3. Turbulent flow was not detected, either in the shale or in the created fractures.
4. Because of the low permeability of the reservoir, the created fractures behave as though they have infinite conductivity.
5. A test period of two weeks, as outlined above, is sufficient to characterize the product of permeability by porosity and the square of the product of the fracture half-length and the fracture height, that is, $(K_g \phi_g x_f^2 h_f^2)$.
6. Within limits, formation damage on the fracture face caused by the frac fluid has a negligible effect on well performance.
7. The method of analysis outlined in the text provides a set of parameters adequate for initializing the reservoir simulator.
8. The history matches obtained by the reservoir simulator are achieved in a few runs (less than 10 in most cases), and the fit is excellent in all cases.
9. The validity of the models must be verified by testing them against the actual monthly production after data have been recorded for 12 to 18 months.

NOMENCLATURE

C_t = total system compressibility, psi^{-1}
 h = formation thickness, ft
 h_f = fracture thickness, ft
 K_g = effective permeability to gas, md
 m = slope of radial flow plot, $\text{psi}^2/\text{cp}/\text{Mcf}/D$
 m' = slope of linear flow plot, $\text{psi}^2/\text{cp}/\text{Mcf}/D$
 $m(p)$ = real gas pseudo potential, psi^2/cp
 $\Delta m(p) = m(P_i) - m(P_n)$, psi^2/cp
 q_i = i th flow rate, Mcf/D
 Δt = shut-in time, hours
 t_i = total elapsed time through i th flow rate, hours
 T_f = formation temperature, $^{\circ}\text{R}$
 x_f = fracture half-length, ft
 x_n = superimposed time rate data at time t_n

$$= q_1 \sqrt{t_n} - \sum_{i=2}^n (q_i - 1 - q_i) \sqrt{t_n - t_i - 1}$$

for linear flow

$$= q_1 \log t_n - \sum_{i=2}^n (q_i - 1 - q_i) \log(t_n - t_i - 1)$$

for radial flow

ϕ_g = gas-filled porosity, fraction

μ_g = gas viscosity, cp

ACKNOWLEDGEMENT

We express our appreciation to Gruy Federal, Inc., and the Morgantown Energy Technology Center of the U.S. Department of Energy for permission to publish this paper. We thank many members of the Gruy Companies' staff for their help from time to time.

REFERENCES

1. Kumar, Raj M., and Hartsock, James H.: "Well Test Analysis for Pacific States Gas and Oil Company L. Bonnett No. 1 Well," report to U.S. Dept. of Energy under contract no. EW-78-C-21-8096, Dec. 6, 1978.
2. Kumar, Raj M., and Hartsock, James H.: "Well Test Analysis for Columbia Gas Transmission Corp. Well No. 20336," report to U.S. Dept. of Energy under contract no. EW-78-C-21-8096, Dec. 19, 1978.
3. Kumar, Raj M., and Hartsock, James H.: "Well Test Analysis for Kentucky-West Virginia Gas Company Well No. 1627," report to U.S. Dept. of Energy under contract no. EW-78-C-21-8096, Jan. 25, 1979.
4. Kumar, Raj M., and Hartsock, James H.: "Well Test Analysis for Morgantown Energy Research Center No. 1 Well," report to U.S. Dept. of Energy under contract no. DE-AC21-78MC08096, Nov. 6, 1979.
5. Kumar, Raj M., and Hartsock, James H.: "Well Test Analysis for Combustion Engineering Well No. 1," report to U.S. Dept. of Energy under contract no. DE-AC21-78MC08096, Jan. 4, 1980.
6. Cullender, M.A., and R.V. Smith: "Practical Solution of Gas-flow Equations for Wells and Pipelines with Large Temperature Gradients," Trans., AIME (1956) 207, 281.
7. Odeh, A.S. and Jones, L.G.: "Pressure Drawdown Analysis, Variable-Rate Case," J. Pet. Tech. (Aug. 1965) 960-964; Trans., AIME (1967) 234. Also Reprint Series No. 9 - Pressure Analysis Methods, Society of Petroleum Engineers of AIME, Dallas (1967) 161-165.
8. Al-Hussainy, R., Ramey H.J., Jr., and Crawford, P.B.: "The Flow of Real Gases Through Porous Media," J. Pet. Tech. (May 1966) p. 624.
9. Al-Hussainy, R., and Ramey, H.J., Jr.: "Application of Real Gas Flow Theory to Well Testing and Deliverability Forecasting," Trans., AIME (1966) 233, 637-641.
10. Millheim, Keith K., and Cichowicz, Leo: "Testing and Analyzing Low-Permeability Fractured Gas Wells," Trans., AIME (1968) 235, 193-198.

TEST RESULTS OF STIMULATED WELLS IN DEVONIAN SHALES

11. Wattenbarger, R.A., and Ramey, H.J., Jr.: "Well Test Interpretation of Vertically Fractured Gas Wells," <u>Trans.</u> , AIME (1969) <u>236</u> , 625-632.	<u>Trans.</u> , AIME (1964) <u>231</u> , 1159.
12. Cinco-L., H., Samaniego-V., and Dominquez-A., N.: "Transient Pressure Behavior for a Well with a Finite-Conductivity Vertical Fracture," <u>Soc. Pet. Eng. J.</u> , (Aug. 1978), pp. 253-264.	14. Hanley, Edward J., and Bandyopadhyay, Pratip: "Pressure Transient Behavior of the Uniform Flux Finite Capacity Fracture," paper SPE 8278 presented at the SPE-AIME 54th Annual Fall Technical Conference and Exhibition, Las Vegas, Sept. 23-26, 1979.
13. Russell, D.G. and Truitt, N.E.: "Transient Pressure Behavior in Vertically Fractured Reservoirs,"	15. Matthews, C.S., and Russell, D.G.: "Pressure Buildup and Flow Tests in Wells," Vol. I, SPE Monograph (1967).

TABLE 1

CHROMATOGRAPHIC ANALYSIS OF SEPARATOR GAS

Operator: Morgantown Energy Technology Center Separator Pressure: 70 psig
Field: Morgantown, West Virginia Separator Temperature: 100°F
Well: MERC No. 1

Date Sampled: September 20, 1979

<u>Composition</u>	<u>Mol %</u>	<u>GPM @ 14.850 psia</u>
Nitrogen	0.25	
Carbon Dioxide	5.78	
Methane	91.98	15.753
Ethane	1.89	0.509
Propane	0.09	0.025
iso-Butane	0.01	0.003
n-Butane	<u>NIL</u>	<u>NIL</u>
	100.00	16.290

BTU per cubic foot: dry 976; wet 959

Specific gravity (air = 1): 0.6220

TABLE 2
SUMMARY OF TEST RESULTS

Property	Pacific States Gas and Oil Co. L. Bonnett No. 1	Columbia Gas Trans. Corp. Well No. 20336	Kentucky- W. Va. Gas Co. Well No. 1627	Morgantown Energy Research Center Well No. 1	C.E. Power Syst. Group Well No. 1
Effective matrix porosity, fraction	0.008	0.01275	0.0068	0.007	0.0095
Effective matrix permeability, md	0.0002	0.015	0.001175	0.0014	0.005
Pay thickness, ft	124	456	228	48	20
Fracture porosity, fraction	0.33	0.33	0.33	0.33	0.33
Fracture half-length, ft					
Fracture 1	195	636	308	35	62
Fracture 2	N.A.	173	308	N.A.	N.A.
Fracture height, ft					
Fracture 1	124	46	20	48	20
Fracture 2	N.A.	154	62	N.A.	N.A.
Fracture permeability, md	125-640 ¹	500,000	500,000	5,000-500,000 ²	500,000
Fracture width, in.	0.1	0.2	0.1	0.1-0.2 ²	0.1

N.A. = not applicable.

¹ At the highest flow rate, the frac water flowed from the fracture to the wellbore, which increased the gas saturation in the fracture; this increased the effective permeability to gas.

² Based on sensitivity runs; the reservoir simulator is not sensitive to calculated pressures in these ranges.

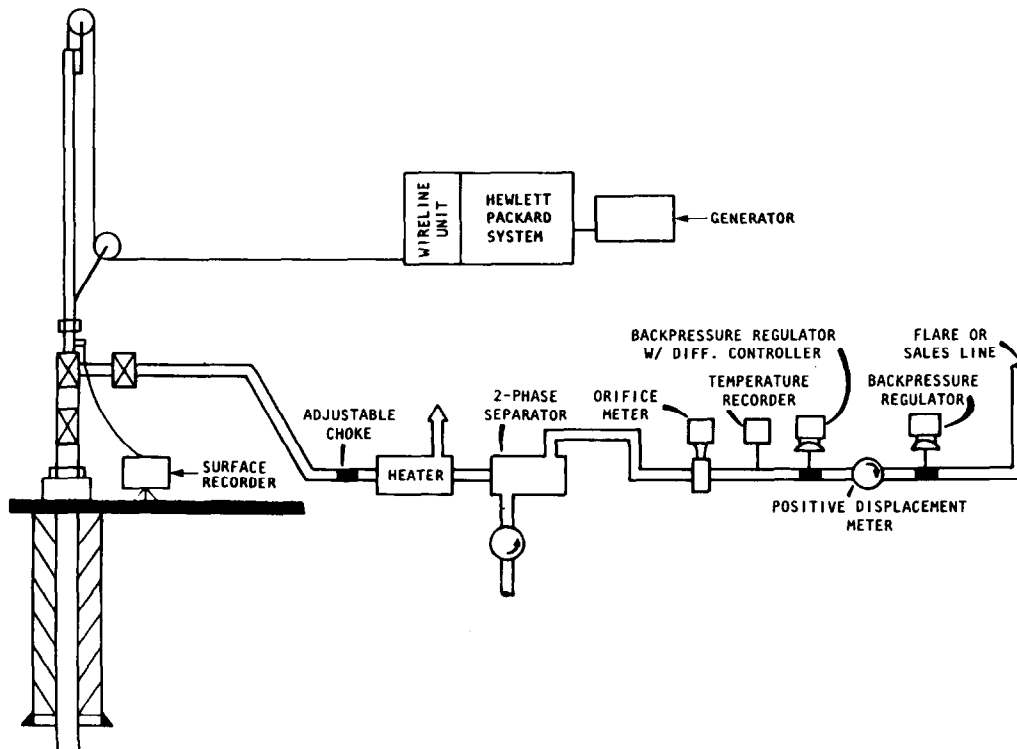


Fig. 1 - Surface facilities for Eastern Devonian Shale Gas Testing Program.

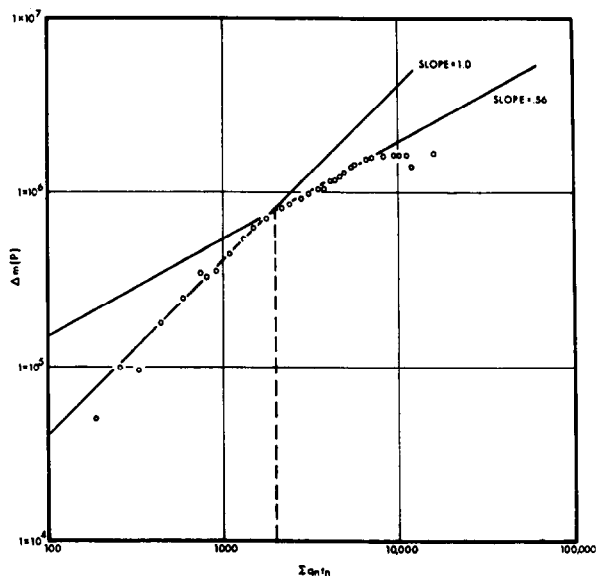


Fig. 2 - Log $\Delta m(p)$ versus $\Sigma q_n t_n$ - first drawdown.

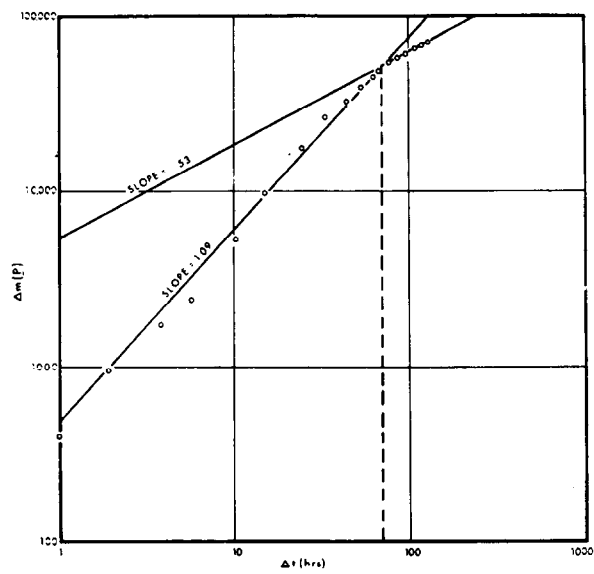


Fig. 3 - Log $\Delta m(p)$ versus log $\Delta t(\text{hrs})$ - buildup.

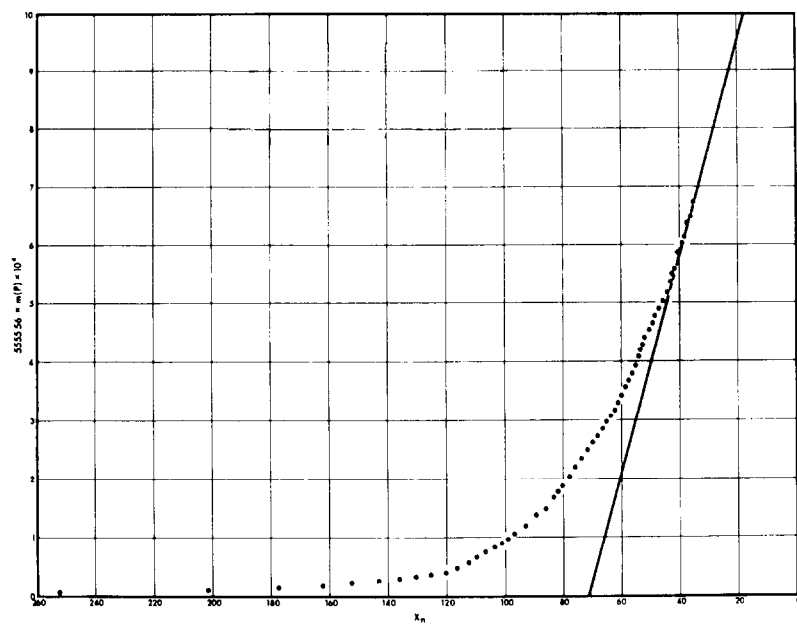


Fig. 4 - Pressure buildup - $m(p)$ versus superimposed time rate data (radial flow).

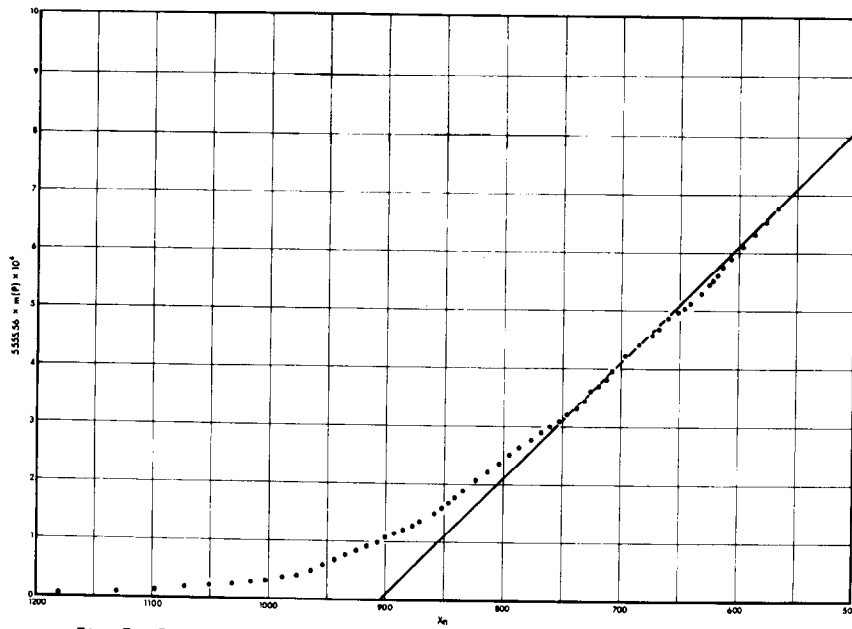


Fig. 5 - Pressure buildup - $m(p)$ versus superimposed time rate data (linear flow).

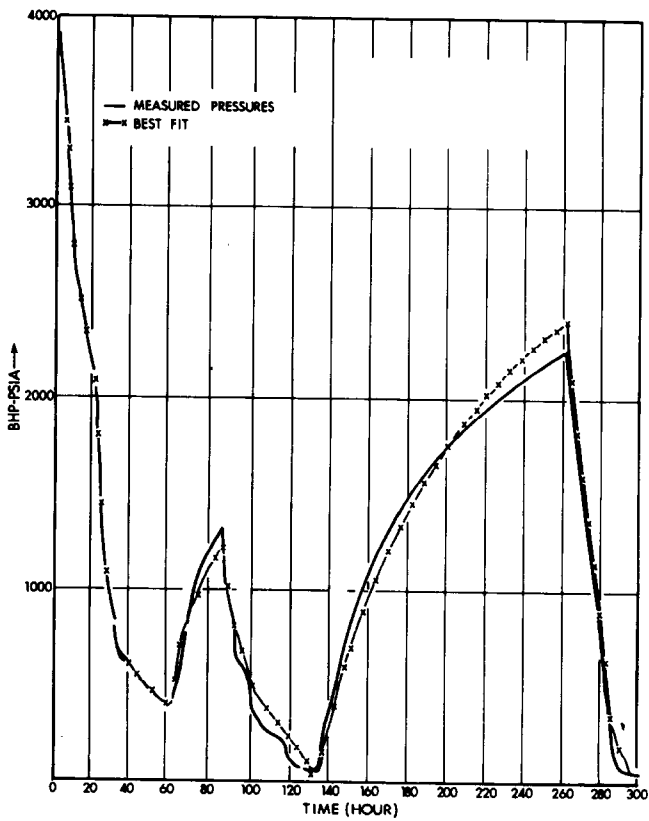


Fig. 6 - History match.

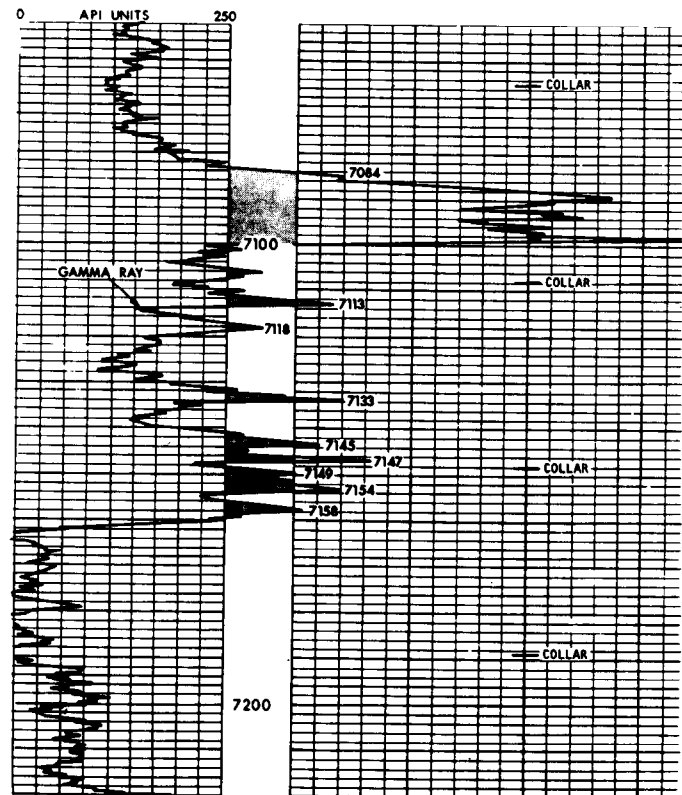


Fig. 7 - Post frac tracer (beads) log.

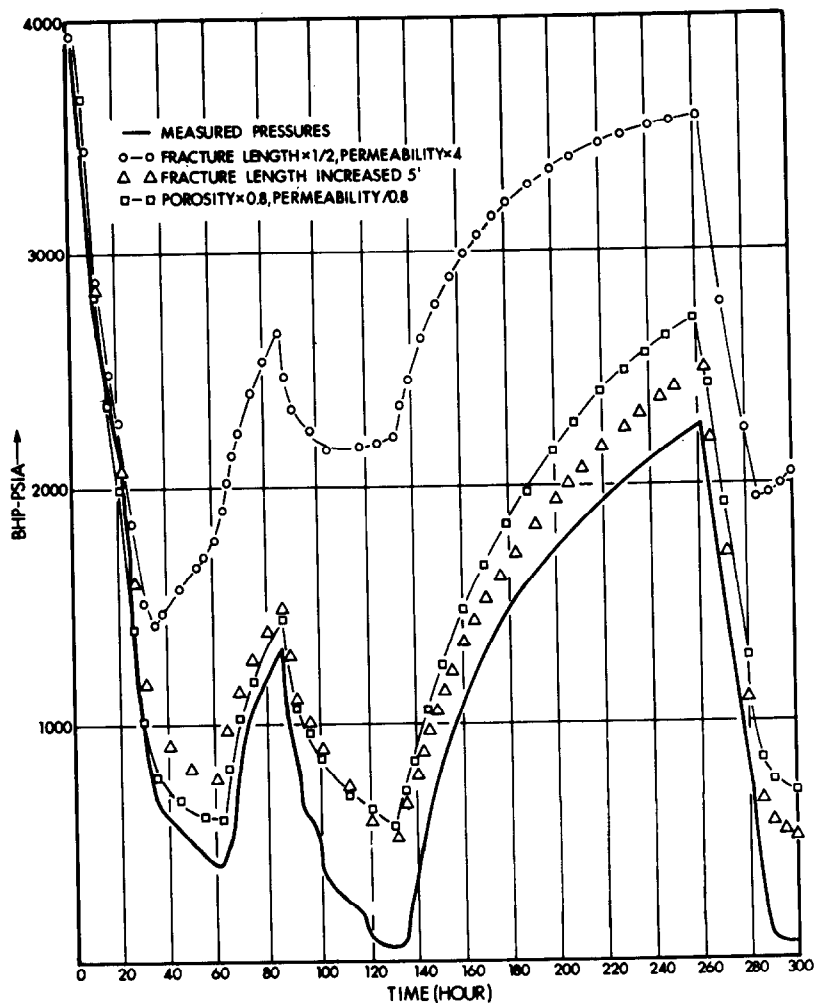


Fig. 8 - Sensitivity analysis.

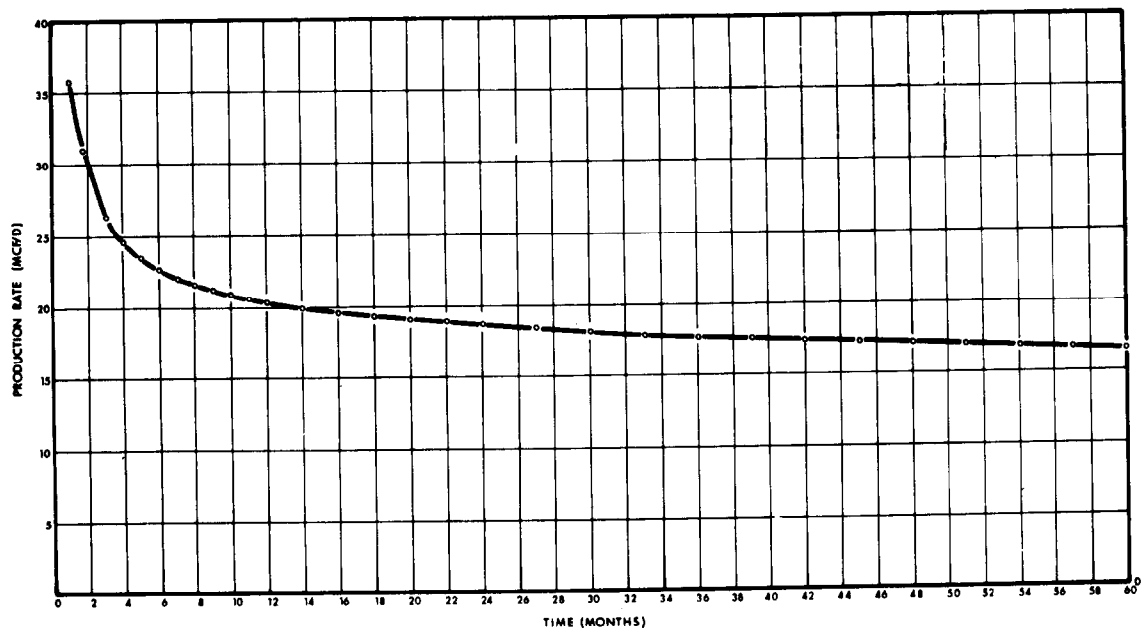


Fig. 9 - Deliverability projections.

METHANE RECOVERY FROM DEEP UNMINEABLE COAL SEAMS

by Larry D. Allred and Ralph L. Coates,
Mountain Fuel Resources, Inc.

This paper was presented at the 1980 SPE/DOE Symposium on Unconventional Gas Recovery held in Pittsburgh, Pennsylvania, May 18-21, 1980. The material is subject to correction by the author. Permission to copy is restricted to an abstract of not more than 300 words. Write: 6200 N. Central Expwy., Dallas, Texas 75206

ABSTRACT

Mountain Fuel Supply Company and the U. S. Department of Energy are conducting a joint project to demonstrate production and recovery of methane gas from deep coal seams in the Book Cliffs coal field of central Utah. The objective is to drill three wells to depths near 3000 feet to determine if commercial quantities of gas can be produced, and then to install production facilities for injecting the gas into the Mountain Fuel Supply gas transmission system.

Two of the three wells have been drilled and testing has been initiated. Five coal seams were encountered at depths between 2681 and 3112 feet. Core samples were obtained and desorption measurements indicate gas contents up to 400 cu ft/ton. The gas is approximately 95 percent methane. Water influx tests were made and water pumping equipment is being installed. Plans are being formulated to hydraulically stimulate the principal coal seams with nitrogen foam to increase production.

INTRODUCTION

Mountain Fuel Supply Company, with joint funding from the Morgantown Energy Technology Center (METC/DOE), is conducting a joint project to demonstrate the economic feasibility of recovering methane from deep unmineable coalbeds in Utah. Different completion techniques and hydraulic stimulation methods are being used to improve the understanding of methane recovery technologies.

Sites for three demonstration wells were selected in Carbon County, Utah. The sites are in a coal field lying in the western 70 miles of an imposing physiographic feature known as the Book Cliffs, which is 185 miles in length. Coal seams are present along its entire length. The western end abuts the Wasatch Plateau and is about 120 miles southeast of Salt Lake City.

References and illustrations at end of paper.

Data from the Bureau of Mines¹ and the Utah Geological and Mineral Survey² have shown coals from this field to contain relatively high volumes of methane gas. The three well sites were selected after carefully reviewing these data. Two of the sites are adjacent to one of Mountain Fuel's major transmission lines.

DRILLING AND WELL LOGGING

The first two of the three planned wells were drilled late in 1979. These two wells are spaced 1800 feet apart in the Whitmore Park area approximately 23 miles northeast of Price, Utah. The wells were drilled to depths of 3000 feet and 3177 feet. Coal was encountered between 2681 and 3112 feet. Because of the depth, location, and other factors, these coals are considered to be unmineable at the present time. Figure 1 is a coal log for Well No. 2, which is typical of the formations encountered in both Whitmore Park wells. The log shows the location and thickness of the coalbeds encountered and the surrounding formations. Only minor variations in thickness and location of the coalbeds exist between the two wells.

Five coal seams were encountered at Whitmore Park Well No. 2. They range in thickness from 2 feet to 13 feet. The shallowest seam is the Sunnyside, which consists of 4 partings varying from 2 to 7 feet thick. Rock Canyon and Fish Creek coals were found to be 5 feet and 2 feet thick, respectively. The Gilson coal is 13 feet thick, and the Kenilworth coal is 2 feet thick.

CORE SAMPLE TESTING

Core samples of each of the upper 4 coals were obtained and are being analyzed for gas content, ASTM rank, and permeability and porosity under in situ conditions.

Desorption of the core samples has been carried out using the standard technique developed by the Bureau of Mines in which core samples are sealed in containers and the desorbed gas is measured by

displacement of water. The gas content of the cores has greatly exceeded previously measured gas content of coals from this area of the Book Cliffs coal field. Table 1 presents a summary of desorption data obtained to date. Some cores from each coalbed indicate very high gas content coal. At least one sample each of the Sunnyside, Rock Canyon, and Gilson coals measured over 375 cu ft/ton of coal. The first sample of Gilson coal taken is continuing to desorb but to date has released 414 cu ft/ton.

Gas from several cores has been analyzed by the Institute of Gas Technology. Table 2 summarizes the results of this analysis. The desorbed gas is 95 to 98 percent methane; carbon dioxide is present in concentrations ranging from 1 to 5 percent. Small amounts of ethane and propane were measured, and only traces of heavier hydrocarbons were noted. Gas samples were taken both in the early stages of desorption and in later desorption stages. In all cases, the methane content of the later samples was higher. This was due to lower carbon dioxide concentrations rather than the desorption of more of the hydrocarbons heavier than methane. No evidence has been noted that heavy hydrocarbons will appear in any significant extent in the final stages of desorption. Samples of the residual gas will be analyzed to see if any heavier hydrocarbons are released when the coal is crushed.

Rank analysis has been completed on several core samples. One typical analysis of the Gilson coal is shown in Table 3. According to ASTM rankings, this coal was ranked as high volatile bituminous A coal.

TESTS ON WELL NO. 1

Figure 2 shows the configuration of the Whitmore Park No. 1 well during the preproduction testing period. The well was completed open hole with respect to the Gilson coalbed. Two Lynes packers were used in the testing in order to isolate the Gilson coal from the formations open above and below the Gilson seam. Separate ports in the Lynes system allowed each of the three zones to be tested independently without repositioning the packers.

Water injection tests were run on each of the three isolated zones in the well. The intent of the injection tests was to determine formation permeability to water. The tests were also intended to show if the formations surrounding the Gilson coal were likely to fracture when the coal was being fractured. Water was injected into each zone at several constant rates. Pressures at the well-head were recorded continuously during the injection testing.

Water was injected into the Gilson coal at rates of 1.5 gal/min, 0.47 bbl/min, .87 bbl/min, and 1.5 bbl/min. Five injection rates ranging from 0.83 to 4.9 bbl/min were tested in the formation above the Gilson coal. Continuous injection was not possible on the formation below the Gilson. Figures 3, 4, and 5 show traces of injection rates and pressure recordings for the Gilson coal, the formation above the Gilson, and the formation below the Gilson, respectively. The pressure response varied dramatically between the three zones. A gradual pressure buildup was observed for all

injection rates into the Gilson coalbed. Injection into the formation above the Gilson resulted in an instantaneous pressure buildup. As soon as injection began, an almost immediate change in surface pressure was noted and no further change in pressure was observed as the injection continued. The formation below the Gilson appeared to be very impervious, so a series of pressure decline tests was run.

Over the range of injection pressures covered during these tests, no indication of a formation breakdown was noted. The maximum injection pressure in the zone above the Gilson was 1750 psig, and in the zone below the Gilson the maximum pressure was 2600 psig. The maximum injection pressure into the Gilson coal was 900 psig.

A series of swab tests was conducted on each of the three zones. A wireline workover rig was used to swab or lift water from each zone being tested. The swab tests were made to reduce the hydrostatic head on the coal formation and then monitor any gas production, and to measure water influx rates from each of the three zones. The water influx data were to be used to calculate formation permeability for each zone. During the swabbing of the Gilson coal zone, relatively large volumes of flammable gas were produced with the water. The series of swab tests was successful in determining the range of water influx from each of the three zones. Water influx data are presented in Table 4.

TESTS ON WELL NO. 2

Figure 6 shows the configuration of the Whitmore Park Well No. 2. This well was completed open hole across the 13-foot thick Gilson coalbed and the smaller Kenilworth coalbed. A Pengo completion system was cased across the 7-foot thick parting of the Sunnyside coalbed. This system is designed to keep the casing cement off the formation and has movable ports to open the zone to production. A series of swab tests was conducted on the open hole formation, including the Gilson and Kenilworth coalbeds. The tests were similar to those run on Well No. 1. Relatively large volumes of flammable gas were produced during the tests. Water influx data from the entire open hole section are presented in Table 4. The average influx rate was 127 B/D.

DISCUSSION OF RESULTS

Each well penetrated from 30 to 35 feet of coal, including two larger seams 7 and 13 feet thick. Using the coal thickness data and the measurements of the gas content of the core samples, it is estimated that this section contains 11. Bcf of gas in place. This quantity of gas indicates good prospects for recovering sufficient quantities of methane to make its recovery commercially profitable.

The swab test data indicate that the water influx into the No. 2 well can adequately be removed with the sucker rod pump purchased for this project. However, the water influx into Well No. 1 is too great to be handled with this type pump. The zone above the Gilson coalbed produced up to 1000 B/D of water under a formation face pressure

of 960 psi. The Gilson coalbed produced a maximum of 80 B/D with a formation face pressure of 380 psi. These high water influx rates have caused a change to be made in the method of completing Whitmore Park Well No. 1. A liner will be run into the open hole, suspended from the existing casing, and cemented in place. The liner will then be perforated adjacent to the Gilson coalbed.

Portions of the data collected from injection tests and swab tests on Well No. 1 were used to calculate coal permeabilities. The longest injection test into the Gilson coal, conducted at 0.47 bbl/min, produced data which indicated a permeability of 20 md. The calculated permeabilities varied with the rate of injection into the Gilson coal, as shown in Table 5. The higher the injection rate and pressure, the higher the calculated permeability. Swab test data on Gilson coal result in a calculated permeability of less than 2 md. The lower permeability from the swab test data is somewhat consistent with the injection permeabilities since swabbing reflects pressures lower than the static formation pressure.

Swab data from Well No. 2 also indicate a calculated permeability of approximately 2 md. One possible explanation for this change in permeability is that coal itself is quite impermeable but contains numerous natural fractures. Coal is also

compressible and, when subjected to injection pressures, the natural fractures are opened. The higher injection pressures therefore result in higher calculated permeabilities. Water injection at very low rates may therefore yield more meaningful data for the permeability of the coal.

FUTURE PLANS

Completion of Whitmore Park Well No. 1, dewatering pump installation, and initial dewatering of both wells will be completed early this year. Dewatering of both wells will continue for three months and gas and water production will be monitored. A nitrogen foam hydraulic stimulation will then be conducted on the coal zones open to production, and an extended test of long-term gas and water production will be conducted over an 18-month period.

REFERENCES

1. Irani, M. C.; Jansky, J. H.; Jeran, P. W.; and Hassett, G. L.: "Methane Emission From U. S. Coal Mines in 1975. A Survey," Bureau of Mines Information Circular 8733 (1977), p 16.
2. Doelling, H. H.; Smith, A. D.; and Davis, F. D.: "Methane Content of Utah Coals," Utah Geological and Mineral Survey Special Studies 49 (August 1979), pp. 15-20.

TABLE 1
SUMMARY OF CORE SAMPLE DESORPTION DATA

Well No.	Sample No.	Coal Seam	Depth feet	Laboratory	Total Gas Desorbed cc/gm	Total Gas Desorbed cu ft/ton	Desorption Complete
WP-1	2	Gilson	3099	IGT	12.9	414	no
WP-2	262	Gilson	3097	UGMS	6.6	212	yes
WP-2	RC-1	Rock Canyon	2865	MFR	10.6	340	no
WP-2	RC-2	Rock Canyon	2867	MFR	12.2	389	no
WP-2	G-3	Gilson	2934	MFR	9.9	317	no
WP-2	261	Sunnyside	2720	UGMS	5.3	169	yes
WP-2	260	Gilson	2935	UGMS	6.7	216	yes
WP-2	10	Lower Sunnyside	2714-20	IGT	8.0	257	no
WP-2	11	Sunnyside	2703	IGT	13.4	429	no
WP-2	13	Fish Creek	2877	IGT	10.9	348	no
WP-2	14	Rock Canyon	2863	IGT	12.3	392	yes
WP-2	16	Gilson	2934-7	IGT	10.4	332	no
WP-2	17	Gilson	2934-7	IGT	10.9	350	no

TABLE 2

DESORPTION GAS COMPOSITION (Mol %)

Sample No.*	Whitmore Park No. 1					Whitmore Park No. 2							
	2A	2C	2D	2E	2F	8A	8B	10B	10C	11B	11C	17A	17B
Volume Desorbed, cc	2,912	9,211	9,642	9,887	10,380	4,361	5,116	2,579	4,452	5,710	10,362	2,725	3,445
<u>Components</u>													
Carbon Dioxide	2.2	2.3	1.7	1.3	1.3	3.3	1.4	4.3	4.1	4.8	3.3	2.4	2.2
Hydrogen		0.2				0.2				0.1			
Methane	97.7	97.3	98.1	98.5	98.5	96.0	98.2	95.2	95.5	94.9	96.3	96.9	97.0
Ethane	0.1	0.1	0.1	0.1	0.1	0.2	0.2	0.4	0.3	0.2	0.3	0.4	0.4
Propane	Tr	0.1	0.1	0.1	0.1	0.3	0.2	0.1	0.1	Tr	0.1	0.3	0.3
n-Butane		Tr	Tr	Tr	Tr	Tr	Tr	Tr	Tr	Tr	Tr	Tr	0.1
i-Butane		Tr	Tr	Tr	Tr		Tr	Tr	Tr			Tr	Tr
Total	100.0	100.0	100.0	100.0	100.0	100.0	100.0	100.0	100.0	100.0	100.0	100.0	100.0

*Numbers indicate core sample, letters indicate gas sample

TABLE 3

 WHITMORE PARK WELL NO. 1
 GILSON COAL RANK ANALYSIS

<u>Proximate Analysis</u>		(He Density = 1.34 gm/cc)	
		<u>Wt %</u>	(As Received)
Moisture		1.8	
Volatile Matter		39.3	40.0 (dry)
Ash		3.1	
Fixed Carbon		<u>55.8</u>	
Total		100.0	
<u>Ultimate Analysis</u>		<u>Wt %</u>	(Dry Basis)
Ash		3.19	
Carbon (total)		80.25	
Organic Carbon			80.16
Mineral Carbon			0.09
Hydrogen		5.50	
Sulfur		0.39	
Nitrogen		1.59	
Carbon Dioxide			0.32
Oxygen (By Diff)		<u>9.08</u>	
Total		100.00	

Gross Calorific Value = 14,270 BTU/lb

TABLE 4

WHITMORE PARK

SUMMARY OF WATER INFLUX FROM SWAB TESTS

Production Zone	Depth ft.	Minimum Water Influx		Maximum Water Influx	
		Rate B/D	Formation Face Pres. psi	Rate B/D	Formation Face Pres. psi
<u>WELL NO. 1</u>					
Gilson Coal	3097-3111	51	430	78	380
Below Gilson Coal	3111-3177	130	340	220	340
Above Gilson Coal	3080-3097	610	1000	1040	960
<u>WELL NO. 2</u>					
Open Hole	2928-3000	71	580	162	620

TABLE 5

 PERMEABILITY FROM WATER INJECTION TESTS ON GILSON COAL
 WHITMORE PARK WELL NO. 1

Test Series	Water Injection Rate, bbl/min	Calculated Permeability millidarcies
1	0.47	20
2	0.87	170
3	1.50	200
4	0.47	73

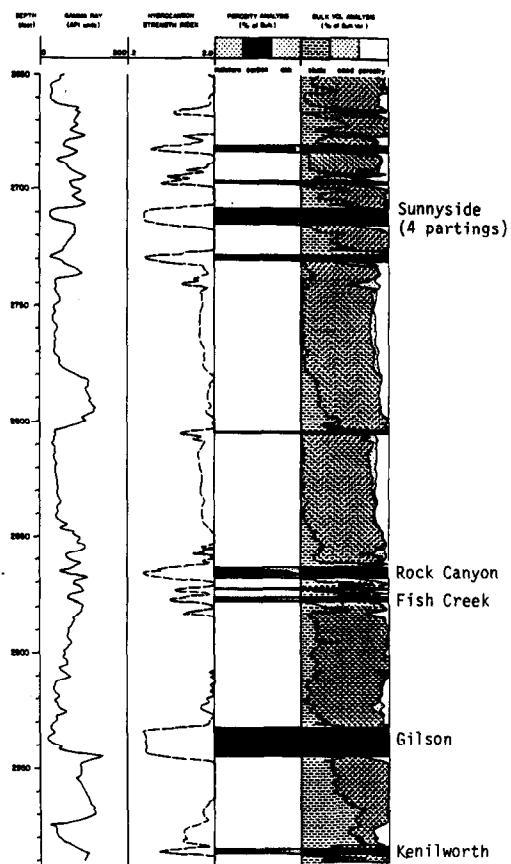


Fig. 1 - Whitmore Park Well No. 2 coal log.

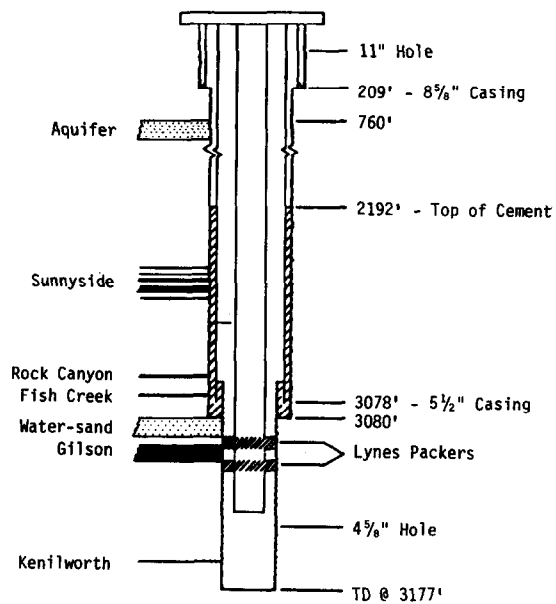


Fig. 2 - Whitmore Park Well No. 1 - preproduction testing configuration.

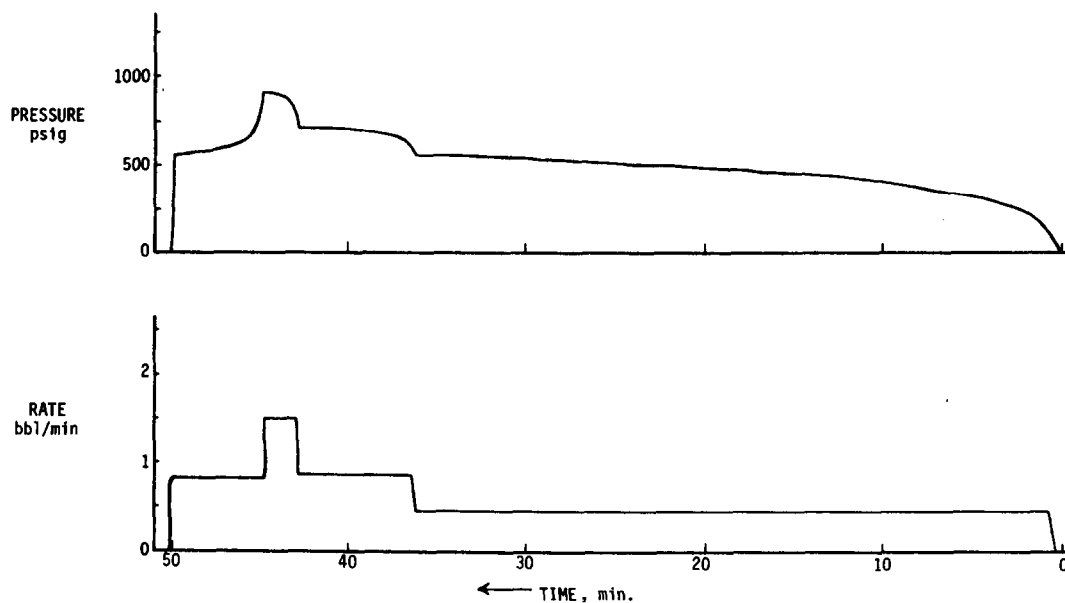


Fig. 3 - Whitmore Park Well No. 1 - Water injection into Gilson coal.

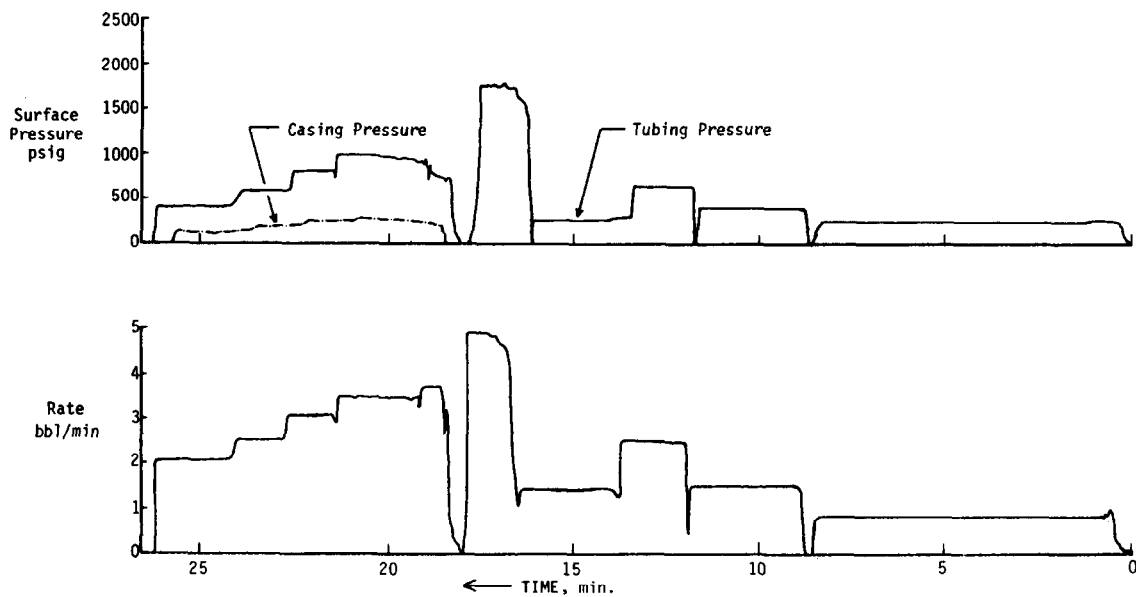


Fig. 4 - Whitmore Park Well No. 1 - Water injection above Gilson coal.

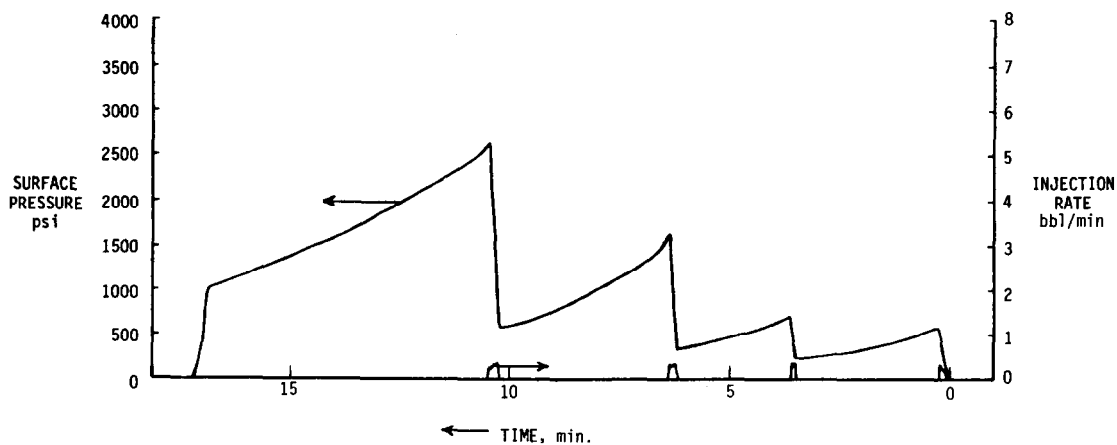


Fig. 5 - Whitmore Park Well No. 1 - Pressure decline tests below Gilson coal.

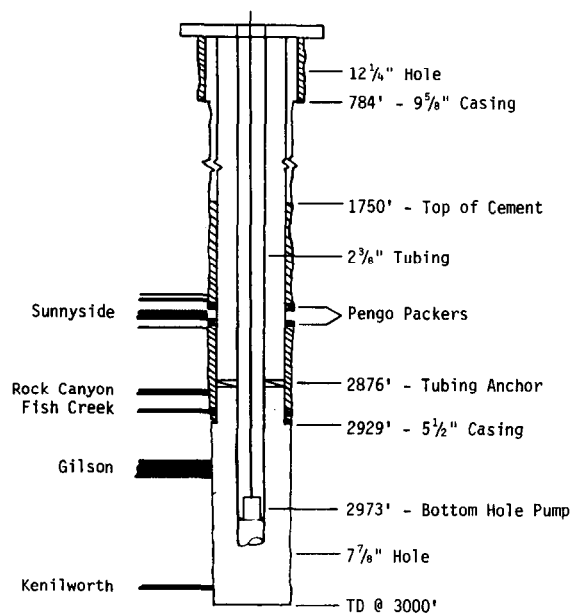


Fig. 6 - Witmore Park Well No. 2 - Completion configuration.

WAYNESBURG COLLEGE MULTIPLE COAL SEAM METHANE EXTRACTION WELL

by James N. Kirr and Greg E. Eddy, Waynesburg College;
Robert Rahsman, Rahsman Geological Services; Norman F.
McGinnis, TRW, Inc.

This paper was presented at the 1980 SPE/DOE Symposium on Unconventional Gas Recovery held in Pittsburgh, Pennsylvania, May 18-21, 1980. The material is subject to correction by the author. Permission to copy is restricted to an abstract of not more than 300 words. Write: 6200 N. Central Expwy., Dallas, Texas 75206

ABSTRACT

Waynesburg College, in cooperation with TRW, Inc. and the Department of Energy, is in the process of completing the drilling of a well through the Upper Pennsylvanian coals near Waynesburg, Greene County in southwestern Pennsylvania. The primary objective of this well was to determine the optimum method for the extraction of methane gas from a multiple number of coal seams, and secondly, to provide Waynesburg College with an alternate source of energy to heat the buildings on the campus. It is anticipated that the gas produced will replace 60 to 70 percent of the peak demand of the College.

The well was drilled to a total depth of 442 meters using rotary percussion with air. After setting a water string of 22 cm casing, a 20 cm hole was drilled to the total depth. Production casing measuring 14 cm was cemented to the surface in a single stage.

Perforation and fracturing were done on an incremental basis using a retrievable bridge plug. Data from the coring and logging operations indicated that only seven of the coal seams present at the site would be suitable for fracturing and gas production. The coals were divided into three zones and perforated and fractured in turn to allow for maximum stimulation. The retrievable bridge plug was used to isolate the lower fractured seams from those above that were to be fractured. Fracturing was done with foam injected at a maximum rate of .03 m³/s using a sand proppant to maintain the openings in the coal.

The well, when completed, will be topped with a standard well head. A downhole positive displacement pump will be used to remove the water produced from the coals. The well is presently undergoing testing to determine its production potential. The gas produced will be run through a separator and dessicator before it is metered into a nearby existing commercial gas line for transportation to the Waynesburg College campus.

Illustrations at end of paper.

INTRODUCTION

In the mid-1970's, gas shortages and rising costs began to have an effect on organizations that used large quantities of natural gas. Waynesburg College, a small, private liberal arts institution located in the center of Greene County in southwestern Pennsylvania (see Fig. 1), was among those that were drastically affected by the increased costs. The College uses natural gas as its primary energy source and consumes an average of 33,000 MCF per year. The budgetary increases that were necessary to pay for the higher costs of the gas were diverting funds that could have been used for other parts of the institution.

Waynesburg College is located in the heart of the Appalachian coal basin and sits on vast, untapped reserves of high grade bituminous coal. The College is rather fortunate in that it owns all of the mineral rights beneath the thirty acre campus in the borough of Waynesburg. It was suggested by a member of the Board of Trustees that the College investigate the possibility of using some of those mineral resources to help alleviate the rising costs of gas. Nearby coal mining operations indicated that the coal beds in this area contained sufficient quantities of pipeline quality gas that could be used in place of commercial gas.

In 1979, Waynesburg College, in cooperation with TRW, Inc., received a grant from the Department of Energy to drill a well for the express purpose of extracting methane gas from the coal beds. The gas would be used to heat the buildings on the Waynesburg College campus. It was estimated that a single, multiple seam completion would produce sufficient gas to satisfy most of the college needs. During the peak demand periods of the winter months, it was estimated that the well would be able to produce sufficient gas to satisfy 60 to 70 percent of the demands of the College. Drilling operations for this project began in October, 1979.

WELL LOCATION AND GEOLOGIC SETTING

The well is located as shown in Figure 1 near the center of the northern boundary of the borough of Waynesburg, Pennsylvania. The well site lies at an elevation of 288 meters in the unglaciated Pittsburgh Plateau section of the Appalachian Plateau Physiographic Province. Topographically, this area contains deeply dissected narrow valleys with relatively steep slopes. Slopes near the well site are approximately 25%. The well site, however, is on the narrow, alluvial floodplain of Purman Run near the contact between the Washington Formation and the underlying Waynesburg Formation, both of which are Dunkard in age. This places the site at about the horizon of the Washington coal.

Structurally, the site is 3 kilometers south-southeast of the axis of the Waynesburg Syncline and 3.5 kilometers west-northwest of the Bellevern Anticline. The axis of both structures trend North 15° East. The dip of the strata at the site is about 1° northwest.

The surface and subsurface rocks in this area are typical of the Pennsylvanian and Dunkard (Permian) rocks in the Appalachian Plateau. They are thin to thick bedded layers of shale, siltstone, sandstone, limestone and coal. These lithologies usually do not persist laterally in thickness or type and are often interbedded with each other.

The well was drilled to a depth of 442 meters, and encountered 22 coal beds and lenses, not counting individual roof coals of the major seams. Most of the coals are thin and of no importance in this project. The major coal seams, including the ones perforated and foam fractured, are listed in Table 1. The Pittsburgh coal is the thickest seam penetrated by the well and is the chief seam mined in Greene County. The shallower coals, including the Waynesburg and Sewickley, are strip mined in the eastern part of the county. At present there are no mines in coals below the Pittsburgh seam, although underground mines in the Upper Freeport and Bakerstown coals have been suggested for the near future in other parts of the county where these coals are thicker.

Several problems developed during drilling because of incompetent shale layers penetrated by the well. The problems which are discussed in a later section were caused by caving of these shales. Two layers caused most of the problems. One layer was between the depths of 239 m and 247 m, and the other was between 258 m and 260 m. These layers were described from the core as red and green claystone containing compaction features. This lithology is extremely incompetent and it is understandable why the problems occurred.

CORING, DRILLING, AND WELL COMPLETION

The original plan was to produce large size coal cores, and, after coring, to ream the resultant well bore to its final size. However, it was determined that the most expeditious and cost-effective approach was to core with a small wireline core barrel. If these coal cores indicated producible seams, then a separate and distinctive methane production well would be drilled and completed. This approach would be faster than the

original plan because a drilling permit would not be required with the attendant approval processing delay. If the coring investigation did not produce the desired results, the only loss would be that of the value of the coring contract.

After core drilling began, a 10 cm surface casing was set with a Longyear NQ wireline core barrel which produced 6.09 m cores 4.8 cm in diameter. Coring activity proceeded uneventfully, except for periods where coring slowed while attempting to pass through the very incompetent red shale zones. These particular shales slowed the process considerably because the diamond core bit "loaded up" and became ineffective. On several occasions the bit became stuck overnight due to caving action of the shale beds.

At approximately 310 m the core barrel failed, circulation was lost, and the drill string became stuck. Bridging of the hole had occurred, because of the caving action of the red shale. The driller was unsuccessful in retrieving his drill string and had to cut off the bottom joint containing the core barrel. He was not able to set a whipstock to deviate around the lost tooling, and was forced to start a new hole. The new core hole was located approximately 10 m from the abandoned and plugged initial core hole.

On the new hole, the driller rapidly pushed down to 310 m and once again began "making core". Coring activity continued uneventfully to a total depth (TD) of 442 m.

Throughout the coring activity the retrieved coal cores of the thicker coal seams were subjected to desorption tests. These tests are a measure of the gas in the coal. The coal is placed in a closed container as soon as possible and the gas liberated by the coal is bled off and measured at prescribed intervals. This procedure usually takes several weeks. The coal is then weighted and crushed and the gas given off at that time is measured and is reported as residual gas. The gas given off in these steps is used to calculate the gas lost between the time the coal was cored and placed in the container. Thus the gas is reported in three categories, lost gas, desorbed gas and residual gas. Table 1 lists these data as well as total gas for the coals sampled in this project.

In general, the gas tests provided reasonably good prospects for methane production. Consequently, a decision was made to proceed with drilling the production well.

The coal thicknesses and gas contents were used to determine the completion method used in the production well. The coal we have tentatively called the Mercer was not sampled because it was not expected to be present in the area. Because of its thickness, it was stimulated in spite of the lack of gas content data. The Waynesburg coal seam is fairly thick and has a relatively high gas content. It was not stimulated because it was thought to be too shallow. The Sewickley seam was not stimulated because it was thought to contain large quantities of water in this area.

The driller mobilized on site on the morning of 22 January with a truck mounted top drive drill rig with

air compressor, a rack of 11.4 cm flush wall drill pipe and a supplemental trailer mounted 1.034 MPa 0.302 - 0.500 m³/s diesel driven air compressor. This supplemental compressed air was required to augment the rig compressor air because the well was to be air drilled.

The well was spudded in, and a 33 cm conductor pipe with an attached blooie line to the pit was set. Following placement of this pipe the crew drilled a 28 cm hole to a depth of 116 m and set a 22 cm water string casing. After cementing in the 22 cm J-55 water string and waiting for the cement to set, the driller began drilling the 20 cm hole for the 14 cm J-55 production casing. Drilling proceeded smoothly to a TD of 442 m.

At this point a variety of logs were run, including, dual induction laterlog/sonic (formation resistivity and hydrocarbon content), formation density (porosity), compensated neutron (precise porosity and lithology), gamma ray (correlation of lithology, depth, bed thickness) and a caliper log (well bore configuration log). Computer log analysis provided additional information on material strength of the rock strata, and carbon, ash and sulfur content of the coal seams. These data confirmed information produced from the analyses and greatly assisted the determination of which coal seams should be completed.

On 6 February the driller rigged up his Bucyrus-Erie-36 L "spudder" rig on the hole. Because of the unavoidable delay between the time the hole was drilled and this date, the well bore had caved and bridged at several depths. This was again caused by the red shales. The condition became clearly evident when the driller attempted to set the 14 cm casing and met tough resistance at approximately 259 m. Consequently, the casing had to be "drilled in" with the rig cable tool and bailer. This process was very slow and the casing was not set and cemented until 16 February. After waiting for the cement to set, a cement bond log was run confirming a good cement job. The well was then ready for the final completion and stimulation steps.

The final well design was to divide the coal seams into three zones and stimulate each zone in turn starting at the bottom of the well. The well completion plan is depicted in Figure 2. Zone 1 (bottom), with approximately 1.68 m of coal, includes the Clarion and two coal layers, tentatively called the Mercer, were perforated with a total of eight shots. The next (middle) zone, with approximately 2.2 m of coal includes the Bakerstown coal which was perforated with four shots, the Upper Kittanning with two shots, and

the Middle Kittanning with two shots. The upper zone included eight shots in the main bench of the Pittsburgh seam's approximately 1.8 m of coal, and two shots in the roof or rider coals of the Pittsburgh coal which includes approximately 0.6 m of coal.

The total thickness of coal stimulated was less than originally forecast. Several coal seams were eliminated by data obtained from the core, the logs, and from a special computerized coal log analysis which was generated by the logging company. Parameters which eliminated certain coals from consideration were; high ash content, low gas content, unanticipated thinness of some of the seams and other reasons mentioned earlier.

When the nitrogen foam frac was completed for the coals in the lower zone (zone 1), a retrievable bridge plug was used instead of the common multi-frac baffles because baffles could not be positioned in the production casing. This was caused by the fact that the casing had to be "drilled in" because of the extensive well bore caving that occurred with the red shales. Data relative to the well fracturing is shown in Table 2.

PRODUCTION DATA

At the time of the writing of this paper the well has not been tested for its potential production capability. The numerous delays caused by the bridging of the red shales and loss of the core pushed the anticipated completion date back by several months. One of the more recent delays occurred at the time the upper most coal unit, the Pittsburgh coal, was being fractured. An unrecorded gas well that was apparently drilled in the period between 1885 and 1900, and never properly plugged when abandoned, was breached during the fracturing operation. The abandoned well, which lies within one hundred fifty meters of the well site, began to eject quantities of mud, water and some gas. It was necessary to delay running the tests of the production capability of the methane extraction well until the proper permits could be obtained and the abandoned gas well properly plugged. This should be completed in the near future and the testing of the gas well can then proceed.

When completed, the well will be topped with a standard well head with a tubing packer. A downhole positive displacement pump will be used to remove the water produced from the coals. After testing, the gas produced will be run through a separator and dessicator before it is metered into a nearby existing commercial gas line for transportation to the Waynesburg College campus.

TABLE 1

COAL SEAM	DEPTH TO TOP [meters]	THICKNESS [meters]	LOST GAS [cc/gm]	DESORBED GAS [cc/gm]	RESIDUAL GAS [cc/gm]	TOTAL GAS [cc/gm]
Waynesburg [2 samples]	46.2	2	0.06 0.02	1.58 1.07	1.15 1.06	2.8 2.2
Sewickley	115	1	0.07	2.66	2.01	4.7
Pittsburgh riders	147	1.8	0.10	2.75	1.33	4.2
Pittsburgh main seam [3 samples]	149	2	0.05 0.08 0.15	1.88 2.15 2.82	2.63 1.89 2.60	4.6 4.1 5.6
Bakerstown	272	1	0.04	2.53	1.78	4.4
Upper Freeport	332	.3	—	1.48	2.12	3.6
Upper Kittaning [2 samples]	363	.5	0.12 0.35	3.07 3.75	1.64 2.00	4.8 6.1
Middle Kittaning	378	.3	—	2.41	0.67	3.1
Clarion	396	.9	0.10	2.93	1.39	4.4
Mercer ? [no samples] [two seams]	429 431	.6 .3				

TABLE 2

COMPLETION ZONE		3		2			1		
COAL SEAM		PITTSBURGH RIDER SEAM	PITTSBURGH MAIN SEAM	BAKERSTOWN	UPPER KITTANNING	MIDDLE KITTANNING	CLARION	MERCER Seam 1	Seam 2
Number of perforations		2	8	4	2	2	4	2	2
BREAKDOWN INPUT	Volume of water [M ³]	1.70		3.75			4.73		
	Casing pressure [mPa]	12,41		13,27			17,75		
	Water pumping rate [M ³ /sec]	0.03		0.03			0.01		
PAD INPUT	Percent nitrogen	45 to 50		75			75		
	Casing pressure [mPa]	11.72		17.92			26.47		
	Water pumping rate [M ³ /sec]	0.01		0.01			0.01		
	Total volume of nitrogen and water [M ³]	37.85		18.93			16.65		
FRAC INPUT	Percent nitrogen	45 to 50		75			75		
	Casing pressure [mPa]	8.96		16.20			26.71 increasing to 27.58		
	Proppant sand 20/40 [kg]	15,875		10,200			1,050		
	Water pumping rate [M ³ /sec]	0.01		0.01			0.01		
	Total volume of nitrogen, water and sand [M ³]	151.40		94.62			17.87		

REMARKS:

ZONE 1 — Frac screened out because of high bottom hole pressure and casing limitation of 27.58 mPa.

— 7M of sand flowed back into the sump.

ZONE 2 — First breakdown attempt failed because of faulty perforation run. Rerun with different shaped charges and perforated Bakerstown only.

— Followed frac with 1.89 M³ water flush.

ZONE 3 — Followed frac with 2.08 M³ water flush.

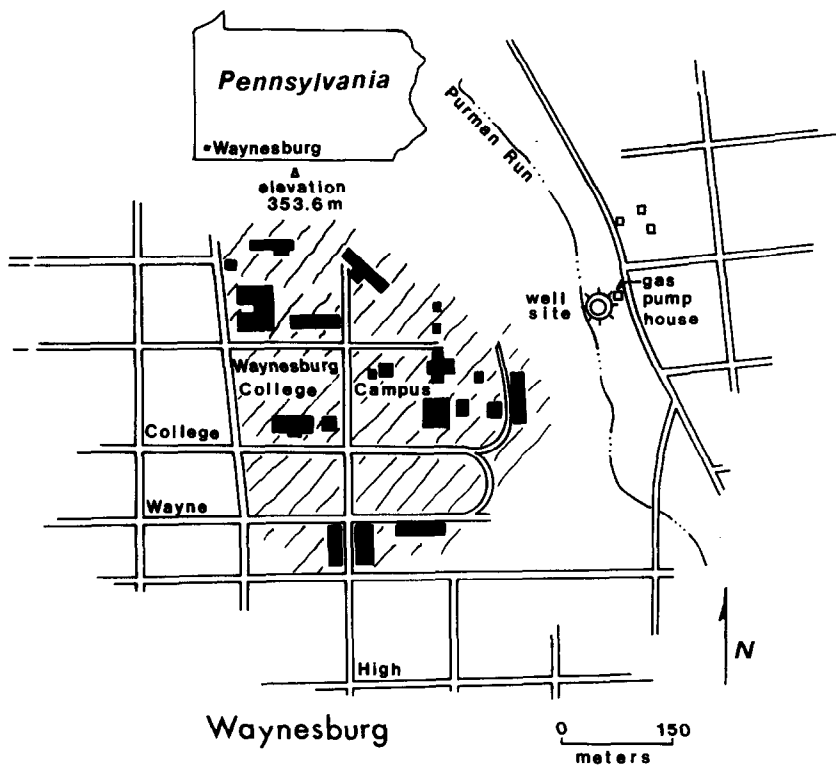


Fig. 1 - Location map of Waynesburg College and the well site.

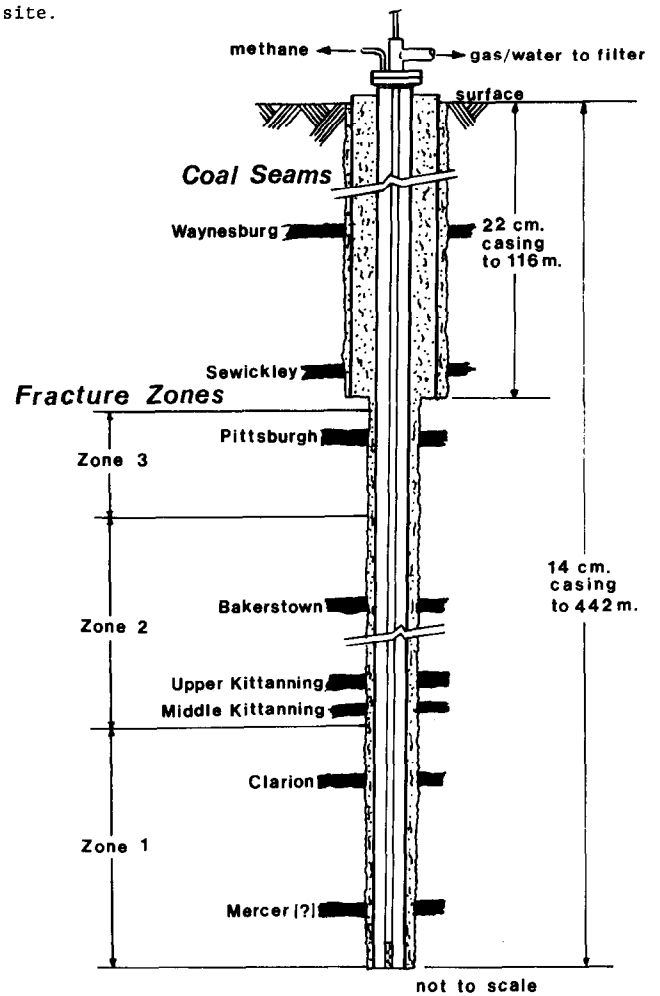


Fig. 2 - Well completion design.

INFLUENCE OF COALBED CHARACTERISTICS AND GEOLOGY ON METHANE DRAINAGE

by Gerald L. Finfinger, Leonard J. Prosser,
Joseph Cervik, U.S. Bureau of Mines

This paper was presented at the 1980 SPE/DOE Symposium on Unconventional Gas Recovery held in Pittsburgh, Pennsylvania, May 18-21, 1980. The material is subject to correction by the author. Permission to copy is restricted to an abstract of not more than 300 words. Write: 6200 N. Central Expwy., Dallas, Texas 75206

ABSTRACT

Methane drainage in advance of mining using horizontal holes continues to expand. Interpretation of coalbed characteristics and geology in relation to drilling procedures and gas flows will provide additional information for further development of this technique. A study conducted in the Pittsburgh coalbed at Bethlehem Mines Corp., Marianna mine 58, showed the effect of coalbed discontinuities, such as clay veins and sandstone channels, on drilling of horizontal boreholes and on gas flows. It has shown the need to adapt drilling techniques to the varying degrees of hardness encountered within the same coalbed.

INTRODUCTION

Over the past 5 years, industry interest in methane drainage has grown and it is expected to accelerate in the next 5 years with the continued development of horizontal drilling technology, long-hole drill equipment, methane sensing and control systems for pipelines, and guidelines for installing, maintaining, and operating underground pipelines. To maximize the development of this methane drainage hardware and technology, the unique geologic and drilling characteristics of each coalbed and each individual horizontal hole must be recognized and further described.

The Bureau conducted a demonstration project at Marianna mine 58 in which an underground piping system was used to safely and effectively transport methane from the coalbed to the surface. A Pittsburgh coalbed (Marianna mine 58) was selected for this project because previous work had shown that large quantities of methane can be drained from this coalbed. The coalbed is characteristically competent, blocky, and has a high fracture porosity and permeability. However, initial gas flows were 2 to 3 times lower than previously reported flows of 23 m³/d/m (250 cfd/ft) of hole length³. Clay veins in the coalbed influenced gas flows. In one hole gas

flow immediately increased over 1,982 m³/day (70,000 cfd) after interception of a clay vein, and in another it increased 906 m³/day (32,000 cfd). Subsequent drilling upon completion of the initial project verified the presence of a sandstone channel outby 2 of the 4 drainage holes, potentially blocking gas flow. Coalbed discontinuities such as clay veins and sandstone channels are usually discovered during the mining process. Vertical core holes can provide general trends for large discontinuities but are seldom spaced close enough to define their limits or locate smaller discontinuities. Since methane drainage work is ideally conducted in virgin areas, encountering such structures is not uncommon.

This paper reports on the effect that coalbed characteristics and discontinuities have on methane drainage and on horizontal drilling techniques.

CASE HISTORIES

In the Sunnyside coalbed, 2 holes were drilled at locations only 106.7 meters (350 feet) apart at an average penetration rate of 15 cm/min (6 in/min) for one hole and 91 cm/min (36 in/min) for the other. Samples of coal were taken from each drilling site to test for hardness. The Hardgrove Grindability Index for samples taken from both sites was the same. There is no explanation, to date, for this difference in penetration rates. The holes were drilled in advance of a section to isolate the coal between them and prevent methane from entering the region from the left and right. As a result, gas flow into the section was expected to decline. After completion of hole 1, flows did decline from about 6,513 m³/day (230,000 cfd) to 4,078 m³/day (144,000 cfd) after 15 days. However, hole 2 appears to have had little or no effect on methane flows. Over a 4-month period, gas flows remained between 3,682 m³/day (130,000 cfd) and 4,078 m³/day (144,000 cfd)².

Holes drilled parallel to the face cleat in the Blue Creek coalbed collapsed or squeezed in 152 meters (500 feet) or less, while holes drilled perpendicular to the face cleat were extended over 305 meters (1,000 feet) and remained opened.

References and illustrations at end of paper.

Because of differences in hardness in part of the Beckley coalbed, drilling changes were required when hole trajectory crossed from the upper to the lower part of the coalbed. Coalbed undulations were common and limited hole depth, because the hole trajectory could not be altered rapidly enough to follow the coalbed³.

Studies in two adjacent mines in the Pocahontas No. 3 coalbed showed that gas flow rates from horizontal holes differed by a factor of 2. A fault crosses one mine which may account for the difference in gas flow rates. In this case, gas flow increased with increasing distance from the fault zone⁴. Drilling long horizontal holes within the confines of a coalbed requires familiarity with the drilling characteristics of the equipment and the particular coalbed. The principles of drilling developed in other coalbeds in the past⁵ were found to be valid, in a general sense, for the Pocahontas No. 3 coalbed. The characteristics governing the flow of methane in this coalbed vary with location on a relatively small scale, and a preliminary study might be required for each mine before committing major capital expenditures for a specific methane drainage program⁶.

MODIFIED DRILLING TECHNIQUES AND EQUIPMENT

Drilling procedures will vary from coalbed to coalbed and even within the same coalbed. When discontinuities exist in a coalbed, drilling operations must either be adjusted in an attempt to re-enter the coalbed or a new site must be selected. If drilling continues, a bit designed to cut through the discontinuity is required. To drill the sandstone channel in the Marianna mine 58, a full face bit constructed of man-made diamonds was used. About 122 meters (400 feet) were drilled in the sandstone with this bit.

The primary objective during drilling is to maintain the trajectory of the hole parallel to the coalbed horizon. If the bit deviates from this course, some means of correcting its path must be applied to prevent the hole from intercepting the floor or roof.

Impurities in coalbeds, such as shale or bony bands and thin stringers of fine pyrite, affect hole trajectory. Bands of impurities tend to be located in the upper half of the coalbed, making the bed harder and penetration slower. In the lower part of the coalbed, which lacks impurity bands, the coal appears softer and penetration rates are much greater. However, the hole trajectory is more difficult to control in softer coal, and the bit tends to arc into the bottom. This distribution of impurity bands is found in parts of the Pittsburgh, Mary Lee, Beckley, and Sunnyside coalbeds. The bands may be related to the depositional environment of the peat-forming materials.

The path of the bit in the vertical plane is controlled by a combination of bit thrust and rotational speed (rpm) and by location of centralizers on a heavy NQ drill collar (fig 1). A drilling assembly with a 9.2 cm (3-5/8 inch) bit tends to wear the bottom side of the hole and arc downward more readily than an assembly with a 8.9 cm (3-1/2 inch) bit⁷.

The Bureau's experience in drilling the Pittsburgh coalbed (Fairview, W.Va. area) revealed marked differences in drilling characteristics of the upper and lower portions of the coalbed⁸. The upper 0.9 to 1.1 meters (3.0 to 3.5 feet) which contains numerous streaks and bands of pyrite, appears harder during drilling than the lower part of the coalbed which is predominately free of impurities and consequently softer. This characteristic of the Pittsburgh coalbed was also in evidence at the Marianna mine 58.

The Marianna mine is located about 48 km (30 miles) north of the Fairview, W.Va. area where overburden thickness is about 244 meters (800 feet). It is 152 meters (500 feet) at the Marianna mine. Comparison of tables 1 and 2 shows that bit penetration rates are greater at the Marianna mine drill site, with a lower rotational speed (rpm) of the bit at comparable levels of thrust. The lower bit penetration rates in the Fairview, W.Va., area may be due to greater overburden pressure on the coalbed.

The penetration rate of a drilling assembly with a 9.2 cm (3-5/8-inch) bit is greater than that of an assembly with a 8.9 cm (3-1/2-inch) bit⁹. Because of the soft nature of the lower portion of the coalbed at the Marianna mine 58 drill site, the drilling assembly with a 9.2 cm (3-5/8-inch) bit arced into the floor repeatedly and could not be controlled with combinations of bit thrust and rotational speed. Removal of the rear centralizer cocked the 5.5 meter (18 foot) drill collar, centralizer, and bit about 0.1° upward in the hole (fig 2). No problems were encountered in controlling this modified drilling assembly. All holes, except hole 1 were drilled with the modified drilling assembly. Table 3 summarizes the effect of the bit thrust and rotational speed on the bit trajectory and penetration rates. Comparison with Tables 1 and 2 shows that penetration rates of the modified drilling assembly are greater by a factor of about two.

The previously discussed data are the result of four horizontal degasification holes drilled in the Marianna mine 58 (fig 3). Total length of the four horizontal drainage holes is 1,737 meters (5,700 feet). The final 671 meters (2,200 feet) of a 762 meters (2,500 feet) hole were drilled at an average rate of 61 cm/min (2 fpm) using the modified drill assembly. This was about double the penetration rate of drill strings previously used (fig 1) under similar conditions.

The Pittsburgh coalbed in the area of the Marianna mine 58 contains a sandstone channel and clay veins¹⁰ which can form cells that limit the drainage area of a horizontal hole. Clay veins are generally associated with fractured roof strata and produce abnormally high methane flows when penetrated by mining or a horizontal hole.

The drill site at the Marianna Mine 58 is in a section abandoned to mining because of severe gas problems. When the study began, the section had been idle for about 2-1/2 years. Consequently, gas flows from holes could be expected to be much lower than flows from holes drilled in an active section.

Hole 3 was drilled to 375 meters (1,238 feet) at a fairly constant rate and gas flows during drilling increased linearly at a rate of $8.3 \text{ m}^3/\text{day/m}$ (89 cfd/ft) of hole drilled (fig 4). Gas flows from hole 4 increased at a rate of $8.0 \text{ m}^3/\text{day/m}$ (86 cfd/ft) to 128 meters (420 feet) and then the rate declined to about $3.3 \text{ m}^3/\text{day/m}$ (35 cfd/ft) between 128 meters (420 feet) and 226 meters (740 feet) (fig 5). Between the depths of 226 and 256 meters (740 and 840 feet) gas flow increased from $1,351 \text{ m}^3/\text{day}$ (47,000 cfd) to $2,266 \text{ m}^3/\text{day}$ (80,000 cfd). This sharp increase in flow of $912 \text{ m}^3/\text{day}$ (33,000 cfd) resulted from interception of a thin clay vein. The lower gas flow rate between 128 meters (420 feet) and 226 meters (740 feet) was probably due to a clay vein which shielded the hole and prevented free migration of gas to the hole. Hole 4 first hit rock at 256 meters (840 feet). Attempts were made to drill through the rock at two other levels in the coalbed. However, both probe holes intercepted rock and were terminated at 277 meters (910 feet) and 299 meters (982 feet) (fig 6). Hole 1 at 290 meters (950 feet) also hit rock and drilling was continued for an additional 37 meters (120 feet) in rock before the hole was abandoned. Both holes 1 and 4 terminated in the projected coalbed horizon (fig 6). Some time later hole 1 was extended over 122 meters (400 feet) in sandstone rock. Based on this data and on information from vertical core hole logs, the discontinuity is assumed to be a sandstone channel. Because rock was encountered in both holes drilled in advance of the face direction, it is possible that this sandstone channel spans the width of the section. Hole 1 was not drilled at a constant rate and, consequently, the flow data are difficult to interpret. The gas flow rate during drilling to 152 meters (500 feet) was $11.1 \text{ m}^3/\text{day/m}$ (120 cfd/ft) of hole. Gas flow rates during drilling of hole 2 were $15.6 \text{ m}^3/\text{day/m}$ (168 cfd/ft) to 134 meters (440 feet) and $3.8 \text{ m}^3/\text{day/m}$ (41 cfd/ft) between 134 meters (440 feet) and 655 meters (2,150 feet) (fig 7). At 677 meters (2,220 feet) gas flow increased from 4,078 to 6,060 m^3/day (144,000 to 214,000 cfd) indicating that a clay vein had been intercepted. Drilling was terminated in the floor at 764 meters (2,505 feet). The lower gas flow rate between 134 and 655 meters (440 and 2,150 feet) again was probably due to a clay vein which shielded the hole and prevented free migration of gas to the hole.

The bearings of the clay veins intercepted by holes 2 and 4 were determined by observing interference effects between holes. All holes were shut in for about 24 hours. Gas pressure at the pressure monitoring hole (hole A) increased from 57.9 to 77.2 kPa (8.4 to 11.2 psig). When hole 1 was opened, gas pressure at hole A immediately began to decline indicating an interference effect. If a clay vein, which obstructs flow, had been located between holes 1 and A, no gas pressure change would have been observed at hole A. Subsequently, hole 4 was opened and a further decrease in gas pressure was immediately observed at hole A. This test indicated that there were no clay veins to obstruct flow laterally between holes 1 and 4.

In about 23 hours, shut-in gas pressures at hole 1 and 2 were 44.1 kPa (6.4 psig) and 53.1 kPa (7.7 psig), respectively. When hole 1 was opened, no change in gas pressure was observed at hole 2. The holes are 3.7 meters (12 feet) apart at the collars.

This indicates that the clay vein intercepted by hole 2 at 677 meters (2,220 feet) is located between holes 1 and 2 (fig 3). Similarly, the gas pressure build-ups for holes 3 and 4 were 32.4 kPa (4.7 psig) and 30.3 kPa (4.4 psig), respectively. When hole 4 was opened, no pressure change occurred at hole 3. The holes are 11.3 meters (37 feet) apart at the collars. This indicates that the clay vein intercepted by hole 4 at 226 meters (740 feet) is located between hole 3 and 4 (fig 3).

GAS AND WATER FLOWS AFTER DRILLING

Initial gas flow from horizontal holes in the Pittsburgh coalbed is about $23.2 \text{ m}^3/\text{day/m}$ (250 cfd/ft) of hole length. The initial gas flows for holes 1 through 4 at the Marianna mine were much less (table 4) and ranged from 7.5 to $11.7 \text{ m}^3/\text{day/m}$ (81 to 126 cfd/ft) of hole. The lower flows at the Marianna mine are due to clay veins and a sandstone channel which isolate large blocks of coal. Degasification is confined only to these large blocks of coal outlined by the clay veins and sandstone channel and subsequently penetrated by a drainage hole. In addition, the section was abandoned for about 2-1/2 years allowing gas to bleed from the coalbed fracture system to the mine opening before the drilling program started.

SUMMARY

Four horizontal drainage holes were drilled ranging in length from 299 meters (982 feet) to 764 meters (2,505 feet). Clay veins and a sandstone channel were located during the drilling phase. The sandstone channel extends over 128 meters (420 feet) along the projected coalbed horizon (in hole 1). Methane flows from the horizontal holes were much less than flows observed in other areas of the Pittsburgh coalbed. The clay veins and sandstone channel isolate large blocks of coal which limit methane flows to the isolated blocks of coal penetrated by the horizontal holes.

Because of the soft nature of the Pittsburgh coalbed at the Marianna Mine 58, all holes except hole 1 were drilled with a modified drilling assembly consisting of a 9.2-cm (3-5/8-inch) bit, centralizer, and 5.5-meter (18-foot) drill collar. Removal of the rear centralizer cocked the assembly 0.1° upward in the hole.

REFERENCES

1. Finfinger, Gerald L., and Cervik, Joseph: "Review of Underground Methane Drainage Technology from U.S. Coalbeds, BuMines IC, 1980.
2. Perry, J. H., Aul, G. N., and Cervik, J.: "Methane Drainage Study in the Sunnyside Coalbed, Utah", BuMines RI 8323, 1978.
3. Cervik, Joseph: "Experience with Methane Control from Horizontal Boreholes", Second International Mine Ventilation Congress, November 1979.
4. Deul, Maurice, and Cervik, Joseph: "Methane Drainage in the Pittsburgh Coalbed", Proc. XVII International Conf. on Safety and Mining Works, Varna, Bulgaria, 1977, 9-15.

INFLUENCE OF COALBED CHARACTERISTICS AND GEOLOGY ON METHANE DRAINAGE

<p>5. Cervik, Joseph, Fields, H. H., and Aul, G. N: "Rotary Drilling of Holes in Coalbeds for Degassification", BuMines RI 8097, 1975.</p> <p>6. Von Schonfeldt, Hilmar: "Methane Recovery from Deep Seams", Pres. at Methane Recovery from Coalbeds Symposium, Pittsburgh, Pa. April 18-20, 1979.</p>	<p>7. McCulloch, C. M., Diamond, W. P., Bench, B. M., and Deul, Maurice: "Selected Geologic Factors Affecting Mining in the Pittsburgh Coalbed", BuMines RI 8093, 1975.</p> <p>8. Prosser, L. J., Jr., Finfinger, G. L., and Cervik, J.: "Methane Drainage at the Marianna No. 58 Mine Using Horizontal Boreholes", BuMines RI in publication.</p>
--	--

TABLE 1

PENETRATION RATES WITH 8.9 CM (3-1/2 INCH) BIT, FAIRVIEW W.VA. AREA

Thrust, N (lb)	Bit rotation, rpm	Penetration rate, cm/min (in/min)
3,558 (800)	700-900	10-18 (4-7)
5,338 (1,200)	400-600	25 (10)
6,672 (1,500). or greater	200-300	38 (15) or greater

TABLE 2

PENETRATION RATES WITH 8.9 CM (3-1/2 INCH) BIT, MARIANNA MINE 58

Thrust, N (lb)	Bit rotation, rpm	Penetration rate, cm/min (in/min)
3,781 (850)	150	20-25 (8-10)
5,449 (1,225)	300	30-36 (12-14)
7,562 (1,700)	150	41-61 (16-24)

TABLE 3

PENETRATION RATES OF MODIFIED DRILLING ASSEMBLY

Thrust, N (lb)	Bit rotation, rpm	Effect on bit trajectory	Penetration rates, cm/min (in/min)
3,781 (850)	300	Downward	30-38 (12-15)
5,671 (1,275)	300	Holds angle	61 (24)
7,562 (1,700)	150	Upward	76-91 (30-36)
11,120 (2,500)	250	Sharply upward	107-122 (42-48)

TABLE 4
INITIAL GAS FLOWS, HOLES 1, 2, 3, AND 4

Hole No.	Hole Length m (ft) (in coal)	Initial gas flow, m ³ /day (cfd)	Initial gas flow, m ³ /day/m (cfd/ft)
1	290 (950)	3,398 (120,000)	11.7 (126)
2	764 (2,505)	7,930 (280,000)	10.4 (112)
3	375 (1,230)	2,832 (100,000)	7.5 (81)
4	256 (840)	2,266 (80,000)	8.8 (95)

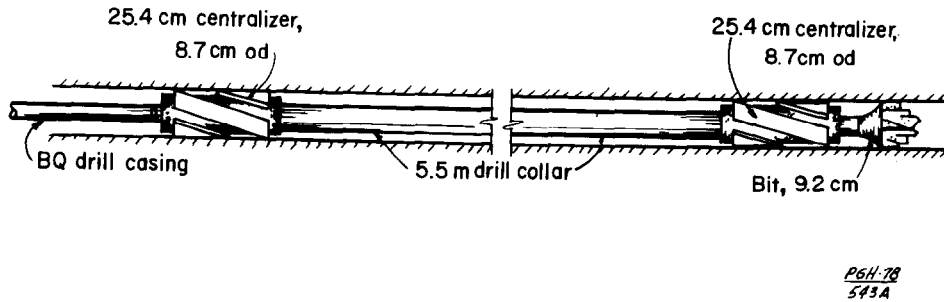


Fig. 1 - Drill string with two centralizers.

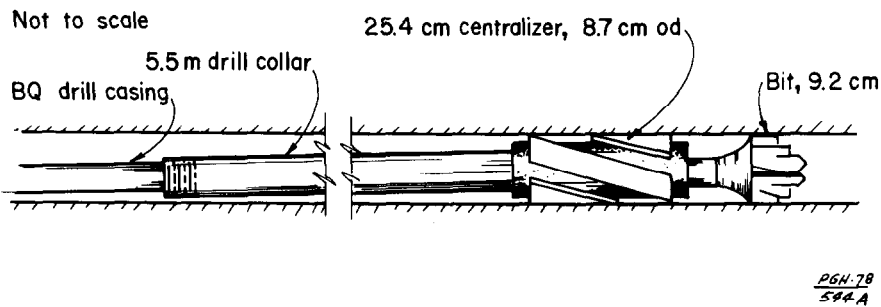


Fig. 2 - Modified drill string.

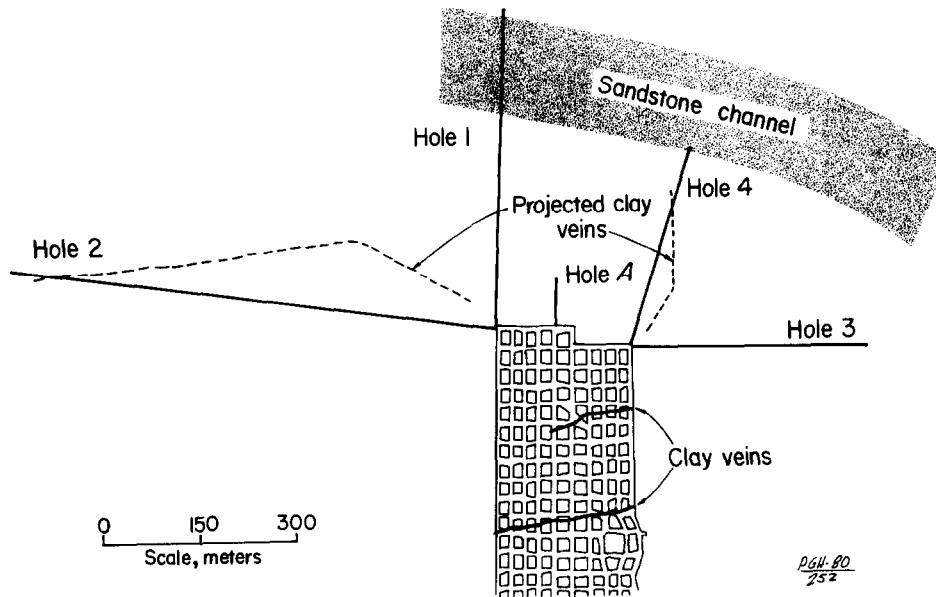


Fig. 3 - Map of sandstone channel and clay veins.

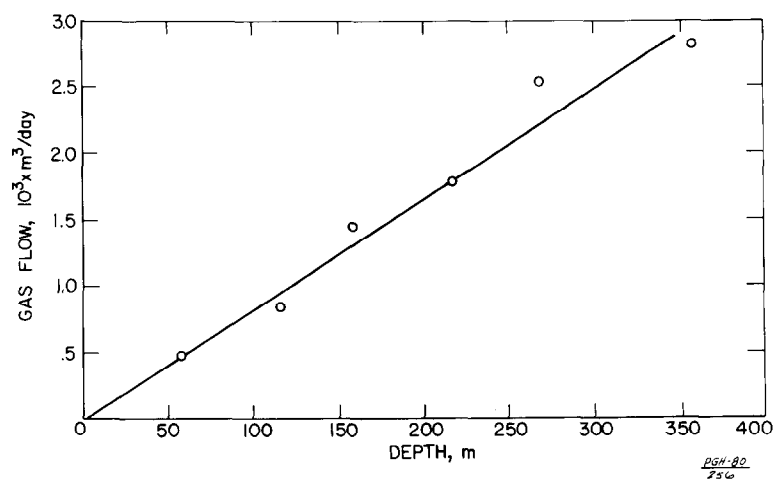


Fig. 4 - Hole 3 gas flow rates during drilling.

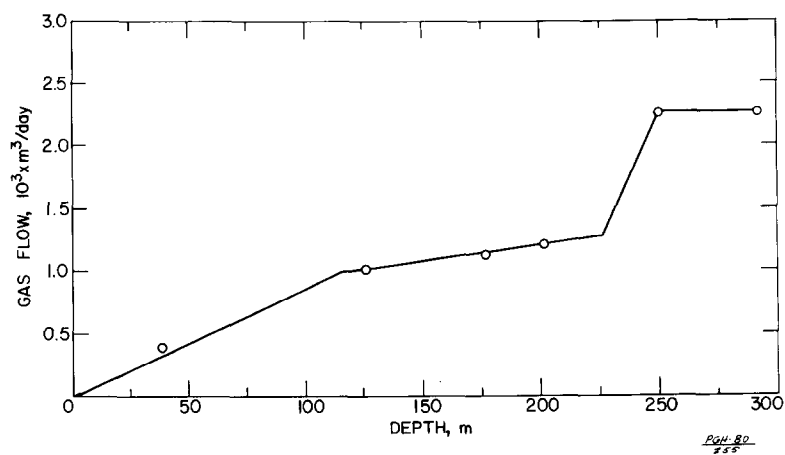


Fig. 5 - Hole 4 gas flow rates during drilling.

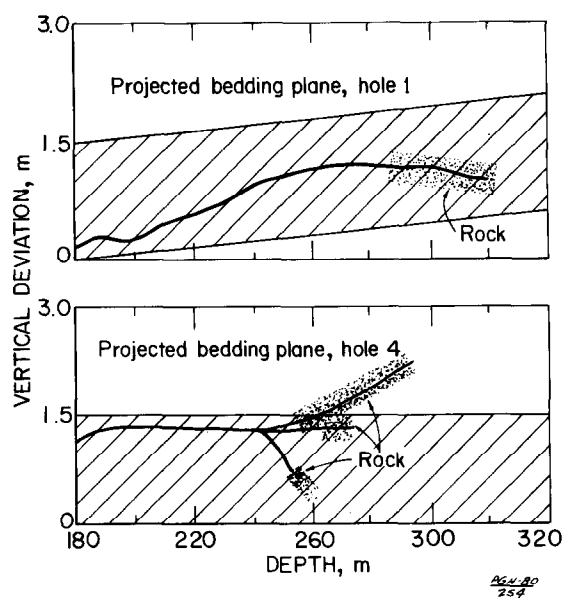


Fig. 6 - Location of holes 1 and 4 with respect to the coalbed.

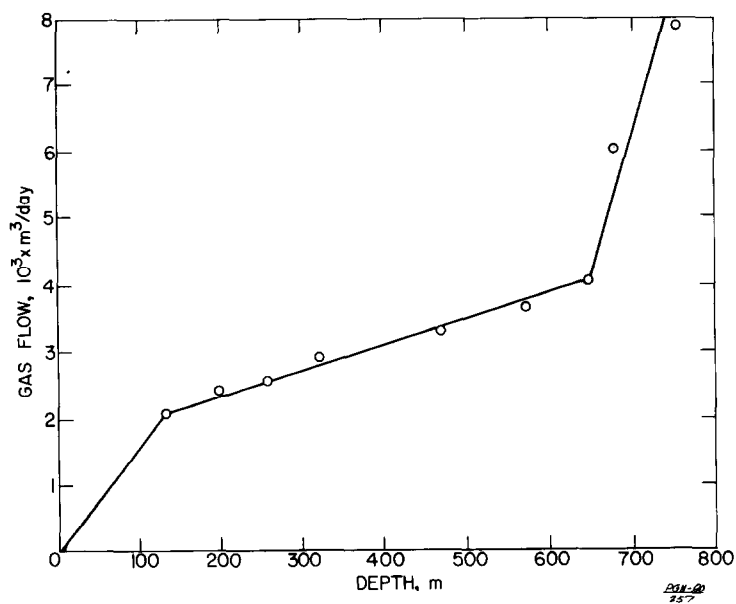


Fig. 7 - Hole 2 gas flow rates during drilling.

COMPLETION TECHNIQUES AND PRODUCTION DATA FROM VERTICAL METHANE DRAINAGE BOREHOLES, JAWBONE COALBED, DICKENSON COUNTY, VIRGINIA

by Peter F. Steidl, Michael A. Trevits, William P. Diamond,
U.S. Bureau of Mines.

This paper was presented at the 1980 SPE/DOE Symposium on Unconventional Gas Recovery held in Pittsburgh, Pennsylvania, May 18-21, 1980. The material is subject to correction by the author. Permission to copy is restricted to an abstract of not more than 300 words. Write: 6200 N. Central Expwy., Dallas, Texas 75206

ABSTRACT

Five vertical methane drainage boreholes have been completed in the Jawbone coalbed at the Clinchfield Coal Co. McClure No. 1 mine in Dickenson County, Va. Foam stimulation treatments were used to increase gas production from the boreholes. After 15 months the cumulative gas production from the first hole was 310,000 cu m (11 MMcf) with production averaging 700 cu m/d (25,000 cu ft/d).

INTRODUCTION

In November 1978 the Clinchfield Coal Co. began mining the Jawbone coalbed in the McClure No. 1 mine in Dickenson County, Va. Direct method desorption tests^{1,4} by the coal company of cores of the Jawbone coalbed indicated in place gas contents of more than 5.3 cu/gm (170 cu ft/ton) of coal. A cost-sharing contract for the drilling and stimulation of vertical degasification boreholes in advance of mining was initiated between the U.S. Bureau of Mines and the Clinchfield Coal Co. Subsequently, the contract was transferred to the Department of Energy with the Bureau of Mines providing technical management and planning. The five degasification boreholes planned for the first phase of the project have been drilled and foam-stimulated to increase gas production. Research in this project is directed toward optimizing both the spacing of boreholes and the stimulation treatment design for vertical degasification boreholes completed in the Jawbone coalbed.

DRILLING PROGRAM

A two-phase degasification project was designed with five boreholes to be completed in the first phase. The first borehole, DG-1A (fig. 1), was drilled close to initial mining so the induced fractures can be observed underground to make certain the mine roof was not damaged by the stimulation treatment. The other four boreholes were to be located in a square pattern about 3 years in advance of mining to allow more time for reducing the in situ gas content and evaluating the effectiveness of the system. After

results from the first phase have been evaluated, a decision will be made on implementing a second phase to drill a large pattern of boreholes in order to continue to reduce the methane hazard and ventilation cost, and to recover methane.

DRILLING

All boreholes were rotary-drilled with air percussion tools. Specific borehole completion data are presented in table 1. During initial drilling operations at boreholes DG-1A, 3B, 4, and 5D significant flows of water were encountered at depths ranging from 25.3 m (83 ft) to 61 m (200 ft). The rate of water inflow was significant enough to prevent controlled drilling activities. Therefore, each borehole was reamed to 203 mm (8 in.) diameter, and an intermediate string of casing was cemented in place from the surface through the water-bearing zones.

Rotary drilling was temporarily suspended in boreholes DG-1A, 2C, and 5D at a point just above the Jawbone coalbed to obtain a core of the coal zone by conventional coring. Air was used as the drilling medium during coring to minimize coalbed formation damage. The coal cores recovered from each well were tested by the Bureau of Mines for in situ gas content^{1,4}.

The results of desorption tests on the coal samples from borehole DG-1A show an estimated in situ gas content of 7.9 cc/gm (250 cu ft/ton). Desorption test results from coal samples collected at boreholes DG-2C and 5D show an estimated in situ gas content of 9.4 cc/gm (300 cu ft/ton). The higher gas content values from boreholes DG-2C and 5D may in part be due to the depth of the coalbed. The coalbed at these two boreholes is approximately 75 m (250 ft) deeper (table 1) than at borehole DG-1A. Bureau of Mines studies¹ have shown that the gas content of a coalbed generally increases at greater depths.

Boreholes DG-1A, 2C, and 5D were rotary-drilled to a total depth of approximately 9.1 m (30 ft) below the base of the Jawbone coalbed after coring was completed. No coal cores were recovered from boreholes

References and illustrations at the end of paper.

DG-3B and 4. These boreholes were drilled with air percussion tools to their total depth below the coalbed.

LOGGING AND CEMENTING PROCEDURES

The boreholes were geophysically logged using gamma ray, density, caliper, and directional surveys. The gamma ray and density surveys provided information on formation depths and rock types present in the boreholes. The caliper survey provided a log of the hole diameter which is used to estimate the amount of cement needed to secure the casing in place. Also an area of good uniform hole above the coalbed can be selected for setting the cement basket where it will seal against the borehole and prevent damage from cement reaching the coalbed below. Directional surveys are important for boreholes completed in minable coalbeds since the bottom hole location must be known before it is intercepted by mining.

The boreholes were cemented by using an automatic-fill basket cementing shoe on the bottom of the casing, a few feet above the coalbed. A tubing cementing basket was placed one joint above the cementing shoe to reduce cement weight on the shoe below. The cement utilized had thixotropic properties and was mixed at a slurry density of 3.2 kg (7 lbs) cement per 3.8 liters (1 gal) of water. The cementing shoe was drilled out after the cement had cured for at least 2 days.

STIMULATION TREATMENTS

Foam stimulation treatments were selected for these boreholes based on favorable results with foam treatments of other vertical coalbed degasification boreholes^{2,3,5}. Advantages of foam treatments include a quick recovery of treatment fluid, low viscosity, and low fluid loss. Summaries of each treatment are given in table 2. Treatment of holes DG-1A, 3B, 4, and 5D used an average of 12.7 cu m (80 bbl) water pad, 3.2 cu m (20 bbl) foam pad, 95.4 cu m (600 bbl) of 70 quality (70 percent nitrogen) foam injected at a rate of 1.9 cu m (12 bbl) /min, and 8,344 kg (18,400 lbs) of 20-40 mesh-sized prop sand. Surface pressure during breakdown on these treatments averaged 5,860 kPa (850 psig) and treating pressure averaged 6,720 kPa (975 psig).

A sandless foam stimulation treatment was used on hole DG-2C in an attempt to determine if proppant, which has caused many downhole pump problems on this and other vertical degasification projects, can be omitted from the treatment and maintain treatment effectiveness. Hole DG-2C was treated with 100 cu m (626 bbl) of 60 quality foam injected at a rate of 1.9 cu m (12 bbl) /min and a surface pressure of 6,890 kPa (1,000 psig). Since no proppant was used, fluorescent paint was added at a rate of 3.8 liter (1 gal) per 15.9 cu m (100 bbl) of foam to facilitate identification of the treated area when it is intercepted by mining. A comparison of production histories and underground observations of the treatment area of the five boreholes will be used to evaluate the effect of the variations in treatment design.

PRODUCTION

The boreholes were equipped with 6 cm (2-3/8-inch) diameter tubing, a downhole sucker rod pump, sucker rods, well head equipment, and a surface rocker-arm pump jack for water production. The pump for the near-mine borehole (DG-1A) was powered by an

electric motor, but the other four boreholes were equipped with methane-fueled engines because of the high cost of supplying electric power to the remote site. These boreholes were not produced continuously until April 1980, due to lack of experience with the methane engines, pump problems, and bad weather.

Production from borehole DG-1A started in August 1978, but pump problems delayed continuous production until October 1978. Gas production peaked in December 1979 at 1,230 cu m/d (43,500 cu ft/d) and began declining. Production through 1979 averaged 720 cu m/d (25,000 cu ft/d) (fig. 2). Cumulative production at the end of January 1980 was estimated at 310,000 cu m (11 MMcf) based on periodic orifice meter readings. Water production (fig. 2) was at the pump capacity of 15.9 cu m/d (100 bpd) for several days before it dropped to 4.7 cu m/d (30 bpd). After a year, it had declined to about 0.5 cu m/day (3 bpd).

The advance of mining to about 180 m (600 ft) from DG-1A reduced pressure in the vicinity of the borehole and increased permeability of the coalbed to gas. This allowed greater gas desorption from the coalbed and accounts for the production increase during August-October 1979 (fig. 2). Mining advanced to within 90 m (300 ft) of the borehole in late February 1979, and gas production declined to 450 cu m/d (16,000 cu ft/d) as the drainage area decreased.

Analyses of gas samples (table 3) show that after hole DG-1A had been produced for a month, most of the nitrogen injected in the stimulation treatment had been removed. Subsequent gas samples showed hole DG-1A was producing a pipeline quality gas averaging 97 percent methane. The results from an analysis of water from the borehole are as follows: Dissolved solids, 27,490 ppm; total iron, 208 ppm; calcium as CaCO_3 , 2,223 ppm; magnesium as CaCO_3 , 1,029 ppm; sodium as Na, 8,100 ppm; chloride as NaCl , 14,330 ppm; sulfate as SO_4 was not detected, and the pH was 7. Since the water is saline, it is pumped into a holding pond.

SUMMARY

Production data from the stimulated near-mine vertical borehole indicates that methane can be drained from the Jawbone coalbed in advance of mining.

Extended production histories will be obtained on the four boreholes located a greater distance from mining to better determine the potential for gas deliverability. The production history of borehole DG-2C which was stimulated without sand proppant will be compared with nearby boreholes stimulated with sand proppant to assess the effectiveness of sandless stimulation treatments in the Jawbone coalbed. Ventilation surveys will be conducted periodically as mining advances towards the four boreholes to evaluate the effect of pre-mining methane drainage on mine methane emissions. The use of engines fueled by methane from the coalbed to power the water pumping equipment will be evaluated for serviceability and durability for possible application for future production facilities.

ACKNOWLEDGMENTS

Thanks and appreciation are expressed for the cooperation of several individuals with the Clinchfield Coal Co., especially Mr. Timothy Wallace,

project engineer, who did most of the field work and planning for this project and collected much of the data.

REFERENCES

1. Diamond, William P.: "Evaluation of the Methane Gas Content of Coalbeds: Part of a Complete Coal Exploration Program for Health and Safety and Resource Evaluation". In Coal Exploration. Proceedings of the Second International Coal Exploration Symposium, Denver, Colorado, Oct. 1-4, 1978, Miller Freeman Publications, Inc., San Francisco, (1979) Volume 2, 211-227.
2. Lambert, Stephen W. and Trevits, Michael A.: "Methane Drainage Ahead of Mining Using Foam Stimulation Mary Lee Coalbed, Alabama". U.S. Department of Energy, RI-PMTC-3(79), (1979), 3-16.
3. Lambert, Stephen W., Trevits, Michael A., and Steidl, Peter F.: "Vertical Borehole Design and Completion Practices Used to Remove Methane Gas From Minable Coalbeds", U.S. Department of Energy, Report in review, 50-131.
4. McCulloch, Charles M., Levine, Jeffrey R., Kissell, Fred N., and Deul, M.: "Measuring the Methane Content of Bituminous Coalbeds". BuMines RI 8043, (1975), 3-10.
5. Steidl, Peter F.: "Foam Stimulation to Enhance Production from Degasification Wells in the Pittsburgh Coalbed." BuMines RI 8286, (1978), 5-7.

TABLE 1

COMPLETION DATA FOR METHANE DRAINAGE BOREHOLES

Completion data	DG-1A	DG-2C	DG-3B	DG-4	DG-5D
Depth of intermediate casing, m (ft)	57.6 (189)	Not used	63.7 (209)	57.6 (189)	25.3 (83)
Intermediate casing outside diameter, mm (inch)	159 (6.25)	Not used	159 (6.25)	159 (6.25)	159 (6.25)
Total depth of production casing, m (ft)	128.6 (422)	203.6 (668)	133.5 (438)	130.8 (429)	203.6 (668)
Production casing outside diameter, mm (inch)	114 (4.5)	114 (4.5)	114 (4.5)	114 (4.5)	114 (4.5)
Depth to Jawbone coalbed, m (ft)	129.5 (425)	206.0 (676)	135.3 (444)	131.1 (430)	205.1 (673)
Coalbed thickness, m (ft) ...	1.5 (5.0)	1.5 (5.0)	1.8 (6.0)	1.5 (5.0)	1.5 (5.0)
Total depth, m (ft) ^{1/}	140.2 (460)	216.4 (710)	146.6 (481)	141.7 (465)	216.4 (710)

^{1/} Ground level used as datum.

TABLE 2
SUMMARIES OF STIMULATION TREATMENTS

Hole no.	Treatment date	Depth to coalbed, m (ft)	Breakdown pressure, kPa (psig)	Treatment pressure, kPa (psig)	Injection rate, cu m/min (bbl/min)	Treatment volume, cu m (gal)	Sand weight, kg (lbs)
DC-1A	07-29-78	130 (425)	6,890 (1,000)	7,580 (1,100)	2.5 (16)	134 (35,300)	12,700 (28,000)
DC-2C	12-12-79	206 (676)	6,200 (900)	6,890 (1,000)	1.9 (12)	100 (26,300)	None
DC-3B	08-20-79	135 (444)	5,510 (800)	5,510 (800)	1.9 (12)	111 (29,400)	7,070 (15,600)
DC-4	09-27-79	131 (430)	6,200 (900)	6,890 (1,000)	1.6 (10)	111 (29,400)	7,170 (15,800)
DC-5D	12-12-79	205 (673)	4,830 (700)	6,890 (1,000)	1.6 (10)	92 (24,400)	6,440 (14,200)

TABLE 3
GAS ANALYSES, PERCENT

Hole no.	Date	H ₂	CO ₂	O ₂	Ar	N ₂	CH ₄	CO	C ₂ H ₆	C ₃ H ₈	C ₄ H ₁₀	C ₅ H ₁₂
DC-1A	08-22-78	ND ^{1/}	1.1	0.60	19.0	79.3	-	0.02	-	-	-	-
DC-1A	08-23-78	ND	1.1	.30	15.4	83.2	-	.02	-	-	-	-
DC-1A	11-01-78	ND	1.3	.06	4.4	94.1	ND	.13	0.001	0.002	-	Tr
DC-1A	06-01-79	-	1.5	.20	1.3	96.9	-	.15	-	-	-	-
DC-1A	06-15-79	-	1.5	.10	0.9	97.4	-	.16	-	-	-	-
DC-1A	08-24-79	-	1.5	.13	.9	97.4	-	.14	-	-	-	-
DC-1A	09-10-79	-	1.5	.13	.8	97.4	-	.15	-	-	-	-
DC-1A	09-27-79	-	1.6	.04	.5	97.8	ND	.13	-	-	-	-
DC-3B	09-27-79	-	0.8	.07	11.1	88.0	ND	.04	-	-	-	-

^{1/} Not detected.

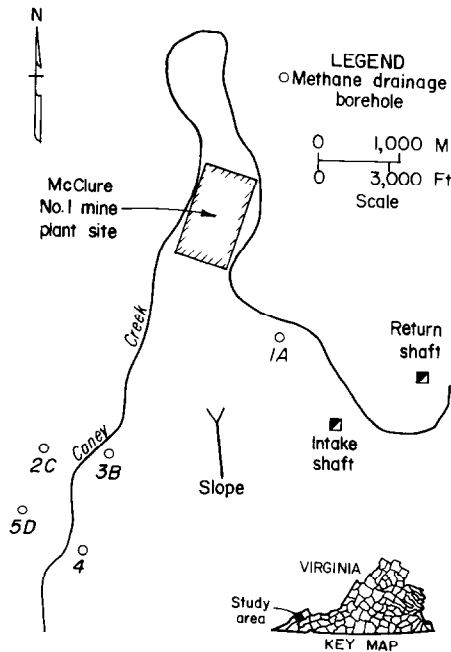


Fig. 1- Borehole location map.

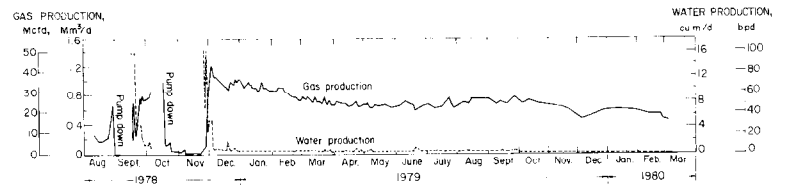


Fig. 2 - Production curves for borehole DG-1A.

P.S. 80
295

DETERMINING THE FEASIBILITY OF USING VERTICAL BOREHOLES TO DRAIN GAS FROM THE POCAHONTAS NO. 3 COALBED, BUCHANAN COUNTY, VA

by Michael A. Trevits, U.S. Bureau of Mines; and
Walter L. Richards and Hilmar A. Von Schonfeldt;
Occidental Research Corporation

This paper was presented at the 1980 SPE/DOE Symposium on Unconventional Gas Recovery held in Pittsburgh, Pennsylvania, May 18-21, 1980. The material is subject to correction by the author. Permission to copy is restricted to an abstract of not more than 300 words. Write: 6200 N. Central Expwy., Dallas, Texas 75206

ABSTRACT

In July 1979, a project was established to determine the feasibility of using vertical boreholes to degasify the Pocahontas No. 3 coalbed in advance of mining. To date, three methane gas drainage boreholes have been completed near the Virginia Pocahontas No. 5 mine in Buchanan County, Va. Various coalbed reservoir tests and in-situ stress determinations have been performed. Hydraulic stimulation treatments were designed and implemented at two boreholes, followed by preliminary gas and water production testing.

INTRODUCTION

In July 1979, a cost-sharing contract was established between the U.S. Bureau of Mines and Occidental Research Corporation to determine the feasibility of using vertical boreholes to degasify the Pocahontas No. 3 coalbed in advance of mining. The test area is located in Buchanan County, Va. where four relatively new deep mines are operating. This geographic area was chosen for the test because the Pocahontas No. 3 coalbed in Buchanan County, Va. ranks among the gassiest coalbeds in the United States. Moreover, the most recent tabulation of mine gas emissions ranks Buchanan County, Va. as number three in total mine emissions.

TEST SITE LOCATION

Three gas drainage boreholes have been drilled, along a straight line, ahead of developing longwall sections of Island Creek Coal Company's Virginia Pocahontas No. 5 Mine (fig 1). Borehole VVH No. 90 is located approximately 91 meters (300 feet) from the mine. Borehole VVH No. 91 is 564 meters (1,850 feet) from the mine and is furthest from mining operations. Borehole VVH No. 92 is positioned between No. 90 and No. 91, 335 meters (1,100 feet) from the mine. The distance between each borehole is approximately 236 meters (775 feet). The boreholes are located and engineered in such a manner as to directly interface with the coal company's gob ventilation program.

References and illustrations at end of paper.

Each borehole is numbered by order of chronological completion according to the coal company's system for vertical ventilation holes (VVH).

DRILLING AND CORING

The drilling phase of the project began on September 30, 1979, and was completed on October 27, 1979. Each borehole was rotary drilled 3 to 6 meters (10 to 20 feet) above the Pocahontas No. 3 coalbed, geophysically logged, cased, and cemented. Pertinent completion data are presented in table 1. The remaining portion of each borehole was then rotary drilled to just above the coalbed. At this point, all rock above the coalbed, the coalbed itself, and a small interval of the rock below the coalbed were cored for various testing procedures.

Conventional coring operations at VVH 90 were completed on October 7, 1979, and at VVH 91 on October 18, 1979. Samples of the coalbed and adjacent strata were recovered for rock mechanics testing. Coal samples were also collected by the Bureau of Mines for direct method gas content determination¹. The results of desorption tests conducted on coal samples from each borehole are presented in table 2. Gas content values generated from desorption testing show that the Pocahontas No. 3 coalbed in Buchanan County, Va., contains the highest amount of in-place gas observed to date for a bituminous coalbed in the United States.

A novel method of coal core recovery was attempted in VVH No. 92. On October 26-27, 1979, a specialized core barrel developed by Exxon¹ and modified by DOWDCO¹ was inserted into VVH No. 92 in an attempt to recover samples of the Pocahontas No. 3 coalbed under in-situ pressure conditions. Unfortunately, during rotary drilling operations, the top of the coalbed was inadvertently exposed. The borehole was immediately filled with water and refilled continuously as the drilling tools were removed.

^{1/} References to specific equipment or companies does not imply endorsement by the U.S. Government or Occidental Research Corporation.

Despite this undesirable downhole condition, coring operations proceeded and two pressurized cores were recovered. Details and results of the pressurized coring operation at VVH 92 are presented in Appendix A.

FORMATION TESTING

A coalbed reservoir evaluation study was conducted by TERRA TEK¹ to identify various coalbed reservoir parameters, measure in situ stress conditions and design hydraulic stimulation treatments. Summaries of tests conducted at each borehole follow:

VVH NO. 90

The coal interval was isolated by means of an inflatable straddle packer. Testing was initiated by isolating the coal interval and allowing coalbed pressure to build. After approximately 42 minutes, downhole pressure increased to 3,415 kPa (495 psig). Pressure was then released and gas flow to the surface was observed. Flow after the initial gas surge was 498 m³/d (17,600 cfd). After two hours of flow, downhole pressure increased from 365 to 1,020 kPa (53 to 148 psig) and the gas flow rate declined to 195 m³/d (6,900 cfd) as coalbed water began to fill the wellbore in the test interval. The coal interval was then retested and pressure build-up was monitored for four hours. Maximum pressure recorded was 3,430 kPa (497 psig). These data were used to determine an estimated coalbed "gas" permeability of 0.3 md and an extrapolated coalbed reservoir pressure of 3,847 kPa (558 psig).

Unique hydraulic fracture testing was also conducted at this borehole to determine in-situ stress conditions. Low injection rate, small volume water treatments or "mini-fracs" were performed on the rock immediately above the coalbed, on the coalbed, and on the rock exposed below the coalbed. During each treatment the test interval was isolated from other exposed formations with a straddle packer. Injection rates were 0.6 m³/h (2.5 gpm), total fluid volume injected was usually less than 0.04 m³ (10 gal). Pressure data were collected by using a downhole sensor. Minimum horizontal stresses as identified during the tests were: 13,450 kPa (1,950 psig) for the rock above the coalbed, 6,240 kPa (905 psig) for the coalbed, and 14,480 kPa (2,100 psig) for the rock below the coalbed.

After the mini-frac tests were completed, an impression packer was placed into the borehole to determine the attitude and height of the induced fractures. Results of the impression survey showed two small, faint, opposing vertical cracks approximately 0.9 to 1.8 meters (3 to 6 feet) above the top of the coalbed. Induced fractures in the coalbed were impossible to distinguish from natural fractures (cleat). No impression survey was made of the rock below the coalbed.

VVH NO. 91

The coal interval was isolated and pressure was allowed to build for 14 hours and 43 minutes. During this period, downhole pressure rose to a maximum of 4,470 kPa (648 psig). Pressure was then released, with no subsequent flow of gas. After a two hour flow period, downhole pressure increased to 1,900 kPa (276

psig) indicating that coalbed water was entering the wellbore in the test interval. The coal interval was retested while monitoring downhole pressure. After 4 hours and 46 minutes downhole pressure was 4,350 kPa (631 psig). These data were used to determine an estimated coalbed permeability of 5.3 md.

VVH NO. 92

After several unsuccessful attempts to conduct a pressure build-up/flow test, it was decided to perform a controlled-rate water injection test. The water injection test was used as a means of checking previous coalbed reservoir data collected at VVH Nos. 90 and 91. At an initial coalbed reservoir pressure of 4,745 kPa (688 psig), fresh water was injected into the coalbed. Injection continued for two hours at a rate of 0.2 m³/h (1 gpm). Following injection, the coalbed was isolated and a pressure decline was observed for about 15 hours. Coalbed permeability, derived from a data analysis, was estimated to be 8.6 md.

It is interesting to note that the permeability value obtained for VVH No. 92 is in close agreement with the 5.3 md value calculated for VVH No. 91. In both cases the results were generated from wells producing coalbed water under single-phase flow conditions. Permeability calculations for VVH No. 90, however, were based only on coalbed gas flow data during the testing period. No calculations were made for the flow of coalbed water during the test.

PRESTIMULATION PRODUCTION

Prior to hydraulic stimulation, VVH Nos. 91 and 92 were produced to determine prestimulation gas and water flow rates. Each testing period was limited to a maximum of 8 to 10 hours of water bailing each day. Production from VVH No. 91 was approximately 115 m³/d (4,000 cfd) gas and less than 0.2 m³/d (1 bpd) water. Production from VVH No. 92 was approximately 115 m³/d (4,000 cfd) gas and 1.7 m³/d (11 bpd) water.

STIMULATION

Hydraulic stimulation treatment designs were generated by TERRA TEK¹ for VVH Nos. 91 and 92. Incorporated into each design was the constraint to contain the induced fractures within the coalbed. This was a necessary prerequisite because mining will eventually intercept each borehole and the mine operator wanted to minimize the possibility of mine roof damage. The results of rock mechanics tests conducted on core samples, coalbed water permeability values and minimum horizontal stress conditions were incorporated in the treatment design. During the computer simulation, it was observed that induced fractures could be propagated in the coalbed provided downhole pressure did not exceed the pressure necessary to fracture the adjacent strata. An indication of the downhole pressure required to fracture adjacent rock was supplied from the "mini-frac" tests performed at VVH No. 90.

Foam was chosen as the stimulation fluid because of its compatibility with coal⁴. Other stimulation fluids, such as guar gum based gels were also considered, but previous degasification tests indicated that the gel system did not "break" as designed (because of low bottomhole temperatures)⁵⁻⁶.

A foam stimulation treatment was performed at VVH No. 90 on October 26, 1979. A small volume was utilized because of the proximity of mining (fig 1). It was felt that a larger volume of treatment fluid might propagate fractures into the mine area.

A high pressure water jet was used to cut a horizontal notch in the middle of the coalbed prior to hydraulic stimulation. The purpose of the notch was to penetrate any coalbed formation damage which might have occurred during coring of the coalbed or drilling of the borehole sump area. At the completion of notching operations, the tool was removed from the borehole and a straddle packer was used to isolate the coalbed.

A total of 0.6 m^3 (150 gals) of water was injected at 8,618 kPa (1,250 psig) surface pressure to breakdown and propagate fractures in the coalbed. Water injection was then temporarily halted and an instantaneous shut-in pressure of 7,585 kPa (1,100 psig) was observed. Pumping resumed at $17.2 \text{ m}^3/\text{h}$ (1.8 bpm) water with nitrogen gas at 57 std m^3/min (2,000 scf/min) and a foaming agent to create a foam pad. As foam was injected into the coalbed, surface pressures rose to 18,615 kPa (2,700 psig). Pumping was immediately stopped and the induced pressure dissipated quickly. Pumping resumed at $12.4 \text{ m}^3/\text{h}$ (1.3 bpm) water and 48 std m^3/min (1,700 scf/min) nitrogen. The resulting surface pressure was 16,550 kPa (2,400 psig). Foam quality, however, dropped from 75 pct to 67 pct. After injection of 1.7 m^3 (450 gals) of foam with no further rise in pressure it was decided to begin sand injection. Sand concentration began at $60 \text{ kg}/\text{m}^3$ (0.5 lb/gal) water and increased to a maximum of $300 \text{ kg}/\text{m}^3$ (2.5 lb/gal) during the final stage of the treatment. The treatment went to completion and the borehole was flushed with water. A total of 15.1 m^3 (4,000 gal) of foam containing 907 kg (2,000 lb) of 20- to 40-mesh sized sand was injected. Average surface pressure was 15,860 kPa (2,300 psig) at an injected rate of $12.4 \text{ m}^3/\text{h}$ (1.3 bpm) water or $38.2 \text{ m}^3/\text{h}$ (4 bpm) foam.

A stimulation treatment was attempted at VVH No. 91 on December 11, 1979. The coal interval was isolated with a straddle packer after successful hydro-slotting operations. Coalbed fracture propagation was initiated at $23.8 \text{ m}^3/\text{h}$ (2.5 bpm) and the resulting surface pressure was 6,895 kPa (1,000 psig). Pumping was then halted and a surface instantaneous shut-in pressure of 6,205 kPa (900 psig) was observed. The injection rate was then increased to $47.7 \text{ m}^3/\text{h}$ (5 bpm) for three minutes producing a surface pressure of 15,860 kPa (2,300 psig).

A foam pad was injected into the borehole at 84 std m^3/min (3,000 scf/min) nitrogen and $23.8 \text{ m}^3/\text{h}$ (2.5 bpm) water and foaming agent, however, because of a rise in surface pressure (maximum of 17,240 kPa (2,500 psig) observed), the nitrogen flow rate was reduced to 70 std m^3/min (2,500 scf/min). After 1.5 m^3 (400 gal) of water and accompanying foam were injected, surface pressure remained at 16,550 kPa (2,400 psig). The nitrogen and water rates were again adjusted to 59 std m^3/min (2,100 scf/min) and $21 \text{ m}^3/\text{h}$ (2.2 bpm). Treatment pressure essentially remained the same as the remainder of the foam pad was injected.

The addition of sand in the stimulation fluid began at a concentration of $90 \text{ kg}/\text{m}^3$ (0.75 lb/gal) for 3.0 m^3 (800 gal) of water or 4.5 m^3 (1,200 gal) foam. The sand concentration was then increased to $180 \text{ kg}/\text{m}^3$ (1.5 lb/gal). Shortly after this increase, water flow to the surface from the annular space between the tubing and casing was noted. This condition continued to increase until sand addition was suspended approximately 6 minutes later (sand addition was terminated because surface recording instruments indicated an approaching sand-out). Gas addition was also suspended and the borehole was flushed with water. Flow back equipment was installed and the lines were opened for flow; stimulation fluid also flowed to the surface through the annular space.

Total volume of treatment fluid utilized was 9.8 m^3 (2,600 gal) water or 17.0 m^3 (4,500 gal) foam and 680 kg (1,500 lb) of 20- to 40-mesh sand. It is assumed that only a fraction of this fluid was actually injected into the coalbed because of the flow to surface.

A combination of the following factors may be responsible for the problems experienced during the stimulation treatment at VVH No. 91. The $47.7 \text{ m}^3/\text{h}$ (5 bpm) injection rate during the water pad stage may have created excessive downhole pressure which may have initiated fractures in the adjacent strata. The 40 to 45 pct quality foam that was injected into the borehole had virtually no proppant-carrying capacity. As this fluid was exposed to the coalbed, a high percentage was probably lost by fluid leakoff. Sand, which was injected with the fluid, undoubtedly began to pack the created fractures and straddled wellbore interval. It is quite likely that the sand pack formed a barrier to fluid flow and caused a significant build-up of pressure in the remaining straddled wellbore space. In addition, the straddle packer may have induced high stresses in the strata exposed to the packer elements (areas above and below the coalbed). Perhaps because of these high stresses, once a fracture began to propagate in the strata above the coalbed near the packer element; it continued to grow upward past the element area and penetrated into the wellbore. The fractures were then widened as the stimulation fluid continued to flow.

Hydraulic stimulation of VVH No. 92 has yet to be attempted.

INDUCED FRACTURE CHARACTERIZATION

A downhole television camera was placed into VVH No. 90 prior to stimulation to identify any natural fractures penetrating the wellbore in the openhole interval. No fractures were observed in the strata above the coalbed. Numerous natural fractures (cleat) and gas bubbles were noted at the coalbed interval. A post-stimulation video survey showed numerous gas producing areas (bubbles) in the upper regions of the coalbed and immediate rock above. Unfortunately, the quality of the pictures were not as good as the prestimulation scan and, therefore, it was impossible to identify induced fractures in the rock immediately above the coalbed. A scan of the slotted coalbed interval vaguely showed a void space approximately 0.5 meters (1.5 feet) high and of

undetermined penetration depth. Further scans at lower levels were impossible because of poor picture quality. No video surveys were conducted at VVH 91 or 92 because of the limited results at VVH No. 90.

An impression packer was placed into VVH No. 91 to identify the openhole areas of the wellbore affected by the stimulation treatment. The impression packer was 3.0 meters (10 feet) in length; the bottom of the packer was located approximately 0.3 meters (1 foot) below the top of the coalbed. Details of the survey are presented in table 3.

A prestimulation impression survey of VVH No. 92 was performed to identify any natural fractures penetrating the wellbore in the openhole interval. The impression packer was 3.0 meters (10 feet) in length; the bottom of the packer was located 1.8 meters (6 feet) below the top of the coalbed. Results of the survey showed no vertical fractures intersecting the wellbore in the rock above the coalbed.

POST STIMULATION PRODUCTION

Installation of production equipment at VVH No. 90 was completed during December 1979. Gas flow from the well was initially measured on November 15, 1979 at 878 m³/d (31,000 cfd) without pumping water from the borehole. By the time production equipment was installed, gas flow rates had declined to 793 m³/d (28,000 cfd). Water production was 0.2 to 0.4 m³/d (1 to 2 bpd). Production continued to decline to 453 m³/d (16,000 cfd) of gas and less than 0.1 m³/h (0.5 bpd) of water observed at the end of February 1980. Analyses of the gas sampled from VVH 90 are presented in table 4.

Gas production data from VVH No. 91 has been obtained after only intermittent water bailing. The highest gas flow rate obtained to date was 241 m³/d (8,500 cfd). This value was noted after a bailing period of only one day. Continuous water pumping for extended periods has yet to be attained.

FUTURE PROJECT PLANS

Project plans call for restimulation of VVH No. 91 and a stimulation treatment at VVH No. 92. If the treatments proceed as planned, fracture characterizations and production will take place shortly thereafter. Results of the stimulation treatment at VVH No. 91 necessitated casing changes in VVH Nos. 91 and 92. An intermediate string of 118 mm (4.5 inches) OD casing has been cemented through the rock interval above the Pocahontas No. 3 coalbed. This casing configuration permits only the Pocahontas No. 3 coalbed and strata below to be exposed to the wellbore. Additionally, the need for a straddle packer will be eliminated in future stimulation treatments at VVH Nos. 91 and 92.

CONCLUSIONS

1. Because of unforeseen project delays, gas production data from vertical gas drainage boreholes completed in the Pocahontas No. 3 coalbed are very limited.
2. Results of coring operations show the Pocahontas No. 3 coalbed in Buchanan County, Va. to contain the highest measured in-place gas

content for a bituminous coalbed in the United States.

3. Various tests of the Pocahontas No. 3 coalbed reservoir have been conducted to determine: permeability, reservoir pressure, in situ stress conditions (adjacent strata and the coalbed), and prestimulation production potential.
4. The "mini-frac" treatments were the first such tests to be utilized in association with methane drainage research. The resulting data have provided the means of unique stimulation design which addresses the specific requirements of the mine operator.
5. The control of bottom-hole treating pressure during hydraulic stimulation of mineable coalbeds is necessary in order to minimize propagation of fractures into adjacent strata.

ACKNOWLEDGMENTS

Grateful acknowledgment is extended to the following for their contributions and cooperation in this endeavor: Island Creek Coal Company, Occidental Research Corporation, Occidental Exploration and Production Co., and the U.S. Bureau of Mines.

REFERENCES

1. Irani, Meherwan C., Jacqueline H. Jansky, Paul W. Jeran, and Gloria L. Hassett: "Methane Emission from U.S. Coal Mines in 1975 - A Survey", BuMines IC 8733 (1977).
2. McCulloch, Charles M., Jeffrey R. Levine, Fred N. Kissell, and Maurice Deul: "Measuring the Methane Content of Bituminous Coalbeds", BuMines RI 8043 (1975).
3. Ibid. McCulloch.
4. Lambert, Stephen W., Michael A. Trevits, and Peter F. Steidl: "Vertical Borehole Design and Completion Practices Used to Remove Methane Gas from Mineable Coalbed", DOE RI (In review) (1980).
5. Lambert, Stephen W., and Michael A. Trevits: "Methane Drainage: Experience with Hydraulic Stimulation Through Slotted Casing", BuMines RI 8295, (1978).
6. Ibid. Lambert, Trevits, and Steidl.

APPENDIX A: PRESSURIZED CORING OPERATIONS AT VVH NO. 92^{2/}

On October 26, 1979, a DOWDCO^{1/} pressure barrel was assembled, tested, and placed into VVH No. 92. Coring operations began after establishing a fresh water circulation rate of 32.9 m³/h (145 gpm).

- ^{2/} In-place gas content determinations and all related experiments were performed by Geochem Research Incorporated (reference does not imply endorsement).

Coring proceeded following a normal schedule at a penetration rate of 0.1 m/min (0.4 ft/min). After approximately 2.7 meters (9 feet) of core was cut, a steel ball was dropped into the drill string, actuating a pressure trip mechanism in the pressure barrel and sealing it from pressure loss. The pressure barrel was then removed from the hole and brought to the surface where the internal barrel pressure was measured. A value of 6,345 kPa (920 psig) was observed indicating the tool had performed as designed.

The pressure barrel was then flushed with gelled kerosene to remove any fresh water drilling fluids contained between the inner and outer barrel of the tool. The entire apparatus was placed in dry ice and frozen for 6 to 7 hours. After this period, the pressure barrel was removed from the dry ice and the free gas trapped inside the inner barrel was released into an auxiliary container. A sample of the gas in the auxiliary container was taken to determine the composition of the pressure barrel reservoir gas.

The pressure barrel was then disassembled and the inner barrel was removed from the outer barrel and cut into 0.3 meter (1 foot) sections. The core sections which contained at least some portion of coal were placed for desorption testing into metal canisters which has been purged with argon gas. A total of four core samples were retained in canisters.

Immediately after canister sealing, a gas sample was taken to determine the composition of the canister headspace gas. Canister pressure was monitored closely as gas desorbed from the core samples. Headspace gas samples were taken whenever canister pressure reached approximately 13.8 kPa (2 psig). This procedure, however, was not used during transport of the canisters. Whenever a gas sample was taken, the canister lid was removed and the canister was purged with argon gas or breath. The canister lid was

immediately resealed and the purging process was repeated. The frequency of gas sampling depended on the rate of canister pressure increase. Air temperature and canister pressure at the time of gas sampling were noted. All gas samples were analyzed by gas chromatography.

The concentrations of hydrocarbon gases, nitrogen, and carbon dioxide in the canister (expressed as cm^3/g of coal) for each time increment were then calculated. Variations in canister pressure and air temperature were accounted for in the calculations. Other factors included in the calculations were the response of the gas chromatograph detector to known hydrocarbon, nitrogen or carbon dioxide mixtures; the volume of the core and gas sample containers; the volumes and densities of coal and shale; and the volume of water included with each core sample. After desorption of the core samples was completed, a ten gram sample of coal from each core sample was crushed in a sealed container and the headspace gas was sampled and analyzed. All core samples were dried in air and the total sample was weighed. Shale was separated from coal and the weight of coal in each sample was determined.

The results of the pressure coring test completed at VVH No. 92 show the Pocahontas No. 3 coalbed to have a maximum in-place methane content of 15 cm^3/g (480 ft^3/ton). The difference between this value and the maximum in-place values obtained from VVH Nos. 90 and 91 (table 2) is attributed to the inadvertent exposure of the coalbed during preliminary drilling operations at VVH No. 92. The drilling operations utilized foam as the circulating medium to facilitate cuttings removal. The medium could not exert sufficient pressure to prevent gas desorption from the exposed coalbed. Therefore, an undetermined volume of gas undoubtedly desorbed from the coalbed and was lost to the atmosphere.

TABLE 1
COMPLETION DATA FOR METHANE DRAINAGE BOREHOLES

Completion data	VVH No. 90	VVH No. 91	VVH No. 92
Total depth of production casing, m (ft).....	560.5 (1,839)	666.0 (2,185)	644.7 (2,115)
Production casing outside diameter, mm (inch).....	178 (7.0)	178 (7.0)	178 (7.0)
Length of liner, m (ft).....	Not used	20.1 (66.0)	20.1 (66.0)
Liner outside diameter, mm (inch).....	Not used	114 (4.5)	114 (4.5)
Depth to Pocahontas No. 3 coalbed, m (ft) ^{1/}	565.1 (1,854)	671.8 (2,204)	648.9 (2,129)
Coalbed thickness, m (ft).....	1.8 (6)	2.1 (7)	2.0 (6.5)
Total depth, m (ft) ^{1/}	585.2 (1,920)	690.7 (2,266)	667.8 (2,191)

1/ Surface casing collar used as datum.

TABLE 2
BUREAU OF MINES DIRECT METHOD TEST RESULTS FOR COAL SAMPLES
RECOVERED FROM BOREHOLES NOS. 90 AND 91

Vertical ventilation hole No.	Sample interval, ^{1/} m (ft)	Preliminary gas content ^{2/} , cm ³ /g	Remaining gas, ^{3/} cm ³ /g	Final gas content, ^{4/} cm ³ /g (ft ³ /ton)
90 ^{5/}	567.8 (1,863.0) to 568.2 (1,864.3)	20.2	1.3	21.5 (685)
90	568.7 (1,865.9) to 569.5 (1,868.3)	13.4	1.5	14.9 (475)
90	569.5 (1,868.3) to 570.0 (1,870.0)	13.5	1.2	14.7 (470)
91 ^{6/}	671.6 (2,203.6) to 671.9 (2,204.6)	19.1	1.2	20.3 (650)
91	671.9 (2,204.6) to 672.4 (2,205.9)	14.8	1.0	15.8 (505)
91	672.4 (2,205.9) to 672.8 (2,207.5)	19.3	1.0	20.3 (650)
91	673.2 (2,208.5) to 673.5 (2,209.6)	16.2	1.2	17.4 (560)

1/ Surface casing collar used as datum.

2/ Includes lost gas plus desorbed gas.

3/ Value obtained by crushing coal sample in a ball mill when desorbed gas equalled 0.01 cm³ for seven days.

4/ Includes preliminary gas content plus remaining gas.

5/ Pocahontas No. 3 coalbed measured from 565.1 meters (1,854 feet) to 566.9 meters (1,860 feet) below datum.

6/ Pocahontas No. 3 coalbed measured from 671.7 meters (2,203.6 feet) to 673.8 meters (2,210.6 feet) below datum.

TABLE 3
DESCRIPTION OF POST-STIMULATION IMPRESSION PACKER SURVEY AT VVH 91

Depth, m (ft) ^{1/}	Description and remarks ^{2/}
668.7 (2,194) to 669.3 (2,176)	Impression packer torn and abraded away from the element. Possibly caused by entry into casing.
669.3 (2,196) to 669.6 (2,197)	Continuous vertical fracture, fracture appears to have become inclined by approximately 10 degrees to borehole axis.
669.6 (2,197) to 670.3 (2,199)	Vertical fracture continuous, multi-branched vertical fractures (not numerous). Fracture width approximately 12.7 mm (0.5 inch).
670.3 (2,199) to 671.5 (2,203)	Multi-branched vertical fracture, not continuous, composed of intersecting branches. Fracture width approximately 12.7 to 19.1 mm (0.5 to 0.75 inch).
671.5 (2,203) to 671.8 (2,204)	Faint impression of cleat structure of coal seam. Vertical fracture in coal seam.

1/ Surface casing collar used as datum.

2/ Description and remarks provided by J. Mark Gronseth, Project Engineer, from TERRA TEK, (reference does not imply endorsement).

TABLE 4
ANALYSES OF GAS SAMPLED FROM VVH NO. 90 ON JANUARY 29, 1980

Sample number	Mole percent (volume percent), dry basis						
	CH ₄	C ₂ H ₆	C ₃ H ₈	Iso-C ₄ H ₁₀	CO ₂	N ₂	O ₂
1	98.17	0.345	0.015	0.001	0.950	0.492	0.030
2	98.20	.346	.014	.001	.981	.450	.006

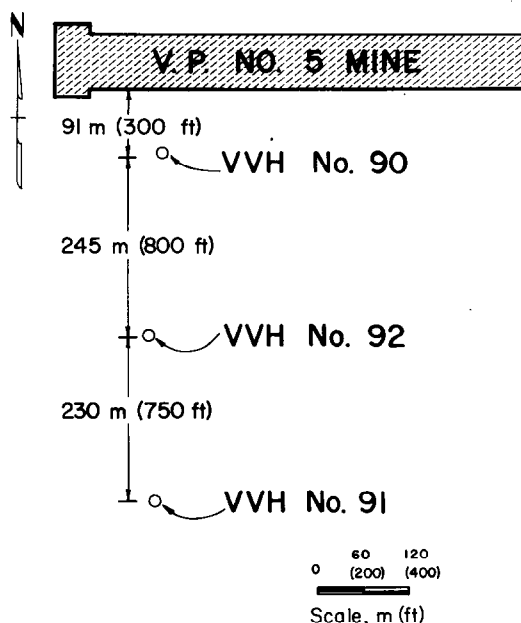


Fig. 1 - Position of test boreholes in relation to active mining at the time of drilling completion.

METHANE DRAINAGE FROM THE MARY LEE COALBED, ALABAMA, USING HORIZONTAL DRILLING TECHNIQUES

by John H. Perry, Leonard J. Prosser, Jr.,
Joseph Cervik, U.S. Bureau of Mines

This paper was presented at the 1980 SPE/DOE Symposium on Unconventional Gas Recovery held in Pittsburgh, Pennsylvania, May 18-21, 1980. The material is subject to correction by the author. Permission to copy is restricted to an abstract of not more than 300 words. Write: 6200 N. Central Expwy., Dallas, Texas 75206

ABSTRACT

The Bureau of Mines has developed several techniques for draining methane from coalbeds in advance of mining. Drilling long horizontal holes from an underground location is one of these techniques which has been successfully demonstrated in the Pittsburgh and Sunnyside coalbeds. A similar project was successfully conducted in the Mary Lee coalbed at Jim Walter Resources Inc., No. 4 mine. In a year about 1.13 million m^3 (40 MMcf) of methane was recovered from the coalbed.

INTRODUCTION

The Bureau of Mines has demonstrated that large quantities of methane can be drained from underground coalbeds through long horizontal holes drilled into the coalbed^{3-4,6}. There are 3 primary factors that determine the amount of gas that can be drained from a coalbed: The volume of methane in the coal, the in-situ pressure, and the permeability. Coalbeds which have relatively high permeability and in-situ pressure can be successfully drained of their methane. The Pittsburgh coalbed is a prime example. Three demonstration projects in this coalbed have removed more than 51 million m^3 (1.8 billion cubic feet) of methane, and about 19.8 million m^3 (700 MMcf) of this gas has been sold³⁻⁴. A single project in the Sunnyside coalbed in Utah removed 1.0 million m^3 (35 MMcf) of methane from that coalbed⁶.

There is a correlation between the volume of gas per ton of coal and the depth of the coalbed. The greater the depth the more methane there will be in a ton of coal⁵. The deepest coal mines in the United States are working the Mary Lee coalbed at a depth of 610 meters (2,000 feet). The Mary Lee coalbed is part of the Black Warrior coal basin which encompasses more than 2,100 km^2 (800 square miles) of Jefferson, Walker, and Tuscaloosa Counties, Alabama (fig 1). The overburden of the Warrior basin varies from 0 to 760 meters (2,500 feet). One area of the basin has an overburden change from 0 to 456 meters

(1,500 feet) within a distance of 800 meters (2,680 feet). The overburden at Jim Walter Resources Inc.'s No. 4 mine is 608 meters (2,000 feet). It has been estimated that there are 198 million m^3 (700 billion cubic feet) of methane in the Mary Lee coalbed. Almost 90 pct of this gas is held in the coal where the overburden exceeds 304 meters (1,000 feet). The average in-situ volume of methane per ton of coal at the No. 4 mine is about 16.7 m^3 (590 ft^3)².

DRILL SITE

This project was designed to degasify a portion of the Mary Lee coalbed from the northeast corner of the No. 4 mine (fig 2). The Mary Lee coalbed is divided into two benches at this location. The upper bench is about 0.5 meters (20 inches) thick and the lower bench about 1.5 meters (5 feet) thick. The binder separating the two is about 0.6 meters (2 feet) thick.

Figure 1 shows the location of the two degasification holes as they were drilled into the lower bench. The first hole was drilled in a N 15° W direction, perpendicular to the face cleat, maximizing the gas flow. This hole was drilled to a depth of 308 meters (1,010 feet). The second hole was drilled to a depth of 165 meters (540 feet) parallel to the face cleat.

CONTROL DURING DRILLING

Normally, with the standard drill string (fig 3) the path of the bit is controlled three ways: (1) By the pressure applied to the bit, (2) by the rotational speed of the bit, and (3) by the location of the centralizers with respect to the heavy NQ drill collar. The drill collar is 5.5 meters (18 feet) long and weighs 90.6 kg (200 pounds). It stiffens the drilling assembly and adds weight to the bottom side of the hole. Depending on conditions, two sizes of drag bits are used, 88.9 mm (3-1/2-inch) or 91.3 mm (3-5/8-inch) in diameter. Drilling with the 91.3 mm (3-5/8-inch) bit tends to wear the bottom side of the hole and arc downward. To compensate for this, more thrust is required to keep the hole horizontal

References and illustrations at end of paper.

with a 91.3 mm (3-5/8 inch) bit than with a 88.9 mm (3-1/2 inch) bit. Table 1 depicts the general drilling parameters used with a 88.9 mm (3-1/2 inch) bit.

The first 36 meters (120 feet) of hole 1 was drilled using these established drilling procedures. At 36 meters (120 feet) the drilling assembly became jammed in the hole. Two possible explanations for jamming are collapse of the hole and squeezing of the hole. Hole collapse is evident when drilling produces excessive coal cuttings and large coal fragments of coal. These coal fragments from the resulting oversized hole wedge between the centralizers and sides of the hole. Normally water is used to flush the coal cuttings out of the hole, but when collapse occurs and the cuttings become wedged around the drill string the water can become blocked in the hole causing a further buildup of cuttings. Hole collapse occurs predominantly in soft coal such as the Mary Lee.

Hole squeezing is attributed to overburden pressure. In this case, the hole flattens due to vertical stresses and the drill string becomes stuck in the undersized hole. The Mary Lee is both a soft and deeply deposited coal, and squeezing and collapse can occur in the same hole.

Because of this situation, an alternative drill string was used in the Mary Lee coalbed. A string consisting of only a 76.2 mm (3 inch) drag bit and BQ rod was used (fig 4). The smaller diameter bit produces less cuttings. Removal of the drill collar and centralizers eliminates the larger items which could be jammed by either squeezing or collapse of the hole. As the hole is drilled beyond the disturbed zone around the mine opening, the potential for collapse and squeezing decreases.

The final 271 meters (890 feet) of hole 1 was drilled with only a 76.2 mm (3-inch) bit and BQ drill rod. Controlling the path of the bit in the vertical plane was attempted by adjusting bit thrust and rotation, without success. The hole 1 trajectory seemed to follow the bottom of the coal, bouncing along the harder floor rock (fig 5).

In an attempt to develop control techniques for drilling the Mary Lee, hole 2 was drilled using two different strings. The first 116 meters (380 feet) of hole 2 was drilled using a 66.7 mm (2-5/8 inch) bit instead of the 76.2 mm (3-inch) bit. This string was tried based on control techniques previously used with the standard drill string. It was hoped the BQ rod, 55.6 mm (2-3/16-inch) OD, would act as a centralizer when combined with the 66.7 mm² (2-5/8 inch) bit. However, this was not the case, and the hole followed the bottom of the coalbed. The second drill string consisted of a 66.7 mm (2-5/8-inch) bit, 63.5 mm (2-1/2-inch) centralizer and BQ rod. Figure 6 illustrates how the centralizer cocks the bit upward in the hole. This drill string showed positive results with an inclination change of +1.7° in 15 meters (50 feet) of drilling. The last 46 meters (150 feet) of hole 2 was drilled using this centralized combination. Table 2 is a log of hole 2. Because of the possibility of hole collapse or squeezing, the entire drill string was pulled from the hole at the end of each shift. When, at a depth of 165 meters (530 feet), the drill string could only be reinserted to a depth of 137 meters (450 feet),

the hole was drilled to its original depth when it collapsed or squeezed a second time trapping the drill string.

PLOTTING HOLES

It is important to know the trajectory of the hole. The vertical changes dictate the drilling parameters take used to keep the hole in the coalbed (fig 5). Combining this data with information as to when the hole hits either the roof or floor, the slope of the coalbed can accurately be defined. Also any wants, rolls, or clay veins encountered can be mapped.

It is also important to plot the hole in the horizontal plane. This plot is transferred to the mine map. Mine management will then know when to seal the hole before it is mined through. Horizontal holes tend to curve left or right. In some cases a hole may turn to the left and then deflect to the right. Figure 7 shows the portion of the 308 meter (1,010 feet) hole as plotted from survey information and the points where it was mined through. There was less than 1.5 meters (5 feet) difference between the location of the hole as plotted and the intercepted locations.

HOLE 1 GAS FLOW AND PRESSURE MEASUREMENTS

Hole 1 (308 meter) was shut-in and an in-situ pressure monitoring hole was drilled 30 meters (100 feet) to its left. This hole was grouted so that the in-situ pressure at a depth of 30 meters (100 feet) could be monitored. Both holes were allowed to reach equilibrium pressures before hole 1 was opened to flow. Hole 1 reached a steady pressure of 484 kPa (70 psig), and the in-situ pressure leveled off at 155 kPa (22.5 psig).

Once hole 1 was opened, its flow and the in-situ pressure began to decline rapidly. The gas flow from hole 1 dropped from an initial value of 5,660 m³/d (200,000 cfd) to 4,386 m³/d (155,000 cfd) in 18 days. The in-situ pressure dropped from 155 kPa (22.5 psig) to 62 kPa (9.0 psig) during the same time period. Both the in-situ pressure and gas flow continued to decline slowly for the next 6 months. The gas flow seemed to level off between 2,122 and 2,038 m³/day (75,000 and 72,000 cfd). The in-situ pressure declined to 11.9 kPa (1.7 psig). The gas flow was at a minimum when section 3 was 152 meters (500 feet) from hole 1. The flow reading taken the day before the hole was grouted and mined through was 1,925 m³/day (68,000 cfd). Figure 8 shows the flow and pressure data for hole 1. Total gas flow from hole 1 for the year was 1.13 million m³ (40 MMcf). The percentage of methane in this gas was between 98 and 99 pct. This remained constant for the life of the hole. The gas was analyzed to have a heat rating of 36.5 Kjoules/m³ (990 Btu/cu ft).

REDUCTION OF FACE EMISSIONS

Ventilation surveys of the No. 3 section show that hole 1 effectively reduced the methane emissions from the faces of that section. When the section was 256 meters (840 feet) from the hole there was a flow of 4.9 m³/min (172 cfm) from the faces. At a distance of 12 meters (40 feet) the flow was 1.9 m³/min (67 cfm), a 60 pct reduction. When the section advanced

36 meters (120 feet) beyond the hole, face flow increased to 2.8 m³/min (100 cfm) of methane. Figure 9 shows the methane history of the No. 3 section as it approached and passed through the 308 meter (1,010 feet) hole.

CASING HORIZONTAL HOLES

To successfully degasify a coalbed not only does the hole have to be drilled but it has to remain open to permit gas flow. The Bureau is now adapting some of the hole casing techniques used in vertical drilling to horizontal drilling of coal. The major departure from the vertical techniques is the use of plastic for the casing. The primary reason for using plastic is that it can be safely mined through when the coal is extracted. Another reason is that it is lighter than steel and therefore easier to handle in the confines of an underground drill site. The Bureau is now testing procedures utilizing casing advancers and underreamers. The casing advancers and underreamers are standard NW casing size.

For both of these techniques the casing is advanced during drilling. When the casing advancer is used the 3-inch schedule 40 plastic pipe is drilled into the coalbed up to 60 meters (200 feet) beyond the disturbed zone around the mine opening. The degasification hole is then completed to depth. The underreamer bit has wings that expand to drill an oversize hole so the plastic can follow directly behind. The entire length of the hole can be cased with slotted plastic pipe for degasification.

CONCLUSIONS

The Mary Lee coalbed can be degasified through the use of long horizontal holes. The advantages are two fold: (1) Vast amounts of methane that can be removed, and (2) reduction of methane emissions at the faces of any section mining through the degasified zone. Jim Walter Resources, Inc. is now planning a degasification program for the No. 4 mine.

REFERENCES

1. Cervik, J., H. H. Fields, and G. N. Aul. Rotary Drilling Holes in Coalbeds for Degasification. BuMines RI 8097, 1975.
2. Diamond, W. P., G. W. Murrie, and C. M. McCulloch. Methane Gas Content of the Mary Lee Group of Coalbeds, Jefferson, Tuscaloosa, and Walker Counties, Ala. BuMines RI 8117, 1976.
3. Fields, H. H., J. Cervik, and T. W. Goodman. Degasification and Production of Natural Gas from an Air Shaft in the Pittsburgh Coalbed. BuMines RI 8173, 1976.
4. Fields, H. H., J. H. Perry, and M. Deul. Commercial-Quality Gas From a Multipurpose Borehole Located in the Pittsburgh Coalbed. BuMines RI 8025, 1975.
5. Irani, M. C., E. D. Thimons, T. G. Bobick, M. Deul, and M. G. Zabetakis. Methane Emissions from U.S. Coal Mines, a Survey. BuMines IC 8558, 1972.
6. Perry, J. H., G. N. Aul, and J. Cervik. Methane Drainage Study in the Sunnyside Coalbed, Utah. BuMines RI 8323, 1978.

TABLE 1

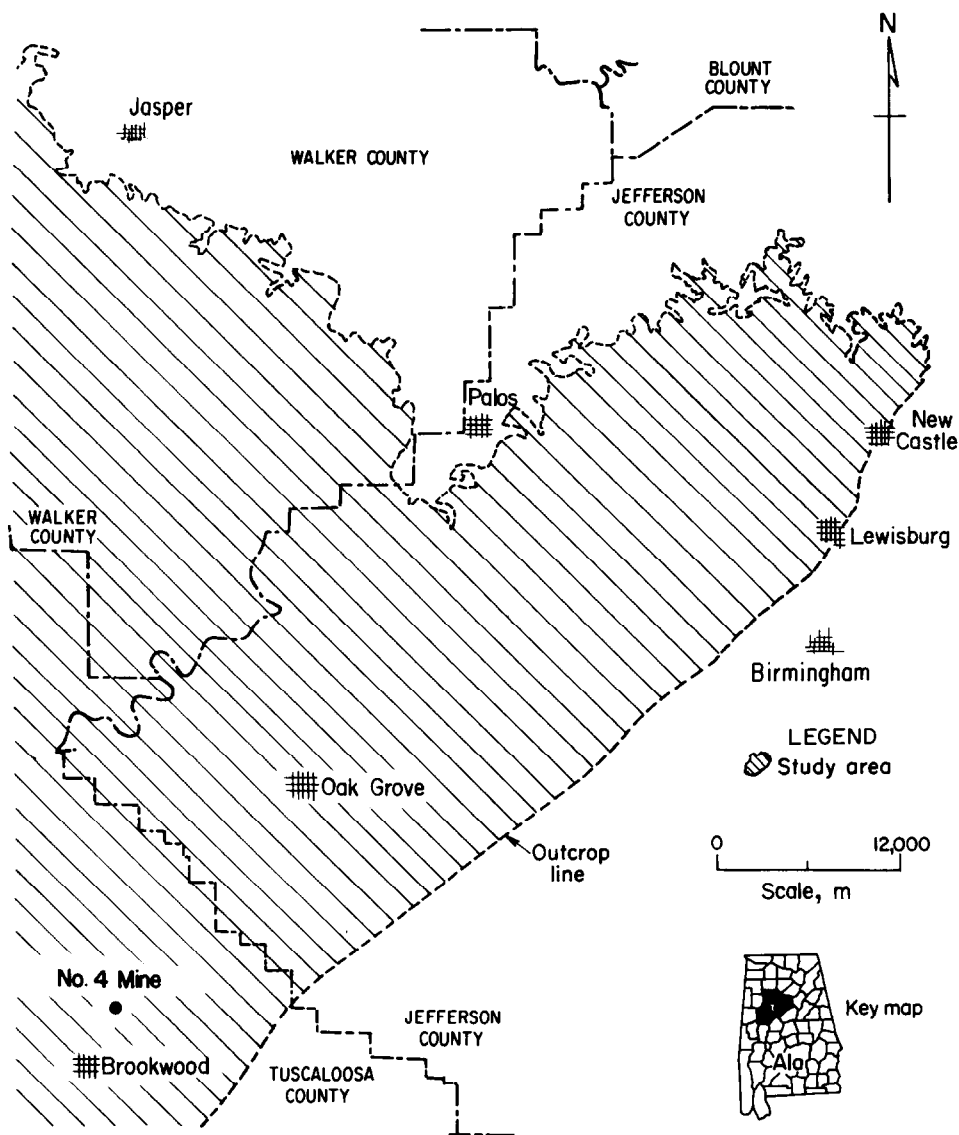
GENERAL DRILL PARAMETERS

88.9 mm bit, drill collar, centralizers, BQ rod.

Thrust, KNewtons	Bit rotation, (rpm)	Hole trajectory
3.5	600	Downward
4.0-5.0	400-600	Holding level
5.2	400	Upward

TABLE 2
DRILL LOG HOLE 2

Depth, meters	Vertical inclination degrees	Thrust KNewtons	RPM	Drill string and remarks
100	89.9	-	-	6.67 cm bit only
116	89.8	14.2	62	Bit & centralizer coal
131	91.5	15.1	75	Bit & centralizer coal
134	-	15.1	75	Bit & centralizer coal
137	-	11.3	100	Gray cutting
146	89.5	11.3	100	Bit & centralizer coal



PGH-75
625

Fig. 1 - Warrior Basin, Alabama.

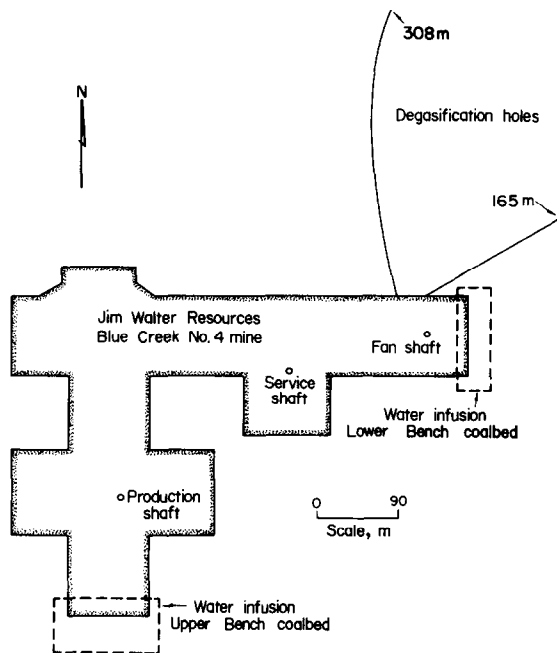


Fig. 2 - Drill site No. 4 mine.

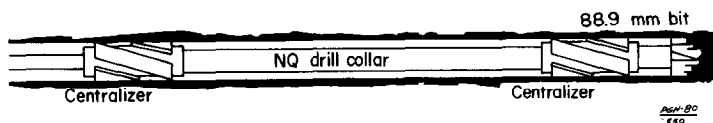


Fig. 3 - Drill string, 2 centralizers, 5.5 meter (18ft) NQ drill collar.



Fig. 4 - 76.9 mm (3inch) bit drill string.

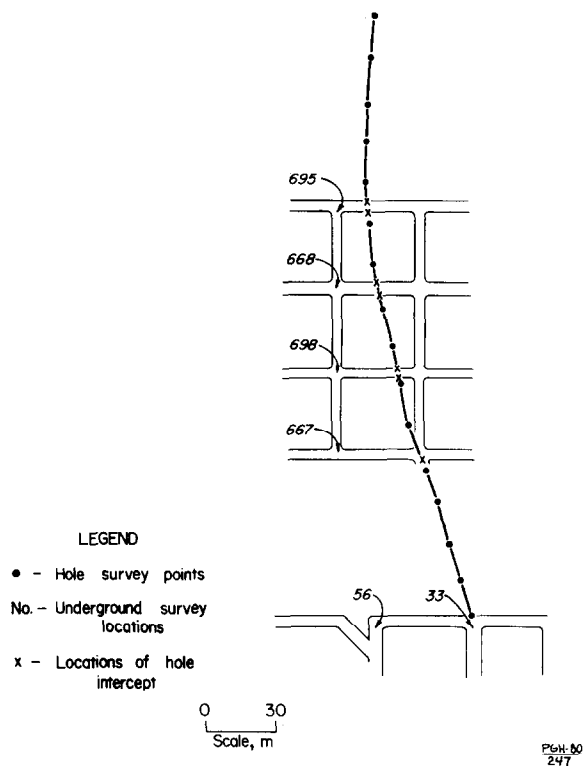


Fig. 5 - Plot of hole No. 1.

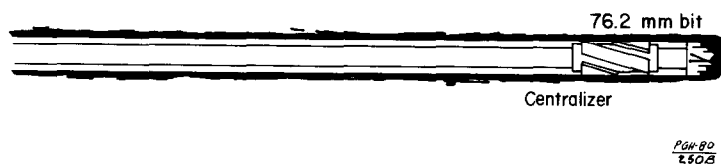


Fig. 6 - Centralized drill string.

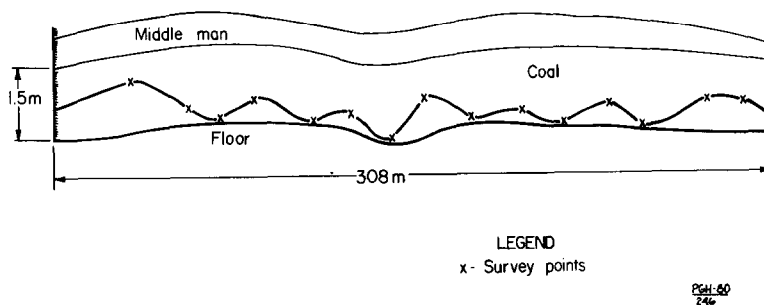


Fig. 7 - Horizontal plot of hole No. 1.

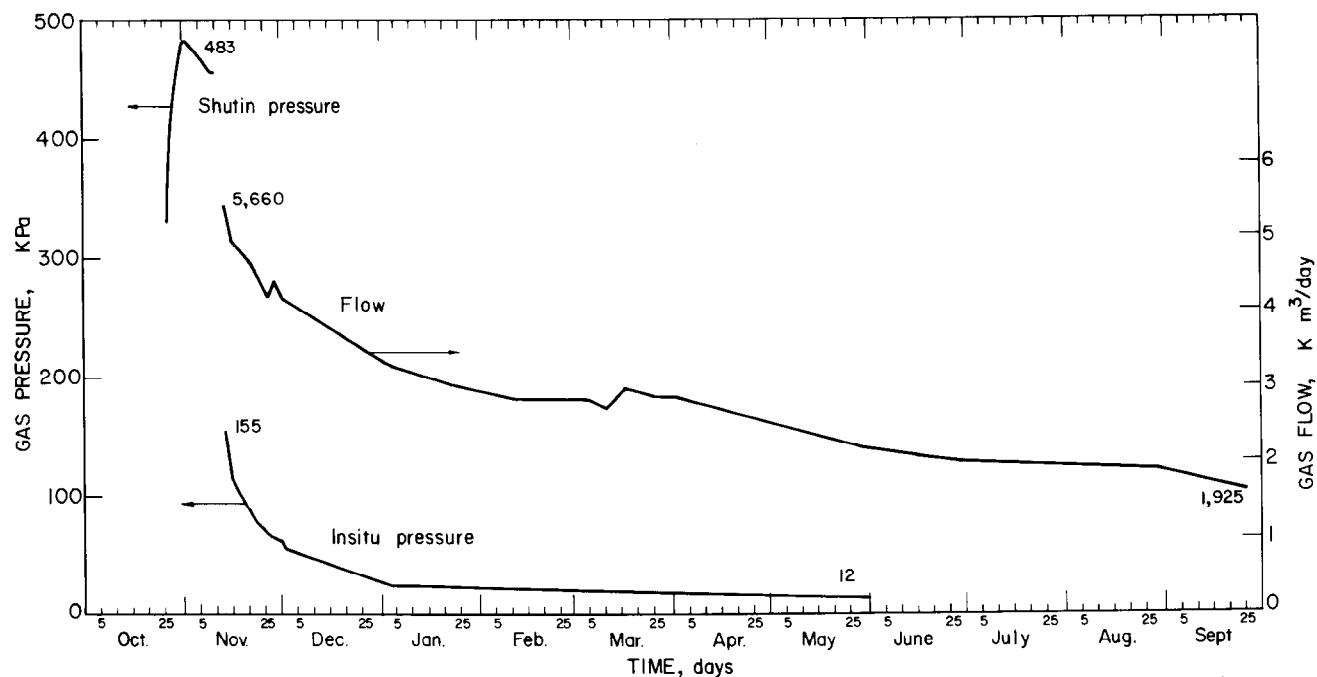


Fig. 8 - Flow and pressure data, hole No. 1.

PGH-80
249

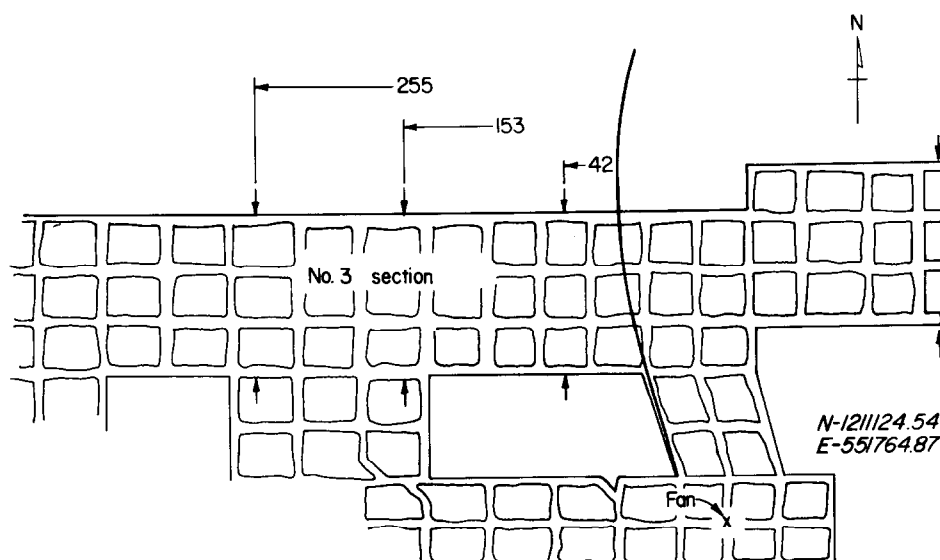
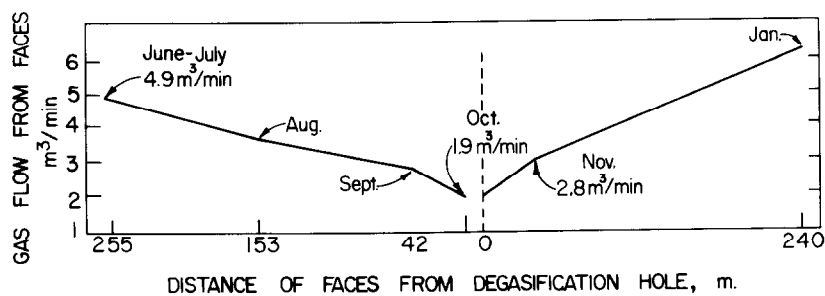


Fig. 9 - Methane history of No. 3 section.

PGH-80
248

DRILLING LONG HORIZONTAL COALBED METHANE DRAINAGE HOLES FROM A DIRECTIONAL SURFACE BOREHOLE

by William P. Diamond and David C. Oyler,
U.S. Bureau of Mines

This paper was presented at the 1980 SPE/DOE Symposium on Unconventional Gas Recovery held in Pittsburgh, Pennsylvania, May 18-21, 1980. The material is subject to correction by the author. Permission to copy is restricted to an abstract of not more than 300 words. Write: 6200 N. Central Expwy., Dallas, Texas 75206

ABSTRACT

Three primary horizontal methane drainage holes totaling 2,428.4 meters (7,967 feet) have been completed in the Pittsburgh coalbed from a directional surface borehole. Directional control and sidetracking techniques developed during the project increased the horizontal drilling rate from 24.4 meters (80 feet) per day initially to 64.9 meters (213 feet) per day on the third horizontal hole. Drilling data indicate that horizontal holes can be drilled substantially longer than the maximum 977 meters (3,207 feet) achieved.

INTRODUCTION

A project to drill horizontal coalbed methane drainage holes from a directional surface borehole was begun in September 1978 at the Emerald Mine near Waynesburg, Pa.¹⁻². Included in the project were a directionally drilled borehole intercepting the Pittsburgh coalbed, three long horizontal degasification holes drilled in the coal from the directional borehole, a vertical borehole for coalbed dewatering and seven vertical boreholes to monitor the progress and extent of degasification with time. The goals of the project were to demonstrate that the technique of directional drilling can be used to degasify coalbeds, to obtain information to improve the technique and to determine the horizontal distance such a hole can be drilled.

GENERAL PROJECT PLAN

The general plan for the directional borehole was to drill a 76-mm (3-inch) diameter pilot hole in a circular arc from the surface to intercept the coalbed horizontally (fig 1). The hole would then be overreamed (using BCQ drill rod as a guide string) to 222.25 mm (8-3/4 inches) in diameter and 139.7-mm (5-1/2-inch) casing would be cemented in place. Three 76-mm (3-inch) diameter horizontal degasification holes would then be drilled, each up to 950 meters (3,100 feet) in length, fanning out from the bottom of the casing. A vertical borehole would be drilled

near the coalbed intercept and equipped with a down-hole plunger pump for dewatering. The vertical borehole would be hydraulically stimulated to create a path for water to flow from the horizontal holes into the vertical dewatering borehole. In addition, seven vertical boreholes (EM 21-27, fig 2) were planned for monitoring the progress of degasification by observing the changes in hydrostatic pressure by measuring the water column over the coalbed at each location.

PILOT HOLE DRILLING

The directional borehole (EM-19) was located at the top of a ridge to allow sufficient overburden above the coalbed for a circular arc of 0.3 to 0.35 radians per 100 meters (5 to 6 degrees per 100 feet) to be drilled to reach the coalbed horizontally. The vertical distance to the coalbed was 304.8 meters (1,000 feet). Of this vertical distance 289.25 meters (949 feet) was required to achieve the required arc to the coalbed. The actual drilled distance of the directional pilot hole well path was 503.5 meters (1,652 feet).

Directional drilling on the pilot hole was begun on November 9, 1978 at a vertical depth of 15.2 meters (50 feet). The directional drilling was accomplished using a 60.3-mm (2-3/8 inch) diameter Dyna-Drill downhole motor and BQ wireline drill rod as the drill pipe. The rate and direction of angle build were controlled by using various bent housings and standoff rings. By orienting the bend in the housing, the tool could be made to drill a hole in the desired direction. The four housing assemblies used to drill the EM-19 pilot hole were, in order of increasing angle build capacity, a 0.0087-radian (30-minute) housing, a 0.013-radian (45-minute) housing, a 0.0087-radian (30-minute) housing with a standoff ring and a 0.013-radian (45-minute) housing with a standoff ring. Control was achieved by changing bent housings and standoff rings as required to keep the hole on the target well path. However, deviations above or below the path were acceptable when it was known that by changing to

References and illustrations at end of paper.

1/ Reference to specific equipment does not imply endorsement by the Bureau of Mines.

another assembly at a later time the hole could be brought back on target without producing severe dog-legs. In general, none of the above assemblies would give a steady 0.32 radian per 100 meter (6 degrees per 100 foot) angle build, so housing changes were required. In all, 10 pipe trips were made on which housings were changed. Some of these trips were also required for other reasons, such as scheduled changes of bearing packages and universal joints on the down-hole motor.

Control of the well path was within specifications, and no plug-backs were required to complete the pilot hole to the coalbed. Thirty (24-hour) working days were needed to drill the 76-mm (3-inch) diameter pilot hole. Directional control operations including orienting, surveying, and pipe trips to change housings consumed approximately 18 percent of the total drilling time.

It was found to be advantageous during the pilot hole drilling to run the Dyna-Drill tool well above its rated operating specifications. The tool is designed to operate at 5.5 m³/hr (24 gpm) at 3,500-6,200 kPa (500-900 psi) with 3,500 kPa (500 psi) preferred. During most of the pilot hole drilling, flow rates of 9 to 11 m³/hr (40 to 50 gpm) averaging 9.5 m³/hr (42 gpm) and 3,500-6,200 kPa (500-900 psig) were found to give better penetration rates and a relatively low rate of tool failure. The low rate of tool failure observed may be partially related to the frequent changing of bearing packages on the tool when it was pulled from the hole at any time for any reason.

Two types of bits were used to drill the pilot hole, a 76-mm (3-inch) diameter diamond plug bit and 76-mm (3-inch) diameter combination Strata-Pax¹ bit with diamonds around the rim to maintain gauge. Most of the pilot hole drilling was completed with the Strata-Pax bit. The two types of bits generally performed comparably, however, since the bits were of about the same initial cost and the diamond bit would probably have a high salvage value while the Strata-Pax has none, the diamond bits probably would be more economical.

The major problem encountered while drilling the pilot hole was lost circulation. The drill site was located on top of a ridge because of the need for approximately 300 meters (984 feet) vertical distance to deviate the well path on an acceptable trajectory. An extensive limestone section through the top third of the drilled distance had apparently developed a high solution permeability. Commercial lost circulation materials were sufficiently effective to permit the successful completion of the pilot hole.

The pilot hole (fig 1) was completed on December 19, 1978, at a total measured depth of 503.5 meters (1,652 feet). Drilling operations took a total of 40 days. Of this time 10 days were off days (drilling was done 24 hours per day with weekends off), 11 days were actually spent drilling, 3.6 days surveying, 1.6 days in normal maintenance, 1.8 days to trip pipe for housing changes, and 12.25 days were down time. The average drilling rate for the 30 actual working days was 16.8 meters (55 feet) per day. Subtracting the down time raises the drilling rate to 28 meters (92 feet) per day.

REAMING OPERATIONS

After the pilot hole was completed, a string of BCQ drill rod was placed in the hole to be used as a guide string for overreaming bits. A gamma ray log was also run to confirm that the pilot hole had reached the top of the Pittsburgh coalbed.

Reaming operations began on January 9, 1979 after a string of a 1-inch pipe was put inside the BCQ rod for added stiffness. The drill pipe used was 88.9-mm (3-1/2-inch) diameter pipe along with 222.25-mm x 63.5-mm (8-3/4-inch x 2-1/2-inch) diamond and Strata-Pax overreaming bits. Lost circulation, which had been a minor problem during the pilot hole drilling, became a major problem during the reaming. In addition, it was found that the large Strata-Pax bits wore out quickly. Two of these bits averaged only 72.5 meters (238 feet) of drilling.

By February 21, 1979 the hole had been reamed to 189 meters (620 feet) despite severe lost circulation problems. At this point, the crown of the third Strata-Pax bit separated from the shank. An attempt to mill up the bit without removing the BCQ guide string failed, and further complicated the down hole problem by cutting the 25.4 mm (1 inch) diameter guide pipe in two (some of the BCQ rod had previously parted and been pulled out of the hole).

It was not until April 4, 1979, that all the "junk" was removed from the hole. The entire string of BCQ guide rod had been pulled during the fishing operations. Although there were apprehensions that without a guide string the pilot hole would collapse, the pilot hole was found to be open and in good condition. It was decided to complete the reaming operation using a "stinger" assembly (fig 3) in front of the reaming bits to keep the reamed hole following the original pilot hole well path. The reaming was successfully completed from 189 to 494 meters (620 to 1,620 feet) using the stinger assembly. A total of 6 bits were used to ream the hole, three diamond and three Strata-Pax (including the one that separated).

CASING AND CEMENTING

The hole was cased on May 10, 1979, using 486.2 meters (1,595 feet) of 139.7-mm (5-1/2-inch) outside diameter K-55 LT&C casing. The casing was run freely to 442 meters (1,450 feet). Below that point it was necessary to push the casing to the desired total depth. The next to the last joint required a maximum of 57,800 newtons (13,000 pounds) down pressure and the last joint required only 8,900 newtons (2,000 pounds). Fifteen centralizers were run in the hole primarily on the bottom 100 meters (300 feet) to give good centralization of the casing in the hole and insure a good cement job. Cementing of the casing was completed on May 11, 1979. A total of 340 sacks of pozzolan cement with gilsonite added to decrease its density were used in an attempt to obtain returns past the lost circulation zones. Good cement returns were obtained.

HORIZONTAL DRILLING

On May 17, 1979, after a tricone bit had drilled out the cement shoe, horizontal drilling was begun. The drilling plan was to drill just enough horizontal hole to reach the vicinity of the vertical dewatering

borehole (EM-20, fig 2). The horizontal hole was drilled to 527.9 meters (1,732 feet) measured depth (MD) on May 23, slightly past EM-20. The dewatering borehole was stimulated on May 25, 1979 with a 79.5 m³ (21,000 gallons) foam treatment. This procedure was designed to increase the flow of water to the vertical dewatering borehole and to attempt to directly connect the horizontal degasification holes with EM-20.

The initial horizontal drilling indicated that an error had been made in the interpretation that the pilot hole had entered the top of the Pittsburgh coalbed. It was found necessary to drop through approximately 0.6 meters (2 feet) of roof rock to enter the main bench of the coalbed. A reevaluation of a gamma ray log of the directional hole in light of the additional drilling information indicated that the pilot hole probably had been drilled through the Pittsburgh rider coal into the roof shale above the Pittsburgh coalbed and then, instead of going into the Pittsburgh coal, the hole had gone back into the rider coal. This error proved to be a major problem for two reasons. First, the vertical dewatering borehole and directional borehole had been placed so that fractures from the stimulation treatment would cross the horizontal hole just beyond the end of the casing. Since the horizontal hole possibly was in roof rock near the anticipated intercept of the stimulated fracture with the horizontal hole, direct communication may not have been achieved. Secondly, this meant that the initial portion of each horizontal hole was in rock which had a tendency to cave or slough, resulting in blockage of the holes. The best method of ensuring that the casing reaches the target coalbed in the future would be to continue the pilot hole after reaching the horizontal and to drill steeply downward until the bottom of the coalbed is reached. This portion of the hole would be abandoned during reaming and casing operations.

Continuous drilling of the first horizontal leg H1 (fig 2) was begun on May 29, 1979. The drilling fluid used was clear water to eliminate any risk of mud additives plugging the coalbed fracture system. However, the use of clear water led to three problems. The first and most important was that removal of drill cuttings was made more difficult because of the low viscosity of water. The problem was made more acute by the low flow rates required by the Dyna-Drill. The flow rates through the tool were increased from 5.5 to 9.0 m³/hr (24 gpm to 40 gpm) and eventually to as high as 13.6 m³/hr (60 gpm). This increase in flow rate eventually led to problems with Dyna-Drill tool life.

A second problem encountered when using clear water was fluid loss. This problem essentially could not be solved without the risk of damaging the coalbed's natural fracture permeability and the future value of the hole for degasification. Fluid losses as high as 57 m³/d (15,000 gpd) were experienced before H1 was completed. The third potential problem was the risk of sloughing of water-sensitive clays in the roof shales that were occasionally drilled through. This problem did not become apparent immediately, but eventually became very serious.

One drilling problem encountered which had been expected was keeping the hole in the coalbed and controlling the hole path. It was decided early in

the drilling that sidetracks were to be avoided if possible since it was felt that it would be difficult to reenter the proper hole after the drilling assembly was removed for any reason. When the hole deviated from the main coalbed, every attempt was made to reenter the coal without sidetracking. Since the directional control engineer was still learning how to control the drilling, and because it was difficult to predict the dip of the coalbed (partially because it was more erratic than expected), large sections of hole H1 were drilled in rock (table 1). One sidetrack was attempted on hole H1 because a section was drilled completely in rock from 685.2 to 801.6 meters (2,248 to 2,630 feet) MD. The new hole was successfully sidetracked in coal at 674.2 meters (2,212 feet) MD and was drilled to 976.6 meters (3,204 feet) MD with only two sections totaling 8.5 meters (28 feet) in rock.

The first horizontal leg H1 (fig 2) was completed on July 13, 1979, at 1,024.7 meters (3,362 feet) MD when it was impossible to reenter the horizontal hole after a pipe trip. The hole had reached a total horizontal length of 538.6 meters (1,767 feet) beyond the end of the casing and was drilled in 26 working days, for an average rate of 20.4 meters (67 feet) per day. Before the leg was completed it had become apparent that many improvements would be required to obtain acceptable daily drilling rates.

Leg H2 was begun on July 16, 1979, and about half of its total length was completed before major changes were made in the drilling techniques. The first changes were made simultaneously. The flow rate through the Dyna-Drill was decreased in an attempt to obtain longer tool life and reduce pipe trips, which at measured depths of 950 meters (3,100 feet) could take as long as 16 hours (round trip). To offset the effect of lower flow rates on removal of cuttings, a concentrated detergent known as Con-det was mixed with the drilling fluid. The Con-det helped to remove cuttings, but presumably did not plug off the coalbed fracture system. Eventually an experimental partial bypass valve just above the Dyna-Drill tool was also used which allowed high flow rates in the annulus, but allowed only 5.5 m³/hr (24 gpm) through the tool. The rest of the flow bypassed the tool through the valve and helped remove cuttings.

The problems associated with drilling in rock were eliminated when it was discovered that it was easier to back up and sidetrack immediately after leaving the coal than to gradually guide the well path back into the coal. Eventually sidetracks could be accomplished in as little as 3 hours. Accepting more sidetracks made staying in the coalbed less critical, increased drilling rates and lengthened directional survey intervals from 6.1 to 12.2 meters (20 to 40 feet). Since it took about 1 hour for a survey, and drilling took 20 to 40 minutes per 6.1 meters (20 feet), this was a significant timesaver.

Leg H2 (fig 2) was completed in 36 working days on August 31 at a total measured depth of 1,463.4 meters (4,802 feet). This was the longest horizontal hole drilled from EM-19, reaching 977.5 meters (3,207 feet) from the end of casing. The average daily footage was 27.1 meters (89 feet).

All of the successful techniques developed in drilling H1 and H2 were used in drilling leg H3, except the use of the bypass valve which had been sent in for repairs when H3 was started. H3 was begun on September 4, 1979. On September 21, 1979, the Dyna-Drill was finally pulled out of the hole after a record 226-hour run. The hole had been drilled to a measured depth of 1,398.4 meters (4,588 feet), a horizontal length of 912.3 meters (2,993 feet) from the end of the casing (fig 2). The average footage per working day (14 days) was over 64.9 meters (213 feet). The hole was sidetracked eight times for an average of 114 meters (374 feet) between sidetracks. Leg H3 was not continued because it could not be reentered due to the apparent sloughing of the shale section at the bottom of the casing. If it could have been reentered, there is every reason to believe that the hole could have been extended substantially greater distances.

After September 21, 1979, unsuccessful attempts were made to reenter the horizontal holes and two additional holes H4 and H5 were drilled. H4 essentially followed H1, and H5 was drilled between H1 and H3 (table 1, fig 2).

The final drilling operation performed on the slant hole was the underreaming of a horizontal sump 215.9 mm (8-1/2 inches) in diameter from the bottom of the casing to a measured depth of 531 meters (1,742 feet) along the center leg, H1. The 215.9-mm (8-1/2 inch) hole entered the coalbed at a measured depth of approximately 521.8 meters (1,712 feet). This underreaming operation took approximately two days, most of which were spent running and pulling drill pipe. The operation was completed on October 9, 1979.

PRODUCTION

Work began on October 9, 1979 to equip the vertical dewatering borehole, EM-20, for dewatering the coalbed, and equip the directional borehole and vertical dewatering boreholes for gas production and monitoring. The dewatering borehole was put on water production November 15, 1979. Water production began at pump capacity of 0.8 m³/h (120 bbl/d) and intermittent gas flows were measured up to a rate of 34 m³/d (1,200 ft³/d). After several days, water production declined drastically without any increase in gas production. It was believed that a barrier to water flow between EM-20 and EM-19 (probably because the portion of the directional borehole at the bottom of the casing was in rock) was directly responsible. During December 1979 and January 1980, several attempts were made to increase water production by flushing out both EM-20 and EM-19, and by trying to extend the fractures in EM-20. Initial indications are that these procedures have partially accomplished the desired results. Current activities to increase the production of water from the system and initiate gas flow are centered on the possible use of a down-hole electric submersible pump in the directional borehole.

RESULTS AND CONCLUSION

HORIZONTAL DRILLING

A number of conclusions can be made from the drilling of the Emerald Mine directional borehole. First, with good directional control personnel, it is

possible to quickly and relatively inexpensively drill a directional pilot hole to a target coalbed. Second, it is important to determine that the hole actually is in the target coalbed by drilling an additional hole completely through the target coalbed. This is necessary because the accuracy of current directional well surveying is at best ± 0.6 to 0.9 meters (2 to 3 feet) vertically (at the measured depth of EM-19). It was found that despite careful attempts to correlate the coalbed depths from the dewatering and monitoring boreholes with the position of the directional borehole, the accuracy of surveying techniques were not sufficient to allow direct depth correlations. Thus it is advisable to use only the results of actual drilling to determine the position of a directional borehole with respect to the target coalbed.

Third, in drilling the horizontal holes in coal, no portion of any hole (except deadends left after sidetracking) should be drilled in rock. The portions of EM-19 drilled in roof and floor shales were a constant source of problems. The best method of drilling the horizontal holes is to attempt to stay at the regional dip of the coalbed and drill as rapidly as possible. When the hole deviates from the coal, a sidetrack, either up or down as required, should be performed as soon as it is certain that the hole actually is in rock. The sidetrack should be initiated back far enough to insure sufficient distance to deviate the hole and avoid immediately drilling out of the coalbed again. The optimum surveying interval for this drilling program is between 12 and 18 meters (40 and 60 feet).

Fourth, it was found that in horizontal drilling, some type of additives are required for removal of cuttings, and that higher flow rates than can reasonably be run through the Dyna-Drill are required for cleaning the hole. It is recommended that a bypass valve capable of delivering 5.7 to 9.1 m³/h (25 to 30 gpm) to the Dyna-Drill at differential pressures of 3,400 to 4,800 kPa (500 to 700 psi) and of bypassing 13.6 m³/h (60 gpm) for cuttings removal should be used in horizontal drilling.

Finally, it was learned during the horizontal drilling that the BQ pipe used was not strong enough for this type of work. The boxes of the pipe began to open up and the pins stretched until even a relatively small pull could separate the pipe at a tool joint. Fortunately, the highest stresses are near the surface and separations usually took place between the surface and depths of approximately 180 meters (600 feet), making it easy to screw back into the separated pipe, pull out of the hole and remove the damaged joint. However, by the end of the project, approximately one-half of the BQ pipe was no longer suitable for further drilling.

REAMING

Both a BCQ guide pipe and a stinger were used to keep the reaming of the 222.25 mm (8-3/4 inch) diameter directional borehole on the pilot hole well path. It is suggested that the use of a stinger is the simplest, easiest, and cheapest method of following the pilot hole. However, precautions should be taken to insure that the pilot hole will stay open during the reaming. These precautions should include the use of muds to prevent fluid loss to water sensitive shales.

BITS

It is recommended that for pilot hole drilling, diamond plug bits be used for predominantly hard formations and Strata-Pax bits for shales. For horizontal drilling, diamond bits would probably be more effective because of their long life and high salvage value. Large diameter Strata-Pax bits are not recommended for reaming unless significant design improvements are made. The diamond reaming bits, although not completely satisfactory, are presently recommended.

ACKNOWLEDGMENTS

Much of the credit for the technical success attained in the drilling of the directional coalbed degasification system belongs to the drilling contractor, drilling crews, and subcontractors. Special recognition is given to Mr. Harold F. Scott, Con-

tractor and Mr. John Gardner, Project Manager; Mr. Verne Nesvacil, Directional Drilling Supervisor, Eastman Whipstock Inc.; and Mr. John Workman, Mining and Industrial Manager, Dyna-Drill Co. The continued assistance of the Emerald Mine Corp. is gratefully appreciated.

REFERENCES

1. Diamond, William P. and Oyler, David C.: "Directional Drilling for Coalbed Degasification in Advance of Mining," In: Proceedings of the Second Annual Methane Recovery from Coalbeds Symposium, Pittsburgh, Pa. April 18-20, 1979, METC/SP-79/9, 162-176.
2. Oyler, David C. and Diamond, William P.: "Directional Drilling for Coalbed Degasification - Program Goals and Progress in 1978." BuMines RI 8380 (1979).

TABLE 1

HORIZONTAL FOOTAGES DRILLED AND ROCK TYPE

Hole No.	Total depth from surface		Horizontal length (end of casing to TD)		Hole in coal (including sidetracks)		Hole in rock (including sidetracks)	
	Meters	(Ft)	Meters	(Ft)	Meters	(Ft)	Meters	(Ft)
H1	1,024.7	(3,362)	538.6	(1,767)	413.0	(1,355)	253.0	(830)
H2	1,463.4	(4,802)	977.5	(3,207)	1,018.6	(3,342)	180.7	(593)
H3	1,398.4	(4,588)	912.3	(2,993)	915.0	(3,002)	73.5	(241)
H4	751.3	(2,465)	265.2	(870)	157.6	(517)	95.1	(312)
H5	701.6	(2,302)	215.5	(707)	180.4	(592)	29.9	(98)
TOTALS			2,909.0	(9,544)	2,684.7	(8,808)	632.2	(2,074)

Total all drilling = 3,311 meters (10,882 ft).

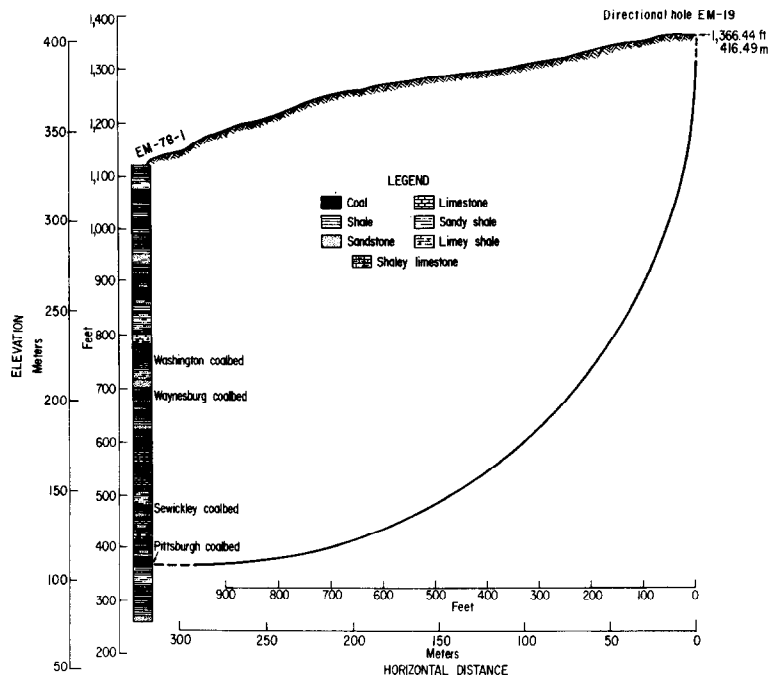


Fig. 1 - Section view of directional well path.

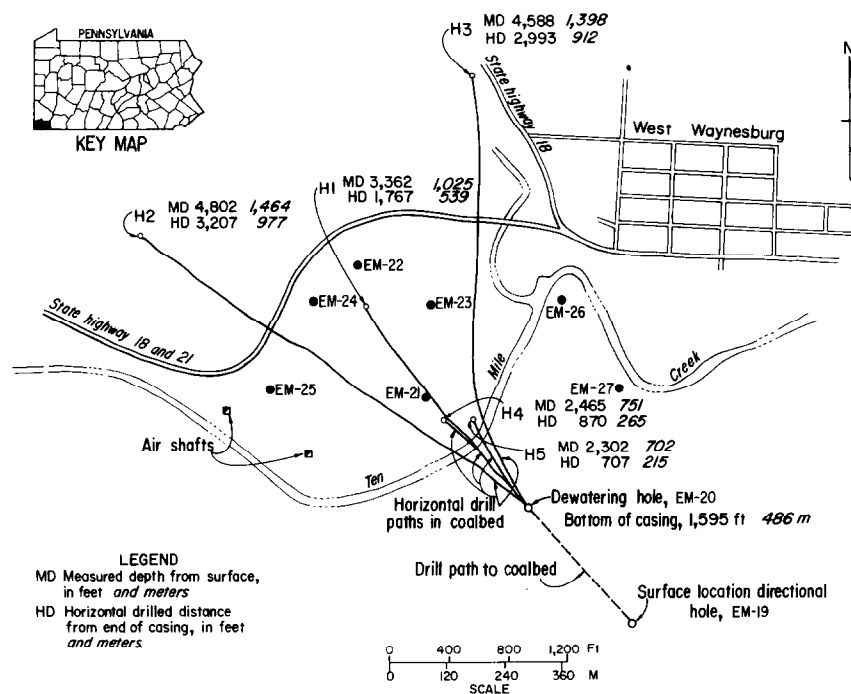


Fig. 2 - Plan view of drill sites and actual well paths.

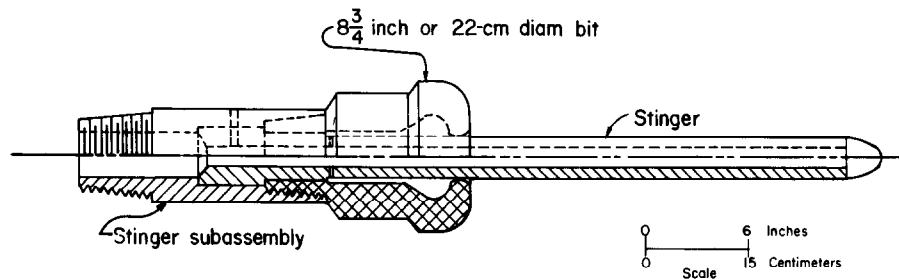


Fig. 3 - "Stinger" assembly for reaming pilot hole.

ADVANCE METHANE CONTROL AND ITS IMPACT ON GAS EMISSIONS IN THE POCAHONTAS #3 COAL SEAM

by Hilmar A. von Schonfeldt, B.R. Pothini, and
George N. Aul, Occidental Research Corporation

This paper was presented at the 1980 SPE/DOE Symposium on Unconventional Gas Recovery held in Pittsburgh, Pennsylvania, May 18-21, 1980. The material is subject to correction by the author. Permission to copy is restricted to an abstract of not more than 300 words. Write: 6200 N. Central Expwy., Dallas, Texas 75206

ABSTRACT

Methane emissions into underground coal mines in certain areas of the United States represent a serious hazard and contribute to lowering mining productivity. In order to reduce methane emissions into some of the deep south west Virginia Coal Mines an advance methane drainage program was developed. This paper gives a state of the art account of drilling long in-seam and slant holes into virgin areas of the Pocahontas #3 and #4 coalbeds. Directional drilling techniques are discussed. Methods to evaluate the drainage effectiveness of this program on the emissions in an operating mine are also covered. It is concluded that an effective methane drainage program can reduce methane emissions significantly thereby improving safety conditions in the mine. It also has the potential for increasing mining productivity. The recovered gas could also lead to a better utilization of our available energy resources.

INTRODUCTION

Methane liberation from the coal seam and surrounding strata in Island Creek Coal Company's deep Virginia Mines has long been a serious problem. The gas represents a safety hazard because it can be ignited in concentrations of 5% to 15% methane in air through sparks generated by the mining equipment.

Under the current safety regulations the methane has to be diluted to below 1% in all working areas by a sufficient amount of fresh ventilation air. In spite of the large ventilation volumes supplied to the working faces, however, the methane content locally can increase to levels above 1% on occasion. In this event all mining operations have to be stopped until the methane content in the air once again falls to safe levels. Also, through experience the mining machine operators have learned to lower the cutting rate sufficiently as to avoid such high methane concentration levels. The presence of the gas, therefore, also forces a lower than technically possible mining productivity. Gas is emitted into the mine workings

at the mining face during the cutting process. Large amounts are also liberated from the roof rock, the floor rock, the mined out areas and all unmined portions of the coal seam, like the barrier pillars for example. Current control techniques to cope with this gas consist of:

1. Dilution of gas to below 1% methane with ventilation air.
2. Drainage of gas from solid coal by short (60 m) bleeder holes in long-wall panels.
3. Water infusion through short holes to block flow of methane.
4. Vertical ventilation holes drilled from the surface over longwall panels to liberate gas from mined out areas.
5. Vertical ventilation holes in advance of mining. These holes, however, represent an experiment on a limited scale only.

In addition to the undesirable effects on safety and mining productivity, the current technique of diluting the methane gas represents a waste of a valuable energy resource. It is our opinion that a suitable methane control technique ahead of mining should be able to recover and utilize much of the gas contained in the coal seam and the rock strata surrounding it. Such a method is currently being developed and was described in some detail elsewhere [1].

DRAINAGE CONCEPT AND OBJECTIVE

The basic technique consists of drilling long horizontal holes into the coal seam one to several years ahead of mining and allowing the gas to drain from the coal through these holes. A variation to this technique is the drilling of underground slant holes into an overlying coalbed from the working mine level. The gas is collected through an approved piping system and moved to the surface through a vertical borehole.

References and illustrations at end of paper.

The objectives of this program are to develop methods of lowering the methane content of the Pocahontas #3 and #4 seams in advance of mining. This is expected to improve mine safety and mining productivity. A further objective is to recover the gas to make the most use of the energy resources available to us.

DRILLING AND COMPLETION

To date a total of 8 drainage holes have been drilled from several locations varying in length from 152 m to 525 m in addition to several shorter holes drilled by the U.S. Bureau of Mines (figure 1). Six of the holes are drilled within the Pocahontas #3 coalbed and 2 are inclined holes drilled from the #3 seam level into the Pocahontas #4 bed some 17 m above. Each of these groups of holes required different techniques for directional control. Presently 5 holes are producing gas and 3 were intersected by mining and are no longer active. All holes are completed with a 102 mm diameter steel standpipe grouted in place between 6 m to 18 m in length. The standpipes serve several functions: During drilling the equipment is bolted directly to the pipe to allow safe handling of the gas and the drilling water; after drilling a pipeline is connected to the standpipe to safely transport the gas to the surface. This insures that no significant amounts of gas from the methane drainage operation are released into the mine at any time.

A typical hole completion is indicated in figure 2.

DIRECTIONAL DRILLING TECHNIQUE

The drilling technique used for maintaining control over long distances in a coalbed depends upon the physical characteristics of the particular seam, the roof and floor rock and the operators ability to use these characteristics to his advantage.

IN-SEAM DRILLING

Experience has shown that drilling in the upper portion of the seam affords the most effective directional control. The Pocahontas #3 coalbed is very soft and friable and, therefore, the bit has a tendency to ream downwards. To counteract this gravity affect the bit must be forced upwards and held close to the roof to prevent drilling into the floor. The comparatively much harder overlying roof strata can be used as a "guiding" horizon. This technique is not without difficulties, especially in areas where the roof of the coal seam changes direction abruptly such as in a "roll". Typical drilling conditions encountered are indicated in figure 3. In this particular example the hole was drilled down dip of the coal seam. As can be seen the actual dip is not constant but varies considerably from point to point. The hole trajectory shows that the bit penetrated the roof on 3 occasions during the early drilling stage while the remainder of the hole was drilled without intercepting the roof rock again. This was achieved by allowing the bit to "bounce" off the roof through proper adjustment of the drilling parameters. The basic tools available to control the inclination of the borehole were the number and spacing of centralizers, thrust and rotational speed of the bit. In order to apply the right drilling parameters frequent surveying of the hole was necessary until the proper centralizer configuration,

bit thrust and speed was established. Once the drill operator found the right combination of these quantities he was able to steer the bit by varying the thrust and rotational speed only. For drilling in the relatively soft Pocahontas #3 coal a drag bit (Hughes Tool Blue Demon) gave excellent penetration rates as well as long bit life. The average drilling rate achieved was 30 m per shift.

SLANT HOLE DRILLING

In the past mining productivity in the Pocahontas #3 coalbed had been hampered in certain areas because of methane migration from the overlying Pocahontas #4 seam through roof fractures into the mine [2]. The decision was made to develop techniques for drain hole drilling in the Pocahontas #4 coalbed because severe methane emission problems are anticipated as soon as longwall mining will induce roof caving.

The two seams are separated by hard sandy shale and sandstones. The key to a successful method was the ability to control borehole direction in the various rock types. The trajectory of one of these holes through a 17 m thick rock interval is illustrated in figure 4. Most of the drilling was done with diamond plug bits 80 mm in diameter. The hole was started at a low angle which was then raised during drilling. The initially low angle was dictated by the size of the drilling equipment and the low clearance available at the drill site. Several drill string configurations with different drill parameters were tried. The directional response of the bit was considerably slower than in coal. It was found, however, that the bit responded well to upward parameters with a concave diamond plug bit and one centralizer behind it. In order to produce downward deflection a relatively high thrust of 2.3 tons had to be applied to the bit.

The Pocahontas #4 seam was intercepted at a depth of 104 m approximately 17 m above the #3 seam. The bit was maintained within the coal seam to a depth of 115 m when it penetrated the roof of the #4 seam. Drilling was terminated at a depth of 201 m when it was concluded that the coal seam had pinched out (figure 4).

Experience gained from drilling the slant holes indicated that the bit angle can be controlled in various rock types. The guidelines developed for changing the borehole direction in rock are found to be valuable for future drilling.

METHANE PRODUCTION

All holes without exception produced a high quality gas. A typical gas analysis is given in Table I. The unit production rates as well as average daily production for 8 drainage holes have been summarized in Table II. It is apparent that the production rates vary over a wide range. The low final flow of the first 3 holes is due to the fact that the mining operation was moving into the drainage area of these holes; as pointed out earlier these holes were eventually mined out. Other factors thought to influence the production rate of drainage holes are productive life of the hole, borehole stability, proximity to other holes and mine workings and to some extent the orientation of the holes relative to the cleat systems. It was generally observed that most holes start producing at a

relatively high rate for the first week or two; thereafter they begin to stabilize at a considerably lower rate. It is felt more work is necessary before reliable estimates can be made regarding long term production decline and drainage radius.

METHANE DRAINAGE EFFECTIVENESS

Two methods were developed to determine the effectiveness of gas removal:

1. Measurement of the gas content of drained and undrained coal through desorption.
2. Measurement of rib emissions through ventilation surveys.

GAS CONTENT MEASUREMENTS

The procedure used to determine the gas content of the coal directly is similar to that developed by the U.S. Bureau of Mines [3]. Coal cuttings were collected from the tail piece of the miner into specially designed desorption canisters. Each sample weighed approximately 4.5 kg. The sample was allowed to desorb over a period of several hundred hours. This allowed the construction of cumulative desorption curves as well as desorption rate curves plotted as a function of time (figure 5, figure 6). After several hundred hours of desorption some of the samples were put into a laboratory ball mill. The residual gas relieved during the grinding process was measured and added to the total volume.

The effect of drainage holes on the gas content of the coal seam is illustrated in figure 5. Three holes, Oxy 1, 2 and 3 (figure 7) were intercepted 310 to 418 days after they were drilled. The curves (figure 5) show the gas content of virgin coal samples (100%) and of samples taken from the coal in the area of the drainage holes. It is indicated that the coal seam was approximately 80% degassed. It should be pointed out that these data are to be understood in a qualitative rather than in a quantitative sense at this early stage of the program. The results show, however, that the horizontal methane drainage holes can lower the gas content of the coal seam significantly. A further important conclusion can be drawn from the desorption data with regard to the rate of desorption which has far reaching implications for coal mining productivity. This is illustrated with the help of figure 6, showing a very high initial desorption rate for virgin coal. The desorption rate of the coal sample from the degassed hole on the other hand is only 5% of the virgin sample over the same time interval.

In mine development it is typically the high methane emission rates near the active mining face that lead to temporary shut down or slow down of the mining process. Mining can resume only after the methane concentration has been diluted to below the required 1% level. The graphs in figure 6 indicate that most of this initially emitted gas could be drained with the help of horizontal drainage holes because it desorbs readily. The remaining residual gas on the other hand is emitted at rates sufficiently low as not to interfere with mining productivity.

VENTILATION SURVEYS

A second way of determining the influence of horizontal methane drainage holes on gas emissions

into the mine was used. Methane concentrations were monitored in freshly mined entries in the area of the drainage holes Oxy 1, 2 and 3. As is illustrated in figure 7 the entries mined into 2 of the 3 drainage holes; the third one was drilled closely along the outside entry in a barrier pillar.

The ventilation system consisted of 2 intaking airways, 1 neutral airway and the return air was taken out in 2 separate splits, one in each of the outside entries.

Ventilation surveys were conducted in each of the return air splits for 7 weeks during which period the holes were intercepted and mined out. It is important to note that the 3 drainage holes were located in the area of the left return split while the right return airway was no closer than approximately 91 m. The results of the survey indicated that the air in the left return contained 25% less methane than the air in the right return (figure 8). It was concluded, therefore, that this difference is due to the presence of the drainage holes near the left return airway.

This result is not as striking as previously indicated by the desorption tests. It is pointed out, however, that in this area unusually high amounts of methane entered the mine through fractured roof strata from the Pocahontas #4 seam [2]. This outburst most certainly reduced the overall effect of the horizontal drainage holes.

METHANE EMISSION AS A FUNCTION OF TIME

It is a well known fact supported by experience of the mining operation that methane emissions at any location decrease with time. In order to quantify this experience methane emissions into an entry were measured at various distances from an active face.

The results are presented in figure 9. Unit methane liberation in cubic meters per day per meter of rib was plotted as a function of the distance from the active mining face. The data show that the daily emission rate per meter of coal face decreased from a maximum of 14 cubic meters at the face to approximately 2 cubic meters 610 m behind the face. These data again indicate that methane emissions from the coal seam into entries could be reduced to 20% or less of the maximum emission rate if a suitable drainage method were provided. Several conclusions regarding methane production and the productive life of a horizontal drainage hole also may be derived from these data. Bearing in mind that it took approximately 40 weeks to advance the particular entry system in which the study was made and assuming that the drainage affect of this entry system is at least as pronounced as that of a horizontal hole of similar length the following can be stated:

1. A minimum of 40 weeks is necessary before the flow from a methane drainage hole has reached steady state conditions provided no interference with the natural drainage radius of the hole exists.
2. Properly spaced methane drainage holes alongside projected mine entries would have to be drilled a minimum of 40 weeks in advance of mining to reduce the methane content of the coal to be mined to 20% or less.

It is also interesting to note that the data in figure 9 seem to indicate a half time of 15 weeks during which the emission rate of the coal face is reduced by 50%. It is not clear at this time whether this trend continues or a steady state emission is reached eventually.

CONCLUSIONS

The concept of advance methane drainage through horizontal holes shows considerable promise for the deep south west Virginia Mines working the Pocahontas #3 coal seam. The capability of drilling in-seam holes in excess of 500 m as well as slant holes into an overlying seam was demonstrated. The holes appeared to be stable. They have produced significant amounts of methane over extended periods of time. It was also concluded that lowering the original gas content of the virgin coal by 80% is feasible provided a sufficient number of drainage holes could be placed. The time required for this drainage is expected to be within reasonable limits of 1 to 2 years. The foregoing work was carried out in 1 mine only; the results therefore, do not necessarily apply to all mines in the Pocahontas #3 coal seam. It is felt, however, that the demonstrated potential reduction of methane emissions into the mine will lead to a significant improvement of the safety environment in very gassy mines. The lowering of emission rates will also have a direct effect on mining productivity especially during mine development into virgin coal areas by

reducing or eliminating downtime. Finally, reduced emissions might eventually allow fewer entries than those currently needed in mine development to move the large amounts of methane.

ACKNOWLEDGEMENTS

This work was performed under a cost sharing agreement between Occidental Research Corporation under a subcontract No. H15730JJ96 with TRW as part of their work on methane drainage for the United States Department of Energy under Contract No. DE-AC21-78MC08089.

REFERENCES

1. von Schonfeldt, H., Methane Recovery from Deep Mines, Proceedings of the Second Annual Methane Recovery from Coalbeds Symposium, R. L. Wise, Editor, Pittsburgh, PA April 18-20, 1979.
2. Finfinger, G. L., Cervik, J., Drainage of Methane from the Overlying Pocahontas #4 Coalbed from Workings in the Pocahontas #3 Coalbed, U.S. Bureau of Mines RI 8359, 1979.
3. Kissell, F. N., McCulloch, C. M. and Elder, C. H., The Direct Method of Determining Methane Content of Coalbeds for Ventilation Design, U.S. Bureau of Mines RI 7767, 1973.

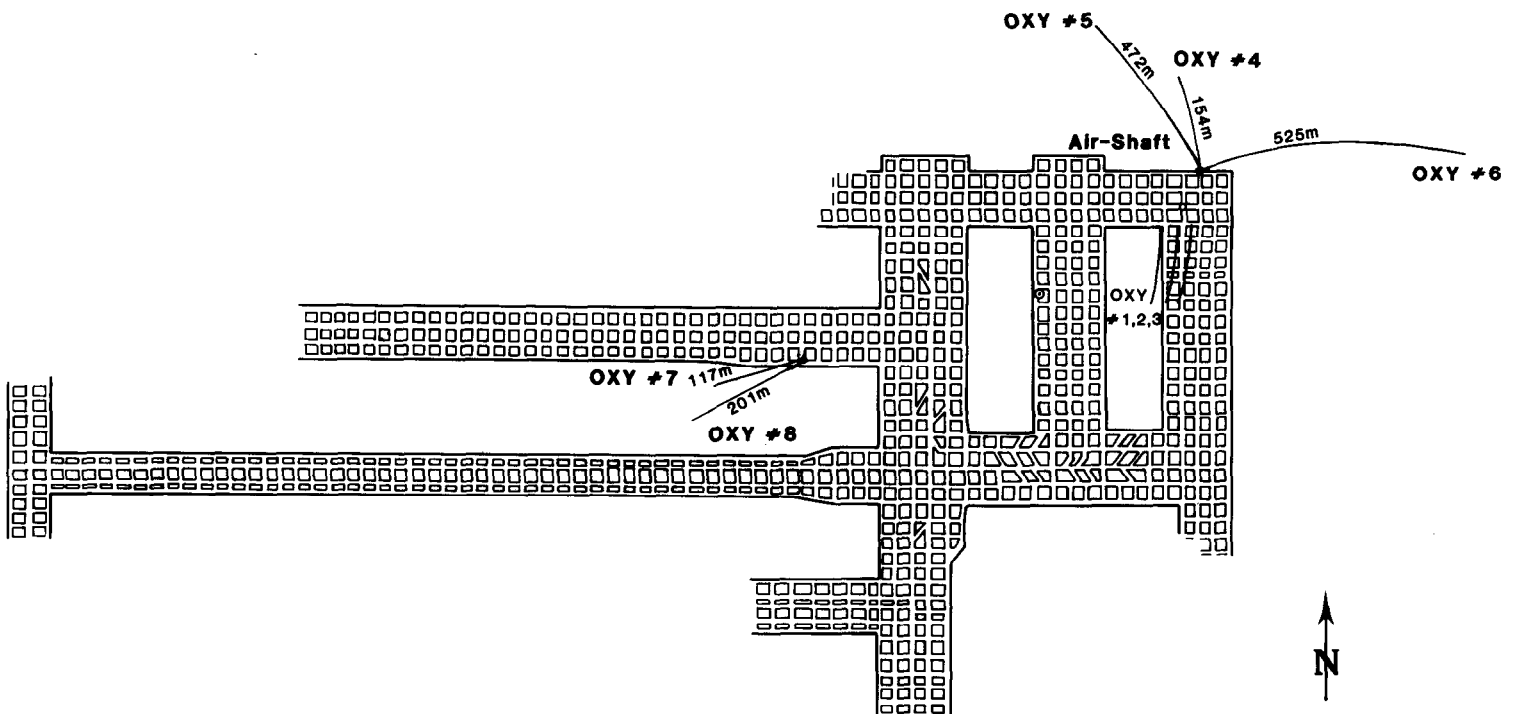
TABLE 1

GAS ANALYSIS DATA

CH ₄	98.026
C ₂ H ₆	0.994
C ₃ H ₈	0.010
ISO-C ₄ H ₁₀	0.001
CO ₂	0.746
N ₂	0.199
O ₂	0.021

TABLE 2

HOLE NUMBER	DEPTH (m)	UNIT PRODUCTION RANGE (m ³ /day/m)	MAXIMUM PRESSURE RECORDED (kg/(cm ²))	LIFE OF HOLE NUMBER OF DAYS FLOWING	AVERAGE DAILY PRODUCTION (m ³ /day)	LENGTH OF STANDPIPE (m)
Oxy #1	152	36 - 1	4.2	418	501	6
Oxy #2	153	40 - 1	3.7	310	673	6
Oxy #3	153	41 - 3	3.5	323	1306	6
Oxy #4	154 (84 in coal)	34 - 14 (363 - 153)	3.5	126	1478	6
Oxy #5	475	30 - 5	3.5	153	6296	15
Oxy #6	525	54 - 15	5.6	167	11,210	12
Oxy #7	117 (11 in coal)	80 - 33	17.6	16	346	4.6
Oxy #8	201 (35 in coal)	41 - 26	12.4	14	1397	4.6



V. P. #5 Mine
Buchanan County, Va.

Fig. 1 - Location of methane drainage holes.

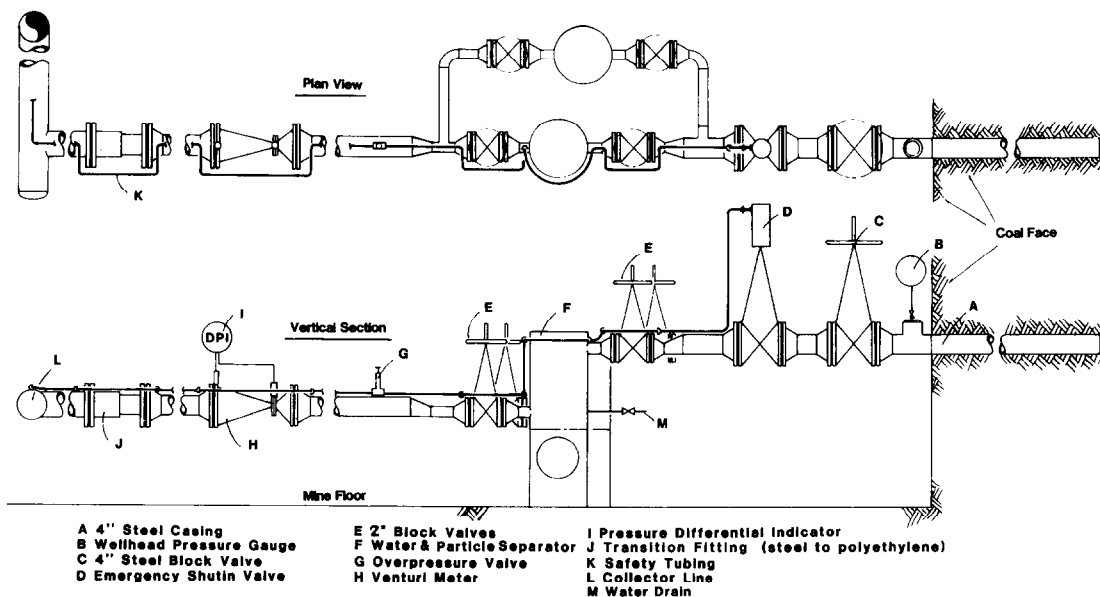


Fig. 2 - Degasification hole completion.

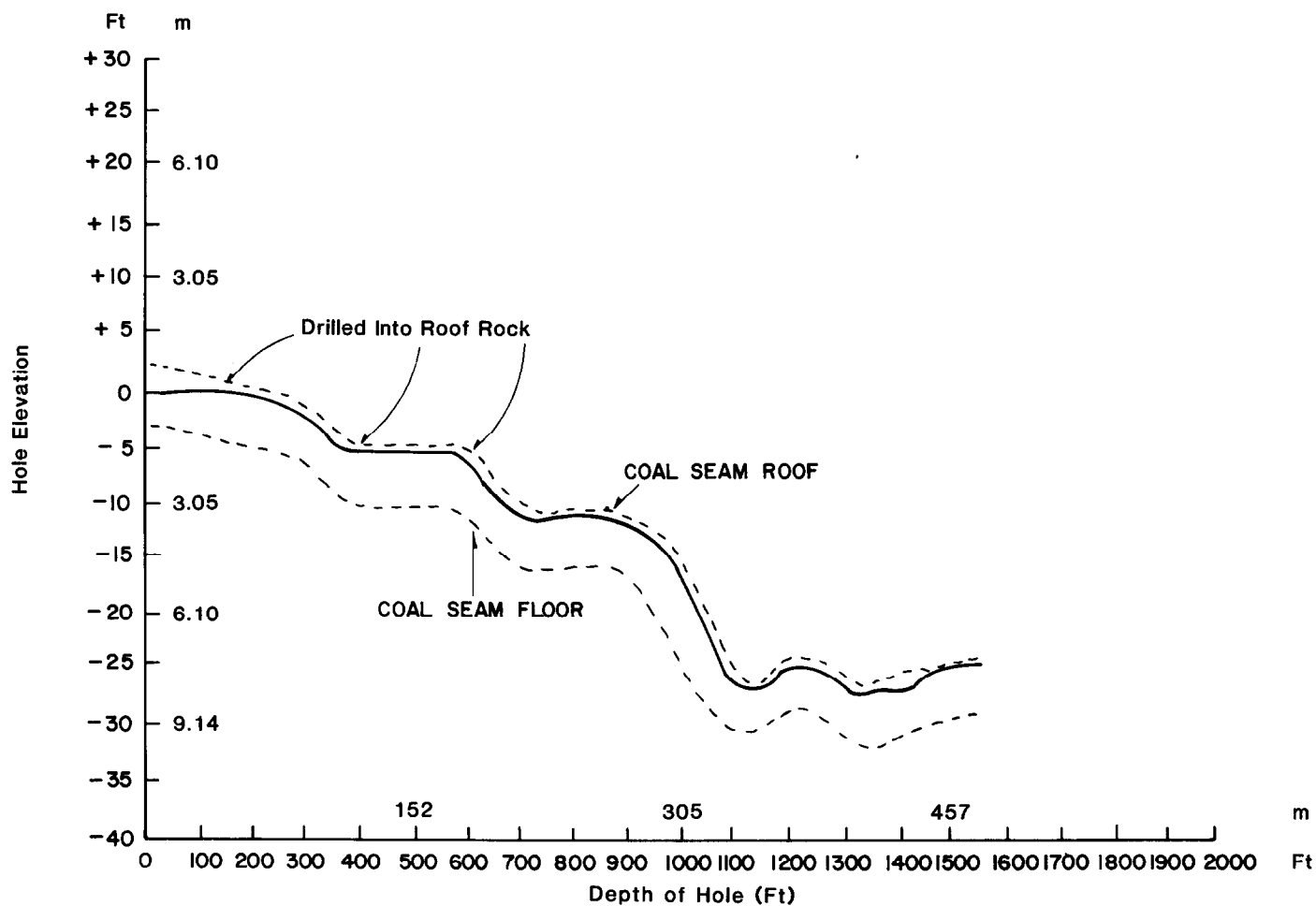


Fig. 3 - Trajectory of Oxy #5 hole.

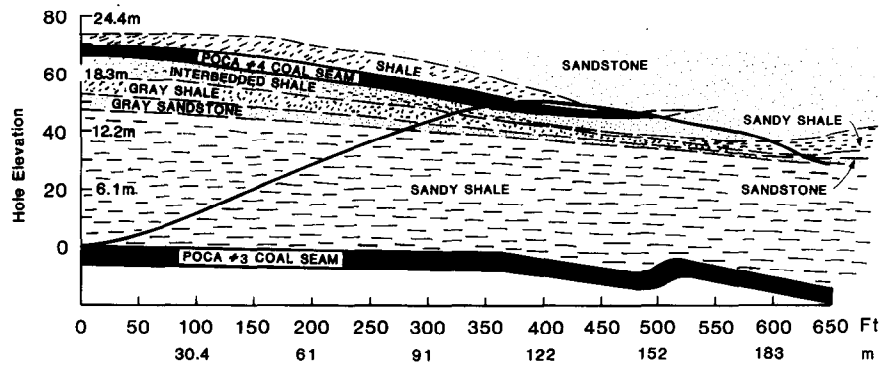


Fig. 4 - Trajectory of Oxy #8 hole.

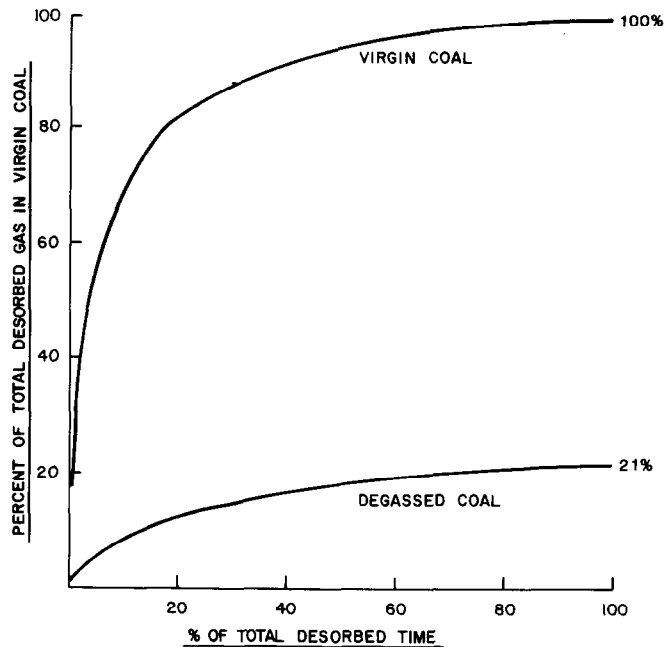


Fig. 5 - Desorption curves for virgin and degassed coal samples.

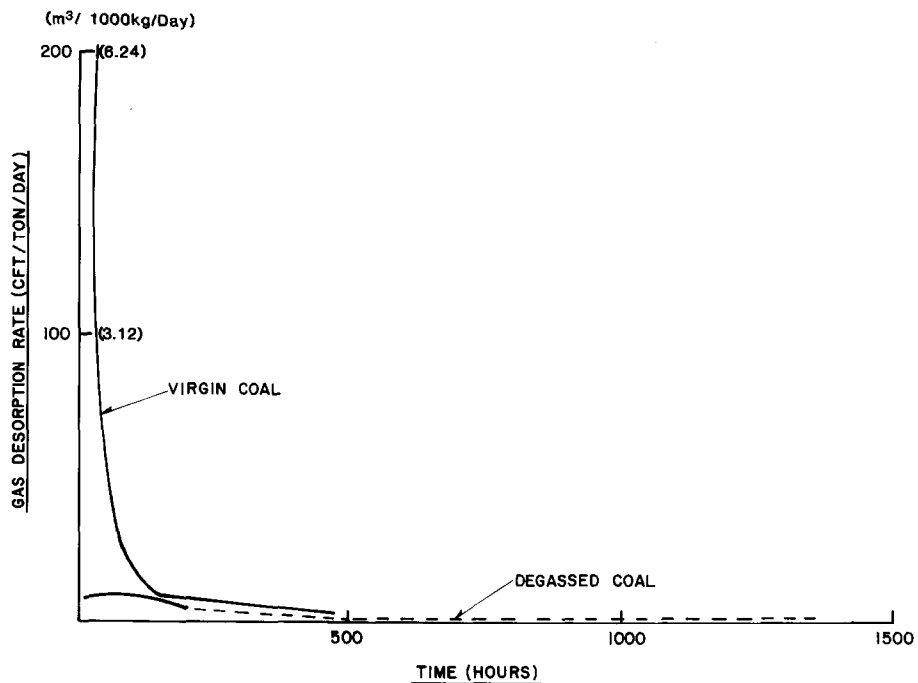


Fig. 6 - Effect of in-seam drainage on gas desorption rate.

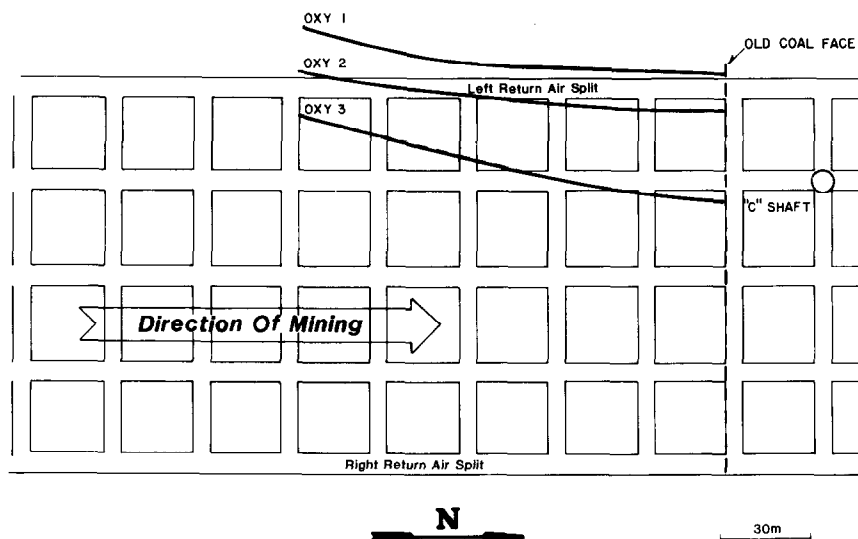


Fig. 7 - Mine plan and location of intercepted holes.

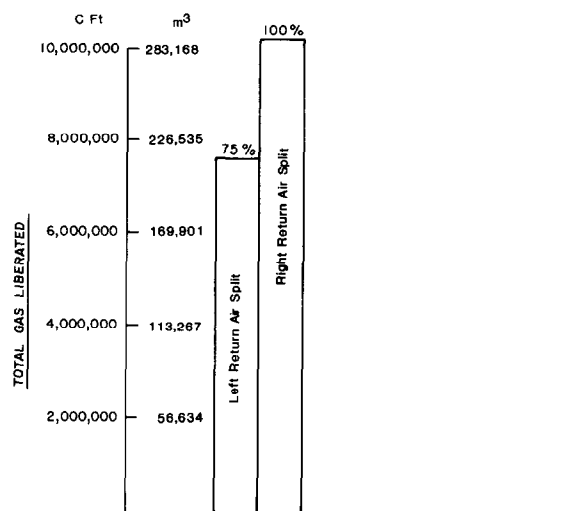


Fig. 8 - Gas in left and right return airway.

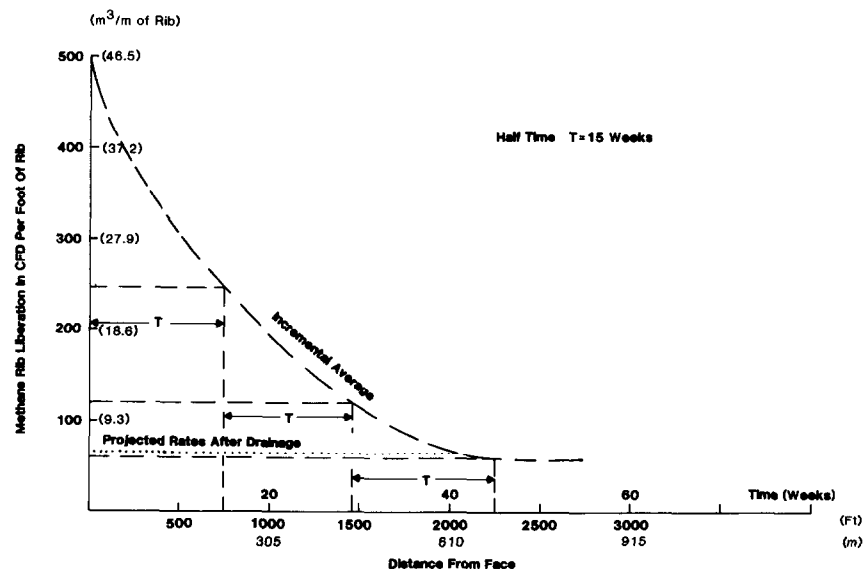


Fig. 9 - Rate of rib liberation of methane as a function of face location.

ANALYSIS OF THE COALBED DEGASIFICATION PROCESS AT A SEVENTEEN WELL PATTERN IN THE WARRIOR BASIN OF ALABAMA

By K.L. Ancell, INTERCOMP; S. Lambert,
U.S. Dept. of Energy; F.S. Johnson,
INTERCOMP

This paper was presented at the 1980 SPE/DOE Symposium on Unconventional Gas Recovery held in Pittsburgh, Pennsylvania, May 18-21, 1980. The material is subject to correction by the author. Permission to copy is restricted to an abstract of not more than 300 words. Write: 6200 N. Central Expwy., Dallas, Texas 75206

ABSTRACT

This paper presents an analysis of the coalbed degasification process. The theoretical and experimental basis of the degasification process are discussed and a simulation model which incorporates all aspects of this process is described. The simulator is demonstrated using actual field data developed by a joint industry/government demonstration project funded by the DOE and U. S. Steel. The basic reservoir description is discussed in detail, including variations of important description parameters with location.

Initial and boundary conditions are demonstrated and analyzed. Initially, the coalbed was saturated with water. With water production, reservoir pressure is lowered, causing gas to desorb from the coal creating a mobile gas saturation. Subsequently, interwell interference effects are demonstrated and the need for such effects explained.

Finally, the long term gas deliverability of the pattern is forecast. This forecast shows that about 45% of the gas within the pattern can be removed if the pattern is in operation six years ahead of mining.

INTRODUCTION

During the process of coalification, considerable quantities of gases are evolved from the indigenous carbonaceous material. These gases include methane and heavier hydrocarbons, carbon dioxide, nitrogen, oxygen, hydrogen, and helium.^{1,2} The primary constituents are methane and carbon dioxide, and these gases have been observed in coal mines since the inception of the industry.

Quantities of methane and air in proper proportions (5 to 15 percent methane) result in explosive mixtures.³ It is these mixtures that when ignited cause the disastrous explosions in coal mines. For many years, the only method of controlling the accumulations of explosive mixtures was a combination of

increasing the ventilation and decreasing the extraction rate. These activities are costly and reduce productivity. With the advent of the energy shortage, the waste of the valuable gas resource makes the practice even more undesirable.

GAS CONTENT OF COALBEDS

Gas can be contained in coal either as free gas in the joints and fractures or as an adsorbed layer on the internal surfaces of the coal.⁴ It is important to understand that the free gas contained in the fracture system will behave according to Boyles and Charles Laws just as gas accumulations in any reservoir rock. On the other hand, the gas which is adsorbed onto the internal surfaces does not behave according to Boyles and Charles Law, but in a very distinctive manner.

It is common knowledge that carbonaceous substances such as charcoal, coke, and coal can adsorb gases preferentially, and this is what gives these substances their filtration properties. It is this same mechanism that stores methane and other gases in coal. In the adsorbed state, the gas molecules are "tightly packed and closely held" to the walls of the minute sized pores in the structure of the coal.⁴

The packing is thought to be only one molecule thick and its density increases with pressure. The large surface area available because of the very fine pore structure of the coal makes it possible to hold large quantities of gas. Fig. 1 is a plot that shows the relationship of the volume of gas that can be retained as a function of pressure for several U. S. coals. This plot is shown as volume in cm³/g of coal as a function of pressure shown in atmospheres and is known as the equilibrium sorption isotherm. At low pressures, the volume adsorbed increases rapidly and almost linearly. At higher pressure when the adsorbed layer becomes more crowded, the adsorption slows and finally, at extremely high pressures, it nearly stops.

References and illustrations at end of paper.

SORPTION KINETICS OF COAL

While the measurement and prediction of the gas that can be stored in coal is very important, it does not tell the complete story of production of methane from coal. If the coalification process makes gas available to the coal surfaces, then the coal-methane system will exist in equilibrium at that temperature, pressure and very probably above the critical moisture value because free water exists as a water saturation in the coal fractures.

If the pressure is lowered by the removal of some of its fluids, the coal will desorb some of its adsorbed gases. The amount that would ultimately be desorbed is calculated by the difference between equilibrium volume at initial conditions and that at the reduced pressure. However, the rate at which this happens is a function of another set of parameters which describe the kinetics of the system.

The emission of gas from coal requires the movement of fluids from their storage place, i.e. the micropores of the coal to a surface, i.e. a well, mine face, outcrop, etc. Patching⁴ and others^{3,5,6,7} postulate that flow in coal can occur in two ways. In solid unfractured coal, the flow is thought to be the very slow diffusion of gas molecules through the pores in response to differences in concentration. In fractured coal, the flow is through fractures in response to pressure gradients. The flow through fractures is much more rapid than the diffusion through solid coal. In large size samples of coal, both types of flow occur simultaneously.

Thimons and Kissell⁸ demonstrated this postulation by flowing methane through very small discs of coal. Their results showed that where fractures existed the flow was laminar flow and could be described by Darcy's Law, and when fractures did not exist the flow was by diffusion.

A system of fractures commonly referred to as "cleat" exists in all coal beds.⁹ This has meaning in the sense that all coal particles are surrounded by fracture planes at some distance. Conclusions from the above references lead to the development of equations which describe the diffusion flow from the solid coal or matrix into the fracture system. Crank and others^{10,11} have shown that utilizing Fick's Laws the differential equation for diffusion into or out of a sphere is

$$\frac{D}{r^2} \frac{\partial}{\partial r} \left(r^2 \frac{\partial C}{\partial r} \right) = \frac{\partial C}{\partial t} \dots\dots\dots (1)$$

where C = concentration, cm³/g
r = distance from the center of sphere, cm
D = diffusion coefficients, cm²/sec
t = time, sec

An analytic solution of Equation (1) for the amount of gas entering or leaving the sphere is given by

$$\frac{M_t}{M_\infty} = 1 - \frac{6}{\pi^2} \sum_{n=1}^{\infty} \frac{1}{n^2} \exp(-Dn^2\pi^2 t/a^2) \dots\dots\dots (2)$$

where M_t = amount sorbed at time, t
 M_∞ = amount sorbed at equilibrium
a = radius of the sphere, cm

Further, it is shown by Crank that the shape of the particle is relatively unimportant and the above equation for a sphere adequately describes the flow for many other shapes as well.

Laboratory investigations of these parameters have been performed by several authors.^{12,13,14} Some of the more important results were presented by Hofer et al.¹³ They showed data that led to the following conclusions:

- (1) The adsorption/desorption process appears to be diffusion controlled.
- (2) The rate curves for adsorption and desorption are the same. The process is reversible.
- (3) The rate of adsorption/desorption is dependent on partial size of the sample.

It is important to note that the solution of the differential equation (1) required the data of diffusion coefficient, D, and the effective fracture spacing, a. However, the system is adequately described by the ratio, D/a² is referred to as the diffusion parameter and is a function of the coal type and the fracture spacing.

RESERVOIR CHARACTERISTICS OF COALBEDS

Although coal beds have several unusual characteristics, the only unique feature about the coal reservoir is the manner in which the gas is stored in the adsorbed state. The mechanisms for the release of the adsorbed gas were discussed in the previous section. Once the gas exists as free gas, the equations applicable to conventional petroleum reservoirs apply.³ These equations are based on Darcy's Law of fluid flow in porous media and the continuity equation. These are discussed in detail later. A discussion of the more important properties of coal beds follows.

1. Cleat in Coal

Coalbeds universally exhibit a natural system of fractures. Except in areas of high tectonic activity, the fracture system is generally perpendicular to the bedding planes of the coal. This system of joints and fractures is commonly referred to as cleat. The origin of cleat in coal is the subject of much discussion; however, it has been observed for many years. Coal mines are traditionally planned to take advantage of the cleat by mining in the direction in which coal breaks most easily.¹²

Frequently there exists a direction in which the cleat system is much better developed than the other. This direction of more frequent fracture spacing and longer, more continuous fractures is called the face cleat. The less developed, shorter fractures are called the butt cleats. The face and butt cleat directions are frequently separated by about 90°.

The variable frequency of fracture spacing with direction yields measurable differences in permeability. Holes or other conduits parallel to the butt cleat direction yield fluid productions up to 10 times greater than those parallel to the face cleat.⁸

2. Porosity of Coal

When determining the porosity of coal, it must be specified that we are looking for the fractional volume of the coal that is capable of being occupied by free gas and not adsorbed gas. This presents somewhat of a problem when measuring porosities of core samples. Taber et al in nearly the only laboratory investigation of coal reservoir properties^{18,19,20,21} reported large differences in porosities between those measured with helium and those measured with water as saturating fluids. Helium porosities on five samples varied from 2.5 to 8.6 percent while water porosities varied from 0.4 to 1.1 percent.

It is thought that this is a function of pore size that the respective molecules could penetrate. The water porosities probably are a better representation of the porosity of the fracture of cleat system. This is consistent with work done by the Bureau of Mines personnel in water infusion experiments. Porosities of fracture systems of about 1 to 4 percent are the best estimates that have been found to date. Kneuper² predicts an effective porosity of 1.3 to 3.9 percent for European coals.

3. Permeability of Coal

Again, the best work on permeability of laboratory samples is by Taber et al.¹⁸ However, it is simply not possible to accurately measure permeabilities of fracture systems in laboratory samples. Cores taken in a virgin coal bed have been broken by the drilling process, and confining stresses have been relieved.

To date, the best estimates of permeability have been made by "history matching" observed production data. This is discussed in a later section. Absolute permeabilities of from 1/10th to 250 millidarcies have been postulated for various coal beds in the U. S.

4. Saturation Distributions in Coal

There are several keys available that lead to the conclusion that initially the cleat system is saturated with water in virgin coal beds. Drill stem test data (unpublished) show recoveries of water with little or no gas. Nearly all data available on vertical wells show that water rates initially start at high levels and decline while gas rates starts at near zero and increase.^{19,20,21,22,23}

Further, field studies have shown that permeabilities to gas must increase with time.²⁴ This has been consistently demonstrated in several mines in different coalbeds. This is readily explained by the concept of relative permeability. As water is produced and gas is desorbed, the water saturation in the fracture system decreases and gas saturation increases. Increased gas saturation with time results in higher permeability to gas.

5. Relative Permeability and Capillary Pressure of Coal

Again, the only recent work has been done by Taber et al.¹⁸ This work is limited to Pittsburgh and Pocahontas coal, but fortunately these coals cover the range of friable and blocky type coals. Gas relative permeability curves are shown on Fig. 2. Their resulting capillary pressure curve is shown as Fig. 3.

6. Pressure-Depth Relationships in Coal

Reservoir pressures increase with depth in coal beds just as in any other geologic formation. What data is available^{19,20,5} indicates that the pressure gradient is generally somewhat less than a hydrostatic gradient. Several examples tend to indicate a gradient of 0.2-0.4 psi/ft based on some drill stem test data (unpublished) and horizontal holes with packers.^{5,24,6}

Caution should be used when using the hydrostatic gradient because most of the data available is from the eastern United States, and other geological basins are likely to show different pressure depth-relationships.

7. Gas Quality of Coal Beds

The gas produced from coal beds is of high quality. In the most comprehensive study on the composition of coal bed gas, Kim¹ reports that all samples contain large amounts of methane. Quantities do vary from 84 to 99 percent methane. Heating value varied from 840 Btu/cuft to 990 Btu/cuft when calculated at 30 inches of mercury, saturated with water vapor.

Quantities of carbon dioxide do exist in nearly all samples, and in some cases there are measurable quantities of heavier hydrocarbons, oxygen, nitrogen, helium, and hydrogen. It is interesting to note that no sulfur dioxide or hydrogen sulfide has been found in any of the coal bed gas samples, even in high sulfur coal beds.

DEVELOPMENT OF SIMULATION MODEL

The previous sections contained a discussion of individual parameters that determine the flow of gas in coal beds. This section relates the parameters to one another in a mathematical manner that allows quantitative evaluation and validates the calculations with field data.

Mathematical Description of the Coal Gas Process

The production of methane from coalbeds is believed to be dependent upon two distinctly different physical processes (1) diffusion from the interior of a solid coal particle to a crack or macropore in the coal, and (2) two-phase (gas-water) Darcy flow through the fracture or macropore structure to a shaft or production well.^{3,6} The two-phase aspect of the fracture flow in coalbeds is evidenced by the increase in permeability with time that has been consistently observed.²⁴ This phenomenon is readily explained by the relative permeability concept used to describe flow in oil and natural gas reservoirs.

1. Methane Diffusion

Diffusion of methane through solid particles of coal is a much slower process than the fracture flow. Depending on particle size, it may or may not be the controlling factor in production.²⁵ Diffusivities have typically been measured by grinding coal particles to a uniformly small size and comparing rates of desorption to analytical solutions for diffusion in a sphere of comparable diameter.

The differential mass balance describing diffusional transport in a sphere is as follows:¹⁰

$$\frac{D}{r^2} \frac{\partial}{\partial r} \left(r^2 \frac{\partial C}{\partial r} \right) = \frac{\partial C}{\partial t} \quad \text{.....(3)}$$

(The nomenclature defining each of the symbols used is found later in this paper.)

The concentration of methane, C , is expressed as moles/unit volume of coal. The boundary conditions for this equation are as follows:

$$\frac{dC}{dr} = 0 \quad \text{at } r = 0 \quad \text{.....(4)}$$

$$C = f(p_g) \quad \text{at } r = a \quad \text{.....(5)}$$

The rate of methane desorption at the surface of the sphere is given by

$$N = (M.W.) 4\pi r^2 D \left. \frac{\partial C}{\partial r} \right|_a \quad \text{.....(6)}$$

or expressed on a unit volume basis:

$$N_v = \frac{3(M.W.)D}{r} \left. \frac{\partial C}{\partial r} \right|_a \quad \text{.....(7)}$$

2. Two Phase Fracture Flow

The differential equations describing the flow of gas and water in a coal bed's fracture system result from combining continuity equations with the Darcy expression for flow in a porous medium:

Continuity Equations

$$-\nabla \cdot (\rho_w v_w) - q_{wv} = \frac{\partial}{\partial t} (\phi \rho_w S_w) \quad \text{.....(8)}$$

$$-\nabla \cdot (\rho_g v_g) + N_v - q_{gv} = \frac{\partial}{\partial t} (\phi \rho_g S_g) \quad \text{.....(9)}$$

Darcy Equations

$$v_w = - \frac{k k_r}{\mu_w} (\nabla p_w - \rho_w g \nabla h) \quad \text{.....(10)}$$

$$v_g = - \frac{k k_r}{\mu_g} (\nabla p_g - \rho_g g \nabla h) \quad \text{.....(11)}$$

Substitution of Equations (10) and (11) into (8) and (9) yields

$$\nabla \cdot \left\{ \frac{\rho_w k k_r}{\mu_w} (\nabla p_w - \rho_w g \nabla h) - q_{wv} \right\} = \frac{\partial}{\partial t} (\phi \rho_w S_w) \quad \text{.....(12)}$$

$$\nabla \cdot \left\{ \frac{\rho_g k k_r}{\mu_g} (\nabla p_g - \rho_g g \nabla h) + N_v - q_{gv} \right\} = \frac{\partial}{\partial t} (\phi \rho_g S_g) \quad \text{.....(13)}$$

These two equations contain five dependent variables -- p_w , p_g , S_w , S_g , and N_v . Two additional equations are required to complete the coal gas model.

$$p_g = p_w + p_c \quad \text{.....(14)}$$

$$S_g = 1 - S_w \quad \text{.....(15)}$$

Equations (14) relates the gas phase pressure to the water phase pressure through a capillary pressure, p_c , which is a measured function of water saturation, S_w (see Fig. 6). Equations (15) just states that the pore space is filled with water and gas.

In order to calculate the gas desorption term, N_v , that appears in Equations (13), it is necessary to solve Equation (3) for concentration. The desorption rate is then calculated from the concentration gradient in accordance with Equations (7). The finite difference approximations to the equations and the solution of these equations is shown in the Appendix.

APPLICATION OF SIMULATION MODEL

Validation of the simulation model was achieved by the analysis of laboratory and field studies. The desorption calculations were identical with the results obtained by Bielicki²⁵ and Hofer¹³. Further, the Coupling of the desorption calculation with the reservoir was tested against the analytic solution to the diffusion equation. The results were that the laboratory experiments, as well as the analytic solution, could be described by the model.

The field example shown here reflects the data from a seventeen well pattern in Jefferson County, Alabama. The project is a joint effort between U. S. Steel Corporation and the Department of Energy.

Example Simulation

Stubbs, et al²⁶ give a description of the pattern and operation. A more complete description of the completion and stimulation methods used in the pattern are given by Lambert, et al.²⁷ The pattern, drilled into the same coalbed being mined is far enough away from the mine to be at least five years in advance of mining.

Fig. 4 shows the surface well pattern with valley creek running through the pattern. Subsurface depths are also indicated with suspected structural faulting. The faults indicated to the east and southeast of the pattern were shown on a core hole map used in deciding prospective mine locations. Both surface and subsurface features indicated possible faulting around well 22. The 1100 ft. deep wells penetrate a 5.2 ft. coal seam. Most of the wells were completed open hole and all were hydraulically fractured. Gas production

began from well 22 on August 5, 1977, but the last well was not put on production until March 1, 1979. Production data was available through October 31, 1979.

Fig. 5 shows the production data for the first 700 days of operation. The first 300 days reflect production from only three wells 7, 9, and 22. As shown on Fig. 4, these wells are widely spaced within the pattern and did not interfere with one another. The result is that 150 - 200 bpd of water was produced with little gas production. As soon as more wells were placed on production, the gas volumes started to increase. This is caused by interference between wells which creates large areas of pressure drawdown.

The purpose of the simulation was the extension of a matched production history to predict future gas production. To simulate the reservoir, a two-dimensional grid was constructed such that two grid blocks would separate each block that contained a well. Since the wells were 1000 feet apart, grid blocks in the pattern area were 333.3 feet square. The grid blocks become larger away from the well area as shown in Fig. 6. Several longer grid blocks were eliminated to the east and southeast simulating the suspected barrier faults in these directions. The gradual increase in depth of the coalbed to the southeast was simulated by tilting the grid in both the x and y directions.

Other data used in the simulation model came from several different sources. The equilibrium sorption isotherm data used are shown in Table 1. The original data, taken on a sample of the Mary Lee coal was adjusted slightly to give an average gas content of 482 SCF/ton at the reservoir pressure of 421 psia. The gas properties were calculated assuming methane as the major constituent of the gas. Data obtained by matching early time desorption rates from the core samples with a simple desorption model showed that the D/a^2 , diffusion parameter, varied over several orders of magnitude. The limited values we had showed D/a^2 increased to the east. Using the same trend, values used in this simulation ranged from 1×10^{-10} to 1×10^{-11} sec^{-1} . A relative permeability curve was developed during the matching process which has a critical gas saturation of 20 percent as shown in Fig. 7. This curve is not dissimilar from the laboratory curve for friable coal shown on Fig. 2.

The primary unknown variables in making the history match were the porosity and the permeability. During the early matching process porosities as high as 5 percent was used for the whole pattern. However, to enable gas saturations to build up high enough to flow gas in most wells, the porosity was eventually lowered to 1.2 percent. Early matching attempts used permeabilities as low as 3 md. Low permeabilities did not allow enough interference between wells and caused the well blocks to decline in pressure too rapidly. A permeability of 75 md. over most of the area corrected this problem although this had to be increased in some areas. Fig. 6 shows areas in which the permeability and porosity were adjusted above these normal values.

The model was initialized with the fracture system saturated with water. The gas content of the coal was at equilibrium with the initial pressure of 421 psia. The individual wells were simulated by a point source at the center of the grid block where the well is

located. The wells were subsequently produced by specifying a water production rate consistent with the wells demonstrated pump capacity. Limiting bottomhole pressures were calculated from liquid level determinations and surface pressures. The well then produced pump capacity or reservoir deliverability against the calculated limiting pressure. The gas-water ratio was then determined by the relative permeabilities of the two phases in the grid block containing the well. The limiting bottomhole pressures were decreased in a stepwise manner consistent with the measured decline in the wells.

The individual wells were assigned production rates at times corresponding to actual first production. The major shut in periods were simulated by periods of zero flow.

The simulation results for the pattern are shown plotted with the actual production in Fig. 8. There are too many wells to show all of the individual wells; however, a few will be shown to illustrate the capabilities of building into the simulation model certain geological and operational features necessary to understand why the wells perform as they do.

For instance, well 22 produced at a fairly constant high water rate and low gas rate. The actual and simulated production rates are shown in Fig. 9. The high water rate compared to other wells in the pattern could indicate a source of water other than that normally in the immediate vicinity of the well. This model allowed us to simulate an area of increased porosity and permeability in the same general area as the possible faulted zone indicated on Fig. 6.

As a different example, well 4 indicates an immediate gas rate response when the well is turned on with the water rate falling off rapidly. See Fig. 10. This indicates the possibility of a barrier near the well which causes rapid pressure draw down along with increased gas saturation. The two faults shown to the east and southeast of the well pattern on Fig. 6 could cause this phenomena. In the model, the symmetrical grid was ended at grid block 21 and the other blocks eliminated on the southeast to simulate these barrier faults.

Well 7, shown in Fig. 11, is located inside the pattern. Its high gas rate beginning after 582 days is indicative of the effect of surrounding wells being placed on production creating interwell interference. Pressure interference between wells results in a rapid lowering of the pressure between wells. Thus, the gas was released at the maximum rate at which the diffusivity function will allow in this interwell area. This well was probably effected by the previously discussed well 4, among others. The high permeability in the area of wells 3, 4, 7, and 8 was necessary to obtain this type of interference. Actually, during fracturing, communications were demonstrated between wells 4 and 7.

Not all the individual wells were good matches. For instance, well 25, shown in Fig. 12 shows that the computed water rate was low. However, looking at the well data, it produced at a very low rate even though the water rate remained high. One reason for this is the well is an outside well in the pattern; thus, it was not subjected to as much interference as internal wells. Limited echometer data indicated that this well was not being pumped off and thus retained a high fluid level in the well. The porosity in this area of the

ANALYSIS OF THE COALBED DEGASIFICATION PROCESS
AT A SEVENTEEN WELL PATTERN IN THE WARRIOR BASIN OF ALABAMA

field was increased to provide more water to be produced before the critical gas saturation was reached. The well finally started producing gas after 735 days when the well began to be pumped off as indicated by the fall off in water rate starting at this time. Although we increased the porosity in the vicinity of this well, the high bottomhole pressure lowered the water rate until the high pressure was removed.

The relatively good match of individual well production rates and the excellent match of the total pattern production rates give credence to predicting what the pattern will produce in the future. Fig. 13 shows the result of continuing to produce the model for 20 years into the future. It can be seen that after only a few months of continued increase in gas production, the rate begins to decline. However, a stable rate of about 400 MCFD is predicted after nine years of production. This rate continues through the remainder of the 20 year period and the recovery at that time is calculated to be 3.8 BCF of gas. At the end of 20 years, about 77percent of the producible gas was removed from the area covered by the 17 well pattern. This means that approximately 2.6 BCF of the gas was produced from the area outside the limits of the pattern.

At the end of six years, which corresponds to the projected time of mining, approximately 45% of the producible gas will be removed from the area covered by the 17 wells. This amount of removal will materially reduce the methane emissions anticipated during mining. Further, the gas recovered is at a rate that is significant from a gas supply standpoint and should be sold or utilized.

This example demonstrates that gas can be recovered from coalbeds at rates that can materially affect the gas content of coal ahead of mining. Further, this rate is significant for a gas supply.

NOMENCLATURE

a	=	radius of coal particle, cm
C	=	Concentration, g.mole/cm ³
D	=	diffusivity, cm ² /sec
g	=	acceleration of gravity, cm/sec ²
G	=	gas gravity, air-1.0
h	=	subsea depth, m
k	=	permeability, md
k _r	=	relative permeability
M	=	volume sorbed, cm ³
M.W.	=	molecular weight, g/g.mole
N	=	rate of methane desorption, g/sec
N _v	=	rate of methane desorption per unit coal volume, g/cm ³ -sec
p	=	hydraulic pressure in the fracture system, g/cm-sec ²
P _c	=	capillary pressure, g/cm-sec ²
q	=	production rate, g/sec
Q	=	flow rate, Mcf/d
q _v	=	rate of production per unit volume, g/cm ³ -sec
r	=	radial distance from the center of a sphere or circle, cm
t	=	time, sec
T	=	transmissibility, Darcy-cm
v	=	velocity, cm/sec
V	=	volume adsorbed, cm ³
V _c	=	grid block volume, cm ³
z	=	compressibility factor
ρ	=	density, g/cc

φ	=	volume of the fracture system relative to total coal volume (effective porosity)
μ	=	viscosity, cp
θ	=	angular displacement, degrees

Subscripts

g	=	gas
i	=	grid block index (x or r direction)
j	=	grid block index (y direction)
k	=	grid block index (z direction)
NR	=	number of grid blocks in radial direction
t	=	time
T	=	total
v	=	volume
w	=	water
x	=	x coordinate values
y	=	y coordinate values
z	=	z coordinate values

Superscripts

n	=	present time level
n+1	=	next time level

REFERENCES

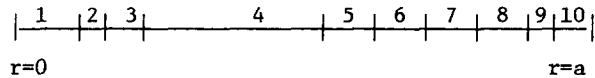
- Kim, A.G.: "The Composition of Coalbed Gas," USBM RI 7762 (1973).
- Kneuper, K., and Huckel, B.A.: "Contribution to the Geochemistry of Mine Gas in the Carboniferous Coal Field of the Saar Region, Germany," Advances in Organic Geochemistry, Pergamon Press, Oxford (1972).
- Cervik, J.: "Behavior of Coal-Gas Reservoirs," paper SPE 1973, (Nov. 1967).
- Patching, T.H.: "The Retention and Release of Gas in Coal - A Review," CIM Transactions, (1970) 73.
- Kissell, F.N.: "Methane Migration Characteristics of the Pocahontas No. 3 Coalbed," USBM RI 7649 (1972).
- Kissell, F.N., and Bielicki, R.J.: "An In Situ Diffusion Parameter for the Pittsburgh and Pocahontas No. 3 Coalbeds," USBM RI 7668 (1972).
- Kissell, F.N., and Edwards, J.C.: "Two-Phase Flow in Coalbeds," USBM RI 8066 (1975).
- Thimons, E.D., and Kissell, F.N.: "Diffusion of Methane Through Coal," FUEL (1973) 52.
- McCulloch, C.M., et al: "Cleat in Bituminous Coalbeds," USBM RI 7910 (1974).
- Bird, R.B., Stewart, W.E., and Lightfoot, E.N.: Transport Phenomena, John Wiley and Sons, (1960).
- Crank, J.: The Mathematics of Diffusion, Second Edition, Oxford Press (1975).
- Bayer, J., Hoyer, L.J.E., and Anderson, R.B.: "Summary of Pertinent Data on Sorbtion of Methane on Some Appalachian Coals," unpublished USBM Report (1963).

13. Hofer, L.J.E., et al: "Rates of Adsorption of Methane on Pocahontas and Pittsburgh Seam Coals," USBM RI 6750 (1966).
14. Sevenster, P.G.: "Diffusion of Gases Through Coal" FUEL, Report No. 9 of 1958 (1959).
15. Dabbous, M.K.: "Gas-Water Capillary Pressure in Coal at Various Overburden Pressures," Soc. Pet. Eng. J. (1976).
16. Dabbous, M.K., et al: "The Permeability of Coal to Gas and Water," Soc. Pet. Eng. J. (1974) 257.
17. Reznik, A.A., et al: "Air-Water Relative Permeability Studies of Pittsburgh and Pocahontas Coals," Soc. Pet. Eng. J. (1974).
18. Taber, J.J., et al: "Development of Techniques and the Measurements of Relative Permeability and Capillary Pressure Relationships in Coal," USBM (1974).
19. Deul, M., and Elder, C.H.: "Degasification of the Mary Lee Coalbed Near Oak Grove, Jefferson County, Alabama, by Vertical Borehole in Advance of Mining," USBM RI 7968 (1974).
20. Deul, M., and Elder, C.H.: "Hydraulic Stimulation Increases Degasification Rate of Coalbeds," USBM RI 8047 (1975).
21. Fields, H.H.: "Degasification and Production of Natural Gas from an Air Shaft in the Pittsburgh Coalbed," USBM RI 8173 (1976).
22. Fields, H.H., et al: "Commercial-Quality Gas from a Multipurpose Borehole Located in the Pittsburgh Coalbed," USBM RI 8025 (1975).
23. Fields, H.H., et al: "Degasification of Virgin Pittsburgh Coalbed Through a Large Borehole," USBM RI 7800 (1973).
24. Kissell, F.N.: "The Methane Migration and Storage Characteristics of the Pittsburgh, Pocahontas No. 3 and Oklahoma Hartshorne Coalbeds," USBM RI 7667 (1972).
25. Bielicki, J.H., et al: "Methane Diffusion Parameters for Sized Coal Particles," USBM RI 7697 (1972).
26. Stubbs, P.B., Dobscha, F.X., and Mahoney, J.V.: "Degasification of the Blue Creek Coal Seam at Oak Grove Mine," Proc., Second Annual Methane Recovery from Coalbeds Symposium, METC/SP-79/9, U.S. DOE (Apr. 1979) 97-113.
27. Lambert, S.L., Trevits, M.A., and Stiedl, P.F.: "Vertical Borehole Design and Completion Practices Used to Remove Methane Gas From Minable Coalbeds," unpublished U.S. DOE Report (Dec. 1979).

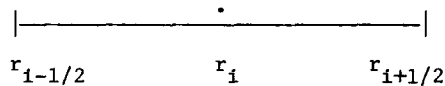
APPENDIX

1. Finite Difference Approximation of the Gas Diffusion Equations

The model sphere on which concentration solutions are to be obtained is subdivided into a series of spherical shells. This subdivision can be illustrated on a line segment, since the solution is one-dimensional and dependent only on the distance from the center of the sphere:



Each of the intervals into which the radius of the sphere is divided is called a grid block. In the coal gas program, the boundaries of the grid blocks are located at $a/8$, $a/6$, $a/4$, $0.5a$, $0.6a$, $0.7a$, $0.8a$, $0.9a$, $0.95a$, and a . To avoid complications that occur at $r=0$, the problem is solved for a hollow sphere with the $a/8$ boundary treated as a no flux boundary as indicated by Equation (4). (Ignoring the particle volume for $r < 0.125a$ is of little consequence since this represents only 0.2 percent of the total volume.) The center of each grid block is taken to be the harmonic average of the block boundaries.



$$\frac{1}{r_i} = 0.5 \left(\frac{1}{r_{i-1/2}} + \frac{1}{r_{i+1/2}} \right) \quad \dots\dots\dots (A-1)$$

A finite difference approximation to Equation (1) can be written for each grid block:

$$A_{i-1/2} (C_{i-1}^{n+1} - C_i^{n+1}) - A_{i+1/2} (C_i^{n+1} - C_{i+1}^{n+1}) = B_i (C_i^{n+1} - C_i^n) \quad \dots\dots\dots (A-2)$$

or rearranged,

$$A_{i-1/2} C_{i-1}^{n+1} - A_{i-1/2} C_i^{n+1} + A_{i+1/2} C_i^{n+1} + B_i C_i^n = A_{i+1/2} C_{i+1}^{n+1} \quad \dots\dots\dots (A-3)$$

where the following definitions apply:

$$A_{i-1/2} = \frac{4\pi D}{\frac{1}{r_{i-1}} - \frac{1}{r_i}} \quad \dots\dots\dots (A-4)$$

$$A_{i+1/2} = \frac{4\pi D}{\frac{1}{r_i} - \frac{1}{r_{i+1}}} \quad \dots\dots\dots (A-5)$$

$$B_i = \frac{4\pi}{3\Delta t} (r_{i+1/2}^3 - r_{i-1/2}^3) \quad \dots\dots\dots (A-6)$$

Equation (A-3) is a backward difference approximation of Equation (1). It is second order correct in space, first order correct in time, and unconditionally stable with respect to

time step size.

This equation can be written for every grid block, except for the first and last, where boundary conditions must be considered. At $i+1$ the first term in Equation (A-2) is dropped because of the no flux boundary, leaving

$$-(A_{i+1/2} + B_i)C_i^{n+1} - A_{i+1/2}C_{i+1}^{n+1} = -B_iC_i^n \dots\dots (A-7)$$

At $i=NR(r=a)$, we have the following equation:

$$A_{NR-1/2}C_{NR-1}^{n+1} - (A_{NR-1/2} + B_{NR})C_{NR}^{n+1} = -B_{NR}C_{NR}^n + N \dots\dots (A-8)$$

where N is the rate of methane desorption. Furthermore, we know that $C_{NR}^{n+1} = f(p_g^{n+1})$.

2. Finite Difference Approximation of the Fracture Flow Equations

Equations (12) and (13) are written in terms of Cartesian coordinates; however, the coal gas simulator can solve them either in Cartesian or cylindrical coordinates. After substitution of Equations (14) and (15), Equations (12) and (13) may be approximated as follows:

$$\Delta \cdot \left\{ T \frac{\rho_w^{n+1} k_{rw}}{\mu_w^n} (\Delta p_w^{n+1} - \rho_w^n g \Delta h) \right\} - q_w^{n+1} = \frac{V}{\Delta t} \{ (\phi \rho_w S_w)^{n+1} - (\phi \rho_w S_w)^n \} \dots\dots (A-9)$$

$$\Delta \cdot \left\{ T \frac{\rho_g^{n+1} k_{rg}}{\mu_g^n} (\Delta p_w^{n+1} + \Delta p_c^{n+1} - \rho_g^n g \Delta h) \right\} + N_T^{n+1} - q_g^{n+1} = \frac{V}{\Delta t} \{ (\phi \rho_g)^{n+1} (1 - S_w)^{n+1} - (\phi \rho_g)^n (1 - S_w)^n \} \dots\dots (A-10)$$

where the following definitions apply:

$$T_x = \frac{k_x \Delta y \Delta z}{\Delta x}; T_y = \frac{k_y \Delta x \Delta z}{\Delta y}; T_z = \frac{k_z \Delta x \Delta y}{\Delta z} \dots\dots (A-13)$$

$$V = x y z \dots\dots (A-14)$$

$$N_T = V c N_v \dots\dots (A-15)$$

$$\Delta \cdot (E \Delta F) = \{ E_{i-1/2} (F_{i-1} - F_i) - E_{i+1/2} (F_i - F_{i+1}) \}_{j,k} + \{ E_{j-1/2} (F_{j-1} - F_j) - E_{j+1/2} (F_j - F_{j+1}) \}_{i,k} + E_{k-1/2} (F_{k-1} - F_k) - E_{k+1/2} (F_k - F_{k+1}) \}_{1,j} \dots\dots (A-16)$$

All relative permeabilities required at grid block boundaries are based on the saturation of the upstream grid block, i.e. the block from which that

is flowing. These finite difference equations are first order correct in both space and time and have no significant stability limitation.

3. Solution of the System of Finite Difference Equations

It is assumed that all of the coal particles can be represented as spheres and furthermore that all of these spheres are identical in size. Thus, the total rate of methane entering the fracture system in a given fracture grid block is the rate of desorption for a typical sphere contained in that block multiplied by the number of such spheres required to make up the total mass of coal in the block.

Thus, to solve the fracture flow equations (Equations (A-9) and (A-10)) we must simultaneously solve the set of equations describing diffusion in a typical sphere of coal (Equation (A-3)), one such sphere for each fracture grid block. The total system of equations consists then of $2 \cdot NX \cdot NY \cdot NZ$ fracture flow equations ($NX \cdot NY \cdot NZ$ equations for both water and gas) plus $(NX \cdot NY \cdot NZ) \cdot NR$ diffusion equations (NR equations for each model sphere).

All of these equations could be collected together in a large matrix equation and solved either directly or iteratively. It is possible, however, to greatly reduce the dimensionality of the problem. The key to this is the fact that none of the equations describing diffusion in a coal particle couple to the equations for other particles, and only the grid block at the exterior boundary of a sphere couples to a fracture system. As a consequence, the following procedure, called static condensation, can be implemented.

- (1) Collect the equations for a given sphere into a tridiagonal matrix equation.
- (2) Factor this matrix into upper and lower halves. (The factors will be identical for every sphere for any given time step, since the same grid is used for all and diffusivity is treated as a constant.)
- (3) Perform the forward elimination for each set of diffusion equations.
- (4) As explained below, the last equation in each set can now be put in the form
$$N = b_1 + b_2 p_{ijk}^{n+1} \dots\dots (A-17)$$
- (5) Substitute Equation (A-17) into Equation (A-10) and solve the resulting set of equations for p_w and S_w . (This is done by either direct elimination or iteration.)
- (6) Use the new pressure solution to get the boundary concentration on the diffusion equations for each typical sphere and perform the back substitutions to generate new concentration distributions.

Steps 4 and 5 of the above procedure require further explanation.

When the diffusion equations for a given sphere are collected together, the resulting set of equations is tridiagonal. The last two equations may be written as follows:

$$E_{NR-1} C_{NR-2}^{n+1} + F_{NR-1} C_{NR-1}^{n+1} + G_{NR-1} C_{NR}^{n+1} = R_{NR-1} \quad \text{.....(A-18)}$$

$$E_{NR} C_{NR-1}^{n+1} + F_{NR} C_{NR}^{n+1} = R_{NR} + N \quad \text{.....(A-19)}$$

where

$$E_i = A_{i-1/2} \quad \text{.....(A-20)}$$

$$F_i = -(A_{i-1/2} + A_{i+1/2} + B_i) \quad \text{.....(A-21)}$$

$$G_i = A_{i+1/2} \quad \text{.....(A-22)}$$

$$R_i = -B_i C_i^n \quad \text{.....(A-23)}$$

After the forward elimination has proceeded through equation NR-1, the last two equations are

$$C_{NR-1}^{n+1} + H_{NR-1} C_{NR}^{n+1} = U_{NR-1} \quad \text{.....(A-24)}$$

$$E_{NR} C_{NR-1}^{n+1} + F_{NR} C_{NR}^{n+1} = R_{NR} + N \quad \text{.....(A-25)}$$

If we algebraically eliminate C_{NR-1}^{n+1} between these two equations, the result is:

$$N = (-R_{NR} + U_{NR-1} E_{NR}) + (F_{NR} - E_{NR} H_{NR-1}) C_{NR}^{n+1} \quad \text{.....(A-26)}$$

We now write C_{NR} as a locally linear function of fracture pressure, p_g :

$$C_{NR}^{n+1} = f(p_g^n) + \frac{df}{dp_g} (p_g^{n+1} - p_g^n) \quad \text{.....(A-27)}$$

When this is substituted into Equation (A-26), we have an equation of the form

$$N = b_1 + b_2 p_g^{n+1} \quad \text{.....(A-28)}$$

After solving for p_g^{n+1} , we calculate C_{NR}^{n+1} , from its equilibrium pressure functionality, insert it in Equation (A-24), and solve for C_{NR-1}^{n+1} . The back substitution for the remaining C_i^{n+1} , then proceeds in the normal fashion.

TABLE 1 - EQUILIBRIUM ADSORPTION ISOTHERM DATA USED IN SIMULATION

Pressure (Atm)	Gas Adsorbed Std. cc/g
0.0	0.0
5.0	4.21
10.0	7.61
15.0	10.43
20.0	12.79
25.0	14.80
30.0	16.54

FIGURE 1
EQUILIBRIUM ADSORPTION ISOTHERMS, U.S. COALS

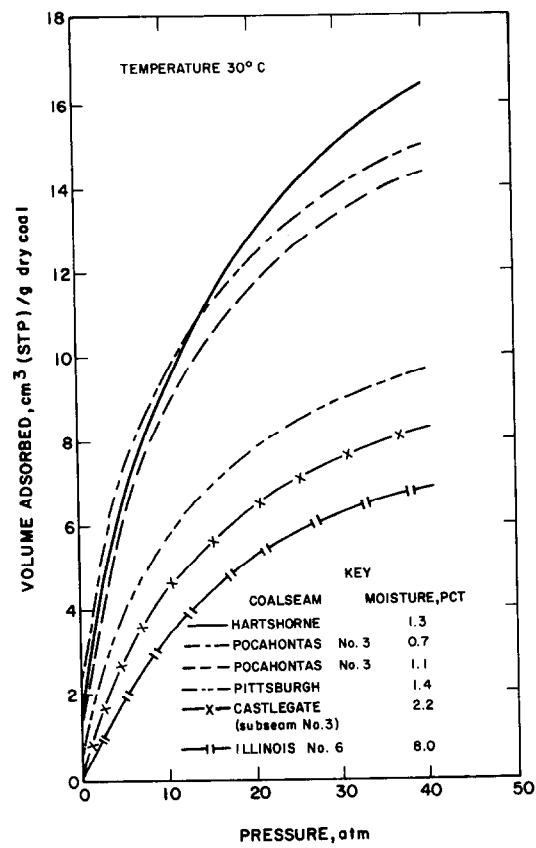


FIGURE 2
GAS RELATIVE PERMEABILITY CURVES

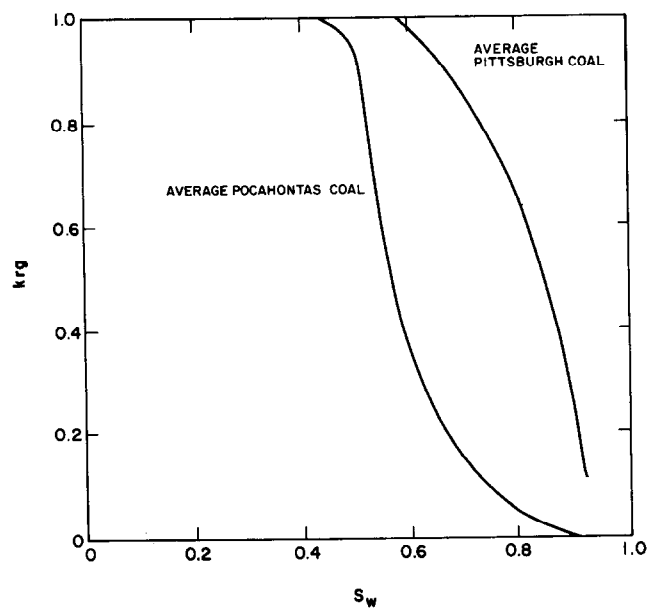


FIGURE 4
OAK GROVE DEGASIFICATION PATTERN
MARY LEE COALBED, JEFFERSON CO., ALABAMA

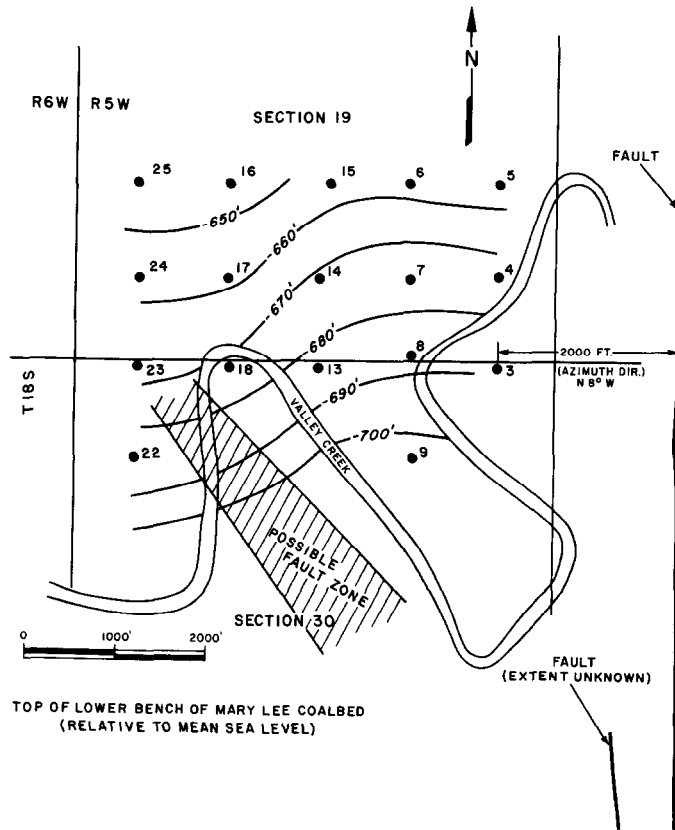
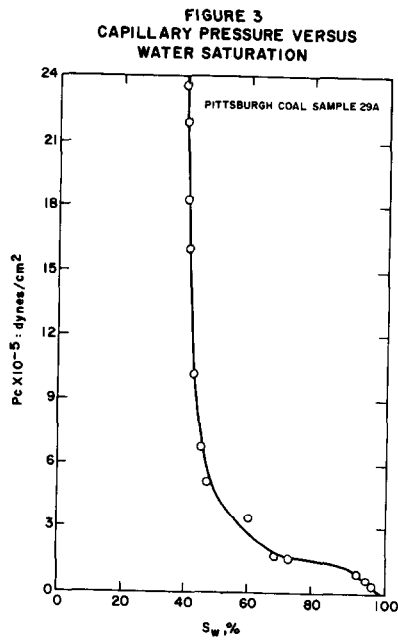


FIGURE 5
TOTAL PATTERN PRODUCTION DATA

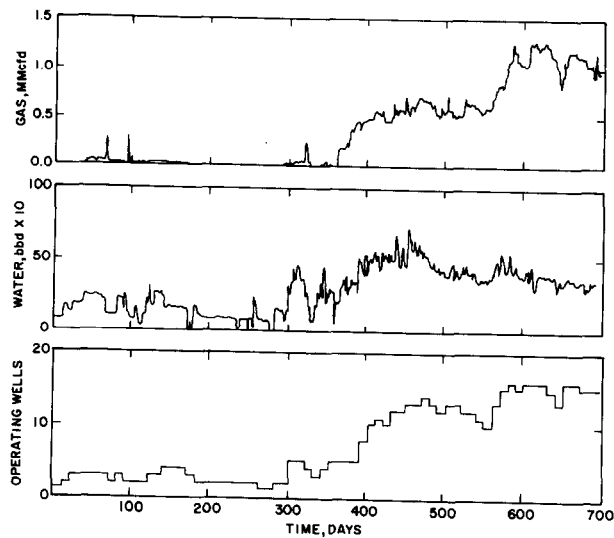


FIGURE 6
GRID USED IN SIMULATION MODEL SHOWING AREAS
OF ADJUSTED PERMEABILITY AND POROSITY

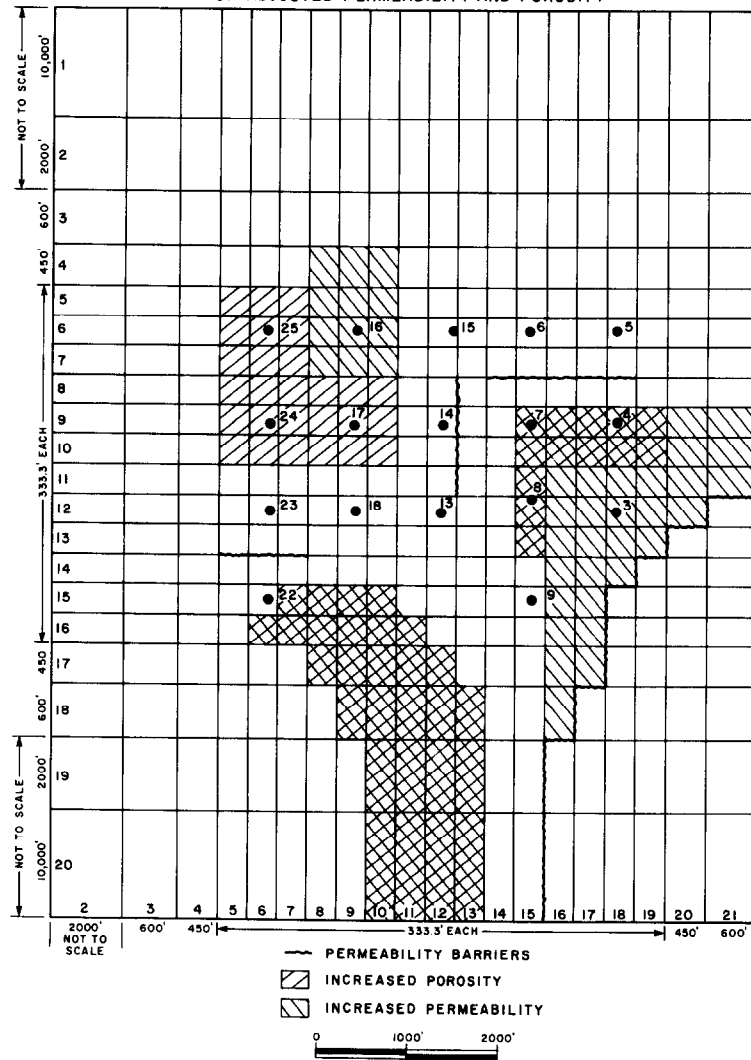


FIGURE 7
RELATIVE PERMEABILITY CURVES USED IN
OAK GROVE PATTERN SIMULATION

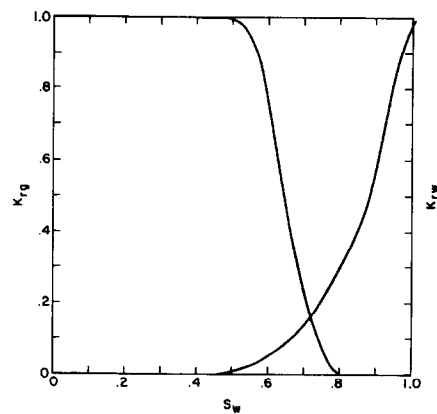


FIGURE 8
TOTAL PRODUCTION RATE FROM PATTERN -
COMPAIRED TO SIMULATION RESULTS

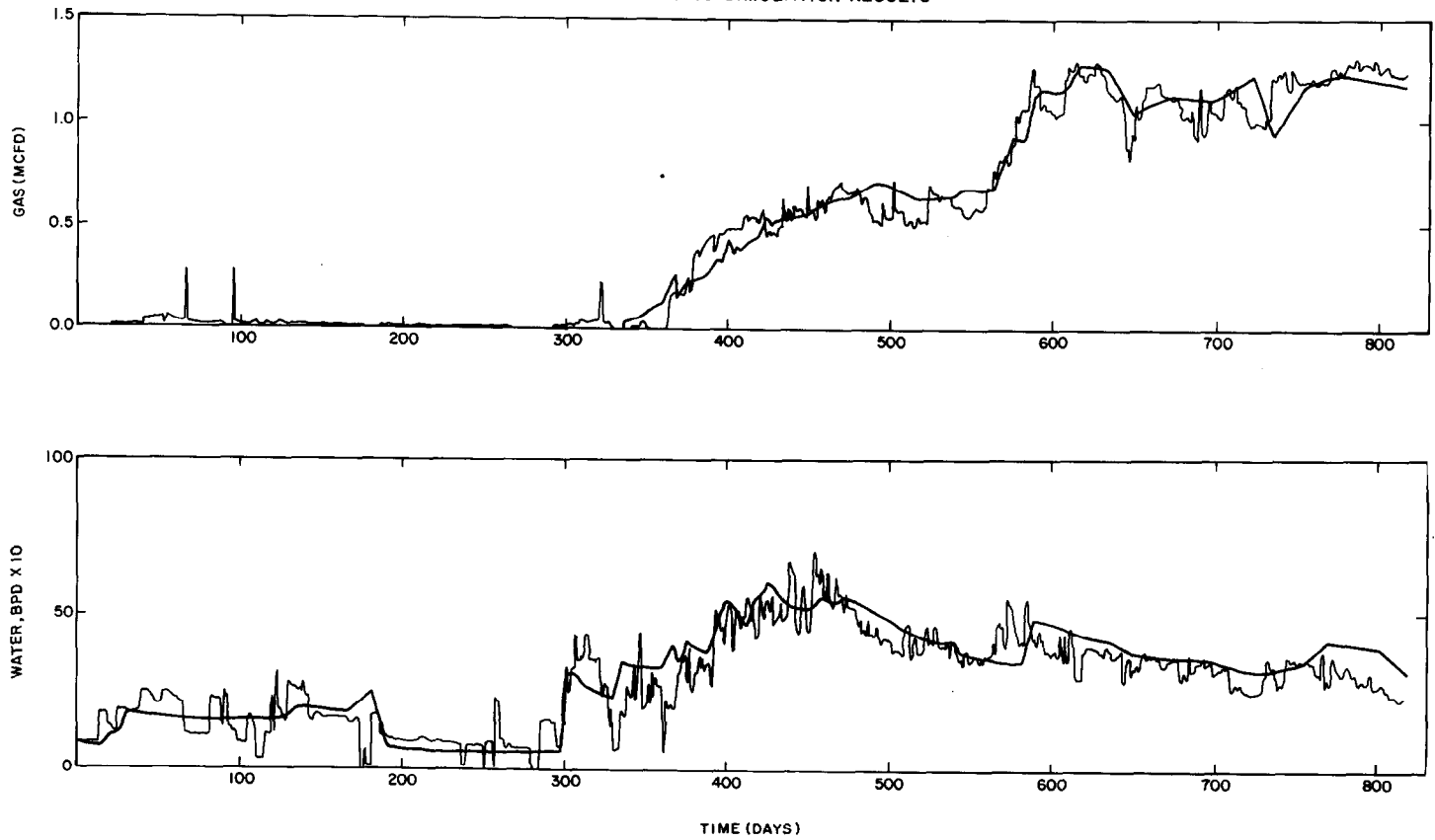


FIGURE 9
WELL 22 PRODUCTION RATES COMPAIRED TO SIMULATION

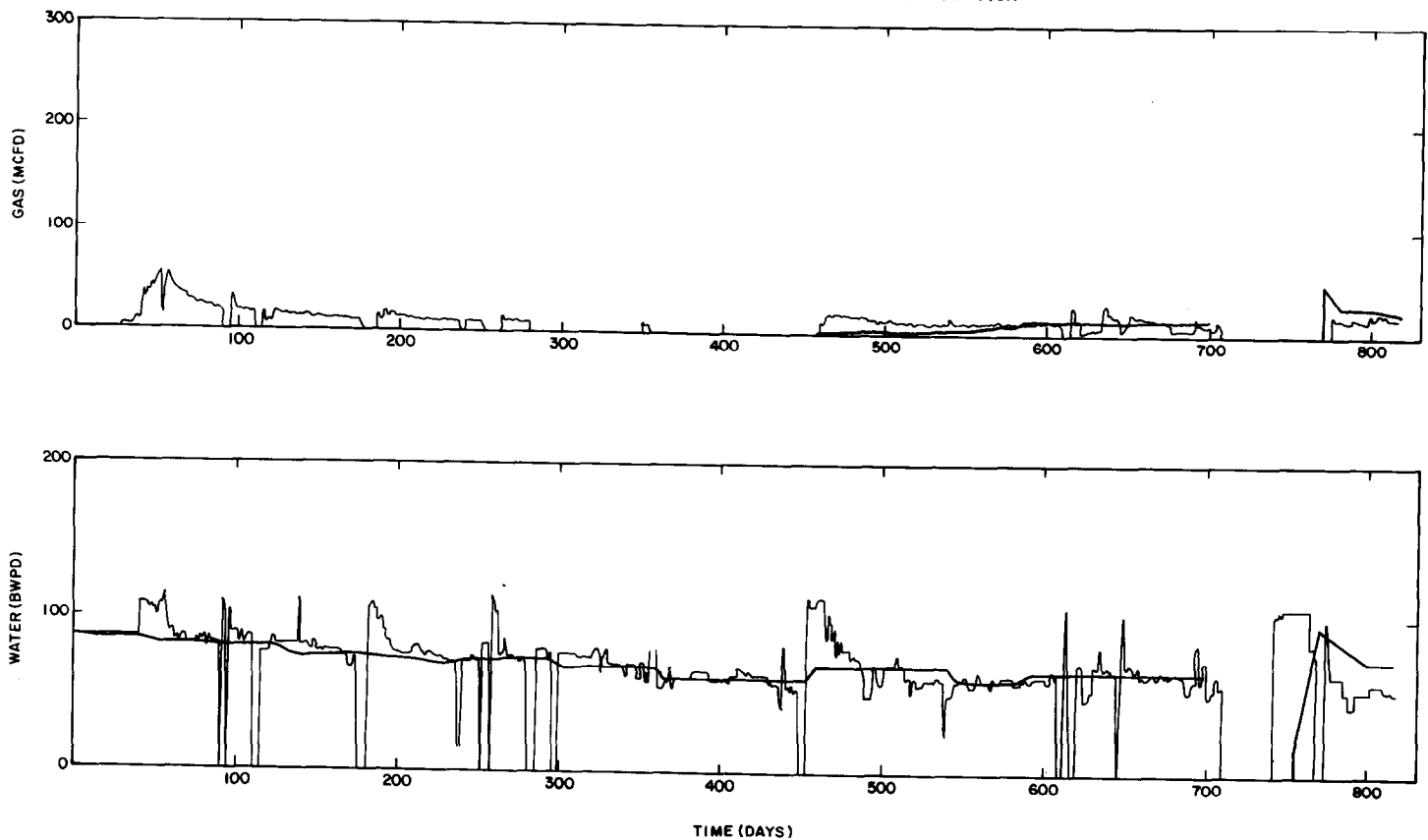


FIGURE 10
WELL 4 PRODUCTION RATES COMPARED TO SIMULATION

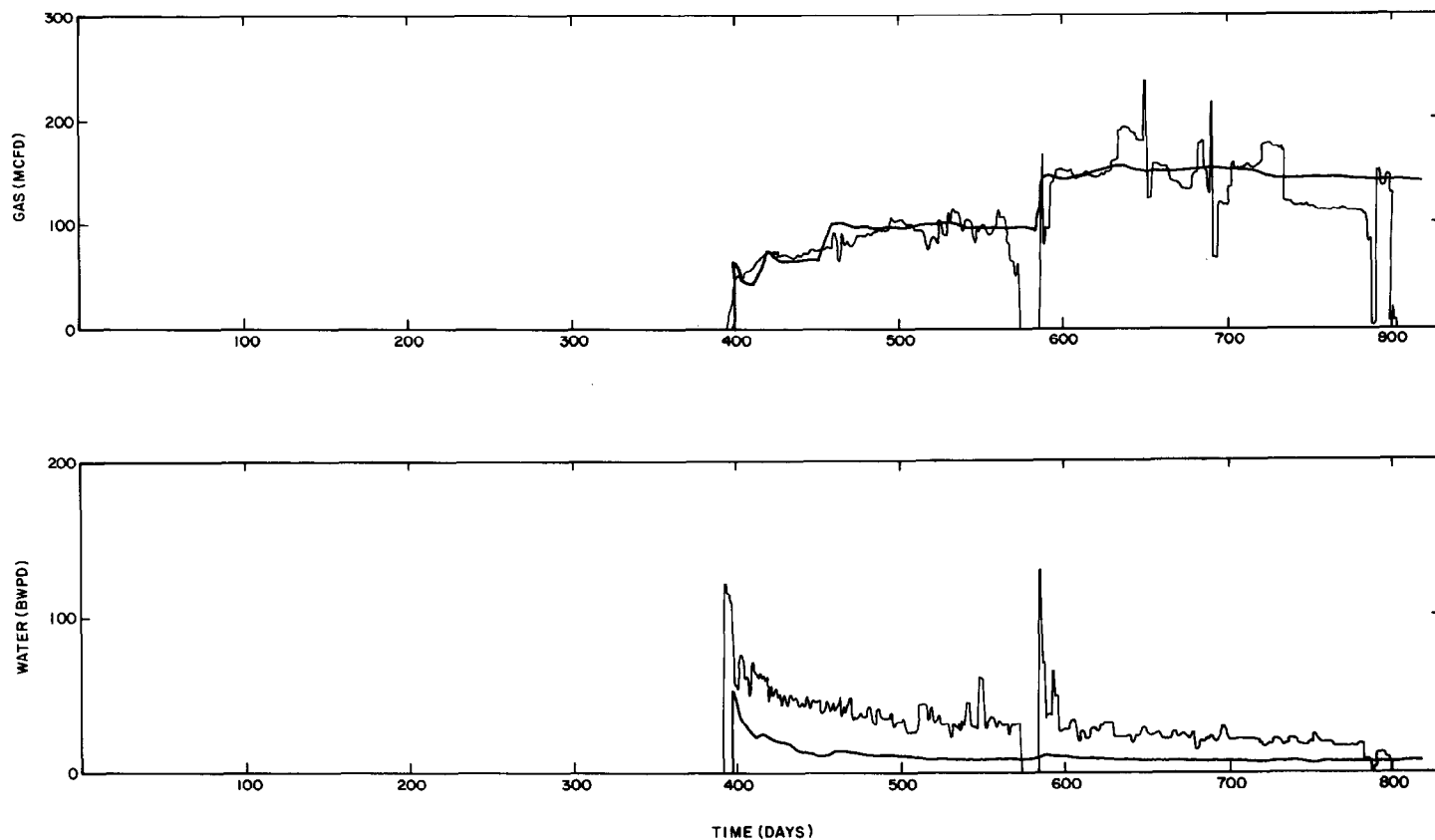


FIGURE 11
WELL 7 PRODUCTION RATES COMPARED TO SIMULATION

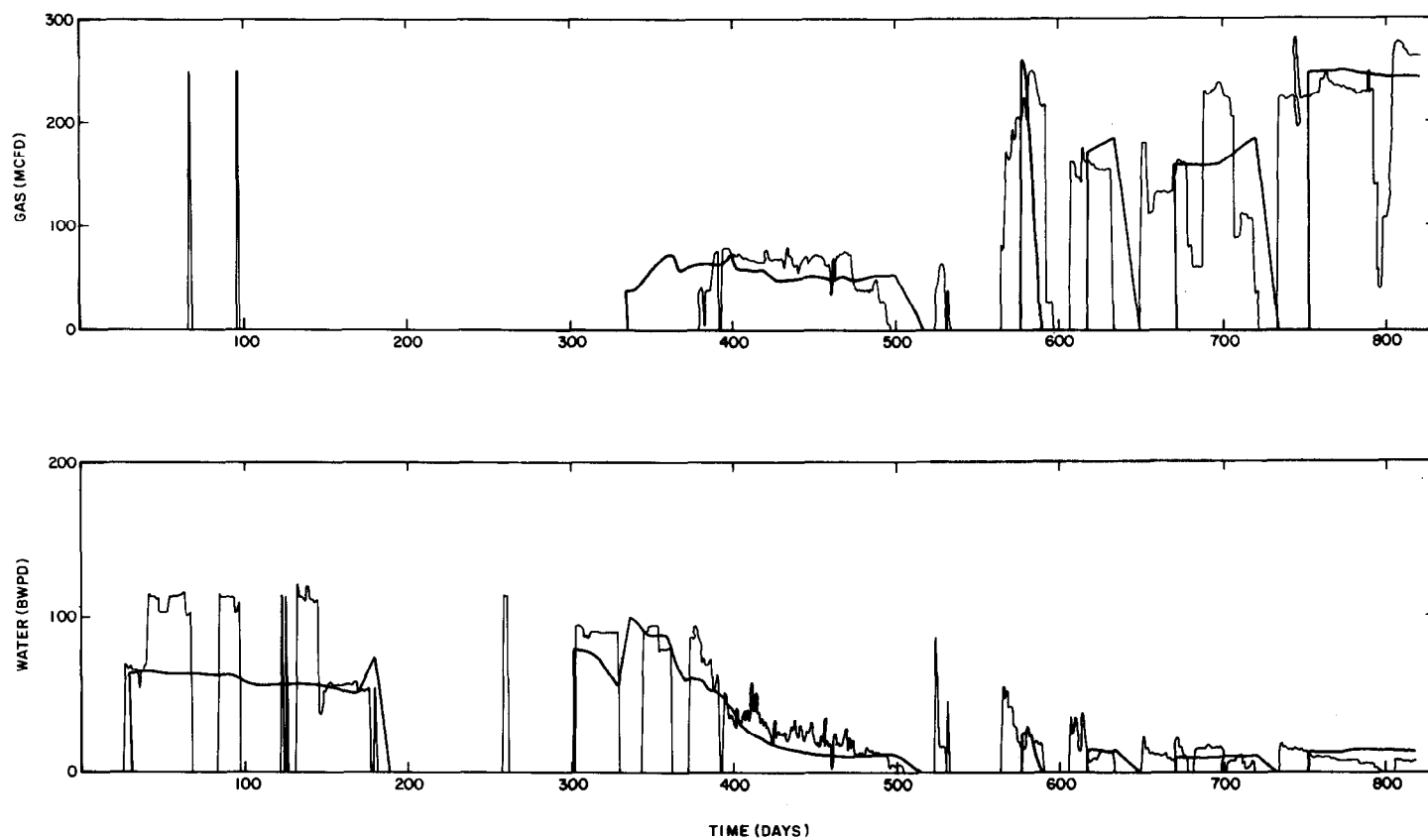


FIGURE 12
WELL 25 PRODUCTION RATES COMPARED TO SIMULATION

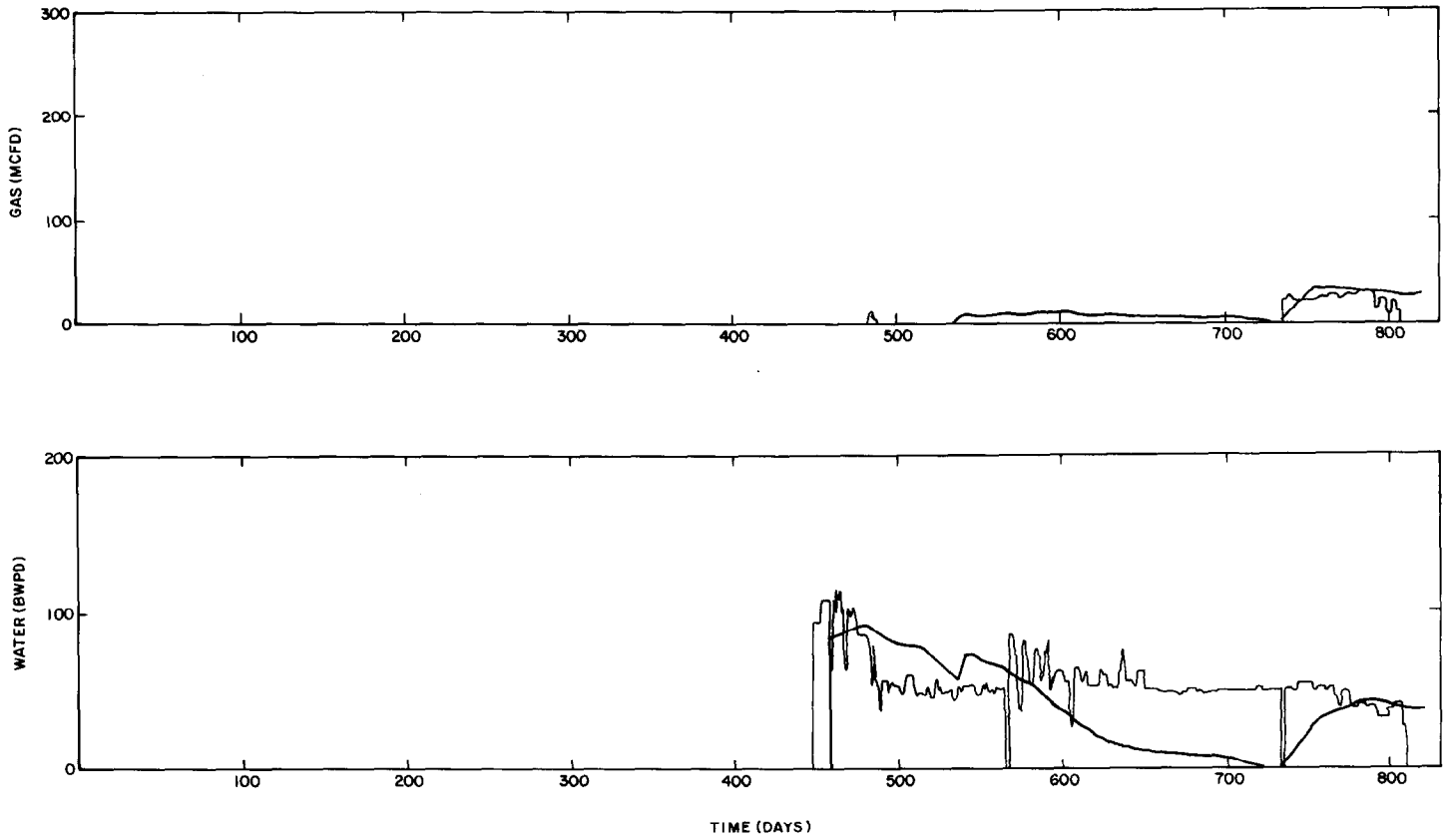
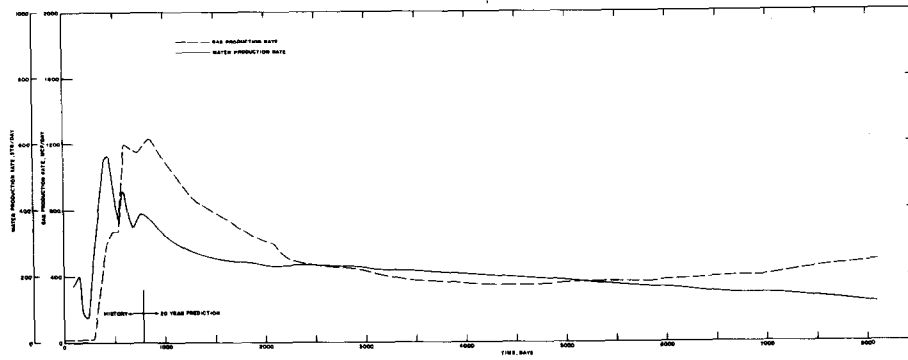


FIGURE 13
20 YEAR PRODUCTION PREDICTION



SEISMIC VELOCITY ANALYSIS TO LOCATE SHALE GAS WELLS

by John St. A. Boyer III, Nigel A. Anstey,
Donohue Anstey and Morrill

This paper was presented at the 1980 SPE/DOE Symposium on Unconventional Gas Recovery held in Pittsburgh, Pennsylvania, May 18-21, 1980. The material is subject to correction by the author. Permission to copy is restricted to an abstract of not more than 300 words. Write: 6200 N. Central Expwy., Dallas, Texas 75206

ABSTRACT

It is known that economic production of shale gas is currently possible only where shale is naturally fractured. The exploration problem is therefore to locate zones of fracture. In principle, extensive zones of natural fracture in a thick shale can be identified by the measurement of seismic velocity from the surface. The technique of reflection velocity analysis uses differential reflection time of reflections observed at the surface (with various source-geophone distances) to infer the extent of the gas saturated fracture zones. This technique has been applied along an available seismic line in Southeastern Ohio. A continuous velocity analysis of the shale interval along this line was prepared, and areas of depressed velocity have been identified. These results, and the results of drilling in the first area of low velocity will be discussed.

INTRODUCTION

Large volumes of shale gas are contained within the Devonian shales of the Appalachian Basin. In general, however, the economics of exploring for and producing this gas are adverse; although the shale is widespread over the basin, only a few fields are currently producing significant gas. Over the years, it has become clear what distinguished the viable shale-gas location from the uneconomic location; a good shale-gas well requires that the shale be fractured so that paths exist for the gas to flow from a large volume of shale to the well bore. A thick section of black gas-source shale is also desirable. By now, the variations of thickness of the source shale over the Appalachian Basin are well documented; maps showing these variations have been prepared under other DOE contracts, and are publicly available. The exploration problem therefore reduces simply to this: How can we locate, from the surface, zones of extensive fracture in the shale?

A current technique for locating zones of fracture includes the use of aerial photographs and satellite images to find linear alignments of surface features,

such as faults, linear valleys, or other surface changes. It is hoped that fractured zones far below the surface can be identified using this technique. One weakness of this approach is its assumption that the faults or fractures are vertical. In general, fractures caused by earth tides can probably be assumed to be vertical, but faults associated with tectonic movements are often not so.

Another weakness of the approach is that fault and fracture planes represent escape paths for gas; if the planes extend to the surface, the inference may be that all the gas has gone. This had led to the suggestion that the best place to drill is not on the lineament itself, but some distance from it; the hope is that the forces which produced a fault or fracture large enough to show at the surface are likely to have produced minor fracturing for some distance from the major feature. There is still no assurance that these minor fractures do not connect to the vent. Nor is anyone quite sure of the "best" distance from the lineament.

A second approach to locating zones of fracture is to use knowledge of faults obtained from subsurface well control or seismics. Since these methods identify a fault only by its displacement, fractures without throw are not revealed. The merit of this approach, however, is that faults can be identified which do not reach the surface.

The age of the faulting is important. Young shales, of course, tend to be plastic; a shale as old as the Devonian becomes brittle and capable of fracture. Only faults much younger than the Devonian are likely to have engendered fracturing; the ideal is probably repeated rejuvenation of deep basement movement. Some feeling for this can be obtained, from well control and seismics, by studying the faulted intervals at different levels.

Further, simple flexure of the whole geologic section, without faulting, may be sufficient to cause fracture in the shale. We speculate that the zone of fracture is likely to be best developed above and just to the downthrown side of the maximum acceleration of dip (see Figure 1); it is the rate-of-change

Reference and illustrations at end of paper.

of dip and not the dip itself, which is likely to be important. In this context the search is for structural hinge-lines and sharp flexes, introduced by tectonic movement after consolidation of the shale.

Considering that over the lone haul only a few significant productive Devonian shale gas fields have been found and that the above mentioned techniques have not improved the finding rate appreciably in recent years, DOE, in February 1978, requested proposals for new approaches to the problem of locating shale-gas wells. The RFP visualized that research projects engendered by this request would seek to develop an exploration rationale, and would then test this rationale by the drilling of one or more wells. In order to maximize the information obtained, selected wells were to be cored and logged in detail, and stimulated with advanced techniques. This comprehensive scheme would not only establish why the exploration rationale succeeded or failed, but also add to the growing fund of information on the character and distribution of the shale-gas resource.

In the RFP seven areas in the Appalachian Basin were delineated as prime candidates for shale-gas exploration, having both a good thickness of black shale and favorable lineament indications. We have directed our efforts at two or these areas in South-eastern Ohio, (see Figure 2) where, using an available 125 mile seismic line, reflection velocity analyses was performed. The results of this velocity analysis and the rationale for selecting up to three drilling sites are discussed below.

THE TECHNIQUE

The essential features of the reflection velocity analysis technique are summarized below:

1. The speed of sound in rocks is called the seismic velocity.
2. The seismic velocity in a shale usually lies in the range 6000-16000 ft/s. The factors accounting for this very wide range are compaction, overpressure, cementation, fracturing, and the presence of gas.
3. In the Devonian shales of the Appalachian Basin, three of these - compaction, fracturing of gas - are likely to be dominant.
4. The dependence on compaction means that the shale velocity is likely to increase with depth; probably the determining factor is the greatest historical depth, rather than the present depth. Where the basin flank is gentle and substantially undisturbed, it is reasonable to hope that velocity variations due to depth are very gradual, and that they may be separated from local variations due to other agencies.
5. The dependence on fracturing arises because the velocity is inversely related to the compressibility of the rock. A fractured rock contains voids, into which the rock can deform under compression; the compressibility of the rock is increased somewhat by the fracture if they are full of

liquid, and increased even more if they contain even a small percentage of gas. There is therefore every hope that a local depression of shale velocity can be equated quite strictly to the presence of a fracture zone containing gas - exactly the condition that we wish to detect.

6. The essence of the seismic method is to make some sort of bang, and to listen for (and time) the echoes; these echoes are the reflections of the bang, bounced off deep rock layers and received at the surface (see Figure 3).
7. Where the depth of a reflecting interface is known from well control, an immediate measure of the average seismic velocity down to that interface is obtained by dividing the depth by half the seismic reflection time. This is the time-depth velocity measurement.
8. Where the depth is not known, a measure of the seismic velocity can be obtained by making two reflection observations of the same piece of reflector. One is the short-offset observation, the other is the long-offset observation (see Figure 4). Of course, the reflection time in the second case is longer, because the seismic pulse has traveled further. The principle of seismic velocity analysis is that the extra distance divided by the extra time gives the velocity. In practice the method uses 12 or more paths of various offset (rather than the two described here); the precision is improved, but the principle is the same.

APPLICATION OF THE TECHNIQUE

Velocity studies were performed on a 125 mile seismic line shot by Petty-Ray Geophysical (now the Exploration Services Division of Geosource Inc.). The Geosource line was recorded along roads, many of which follow winding river valleys. The north-west part of the line is over glaciated topography. The shale becomes shallow and thin to the west. It was understood from the onset that the velocity measurements would be very dependent on the quality of the original seismic data, and that they would be adversely affected by rough topography, bends in the line, gaps associated with houses or villages, surface transitions from bedrock to thick alluvium, and glacial fill. Nevertheless it was hoped that broad regional trends in velocity would remain clearly visible, and that local anomalous departures from these trends would also be clear. A full velocity analysis through the shale interval was commissioned.

The velocity analysis was performed using conventional techniques. Common-depth-point gathers were made every 150 feet. For each of several successive cdp gathers, a sequence of stacked traces, representing several constant velocities were obtained. The velocity which yields the best-looking stack, over a particular group of cdp gathers and at a particular time, is judged to be the correct one.

Velocity displays are shown in Figures 5, 6 and 7. Figure 5 represents a three-dimensional surface in time, velocity and absolute summed amplitude. Figure 6 represents the same data, but contoured by computer; this type of display probably gives the easiest measurement of velocity. Figure 7 shows several velocity stacks at the same station and probably gives the greatest degree of comfort in terms of determining the actual change of velocity through the shale interval. For the present project, Geosource provided one display like Figure 6 and one like Figure 7 every 3000 ft along the line. Ten depth-points were used in each display, spaced at 150 ft; the data entering velocity analysis were therefore one-half of all the data recorded on the line.

INTERPRETATION

The first interpretive step of the seismic analysis was to correlate the seismic reflections with the known geological interfaces as shown in Figure 8. This was unusually straightforward, thanks to the well-spaced nature of the reflections and the high velocity of the Big Lime interval. Figure 9 is a short sequence of seismic cross-section near the southeast end of the line, annotated to show the top-shale (Berea) reflection, the base-shale (Big-Lime) reflection, and the deep Trenton reflection.

This segment of seismic section is unusually good — particularly in that it shows the Berea complex at the top of the shale. Only a few miles from the southeast end of the line the top-shale reflection becomes too shallow and/or too weak to be seen. Also visible in the figure are two or three reflections from within the shale; reflections like these (though not necessarily their stratigraphic equivalents) are seen intermittently along the line.

The observed weakness or absence of the top shale reflection forced a change in the approach visualized in the proposal. It became clear that the velocity measurement would have to be that from surface to Big Lime, rather than that of the shale interval itself (from Berea to Big Lime). Of course this would make the measurement less sensitive to velocity anomalies originating in and confined to the shale; however, by this stage of the work it was apparent that the measurement from surface to Big Lime shows significant anomalies, and that a small sacrifice of sensitivity was immaterial.

Figure 10 shows the velocity analysis corresponding to Figure 9. The contour maxima representing the main reflections are annotated, and the dashed line joining these maxima yields the velocity-time relation. Where the dashed line has a small inclination to the vertical (as within the shale), the interval velocity is comparatively low; where it deflects off to the right (as within the Big Lime) the interval velocity is high. This high velocity in the lime sequence is an important corroboration of the reflection identifications.

RESULTS

The broad results of the whole project are com-

pressed into an illustration similar to Figure 11. This display represents a small section of the profile along the path of the seismic line.

The three graphs are the seismic velocity values for the Big Lime reflection. The upper one shows the raw velocity values as picked from the velocity analyses. The code is as follows:

- a very clear maximum, with no interference and small spread,
- a clear maximum, with little or no interference, but with somewhat broader spread,
- subject to interference, but with the "best" pick, well resolved; or a clear maximum without interference but with widespread,
- subject to obvious interference, with some ambiguity of pick,
- ? questionable, no pick at all.

The pronounced and abrupt deviations from a smooth curve are associated with an edge-effect which plagues seismic velocity measurements straddling the edge of anomalies. A discussion of these is beyond the scope of this paper. However, at a first level, it is defensible to smooth out these deviations by an appropriate smoothing operator, and this has been done (to two degrees) in the second and third curves. Here we concentrate on the third lowest curve, which shows a pronounced and broad velocity minimum.

The first message of the Big Lime velocity profile, in its doubly-smoothed form, is a regional increase of velocity with depth. This is to be expected, as a corollary of the compactibility of a predominantly-shale section. At the northwest end of the line the velocity to Big Lime is about 14000 ft/s; at the southeast end it probably approaches 16000 ft/s. All local variations of velocity are to be seen against the background of this expected regional variation.

The next message is that local variations are apparent. Several of these have a magnitude approaching 1000 ft/s; a few exceed 1500 ft/s. This is at least as good as we could have hoped for, realistically. The temptation, therefore, is to nominate each local minimum of Big Lime velocity as a location for a shale-gas test.

The local minimum of Big Lime velocity shown in Figure 11 is where the first experimental well is being drilled. Other local minimum velocity areas have been identified along the seismic line but detailed discussion of them at this time would be premature. Drilling of the first well is underway at the time of this writing and actual results will be presented at the SPE meeting.

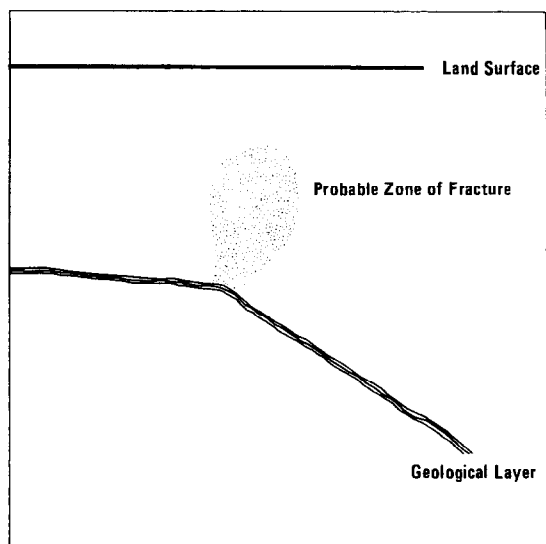


Fig. 1 - Zone of flexure.

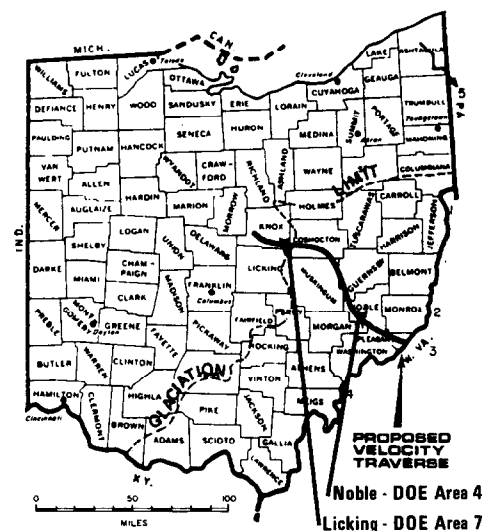


Fig. 2 - Areas in Ohio from RFP.

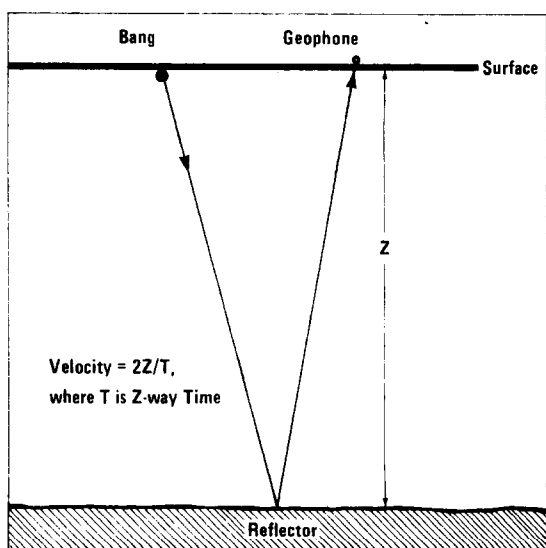


Fig. 3 - Basics of seismic method.

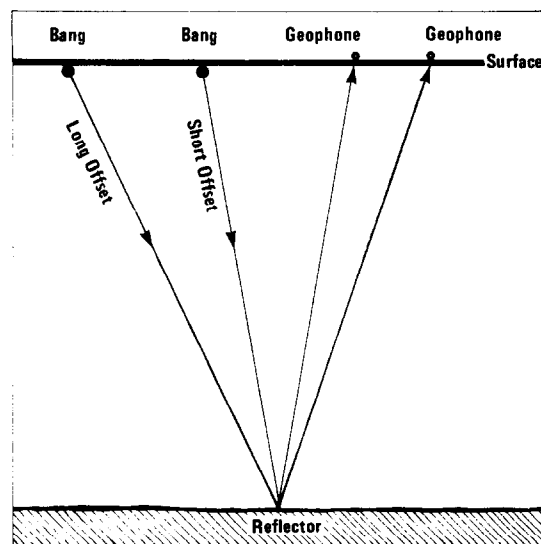


Fig. 4 - Short offset and long offset observations.

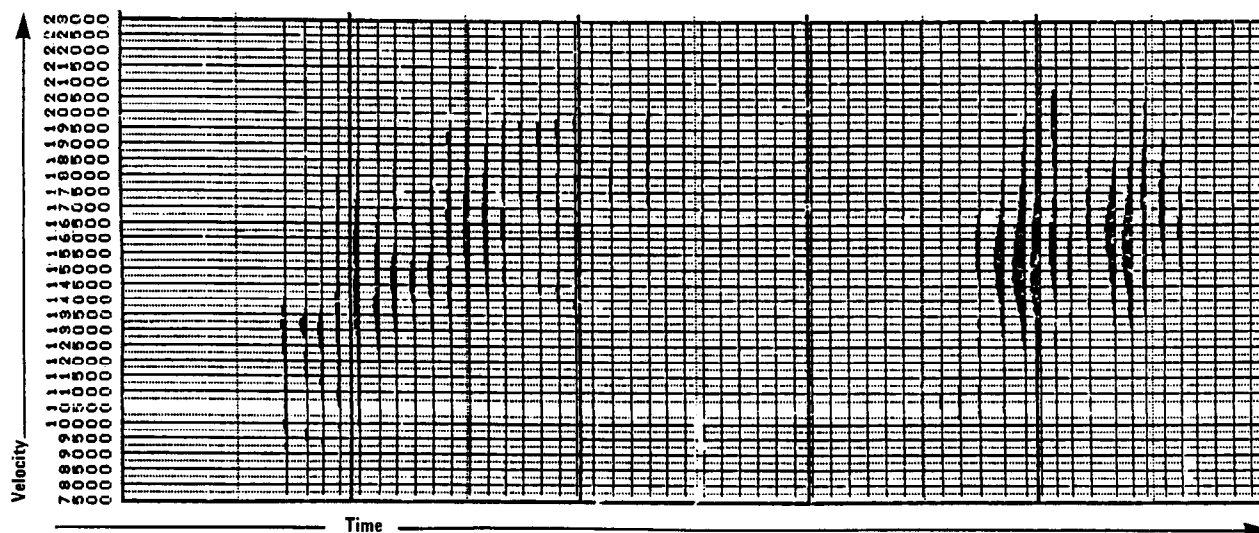


Fig. 5 - Velocity analysis display, three-dimensional surface.

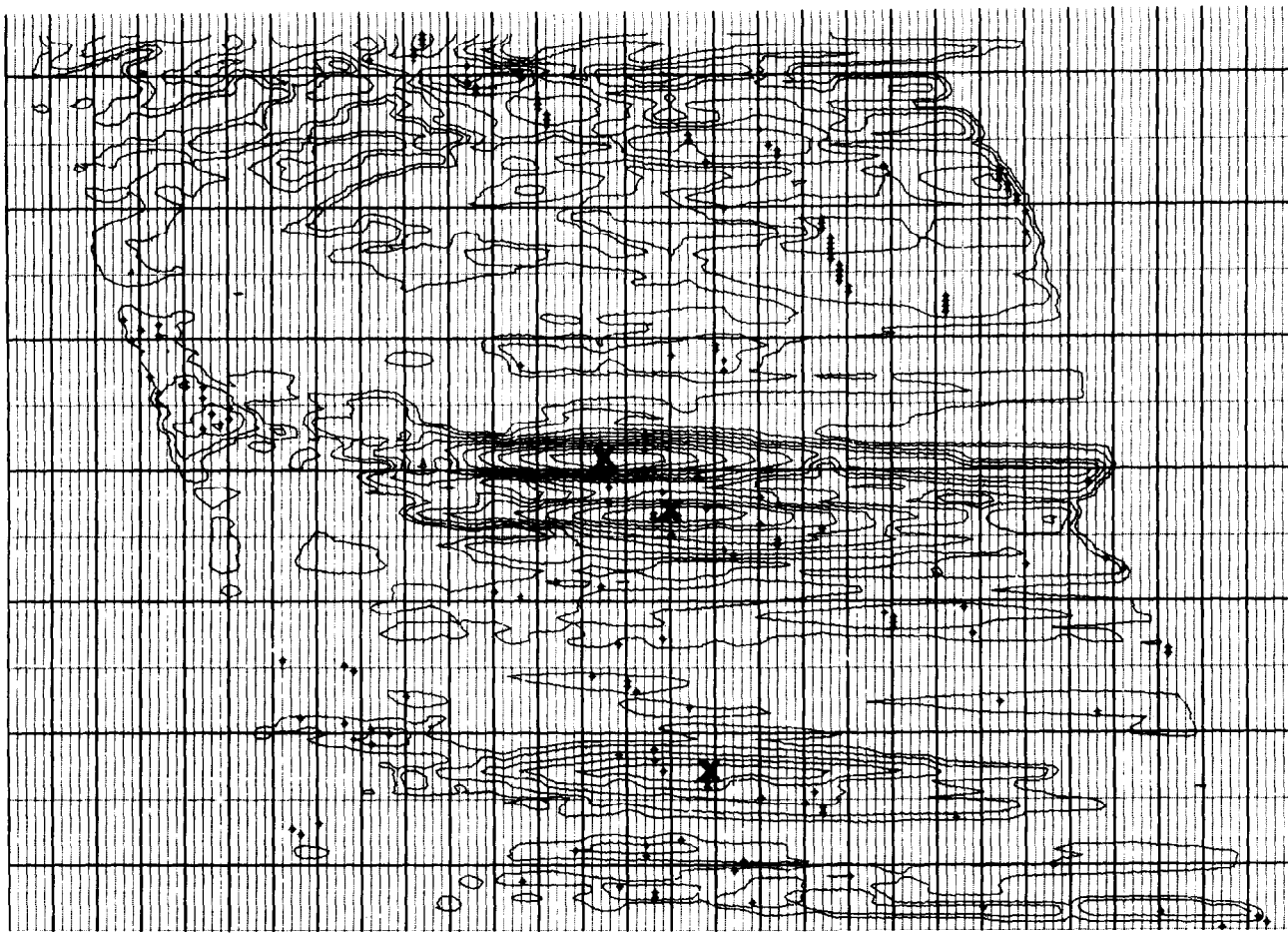


Fig. 6 - Velocity spectrum.

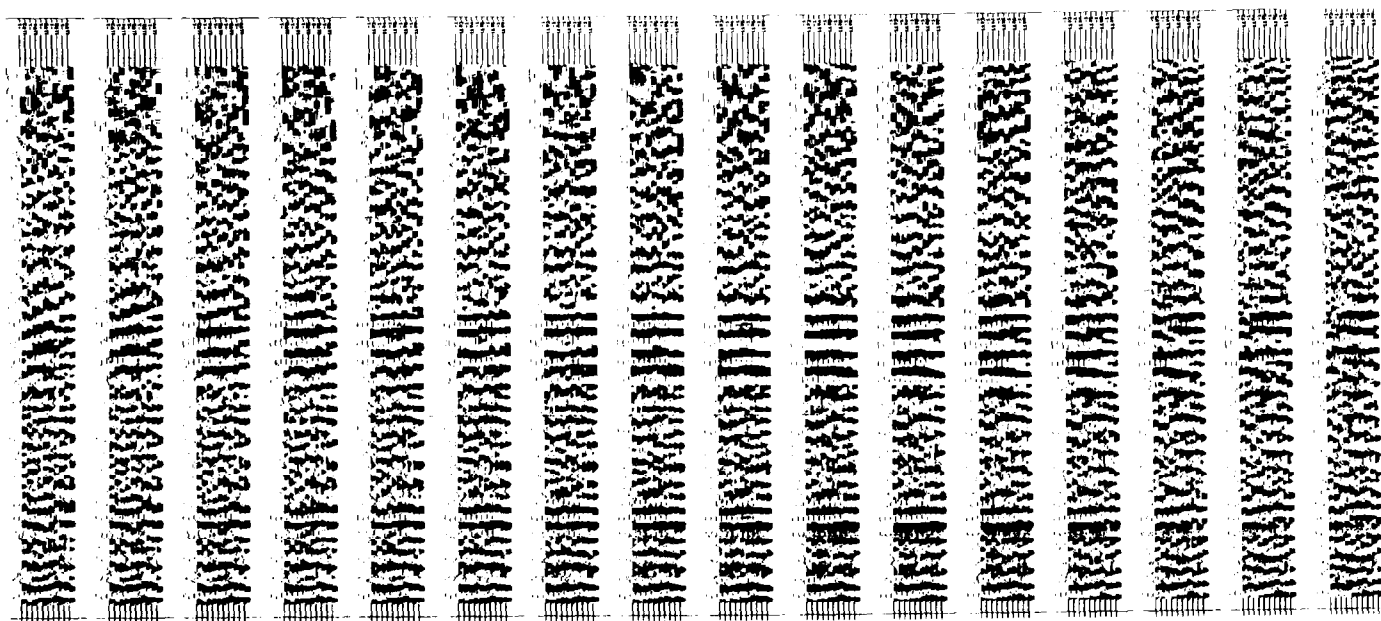


Fig. 7 - Velocity stacks.

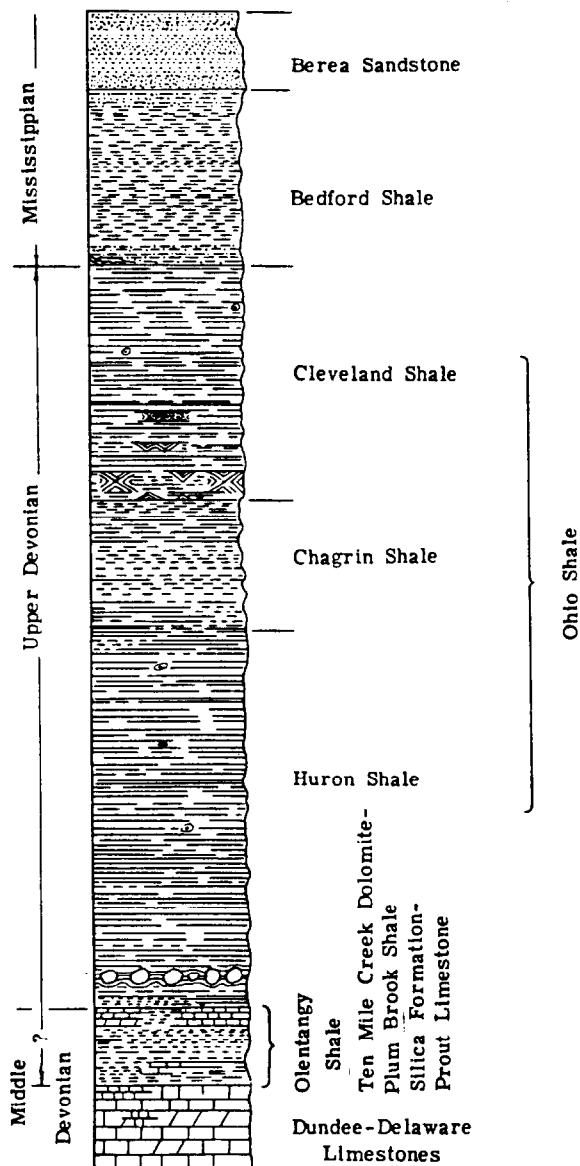


Fig.8 - Generalized columnar section of the Devonian-Missippian shale sequence (from Hoover, 1960).

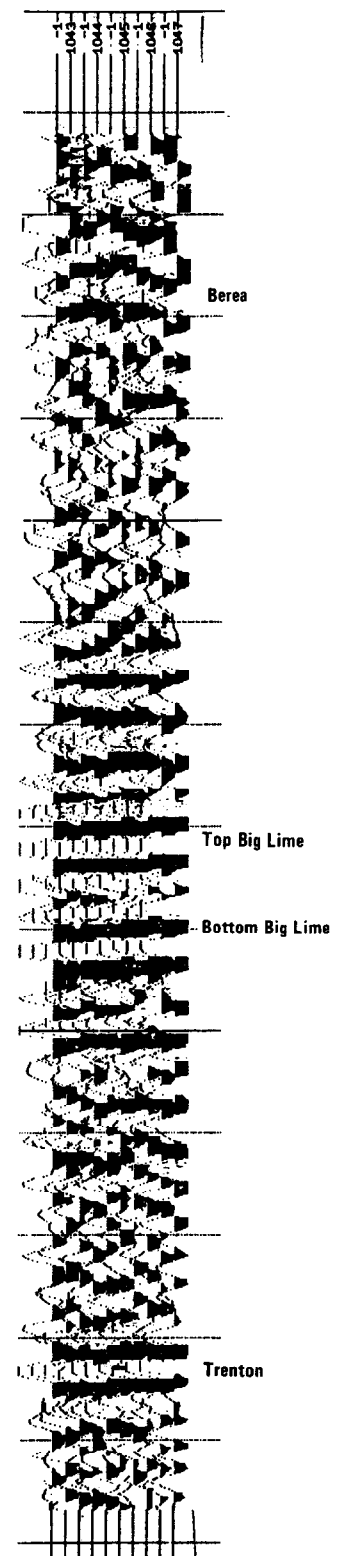


Fig. 9 - Velocity stacks showing Berea, Big Lime and Trenton.

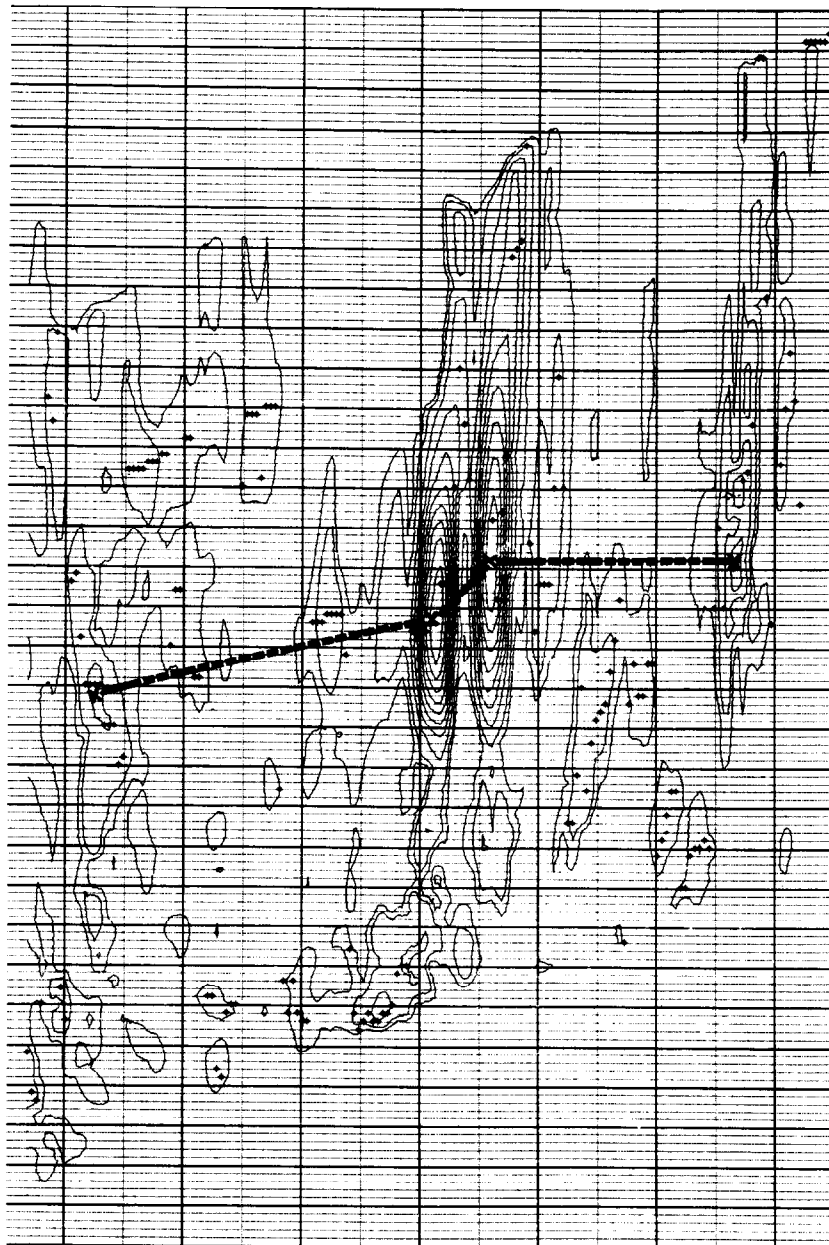


Fig. 10 - Velocity spectrum.

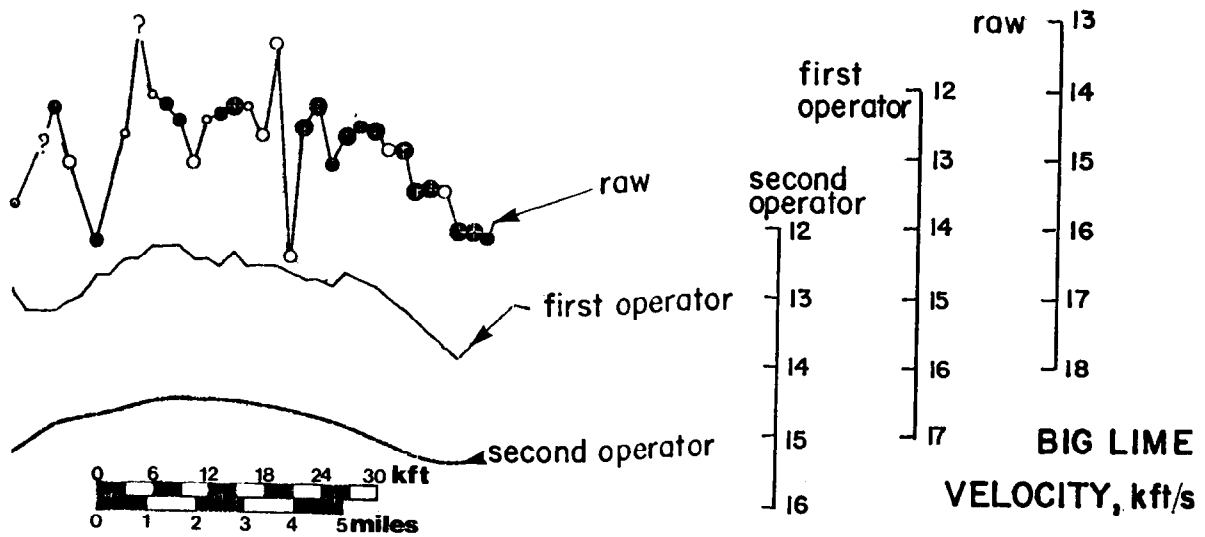


Fig. 11 - Velocity analysis curves - Big Lime.